CHEMICAL CHARACTERISATION

OF THE

SOILS OF EAST-CENTRAL NAMIBIA

Marina Elda Coetzee

Thesis presented in partial fulfilment of the requirements for the degree of Master of Science in Agriculture at Stellenbosch University

Study Leader:	F Ellis
Date:	March 2009

Declaration

By subitting this thesis electronically, I declare that the entirety of the work contained therein is my own, original work, that I am the owner of the copyright thereof (unless, to the extent explicitly otherwise stated) and that I have not previously in its entirety or in part submitted it for obtaining any qualification.

Date: 22 February 2009

ABSTRACT

A number of chemical and physical features of Namibian soils in a 22 790 km^2, two degree-square block between 17 – 19 ^{o}E and 22 – 23 ^{o}S in eastern central Namibia, had been investigated, and the fertility status established.

In 80 % of samples the nitrate, nitrite, and sulfate concentrations of the saturated paste extract are 0 – 54.6 mg l^{-1} NO_3^-, 0 – 24.7 mg l^{-1} NO_2^-, and 5.4 – 20.9 mg l^{-1} SO_4^{2-} respectively. In 90 % of samples the plant-available phosphorus is below 12 mg kg^{-1}, which is low for a soil under natural grassland, but in line with the prevailing semi-arid climate and low biomass production of the study area. In 80 % of samples the extractable calcium, magnesium, potassium, and sodium concentrations are 0.61 – 5.73 $cmol_c kg^{-1}$ Ca (122 – 1 146 mg kg^{-1} Ca), 0.12 – 2.28 $cmol_c kg^{-1}$ Mg (15 – 278 mg kg^{-1} Mg), 0.13 – 0.54 $cmol_c kg^{-1}$ K (51 – 213 mg kg^{-1} K) and 0.05 – 0.38 $cmol_c kg^{-1}$ Na (11 – 87 mg kg^{-1} Na) respectively, while the exchangeable calcium, magnesium, potassium, and sodium concentrations are 0.21 – 6.02 $cmol_c kg^{-1}$ Ca, 0.12 – 2.01 $cmol_c kg^{-1}$ Mg, 0.12 – 0.49 $cmol_c kg^{-1}$ K and 0 – 0.13 $cmol_c kg^{-1}$ Na respectively. The mean ± 1 standard deviation is 3.57 ± 3.57 $cmol_c kg^{-1}$ for cation exchange capacity, 3.48 ± 3.61 for sum of exchangeable bases and 4.53 ± 4.39 for sum of extractable bases. The cation exchange capacity and the sum of exchangeable bases are virtually identical, which indicate the almost complete absence of exchangeable H^+ and Al^{3+} in the soils of the study area, as expected from a semi-arid climate. None of the profiles were classified as saline or sodic. In 80 % of samples the plant-available iron, manganese, zinc and copper concentrations are 7.2 – 32.8 mg kg^{-1} Fe, 13.6 – 207.5 mg kg^{-1} Mn, 0 – 1.80 mg kg^{-1} Zn and 0 – 4.0 mg kg^{-1} Cu respectively. Soil organic matter content of the study area soils ranges between 0.05 – 2.00 %, with most (80 % of samples) containing 0.25 – 1.20 % organic matter. This is considerably lower than values reported in literature, even for other southern African countries. The reason lies with the hot, semi-arid climate. The pH distribution is close to normal, with 80 % of samples having pH (H_2O) of 5.54 – 8.18, namely moderately acid to moderately alkaline. Sand, silt and clay content of most (80 %) samples varies between 60.3 – 89.7 % sand, 4.6 – 25.2 % silt and 3.5 – 19.1 % clay. The soils of the study area are mainly sandy, sandy loam and loamy sand. In 80 % of samples the coarse sand fraction ranges from 3.5 – 34.5 %, the medium sand fraction from 20.5 – 37.3 %, the fine sand fraction from 38.7 – 54.5 % and the very fine sand fraction from 0.0 – 12.9 % of all sand. The fine sand fraction, thus, dominates, with very fine sand being least abundant. The topsoil contains relatively more coarse sand and less very fine sand than the subsoil. Instances of sealing, crusting and hardening occur sporadically in the study area. Cracking is only found in pans, while self-mulching is not evident. No highly instable soils were encountered in the study area. The water-holding capacity is generally low, with depth limitations in the western highlands, the Khomas Hochland, and texture limitations in the eastern Kalahari sands. The central area has soils with a somewhat better water-holding capacity, but it is still very low when compared to arable soils of temperate, sub-humid and humid zones elsewhere in southern Africa.

Soil characteristics are perceptibly correlated with climate, parent material, topography, degree of dissection of the landscape and position in the landscape. The most obvious differences are between soils formed in schistose parent material of the Khomas Hochland in the west and those of the Kalahari sands in the east. The soils of the study area are unsuitable to marginally suitable for rainfed crop production, due to low

fertility. The study area is climatologically unsuited for rainfed crop production, so the present major land use is extensive livestock production on large farms. The natural vegetation is well adapted to the prevailing conditions.

The methodology followed to delineate terrain units, with a combination of procedures involving digital elevation data and satellite imagery, seems to work well in the Namibian landscape. This study thus served as a successful proof-of-concept for the methodology, which can in future be rolled out for the remainder of the country. The site and analytical information is available in digital format as spreadsheets and in a geographical information system, as well as in a variety of digital and printed maps.

UITTREKSEL

'n Aantal chemiese en fisiese eienskappe van Namibiese gronde in 'n 22 790 km^2, 1^o x 2^o blok tussen 17 – 19 ^{o} Oos en 22– 23 ^{o} Suid in oostelike sentraal-Namibië is ondersoek en die grondvrugbaarheidstatus bepaal.

In 80 % van monsters is die nitraat-, nitriet- en sulfaatkonsentrasies van die versadigde pasta ekstrak 0.0 – 54.6 mg l^{-1} NO_3^-, 0.0 – 24.7 mg l^{-1} NO_2^-, en 5.4 – 20.9 mg l^{-1} SO_4^{2-}onderskeidelik. In 90 % van monsters is die plant-beskikbare fosfor minder as 12 mg kg^{-1}, wat laag is vir gronde onder natuurlike grasveld, maar dit is verklaarbaar deur die heersende semi-ariede klimaat en lae biomassa produksie in die studiegebied. In 80 % van monsters is die konsentrasies van ekstraheerbare kalsium, magnesium, kalium en natrium 0.61 – 5.73 $cmol_c kg^{-1}$ Ca (122 – 1 146 mg kg^{-1} Ca), 0.12 – 2.28 $cmol_c kg^{-1}$ Mg (15 – 278 mg kg^{-1} Mg), 0.13 – 0.54 $cmol_c$ kg^{-1} K (51 – 213 mg kg^{-1} K) en 0.05 – 0.38 $cmol_c kg^{-1}$ Na (11 – 87 mg kg^{-1} Na) onderskeidelik, terwyl die uitruilbare kalsium, magnesium, kalium en natrium konsentrasies onderskeidelik 0.21 – 6.02 $cmol_c kg^{-1}$ Ca, 0.12 – 2.01 $cmol_c kg^{-1}$ Mg, 0.12 – 0.49 $cmol_c kg^{-1}$ K and 0.0 – 0.13 $cmol_c kg^{-1}$ Na is. Die gemiddelde ± 1 standaardafwyking is 3.57 ± 3.57 $cmol_c kg^{-1}$ vir katioonuitruilvermoë, 3.48 ± 3.61 vir die som van uitruilbare basisse en 4.53 ± 4.39 vir die som van ekstraheerbare basisse. Die katioonuitruilvermoë en som van uitruilbare basisse is feitlik identies, wat 'n feitlik algehele afwesigheid van uitruilbare H^+ and Al^{3+} in die gronde van die studiegebied aandui, soos verwag word weens die semi-ariede klimaat. Geeneen van die profiele is geklassifiseer as soutbrak of natriumbrak nie. In 80 % van monsters is die plant-beskikbare yster, mangaan, sink en koper konsentrasies onderskeidelik 7.2 – 32.8 mg kg^{-1} Fe, 13.6 – 207.5 mg kg^{-1} Mn, 0.0 – 1.80 mg kg^{-1} Zn en 0.0 – 4.0 mg kg^{-1} Cu. Grond organiese material inhoud in die studiegebied wissel tussen 0.05 – 2.00 %, met 80 % van monsters wat 0.25 – 1.20 % organiese material bevat. Dit is aansienlik laer as die waardes gevind in literatuur, selfs vir ander Suider-Afrikaanse lande. Die oorsaak is die warm, semi-ariede klimaat. Die pH verspreiding is feitlik normal, met 80 % van monsters wat pH (H_2O) van 5.54 – 8.18 het, met ander woorde matig suur tot matig alkalies. Sand, slik en klei inhoud van die meeste (80 %) monsters varieer tussen 60.3 – 89.7 % sand, 4.6 – 25.2 % slik en 3.5 – 19.1 % klei. Die gronde van die studiegebied is hoofsaaklik sand, sand-leem en leem-sand. In 80 % van monsters beslaan die growwe sandfraksie 3.5 – 34.5 %, die medium sandfraksie 20.5 – 37.3 %, die fyn sandfraksie 38.7 – 54.5 % en die baie fyn sandfraksie 0.0 – 12.9 % van die totale sandfraksie. Die fyn sandfraksie is dus dominant, terwyl die baie fyn sandfraksie die skaarsste is. Die bogronde bevat relatief meer growwe sand en minder baie fyn sand as die ondergronde. Gevalle van verseëling, korsvorming en verharding kom sporadies in die studiegebied voor. Krake kom net in panne voor en self-omkering is nie opgemerk nie. Geen hoogs-onstabiele gronde is in die studiegebied gevind nie. Die waterhouvermoë is in die algemeen laag, met dieptebeperkinge in die westelike hooglande, die Khomas Hochland, en tekstuurbeperkinge in die oostelike Kalahari sande. Die sentrale gedeelte het gronde met 'n ietwat beter waterhouvermoë, maar dis steeds baie laag in vergelyking met akkerbougronde van gematigde, sub-humiede en humiede sones elders in Suider-Afrika.

Grondeienskappe is ooglopend verwant aan klimaat, moedermateriale, topografie, graad van gebrokenheid van die landskap en posisie in die landskap. Die duidelikste verskille kom voor in die gronde wat van

skisagtige moedermateriaal van die Khomas Hochland in die weste en dié wat in die Kalahari sande in die ooste gevorm het. Die gronde van die studiegebied is ongeskik tot marginal geskik vir droëland akkerbou, weens die lae vrugbaarheid. Aangesien die studiegebied klimatologies ongeskik is vir droëland akkerbou, is die huidige hoof landgebruik ekstensiewe veeproduksie op groot plase. Die natuurlike plantegroei is goed by die heersende omstandighede aangepas.

Die metodiek wat gevolg is om terreineenhede af te baken, wat ‘n kombinasie van prosedures met digitale hoogtedata en satellietbeelde is, blyk goed te werk vir die Namibiese landskap. Hierdie studie dien dus as ‘n suksesvolle bewys-van-konsep van die metodiek, wat in die toekoms uitgebrei kan word na die res van die land. Die veld- en ontledingsinligting is beskikbaar in digitale formaat, in ‘n geografiese inligtingstelsel en ‘n verskeidenheid digitale- en gedrukte kaarte.

ACKNOWLEDGEMENTS

I would like to acknowledge the contributions and support of a number of people, and thank them all profoundly:

My present and former colleagues at the Ministry of Agriculture, Water and Forestry deserve medals for their hard work, enthusiasm, perseverance and putting up with me. The Agro-Ecological Zoning Team consists/consisted of Albert Calitz, Celeste Espach, Louis du Pisani, Heleon Beukes, Heiner Mouton, Josephath Kutuahupira and Serafia Ashipala. Without this great team there would not have been anything to write about. I would like to particularly thank Josephath and Heiner for the site and profile descriptions. Joleen Pretorius, Meriam Endjala and Elizabeth Campbell provided administrative support to the AEZ Team. In the Agricultural Laboratory, Albertha Dausas, Malvern Kachote, Herbicious Tiyeho, Negamba Sheya, Else Stanley, Sara Nanus and Elizabeth Kondombolo at various times carried out the thousands of analyses necessary to characterise the soils and build up a good database. Michael Rowell and Willi Nauhaus compiled the Standard Operating Procedures for analytical methods as part of the Agricultural Laboratory's Quality System. Nico de Klerk, Hans Venter, Paul Jessen and Sheehamandje Ipinge gave their unstinting support to the AEZ Programme. Ben Strohbach, Bessie Bester and Leon Lubbe gave very valuable feedback.

Jürgen Kempf from the Univeristy of Würzburg generously shared his knowledge and data. I also made use of the work that Silke Bertram and Markus Broman did on Bergvlug. Eddy de Pauw, Catherine Vits, Frank Beernaert, Willy Verheye, Bernard Yerima and Andrea Kütter all assisted in various ways to kick-start soil mapping and land evaluation in Namibia. Freddy Nachtergaele and colleagues of the Food and Agriculture Organisation entrusted the AEZ Team with the task to compile a SOTER database for Namibia and gave all the assistance and advice we asked for. The National Soil Survey of Namibia (phase I) was carried out with technical assistance from the Cartographic Institute of Catalonia, and financial support by the Cooperacion Española. This support project was headed by Antoni Roca i Adrover and co-ordinated in Barcelona by Pere Oller i Figueras. The field staff in Namibia consisted of Emilio Ascaso Sastrón, Juan Francisco García Ruíz and Gustavo Carrillo Mahiques, assisted by Paulus Amukwaya Festus and Gabriel Ngungaa Hangara. Database development and GIS integration were carried out by Jordi Marturià Alavedra. In Windhoek, assistance was provided by Carlos Rubio Basabe and Juan Arroyo Fernández, Harald Eichlseder and Roelof Kunst. Vincent van Engelen and his colleagues at the International Soil Reference and Information Centre provided the SOTER database structure, trained Namibian staff and assisted whenever we got stuck. GTZ staff and consultants provided technical and financial assistance at various stages of the QLPP project: Albert Engel, Marysia Avis, Sharon Gomez and Willy Verheye (again!) Theo Dohse from the Institute for Soil, Climate and Water helped the AEZ technicians sort out their fieldwork methodology. Nicolas Ganzin has been collaborating for a long time on biomass production estimation. Johan van Rensburg gave continuous support in GIS. Gabi Schneider and Ute Schreiber from the Geological Survey of Namibia kindly provided digital geological data.

Freddie Ellis, Jan Lambrechts and Martin Fey provided me with the opportunity to enrol for a Masters at the University of Stellenbosh. To Freddie and Jan, specifically, I would like to express my appreciation for their guidance. Annatjie French kept the administrative cogs oiled. Matt Gordon kindly carried out the nitrate-, nitrite and sulfate analyses.

My parents, Bertus and Bertha Visser, gave me both the anchors and the wings to pursue my dreams. My sister, Elmarie, bolstered my ego and cut me down to size, as the occasion required (a necessary activity!). Santjie Garises kept the household afloat while I worked on the thesis.

My husband, Johan, and sons, Gian and Altus, are my inspiration. Thank you for all your love, support, patience and tea. I love you and am immensely proud of you all.

To the Lord, my God, thank you for every blessing.

TABLE OF CONTENTS

LIST OF TABLES

LIST OF FIGURES

LIST OF ACRONYMS, ABBREVIATIONS AND SYMBOLS

%	percentage
	in concentration: 1 % (mass/mass) = 10 000 mg kg^{-1}
~	approximately
“	second
∑	sum of
a.m.s.l	above mean sea level
AECI	Cooperacion Española (Spanish Cooperation Office)
AEZ	Agro-ecological Zoning
AgriLASA	Agricultural Laboratory Association of Southern Africa
AW	available water
BD	bulk density
BShw	Köppen classification: semi-arid hot steppe / savanna climate with summer rains
CEC	cation exchange capacity, measured in $cmol_c$ kg^{-1}
cm	centimetre (1 cm = 10 mm = 0.01 m)
$cmol_c$ kg^{-1} *or* cmol(+) kg^{-1}	centimol charge per kilogram
CV	coefficient of variation
dekad	10 days; a 10-day interval
DWA	Department of Water Affairs, Namibia
EC	Electrical conductivity, measured in (micro / milli / desi-) siemens per cm or m
	1 mS cm^{-1} = 100 mS m^{-1} = 1 dS m^{-1} = 1 000 µS cm^{-1}
ESP	exchangeable sodium percentage (exchangeable sodium, as a percentage of cation exchange capacity)
ESRI	Environmental Systems Research Institute
FAO	Food and Agriculture Organisation of the United Nations
FC	field capacity
GIS	geographical information system
h	hour
ha	hectare (1 ha = 100 m^2; 100 ha = 1 km^2)
ICC	Institut Cartogràfic de Catalunya (Cartographic Institute of Catalonia)
INQUA	International Union for Quaternary Research
ISRIC	International Soil Reference and Information Centre
ISSS	International Soil Science Society
ITCZ	Intertropical Convergence Zone
kg	kilogram (= 1000 g)
kg ha^{-1} *or* kg/ha	kilogram per hectare
km	kilometre
km/h	kilometre per hour
kWh/m^2/day	kilowatt-hours per square meter per day

m	meter
M	Molar mass, kg mol^{-1}
m^3/h	cubic meter per hour
Ma	million years (before present)
MAWF	Ministry of Agriculture, Water and Forestry (since 1st of April 2005)
MAWRD	Ministry of Agriculture, Water and Rural Development (until 31st of March 2005)
mg kg^{-1}	milligram per kilogram
mg l^{-1}; mg/l	milligram per liter
mm	millimetre
mS	millisiemens
n	number of samples, as in n = 61
NAMSOTER	Namibian SOTER Database and GIS
NARIS	Namibian Agricultural Resources Information System
NDVI	Normalised difference vegetation index
nm	nanometer = 10^{-9} meter
NOAA	United States National Oceanic and Atmospheric Administration; also the name of their series of earth observation satellites
NSS	National Soil Survey (of Namibia)
Ø	diameter
^oC	centigrade (degree celcius)
^oE	degree east
^oW	degree west
OC	organic carbon
OM	organic matter
omuramba	local name for a broad, shallow, grassy drainage line. plural: omiramba
PA	previously advantaged
PD	previously disadvantaged
ppm	parts per million = mg kg^{-1}
Q	quartile, as in 'lower Q', 'upper Q', Q range
QLPP	Quantification of Land Production Potential
RDMS	relational database management system
RSA	Republic of South Africa
Sat / sat	saturation / saturated
SHC	saturated hydraulic conductivity
SMAR	Sustainable Management of Arid Rangelands
SOM	soil organic matter
SOP	Standard operating procedure from the MAWRD / MAWF Agricultural Laboratory's Quality Manual
SOTER	World Soils and Terrain Digital Database
SRI	Surface roughness index
SRTM	Shuttle Radar Topography Mission
Std. Dev.	standard deviation

STHPZ	Subtropical High Pressure Zone
Street	local name for an interdunal valley, Afrikaans: straat
S-value	sum of exchangeable Ca, Mg, K and Na
TM	Thematic Mapper, a specific type of radiometric sensor on Landsat satellites
TPI	topographic position index
TWI	topographic wetness index
UNEP	United Nations Environmental Programme
UK	United Kingdom
UNESCO	United Nations Educational, Scientific and Cultural Organization
USA	United States of America
USDA	United States Department of Agriculture
USDA-SCS	USDA Soil Conservation Service
WP	wilting point
WRB	World Reference Base
µ	micro (10^{-6}), as in µS/cm

CHAPTER ONE

INTRODUCTION

1.1 PROBLEM STATEMENT

The soils of Namibia had not yet been fully and systematically mapped and characterised and very little is known about their properties and fertility status. This study aimed to investigate a number of chemical and physical characteristics of Namibian soils in a 22 790 km^2, two degree-square block between 17 – 19 ^{o}E and 22 – 23 ^{o}S in eastern central Namibia, to establish their fertility status. These characteristics are: nitrate, nitrite, and sulfate of the saturated paste extract; plant-available phosphorus, iron, manganese, zinc and copper; extractable and exchangeable calcium, magnesium, potassium and sodium; the cation exchange capacity, sum of extractable and exchangeable bases; the pH measured in water; particle size (sand, silt and clay content), as well as the various sand fraction; soil organic matter; base status, total base saturation and saturation by calcium, magnesium, potassium and sodium, repectively; and salinity.

Secondly, a methodology for delineation of terrain units according to SOTER terminology (ISRIC, 1991, 1993; FAO, 1995)), making use of digital elevation data and satellite imagery, was developed and tested. Namibia is a very large country with very few soil scientists. Such a method for rapid delineation of areal units, to serve as basis for soil characterisation, would accelerate the pace of soil mapping and description in the country.

1.2 CONTEXT

The present study was carried out under the auspices of the *Agro-Ecological Zoning of Namibia (AEZ) Programme*, of which the author is the Programme Manager. This programme is being implemented by agricultural researchers and technicians of the Directorate of Agricultural Research and Training of the Namibian Ministry of Agriculture, Water and Forestry (MAWF), prior to 2005 known as the Ministry of Agriculture, Water and Rural Development (MAWRD).

The study was carried out within the broader context of *Land Reform in Namibia*. Quantitative biophysical and socio-economical data are essential for selecting commercial farms to be bought or expropriated for resettlement of the landless, for calculating a realistic price and for deciding on the number of people and livestock to be resettled per farm. It is also indispensable for land use planning of resettlement farms and for computing the amount of land tax to be levied per commercial farm in order to help finance the Land Reform Programme. In response to this need for scientific data for sound, objective decision-making, a pilot project was designed by the AEZ Programme team to develop concepts and methodologies for land production potential assessment in the Namibian context. A pilot project, *Quantification of Land Production Potential (QLPP)*, was carried out in a two-degrees by one-degree block east of Windhoek, the capital of Namibia. The topic of this thesis, characterisation of the soils, is one component of the wider QLPP project. It contributes in

a small way to peace and stability in Namibia, by providing unbiased scientific data on soil fertility to assist the decision-making process and thus contribute to orderly land reform.

The author has been the architect, manager, main implementer and chief reporter of the AEZ Programme since its inception in 1993. Where team members of the AEZ Programme have carried out the fieldwork, laboratory work and construction of map legends, maps and reports, their contributions are fully acknowledged. The characterisation of the soils in terms of their physical and chemical properties is exclusively the work of the author.

1.3 APPROACH

All extant data on the study area were gathered and assessed as to their relevance and essence. A literature review was carried out on the infrastructure, land tenure, land use, climate, vegetation and water resources (Chapter 2), and the topography, geomorphology and geology (Chapter 3) of the study area. Literature on the soils of the area (Chapter 3) and on physical and chemical characterisation of soils in general, was examined. Gaps in the present soils data were identified. Terrain units were delineated (Chapter 5). A soil survey was carried out by a technician under guidance of the author. Soil samples were collected from profile pits and analysed by the Namibian Ministry of Agriculture, Water and Forestry's Agricultural Laboratory for a variety of chemical and physical attributes. All field observations and laboratory results were databased and mapped (Chapter 5 and Appendix A). The various methods used in this process were summarised in Chapter 4. Soil characteristics were described and statistically analysed to find relationships with parent material and topography (Chapters 6 - 10). Soils were evaluated as to their fertility status (Chapter 11).

The discussion of relevant literature was not concentrated in a single chapter, but appears where particular subjects are elaborated. Efforts had been concentrated on literature on soils of arid and semi-arid zones, preferably in southern Africa. As expected, very little information was available on the soils of Namibia and even less on the soils of the study area. The only pedological work done in the study area or surrounds was by Ganssen (1960, 1963), Ganssen and Moll (1961), Scholtz (1968a, 1968b, 1973), Leser (1971, 1982), Loxton, Venn and Associates (1971) and Petersen (2008). Kempf (1994, 1999a, 1999b, 1999c 2008), Bertram and Broman (1999), and Bertram and Kempf (2002) carried out investigations into the geomorphology of the area. Soil information from these sources was reviewed in Chapter 3.

To gain a better understanding of the study area, of the soils it could conceivably contain and of their genesis and characteristics, the literature review was extended to the geology and geomorphology of the study area (Chapter 3). This broader framework provided insights into the origin and ages of rock types and lineaments, the occurrence of erosional and depositional surfaces, particular landforms and the underlying lithology. The work of Grünert (2000) and Schneider (2004), as well as the Atlas of Namibia by Mendelsohn, Jarvis, Roberts and Robertson (2002) provided good overviews of the geological development of Namibia. The work of Kasch (1983a, 1983b, 1986, 1988), Miller (1983) and Kukla (1992) fostered understanding of the Damara Orogen and appreciation of how most of the western part of the study area was formed, while the work of Kasch (1983a, 1983b, 1986, 1988) and Hegenberger (1993) also illuminated the subsequent Karoo and Kalahari periods that dominate the surface geology towards the east. The geomorphological setting started

with old observations by Gevers (1932a, 1932b, 1934, 1942). The erosional cycle of King (1967, 1978) and its re-interpretation by Partridge and Maud (1987, 1988) followed. Kempf's (1999) more recent work on the central parts of Namibia provided additional information and alternative perspectives. Broad landforms, like the Kalahari, as well as medium-sized and small feature, such as pans and dunes, were briefly discussed.

Soil chemistry, soil analysis and soil fertility were studied from a large number of sources. Preference was given to literature from Europe and southern Africa, as the support network of the author draws mostly from soil scientists in South Africa, Belgium, Germany, the Netherlands and the Food and Agriculture Organisation (FAO) of the United Nations in Rome. This Euro-African focus of the study can be seen in the use of the World Reference Base, WRB (FAO, 1998a and 2001), for classification purposes, the FAO methodology of soil profile description (FAO, 1990), the digital format for soil data storage (SOTER), developed by the FAO (FAO 1989, 1991, 1995, 1996, 2003) and International Soil Reference and Information Centre (ISRIC, 1991, 1993), and the use of standard methods for soil analysis from the Non-Affiliated Soil Analysis Working Committee (1990) and ISRIC (Van Reeuwijk, 1992, 2002) .

1.4 PRODUCTS

The tangible products of the study are:

- Soil profile data in an accessible digital format
- Analytical data of geo-referenced soil profiles in accessible digital and hardcopy format
- Chemical and physical characterisation of the soils, in the context of the lithology and topography
- A number of maps and images of the study area in digital and hardcopy format
- A geographical information system of all the available raw and processed data.

CHAPTER TWO

DESCRIPTION OF THE STUDY AREA

2.1 LOCATION

The study area lies within a one degree by two degrees block, 22^{o} – 23^{o} south, 17^{o} – 19^{o} east, in eastern central Namibia. It spans approximately 100 km (north-south) by 200 km (east-west) and covers 22 790 km^2 or 2 279 million ha. It includes parts of three administrative regions, *viz*. Khomas (western half), Omaheke (eastern half) and Otjozondjupa (northwestern corner) (Figure 2.1).

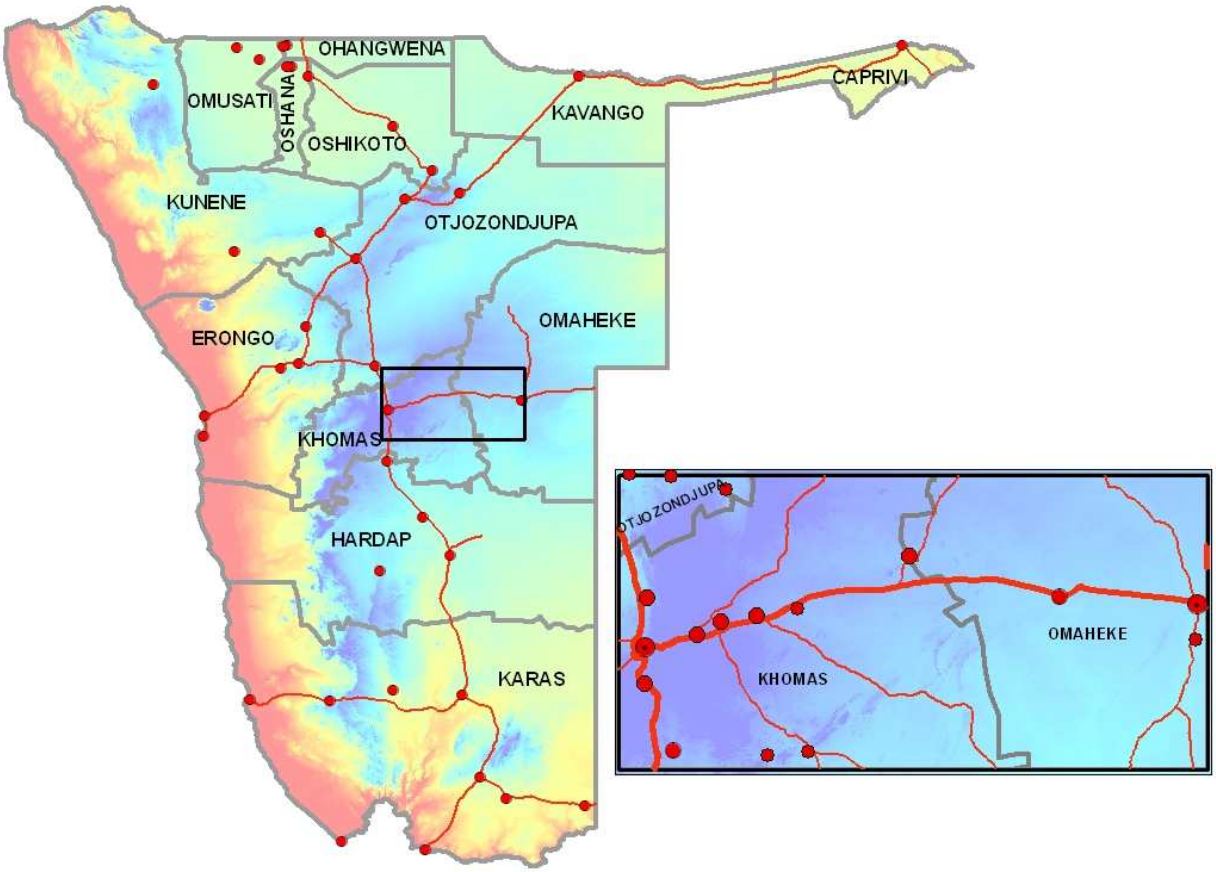

Figure 2.1. Namibia and study area (MAWF, 2005)

2.2 INFRASTRUCTURE

Infrastructure is the facilities and services that support day-to-day economic activities and functioning of a community, such as transportation and communication systems, water and electricity. Windhoek, the capital of Namibia, is the main urban centre. More than 90 % of the population in the study area is concentrated in Windhoek. Gobabis is a substantial town with municipal status and most of the essential facilities. Witvlei is officially classified as a village. Omitara, Aris, Groot Aub and Kapps Farm are settlements; Otjivero, Seeis, Dordabis, Ovitoto, Döbra, Okamboro, Blaukrans, Midgard and Doringveld are informal settlements. Neudamm houses an agricultural college and the Faculty of Agriculture and Natural Resources of the

University of Namibia, while Hosea Kutako comprises an international airport with its associated infrastructure (Figure 2.2). The road network (Figure 2.2) consists of 500 km tarred trunk roads, 1 028 km gravel main roads and 820 km graded earth district roads (Roads Authority, 2004). The area has 335 km of railways (Figure 2.2), though rail transport of agricultural produce is minimal. Air transport facilities are provided by Hosea Kutako International Airport, Eros Airport, which is a busy regional hub, Gobabis Aerodrome and at least 14 officially recognised landing strips on farms (Figure 2.3).

2.3 LAND TENURE

Title deeds have been registered on all the land parcels within the study area. Around urban centres, some land parcels belong to local authorities (municipal, village and town councils) and there are also a large number of privately owned smallholdings for residential-, recreational- and light industrial use. Many parcels contain utilities, e.g. road-, rail- and power-line reserves. These belong to the respective state-owned enterprises (Roads Authority, Transnamib and Nampower) or Ministries responsible for those functions. Government land houses an agricultural college at Neudamm, quarantine station at Bergvlug, schools, resettlement farms and Ovitoto, the largest single parcel that is farmed communally at subsistence level. On resettlement farms a number of previously disadvantaged families are farming through leasehold agreements, mostly at subsistence level. Some of the land in the southwest of the study area belongs to individuals from the Baster ethnic group, in the area formerly known as the 'Baster Gebiet' or 'Basterland'. Some private property belongs to non-profit organisations (e.g. farmers associations, churches, etc.), while most are commercial farming enterprises owned by corporate entities (closed corporations, limited companies, trusts, etc.) and individuals (Figure 2.4; Table 2.1).

Table 2.1: Land ownership in the study area (MAWF, 2005).

OWNERSHIP	NUMBER	AREA (ha)	% of AREA
Government of the Republic of Namibia	65	93992	3.6
Local Authorities	15	75309	2.9
Organisations	11	12778	0.5
Black Individuals ('previously disadvantaged')	105	281090	10.8
White Individuals ('previously advantaged')	512	1590318	60.9
Foreign Individuals	3	9485	0.4
Corporate Entities	162	538761	20.6
Unspecified	123	7846	0.3

2.4 LAND USE

The study area, excluding proclaimed urban areas, consists of 996 land parcels of which 113 are peri-urban smallholdings, road and rail reserves and other non-agricultural land of less than 10 ha each. A further 278 land parcels are less than 100 ha and another 77 between 100 and 1 000 ha. There are 523 parcels of more than 5 000 ha that can be considered economically viable farmland and 306 parcels of 1 000 – 5 000 ha on which extensive livestock farming is a precarious enterprise in the prevailing semi-arid climate (Figure 2.5;

Table 2.2).

Table 2.2: Land parcels in the study area (MAWF, 2005).

Land Parcel Size (ha)	Number of Land Parcels
< 1	34
1 – 10	79
10 – 100	278
100 – 1000	77
Subtotal < 1000	468, covering < 2 % of surface area
1 000 – 5 000	306
5 000 – 10 000	204
10 000 – 15 000	13, of which 2 belong to a municipality and 1 to Government
15 000 – 20 000	3, all municipal property
20 000 – 55 000	2, of which one is the communal land of Ovitoto
Subtotal > 1000	528, that can be considered 'farms'
Total	996

Farming in central Namibia is based on the utilisation of natural pasture by livestock or game, with the objective of profit-maximisation (Buß, 2006). More than 98 % of the land area is under natural rangeland and is used for extensive, low pressure livestock production. Cattle-farming is dominant (> 90 % of all farms), while mixed cattle- and sheep-farming, small stock- (sheep and goats) and game-farming-*cum*-eco-tourism also take place (IDC, 2005). Live cattle and beef exports account for 7 % (in gross income) of all Namibian exports (Buß, 2006). An investigation by International Development Consultants (IDC, 2005) found that average meat production is 4.28 kg/ha for cattle and 5.3 kg/ha for sheep in the study area. It has potential for the production of cactus pear, ethno-botanicals (e.g. devil's claw), oleo-resins, small citrus orchards, small olive groves, and tunnel-cultivated cut-flowers and vegetables where sufficient groundwater for irrigation is available (IDC, 2005). Harvesting of wood and charcoal production from invader bush are possible (IDC, 2005). Towards the northeast, crops such as maize, sunflower, groundnuts, oriental tobacco, cotton, pearl millet, sorghum and cultivated pastures can be planted to a limited extent, but only if the farmer has sufficient groundwater for supplementary irrigation and/or a high risk tolerance, as crop failures occur 30 – 40 % of the time on farms just outside the study area.

Trophy hunting, venison hunting, non-consumptive eco-tourism and the accompanying hospitality industry are valuable additional sources of income for farmers of the area. These wildlife-based tourism enterprises require high capital inputs for accommodation and catering facilities, game fencing, construction of waterholes and hides, off-road game-viewing and hunting vehicles and rare game species. It also calls for skilled labour and good marketing skills. Game management in a conservancy, a loose merger of a number of farms (often with a surface area in excess of 100 000 ha) and a single wildlife management plan, is economically more efficient (Barnes and De Jager, 1996). The study area covers parts of 12 conservancies consisting of more than 150 farms.

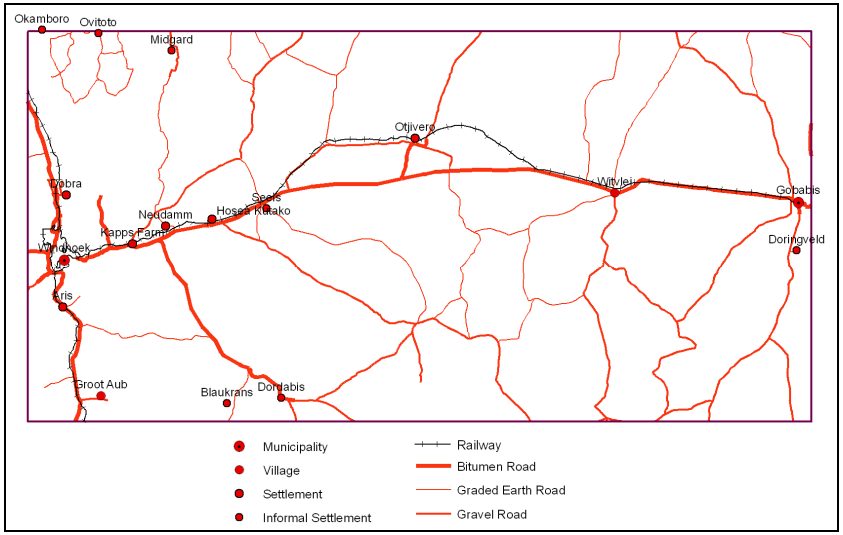

Figure 2.2. Urban centres, rail and road network (MAWF, 2005)

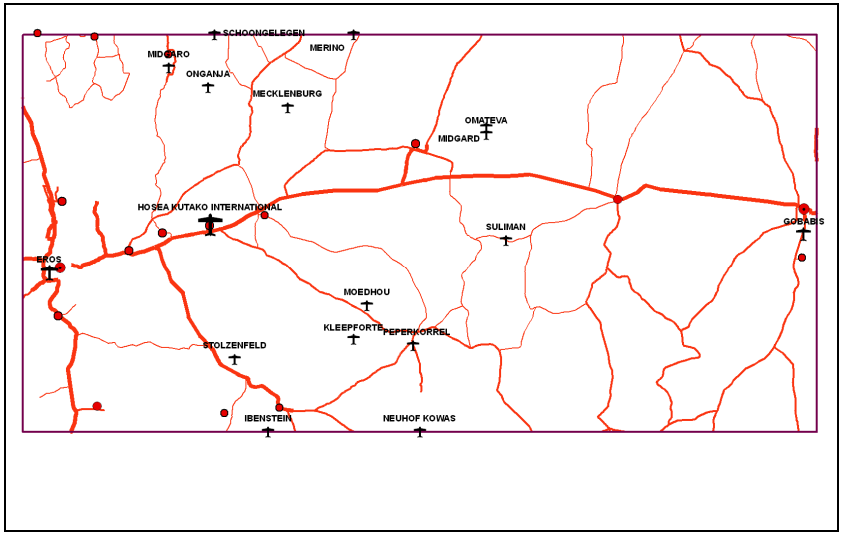

Figure 2.3. Air transport facilities (MAWF, 2005)

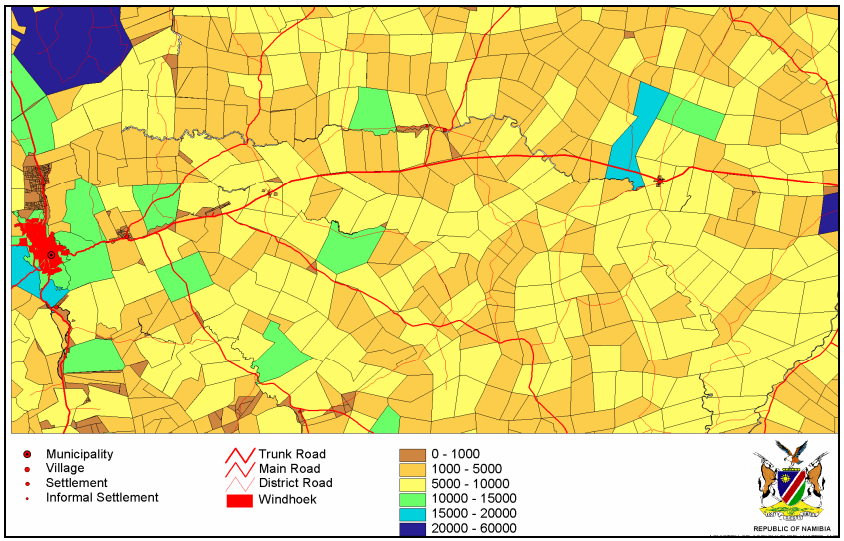

Figure 2.4. Land ownership in the study area (MAWF, 2005) (PA = previousoly advantaged; PD = previously disadvantaged)

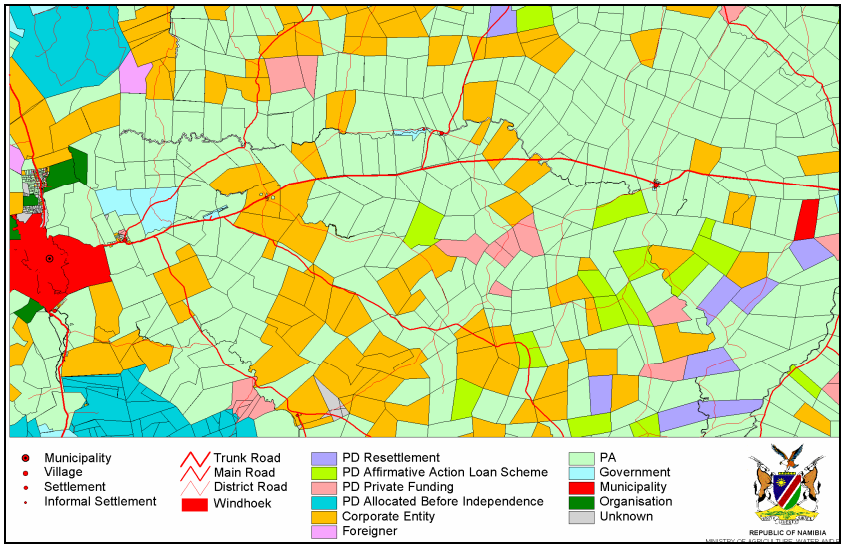

Figure 2.5. Size of land parcels (in ha) in the study area (MAWF, 2005)

2.5 CLIMATE

The study area is situated in the tropics on the south-western flank of Africa. This position, in conjunction with the cold Benguela Current along the west coast, dictates the climate. Köppen (1936) classified it as a *semi-arid hot steppe / savanna climate with summer rains*. He used the code BShw, which he defined as "a dry climate (B) where the potential evaporation is more than average rainfall for the year, there is no water surplus, therefore no permanent water streams will develop; steppe climate (S) that is semi-arid with an annual rainfall of 380 – 760 mm; dry and very hot (h), with the average annual temperature > 18 ^{o}C; and the dry season in winter (w)". Papadakis (1970a and 1970b) classified the Kalahari as a *Hot Subtropical Desert*, and central Namibia a *Tropical Highland Desert*.

According to Mendelsohn, Jarvis, Roberts and Robertson (2002), the climate is governed by three systems: the Subtropical High Pressure Zone (STHPZ), Inter-tropical Convergence Zone (ITCZ) and Temperate Zone. The STHPZ is expressed by the Botswana Anticyclone – a high-pressure cell located over the centre of the subcontinent during most of the year, causing dry stable conditions – and the South Atlantic Anticyclone that feeds cool air from the Atlantic Ocean onto the Namibian coast in the form of south-westerly winds. During summer the Botswana Anticyclone weakens and migrates off the coast of southern Africa, allowing moisture-bearing air from the ITCZ to move south from the equatorial regions, bringing summer rains to Namibia. These fall as convection thunderstorms with highly variable spatial and temporal distribution. The Temperate Zone of moist air carries a succession of low-pressure systems and cold fronts on the prevailing westerly winds past the southern tip of the subcontinent. During winter, the Temperate Zone moves further north and cold fronts sweep across southern Namibia, bringing a little winter rain to the southernmost parts of Namibia, as well as cold spells further north (Mendelsohn *et al.*, 2002).

Within the study area, first order weather stations are located in Windhoek (at the Namibia Meteorological Service) and at Hosea Kutako International Airport. A substantial number of second and third order stations are also found in the area. However, these stations normally only record rainfall, the critical climatic factor governing the environment and land use in Namibia.

2.5.1 RAINFALL

The mean annual rainfall of the study area increases from 300 mm in the south to 410 mm in the north, according to the relatively old *Updated Isohyetal Rainfall Map for Namibia* (DWA, 1992) (Figure 2.6).

Du Pisani (2005a) constructed 'virtual stations' (*sic*) for each half-degree block in and adjacent to the study area (21^{o}30' – 23^{o}30' S and 16^{o}30' – 19^{o}30' E) and interpolated daily rainfall data from 172 actual stations for the period 1941 – 2000. Mean annual (January – December) (Figure 2.8), and mean seasonal (July – June) rainfall are higher than median annual (Figure 2.7) and median seasonal rainfall. This is typical for arid and semi-arid environments where rainfall is not normally distributed, but usually best described by a gamma distribution function. Rainfall increases from south to north and shows a discernible orographic influence over

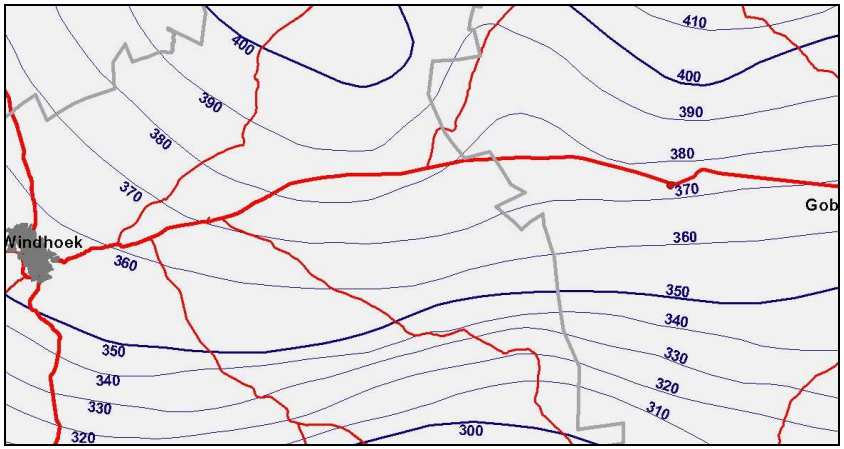

Figure 2.6. Rainfall isohyets (MAWF, 2005, based on DWA, 1992)

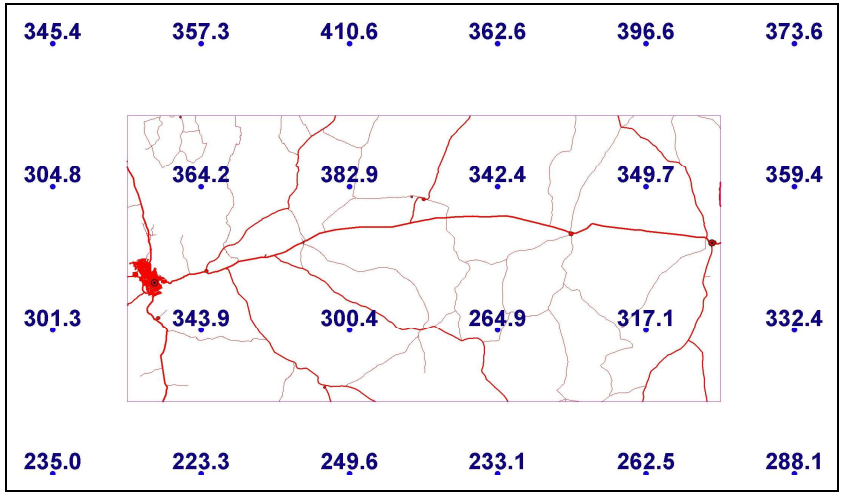

Figure 2.7. Median annual rainfall over a 60-year period (1941 – 2000) (Du Pisani, 2005a)

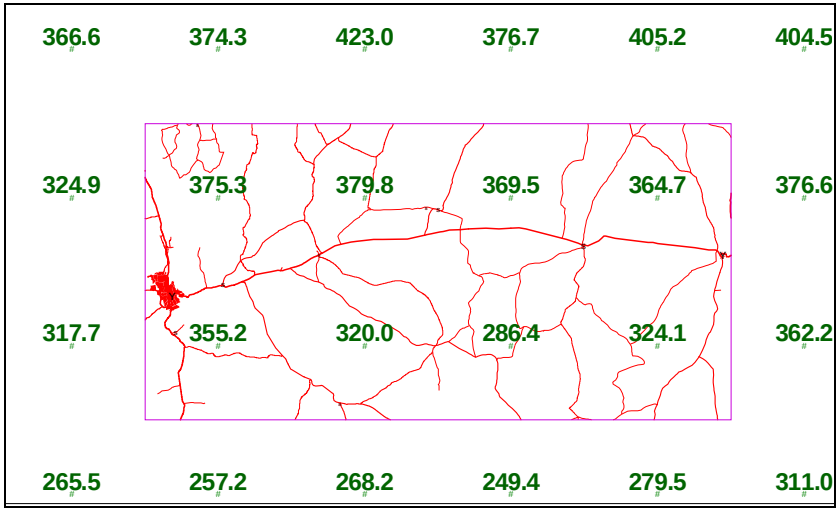

Figure 2.8. Mean annual rainfall over a 60-year period (1941 – 2000) (Du Pisani, 2005a)

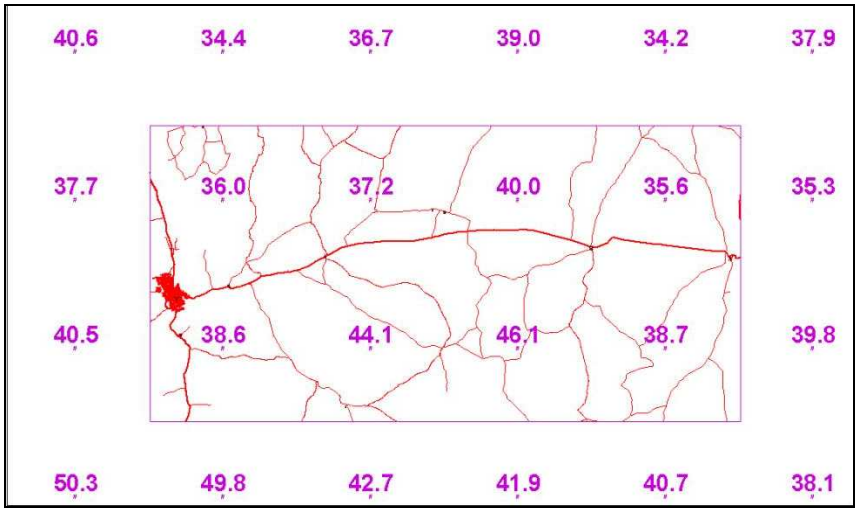

Figure 2.9. Coefficient of variation of annual rainfall over a 60-year period (1941 – 2000) (Du Pisani, 2005a)

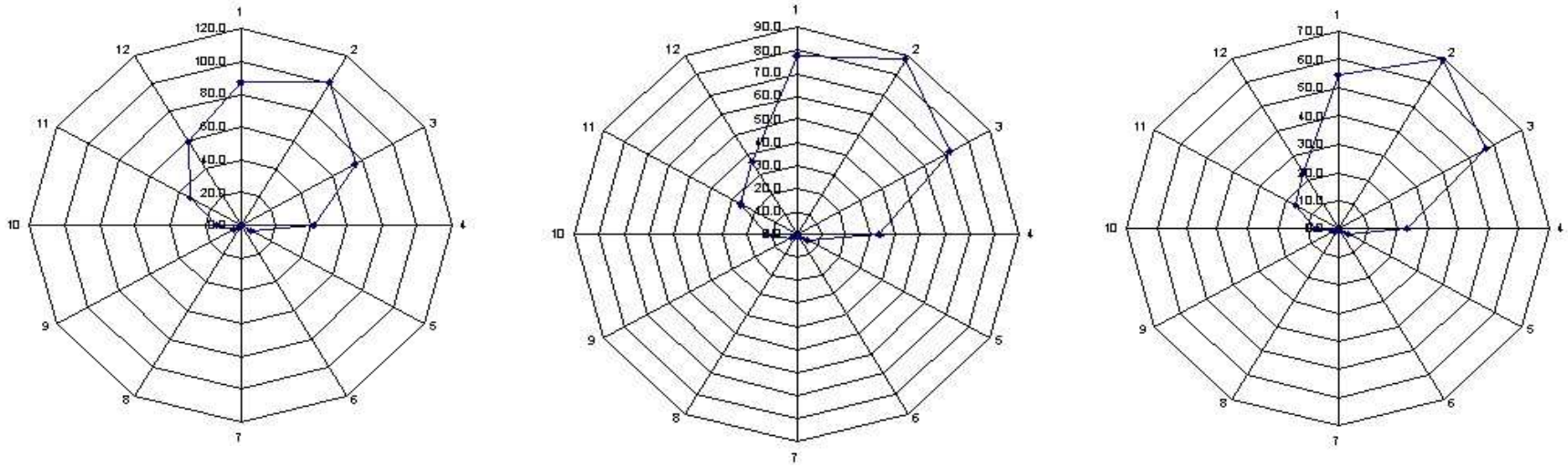

Figure 2.10. Monthly rainfall distribution of 'virtual stations' representing high, average and low rainfall in the study area (Du Pisani, 2005a)

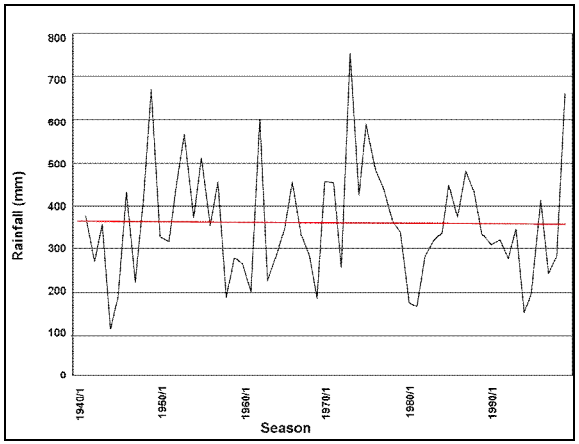

Figure 2.11. Median seasonal rainfall (1940/1 – 1999/2000) from the 'wettest' virtual station (Du Pisani, 2005a)

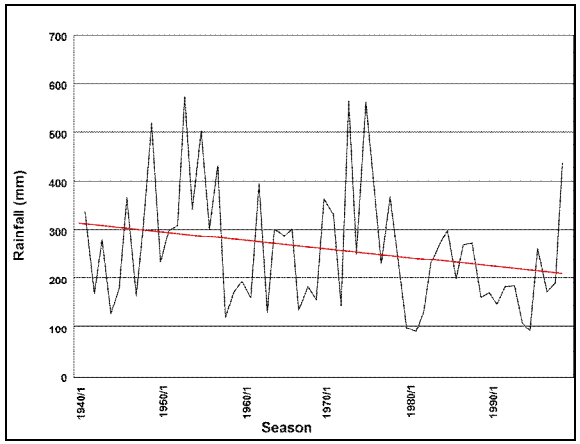

Figure 2.12. Median seasonal rainfall (1940/1 – 1999/2000) from the 'driest' virtual station (Du Pisani, 2005a)

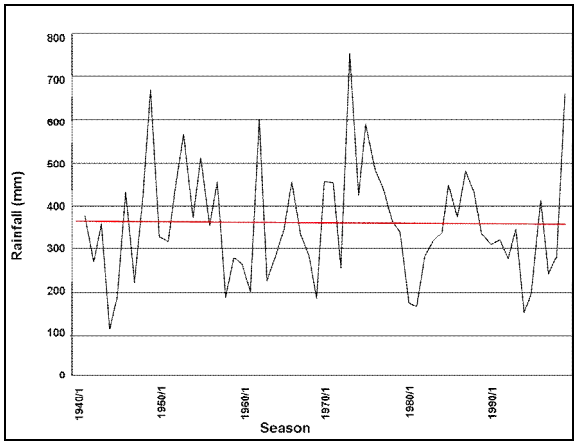

Figure 2.13. Median seasonal rainfall (1940/1 – 1999/2000) from the 'average' virtual station (Du Pisani, 2005a)

the central high ground, the Khomas Hochland, and particularly over the mountains east of Windhoek.

The high temporal variability of rainfall is illustrated in Figure 2.9 by the coefficient of variation (CV), which is inversely related to the amount of rain. The CV ranges from 34 % for the area of highest rainfall, to more than 50 % for the area of lowest rainfall.

Rainfall is concentrated in summer with most occurring during the period from January until March, as is evident from the three radar graphs in Figure 2.10. The radial axes numbered 1 – 12 represent the months from January to December, with the millimetres of monthly rainfall marked on each of them. The graphs represent three 'virtual stations' with high, average and low median annual rainfall respectively, as typical examples from the study area.

The high inter-annual variability of rainfall in the study area is evident from Figures 2.11 - 2.13. The three graphs illustrate median seasonal rainfall from the virtual station with the highest mean (423.0 mm) and median (410.6 mm) rainfall, the station with the lowest mean (249.4 mm) and median (223.3 mm) rainfall, and a third station that represents the block with rainfall closest to the average of the whole study area (mean of 355.2 mm and median of 343.9 mm). A downward trend in rainfall over the 60-year period is evident for stations with lowest rainfall (Figure 2.12).

When rainfall is expressed in dekadal (10-day) format, as in Figures 2.14 – 2.16, the rainfall patterns of the wetter, drier and average parts of the study area are similar throughout the study area: a dry winter, a slow start in October, significant showers occurring from January until end of March, and a rapid decline throughout April.

2.5.2 TEMPERATURE

Temperatures are generally lower than what would be expected from the latitude and aridity, due to the elevation. Du Pisani (2005b) used two stations to characterise the temperature of the study area, *viz*. Windhoek Meteorological Office and Hosea Kutako International Airport, as those are the only stations with good quality temperature data. Temperature profiles are fairly similar at the two stations (Figures 2.17 – 2.22), with the maxima slightly higher at Hosea Kutako than in Windhoek. Minima are consistently lower at the airport, with the difference in the winter months exceeding 3 ^{o}C. December and January are the hottest months, while June and July are the coldest.

2.5.3 GROWING PERIODS

Most of the study area has an average growing period of between 40 and 60 days, while the north-eastern corner has an average growing period of between 60 and 90 days, with only a very short dependable growing period (Figure 2.23). The Windhoek – Okahandja Valley has between 40 and 60 days of adequate soil moisture for plant growth (De Pauw, 1996; De Pauw and Coetzee, 1999; De Pauw, Coetzee, Calitz, Beukes and Vits, 1999; Coetzee, 2001a, 2001b).

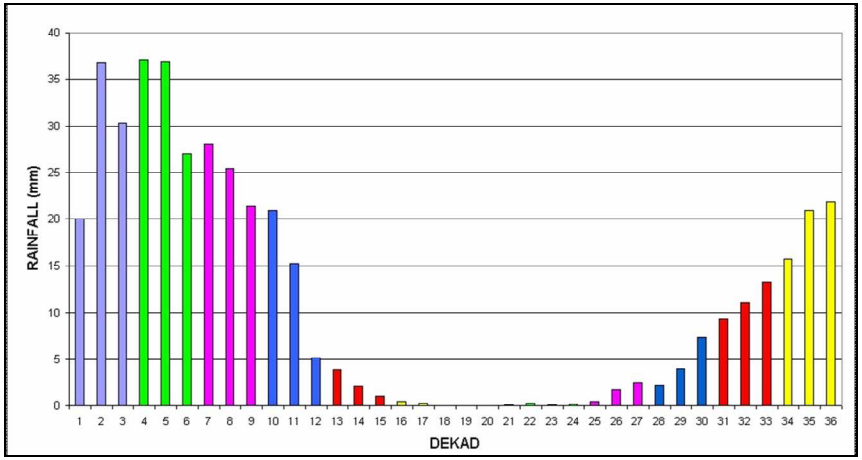

Figure 2.14. Decadal rainfall from the 'wettest' virtual station (Du Pisani, 2005a)

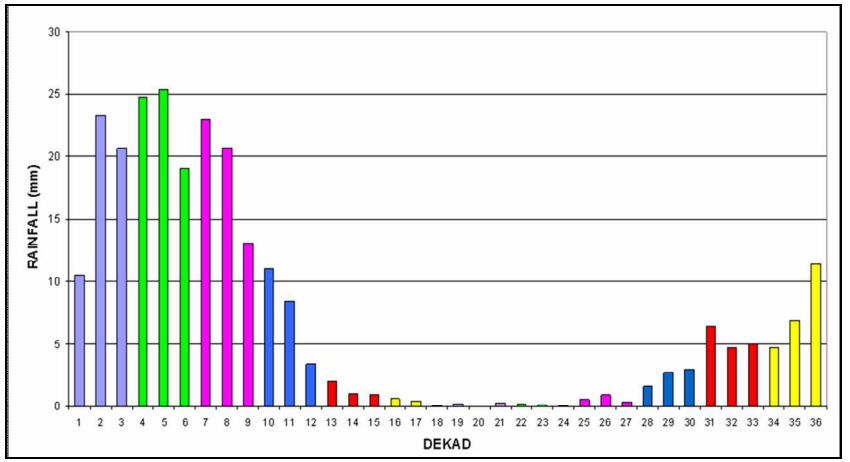

Figure 2.15. Decadal rainfall from the 'driest' virtual station (Du Pisani, 2005a)

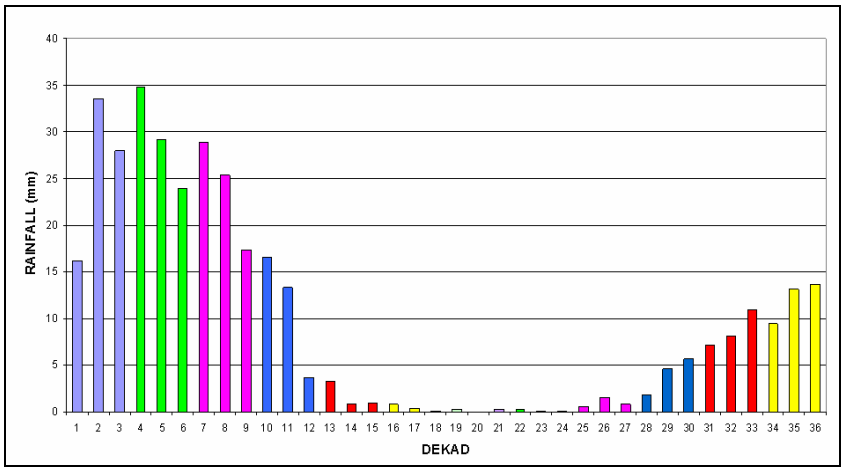

Figure 2.16. Decadal rainfall from the 'average' virtual station (Du Pisani, 2005a)

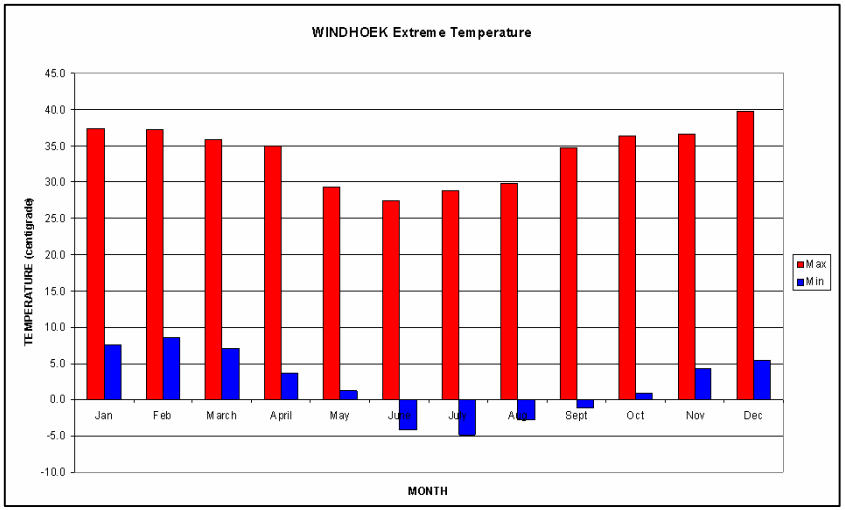

Figure 2.17. Monthly temperature extremes – Windhoek (Du Pisani, 2005b)

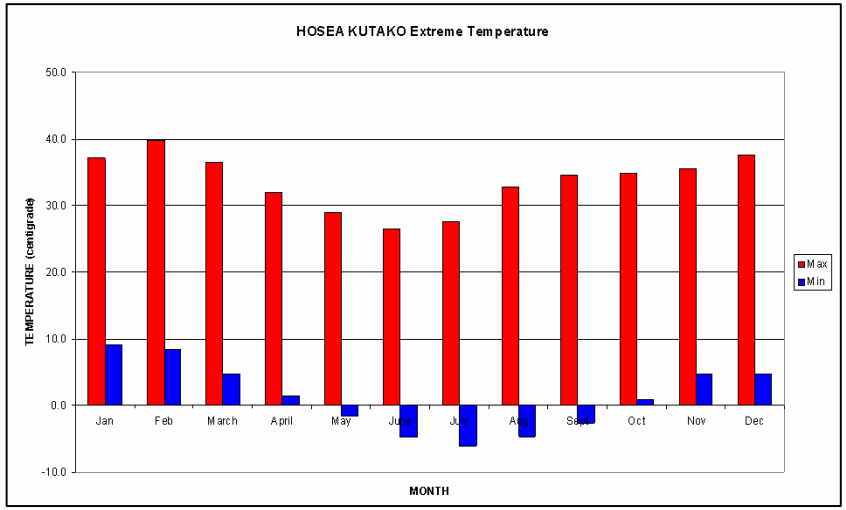

Figure 2.18. Monthly temperature extremes – Hosea Kutako (Du Pisani, 2005b)

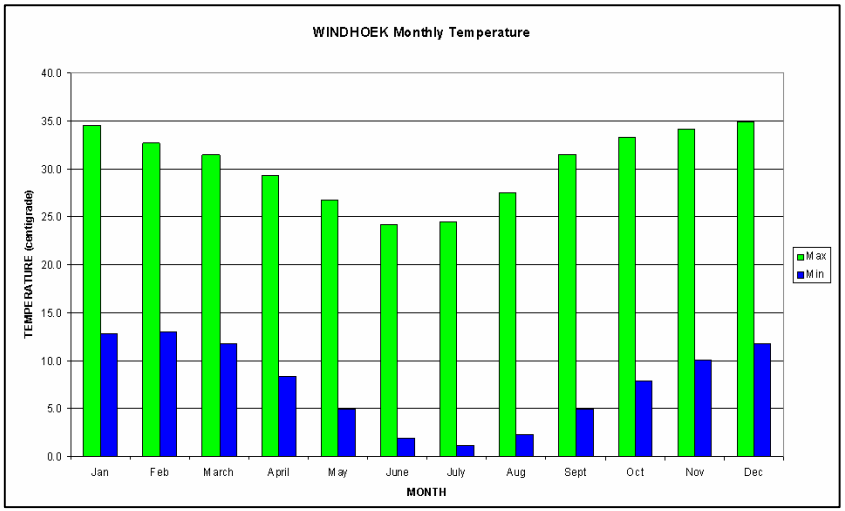

Figure 2.19. Monthly maximum and minimum temperature – Windhoek (Du Pisani, 2005b)

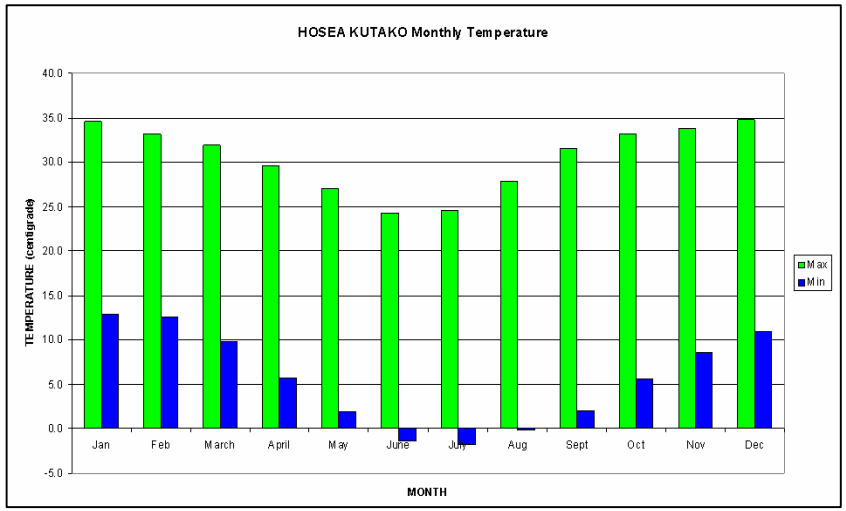

Figure 2.20. Monthly maximum and minimum temperature – Hosea Kutako (Du Pisani, 2005b)

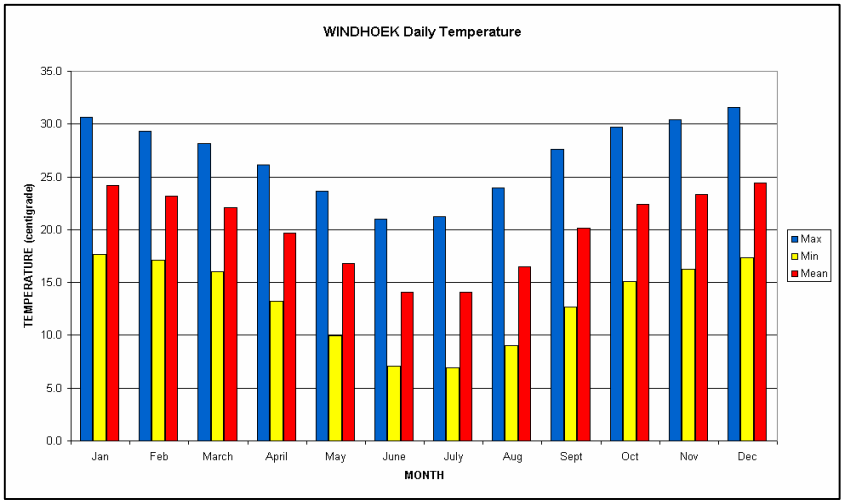

Figure 2.21. Daily maximum, minimum and mean temperature – Windhoek (Du Pisani, 2005b)

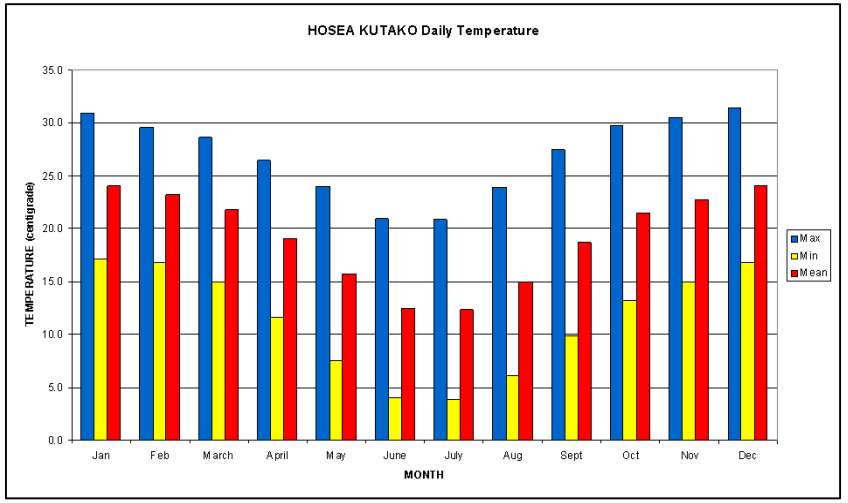

Figure 2.22. Daily maximum, minimum and mean temperature – Hosea Kutako (Du Pisani, 2005b)

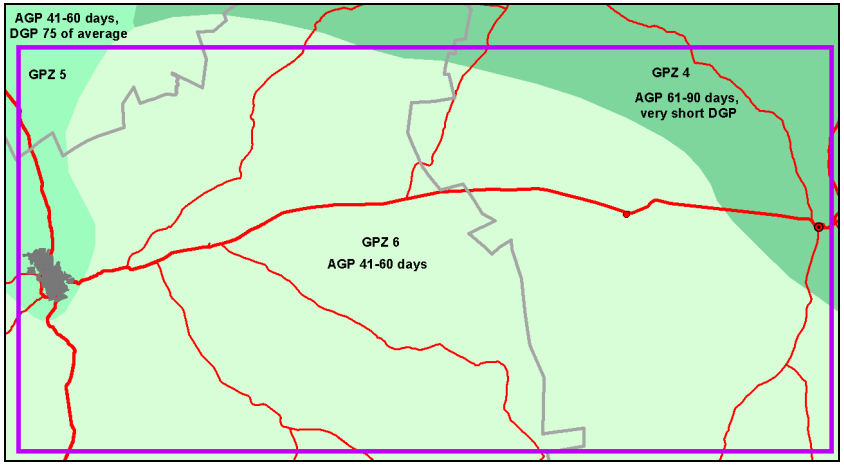

Figure 2.23. Growing period zones (MAWF, 2005) (AGP = average growing period; DGP = dependable growing period)

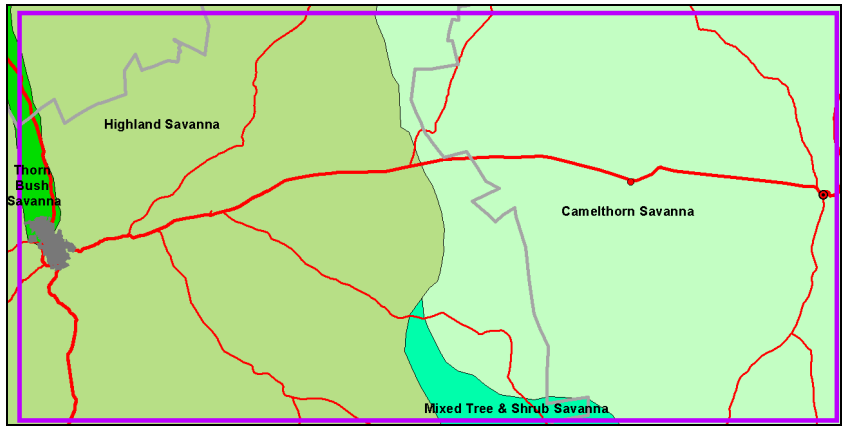

Figure 2.24. Vegetation zones (MAWF, 2005, based on Giess, 1998

2.5.4 OTHER CLIMATIC PARAMETERS

Solar radiation varies between ~5.8 kWh m^{-2} day^{-1} in the east and ~6.2 kWh m^{-2} day^{-1} in the west of the study area (Mendelsohn *et al.*, 2002). The number of sunshine hours per day varies between 8 h in March, the time of maximum cloud cover, and slightly more than 10 h from May until September when skies are clear (Mendelsohn *et al.*, 2002). Relative humidity varies from below 20 % in September to 70 – 80 % in March (Mendelsohn *et al.*, 2002). Mean annual evaporation lies between 1 820 mm and 1 960 mm in the study area roughly north of the Windhoek – Gobabis road, while it varies between 1 960 mm and 2 100 mm in the southern half of the study area (Mendelsohn *et al.*, 2002). Monthly evaporation is highest during December, closely followed by October, November and January, and lowest in June and July (Mendelsohn *et al.*, 2002). On ~20 % of days Windhoek experiences wind from the east, ~10 % from the northeast and ~10 % from the west, while ~35 % of all days are calm (Mendelsohn *et al.*, 2002). In the vicinity of Gobabis, on ~15 % of days wind blows from the northeast, and roughly 10 % each from the east, south and northwest, with 44 % of days being calm. Wind speeds are on average well below 20 km/h (Mendelsohn *et al*, 2002). The north-western quarter of the study area experiences 10 – 20 days of frost, while the remainder has up to 30 days of frost, per year (Mendelsohn *et al.*, 2002).

2.6 VEGETATION

FAO-UNESCO (1977) classifies the whole study area as *Thornbush Savanna* and describes it as an intermediate vegetation type between the moister wooded types and the subdesert types, with grasses generally less than a metre high and trees mainly of the *Acacia* genus and *Commiphora* genus. According to Giess (1971, 1998) the study area has four main vegetation zones, *viz*. the *Highland Savanna* around Windhoek, *Thornbush Savanna* in the Windhoek–Okahandja Valley, *Camelthorn Savanna* east of the Hosea Kutako International Airport and *Mixed Tree- and Shrub Savanna* towards the southern edge of the study area (Figure 2.24).

Mendelsohn *et al.* (2002) label the corresponding vegetation types *Highland Shrubland*, *Thornbush Shrubland*, *Central Kalahari* and *Southern Kalahari* respectively. All four vegetation zones form part of the *Acacia Tree- and Shrub Savanna Biome*. Elements of both the *Sudano-Zambezian Flora* and *Namib-Karoo Flora* can be found, depending on small-scale environmental factors (Kempf, 1994).

2.6.1 DOMINANT PLANT SPECIES

The eastern half of the area – the **Camelthorn Savanna** or Central Kalahari – is characterised by *Acacia erioloba* (Camel-thorn; Kameeldoring) trees, which lend their name to the zone in the Giess classification. *Terminalia sericea* (Silver cluster-leaf; Sandgeelhout) occurs on deep sandy soil. *Acacia mellifera* (Black-thorn acacia; Swarthaak) and *Dichrostachys cinerea* (Sickle bush; Sekelbos) are indigenous invasive ('encroacher') species most often implicated in bush encroachment (Section 2.6.2). *Ziziphus mucronata* (Buffalo-thorn; Blinkblaarwag-'n-bietjie), *Boscia albitrunca* (Shepherd's tree; Witgat), *Acacia hereroensis* (Mountain-thorn; Bergdoring), *Acacia karoo* (Sweet-thorn; Soetdoring) and *Albizia anthelmintica* (Worm-cure

albizia; Aroe) are also abundant (Curtis and Mannheimer, 2005). *Prosopis* (Mesquite), an invasive alien, is common along watercourses, especially the Nossob River (Smit, 2002; Bethune, Griffin and Joubert, 2004).

The most common shrubs in this vegetation zone are *Acacia hebeclada* (Candle-pod acacia; Trassiebos), *Grewia flava* (Velvet raisin; Fluweelrosyntjie); *Grewia flavescens* (Sandpaper raisin; Skurwerosyntjie); *Phaeoptilum spinosum* (Brittle-thorn; Brosdoring); *Tarchonantus camphorates* (Camphor bush; Wildekanferbos); *Ozoroa paniculosa* (Common resin-bush); *Rhigozum brevispinosum* (Simple-leaved rhigozum; Granaatbos); *Rhigozum trichotomum* (Three-thorn rhigozum; Driedoring) and *Catophractes alexandri* (Trumpet-thorn; Ghabbabos) (Curtis and Mannheimer, 2005).

Where rangeland is in good condition, the sward is dominated by *Eragrostis pallens* (Broom grass; Gemsbokgras / Besemgras), *Eragrostis rigidior* (Curly-leaved love grass; Krulblaarpluimgras), *Eragrostis lehmanniana* (Lehmann's love grass / Common love grass; Knietjiesgras), *Anthephora pubescens* (Woolgrass; Borseltjiegras) and *Schmidtia pappophoroides* (Kalahari sand quick; Kalaharisandkweek) (Klaassen and Craven, 2003; Lubbe, 2006), *Brachiaria*- and *Digitaria* species (Müller, 1983). Degraded veldt is typified by *Aristida* (Steekgras) species, such as *Aristida congesta* (Tassel three awn / perennial bristlegrass; Katstertsteekgras) and *Aristida stipitata* (Sandveld long-awned stick grass / Sandveld bristlegrass; Langnaaldsteekgras) (Lubbe, 2006; Klaassen and Craven, 2003), *Schmidtia kalahariensis* (Annual Bushman grass; Kalaharisuurgras / Eenjarige vyfnaaldgras) and *Stipagrostis uniplumis* (Silky Bushman grass; Blinkhaarboesmangras) (Müller, 1983; Klaassen and Craven, 2003).

The western half of the study area – the **Highland Savanna** or Highland Shrubland – is dominated by *Acacia mellifera*, *Acacia erioloba*, *Acacia hereroensis*, *Acacia karroo, Acacia erubescens* (Yellow-bark acacia; Withaak), *Acacia recifiens* (Red-thorn; Rooihaak), *Combretum apiculatum* (Kudu-bush; Koedoebos), *Ziziphus mucronata; Boscia albitrunca* and *Albizia anthelmintica* trees*. Prosopis* is a common tree throughout the whole study area, predominantly along watercourses (Smit, 2002; Bethune *et al.*, 2004; Curtis and Mannheimer, 2005).

The most abundant shrubs of this vegetation type are *Croton gratissimus* (Lavender croton; Laventelbos); *Grewia bicolor* (Two-coloured raisin-bush; Basterrosyntjie); *Grewia flava; Lycium bosciifolium* (Limpopo honey-thorn; Wolfdoring, Slapkriedoring); *Lycium eenii* (Broad-leaved honey-thorn; Breëblaarkriedoring); *Manuleopsis dinteri* (Dinter's bush); *Rhigozum brevispinosum*; *Rhigozum trichotomum*; *Catophractes alexandri*; *Tarchonantus camphorates*; *Phaeoptilum spinosum, Montinia caryophyllacea* (Wild clove-bush; peperbos) (Curtis and Mannheimer, 2005) and *Rhus ciliata* (Sour karee) (Müller, 1983).

Good condition rangeland contains *Anthephora pubescens*, *Brachiaria nigropedata* (Blackfooted Brachiaria / Spotted Brachiaria; Swartvoetjie), *Cenchrus ciliaris* (Buffalo grass; Bloubuffelgras), *Digitaria eriantha* (Finger grass / Wooly finger grass; Wolvingergras / Kleinvingergras), *Eragrostis nindensis* (Wether love grass /, perennial love grass; Agtdaepluimgras), *Stipagrostis uniplumis* and *Heterogpogon contortus* (Spear grass; Assegaaigras) as the most prominent grass species (Müller, 1983; Klaassen and Craven, 2003; Lubbe, 2006). Poor rangeland is characterised by *Enneapogon cenchroides* (Common nine-awned grass; Eenjarige negenaaldgras), *Chloris virgata* (Feather-top Chloris; Klossiegras), annual and perennial *Melinis repens*

(Red-top; Ferweelgras) and various *Aristida* species (Klaassen and Craven, 2003; Lubbe, 2006).

The **mixed tree and shrub savanna** (in the south) typically has *Acacia haematoxylon* (Grey camel-thorn; vaalkameel) on the sand dunes, *Rhigozum trichotomum* in the hard dune valleys ('streets'), and a good quantity of *Acacia erioloba*, *Boscia albitrunca*, *Acacia mellifera* subsp. *detinens*, *Acacia reficiens*, *Acacia hebeclada* subsp. *hebeclada* and *Grewia flava* (Curtis and Mannheimer, 2005).

Asthenatherum glaucum (Gha grass; Ghagras), *Anthephora argentea* (Silver wool grass; Silwerborseltjiegras), *Eragrostis lehmanniana*, *Stipagrostis uniplumis* and *Stipagrostis ciliata* (Tall Busman grass; Langbeenboesmangras), personify well-maintained veldt, while *Schmidtia kalahariensis* dominates on degraded land. *Stipagrostis amabilis* (Kalahari coach; Duinekweek) stabilises dune crests (Müller, 1983).

The Windhoek – Okahandja valley, comprising **Thorn Bush Savanna** (tree and shrub savanna; thornbush shrubland) is dominated by *Acacia* species, such as *Acacia reficiens*, *Acacia hebeclada* subsp. *hebeclada*, *Acacia erubescens* and *Acacia fleckii*. *Acacia tortillas* subsp. h*eteracantha* also occurs. *Boscia albitrunca* and *Ziziphus mucronata* are common (Curtis and Mannheimer, 2005).

In good condition rangeland one finds *Anthephora pubescens*, *Brachiaria nigropedata*, *Digitaria* species and *Urochloa bolbodes* (Gonya grass; Meerjarige beesgras). In degraded veldt *Stipagrostis uniplumis* and *Schmidtia pappophoroides* are abundant (Müller, 1983).

In-depth studies of the vegetation, in the form of Braun-Blanquet relevés, had been carried out by Volk and Leippert (1971) on the farms Voigtland, Brack and Binsenheim, while Kellner (1986) concentrated on farm Neudamm. Extensive vegetation data have also been collected by Strohbach (2008).

2.6.2 BUSH ENCROACHMENT

Bush encroachment, chiefly by *Acacia mellifera* subsp. d*etinens*, is already a substantial problem in some parts of the study area and has the potential to become a major dilemma as it is in other parts of Namibia. Bush encroachment is the invasion and/or increase in density and size of aggressive undesired woody species resulting in an imbalance of the grass-to-bush ratio, a decrease in biodiversity and a decrease in carrying capacity (IDC, 2005). Desirable grass-, forb- and fodder bush species are out-competed by undesirable, often thorny, bush species. As a rule of thumb, bush densities of more than 1.5 times the mean annual rainfall (expresses as number of bush per hectare) are considered to be encroachment. That would translate into 375 – 550 bushes / ha in the study area. In reality, densities of 1 500 – 3 000 bushes / ha are found (IDC, 2005). For chemical bush control, the clay content of soils must be known to calculate the required quantity of herbicide (Horsthemke, 2000) thus the present study will contribute to the control of bush encroachment in the area. Extensive work on bush encroachment in Namibia, including the study area, had been published by Bester (1996; 1997a; 1997b; 1999a), De Klerk (2004), and Joubert, Rothauge and Smit (2008).

2.6.3 GRAZING CAPACITY

The concepts *carrying capacity* and *grazing capacity*, as employed by the pasture scientists of MAWF (Lubbe, 2006), are defined as follows (Trollope, Trollope and Bosch, 1990):

- *Carrying capacity* is the potential of an area to support livestock through grazing and/or browsing and/or fodder production over an extended number of years without deterioration to the overall ecosystem.
- *Grazing capacity* is the productivity of the grazeable / browsable portion of a homogeneous unit of vegetation expressed as the area of land required to maintain a single animal unit over an extended number of years without deterioration to the soil.

Morris, Hardy and Bartholomew (1999) stated that the stocking rate is the single most important management factor influencing animal, performance and profitability of a livestock farming system. The Ministry of Agriculture, Water and Forestry promotes the use of the biomass concept (Bester 1988, 1999b, 2003) to determine the ideal stocking rate annually.

Grazing capacity of the study area varies between 12 kg live animal mass per ha in the south-western corner, to 30 kg/ha in the northeast (Figure 2.25). These values are under revision at present (Lubbe, 2005), and are highly variable in space and time. Actual stocking rates vary from 84 kg/ha in the Ovitoto communal area – which is grossly overstocked – to 24 kg/ha on average on commercial farms (IDC, 2005).

2.6.4 BIOMASS PRODUCTION

Cumulative seasonal biomass production estimates had been calculated for the study area since 1985/6 (Ganzin, Coetzee, Rothauge and Fotsing, 2005; MAWF, 2005). The method is based on the Monteith model (1972) of biomass production calculated from solar radiation and uses NOAA and SPOT *Vegetation* satellite imagery in the form of normalized different vegetation indices (NDVI) and the Sustainable Management of Arid Rangelands (SMAR) software (Ganzin, 1999).

Figures 2.26 – 2.29 show the mean estimated seasonal biomass production over the 20-year period 1985/6 - 2004/5 (Figure 2.26) and comparisons of the 2001/2 (Figure 2.27), 1994/5 (Figure 2.28) and 1999/2000 (Figure 2.29) growing seasons with the mean, expressed as a percentage of the mean. These three seasons were average, very poor and very good respectively. At present the method does not differentiate between trees, shrubs, grass and forbs, but research is in progress to refine the method into estimating grass and forb production (Lubbe, 2005; Espach, Lubbe and Ganzin, 2006). This will greatly assist in determining seasonal livestock carrying capacity, as well as long-term grazing capacity.

2.6.5 LAND COVER

Land cover is defined as 'the observed (bio) physical features on the earth's surface' (Di Gregorio and Jansen, 1997) and can include vegetation and man-made features, as well as bare rock, soil and inland water systems. Espach (2006) has mapped the land cover of the eastern half of the study area, roughly from

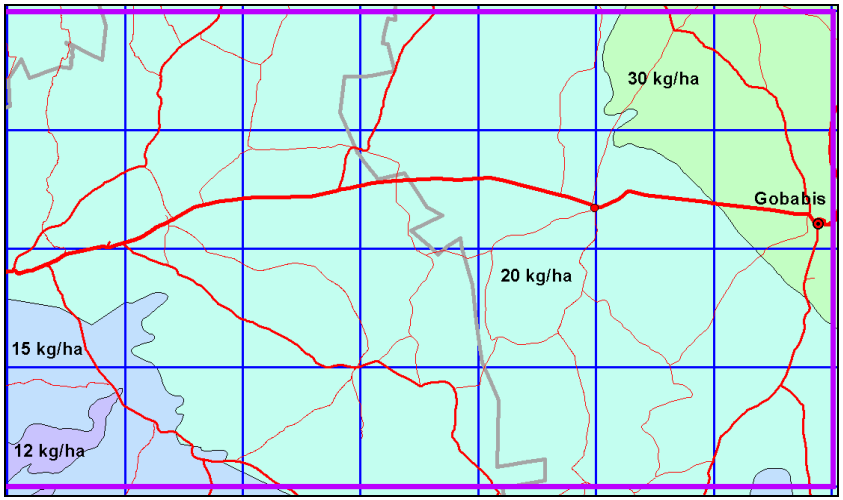

Figure 2.25. Grazing capacity, in kg live animal mass per ha (MAWF, 2005)

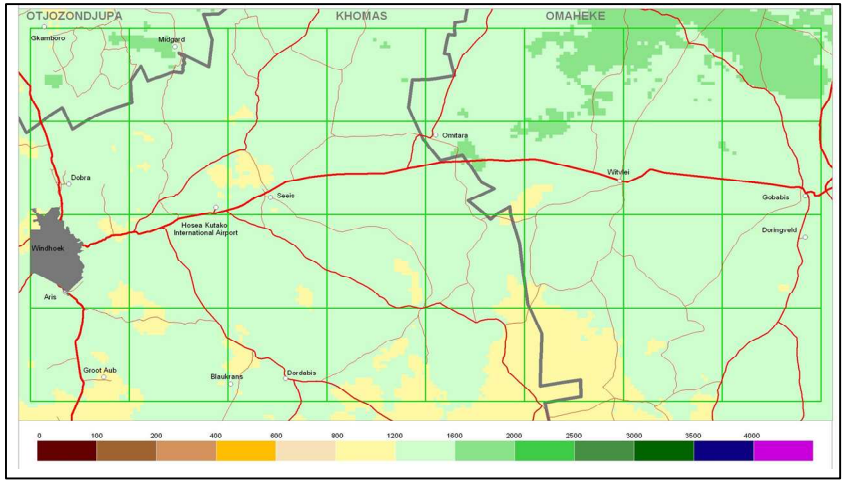

Figure 2.26. Estimate of total seasonal above-ground biomass production (kg/ha) – 20-year mean (1985/6 – 2004/5) (MAWF, 2005)

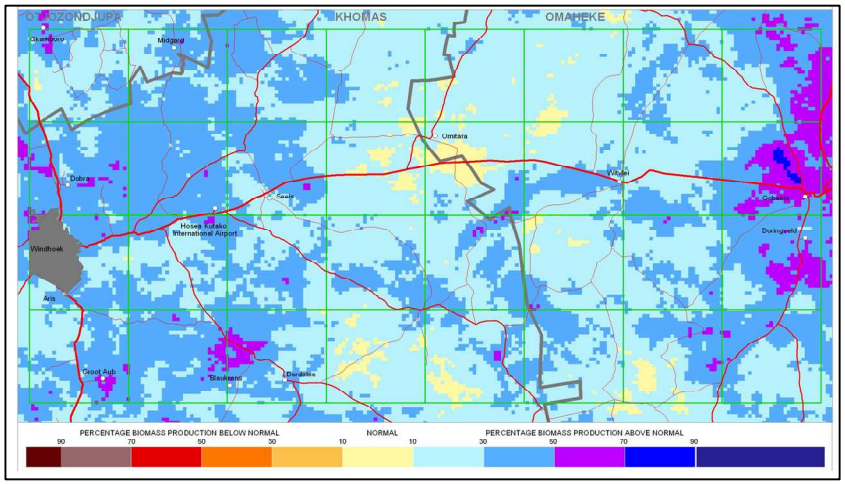

Figure 2.27. Estimated total season above-ground biomass production of the 2001/2 growing season (1 October 2001 – 30 April 2002), compared to the 20-year mean (1985/6 – 2004/5), expressed in percentage biomass production above normal (MAWF, 2005)

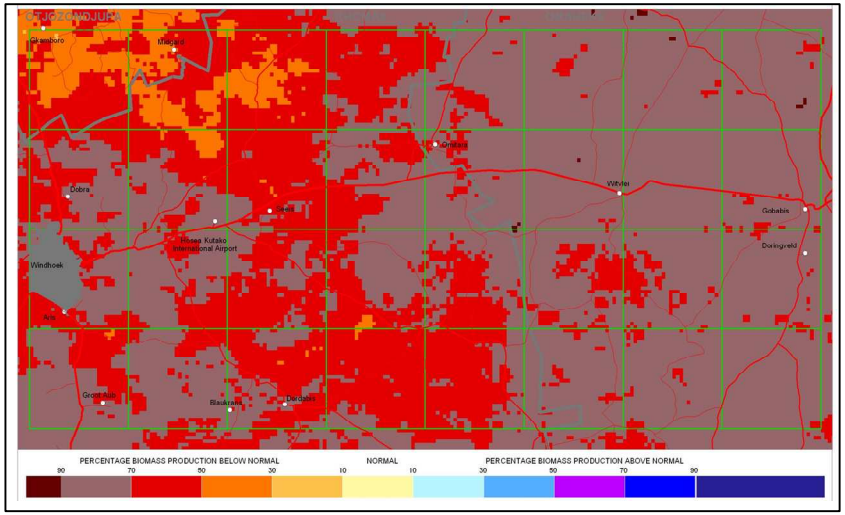

Figure 2.28. Estimated seasonal biomass production: deviation from the 20-year mean (1985/6 – 2004/5) during a very poor growing season (1994/5) (MAWF, 2005)

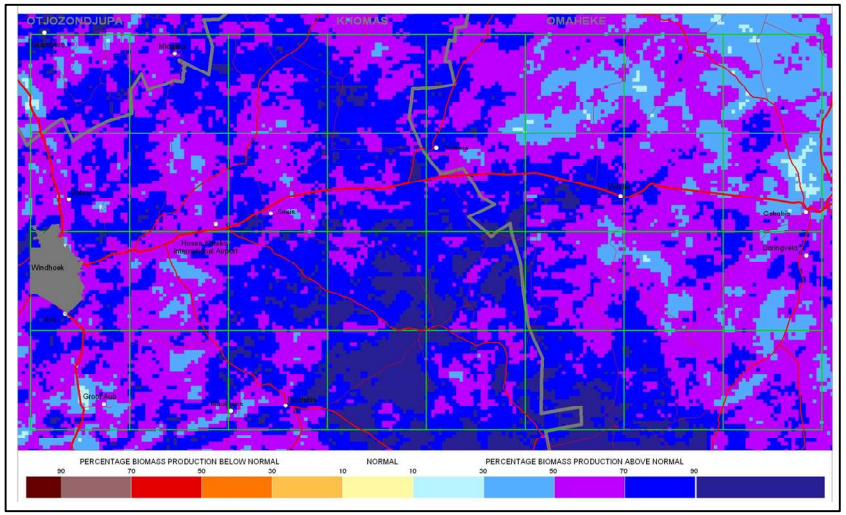

Figure 2.29. Estimated seasonal biomass production: deviation from the 20-year mean (1985/6 – 2004/5) during a very good growing season (1999/2000) (MAWF, 2005)

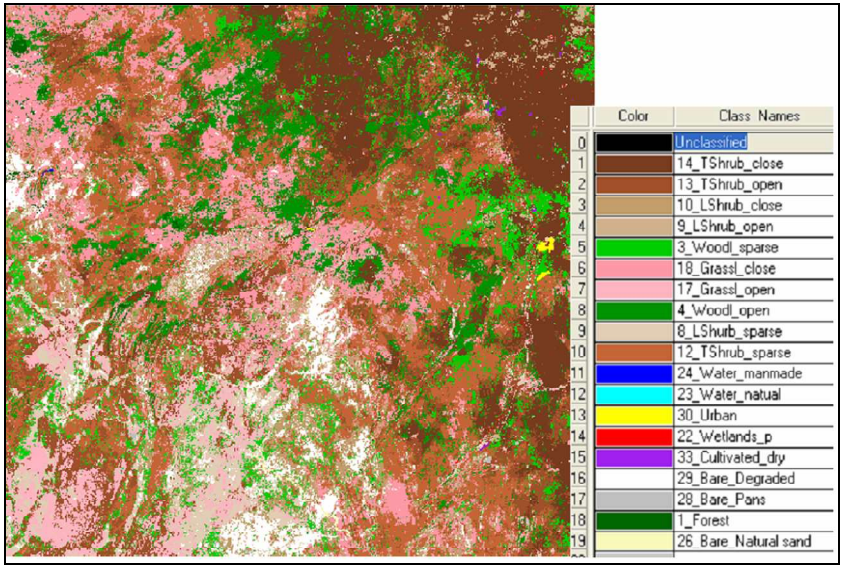

Figure 2.30. Land cover of the eastern half of the study area (Espach, 2006)

Witvlei to Gobabis (Figure 2.30), by means of supervised classification of multi-seasonal Landsat satellite images and field sample data. Verification was done through point-based field sampling, an area-based assessment using recent digital orthophotos, a comparison with the MODIS continuous field vegetation dataset and digital photographs taken from a low-flying gyrocopter (Espach, 2006; Espach, Lubbe and Ganzin, 2006). The study area consists of grasslands, shrubland, woodland and forest, according to the classification in Table 2.3.

Table 2.3: Landcover classification (Espach, 2006).

LANDCOVER TYPE	**MINIMUM THRESHOLD PARAMETERS**	**MODIFIERS FOR EACH VEGETATION GROUP**
Forest (dominated by single-stemmed trees)	Canopy cover > 70 % and canopy height > 5 m	Canopy cover thresholds (all types): 0 – 10 % Very Sparse 10 – 40 % Sparse 40 – 70 % Open 70 – 100 % Closed Forests are by definition closed with > 70 % canopy cover. The 0 – 10 % modifier is not applicable to tree and shrub dominated classes – these automatically qualify for one of the herbaceous classes
Woodland (dominated by single-stemmed trees)	Canopy cover > 10% and < 70 % and canopy height > 5 m	
Shrubland (tree / multi-stemmed shrub mix)	Canopy cover > 10 % and height > 0.5 m Canopy height: < 2 m: low shrubland; > 2 m: tall shrubland	
Herbaceous: Grassland	Tree / shrub cover < 10 % and > 1 % vegetation cover	
Herbaceous: Forbs	Tree / shrub cover < 10 % and > 1 % vegetation cover	

Areas of low grass cover are interspersed with open and closed grassland, sparse tall shrub and open tall shrub in the centre and western sections of the study area (Figure 2.30). Sparse and open woodland, intermingled with open and closed tall shrub and forest dominate in the east and north-east of the study area.

2.7 WATER RESOURCES

2.7.1 GROUNDWATER

Water availability is the major constraint on all types of land use in Namibia. Farmers predominantly make use of boreholes to access groundwater (Figure 2.31). Groundwater resources are inadequate for irrigation purposes, except on very small scale for vegetable gardens, greenhouses and small orchards of high-income crops.

Groundwater quality is generally good (Figure 2.32), though the depth to aquifers with sufficiently high yields (Figure 2.33) often makes pumping uneconomical.

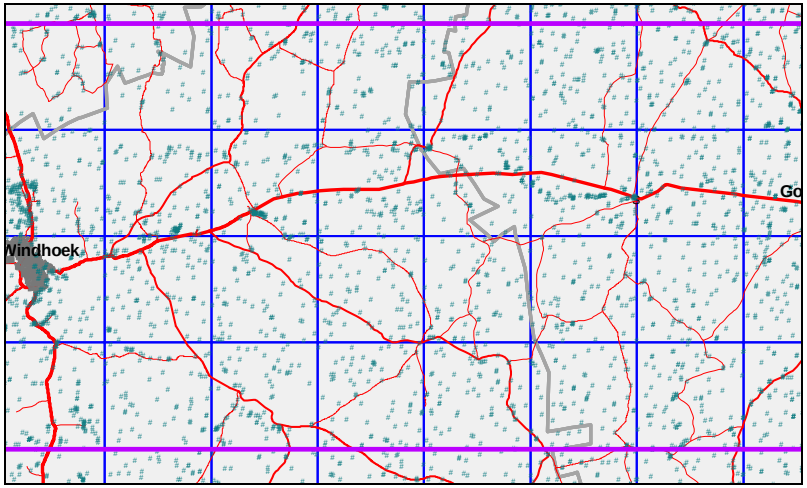

Figure 2.31. Boreholes locations (MAWF, 2005)

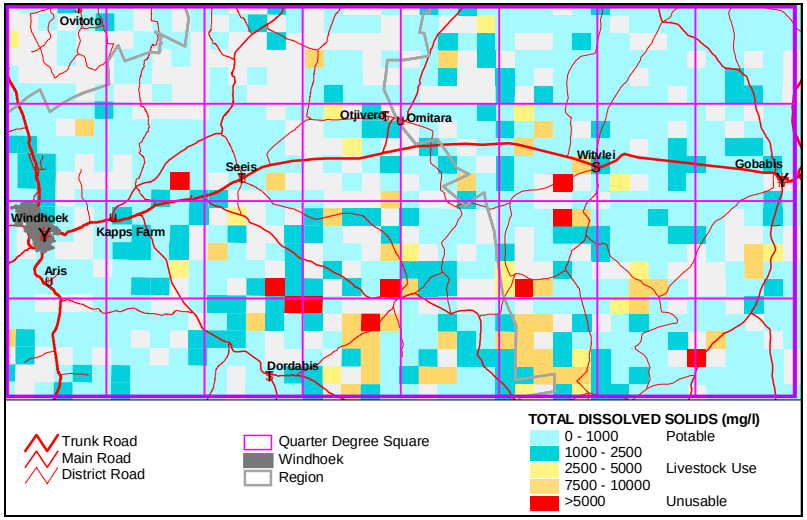

Figure 2.32. Quality of groundwater (MAWF, 2005, from Mendelsohn *et al.*, 2002)

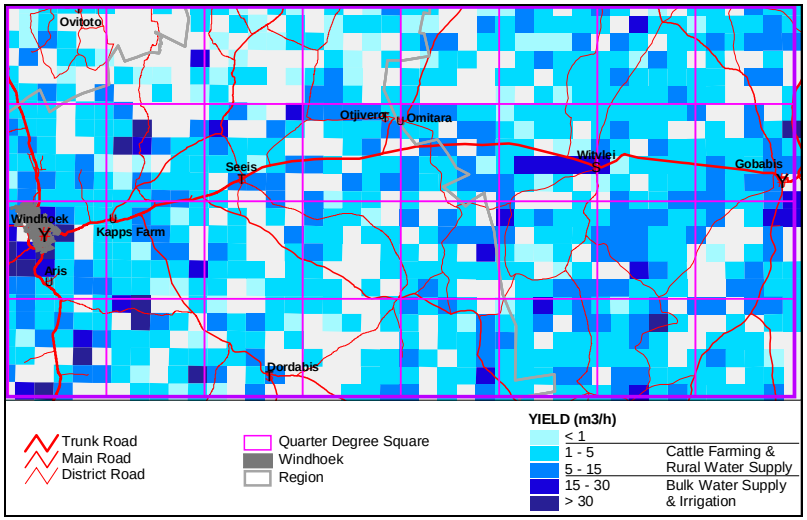

Figure 2.33. Borehole yield (MAWF, 2005, based on Mendelsohn *et al.*, 2002)

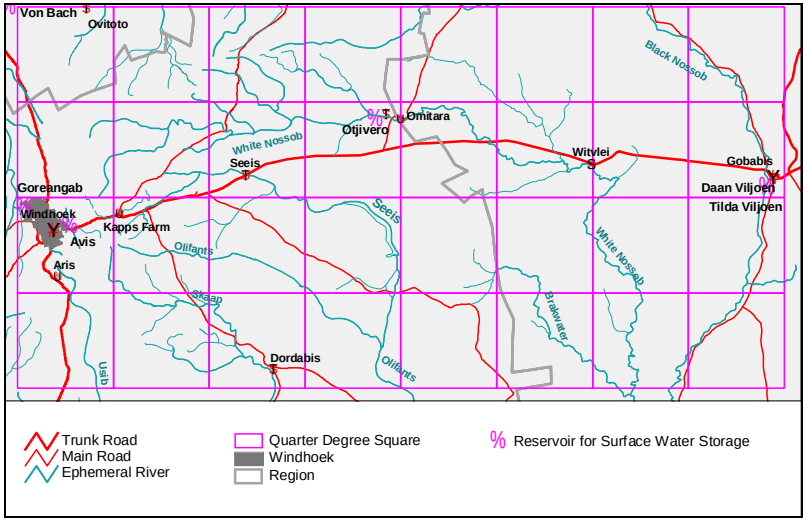

Figure 2.34. Surface water – rivers and reservoirs (MAWF, 2005)

2.7.2 SURFACE WATER

The study area has no permanent rivers. Runoff from episodic rivers is stored in surface reservoirs operated by the Namibia Water Corporation, Namwater, namely Goreangab, Avis, Otjivero, Tilda Viljoen and Daan Viljoen Reservoirs, with Oanob and Sartorius von Bach Reservoirs just outside the study area (Figure 2.37). All of the surface water is distributed to urban areas for domestic and industrial use. There are a few relatively large private earth dams on farms, e.g. on Hoffnung, Midgard and Neudamm.

CHAPTER THREE

GEOMORPHOLOGY, GEOLOGY AND SOILS

3.1 GEOMORPHOLOGICAL CONTEXT WITHIN SOUTHERN AFRICA

Shaw (1997) described Africa as a massive fragment of continental crust, tectonically stable relative to other continents and moving northwards since the break-up of Gondwana, characterised by a strong Precambrian tectonic legacy, vast ancient erosional surfaces and sedimentary basins that give it an unusually flat aspect.

In southern Africa, Precambrain rocks provided the basement upon which later sedimentation occurred, particularly the Karoo Sequence – from the Dwyka glaciation to the deposition of the terrestrial sandstones of the Ecca Formation. The Ecca formation is believed to be the source rock of the Kalahari sands (Smith, 1984). The fragmentation of Gondwana lead to the formation of pericratonic basins around the African coastline and flexuring of the continental crust which resulted in the formation of the Great Escarpment of southern Africa and the development of the inter-cratonic Kalahari-Cubango-Congo Basin (Thomas 1988), in which accumulation of Kalahari sediments commenced in the Cretaceous (Thomas and Shaw, 1991).

By the end of the Cretaceous, the interior of southern Africa had been eroded to a vast peneplain, the *African Erosion Surface* (Partridge and Maud, 1987, 1988), with deeply leached tropical soils and silicification that is still evident in parts of southern Africa today. The eroded material had been deposited on the continental shelf. The marginal escarpment retreated, forming a broad, gently sloping coastal plain (McCarthy and Rubidge, 2005). At this time, the southern African crust began to flex, forming large swells and depressions, probably as the result of mantle convection or compression from seafloor spreading from the mid-ocean ridges surrounding much of Africa (McCarthy and Rubidge, 2005). Uplift along the Kalahari-Zimbabwe Axis diverted much of the ancient Limpopo River headwaters towards a series of intra-continental lakes, including the ancestral Lake Makgadikgadi (McCarthy and Rubidge, 2005). This marks the start of the Kalahari Basin. The subsequent uplift of the Transvaal-Griqualand Axis further south diverted the Kalahari River towards the southeast, where it captured the Karoo River to form the Orange River (McCarthy and Rubidge, 2005).

By ~20 Ma ago, the influence of the East African Rift System spread into the Luangua and Zambezi Valleys, with the Zambezi systematically capturing the headwaters of the lake system. The Kafue and Upper Zambezi had already joined the Lower Zambezi, while the Kwando-Linyanti-Chobe is currently being captured. The Quito and Cubango-Kavango will eventually join the Zambezi. The depression into which the Okavango River debouches, with its accompanying faults, indicate that the rift system is still propagating (McCarthy and Rubidge, 2005). The tectonic quiescence was interrupted by two periods of uplift resulting in renewed erosion. Around 20 Ma ago the eastern part of the subcontinent rose by ~250 m, while the west rose by ~150 m (McCarthy and Rubidge, 2005). The subsequent erosion gave rise to the *Post-African I Erosion Surface* in the interior (Partridge and Maud, 1987, 1988).

The second uplift, around 5 Ma ago, culminated in a further tilting of the subcontinent – around 900 m in the east and only around 100 m in the west – and formation of the *Post-African II Erosion Surface* (Partridge and Maud, 1987, 1988). The increase in gradient added energy to rivers draining the escarpment towards the ocean, causing rapid down-cutting into gorges and submarine deposition of eroded material on the continental shelf (Figure 3.1).

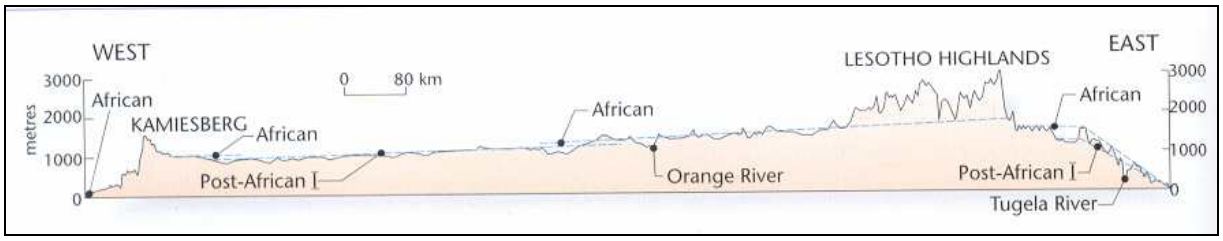

Figure 3.1. Transect through southern Africa, showing erosional surfaces (McCarthy and Rubidge, 2005)

During the Pleistocene (the last 2 Ma) a succession of ice ages caused variation in sea levels, allowing alternate periods of erosion and deposition on the coastal plains. During cold periods coastal rivers cut down into bedrock to form deep valleys, while warm periods produced estuaries and coastal lakes. Ice ages also increased aridity of the southern African interior, with formation of the Kalahari sands (or Mega Kalahari, see paragraph 3.6) stretching across parts of the southern Congo, Angola, Zambia, Zimbabwe, Namibia, Botswana and the Northwest and Northern Cape Provinces of South Africa (McCarthy and Rubidge, 2005).

3.2 TOPOGRAPHY

The western part of the study area is relatively high and strongly dissected where it forms part of the *Khomas Hochland* (= Highland) (Figures 3.2 and 3.3). The second highest point in Namibia is the Moltkeblick (2 479 m) in the Auas Mountains southeast of Windhoek (Surveyor General, 1983).

The land slopes down towards the southeast of the study area, where the minimum elevation is roughly 1 310 m (Figure 3.3) and the landscape almost flat (Figure 3.2). The Windhoek – Okahandja Valley is a graben at lower elevation (1 400 – 1 700 m) within the Khomas Hochland.

Figures 3.4 – 3.11 show altitudinal profiles from west to east (A1 – A2, B1 – B2, C1 – C2) and north to south (D1 – D2, E1 – E2, F1 – F2, G1 – G2, H1 – H2). The vertical scale is greatly exaggerated.

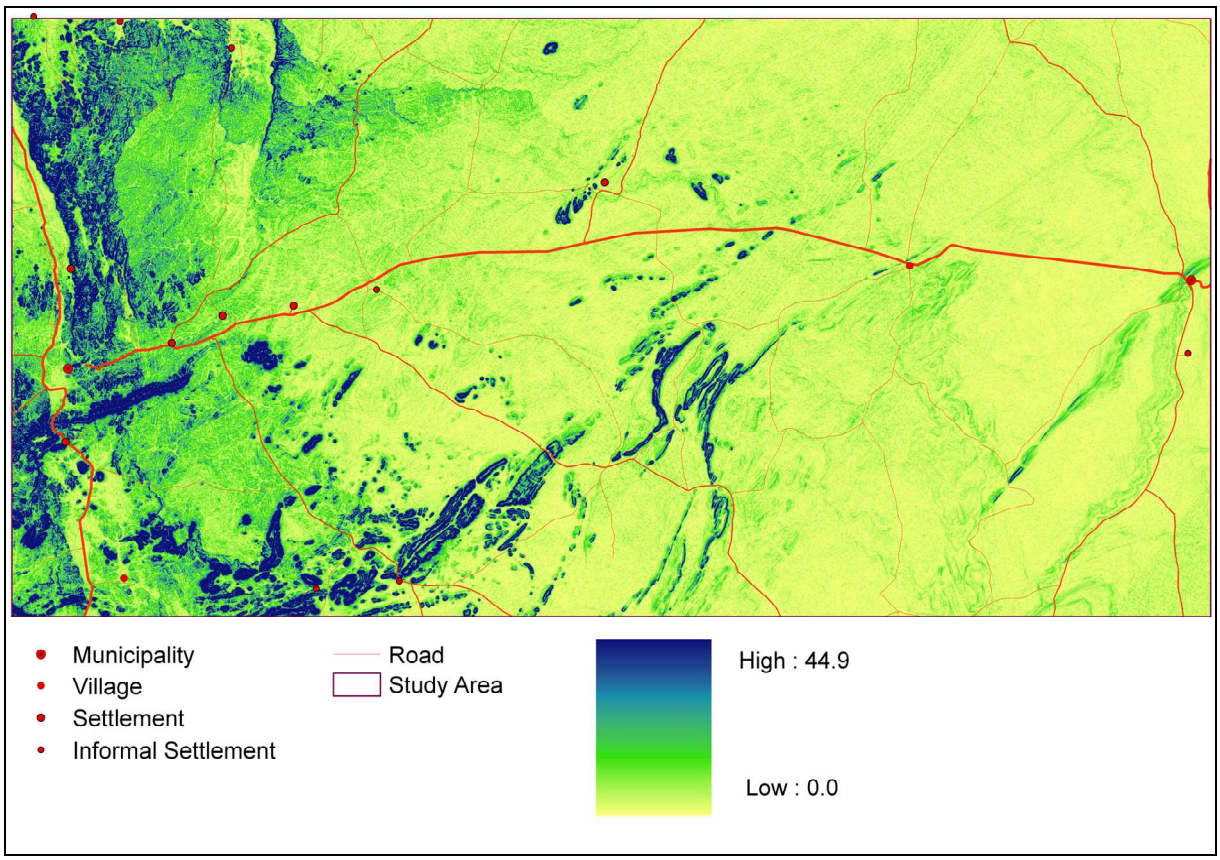

Figure 3.2. Slope (%) of the study area

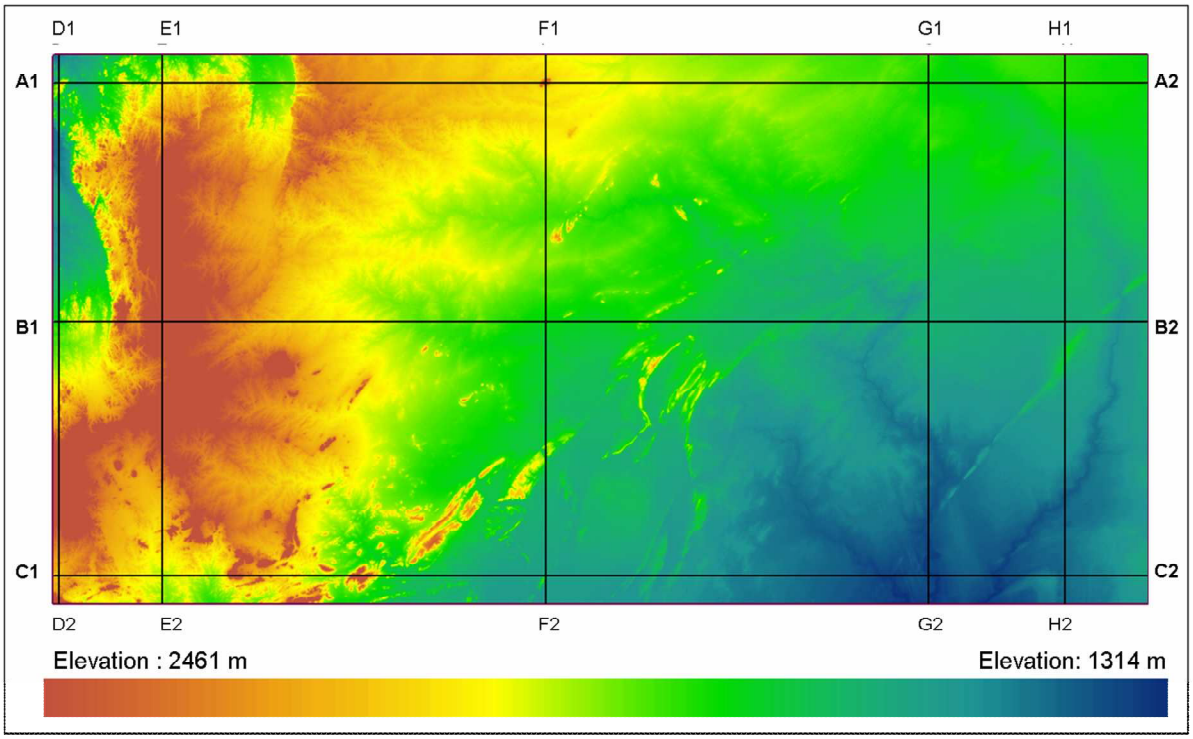

Figure 3.3. Elevation (m) and location of transects used to construct altitudinal profiles

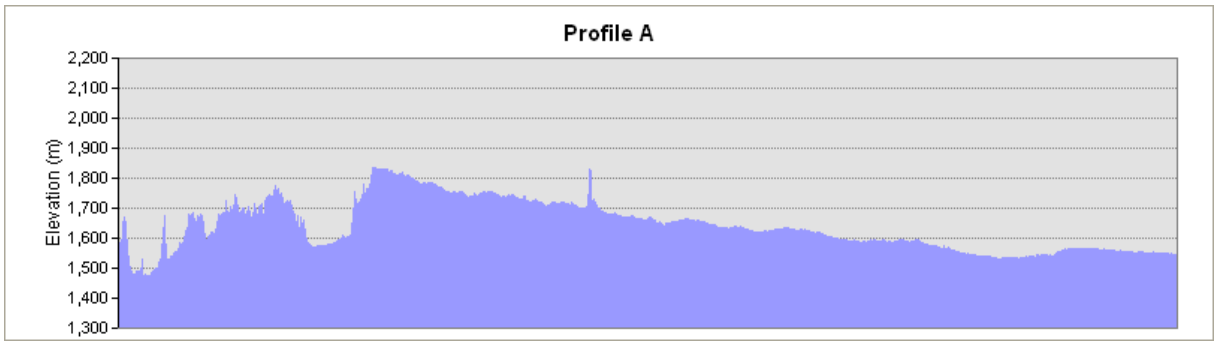

Figure 3.4. Altitudinal profile of transect A1 – A2

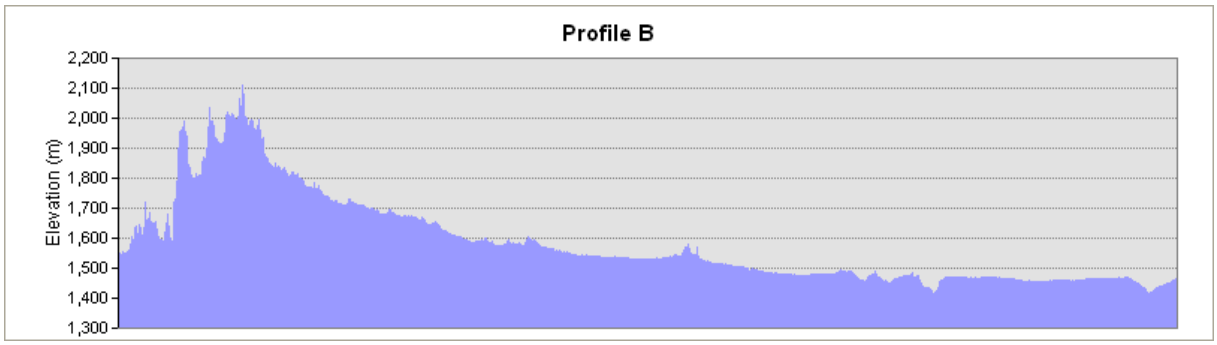

Figure 3.5. Altitudinal profile of transect B1 – B2

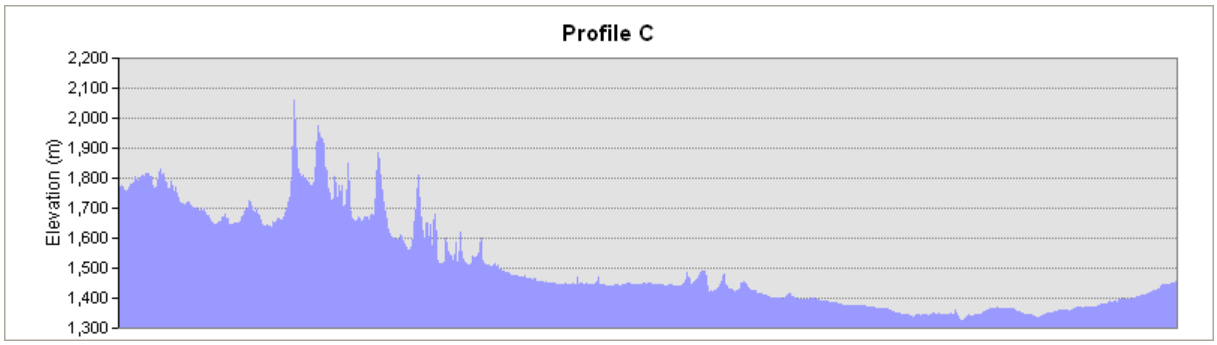

Figure 3.6. Altitudinal profile of transect C1 – C2

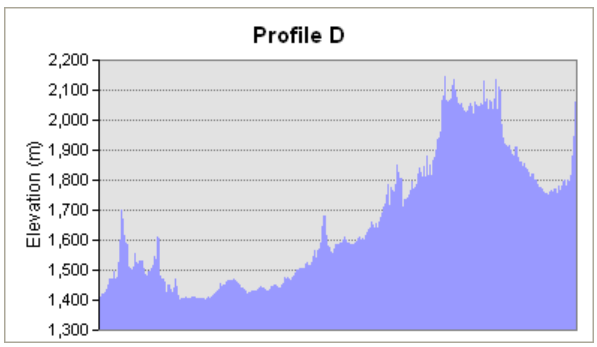

Figure 3.7. Altitudinal profile of transect D1 – D2

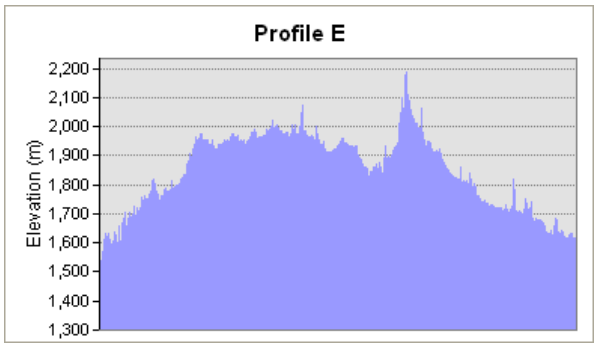

Figure 3.8. Altitudinal profile of transect E1 – E2

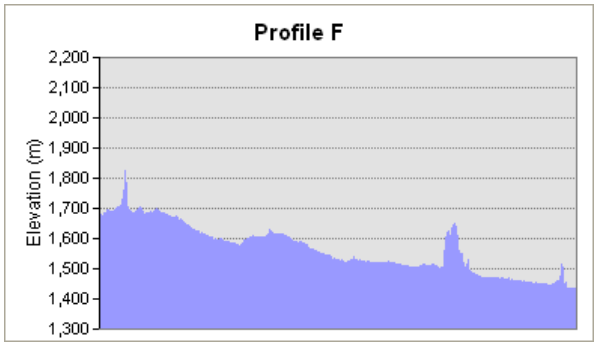

Figure 3.9. Altitudinal profile of transcect F1 – F2

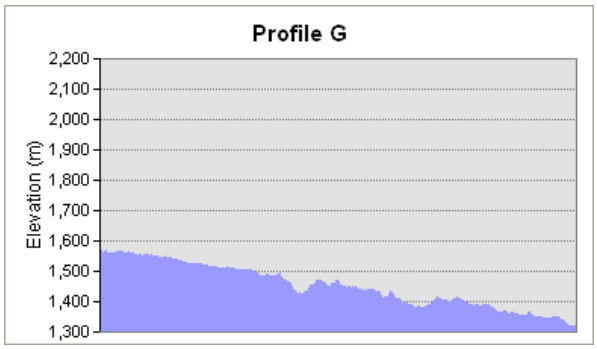

Figure 3.10. Altitudinal profile of transcect G1 – G2

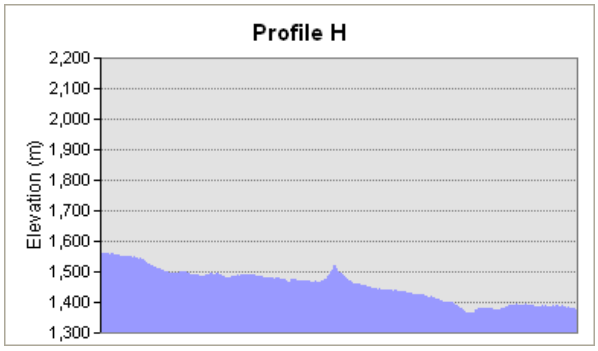

Figure 3.11. Altitudinal profile of transcect H1 – H2

3.3 AGRO-ECOLOGICAL ZONES

De Pauw, Coetzee, Calitz, Beukes and Vits (1999; AEZ Programme, 1999) divided the study area into 3 broad physiograpic zones, namely the *Escarpment*, *Central Plateau* and *Kalahari*, and further into 10 agro-ecological zones (Figure 3.12; Table 3.1).

Table 3.1: Codes and short descriptions of agro-ecological zones (MAWF, 2005; De Pauw *et al.*, 1999; AEZ Programme, 1999).

ESC2	Escarpment, high mountains on Basement Complex rocks
ESC4	Escarpment, high plateaux on Basement Complex rocks
CPL3-4	Central Plateau, strongly dissected inselberg plains, average growing period 61-90 days, very short dependable growing period
CPL3-6	Central Plateau, strongly dissected inselberg plains, average growing period 41-60 days
CPL3-7	Central Plateau, strongly dissected inselberg plains, average growing period 21-40 days
CPL5	Central Plateau, flat plains on metamorphic rocks
KAL2-7	Kalahari Sands Plateau, stabilized northwest – southeast dunes with common pans, average growing period 31-40 days
KAL3-4	Kalahari Sands Plateau, stabilised sand drift with few pans, average growing period 61-90 days, very short dependable growing period
KAL3-6	Kalahari Sands Plateau, stabilized sand drift with few pans, average growing period 41-60 days, no dependable growing period
R	Undifferentiated rocky hills and inselbergs

3.4 KHOMAS HOCHLAND

The Khomas Hochland is a rugged dissected plateau, on average 1 700 – 2 000 m above sea level, located roughly between the Swakop River in the north and Aris in the south, the Great Escarpment in the west and the Neudamm Kuppe in the east. The highest peaks and ridges of the Khomas Hochland are found around Windhoek, *viz*, the Kaiser Wilhelmberg, Kupferberg, Regenstein, Lichtenstein, Liebenstein and Grossherzog Frederick Mountains to the southwest, Auas Mountains to the southeast, Eros Mountains to the east and Otjihavera Mountains to the northeast respectively. East of the Swakop River is an isolated and unnamed remnant of the Khomas Hochland, with the Kunistein at 1 924 m as the highest point. The summit level slopes eastward until the land gradually sinks below the Kalahari sand east of the Neudamm Highland. Three of the most important ephemeral rivers in Namibia – the Swakop, Kuiseb and Nossob – arise in the Khomas Hochland.

The Khomas Hochland was created by an east-west axis of up-arching from the Windhoek area to the Great Escarpment. All the cyclic erosion surfaces slope eastward, the older ones progressively more so. King (1967) described the Khomas Hochland as an ancient, repeatedly-upwarped segment of Gondwana with locally elevated eastwardly tilted berms (partial bevels) and valleys that open into the main plain when followed eastward. He postulated that an early warp is indicated by the summit heights of inselbergs and mountain ranges on the Khomas plateau, which decrease in elevation eastwards more rapidly than the Khomas surface. He stated that when a land-surface has been deformed by tilting to a differential greater than the critical height for the local rock type and pediplanation continues to operate at the same base-level as before, a scarp may be developed separating what appear to be surfaces due to two distinct cycles of erosion. King assigned the smooth ridge crests of the Khomas Hochland to the Jurassic age *Gondwana Erosion Surface*. The extensive post-Gondwana valley system between them corresponds to the *African Erosion Surface* of Partridge and Maud (1987, 1988).

Kempf (1999c) and Bertram and Kempf (2002) suggested that the western part of the study area (Khomas Hochland and Neudamm Highlands) forms part of a large lenticular upwarp, dissected into a flight of distinct etchplain levels. They postulated that the oldest has been preserved in the silcrete capped plateau of the Gamsberg. They concluded that upwarping continued throughout much of the Tertiary up to the Early Quaternary, with a most active phase during the Oligocene. They identified three major levels and called these the *Otjihavera*, *Khomas* and *Seeis niveaux*. The Khomas niveau consists of the deeply dissected block of the Khomas Hochland. Its planation must have ceased in Mid-Oligocene to Mid-Miocene, as it cuts across Oligocene volcanic plugs and trachyte veins. East of Windhoek, the Khomas niveau continues, amongst others, as the top level of the Eros Mountains, the flat top of the Neudamm Kuppe and the Onyati Mountains. The undissected part of the Khomas niveau east of the regional watershed had been rejuvenated during the Pliocene and now forms the Seeis niveau, some 50 – 100 m below the Khomas niveau. The Neudamm Highlands is an example of the Seeis niveau (Bertram and Kempf, 2002).

3.4.1 WINDHOEK-OKAHANDJA VALLEY

The Windhoek-Okahandja Valley lies about 350 m below the surrounding plateau, with a width of 10 to 15 km over a length of more than 60 km. Gevers (1932a, 1932b, 1934, 1942) and King (1967, 1978) ascribed the Windhoek Valley to erosion during the African cycle in the Cretaceous, mainly by the Otjihavera and Usib Rivers. However, Miller (1983), Grünert (2003) and Schneider (2004) explained the Windhoek-Okahandja Valley as a halfgraben – a tectonic feature formed in the mid-Tertiary (~35 Ma ago) by north-south-trending faults. They argued that its origin lies in the major extensional forces exerted on the continental crust in the Mid-Jurassic (~170 Ma ago), before the break-up of Gondwana. They asserted that the graben can actually be followed for a length of 150 km.

Kempf (1999c) referred to radiometrically dated Oligocene volcanic plugs and intrusive dykes near Windhoek, which are saprolised and peneplanated in both the Khomas and Seeis niveaux. The peneplanation is also signified by relicts of fossil ferralitic soils on the highlands, which are proposed to be of post-Oligocene to Miocene age. According to Kempf's interpretation, the Windhoek Valley forms an intramontane basin associated with a tectonic stressfield with numerous rupture fissures induced by upwarping, where peneplanation, rather than fluvial incision, was the dominant process until the end of the Miocene. The Windhoek-Okahandja Valley constitutes the third and lowest peneplanation level postulated by Bertram and Kempf (2002) and Kempf (2008), namely the Otjihavera niveau. They suggested that it shows very similar pedological and weathering features as the Seeis niveau (Kempf, 2008). This is most likely due to the fact that the tectonically induced basin and the undissected Neudamm highlands were experiencing similar environmental conditions that caused deeper chemical weathering with desilification in the middle Pliocene (Kempf, 2008). In contrast, the very active and steep westward drainage of the Khomas level caused strong dissection along rupture fissures due to tectonic uplift since the mid Tertiary. In Kempf's opinion (2008) this dissection was a consequence of the end-Miocene Messinian crisis, with final development of intensive Benguela upwelling. Namibia was very dry at around 7 – 4 Ma ago, but became wetter in the mid Pliocene (~ 4 – 3 Ma), which rejuvenated intensive weathering on the undissected and poorly drained Seeis- and Otjihavera niveaux and caused deep valley incision on the already dissected and well drained Khomas niveau. The end of the Tertiary (~ 3 – 2 Ma) was very dry again and caused extensive dune development in the Namib. This climatic history matches what is known from offshore Benguela drilling cores (Kempf, 2008).

3.4.2 AUAS MOUNTAINS

These are composed of the Auas Formation sediments that were laid down ~730 Ma ago in a spreading ocean on the continental shelf of a passive margin (Schneider, 2004). During the Damaran Orogeny they underwent intense folding and thrusting towards the southwest. The highest peaks of the Auas Mountains, which are among the highest in Namibia, are capped with weathering-resistant quartzites forming steep south-facing cliffs (Schneider, 2004).

3.5 CENTRAL PLATEAU TRANSITION ZONE

This is the area east of Neudamm up to Witvlei, corresponding with the agro-ecological zones *CPL3-4*, *CPL3-6*, *CPL3-7* – strongly dissected inselberg plains with growing periods varying between 21 and 90 days – and *CPL5* – flat plains on metamorphic rocks of the Central Plateaux of Namibia. The area is lower and less dissected than the Khomas Hochland.

Small mountain ranges are found between the Windhoek-Rehoboth road and Dordabis: Hoher Schein, Kransneus-, Kransnek-, Blaukrans- and the Hatsamas Mountains. East of Dordabis the small mountains are the Grimmrücken, Kleeberge, Groot Kleeberg, Buschmannsklippe, Okambaraberg and Hartbeest-Rücken. Some of the more prominent inselbergs are the Schildkrötenberg at Aris, and the Bismarckfelsen, Oamites Mountain and Billstein west of the Windhoek-Rehoboth road. In the area north of Dordabis and south of the Windhoek-Gobabis road one finds the Bismarckberge, Paviansberg, Elisenhöhe, Koanusberg, Humansberg, Richtberg, Seeisberg and Dreispitz – all inselbergs. Further east, the most prominent inselbergs are the Otjiveroberg, Omieveberg, Ozombaheberg, Koedoeberg, Losberg and Heliographenberg .

3.6 KALAHARI

The definition of the Kalahari depends upon the criteria used, from physiographic region to eco-zone to an area occupied by Kalahari Group Sediments. The Mega Kalahari refers to the extent of the Kalahari erg from the northern Cape to Gabon and Congo north of the equator, an area of more than 2.5 million km^2 (Thomas, 1984). The drier parts occur south of the Zambezi River. The Kalahari is an edaphic desert. The absence of surface water is the result of a combination of relatively low mean annual rainfall, high temporal and spatial variability in rainfall, high evaporation rates and high infiltration rates. The sand mantle is generally 80 to 100 m deep, but in places up to 300 m (Schneider, 2004). It overlies Karoo sediments and volcanics, with very few rock outcrops (Grünert, 2003, Schneider, 2004).

The Kalahari is a gently undulating sand plain at approximately 1 000 m above mean sea level, with occasional inselbergs or minor hill chains. The central Kalahari has an endoreic network of ephemeral and dry channels draining towards the Makgadikgadi Basin and Okavango Delta. The southern Kalahari does not have an integrated drainage system, but rather a large number of small pans and dry rivers, locally known as *omiramba*. Lancaster (1978a, 1978b, 1986a), Goudie and Thomas (1985), Shaw (1988), Thomas, Nash, Shaw and Van der Post (1993), Shaw and Thomas (1997) and Mosweu (2008) described the distribution and characteristics of the pans and their lunette dunes, while Shaw and De Vries (1988), Nash (1995, 1997), Nash, Shaw and Thomas (1994a, 1994b, 1994c), and Nash and McLaren (2003) and discussed the morphology and function of the dry valleys.

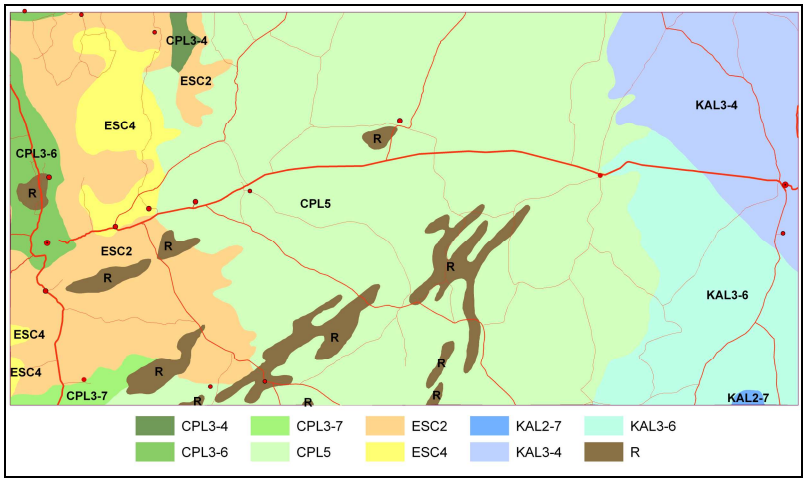

Figure 3.12. Agro-ecological zones (MAWF, 2005). See Table 3.1 for full legend.

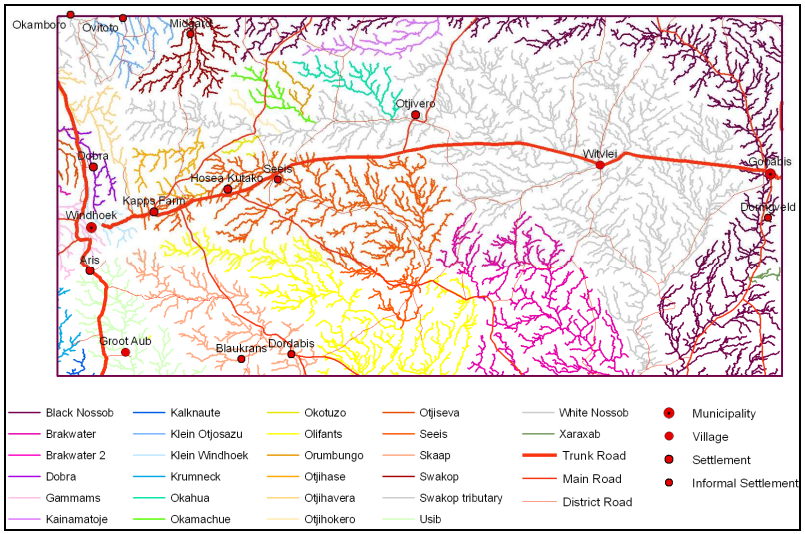

Figure 3.13. Drainage of the study area

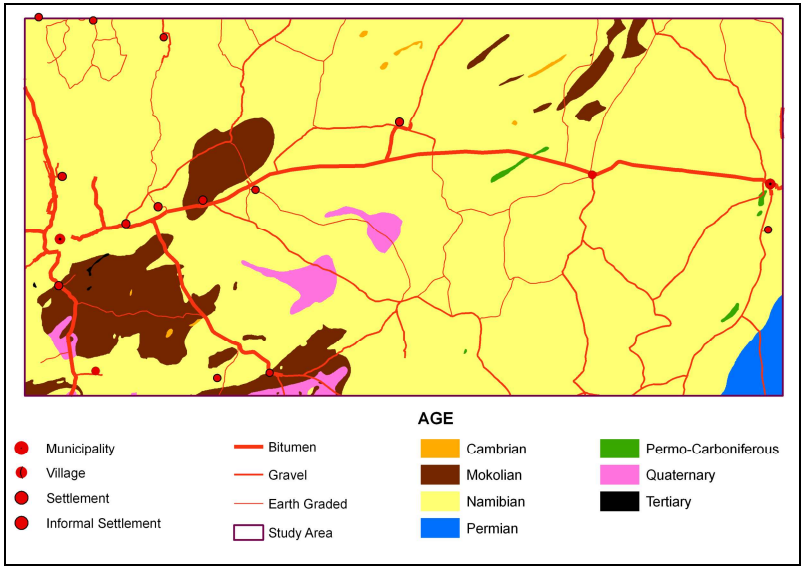

Figure 3.14. Geology – age (Geological Survey of Namibia, 2008)

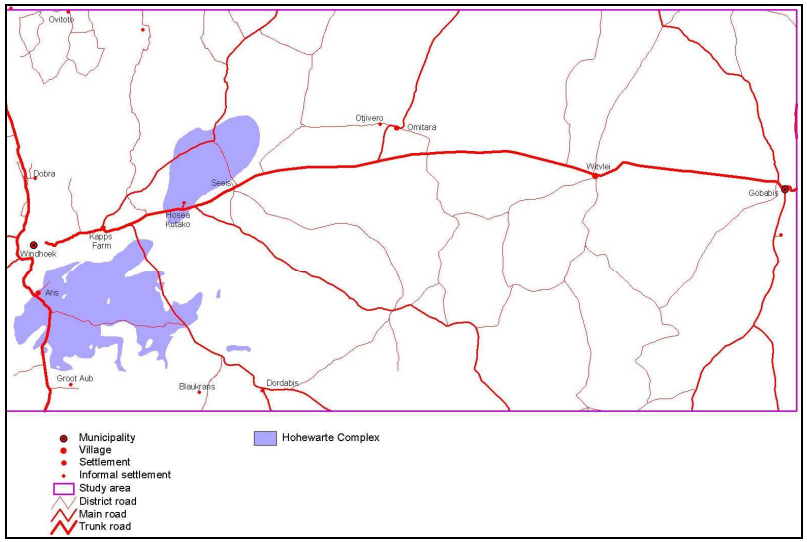

Figure 3.15. Geology – Höhewarte Complex (Geological Survey of Namibia, 2008)

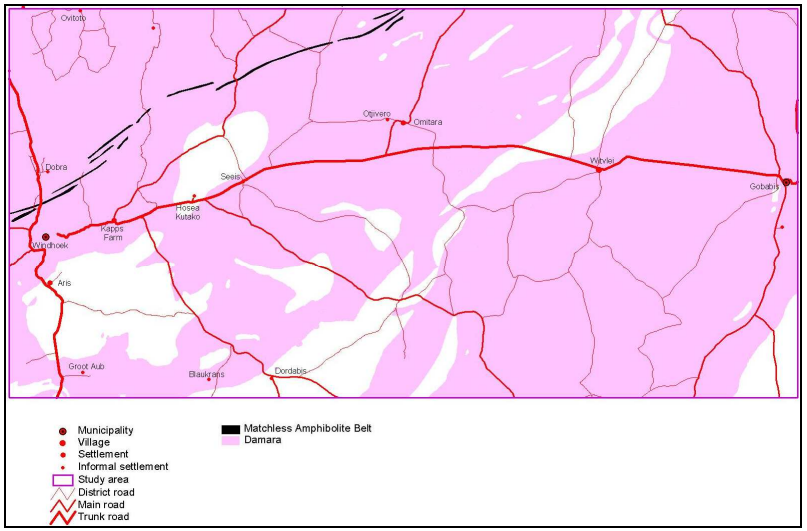

Figure 3.16. Geology – Damara Sequence (Geological Survey of Namibia, 2008)

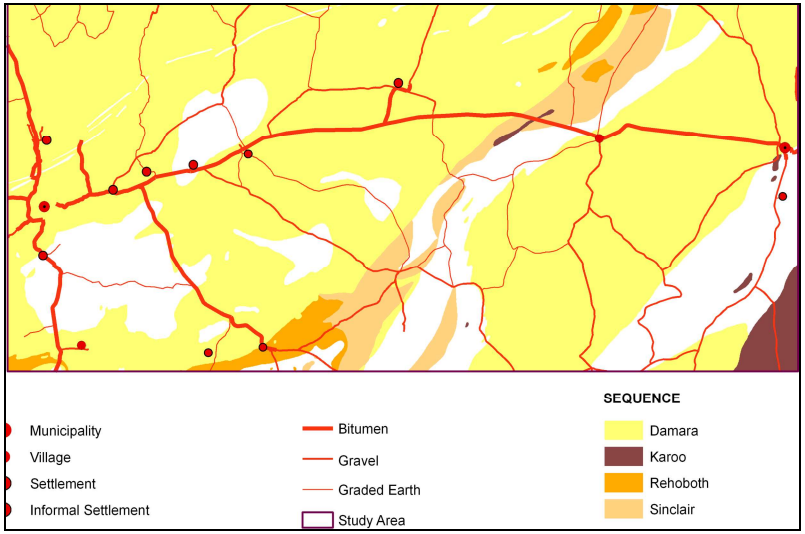

Figure 3.17. Geology – Sequences (Geological Survey of Namibia, 2008)

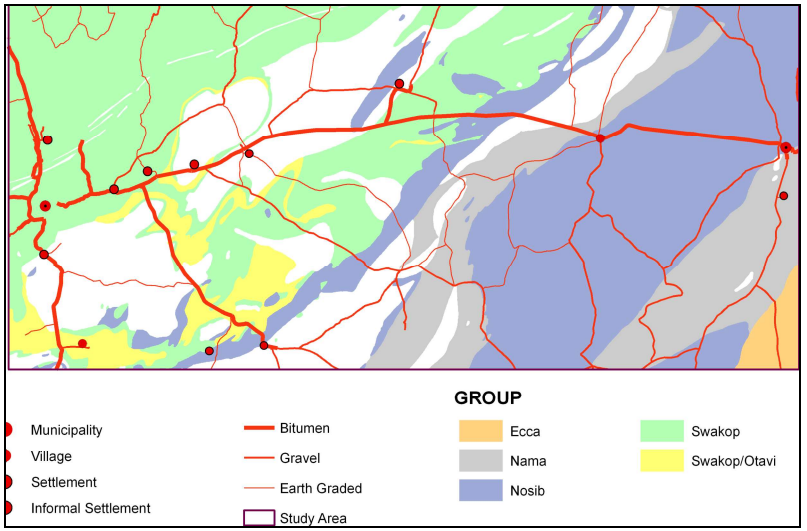

Figure 3.18. Geology – Groups (Geological Survey of Namibia, 2008)

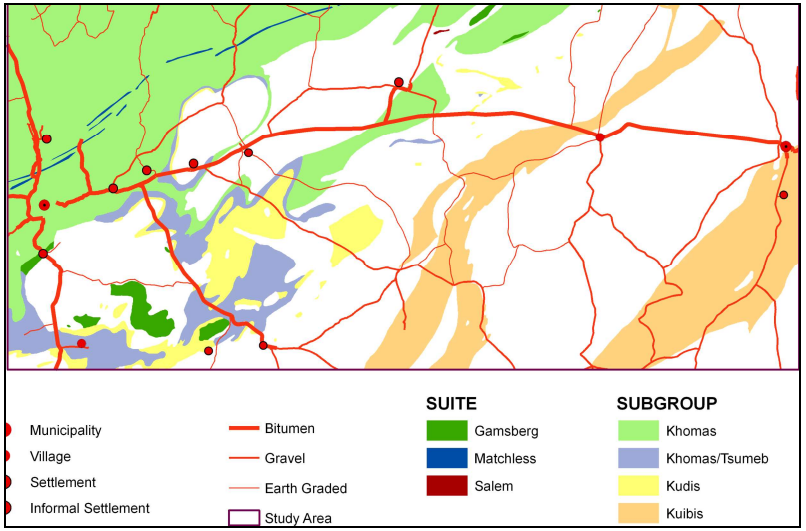

Figure 3.19. Geology – Suites and Subgroups (Geological Survey of Namibia, 2008)

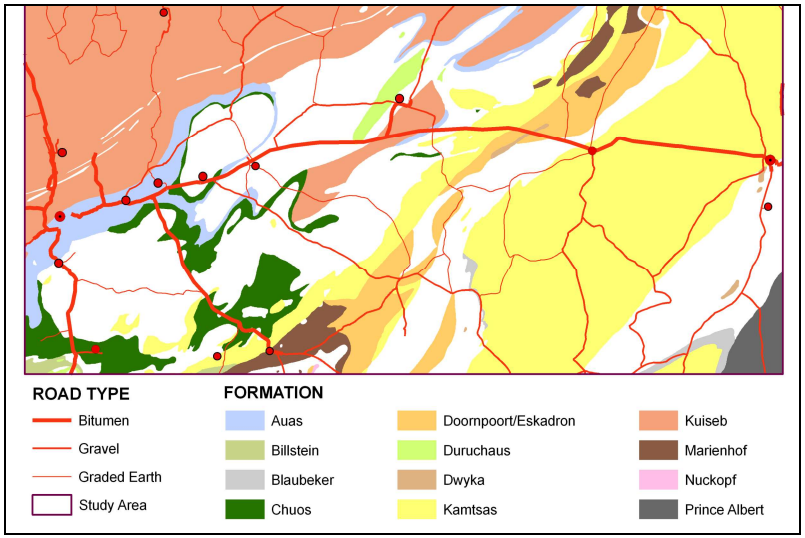

Figure 3.20. Geology – Formations (Geological Survey of Namibia, 2008)

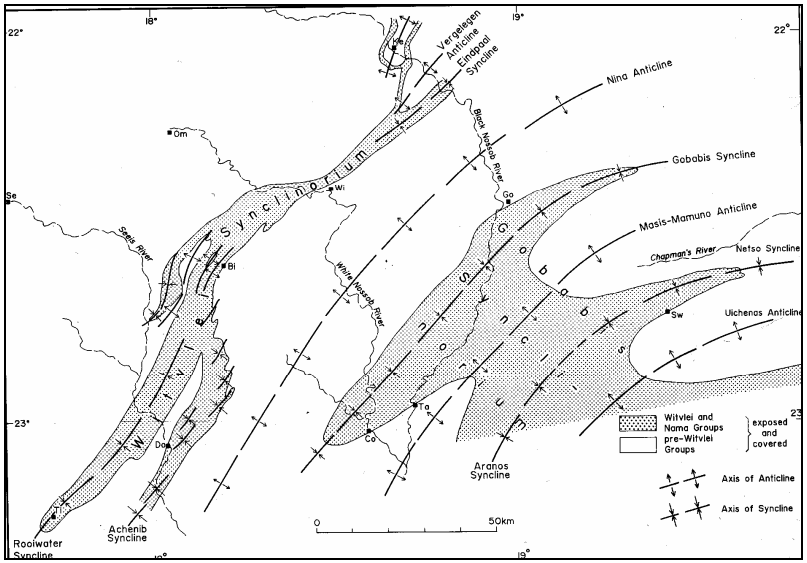

Figure 3.21. Witvlei and Gobabis Synclinoria (Hegenberger, 1993)

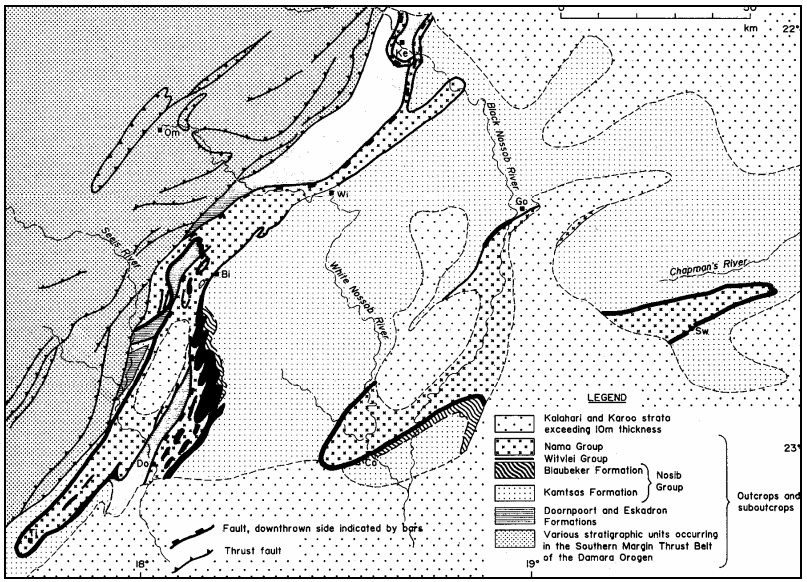

Figure 3.22. Stratigraphy of Witvlei and Nama Groups (Hegenberger, 1993)

3.6.1 DUNES

The dunes of the central and southern Kalahari are mainly linear (Thomas and Shaw 1991), with small areas of parabolic dunes and pan lunettes (Shaw, 1997). They were formed during the last glacial maximum in the Northern Hemisphere (20 000 – 16 000 years ago), when a large high-pressure cell circulated over the sub-continent and resulted in strong, cold dry winds (Schneider, 2004), the mean temperature was approximately 5 ^{o}C lower than today; there was less water vapour in the atmosphere and consequently lower precipitation and an expansion of the world's deserts (Grünert, 2003). Annual rainfall in the region was less than 150 mm, the threshold for sand movement in a vegetation-free environment (Heine 1982). The dunes are now stabilised by typically savannah vegetation. The alignment of linear (longitudinal) dunes is the result of acute bimodal wind regimes, with overall dune orientation parallel or sub-parallel to the resultant direction of sand transport (Thomas and Goudie, 2000). Linear dunes can also develop in wide unimodal wind regimes, where the single wind direction swings through an arc of less than 90^{o} (Lancaster, 1978b ; Wilkinson, 1988). The origin of the sand is streams flowing into the Kalahari depression over millions of years (Wilkinson, 1988). The sand consists mainly of physically hard and chemically inert quartz (Wilkinson, 1988).

Lunettes are crescent-shaped dune features found on the lee (downwind) margins of many pans in the Kalahari (Thomas and Goudie, 2000). The horns of these dunes face into the wind and result from deflation of sand and silt from the pan floor during windier or drier periods in the past (Wilkinson, 1988).

3.6.2 PANS

Pans ('*playas*') are abundant in the Kalahari. They occupy the lowest points in the topography and have flat basin floors (Wilkinson, 1988). Pans are hydrologically closed dryland depressions that may hold an ephemeral shallow water body or which may have been occupied by a lake under past positive water balance conditions (Thomas and Goudie, 2000). Hydrological inputs are provided by direct precipitation, surface or subsurface inflow, or a combination of these, and there is no surface outflow (Thomas, 1997). Calcretes beneath many pans support perched water tables.

According to King (1967), some pans are back-tilted sections of former drainage systems; others are deflation hollows, while some are the products of surface or subsurface solution of lime-bearing deposits. Goudie and Thomas (1985) integrated a number of hypotheses of pan formation into a model that should be applicable wherever conditions for pan formation are favourable: drainage impedance, the presence of suitable sediment or rock types and a semi-arid climate. The model includes, *inter alia*, erosion by animals concentrating around water and salt deposits, reduction of vegetation cover, deflation, lack of integrated surface drainage and tilting of old planation surfaces leading to drainage disruption. Lancaster (1986) noted that some of the higher-level pans in the Aminuis area contain algal mats and stromatolites, suggesting an origin as spring tufas at points of high groundwater discharge.

Pans are usually vegetation-free, particularly at the lowest elevations. Episodic flooding, vertisol and solonchak formation and salt accumulation discourage vegetation growth, although halophytic plants and shallow-rooting grasses may be established. Grassed pans exist alongside bare clay surfaces, suggesting

small variations in soil alkalinity and wind direction (Shaw and Thomas, 1997). The dominant salts in pans are sodium and calcium sulfates, sodium chloride and sodium carbonate.

3.6.3 DURICRUSTS

Duricrust occurrence is correlated with rainfall and usually associated with pans, drainage lines and valley sides (Goudie, 1973). Three types of duricrust are found in the Kalahari Group sediments: calcrete, silcrete and ferricrete, with thicknesses of up to 100 m in the southern Kalahari (Shaw and De Vries, 1988). The origin, distribution and characteristics of calcretes had been studied by Netterberg (1980) and reviews on the subject had been written by Goudie (1973), Watts (1980) and Summerfield (1982). Many Kalahari duricrusts date from the Tertiary, showing long-term geomorphological stability (Goudie, 1973), but some types are of Quaternary or recent age.

Calcretes are widespread in southern Africa where mean annual precipitation is in the range 150 – 600 mm, and annual free surface evaporation is above 1 000 mm (Goudie and Thomas, 1985). Calcrete develops in deserts due to progressive accumulation of calcium carbonate, either supplied by groundwater along valley bottoms, or on hillsides as airborne carbonate dust (Wilkinson, 1988). In the Kalahari they are plentiful in the interdune valleys, locally known as '*streets'* (English) or '*strate'* (Afrikaans). Goudie (1973, 1983) and Netterberg (1980) found that the Kalahari calcretes range from calcic soils to massive hardpan calcretes, and from precipitates to alteration products. They may form ridges and terraces on pan edges.

Silcretes are frequently encountered as layers of nodules within the calcrete, due to direct precipitation or calcium displacement (Summerfield, 1982).

3.7 DRAINAGE

The Khomas Hochland constitutes a regional watershed (Figure 3.13). All the rivers draining the land east and southeast of the Auas and Otjihavera Mountains and east of the Swakop River valley are *endoreic* – they do not reach the ocean, but gradually disappear in the sand of the Kalahari. Endoreic systems are independent of the worldwide base level determined by the world ocean. By creating their own base levels, they are not influenced by eustatic changes, and erosion can only proceed to the local base level – pans in the case of the Kalahari (Wilkinson, 1988). The Usib and its tributaries drain the area south of Windhoek. The Auas Mountains and area around Dordabis are drained by the Skaap River. Both the Usib and the Skaap flow into large pans near Duineveld, southeast of Rehoboth, in exceptionally good rainy seasons before disappearing into the Kalahari sand. The Seeis River joins the Olifants on the farm The Dunes at the southern edge of the study area. The Olifants subsequently joins the Auob at Tweerivieren southeast of Gochas. The confluence of the White- and Black Nossob is on the farm A-Ais, just south of the study area. The Auob and Nossob Rivers flow towards the Orange River, but do not reach it nowadays.

Exoreic rivers, with gradients three to four times that of the southern and eastern rivers, drain the Khomas Hochland towards the Atlantic Ocean. The Windhoek-Okahandja Valley is drained by the Otjihavera River

and its tributaries, which in turn joins the Swakop River that drains the area around Midgard and Ovitoto. The Swakop occasionally reaches the Atlantic Ocean at Swakopmund.

Large parts of the Kalahari, particularly in the areas of longitudinal dunes, are *areic* – without drainage lines. Ephemeral rivers that flow only occasionally and fossil drainage lines are locally known as *omiramba* (singular *omuramba*). They are often wide and shallow grassy valley bottoms without discernable streambeds.

Many drainage lines, particularly in the Khomas Hochland and Neudamm Highlands, correspond with tectonically disturbed zones such as rupture fissures resulting from upwarping (Kempf, 1999c). Valleys often meet at right angels, especially in proximal areas of elevated highlands (Bertram and Kempf, 2002).

3.8 MAIN STRATIGRAPHIC UNITS OF THE STUDY AREA

The present state of the study area is the end-result of the Mokolian and Damaran Orogenies and the deposition of Kalahari sediments.

3.8.1 HÖHEWARTE METAMORPHIC COMPLEX

The oldest rocks in the study area occur in the Paleoproterozoic Höhewarte Complex (Figure 3.15). The complex formed during development of the Kalahari Craton in Vaalian (> 2 000 Ma) to Early Mokolian (2 000 – 1 800 Ma) times, and through several cycles of subsequent metamorphism. The Höhewarte Complex forms a roughly circular dome structure with a diameter of approximately 40 km southeast of Windhoek (Schneider, 2004). It also underlies the extensive peneplain in the area of the Hosea Kutako International Airport. The lithology is dominated by mica schist, porphyro-blastic ortho- and para-gneiss, migmatite, granite gneiss and amphibolite (Schneider, 2004).

3.8.2 DAMARA SEQUENCE

The late Precambrian to early Palaeozoic Damaran Orogeny (1 000 – 500 Ma ago, Scheider, 2004) is part of the pan-African mobile belt system and connects with the Zambezi and Mozambique Belts. It underlies a vast tract of Namibia, where it can be subdivided into several geological provinces. Miller (1983) grouped the intra-continental branch of the Damaran Orogeny into seven zones bases on stratigraphy, structure, grade of metamorphosis, plutonic rock and geochronology (Schneider, 2004). Three of these zones run through the study area, namely the *Okahandja Lineament*, *Southern (Khomas) Zone* and the *Southern Margin (Hakos) Zone*. The Okahandja Lineament is the most important boundary in the Orogeny, with major changes in stratigraphic succession, structural style and age of deformation (Schneider, 2004). Both the Okahandja Lineament and the Southern Zone (Khomas Zone) are composed of the Kuiseb Group, but with different metamorphic characteristics. The Southern Margin Zone (Hakos Zone) shows intense thrusting, the result of continental collision (Schneider, 2004).

During its history, the Damaran Orogeny passed through a Wilson cycle, evolving through the successive

stages of rifting, spreading, plate convergence, subduction and continental collision (Miller, 1983). Kukla's model (1992) supports this concept of convergence and collision of the Kalahari and Congo Cratons following a rifting and spreading phase, and includes formation of the Khomas Hochland accretionary prism of Late Proterozoic age, developed in the Khomas Trough.

- *Rifting*: Initial rifting started around 750±65 Ma ago (Miller, 1983), and was characterised by formation of fault grabens filled with fluvial, lacustrine, shallow marine and volcanogenic deposits with rapid facies changes (Hegenberger, 1993).
- *Spreading*: Advanced rifting led to crustal thinning and the development of an oceanic spreading centre in the Khomas Sea. This phase has been confirmed by the presence of tholeiitic, mid-ocean ridge-type metabasalts and pillow lavas of the Matchless Amphibolite (Kukla, 1992). Breccias, meta-gabbros and ultramafic lithologies also occur within the oceanic sequence. The amount of tectonic shortening indicates that the basin had a minimum width of several hundreds of kilometres, once spreading ceased (Kukla, 1992).
- *Convergence*: The next phase was convergence and subduction of Khomas Sea oceanic crust beneath the Congo Craton. An oceanic trench developed along the southern margin of the Congo Craton, where sedimentary precursors of the Kuiseb schists accumulated as turbidites on an elongated submarine fan, incorporating large amounts of clastic sediments (Kukla, 1992). The trench sediments accreted against the Congo cratonic margin.
- *Subduction*: The Khomas Hochland accretionary prism evolved through the offscraping of submarine fan lithologies from the descending oceanic slab. The dominance of metasediments relative to basalts within the present-day Khomas Trough confirms high sediment input into the oceanic trench. Clastic sediments were preferentially accreted whereas oceanic basalts and pelagics were mostly subducted (Kukla, 1992). During accretion, early isoclinal folding occurred within the accretionary prism, the D_1-phase of deformation. The backstop of the accretionary prism was located at the southern margin of the Congo Craton and Kukla suggests that this structure was the initial expression of the Okahandja Lineament. Small amounts of pre-, syn- and post-tectonic alkaline and calc-alkaline granites, diorites and metagabbro intrusions occurring in the southern Central Zone within 30 km from the Okahandja lineament represents the magmatic arc associated with the subduction zone (Miller, 1983).
- *Continental collision*: Collision between the two cratons caused onset of major compressive stresses in the lithosphere, causing the D_2, D_3 and D_4 deformation patterns in the Khomas Trough. The Us Pass Lineament, forming the northern edge of the Southern Margin Zone, is interpreted as representing the continental suture zone (Hoffmann, 1983, 1989).

The *Matchless Amphibolite Belt* (Figure 3.19) is a striking and economically important linear feature running southwest to northeast through the Khomas Hochland, from Homeb in the Namib to near Steinhausen, where it disappears under Kalahari sand, over a distance of ~350 km (Schneider, 2004). Killick (2000) describes it as a relatively thin, but laterally continuous belt of metamorphosed, subalkaline, tholeiitic, ocean-floor basalt within metapelitic schist. It is up to 3 km wide, forming lenses and layers of amphibolites interbedded with Kuiseb Formation schist. Its estimated maximum stratigraphic thickness is 10 km. The belt is a remnant of the basaltic ocean floor of the ancient Khomas Sea (or Damaran Southern Zone Ocean), which was sheared off during the subduction of the oceanic crust beneath the continental crust of the Congo Craton (Schneider, 2004). One proposed mechanism is that the Matchless Amphibolite was incorporated into

the prism during the late stages of the accretionary processes by off-scraping from an oceanic crustal high such as the mid-ocean ridge, an aseismic ridge or an oceanic plateau (Killick, 2000). A second possible emplacement mechanism is that it may have been structurally emplaced during obduction of the accretionary prism onto the Kalahari Craton during the D_3 deformation, with fluids actively participating in the development of shear zones. It has a mid-ocean rift basalts geochemical signature, interpreted as metamorphosed, syn-sedimentary submarine volcanics emplaced into sediments covering a mid-ocean ridge (Schneider, 2004). Killick (2000) sites evidence that the belt is stratigraphically inverted over most of its length. The Matchless Amphibolite Belt contains 18 known base metal deposits, grouped into four clusters, which formed as part of the hydrothermal system during spreading. These are classified as Besshi-type volcanic hosted massive sulfide deposits, and it is estimated that the water depth at the time of their formation must have been at least one kilometer (Killick, 2000). In the study area, copper is mined from one such cluster of three sulfide lenses at Otjihase Mine (Schneider, 2004).

The sedimentology and stratigraphy of the Witvlei and Nama Groups (Figure 3.18) of the upper Damara Sequence had been studied extensively by Hegenberger (1993). These sediments are found towards the centre and east of the present study area. They were deposited on the Southern Foreland some 650 – 530 Ma ago (Miller, 1983) and preserved from erosion by being buried under Karoo sediments in the Witvlei and Gobabis Synclinoria (Figure 3.21). The Witvlei Synclinorium consists of the Rooiwater, Achenib and Eindpaal Synclines and the Vergelegen Anticline. The Synclinorium is approximately 180 km long and up to 20 km wide. The marginal thrust plane of the Damaran Orogeny forms the northwestern boundary of the Witvlei Synclinorium. Steep hills and ridges are formed in the central part of the synclinorium by erosion-resistant quartzite of the Weissberg Member. The overlying shales are deeply eroded. They occupy the inter-montane valleys and plains. Several anticlines show relief inversion: once erosion had removed the resistant Weissberg Member quartzite, the softer rocks of the underlying Buschmanns-klippe Formation (Figure 3.22) eroded quickly, forming oblong valleys within the centres of anticlines. In the southwest the Witvlei Synclinorium is underlain by the Doornpoort and Kamtsas Formations (Figures 3.21 and 3.22) that are exposed at the southwestern tip of the Rooiwater Syncline. The broad Nina Anticline (Kamtsas Formation arenites of the Nosib Group) separates the Witvlei and Gobabis Synclinoria. The latter consists, from west to east, of the Gobabis Syncline, Masis-Mamuno Anticline (which further north forms the Ganzi Ridge), Aranos Syncline and Uichenas Anticline, all trending southwest to northeast and mostly covered by Karoo and Kalahari sediments. Witvlei and Nama Group exposures are found along the Black and White Nossob River valleys (Hegenberger, 1993).

Hegenberger's stratigraphic sequence (Hegenberger, 1993), from the bottom upwards (see Table 3.2), is as follows:

- The *Tsumis Group* (Bitterwater, Aubures, Doornpoort, Klein Aub and Eskadron Formations) (Figures 3.20 and 3.22) contains the oldest sediments. These were deposited on the Kalahari Craton as fluvial, lacustrine, shallow marine and volcanogenic sediments of the early Damara rifting phase (Hoffmann, 1989). They consist of conglomerate, sandstone, shale and carbonates.
- The succeeding *Nosib Group* (Kamtsas Formation) represents later rift filling and consists mainly of fluvial arenites (Figures 3.18, 3.20 and 3.22).
- A patchy mixtite of glacial origin (diamictite), the *Blaubeker Formation*, indicates major unconformities

between the underlying Nosib and overlying Witvlei Groups (Figures 3.20 and 3.22).

Table 3.2: Lithostratigraphic units of the Damara Sequence in the study area (Hegenberger, 1993).

Group	Formation	Member	Main Lithology (facies in brackets)	Depositional Environment
Nama	Zaris	Grünental	Sandstone (b) Shale, dark limestone (c) Dark limestone (c)	Shallow subtidal (c) Offshore to subtidal lagoonal (a) Fluviatile (b)
		Zenana	Quartzite (upper unit) Dark dolomite (lower unit)	Sandy tidal delta fan (distal) Shallow subtidal
	Dabis	Weissberg	Orthoquartzite (a) Submature quartzite (b) Conglomerate (c)	Protected intertidal to shallow subtidal (a) Onshore tidal flat (b) Proximal delta fan (c)
Unconformity, in places paraconformity or conformity				
Witvlei	Busch-manns-klippe	Okambara	Light-grey dolomite (upper unit) Quartzite (middle unit) Light-grey limestone (lower unit)	Inter to supratidal (upper) Tidal channels (middle) Shallow subtidal (lower)
		La Fraque	Shale, marl, subordinate carbonates	Muddy shallow subtidal (shelf lagoon)
		Bildah	Light-grey and pink dolomite	Shallow subtidal; intertidal, locally shallow subtidal
	Unconformity			
Witvlei	Court	Simmenau	Quartzite (main) Conglomerate (subordinate)	Braided fluvial; Alluvial fan
		Constance	Shale, siltstone, subordinate carbonates	Muddy shallow lagoonal or flood-plain
		Gobabis	Dark carbonates (laminated or massive)	Lacustrine, shallow-water (b) Anoxic lacustrine, deepwater (a)
		Tahiti	Quartzite	
Unconformity				
	Blaubeker		Mixtite (diamictite)	
Unconformity				
Nosib	Kamtsas		Quartzite, conglomerate	
Unconformity				
Tsumis	Eskadron		Quartzite, shale carbonate	
	Doornpoort		Quartzite, conglomerate	

- The *Witvlei Group* was deposited on the southern shelf of the Damara trough, on the northern and western edge of the Kalahari Craton. It shows two sedimentary cycles, represented by the Court and Bushmannsklippe formations (Figures 3.20 and 3.22). Sedimentation of the Witvlei Group was terminated by a transgression. The Court formation was probably deposited towards the end of the rifting stage, firstly as deepwater laminate carbonate, passing into shallow-water carbonate (both of the Gobabis Member), followed by floodplain mudstone with carbonate intercalations (Constance member) and then by fluvial sandstone (Simmenau member). The Bushmannsklippe Formation was most likely deposited during the drifting stage, in a flexure basin of a passive margin. It starts with light-coloured intertidal dolomite (Bildah Member), grading into shallow subtidal limestone towards the top, followed by marl (La Fraque Member), which was deposited in a muddy lagoonal to subtidal environment. This is followed by three units of the Okambara Member, namely a shallow subtidal lower unit consisting of limestone with arenaceous intercalation, showing edgewise conglomerate and hummocky cross-

stratification; an arenaceous middle unit also showing crossbedding; and an upper unit consisting of dolomite with sandy intercalations containing flat-pebble conglomerate and, near the top, stromatolites and pseudomorphs after an evaporite mineral, indicative of regression.

- The Dabis and Zaris Formations of the *Nama Group* were mostly deposited in peritidal and shallow subtidal environments, with clastic material derived from the Kalahari Craton (Figures 3.20 and 3.22). The basal unconformity probably indicates the reversal of plate motion from spreading to convergence.

3.8.3 KAROO SEQUENCE

Karoo Sequence (Figure 3.17) sediments are mostly buried under the Cenozoic Kalahari Group. A few scattered Dwyka diamictites of the lower Karoo Sequence are found on the Nossob Valley floor (Schneider, 2004).

3.8.4 KALAHARI SEQUENCE

The deposition of the Kalahari Sequence (Figure 3.17) followed on the disintegration of Gondwana and the subsequent isostatic uplift of the continental edges about 120 Ma ago. It covers roughly one third of Namibia's surface and includes stabilised red sand dunes and flat sand plains, conglomerates, sandstones, shales and siliceous calcretes. Clay-filled pans of Cenozoic to recent age are often found among the Kalahari Sequence sediments (Schneider, 2004).

3.9 LITHOLOGY

3.9.1 KHOMAS HOCHLAND

Schneider (2004) describes the origin of the Khomas Hochland as a narrow elongated branch of the Khomas Sea which eventually became the Damara Mobile Belt. Clayey-sandy sediments were eroded from the Congo Craton towards the north and the Kalahari Craton towards the southeast and deposited to a thickness of 10 000 m in this narrow sea. During the subsequent Damaran Orogeny these sediments were intensely folded and metamorphosed to intercalated mica-schist, quartzite and meta-greywacke, presently known as the Kuiseb Formation (Figure 3.20) of the Damara Sequence (Schneider, 2004).

The Damara Mountains were eroded over the aeons to form a vast peneplain. After the break-up of Gondwana the area was extensively uplifted. Further erosion over millions of years resulted in the present plateau with its rolling topography (Schneider, 2004).

3.9.2 WINDHOEK-OKAHANDJA VALLEY

The Windhoek-Okahandja Graben was formed as a result of powerful extensional forces applied on the continental crust since the Mid-Jurassic (~170 Ma ago), before the break-up of Gondwana, which created

north-south-trending faults. Crustal stress was relieved by vertical (and minor horizontal) displacement of individual blocks in the mid-Tertiary (~35 Ma ago). The valley is covered by Cenozoic sediments deposited on the schist of the Kuiseb Formation of the Damara Sequence (Schneider, 2004).

3.9.3 AUAS MOUNTAINS

Auas Formation (Figure 3.20) sediments were laid down ~730 million years (Ma) ago in a spreading ocean on the continental shelf of a passive margin. During the Damaran Orogeny they underwent intense folding and thrusting towards the southwest. The highest peaks of the Auas Mountains are capped with weathering-resistant quartzites forming steep south-facing cliffs (Schneider, 2004).

3.9.4 AREA SOUTH OF WINDHOEK TOWARDS REHOBOTH

The mountain pass between Windhoek and Usib Valley towards the south is a surface manifestation of the block faulting that originally caused the formation of the Windhoek-Okahandja Graben. The accompanying volcanism resulting in the emplacement of thrachytes and phonolites of mid-Tertiary age, such as the Schildkrötenberg and Huquanis phonolites north of Aris and the Gocheganas trachyte (also known as the 'Backenzahn' or 'Kiestand'). Older granitic intrusions from the Kibaran (1 200 Ma) and Damaran (500 Ma) Orogenies also occur in the Aris area, such as Falcon Rock. This whole area is underlain by the Höhewarte Complex, composed of quartz-feldspar gneisses inter-layered with meta-carbonates and amphibolites. The Bismarckfelsen and surrounding hills towards the west are composed of erosion-resistant quartzite of the Melrose Formation (Figure 3.20). Further south of Aris, the glacial Naos Formation (Figure 3.20) is visible west of the trunk road towards Rehoboth, while the Nosib and Hakos Groups (Figure 3.18) of the Damara Sequence are exposed towards the east. These were thrust to the southwest onto the Höhewarte Complex, where they now form tectonic nappes (Schneider, 2004).

3.9.5 AREA BETWEEN WINDHOEK AND HOSEA KUTAKO INTERNATIONAL AIRPORT

The Kleine Kuppe Formation (Wasserberg Member) (Figure 3.20) just east of Windhoek, contains mainly micaceous quartzites intercalated with Kuiseb Formation schists. Between the Dordabis turn-off and Hosea Kutako International Airport, a series of thrusts towards the southwest, in schist and quartzite of the Hakos Group, is found. The schist and quartzite are extensions of the Auas Mountains south of the road (Schneider, 2004).

3.9.6 AREA NORTH OF HOSEA KUTAKO AIRPORT (TOWARDS STEINHAUSEN)

North of the airport one finds intercalated mica schist and quartzite of the Kuiseb Formation, including the mountains Lydiakop, Ludwigskop and Neudammkuppe. These mountains are the products of block faulting caused by the extensional tectonics that operated during the mid-Tertiary. Further east on the Kapps Farm – Steinhausen road, the terrane is underlain by gneisses of the Höhewarte Complex. One also finds extensive thrusting, underlain by graphitic schist of the Hakos Group, Kudis Subgroup, before coming across more of

the Kuiseb Formation. The Matchless Amphibolite Belt (Figure 3.19) runs through this area, but without prominent outcrops (Schneider, 2004).

3.9.7 BISMARCK MOUNTAINS AND TOWARDS DORDABIS

The Bismarck Mountains southeast of the Dordabis turn-off had been formed by the thrusting of Auas Formation (Figure 3.20) quartzite onto Nosib Group schist. The road passes over a few outcrops of quartz-feldspar gneiss inter-layered with marble and amphibolite of the Höhewarte Complex. These are locally intruded by Mesoproterozoic Rietfontein Granite which forms hills such as the Dassiekuppe. Rosaberg is composed of quartzite of the Auas Formation (Figure 3.20) thrust onto schist and marble of the Hakos Group, Kudis Subgroup (Figure 3.19). Dreispitz is composed of schist and quartzite of the Kudis Subgroup thrust onto the younger Vaalgras Subgroup (Figure 3.19) and the Höhewarte Complex. Humansberg is composed of feldspathic quartzite of the Kamtsas Formation of the Nosib Group. The Kamtsas Formation was deposited in a half-graben during early stages of rifting 750Ma ago. The Elisenhöhe Mountain and its surrounding mountains are composed of marbles of the Kudis Subgroup, with Kamtsas Formation quartzites thrust onto them. The Höhewarte Complex underlies all of this terrrane.

The Koedoeberg and Hatsamas Mountains are composed of Kamtsas Formation quartzite thrust onto younger Vaalgras Subgroup lithologies. The Grimmrücken is composed of Kamtsas Formation quartzite. At Dordabis there is a major thrust along which quartzite of the Kamtsas Formation has been thrust onto quartzite and phyllite of the Rehoboth Sequence (Figure 3.17) (of Palaeoproterozoic age). South of Dordabis the landscape flattens out and Kalahari sediments take over. The Eskadron Formation (Figure 3.20) (of Mesoproterozoic age) of the Sinclair Sequence (Figure 3.17), with red-brown quartzite, crops out as a range of small hills about 15 km southeast of Dordabis, as a result of a fault. The Karubeamsberge and the Hartebeestrückenkuppe are composed of quartzite of the Eskadron Formation, while the flat area between the two ranges is underlain by black limestones of the Kuibis Subgroup (Figure 3.19), Nama Group. The northeastern extension of the Karubeamsberge consists of metasediments of the Doornpoort Formation of the Sinclair Sequence, overlying the Eskadron Formation (Schneider, 2004).

3.9.8 AREA FROM HOSEA KUTAKO INTERNATIONAL AIRPORT TO WITVLEI

Cenoizoic age sediments of the Kalahari Group, with some ridges of Nosib Group quartzite are found east of the airport. Northeast trending folds and thrusts with large displacements occur, and several deformation events have been recognized in the Omitara area. Near Omitara a 10 km wide zone of quartzites with heavy mineral layers, conglomerate bands and scattered pebbles of the Kamtsas Formation, Nosib Group, are found. Further east, these quartzites are thrust over the red-brown quartzites of the Eskadron Formation, Sinclair Sequence of Mesoproterozoic age. The latter contains copper deposits in three broad zones, which were most probably deposited in shallow basins. Witvlei is located in a gap between a ridge of sandstone Kuibis Subgroup of the lower Nama Group, and quartzite of the Nosib Group (Schneider, 2004).

3.9.9 WITVLEI TO GOBABIS

Feldspatic quartzites of the Kamtsas Formation underlie the area between Witvlei and Gobabis. Gobabis lies on the contact between the Nosib Group, which is visible in isolated low hills, and the Nama Group, which is partially followed by the road towards Buitepos, as a syncline (Schneider, 2004).

3.9.10 GOBABIS TO LEONARDVILLE

The flat landscape south of Gobabis is underlain by sandstones of the Kuibis Subgroup, Nama Group, and towards the southern edge of the study area, by the Nosib and Witvlei Groups. Dwyka diamictites of the lower Karoo Sequence are found in the valley floors of the White and Black Nossob Rivers, indicating that these parts of the drainage system are probably quite old. Downstream of the confluence of these two ephemeral rivers on the farm A-Ais (just south of the study area), the river is known as the Nossob. The lower part of the Nossob, as well as the Olifants and Auob Rivers are thought to date to the end of the last ice age (Schneider, 2004).

The lithology of the study area is summarised in Figure 3.23 and Table 3.3

Table 3.3: Lithology (Geological Survey of Namibia, 2008)

CODE	ROCK TYPES
Cd	Tillite, boulder shale, shale, sandstone, limestone
Egdb	Granite
Eu	Serpentinite, chlorite schist, talc schist
Mbi	Quartzite, schist, conglomerate, quartz porphyry
Md	Quartzite, conglomerate, shale, basalt, rhyolite, ignimbrite
Mgg	Granite
Mho	Para-/orthogneiss, metasedimentary rocks, granite, metabasite dykes
Mm	Quartzite, phyllite, rhyolite, basalt, conglomerate, intrusive metabasite dykes
Mnu	Rhyolite, ignimbrite, conglomerate, quartzite, shale, basalt
Nau	Marble, schist, ortho-amphibolite, quartzite
Nb	Mixtite
Nc	Mixtite, minor schist, shale, quartzite, iron-formation, ortho-amphibolite, graphitic schist
Nd	Schist, marble, quartzite, conglomerate, graphitic schist
Ndu	Quartzite, conglomerate, schist, marble
Ngl	Syntectonic gneissic leucogranite
Nk	Mica schist, minor quartzite, graphitic schist, marble
Nka	Quartzite, conglomerate, schist, marble
Nka_uc	Quartzite, conglomerate, schist, marble
Nks	Sandstone, black limestone, conglomerate, shale
Nks_uc	Sandstone, black limestone, conglomerate, shale
Nku	Marble, schist, quartzite, graphitic schist
Nml	Ortho-amphibolite
Nsc	Marble, schist, quartzite, calc-silicate, graphitic schist
Pp	Shale, mudstone
Pp_uc	Shale, mudstone
Q	Alluvium, sand, gravel, calcrete
Tr	Trachyte, phonolite

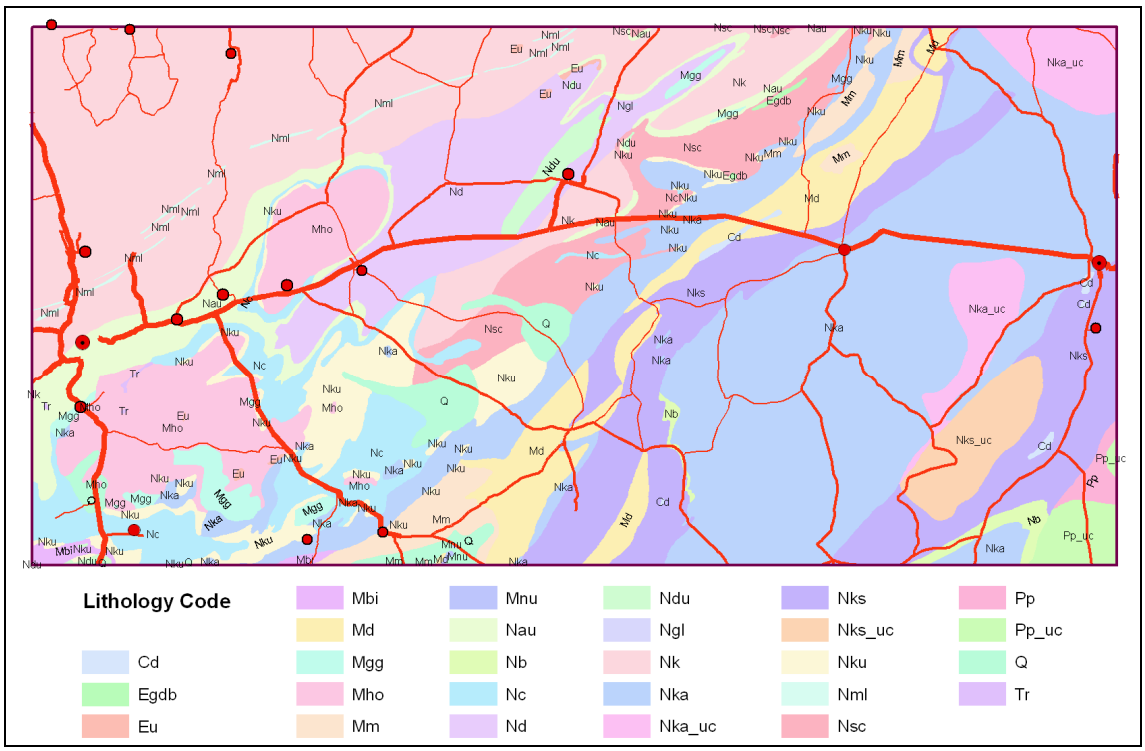

Figure 3.23. Lithology map (Geological Survey of Namibia, 2008). See Table 3.3 for full legend.

3.10 SOILS OF THE STUDY AREA – EXTANT INFORMATION

Scholz (1968a) described some soil types of the southern Khomas Hochland and a small plot further to the east (Scholz 1968b). He noted (1973) that the soils are generally rich in materials derived from physical weathering. Organic matter content is very low (OC < 1 %) as a result of low litter supply and rapid mineralization, with low water-holding capacity. Ganssen (1960, 1963) and Ganssen and Moll (1961) recorded that the soils are shallow and also often skeletic, especially on slopes, where they can turn into blockfields and bare bedrock. Blümel (1991) mentioned that pedogenic duricrusts like calcrete, silcrete and ferricrete are common compounds in the soils, usually genetically unrelated to the host sediment.

Soils evolved from Kalahari sand are weakly developed. Profile development is almost absent and the soils are characterized by low levels of nutrients and organic matter (Thomas and Shaw, 1991). In the linear dunefields, nutrient content and sand grain size vary along catenas across the dune ridges, with the highest nutrient concentrations and the finest grain sizes being found in the inter-dune areas (Lancaster 1986; Thomas and Shaw, 1991). Kalahari sands have a high hydraulic conductivity, which allows for potential recharge but poor storage. Most of the soils formed from Kalahari sands are classified as Arenosols (FAO-UNESCO, 1974, 1977; FAO 1998a) or quartzipsamments in the USDA nomenclature (Soil Survey Staff, 1975, 1998).

The FAO-UNESCO Soil map of the World (FAO-UNESCO, 1974, 1977) contains information on Namibian soils supplied by Scholz (1963c). The study area is mainly divided between two broad soil regions. The Kalahari Desert towards the east is generally occupied by luvic and cambic Arenosols, with intensely leached sand found in depressions, and some albic Arenosols with deep-lying duripans in some cases. Calcic Xerosols, Vertisols and Solonchaks are found in less sandy areas, which are often of alluvial origin. The

western part is mainly covered by stony calcic Xerosols (typical soils of an aridic moisture regime, having weak ochric A horizons and calcium carbonate enrichment within 125 cm of the surface), with Lithosols (soils limited in depth by continuous hard rock within 10 cm of the surface and develop mainly in mountainous areas) and rock outcrops. The cambic Arenosols are described as generally poor in organic carbon, nitrogen, exchangeable bases and phosphorus, with slightly acidic pH at the surface, but they become less acidic with depth. According to this source, Xerosols contain high concentrations of cationic nutrients, but high levels of soluble salts may be present, while trace element deficiencies, especially zinc and iron, are common. These soils may suffer from imperfect drainage due to the presence of petrocalcic or argillic B horizons. Lithosols are found in areas of dissected topography with steep slopes. They are shallow and very stony, thereby limiting their use mostly to extensive livestock production (FAO-UNESCO, 1974, 1977).

Loxton, Venn and Associates (1971) mapped the soils and irrigation potential of northern and central Namibia at small scale, using the South African classification system that would later be published as the Binomial System (McVicar, *et al.*, 1977). Figures 3.24 – 3.27 depict their maps of the topography, soil depth, soil potential for irrigation and dominant soils of the present study area.

Bertram and Broman (1999) and Bertram and Kempf (2002) carried out studies on seven farms, viz. Neudamm, Bergvlug, Bellerode, Sonnleiten, Hoffnung, Höhewarte and Ondekaremba, concentrating on the first two in the Neudamm Highlands east of Windhoek. Bertram and Kempf (2002) found that classification of the soils of the Khomas Hochland according to the FAO Revised Legend (FAO-UNESCO-ISRIC, 1988) or World Reference Base (FAO, 1998a) only key out as Regosols and Leptosols. They argued that this is not meaningful, as these Reference Groups, strictly speaking, only differ in solum depth. They suggested the creation of a new Reference Soil Group in the World Reference Base, namely Colluvisols, for finely textured soils developed in young colluvium, to emphasise the importance of landscape evolution for pedogenesis. They also suggested that a new soil qualifier should be adopted for weakly developed skeletic soils on saprolite, namely saprolitic Leptosols.

According to Bertram and Kempf (2002), typical catenas showed saprolitic Leptosols on top, through lithic Leptosols and cambic Leptosols on slopes, to Colluvisols on valley floors. Fluvisols were found on terraces. Kempf (1994, 1999a, 1999b, 1999c), in his wider analysis of the central Namibian geomorphology, described recent Cambisols and Arenosols, denudated Leptosols, young Fluvisols, Vertisols and Regosols as the most common soil types.

Bertram and Broman (1999) mentioned remnants of older Ferralsols and Acrisols in pockets on the pediment furthest from drainage lines on the farms Neudamm, Höhewarte, Sonnleien and Ondekaremba. These are usually preserved by colluvial cover of similar material, derived from sites further upslope. The type specimen is on farm Höhewarte, where the colluvium contains Mid-Paleolithic artefacts on top of a fossil surface containing Acheulian tools *in situ* (Kempf 1999a; 1999c). This may indicate a middle Pleistocene colluvial phase during which much of the original ferralic substrates were eroded from local watersheds. Kempf (1994, 1999a, 1999b) also found old Ferralsols, derived mainly from deeply weathered saprolitic country rock, with occasional ferricrete remnants. He noted that postgenetic aeolian and fluvial activity changed many of the ferralitic or fersialitic substrates, presumably during the Quaternary.

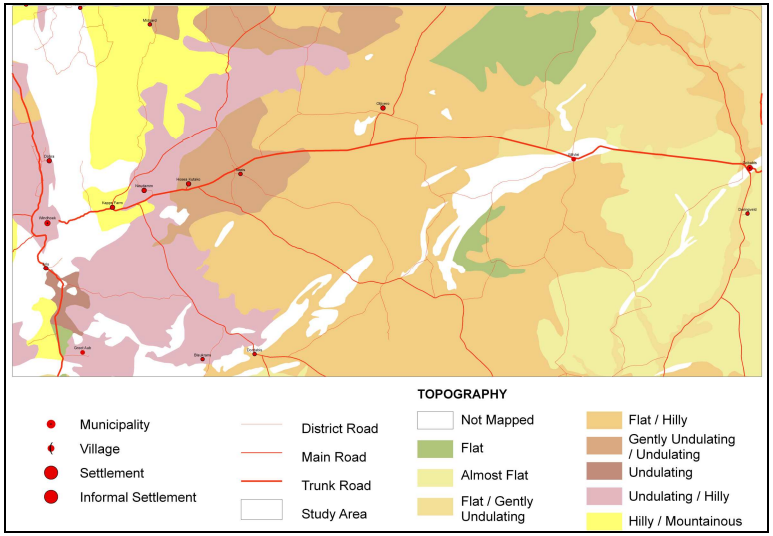

Figure 3.24. Topography (MAWF, 2005, based on Loxton *et al.*, 1971)

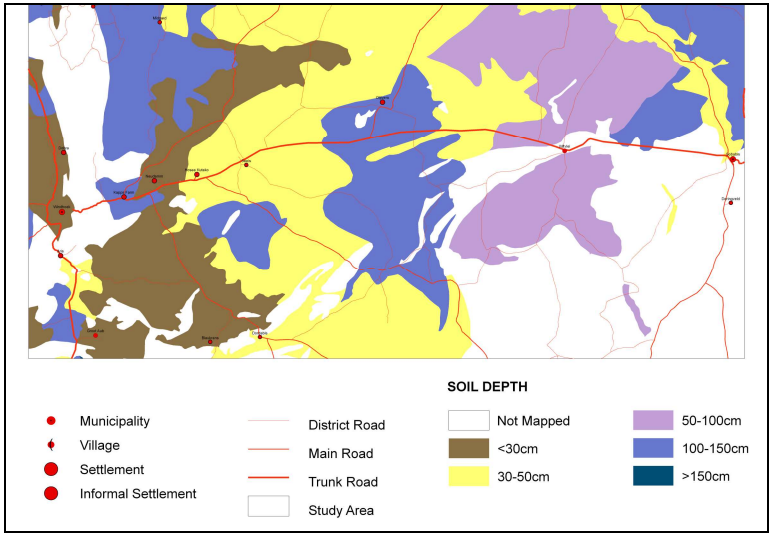

Figure 3.25. Soil depth (MAWF, 2005, based on Loxton *et al.*, 1971)

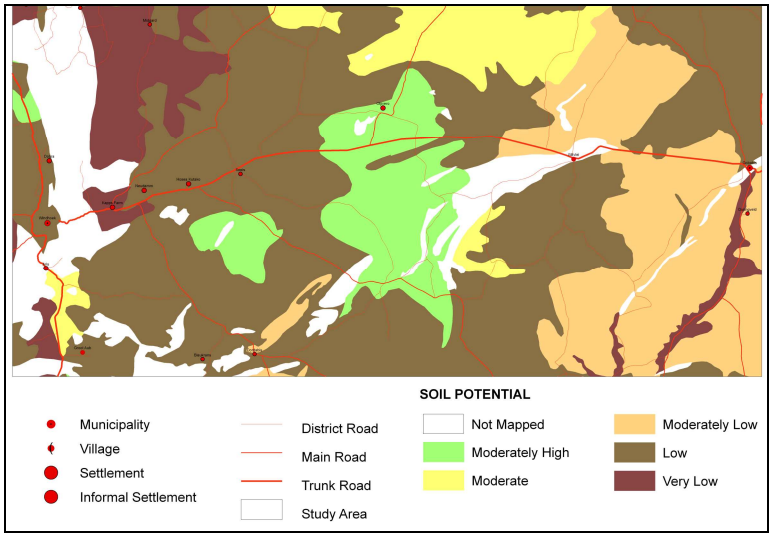

Figure 3.26. Soil potential for irrigation (MAWF, 2005, based on Loxton *et al.*, 1971)

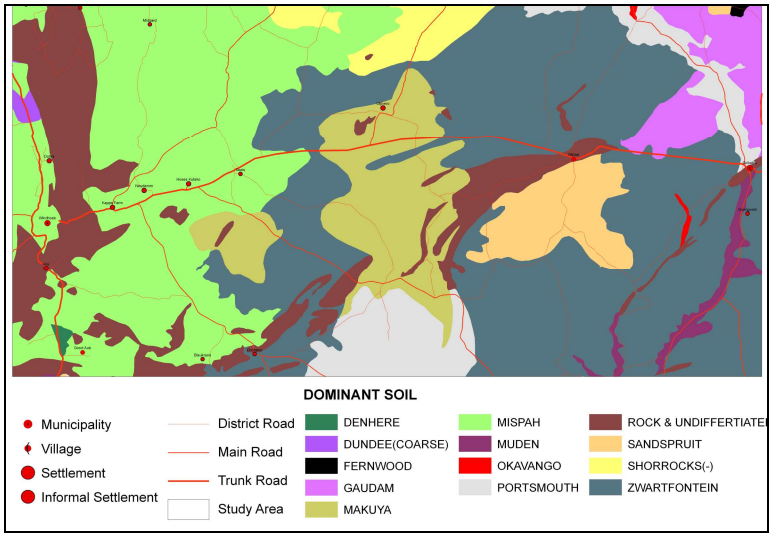

Figure 3.27 Dominant soil (MAWF, 2005, based on Loxton *et al.*, 1971)

Saprolite, deeply chemically weathered bedrock, is a very characteristic component of the central highlands of Namibia. Kempf (2000) mentioned signs of saprolitisation down to a depth of 60 – 80 m in the Khomas niveau. Kempf considered saprolitisation as an important factor in any recent and ongoing soil formation, and as compelling evidence for the occurrence of etchplanation. He proposed (Kempf, 2008) that the most recent phase of environmental conditions allowing deep chemical weathering occurred during the mid-Pliocene. He suggested that an earlier, more physical weathering phase during the Late Miocene / Early Pliocene caused the deep dissection of the greater (western) part of the Khomas planation level, as a result of the steep gradient towards its base level, the Atlantic Ocean. The eastern part of the highlands with its lower absolute height above its base level – the Kalahari endorheic system – consequently had lower drainage line gradients and was less affected by linear erosion processes. This eastern part of the previous Khomas niveau thus underwent gradual planation rather than deep vertical incision to form the present Seeis niveau. Exposed outcrops of the deeply weathered bedrock are prone to erosion and bedrock-cut gullies are common. The saprolite and overlying weathering substrates show alteration by subsequent physical weathering during the End-Pliocene to Quaternary (Bertram and Kempf, 2002).

Kempf (1999) observed strong relationships between soil types, weathering status, pedochemistry and morpho-position of the soil profile. He concluded that the morpho-position is the most important factor for pedogenesis and soil dynamics in this semi-arid climate, with little soil formation today. He postulated that Quaternary pedogenesis and soil dynamics as well as morphological development of central Namibia are characterised by:

- Deeply weathered peneplanation relief, probably until the Miocene
- Existence of fossil ferralitic and fersialitic paleosoils
- Discrete erosive, periods with temporary re-deposition
- Quaternary imprint due to intensified physical weathering and more pronounced topography.

Bertram and Broman (1999) and Bertram and Kempf (2002) concluded that slope profiles are mainly convex on the crest, sometimes straight in the mid-slopes, with concave footslopes in the eastern Khomas Hochland. They found a slight tendency for lithic and skeletic phases to be more frequent on convex slopes. Bertram and Broman (1999) found some clay enrichment on convex slopes. They did not find a significant correlation between slope angle and soil characteristics. Colluvial soils were not found on slopes above 11^{o}; all of those (up to 36^{o}) were Leptosols. However, they did find some Leptosols on valley floors and on slopes of only 1^{o}. They mentioned that soil profiles on watersheds show truncation, being eroded down to a thin saprolitic layer. Soils were weakly developed and particularly shallow on slopes. Abundance of rock fragments varied from 0 to 91 %. Weathering substrates were highly skeletic, especially on scree cones of main scarps, in valleys and on steep upper slope positions. The dominant textural class was sandy loam, followed by loam and silt loam. Clay content was lower than 5 % and organic matter content was negligible. Soil colours were brownish (yellowish brown, bright brown, dull yellowish brown) and greyish and the colluvia had lower chromas than the weathering substrate. Surface pavements were common, especially on slopes and high planation remnants. Those were composed of strongly weathered schistoid bedrock debris and weathering-resistant vein quartz.

Bertram and Broman (1999) described catenary relationships derived from 89 samples from 56 profiles,

arranged according to position (upper slope, middle slope, lower slope and valley floor) from 15 slope transects. They found that the absolute content of skeletal material (Ø > 2 mm) markedly increased upslope. They noticed a tendency for the majority of upper slopes and about two thirds of middle slopes to key out as Leptosols. Soils not fully satisfying all criteria for classification as Leptosols, still had leptic and or skeletic phases. Lower slopes and valley floors contained weakly developed fine grained brownish grey soil on colluvial sediments, classified as Regosols (or Colluvisols, if one follows the suggestion of Bertram and Kempf, 2002). They mentioned that coarse material is often found arranged in stonelines, representing previous erosion surfaces.

Bertram and Broman (1999) observed that the absolute clay percentage was equally high on lower slopes and valley floors, but relative clay content (% of fine earth fraction) was higher on lower slopes than valley floors. The absolute sand content decreased rapidly upslope, though the relative sand content was similar in all positions. The absolute silt content also decreased upslope, with the relative silt content being lowest on lower slopes. In general, sandy loam was the predominant textural class on all slope positions, with especially medium sand content being constant throughout most catenas. Sodic properties were mainly found in valley floor substrates, which proved to be very susceptible to gully erosion due to rapid colloid dispersion on wetting, especially after loosening of topsoil by overgrazing and trampling. Luvic properties – clay enrichment in the subsoil – were not restricted to particular slope positions, though it was somewhat higher in valley floors (Kempf 1993, 1994). In general, base saturation and pH were found to be higher on valley floors and lower slopes. Base saturation, Mg and K peaked in lower slopes positions. However, Bertram and Broman could not establish an unambiguous pattern of base saturation (and thus eutric or dystric status) with regard to slope position. They found that the variation in chemical characteristics within slope classes was larger than between classes. None of the chemical parameters showed continuous increase or decrease from the upper slope to the valley floor. Lower slopes seemed to be anomalous in many respects (higher or lower than middle slope and valley floors). Most pronounced differences were observed between middle slope and lower slopes. They concluded, in contrast to Kempf (1999), that there was no good correlation between slope position and soil characteristics.

ꕥ ꕥ ꕥ ꕥ

CHAPTER FOUR

METHODOLOGY

4.1 INTRODUCTION

Digital elevation data and satellite imagery were used to delineate terrain units, based on the FAO/SOTER methodology (FAO, 1977, 1989, 1990, 1995, 2003; ISRIC, 1991). Analytical data from soil samples collected from 392 soil profiles in the study area, were extrapolated to these terrain units.

4.2 DATA SOURCES

4.2.1 TOPOGRAPHICAL MAPS

The study area is covered by 32 topographical maps at 1:50 000 scale (Surveyor General, 1972 – 1976) (Figure 4.1) and two maps (2216 Windhoek and 2218 Gobabis) at 1:250 000 scale (Surveyor General, 1983 – 1984). These were digitally scanned and used as background layers in the GIS to visually delineate terrain types, which were subsequently digitized on-screen (Kutuahupira and Mouton, 2006).

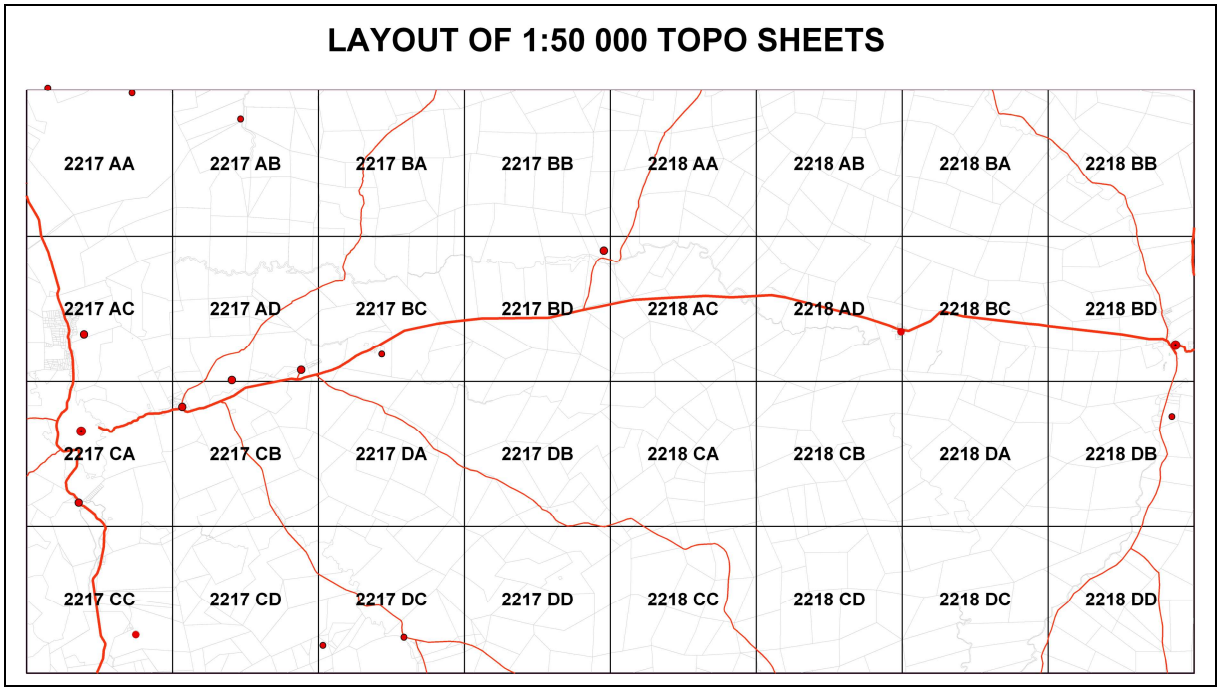

Figure 4.1. Layout of 1:50 000 topo sheets

4.2.2 SATELLITE IMAGES

Landsat 5 TM and *Landsat 7 ETM+* images of 1998 - 2000, geo-referenced, radiometrically corrected,

mosaiced and cut on the 1:250 000 topographical sheet templates (ICC, MAWRD and AECI, 2000), were used to visually interpret and delineate homogeneous terrain and soil units at a scale of 1:50 000 (Kutuahupira and Mouton, 2006). On-screen digitising was carried out using *ArcView™ 3.2* GIS software (ESRI, 1999).

Landsat 7 ETM+ images (P177/R075 2002-08-20; P177/R076 2002-08-20; P178/R075 2001-05-04; P178/R076 2001-05-04), with 28.5 m resolution, were used to carry out supervised classification of soil colour and oxides, employing *ERDAS Imagine™ 9.1 Professional* image processing software (Leica, 2006). For that purpose, 217 field observations were used as training pixels. In addition, *Definiens Professional™ 5* image processing software (Definiens Software, 2006) was used for segmentation of the study area into homogeneous units.

4.2.3 DIGITAL ELEVATION DATA

The methodology employed by the author to delineate Terrain Units, was loosely based on that of Dobos, Daroussin and Montanarelle (2005). Shuttle Radar Topography Mission (SRTM) digital elevation data, dated 2004, with 1 arc-second (approximately 30 m) resolution and in WGS84 geographical latitude / longitude coordinates, were used in a digital elevation model. Tiles S22E16, S22E17, S22E18, S22E19, S23E16, S23E17, S23E18, S23E19, S24E16, S24E17, S24E18 and S24E19 covered the study area, as well as one degree extra on each side.

4.3 FIELD OBSERVATIONS

Soil profile descriptions, collection of soil samples, preliminary classification of the soils, delineation of terrain and soil units, mapping of these units on topographic sheets, and transfer of the data into digital format were done by Kutuahupira and Mouton, agricultural research technicians of the AEZ Programme, during 2004 and 2005 (Kutuahupira and Mouton, 2006). Field and analytical data were also obtained from J. Kempf, a lecturer from the University of Würzburg, Germany, and long-time collaborator of the AEZ Programme (Kempf, 1999c, 2008). The author found it difficult to interpret and apply the terrain and soil units of Kutuahupira and Mouton. The author decided to re-map the area in terms of terrain units, in terms of SOTER classes, by employing digital elevation data and satellite imagery. Additional fieldwork was undertaken during 2008, to verify computer-generated maps and to obtain data for supervised classification of satellite images.

Kutuahupira and Mouton (2006) described their mapping methodology in detail, so only a summary is given here. A subjective sampling strategy was followed: observations were made at sites which were considered to be representative of distinct terrain units, identified on the maps prepared in the office and by the investigators in the field. A catenary transect approach was used to gain insight into the relationship between soils and terrain features, by driving and walking through the identified units. Roadcuts, augurings and minipits were employed to test the homogeneity of a unit, where after a full site and profile description was made at a representative site. A total of 344 profile descriptions, comprising 1013 horizons, were completed. An additional 48 profile descriptions, with analytical data, were obtained from Kempf (1999c, 2008).

Field observations and profile descriptions were carried out according to the FAO Guidelines for Soil Description (FAO, 1990). The following parameters were recorded on field forms:

- **Location:** Profile number; latitude; longitude; elevation; year of profile description; month of profile description; location (farm name or relevant description); farm identification (title deed number); topographical sheet; land use; vegetation
- **Terrain:** slope; landform; land element; position in landscape
- **Lithology:** origin of parent material; lithology[1]; abundance and type of rock outcrops; abundance and type of surface fragments; underlying rock.
- **Erosion:** surface sealing thickness and hardness; width and abundance of surface cracks; erosion type, degree and area affected
- **Profile**: effective depth; horizon number; horizon designation; horizon depth; distinctness of horizon transition; diagnostic horizon; abundance, type and size of rock fragments; moist matrix colour (some descriptions of dry matrix colour); type, grade and size of structure; dry consistence (very few descriptions of moist consistence); estimation of clay content, sand grade and textural class; estimation of drainage category; mottles; nodules; cutans; cementation; presence of roots; presence of carbonates (reaction with 10 % hydrochloric acid); any additional profile information
- **Classification**: provisional classification - WRB (FAO, 1998a)

Soil colour was determined using standard soil colour charts (Eijkelkamp, 1998) based on the original Munsell charts. The World Reference Base was used for classification of the soils (FAO, 1998a), with further reference to FAO (2001) and the ISSS Working Group RB (1998).

Digital photos were taken of profiles and the surrounding landscape. Representative soil samples were collected from the respective horizons for analysis. Not all profiles were sampled, and not all samples analysed for all chemical and physical properties, due to time and financial constraints.

4.4 LABORATORY METHODS

Analyses were carried out to measure the following: pH in a 2:5 soil:water suspension; electrical conductivity in a 2:5 soil:water suspension; electrical conductivity in the saturated paste extract; organic carbon; extractable calcium, magnesium, potassium and sodium; exchangeable calcium, magnesium, potassium and sodium; cation exchange capacity; plant-available phosphorus; extractable iron, manganese, zinc and copper; nitrate, nitrite and sulfate of the saturated paste extract; sand, silt and clay; coarse-, medium-, fine- and very fine sand fractions.

The bulk of the chemical and physical analyses were carried out by Ms A. Dausas, Mr T Kachote, Ms N. Sheya and Ms E. Stanley, agricultural research technician and technical assistants from the Agricultural

[1] In the respective analyses (Chapters 6 – 10), only three lithological units were considered, namely schist, quartzite and Kalahari sand. These were the only units recorded in sufficient numbers and with complete confidence by the technicians carrying out the profile descriptions.

Laboratory of the Namibian Ministry of Agriculture, Water and Forestry in Windhoek. The laboratory is a member of the Agricultural Laboratory Association of Southern Africa, and participates in their inter-laboratory quality control scheme. Standard Operating Procedures, compiled into a Quality Manual (MAWRD, 2000), were followed for all analyses. Nitrate, nitrite and sulfate were measured by Mr M. Gordon from the laboratory of the Department Soil Science, University of Stellenbosch.

Organic matter content, sum of extractable bases (Ca, Mg, K, Na), sum of exchangeable bases and base saturation were calculated, while textural classes and sand classes were determined from texture triangles. Soil hydraulic properties were calculated from particle size data.

4.4.1 SAMPLE PREPARATION

Samples were dried at room temperature or using mild heat (< 30 ^{o}C). Clods were lightly crushed by hand with a mortar and pestle, whenever necessary. Samples were sieved to 2 mm (the fine earth fraction) and stored in inert plastic jars with screw caps. Stones and gravel were removed by sieving and weighed separately where they constituted a significant proportion of the sample.

4.4.2 PH (H_2O)

The pH of the soil was potentiometrically measured in the supernatant of a 2:5 (= 1:2.5) soil:deionised water suspension, on a mass to volume basis. This Standard Operating Procedure Soil-109 (MAWRD, 2000) had been adapted from the methods of the Non-Affiliated Soil Analysis Work Committee (1990) and Hendershot, Lalande and Duquette (1993). A Mettler Toledo MA 235 pH / ion Analyzer was used.

4.4.3 ELECTRICAL CONDUCTIVITY

Electrical conductivity was measurement in the supernatant of a 2:5 (=1:2.5) soil:deionised water suspension, using an Eijkelkamp EC 18.33 meter. It was also measured in the saturated paste extract. To prepare a saturated paste extract, water was added to a soil sample until a given mechanical property of the soil was attained, equivalent to the liquid limit. Unit of measurement: µS/cm. This Standard Operating Procedure Soil-112 (MAWRD, 2000) is based on the work of the Non-Affiliated Soil Analysis Work Committee (1990), Bower and Wilcox (1965), Van Reeuwijk (1992) and Richards (1954).

4.4.4 PLANT-AVAILABLE PHOSPHORUS

The Olsen method of extraction was used, namely a 0.5 M sodium bicarbonate solution at pH 8.5. This method is suitable for alkaline to neutral soils. Phosphate in the extract was measured colourimetrically at 882 nm, using the blue ammonium molybdate method of Murphy and Riley (1962), with ascorbic acid as reducing agent. A GBC UV / VIS 916 spectrophotometer was used. Unit of measurement: mg kg^{-1} P. This Standard Operating Procedure Soil-104 (MAWRD, 2000) is based on the work of the Non-Affiliated Soil

Analysis Work Committee (1990), Olsen and Dean (1965), Shoenau and Karamanos (1993) and Murphy and Riley (1962).

4.4.5 EXTRACTABLE BASES (CA, MG, K, NA)

Extraction was carried out with 1M ammonium acetate at pH 7. Lanthanum chloride was added as a suppressant. Measurement was done with a GBC Avanta atomic absorption spectrometer. Calcium was aspirated in a nitrous oxide-acetylene flame, while magnesium, potassium and sodium were aspirated in an air-acetylene flame. The respective wavelengths at which adsorption was recorded, were 422.7 nm for calcium, 285.2 nm for magnesium, 589.0 for sodium and 766.5 nm for potassium. Unit of measurement: mg kg^{-1} Ca, Mg, Na and K respectively. This Standard Operating Procedure Soil-124 (MAWRD, 2000) was developed by Rowell, based on the methods of the Non-Affiliated Soil Analysis Work Committee (1990), USDA-SCS Staff (1972) and Van Reeuwiljk (1992).

4.4.6 EXCHANGEABLE BASES (CA, MG, K, NA) AND CATION EXCHANGE CAPACITY

Soil samples were pre-washed with deionised water to remove soluble salts. Thereafter they were leached with ammonium acetate to replace exchangeable bases with ammonium ions. Exchangeable calcium, magnesium, sodium and potassium were measured in this effluent by atomic absorption spectroscopy, according to Standard Operating Procedure Soil-124. Samples were then leached with sodium acetate to saturate the cation exchange complex with sodium ions. The excess sodium was removed by leaching with ethanol and the cation exchange capacity determined by measuring the sodium subsequently de-sorbed by a further leaching with ammonium acetate. The method used an automatic extractor (SampleTex 24VE programmable vacuum extractor) where the soils were mounted in plastic syringes for the leaching operations. The method allows some modification for soils containing carbonates and being either saline or non-saline.

Carbonate / non-saline soils: If the pH of the 2:5 soil:water extract is higher than 7, with carbonates present, and EC (2:5) is lower than 0.4 mS cm^{-1}, no pre-washing is needed. A 50:50 mixture of ammonium acetate at pH 7 and ethanol is used to displace the bases. This prevents carbonate dissolution.
Carbonate / saline soils: If the pH of the 2:5 soil:water extract is higher than 7, with carbonates present, but EC (2:5) is higher than 0.4 mS cm^{-1}, then a pre-washing must be done, followed by application of a 50:50 mixture of ammonium acetate at pH 7 and ethanol to displace the bases. Unit of measurement: $cmol_c$ kg^{-1}. This Standard Operating Procedure Soil-116 (MAWRD, 2000) was adapted by Rowell, based on the methods of the Non-Affiliated Soil Analysis Work Committee (1990), Van Reeuwiljk (1992), Rhoades (1982) and Thomas (1982).

4.4.7 PARTICLE SIZE ANALYSIS

Particle size analysis was carried out by the Rowell (2000a) autopipette method. Samples were pre-treated

when necessary and dispersed by shaking with a sodium carbonate and sodium hexametaphosphate solution. Silt and clay sized particles were separated by sampling with an autopipette at a depth of 6 cm after specific time intervals (related to ambient temperature) determined using Stoke's Law of Sedimentation. These were dried and weighed. Sand was separated by wet sieving through a 53 µm sieve. The sand was further separated into very fine, fine, medium and coarse fractions by dry sieving. All particle size fractions were expressed as percentage of the fine earth fraction (Ø < 2 mm) (Table 10.12). The textural class was determined from the USDA Soil Textural Classes Triangle and Sand Classes Triangle (Non-Affiliated Soil Analysis Work Committee, 1990; Van der Watt and Van Rooyen, 1995) (Figure 10.36). The method is suitable to determine the proportion of sand, silt and clay in most mineral soils but treatments are needed for soils with organic carbon contents of more than 2 % and soils containing high concentrations of soluble salts and cementing agents such as calcium carbonate and gypsum. This Standard Operating Procedure Soil-120 (MAWRD, 2000) was developed by Rowell (2000a), based on the method of Miller and Miller (1987).

4.4.8 ORGANIC CARBON AND ORGANIC MATTER

An adaptation of the Walkley-Black method was used. Organic matter was oxidised with an excess of a concentrated oxidising mixture, containing sulfuric acid and potassium dichromate. The amount of unused potassium dichromate was determined colourimetrically at 600 nm with a GBC UV / VIS 915 spectrophotometer. Results were calibrated against glucose. Unit of measurement: g kg^{-1} C, which was converted to percentage. A factor was used in calculations to take account of incomplete oxidation: organic matter (in %) content was calculated as organic-C (in %) x 1.74. The method is suitable for soils low in organic matter content. This Standard Operating Procedure Soil-125 (MAWRD, 2000) is based on the work of the Non-Affiliated Soil Analysis Work Committee (1990), Sims and Haby (1971), Nelson and Sommers (1982), Walkley and Black (1934), DeBolt (1974), as adapted by Rowell (2000b).

4.4.9 AVAILABLE MICRONUTRIENTS (FE, MN, ZN, CU)

The micronutrients were extracted with a reagent consisting of 0.5M ammonium acetate : 0.5M acetic acid : 0.02M EDTA, at pH 4.65, using an extraction ratio of 1:5 (soil mass:extractant volume). Fe, Mn, Cu and Zn were measured on a GBC Avanta atomic absorption spectrometer. Unit of measurement: mg kg^{-1}.

4.4.10 NITRATE, NITRITE, SULFATE

Saturated paste extracts were prepared, and the anions measured on a Dionix DX 120 Ion Chromatograph. Unit of measurement: mg l^{-1}.

4.4.11 CARBONATE (ESTIMATION)

Air-dried soil was treated with 10 % hydrochloric acid and effervescence was noted on a scale from 1 (none) to 5 (very strong), following the method of Allison and Moodie (1965).

4.4.12 SOIL HYDRAULIC PROPERTIES

Bulk density (g cm^{-3}), saturation (cm^3 water cm^{-3} soil), field capacity (cm^3 water cm^{-3} soil), wilting point (cm^3 water cm^{-3} soil), available water (cm^3 water cm^{-3} soil) and saturated hydraulic conductivity (cm h^{-1}) were calculated (Hydraulic Properties Calculator website), based on the equations of Saxton, Rawls, Romberger and Papendick (1986).

4.5 DATABASING AND DATA PROCESSING

Field observations and profile descriptions were captured on field forms, while analytical data were entered into laboratory forms. These data were subsequently transferred into digital format. Databases were structured according to the FAO SOTER methodology (FAO, 1989, 1991, 1995, 1996, 2003; ISRIC, 1991, 1993; Van Engelen and Wen, 1995; Coetzee, 2001a, 2001b), making use of *Microsoft® Office Access 2003* and *Microsoft® Office Excel 2003* (Microsoft Corporation, 2003) software. Data were cleaned, edited and validated.

Analytical data were not available for all profiles. The final analytical dataset, used for descriptive statistics, consisted of 702 records. The geospatial dataset consisted of 655 records.

4.6 STATISTICAL ANALYSIS

Statistical analysis was carried out with *Statistica version 7* (StatSoft, Inc., 2004) and *StatFi 2007 Professional Build 4.8.6.0 for Excel* software (AnalystSoft, 2007).

Descriptive statistics, consisting of the number of valid observations, arithmetic mean, median, standard deviation, coefficient of variance, minimum, maximum, range, top and bottom quartiles, inter-quartile range; top and bottom deciles, kurtosis and skewness, were compiled for the respective soil characteristics. Distribution patterns were made visible through the use of scatter diagrams, decile distribution graphs and histograms. Box-and-whisker plots were drawn for all characteristics, but not included in this document. As the mean is sensitive to extreme values, the median is considered to be a better measure of central location (Keller and Warrack, 1997). Most variables were not normally distributed; therefore, non-parametric statistical methods had to be used.

As measure of association between the various chemical and physical characteristics, correlations were tested with the Kendall-Tau, Gamma and Spearman methods. As the degree of correlation increases in this order (between the three methods), it was decided to use the most conservative one, namely Kendall-Tau. Scatterplots were included in the thesis whenever the r^2 exceeded 0.30.

The relationships between the chemical and physical characteristics of the soils, and the position in the profile (topsoil / subsoil), position in the landscape, slope, land element, topographic class, degree of dissection of the landscape, origin and type of parent material and WRB reference soil group, were investigated. Means-and-error plots were used to visualise these relationships.

4.7 GEOSPATIAL ANALYSIS

ArcGIS™ 9.2 (ESRI, Inc., 2006) geographical information system (GIS) software, including the modules *ArcMap™ 9.2*, *ArcCatalogue™ 9.2*, *Spatial Analyst™ 9.2*, *3D Analyst™ 9.2* and *GeoStatistical Analyst™ 9.2*, as well as *ArcView™ 3.2* (ESRI, Inc., 2006) GIS software, including the extensions *ArcView Image Analyst™*, *ArcView Spatial Analyst™* and *ArcView 3D Analyst™*, were used to carry out geospatial analysis. In addition, several extensions and scripts written for ArcView and available on the Internet were employed: *Texture Analysis and Neighbourhood Statistics for Grids* (Behrens, 2005), *DEMAT - DEM Analysis Tool*. (Behrens, 2005), *Xtools* (DeLaune, 2003), *Grid Pig* (Hare, 2007), *Surface Areas and Ratios from Elevation Grid* (Jenness, 2002), *Surface Tools* (Jenness, 2004), *Grid Tools version 1.7* (Jenness, 2006), *Topographic Position Index TPI version 1.3a* (Jenness, 2006), *Batch Grid Toolbox* (Magadzire, 20006), *Grid Projector* (McVay, 1999), *Image-Tools version 2.6* (Patterson, 2004), *Basin1* (Petras, 2003), *Image Georeferencing Tools* (Raber, 1999), *Grid Analyst Extension version 1.1* (Saraf, 2002), *FeatureDensity* (Schaub, 2004), *Terrain Analysis* (Schmidt, 2002), *Grid Converter version 2.2.* (Weigel, 2002) and *Gridmachine version 6.77* (Weigel, 2005). *Global Mapper™* software (Global Mapper Software, LCC.,2005) was used to convert the SRTM elevation data into a format accepted by ArcView and ArcGIS.

A digital terrain model was created in ArcView. From that a slope map was created. This formed the basis for further analysis. The continuous slope data were reclassified into slope classes, according to the FAO/SOTER methodology (FAO, 1977, 1989, 1990, 1995, 2003; ISRIC, 1991). These were, in turn, reclassified into two slope classes, with 8 % slope as the division point. Slopes of less than 8 % are generally considered to be 'level land' and suitable for mechanised agriculture. Height differences within the cells of a 33-second grid were calculated, to obtain a map of local relief, making use of majority filters to weed out extremes. The 1 750 m contour was used to differentiate between highlands (plateaux) and lowlands (plains). This contour was selected by visual observation in the field, and studying the change in contour density over distance.

Topographic position index (TPI) was calculated according to the methodology of Jenness (2006b), which was based on work by Guisan *et al.* (1999), Jones *et al.* (2000), Weiss (2001), and Dickson and Beier (2006). From the TPI, both position in the landscape (e.g. ridge crest, valley bottom, mid-slope, etc.) and landform category (i.e. steep narrow canyons, gentle valleys, plains, open slopes, mesas, etc.) could be classified.

Topographic roughness and convolutedness can be estimated from the ratio of the surface area, as calculated in three dimensions, and the planimetric area (as if the land is completely flat). The methodology of Jenness (2002, 2004a) was employed. His method was based on earlier work by Hobson (1972), Beasom (1983), Mandelbrot (1983), Polidori *et al.* (1991), Lam and De Cola (1993), Lorimer *et al.* (1994), Berry (2000), Hodgson (1995) and Jenness (2000). A surface roughness index (SRI), derived from the surface ratios and reclassified in terms of quintile classes, together with feature density analyses of contours and the drainage network, were used to delineate areas of high, moderate and low degree of dissection of the landscape.

Stream flow, flow accumulation and stream order functions were used to derive a drainage network map for

the study area. It was compared with existing digital data (MAWF, 2005) and topographic maps (Surveyor General, 1972 – 1976) and proved to be more accurate than those sources. Topographical Wetness Index (TWI) was calculated. Topographic classes were calculated from the SRI, TWI and TPI.

The segmentation of the study area, using *Definiens Professional 5* image software (Definiens Software, 2006), culminated in 2249 homogeneous units. For each of these, the FAO slope, topography, local relief, degree of dissection, level land and highland / lowland classes were calculated, the respective codes assigned (Tables 5.1 – 5.6) and a concatenated terrain code compiled. For example, terrain code 112111 means FAO slope class 1 (< 0.5 %), topography class 1 (flat), local relief class 2 (5 – 10 m), degree of dissection class 1 (low), level land class 1 (< 8 % slope) and highland / lowland class 1 (elevation < 1750 m, lowland). Adjacent homogenous units with the same terrain code were merged, to finally form a total of 107 distinct terrain units (Chapter 5).

Table 4.1: Classes and codes within terrain units.

FAO slope class	Code
Slope < 0.5 %	1
Slope 0.5 – 2 %	2
Slope 2 – 5 %	3
Slope 5 – 8 %	4
Slope 8 – 15 %	5
Slope > 15	6
Topography	Code
Flat	1
Almost flat	2
Undulating	3
Rolling	4
Hilly	5
Mountainous	6
Local Relief	Code
< 5 m	1
5 – 10 m	2
10 – 30 m	3
30 – 60 m	4
60 – 100 m	5
100 – 300 m	6
> 300 m	7
Degree of dissection	Code
Low	1
Medium	2
High	3

Level land	Code
Slope > 8 %	0
Slope < 8 %	1
Highland / lowland	Code
Elevation < 1750 m	1
Elevation > 1750 m	2

The 655 geo-referenced analytical records were imported into the GIS software and spatially joined with the terrain units. Maps of the various chemical and physical characteristics were drawn in the format of point data (Chapters 6 – 10).

CHAPTER FIVE

SPATIAL CHARACTERISATION

5.1 TERRAIN UNITS

The study area had been divided into 107 terrain units (Figure 5.1; Appendix A), each with a code and specific description in terms of FAO slope, topography, local relief, degree of dissection, level land and highland/lowland classes. These respective characteristics, in the format of 'continuous' raster data as originally derived from digital elevation data, are shown below. in addition, these characteristics are also represented as they have been allocated to the terrain units, in the format of vector data. Terrain unit codes are a combination of the respective codes of FAO slope, topography, local relief, degree of dissection, level land and highland / lowland classes *in that order*. Appendix A contains a large map of terrain units with profile positions and a full legend.

5.2 SLOPE

The slope map (Figure 5.2), containing continuous slope values, shows that the steepest areas occur in the western quarter of the study area, with a further southwest to northeast trending series of mountains and hills running through the centre of the area. The Witvlei and Gobabis synclinoria can be distinguished, as well as the oval valleys within the centres of some anticlines.

Figure 5.3 is the slope map in terms of FAO/SOTER classes. The continuous slope values had been reclassified into six distinct slope classes (Table 5.1).

Table 5.1: FAO slope classes.

FAO Slope Class	Code
Slope < 0.5 %	1
Slope 0.5 – 2 %	2
Slope 2 – 5 %	3
Slope 5 – 8 %	4
Slope 8 – 15 %	5
Slope > 15	6

The majority FAO slope class value of cells within each terrain unit was calculated and assigned to the respective units. Thus, Figure 5.4 is another representation of the original slope map, this time of FAO slope classes according to terrain units.

5.3 TOPOGRAPHY

The topography changes from flat in the east, through almost flat in the central areas, to undulating, rolling, hilly and mountainous in the west. Very few areas keyed out as rolling or hilly. Figure 5.5 is the map of the raster data, while Figure 5.6 is the map of the vector data, namely the terrain units classified as to topography class (Table 5.2).

Table 5.2: Topography classes.

Topography	**Code**
Flat	1
Almost flat	2
Undulating	3
Rolling	4
Hilly	5
Mountainous	6

5.4 LOCAL RELIEF

The local relief refers to the height difference (in m) within an area of 33" x 33" (approximately 0.9 km x 0.9 km). Mountains, hills, ridges and river valleys can be distinguished quite plainly. Figure 5.7 is a map of the raster data, while Figure 5.8 is a map of the vector data, namely the terrain units classified as to local relief of the landscape (Table 5.3).

Table 5.3: Local relief classes.

Local Relief	Code
< 5 m	1
5 – 10 m	2
10 – 30 m	3
30 – 60 m	4
60 – 100 m	5
100 – 300 m	6
> 300 m	7

5.5 DEGREE OF DISSECTION

The degree of dissection is a more localised feature on top of the broader topography class. Figure 5.9 is a map of the raster data, while Figure 5.10 is a map of the vector data, namely the terrain units classified as to degree of dissection of the landscape (Table 5.4). Figures 5.11, 5.12 and 5.13 are maps of topographic wetness index (original and filtered data) and surface roughness index, which were calculated during the process of deriving the topography and degree of dissection classes.

Table 5.4: Degree of dissection classes.

Degree Of Dissection	Code
Low	1
Medium	2
High	3

5.6 LEVEL LAND

The slope map was reclassified into two classes: slopes up to and including 8 %, and slopes greater than 8 % (Table 5.5; Figure 5.14). Terrain Units were classified as to the percentage of level land (with slope < 8 %), within each unit (Figure 5.15).

Table 5.5: Level land classes.

Level Land	Code
Slope > 8 %	0
Slope < 8 %	1

5.7 HIGHLAND / LOWLAND

The 1750 m contour was used to separate highlands (plateaux) from lowlands (plains) (Table 5.6; Figure 5.16). The Khomas Hochland is quite evident.

Table 5.6: Highland / lowland classes.

Highland / Lowland	Code
Elevation < 1750 m	1
Elevation > 1750 m	2

5.8 LANDFORMS

The landforms derived by using the methodology of Jenness (2006), were reclassified into nine classes (Table 5.7; Figure 5.17). Figure 5.18 is an enlargement of part of Figure 5.17, to show the landforms more clearly.

Table 5.7: Landform categories, according to the classification of Jenness (2006).

Landforms
Mountain tops and high ridges
Mesas and upper slopes
Mid-slope ridges and small hills in plains
Local ridges and hills in valleys
Plains and open slopes
Upland drainages

Landforms
Shallow valleys and mid-slope drainages
U-shaped valleys
Deep valleys and deeply incised streams

These categories are, arguably, not the most suitable for the Namibian landscape and will most likely be revised in future. They were not used in any further analyses.

5.9 POSITION IN THE LANDSCAPE

Position in the landscape, as derived with the methodology of Jenness (2006), correlated very well with field data. These are shown in Figure 5.19 and Figure 5.20 (which is an enlargement of part of Figure 5.19).

5.10 SOIL DEPTH

Soil depths as recorded by Loxton, Venn and Associates (1971), Kutuahupira and Mouton (2006), Kempf (1999c, 2008), Bertram and Broman (1999), Bertram and Kempf (2002) and fieldwork by the author, were spatially joined to terrain units, making use of kriging for interpolation of point data. These are shown in Figure 5.21.

5.11 SOIL AND TERRAIN UNITS OF KUTUAHUPIRA AND MOUTON

The soil and terrain units delineated by Kutuahupira and Mouton (2006) are included for the sake of completeness (Tables 5.8 – 5.9; Figures 5.22 – 5.23). They were taken into account during preparation of the present terrain units, but with some circumspection.

Table 5.8: Terrain units, according to Kutuahupira and Mouton (2006).

Terrain types			Percentage of level land			Local relief			Profile type
Code	Map ID	Class	% of area with slopes < 8 %	Av slope (%)	Class	Height difference (m)	Av slope length (m)	Class	% of level land on low/high – land
Plains									
A1a	1	A	> 75 % of area level	1	1	0 – 30	11	a	> 75% lowland
A1d	2	A	> 75 % of area level	1	1	0 – 30	18	d	> 75% highland
A2a	3	A	> 75 % of area level	1.4	2	0 – 30	16	a	> 75% lowland
A2c	4	A	50 – 75 % of area level	1	2	0 – 30	23	c	50 – 75% highland

Terrain types			Percentage of level land			Local relief			Profile type
Code	Map ID	Class	% of area with slopes < 8 %	Av slope (%)	Class	Height difference (m)	Av slope length (m)	Class	% of level land on low/high – land
A2d	5	A	> 75 % of area level	1.5	2	0 – 30	19	d	> 75% highland
B1c	6	B	50 – 75 % of area level	3	1	30 – 100	56	c	50 – 75% highland
B1d	7	B	50 – 75 % of area level	3.3	2	30 – 100	38	d	50 – 75% highland
B2b	8	B	50 – 75 % of area level	3.3	2	30 – 100	38	b	50 – 75% lowland
B2d	9	B	50 – 75 % of area level	2 – 4	2	30 – 100	66	d	50 – 75% highland
Highlands of the central plateau									
A3c	10	A	50 – 75 % of area level	1.5	3	0 – 30	19	d	50 – 75% highland
A3d	11	A	50 – 75 % of area level	1 – 2	3	0 – 30	25	d	50 – 75% highland
A4c	12	A	50 – 75 % of area level	1.4	4	0 – 30	19	d	50 – 75% highland
A5c	13	A	50 – 75 % of area level	2	5	0 – 30	25	d	50 – 75% highland
Plains with hills, ridges and koppies									
B3c	14	B	50 – 75 % of area level	2 – 3	3	100 – 170	130	c	50 – 75% highland
B3d	15	B	50 – 75 % of area level	5	3	100 – 170	145	d	50 – 75% highland
Open or isolated hills, ridges, koppies and mountains									
C1c	16	C	50 – 75 % of area level	8	1	170 – 300	210	c	50 – 75% highland
Hills and mountains									
D1c	17	D	< 20% of area is level	33	1	100 – 170	130	c	> 75% highland
D1d	18	D	< 20% of area is level	33	1	100 – 170	130	d	> 75% highland
D2c	19	D	< 20% of area is level	31	2	170 – 300	290	c	> 75% highland
D3c	20	D	< 20% of area is level	33	3	170 – 300	130	c	> 75% highland
D3c	21	D	< 20% of area is level	33	3	170 – 300	130	c	> 75% highland
D4c	22	D	< 20% of area is level	31	4	170 – 300	290	c	> 75% highland
D5c	23	D	< 20% of area is level	53	5	300 – 1000	309	c	> 75% highland

Table 5.9. Soil mapping units, according to Kutuahupira and Mouton (2006).

Code	Soil mapping units
R	Rock outcrops such as the mountains, hills and ridges
1	Mica-schist outcrops; very shallow soils; unweathered quartz gravels; inclusions of lithic Leptosols and hyperskeletic (saprolitic) Leptosols
2	Very shallow, gravelly, on mica schist; hyperskeletic Regosols (valleys, foot- and midslopes); inclusions of hyperskeletic Leptosols and lithi-skeletic Leptosols (ridge crests, hills)
3	Association of shallow, gravelly hyperskeletic Leptosols, haplic Leptosols and calcaric Cambisols; inclusions of moderately deep ferralic Arenosols
4	Rock outcrops (20%); hyperskeletic Leptosols; inclusions of lithi-skeletic Regosols; shallow and gravelly (quartzite)
5	Rock outcrops (granite, gneiss); lithic Leptosols; lithi-skeletic Leptosols
6	Association of lepti-skeletic Regosols and lepti-arenic Regosols; inclusions of haplic Luvisols lithi-skeletic Leptosols; on mica-schist
7	Association of moderately deep lepti-arenic Regosols, haplic Regosols, eutric Cambisols and leptic Cambisols; inclusions of haplic Calcisols and skeletic Leptosols
8	Association of lepti-skeletic arenic, lithic and haplic Regosols (high); inclusions of eutric Cambisols and haplic Luvisols (low)
9	Shallow skeletic Regosols (high); inclusions of moderately deep haplic Cambisols and lepti-petric Calcisols (low)
10	Deep ferralic Arenosols (flat areas); inclusions of moderately deep arenic Regosols (hummocks, ridges)
11	Associations of moderately deep to deep haplic Cambisols and ferralic Arenosols (lower); inclusions of lithic Leptosols, haplic Regosols and skeletic Regosols (higher) [Kalahari]
12	Association of moderately deep to deep arenic Regosols, ferralic Arenosools, haplic Cambisols; inclusions of lithic Leptosols and haplic Regosols
13	Association of shallow gravelly to moderately deep skeletic Regosols, arenic Regosols, haplic Leptosols, lithic Leptosols; inclusions of haplic Cambisols and ferralic Arenosols
14	Deep to very deep haplic Arenosols; inclusions of ferralic Arenosols (higher) [Kalahari sand plateau]
15	Shallow to moderately deep ferralic Arenosols; inclusions of skeletic Regosols and lithi-skeletic Leptosols [highly eroded river terrace]
16	Association of moderately deep to deep skeletic , leptic and haplic
17	Very deep ferralic Arenosols; inclusions of haplic Arenosols
18	Shallow to moderately deep areni-skeletic Regosols; inclusions of petric Calcisols
19	Association of ferralic Arenosols and skeletic Regosols (higher); inclusions of lithic Leptosols(higher) and petric Calcisols (watercourse, depressions)
20	Association of shallow to moderately deep haplic Arenosols and chromic Cambisols; inclusions of lepti-petric Calcisols and lithic Leptosols
21	Association of shallow to moderately deep lepti-skeletic Cambisols and haplic Cambisols; inclusions of lithic Leptosols
22	Shallow to moderately deep ferralic Arenosols; inclusions of haplic Calcisols and petric Calcisols (low)

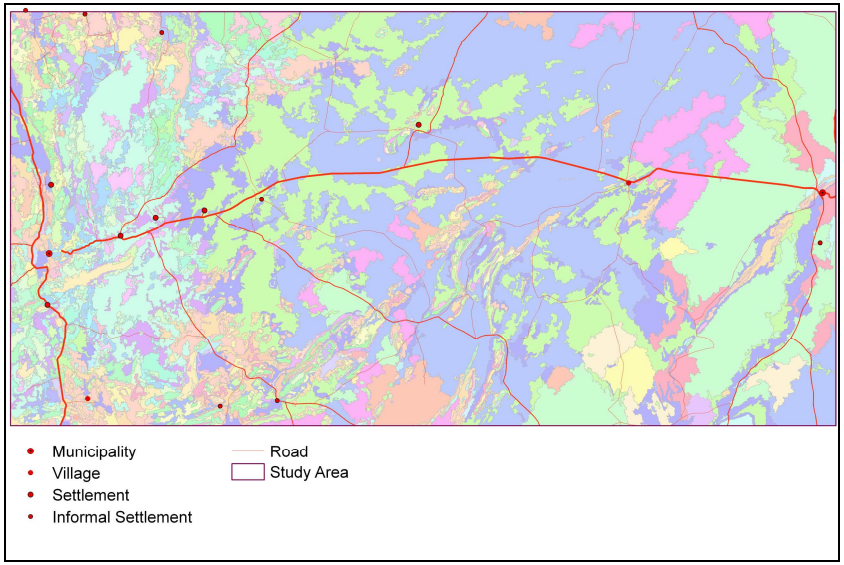

Figure 5.1. Terrain units (see Appendix A for large map and legend)

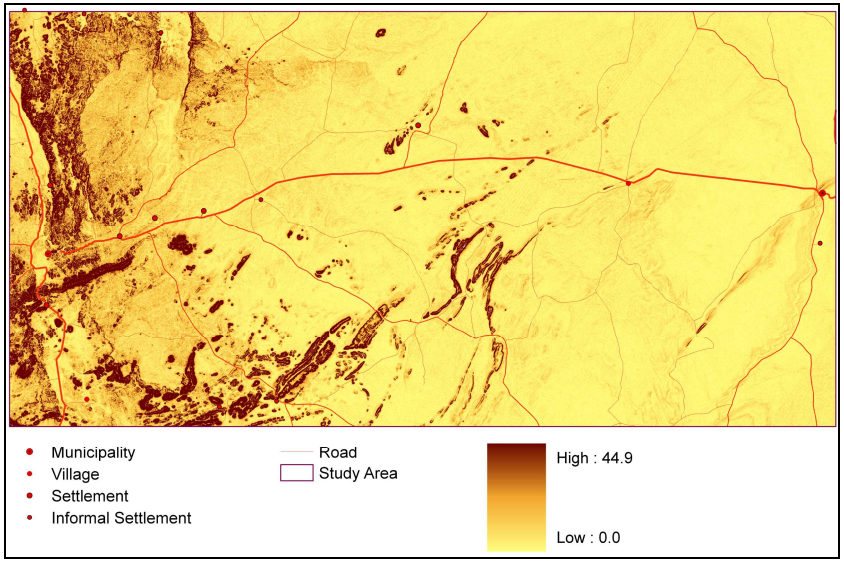

Figure 5.2. Slope (%)

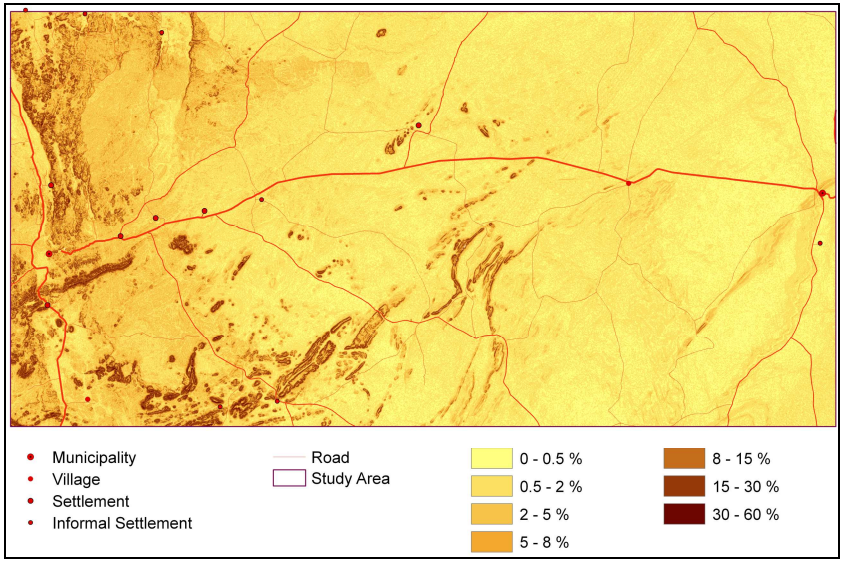

Figure 5.3. FAO slope classes (%)

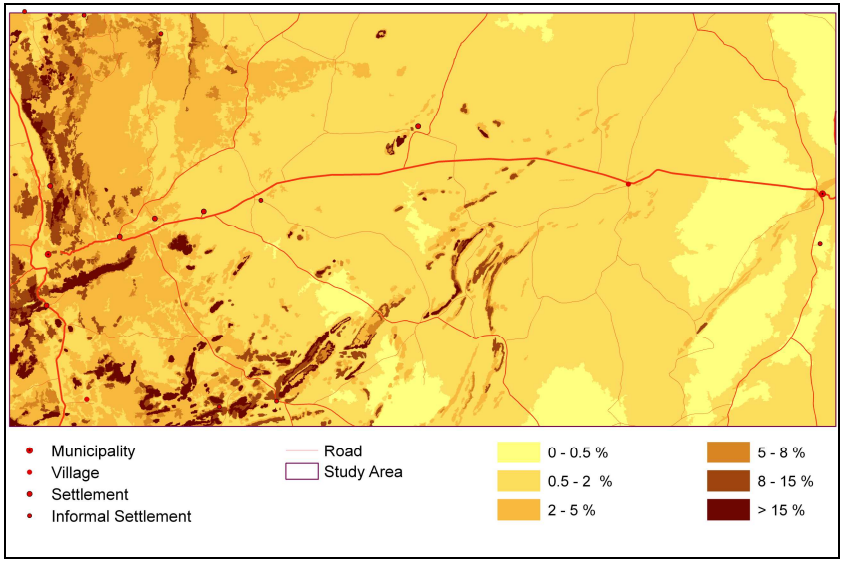

Figure 5.4. FAO slope classes (%), per terrain unit.

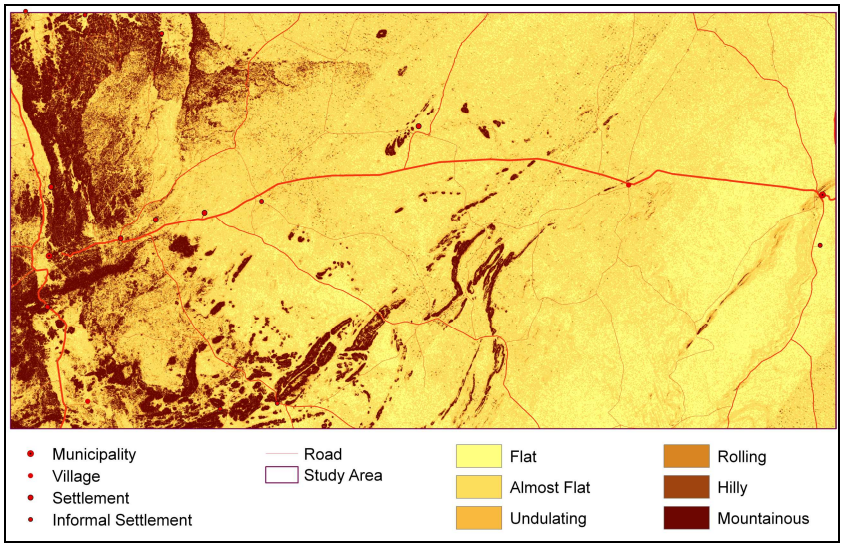

Figure 5.5. Topography classes

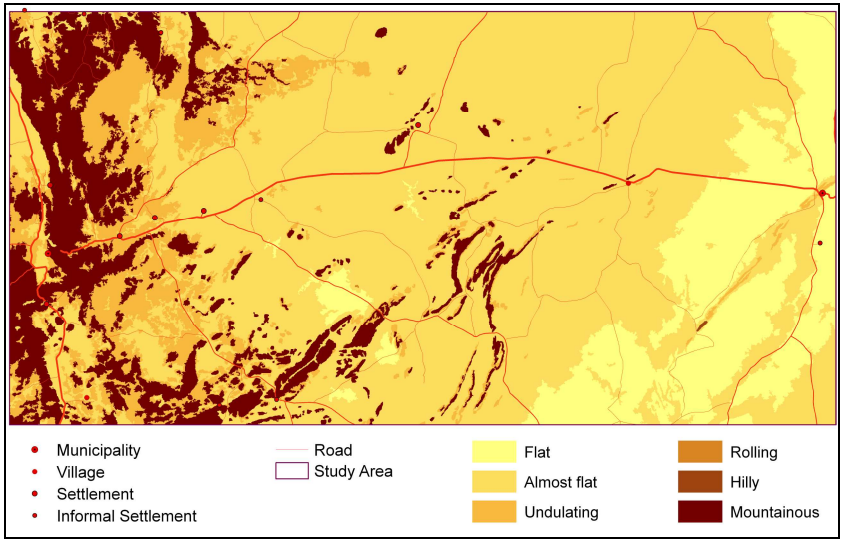

Figure 5.6. Topography classes, per terrain unit

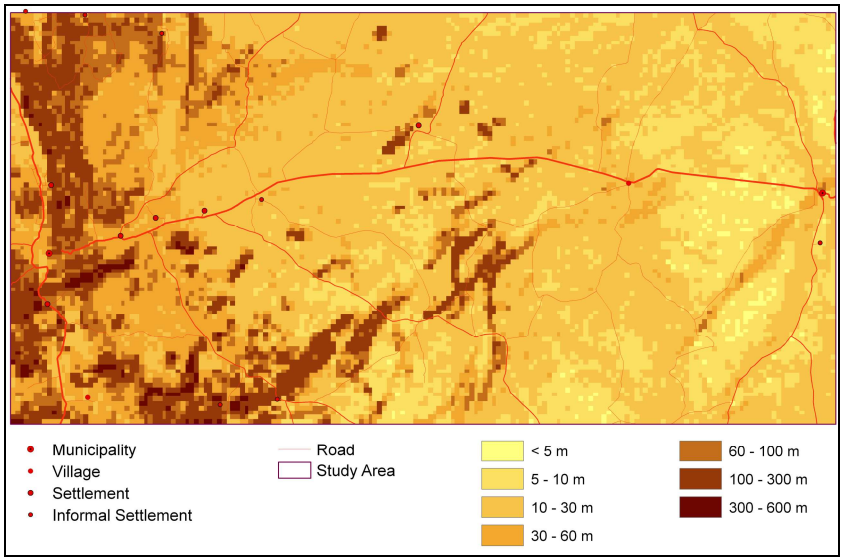

Figure 5.7 Local relief

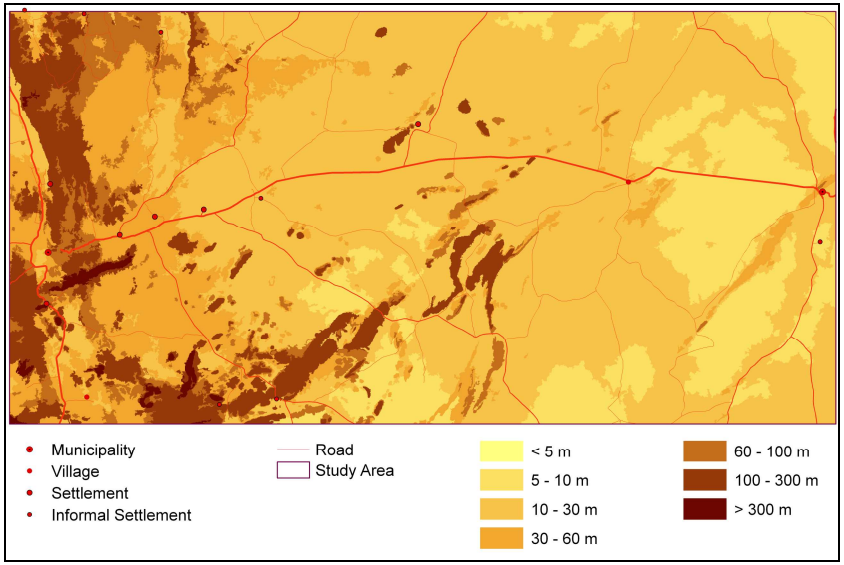

Figure 5.8. Local relief, per terrain unit

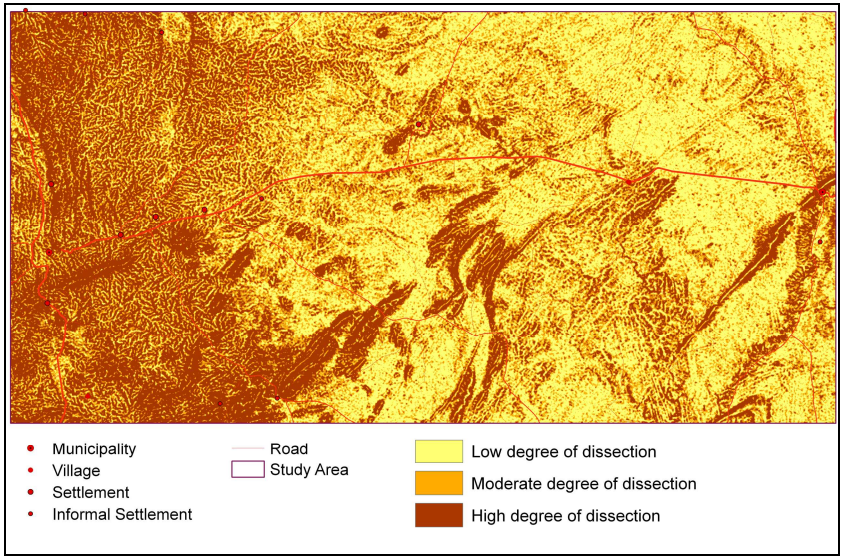

Figure 5.9. Degree of dissection of the landscape

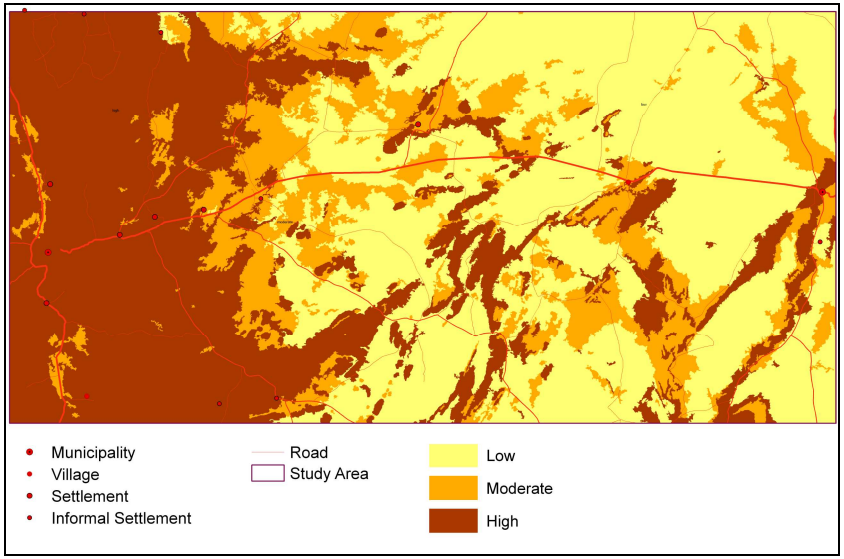

Figure 5.10. Degree of dissection of the landscape, per terrain unit

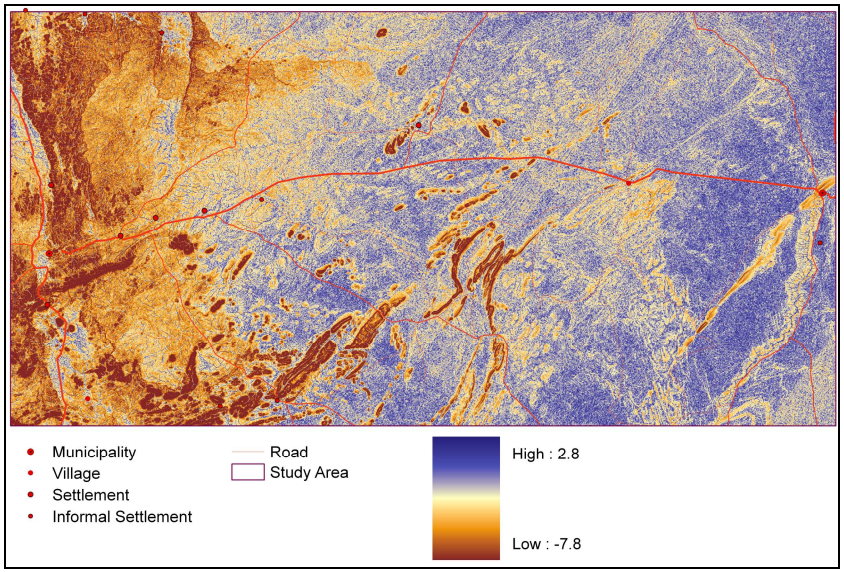

Figure 5.11. Wetness index (unfiltered)

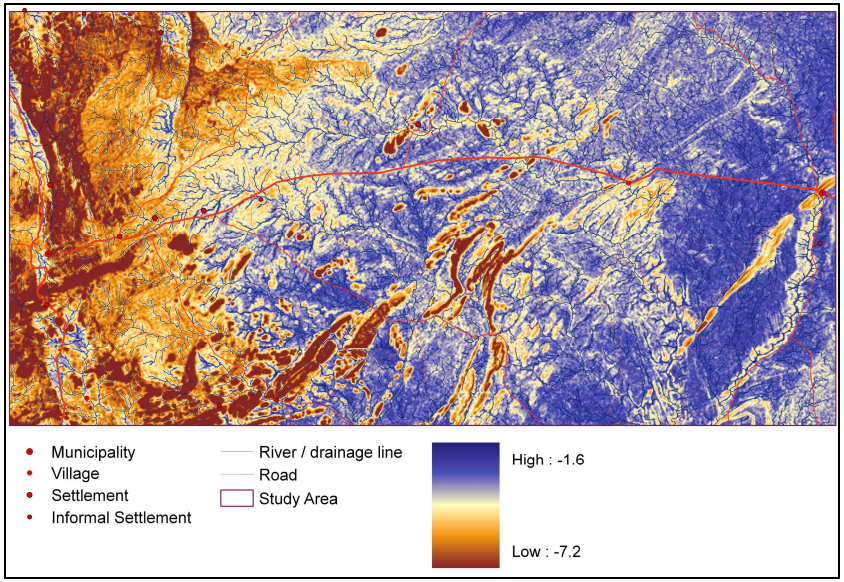

Figure 5.12. Wetness index (filtered) and drainage network

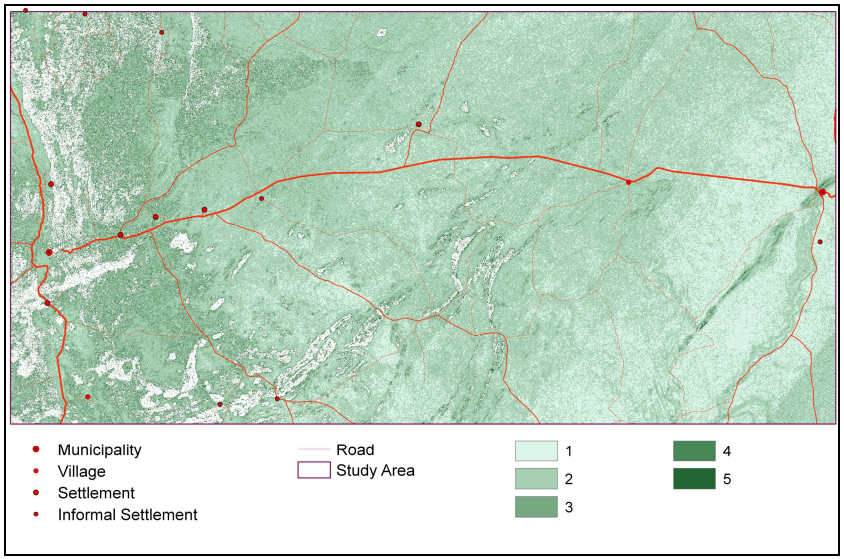

Figure 5.13. Surface roughness index

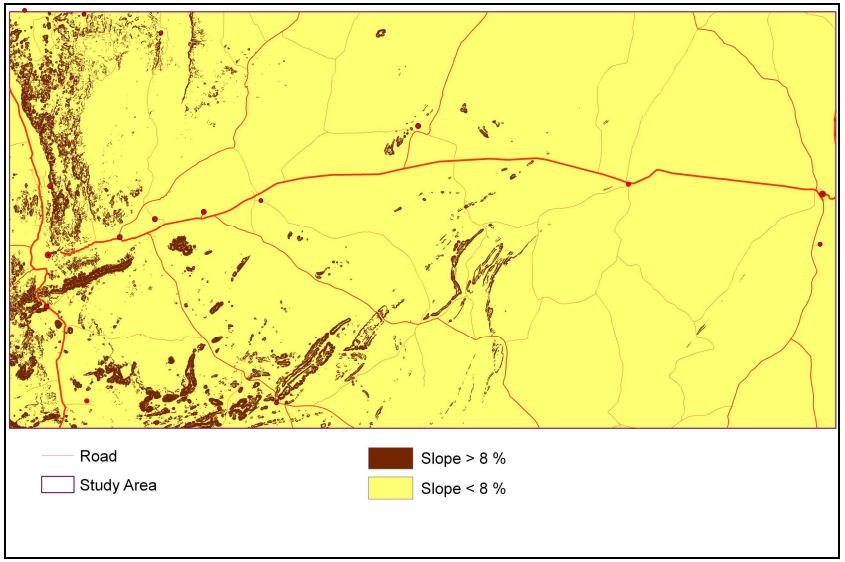

Figure 5.14. Level land, with a slope of less than 8 %

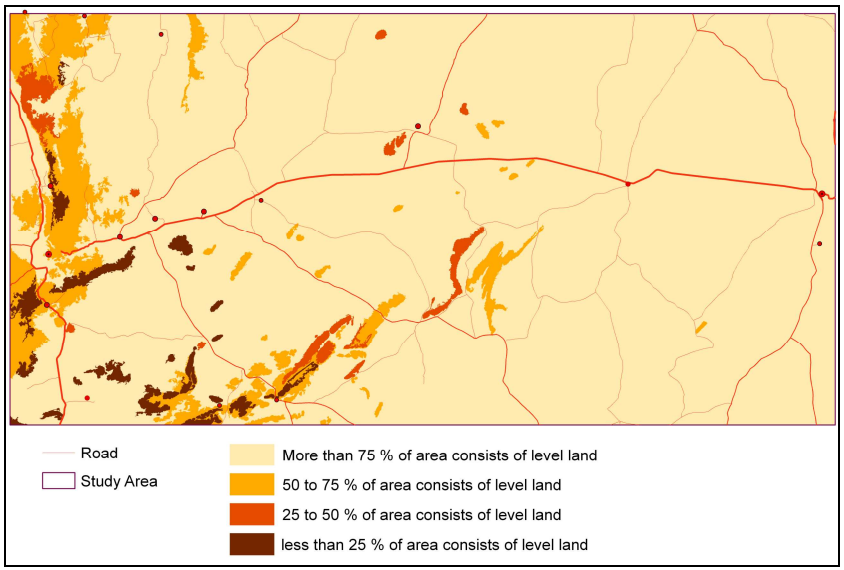

Figure 5.15. Percentage of level land, per terrain unit

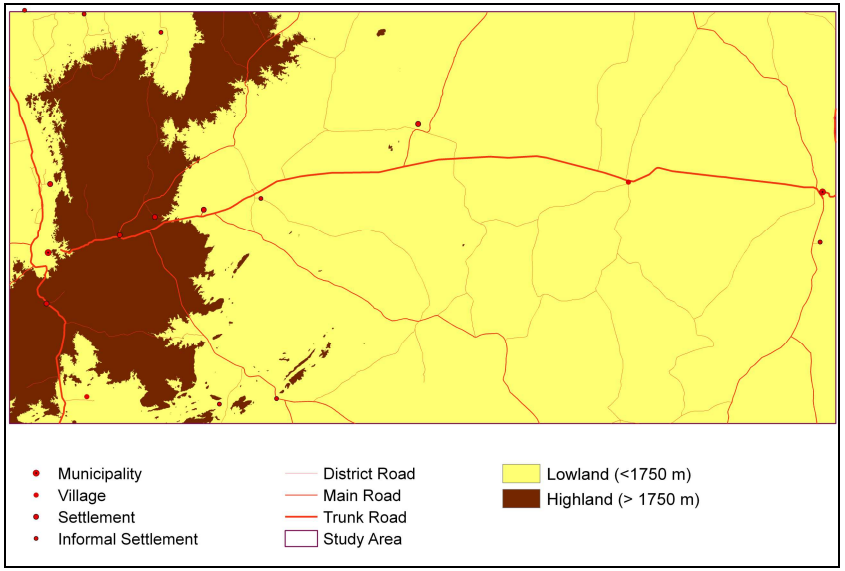

Figure 5.16. Highlands and lowlands

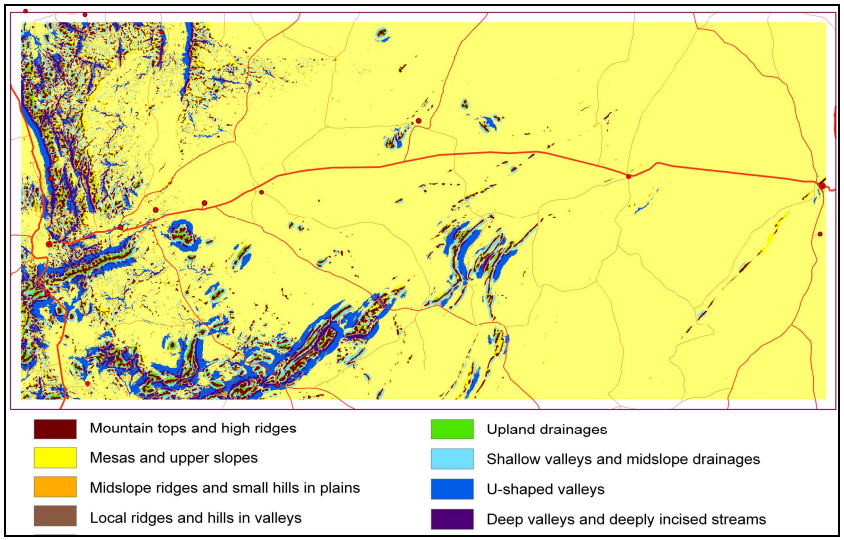

Figure 5.17. Landforms (Jenness classification)

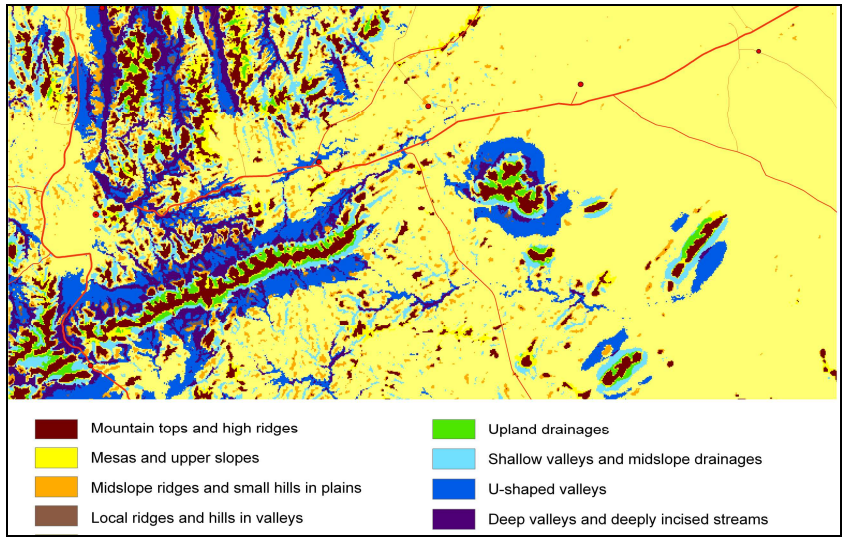

Figure 5.18. Detail of landforms (centre, left of Figure 5.17 – area around Windhoek)

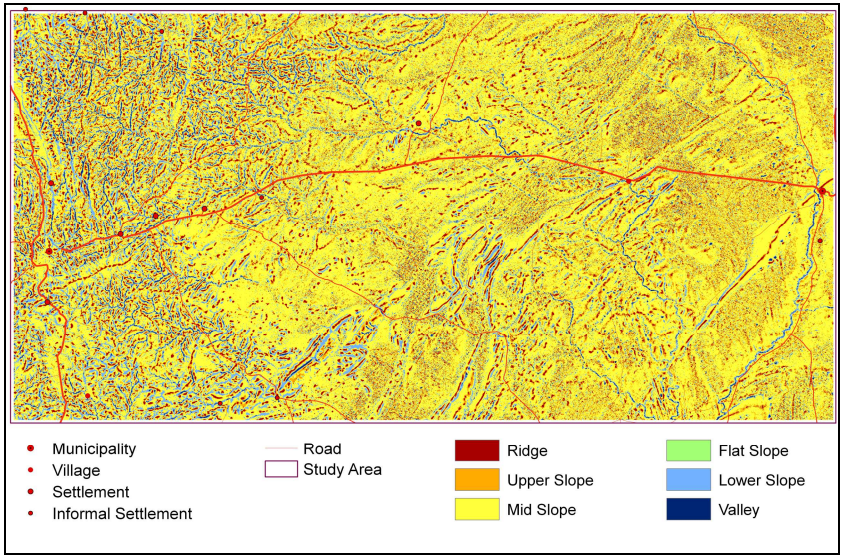

Figure 5.19. Position in the landscape

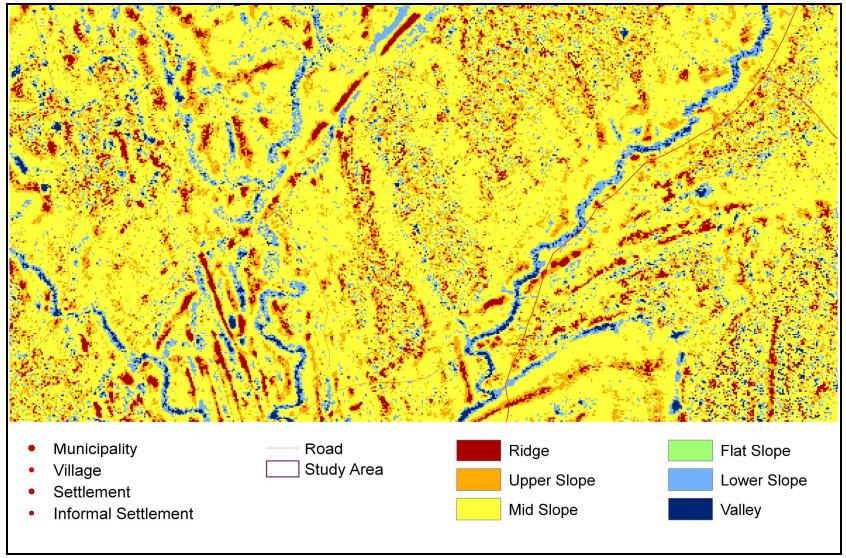

Figure 5.20. Detail of position in the landscape (bottom, right of Figure 5.19 – showing White Nossob and Black Nossob Rivers with tributaries)

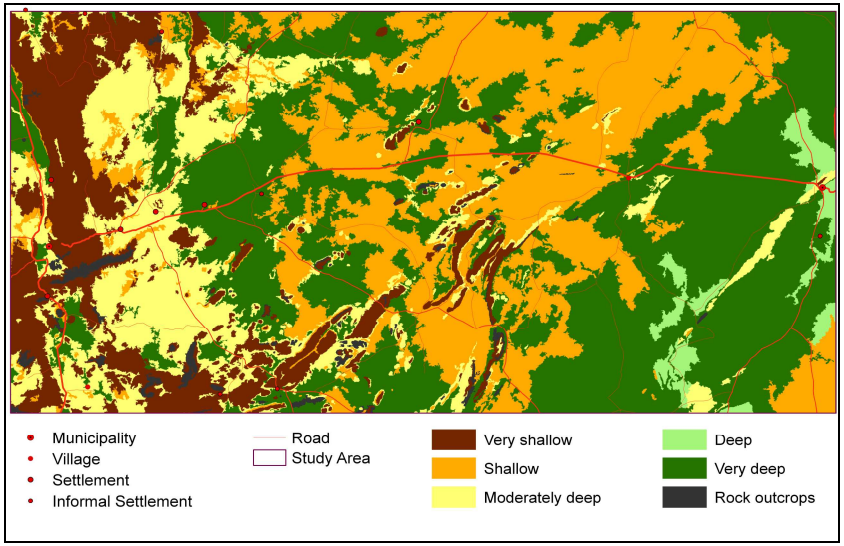

Figure 5.21. Depth classes, per terrain unit

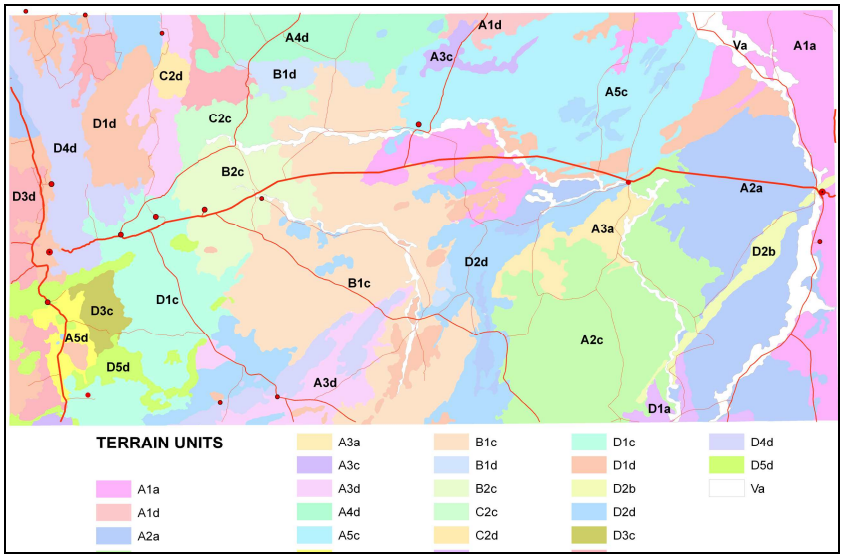

Figure 5.22. Terrain units, according to Kutuahupira and Mouton (2006) (See Table 5.8 for legend)

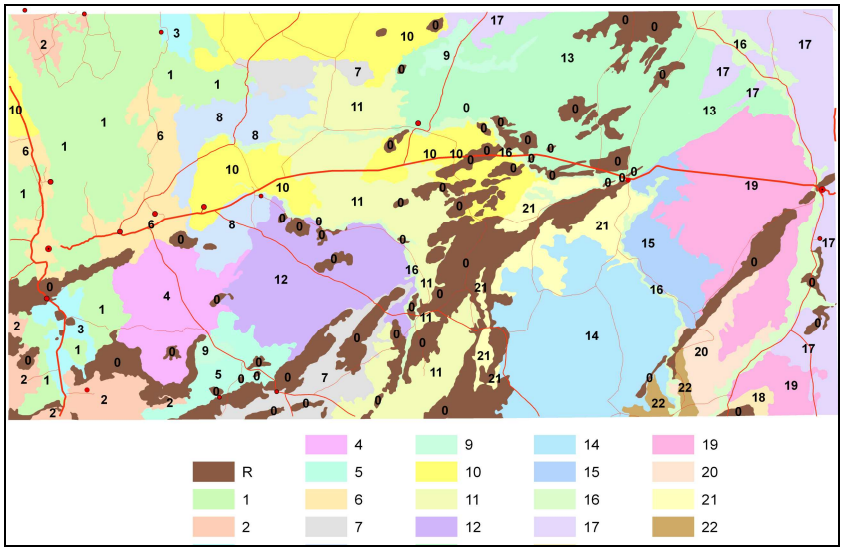

Figure 5.23. Soil mapping units, according to Kutuahupira and Mouton (2006) (See Table 5.9 for legend)

CHAPTER SIX

CHEMICAL CHARACTERISATION – NITROGEN, PHOSPHORUS, SULFUR

6.1 INTRODUCTION

Data on the chemical composition of the Earth's crust, soils from all over the globe and several different soil orders were reviewed by Helmke (2000). He named the ten most abundant elements in most dry soils as oxygen, silicon, aluminium, iron, calcium, potassium, sodium, magnesium, titanium and carbon. He also listed typical concentrations of major dissolved components in soils solution, which he defined as the aqueous phase of the soil at or below field moisture capacity (in contrast to soil water, which he defines as the moisture that fills the pores between soil particles at above field moisture capacity). For the purpose of soil fertility assessment, availability of the 13 mineral elements essential for plant growth needs to be assessed (Sims, 2000), namely nitrogen (N), phosphorus (P), potassium (K), calcium (Ca), magnesium (Mg), sulfur (S), boron (B), chlorine (Cl), copper (Cu), iron (Fe), manganese (Mn), molybdenum (Mo) and zinc (Zn). Chemical extractants – usually dilute solutions or mixtures of acids, bases, salts and chelates – are employed to simulate the absorption of these nutrients by plants. Nutrient availability in soils depends on inherent soil properties, such as texture, sesquioxides, carbonates and organic matter, as well as properties more sensitive to natural and anthropogenic inputs, such as pH, CEC and Eh (Sims, 2000).

This chapter deals with the macronutrients nitrogen, phosphorus and sulfur. The bases potassium, calcium, magnesium and sodium are discussed in Chapter 7, CEC, base saturation and salinity in Chapter 8, while the micronutrients iron, manganese, copper and zinc are examined in Chapter 9, and soil organic matter, pH and texture in Chapter 10.

6.2 NITROGEN [N]

Nitrogen constitutes around 0.02 % (200 mg kg^{-1}) of the Earth's crust. Non-exchangeable nitrogen is found in primary silicates, secondary silicates such as illite and vermiculite (Stellenbosch University [US], 2002). Insignificant amounts are produced from weathering of rocks, so that soil nitrogen content is virtually independent of the nature of the inorganic parent material.

Table 6.1: Typical nitrogen concentrations (in mg kg^{-1}) found in the earth's crust, some common rocks and soils.

SOURCE	Whitehead, 2000	Sims, 2000	Bowen, 1966
Earth's Crust	200		
Granite	59		
Basalt	52		
Shale	60		
Soils (Total N)	800 – 5 000 [2 800]	500 to 1 500	200 - 2 500 [1 000]

The main source of soil nitrogen is atmospheric molecular nitrogen gas [N_2] occurring in soil air, the soil solution and adsorbed as gas on the solid phase. The conversion of N_2 to ammonia [NH_3] and subsequently

to organic forms readily available for biological processes, is known as nitrogen fixation (Foth, 1990; Van der Watt and Van Rooyen, 1995). It is carried out by symbiotic micro-organisms – such as the actinomycete *Frankia* associated with the non-leguminous casuarinas, and the *Rhizobium* bacteria associated with roots of legumes – and free-living soil organisms, such as *Azotobacter* and *Clostridium* bacteria, and *Azolla*, *Nostoc* and *Calothrix* blue-green algae (Foth, 1990). Under natural grassland, rhizobial bacteria fix ~10 kg N ha^{-1} $year^{-1}$, while free-living bacteria fix ~1 – 2 kg N ha^{-1} $year^{-1}$ (Whitehead, 2000).

According to Sims (2000), the soil nitrogen cycle basically consists of:

- *mineralization* – conversion of organic nitrogen into ammonium by microbial decomposition, also known as *ammonification*
- *immobilization* – assimilation of ammonium and nitrate from the soil solution by microbes, for growth and biomass production
- *nitrification* – conversion of ammonium to nitrate by some soil bacteria under aerobic conditions
- *ion-exchange* – retention of ammonium and nitrate on soil clays or soil organic matter through cation exchange, and incorporation into micaceous clays
- *denitrification* – conversion of nitrates to molecular nitrogen or various nitrogen oxides by some soil bacteria under anaerobic conditions, and subsequent loss of these gases from the soil
- *volatilization* – conversion of ammonium to gaseous ammonia under conditions of high pH, and subsequent loss to the atmosphere, and
- *leaching* – downward loss of nitrate with percolating water.

Most plants take up almost all their nitrogen through the roots as nitrate [NO_3^-] and ammonium [NH_4^+] ions. The exception is legumes, which obtain their nitrogen from symbiotic nitrogen-fixing bacteria. Urea and amino acids can be absorbed by roots, but this plays a very minor role in nitrogen uptake. Plants can absorb some (< 5 %) of their required nitrogen through their stomata, as the gasses ammonia [NH_3] and nitrogen dioxide [NO_2] (Whitehead, 2000). Atmospheric ammonia originates from volatilisation of urea in livestock urine and from nitrogenous fertilizers applied elsewhere. Atmospheric nitrogen oxides [NO, NO_2] come from combustion of fossil fuels and from lightning discharges (Whitehead, 2000). Volcanic eruptions also contribute atmospheric sources of nitrogen to soils (Sims, 2000). The study area, being remote from crop producing areas, large urban or industrial centres and volcanoes, receives very few atmospheric inputs apart from nitrogen gas.

According to Sims (2000), total nitrogen values in soils typically range from 0.05 to 0.15 % (500 to 1 500 mg kg^{-1}) of which more than 98 % is organic in nature. Other writers, such as Whitehead (2000) and Blackmer (2000), put the organic nitrogen at around 95 % of total soil nitrogen, and estimate that nitrogen constitutes about 5 % of soil organic matter (dry weight). Roughly 35 % of these complex nitrogen-containing organic polymers are heterocyclic nitrogen compounds and ~20 % are ammoniacal, while hydrolysis would change the remainder into amino acids (~30 – 40 %) and amino sugars (~5 – 6 %) (Whitehead, 2000). The heterocyclic nitrogen compounds derive mainly from humus, which forms through biochemical modification of plant residues and the reactions of amino compounds and ammonia with phenolic compounds derived from lignin (Stevenson, 1994). These organic molecules are for the most part insoluble in water, and their nitrogen thus unavailable to plants. Only when they are mineralised to inorganic nitrogen compounds does their

nitrogen become accessible for plant uptake. Heterocyclic nitrogen compounds mineralise more slowly than linear humus polymers. Mineralisation of organic nitrogen provides a steady supply of plant-available nitrogen under natural systems in equilibrium (Whitehead, 2000).

The inorganic mineral fraction of nitrogen in soil consists of ammonium [NH_4^+], nitrite [NO_2^-] and nitrate [(NO_3^-] ions. In well-aerated warm soils, such as those found in the study area, NO_3^- is the dominant nitrogen compound in the soil solution, and the preferred form of nitrogen for uptake by most plants (Blackmer, 2000). NO_2^- is taken up in small quantities by plants, but higher concentrations are toxic to them. NH_4^+ is preferred by young plants, acid-loving plants and those adapted to waterlogged soils (US, 2002). Ammonium in the soil solution is in equilibrium with a much larger quantity of exchangeable ammonium adsorbed on the exchange complex (Blackmer, 2000). Mineralization of inaccessible organic forms of soil nitrogen is brought about through the biochemical process of *ammonification*:

$$\text{Organic N} \rightarrow NH_4^+ + OH^-$$

Some ammonium is used by plants, some is lost to the atmosphere, but the bulk is further transformed through the aerobic biological process of *nitrification*. *Nitrosomonas* bacteria transform ammonium into nitrites, followed by *Nitrobacter* bacteria transforming the nitrites to nitrates.

$$2NH_4^+ + 3O_2 \rightarrow 2NO_2^- + 4H^+$$
$$2NO_2^- + O_2 \rightarrow 2NO_3^-$$

$$NH_4^+ + 2O_2 \rightarrow NO_3^- + 2H^+ + H_2O$$

The rate of *mineralisation* is enhanced by heat, presence of earthworms, a low carbon to nitrogen ratio and soils with good water holding capacity without easily becoming waterlogged. Nitrate, being an anion, is not readily adsorbed onto the exchange sites of clay and organic matter. It remains in the soil solution and is thus mobile and accessible to plants, but susceptible to leaching and denitrification. *Denitrification* is the biochemical reduction of nitrite and nitrate to gaseous nitrogen, either in the form of molecular nitrogen or oxides of nitrogen (Van der Watt and Van Rooyen, 1995): $NO_3^- \rightarrow NO_2^- \rightarrow NO \rightarrow N_2O \rightarrow N_2$
Denitrification is favoured by anaerobic conditions and needs electron-donating substrate, such as organic residues, to support microbial respiration (Blackmer, 2000).

Ammonium, a cation, is adsorbed on the exchange complex. This restricts its mobility and availability to plant roots to some extent, but also protects it from fast leaching and volatilisation. Ammonium in the soil solution is readily nitrified.

Nitrogen concentrations are highest in the upper few centimetres of soil, due to the presence of nitrogen-containing leaf litter and animal excreta, decreasing with depth and practically absent below 30 – 40 cm (Whitehead, 2000). Micro-organisms play a crucial role in the nitrogen cycles involving soil and rangeland under extensive livestock grazing. They are responsible for the digestion of plant material by ruminants, the transformation of plant residues and animal excreta into soil organic matter and the mineralization of nitrogen from the latter. Maximum nitrogen availability is between pH 6 and 8, as this is the optimal range for the soil microbes that fix nitrogen symbiotically and mineralise organic matter (Foth, 1990). Losses through leaching and volatilisation are low in extensively managed grassland systems (Whitehead, 2000). Figure 6.1 shows

the various forms and pathways of nitrogen in grassland, which would also be applicable to the present study area.

Plants contain 1 – 5 % nitrogen on a dry weight basis. It is essential to plants as a constituent of amino acids, proteins, nucleic acids, nucleotides, chlorophyll and coenzymes (Foth, 1990; Reuter and Robinson, 1997). Some of these proteins function as enzymes, such as the essential photosynthetic enzyme ribulose biphosphate carboxylase-oxygenase (Whitehead, 2000).

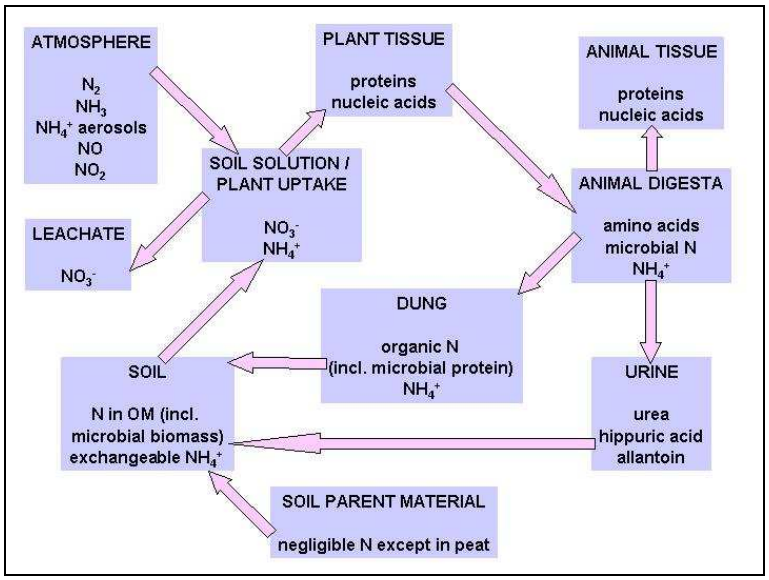

Figure 6.1. The major forms of nitrogen involved in the cycling of nitrogen in grassland (from Whitehead, 2000)

Table 6.2: Estimated nitrogen balances (kg ha^{-1} $year^{-1}$) from an extensively managed grassland, grazed by cattle, in the United Kingdom (Whitehead, 2000, quoting data from Dampney and Unwin, 1993).

	ESTIMATED N (KG HA^{-1} $YEAR^{-1}$)
INPUTS	
Fixation of atmospheric N_2	8
Deposition from atmosphere	15
Fertilizer	0
Supplementary feeds	0
ASPECT OF RECYCLING	
Uptake into herbage	60
Consumption of herbage by animals	30
Dead herbage to soil	30
Dead roots to soil	30
Excreta to soil of grazed area	25
OUTPUTS	
Milk / live-weight gain	3
Leaching / runoff	5
Volatilisation of ammonia	3

Denitrification / nitrification	2
Loss through excreta off sward	0
GAIN TO SOIL	10

6.2.1 STATISTICAL ANALYSIS: NITRATE AND NITRITE OF THE SATURATED PASTE EXTRACT

Normality was rejected for nitrate and nitrite of the saturated paste extract by the statistical tests employed, namely the Shapiro-Wilk W test, Kolmogorov-Smirnov / Lilliefors test, and three D'Agostino tests based in skewness, on kurtosis, and on a combination of skewness and kurtosis (AnalystSoft, 2007).

Table 6.3: Descriptive statistics – nitrate (n = 79) and nitrite (n = 80) content of the saturated paste extract.

	Nitrate	**Nitrite**
	mg l^{-1}	mg l^{-1}
Mean	16.28	6.15
Median	1.80	1.30
Standard Deviation	29.88	11.13
Minimum	0.00	0.00
Maximum	166.70	49.70
Range	166.70	49.70
Lower Quartile	0.20	0.00
Upper Quartile	20.80	5.75
Quartile Range	20.60	5.75
Percentile 10	0.00	0.00
Percentile 90	54.60	24.65
Skewness	2.83	2.38
Kurtosis	9.29	5.06

Table 6.4: Distribution in terms of deciles – nitrate (n = 79) and nitrite (n = 80).

	Decile	**NO_3^-**	**NO_2^-**
		mg l^{-1}	mg l^{-1}
minimum		0.0	0.0
	1	0.0	0.0
	2	0.0	0.0
	3	0.3	0.2
	4	0.6	0.7
median	5	1.8	1.3
	6	6.3	2.3
	7	15.9	3.5
	8	25.6	6.7
	9	56.4	24.0
maximum	10	166.7	49.7

The **nitrate** content of 79 samples varies between 0 and 166.7 mg l^{-1}, with a mean of 16.28, median of 1.80 and standard deviation of 29.88. The quartile range is 20.60, from 0.20 (lower quartile) to 20.80 mg l^{-1} (upper quartile). The distribution is greatly skewed, with skewness of 2.83 and kurtosis of 9.29 (Table 6.4; Figures 6.2 – 6.3).

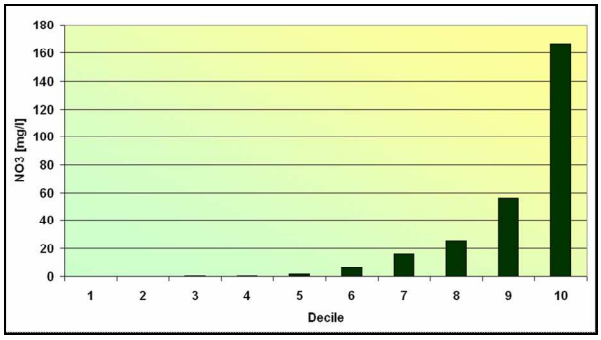

Figure 6.2. Decile distribution of nitrate content (mg l^{-1})

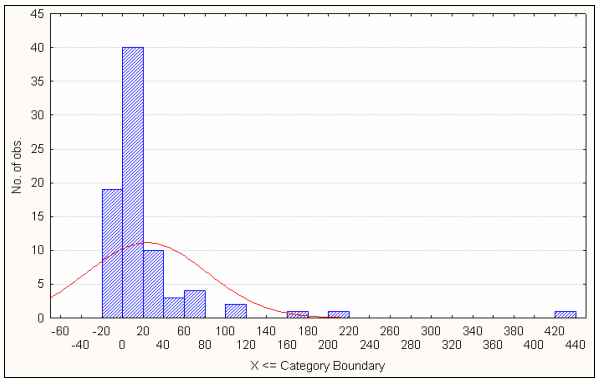

Figure 6.3. Histogram of nitrate content (mg l^{-1})

Statistically significant, but weak, correlations, at $p < 0.05$, were found between nitrate content and electrical conductivity measured in the saturated paste extract ($r^2 = 0.21$) (Figure 6.4), sulfate content of the saturated paste extract ($r^2 = 0.10$), and electrical conductivity measured in a 2:5 soil:water suspension ($r^2 = 0.10$).

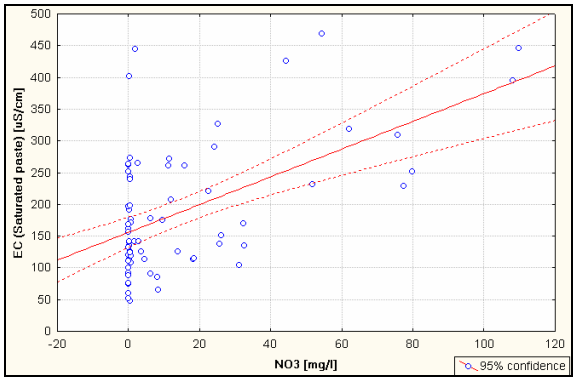

Figure 6.4. NO_3^- (saturated paste) content (mg l^{-1}) vs EC (saturated paste) (uS cm^{-1})

The **nitrite** content of 80 samples varies between 0 and 49.70 mg l^{-1}, with a mean of 6.15, a median of 1.30 and a standard deviation of 11.13. The quartile range is 5.75, from 0.00 (lower quartile) to 5.75 (upper quartile). The distribution is greatly skewed, with skewness of 2.38 and kurtosis of 5.06 (Table 6.4; Figures 6.5 – 6.6).

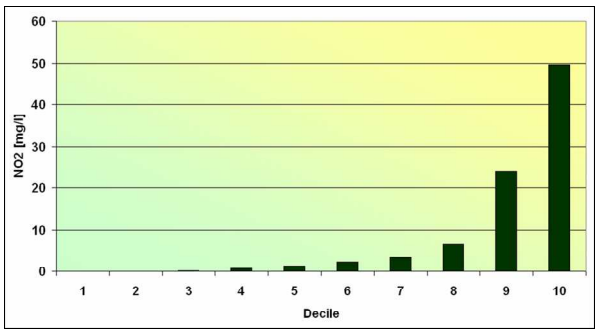

Figure 6.5. Decile distribution of nitrite content (mg l^{-1})

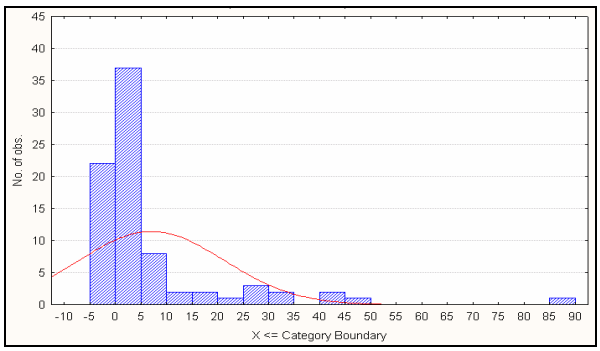

Figure 6.6. Histogram of nitrite content (mg l^{-1})

A statistically significant, but weak, correlation, at $p < 0.05$, was found between nitrite content and electrical conductivity measured in the saturated paste extract ($r^2 = 0.20$).

Both nitrate and nitrite concentrations are higher in the topsoil than the subsoil (Table 6.5; Figures 6.7, 6.81), as expected from the contribution of leaf litter and animal excreta to soil nitrogen, and in line with literature, e.g. Whitehead (2000), Hartemink and Hunting (2008).

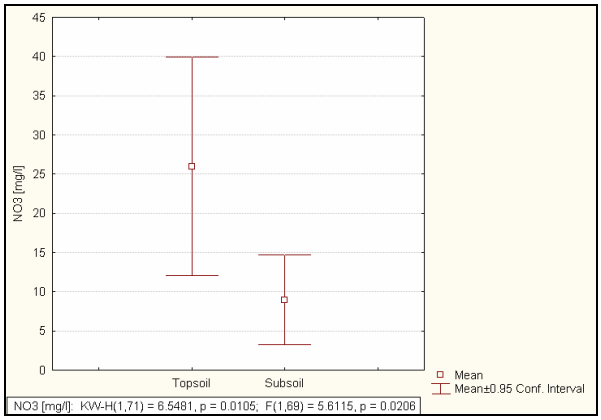

Figure 6.7. Nitrate content (mg l^{-1}), per topsoil and subsoil

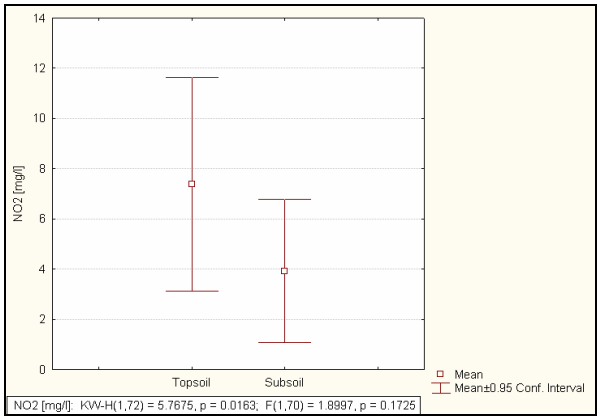

Figure 6.8. Nitrite content (mg l^{-1}), per topsoil and subsoil

Table 6.5: Nitrate and nitrite content, per topsoil (n = 35) and subsoil (n = 37) .

	NO_3^- mg l^{-1}		NO_2^- mg l^{-1}	
	Topsoil	**Subsoil**	**Topsoil**	**Subsoil**
Mean	26.00	8.96	7.38	3.93
Median	6.31	0.44	2.42	0.26
Standard Deviation	39.93	17.16	12.43	8.57
Minimum	0.00	0.00	0.00	0.00
Maximum	166.70	75.79	49.69	34.81
Range	166.70	75.79	49.69	34.81
Lower Quartile	0.58	0.00	0.67	0.00
Upper Quartile	31.30	9.53	7.81	3.20
Quartile Range	30.72	9.53	7.14	3.20
Percentile 10	0.00	0.00	0.00	0.00
Percentile 90	79.74	32.53	28.38	15.00

When disregarding clay loam and sandy clay soils, of which there are too few samples to be representative, it emerges that sandy soils have relatively low mean nitrate and nitrite concentrations (Figures 6.9 and 6.10). Sand also has the smallest spread of nitrite values in the ±0.95 confidence interval.

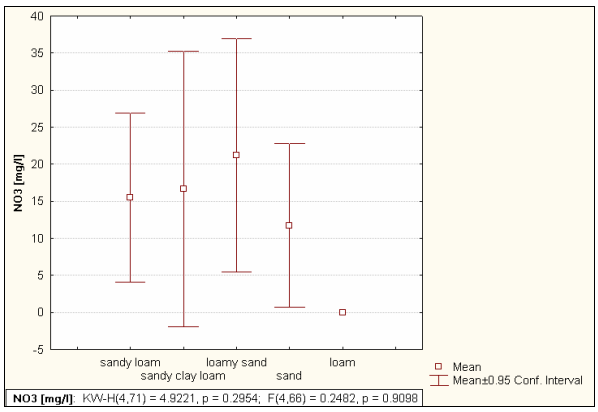

Figure 6.9. Nitrate content (mg l^{-1}), per textural class

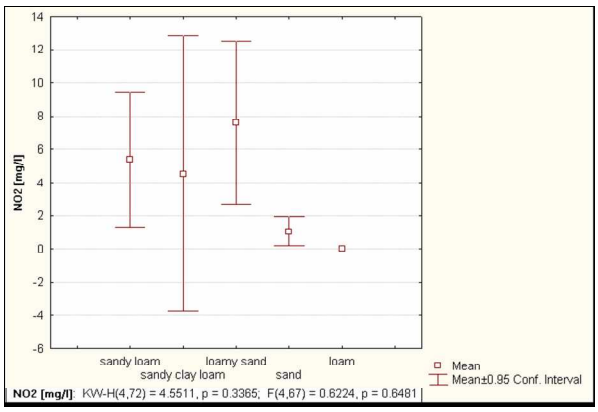

Figure 6.10. Nitrite content (mg l^{-1}), per textural class

Nitrate concentrations are highest in Leptosols, Cambisolsand Arenosols, and lowest in Calcisols en Luvisols (Table 6.6; Figure 6.11). The spread in values is very large in Leptosols. Nitrite concentrations are highest in Leptosols, and lowest in Luvisols, Arenosols and Calcisols (Table 6.6; Figure 6.12). In most cases the mean values are much higher than the medians, as the result of a few high extremes. The spread in values is very large in Leptosols.

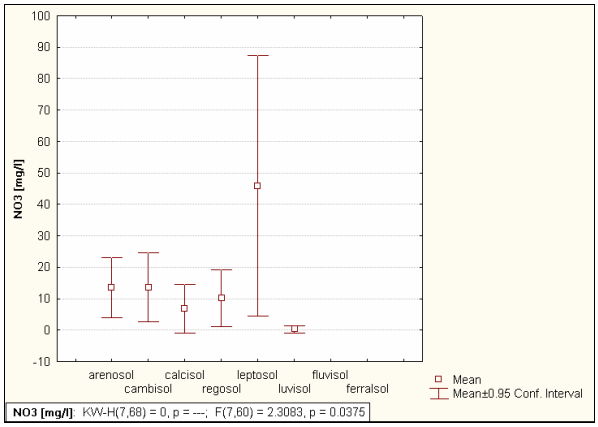

Figure 6.11. Nitrate content (mg l^{-1}), per WRB reference soil group

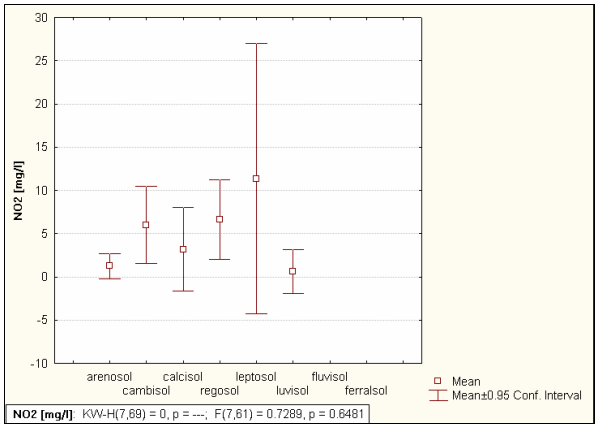

Figure 6.12. Nitrite content (mg l^{-1}), per WRB reference soil group

Table 6.6: Nitrate and nitrite content, per WRB reference soil group.

NO_3^- mg l^{-1}	**Arenosols** (n = 9)	**Calcisols** (n = 9)	**Leptosols** (n = 8)	**Cambisols** (n = 14)	**Regosols** (n = 25)	**Luvisols** (n = 3)
Mean	13.50	6.77	45.84	13.57	10.13	0.26
Median	8.37	0.75	34.21	3.61	0.43	0.00
Std. Dev.	12.38	10.11	49.57	19.04	21.72	0.45
Minimum	0.00	0.00	0.00	0.00	0.00	0.00
Maximum	32.53	24.24	109.85	54.55	77.46	0.78
Range	32.53	24.24	109.85	54.55	77.46	0.78
Lower Quartile	3.62	0.00	0.31	0.26	0.00	0.00
Upper Quartile	18.43	11.40	93.92	25.13	6.32	0.78
Quartile Range	14.81	11.40	93.61	24.87	6.32	0.78
Percentile 10	0.00	0.00	0.00	0.00	0.00	0.00
Percentile 90	32.53	24.24	109.85	51.80	32.29	0.78
NO_2^- mg l^{-1}	**Arenosols** (n = 9)	**Calcisols** (n = 9)	**Leptosols** (n = 9)	**Cambisols** (n = 14)	**Regosols** (n = 25)	**Luvisols** (n = 3)
Mean	1.25	3.18	11.36	6.01	6.61	0.59
Median	0.67	0.25	1.17	4.03	0.68	0.00
Std.Dev.	1.88	6.29	20.38	7.68	11.21	1.03
Minimum	0.00	0.00	0.00	0.00	0.00	0.00
Maximum	6.04	19.54	49.69	28.38	34.81	1.78
Range	6.04	19.54	49.69	28.38	34.81	1.78
Lower Quartile	0.26	0.00	0.38	0.95	0.00	0.00
Upper Quartile	1.34	2.71	2.87	6.61	9.62	1.78
Quartile Range	1.08	2.71	2.49	5.66	9.62	1.78
Percentile 10	0.00	0.00	0.00	0.00	0.00	0.00
Percentile 90	6.04	19.54	49.69	15.90	28.48	1.78

The nitrate and nitrite levels of profiles, of topsoil and subsoil respectively, are shown in Figures 6.13 – 6.16.

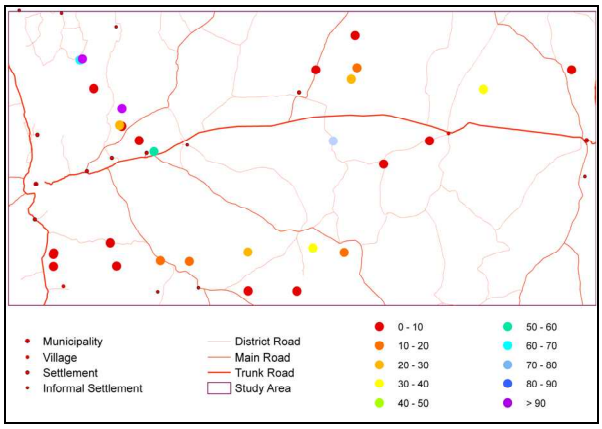

Figure 6.13. Nitrate content (mg l^{-1}) of topsoil

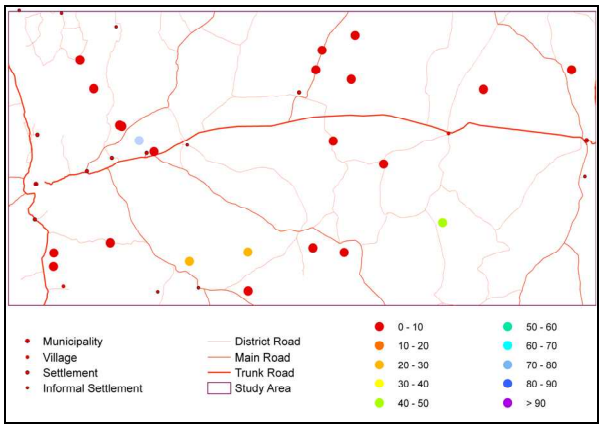

Figure 6.14. Nitrate content (mg l^{-1}) of subsoil

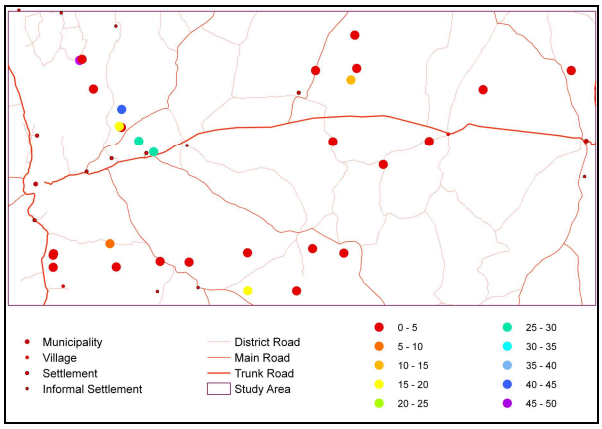

Figure 6.15. Nitrite content (mg l^{-1}) of topsoil

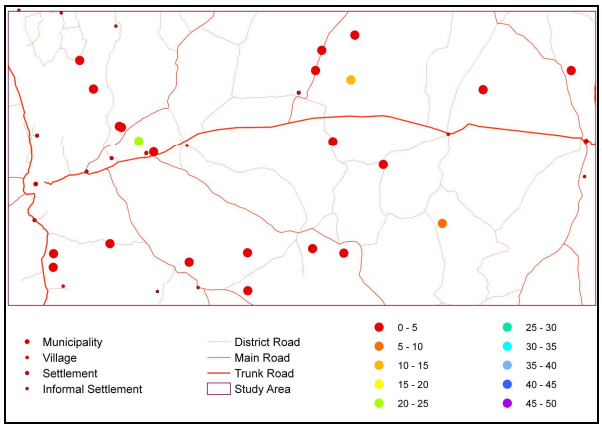

Figure 6.16. Nitrite content (mg l^{-1}) of subsoil

6.3 PHOSPHORUS [P]

Phosphorus occurs in more than 60 minerals. It is abundant in the apatite group [$3\{Ca_3(PO_4)_2\}.CaX_2$, where $X = CO_3^{2-}$ / OH^- / F^- / Cl^-], for example hydroxylapatite [$Ca_5(PO_4)_3OH$], fluorapatite [$Ca_5(PO_4)_3F$] and chlorapatite [$Ca_5(PO_4)_3Cl$]. It occurs to a lesser extent in strenghite [$FePO_4.2H_2O$], variscite [$AlPO_4.2H_2O$] (Whitehead, 2000) and phosphophyllite [$Zn_2(Fe,Mn)(PO_4)_2.4H_2O$].

Table 6.7: Typical P concentrations (in mg kg^{-1}) found in the earth's crust, some common rocks and soils.

SOURCE	Whitehead, 2000	Sharpley, 2000	Helmke, 2000
Earth's Crust	800		
Granite	390		
Basalt	610		
Shale	700		
Sandstone	170		
Limestone	400		
Soils From Granite	900		
Soils From Shale	1 200		
Soils From Sandstone	400		
Entisol			662
Spodosol			3 000
Alfisol			455

Mollisol			880
Soils (Total)	400 – 4 000	100 – 3 000	650
Soils (plant-available P)		5 – 80 (North America)	

Inorganic phosphorus, which usually constitutes between 50 and 70 % of the total P in grassland soils (Whitehead, 2000; Sharpley, 2000), occurs as phosphates in unweathered minerals, adsorbed by 1:1 lattice clays (e.g. kaolinite), adsorbed by Fe and Al oxides and hydroxides, precipitated by Ca (e.g. in apatite) and as soluble $H_2PO_4^-$ and HPO_4^{2-} ions in the soil solution (Whitehead, 2000). On weathering, soluble $H_2PO_4^-$ and HPO_4^{2-} are formed, but most are soon adsorbed or re-precipitated by calcium (at neutral or high pH) or iron and aluminium (at low pH) (Sharpley, 2000; Whitehead, 2000). This causes low mobility of phosphorus in soil, with low levels of leaching. Phosphorus can be lost from grassland through surface runoff, both in soluble form and in suspended particles (Whitehead, 2000).

Maximum phosphorus availability is between pH 6.5 and 7.5. It is also highly available above pH 8.5 due to sodium phosphates having high solubility. Between pH 7.5 and 8.3 bioavailability is reduced by the presence of calcium carbonate that represses the dissolution of calcium phosphate. Below pH 6.5, acidity allows more iron and aluminium to go in solution, allowing the formation of relatively insoluble iron and aluminium phosphates (Foth, 1990). Most organic soil P occurs as the insoluble Ca, Fe and Al salts of inositol phosphates, with some P immobilized in complex humus polymers, nucleotides, nucleic acids and phospholipids (Whitehead, 2000). There is more organic phosphorus in microbial matter than in plant material in the soil (Whitehead, 2000). The rate of mineralisation of organic soil phosphorus is increased by high temperatures and distinct wet and dry cycles (Sharpley, 2000).

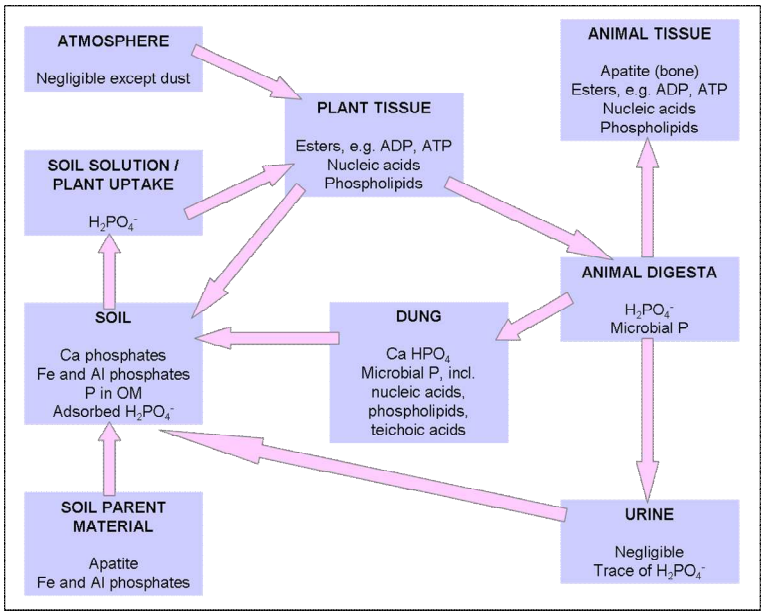

Figure 6.17. The major forms of phosphorus involved in the cycling of phosphorus in grassland (from Whitehead, 2000)

Soil P is well correlated with P of the parent material (Whitehead, 2000), but is also influenced by soil texture, extent of pedogenesis and management factors (Sharpley, 2000). According to Whitehead (2000) and Sharpley (2000), P concentrations are highest in the surface horizons of grassland soils, due to the

contribution from leaf litter and animal excreta, and greater biological activity. A typical extensively managed natural grassland, such as the study area, producing around 1 000 kg dry dead herbage material, per ha, per annum, containing about 0.1 % P, would see replacement of about 1 kg P per ha per year in the soil (Whitehead, 2000). Figure 6.17 shows the various forms and pathways of phosphorus in grassland, which would also be applicable to the present study area.

Table 6.8: Estimated phosphorus balances (kg ha^{-1} $year^{-1}$) from an extensively-managed grassland, grazed by beef cattle (Whitehead, 2000).

	ESTIMATED P (KG HA^{-1} $YEAR^{-1}$)
INPUTS	
Deposition from atmosphere	0
ASPECT OF RECYCLING	
Uptake into herbage	6
Consumption of herbage by animals	3
Dead herbage to soil	5
Dead roots to soil	2
Excreta to soil of grazed area	2.7
OUTPUTS	
Milk / live-weight gain	0.8
Leaching / runoff	0.1
Loss through excreta off sward	0
GAIN TO SOIL	0.1

Phosphorus is important in energy transfer as a constituent of adenosine triphosphate (ATP). It is also a component of many proteins, coenzymes, nucleotides, nucleic acids, metabolic substrates (Foth, 1990) and phospholipids (Reuter and Robinson, 1997). It plays essential roles in cell division and germination of seeds (Whitehead, 2000).

6.3.1 STATISTICAL ANALYSIS: PLANT-AVAILABLE PHOSPHORUS (OLSEN-METHOD)

Normality was rejected for plant-available phosphorus by the statistical tests employed, namely the Shapiro-Wilk W test, Kolmogorov-Smirnov / Lilliefors test, and three D'Agostino tests based in skewness, on kurtosis, and on a combination of skewness and kurtosis (AnalystSoft, 2007).

Table 6.9: Descriptive statistics – plant-available phosphorus content (n = 555)

	Plant-available P
	mg kg^{-1}
Mean	4.50
Median	2.00
Standard Deviation	5.93
Coefficient of Variation	1.32
Minimum	0.00
Maximum	49.00

Range	49.00
Lower Quartile	0.50
Upper Quartile	6.40
Quartile Range	5.90
Percentile 10	0.10
Percentile 90	12.00
Skewness	2.50
Kurtosis	9.72

Table 6.10: Distribution in terms of deciles – plant-available phosphorus content (n = 555).

	Decile	Plant-available P
		mg kg^{-1}
minimum		0.0
	1	0.1
	2	0.3
	3	0.7
	4	1.3
median	5	2.0
	6	3.1
	7	5.3
	8	8.0
	9	12.0
maximum	10	49.0

The plant available phosphorus content of 555 samples from the study area ranges from 0 to 49.0 mg kg^{-1}. The distribution is positively skewed, with skewness of 2.50 and kurtosis of 9.72, thus the mean (4.5) is less useful as a measure of central location than the median (2.0). The standard deviation is 5.93. Half the samples have phosphorus concentrations of between 0.5 (1^{st} quartile) and 6.4 (3^{rd} quartile), for a quartile range of 5.9. In 90 % of samples, the P content is below 12 mg kg^{-1}, which is low for a soil under natural grassland, but in line with the prevailing arid climate and low biomass production. The frequency distribution is shown in Table 6.10 and Figures 6.18 - 6.19.

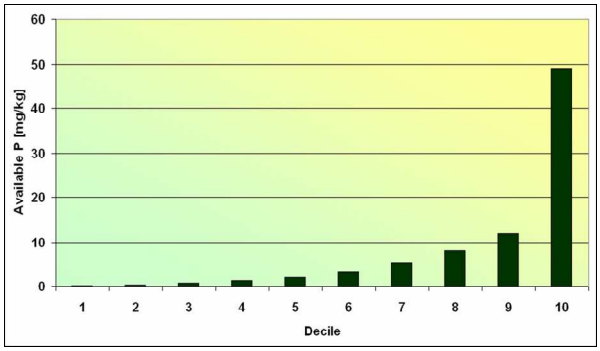

Figure 6.18. Decile distribution of plant-available P content (mg kg^{-1})

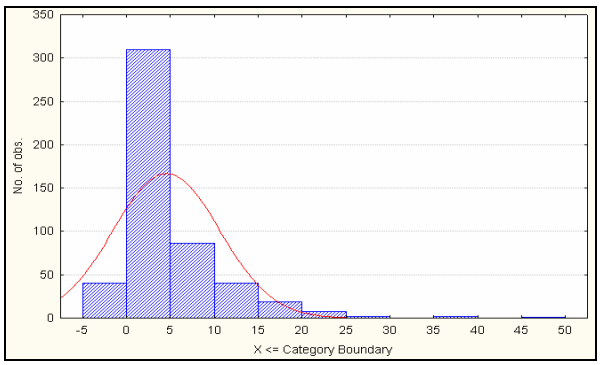

Figure 6.19. Histogram of plant-available P content (mg kg^{-1})

The concentrations of P found in the study area are lower than those found by Ellis (1988) in comparable areas in southern Africa: median 17 mg kg^{-1} and range 73 mg kg^{-1} for A horizons, median 9 mg kg^{-1} and range 52 mg kg^{-1} for B horizons in the eastern Boesmanland; median 28 mg kg^{-1} and range 137 mg kg^{-1} for A horizons, median 8 mg kg^{-1} and range 292 mg kg^{-1} for B horizons in western Boesmanland, South Africa. It is also slightly lower than the concentrations found by Kotze and Du Preez (2008) in soils from the eastern Free State in South Africa, namely 12.1 to 6.0 mg kg^{-1}, from the surface to a depth of 45 cm. It does,

however, agree with P concentrations recorded elsewhere in Namibia (Coetzee, Beernaert and Calitz, 1999; Kempf, 1999a, 1999b, 1999c; Coetzee, 2001b; Kutuahupira, Mouton and Coetzee, 2001a, 2001b; Kutuahupira, Mouton and Beukes, 2003) and in South Africa (Materechera, Mandiringana and Mbokodi, 1998).

Statistically significant, but weak, correlations, at $p < 0.05$, were found between plant-available phosphorus content and electrical conductivity measured in a 2:5 soil:water suspension ($r^2 = 0.20$), zinc ($r^2 = 0.17$), iron content ($r^2 = 0.14$) (Figures 6.20 – 6.22), organic matter content ($r^2 = 0.16$), extractable sodium content ($r^2 = 0.13$), and electrical conductivity measured in a saturated paste ($r^2 = 0.10$).

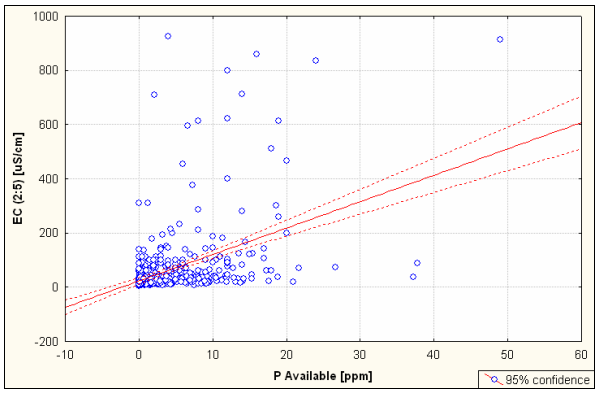

Figure 6.20. Plant-available P content (ppm = mg kg^{-1}) vs EC (2:5 soil : water) (uS cm^{-1})

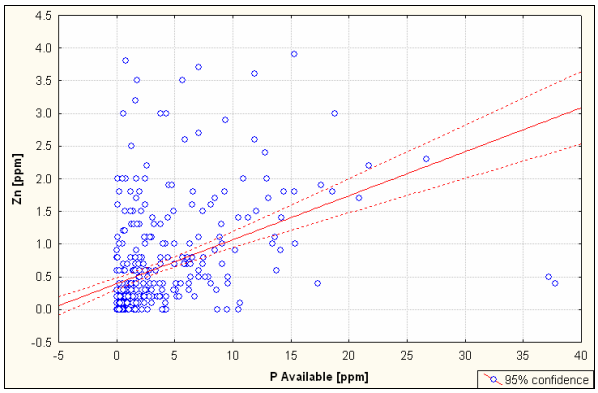

Figure 6.20. Plant-available P (ppm = mg kg^{-1}) content vs Zn content (ppm = mg kg^{-1})

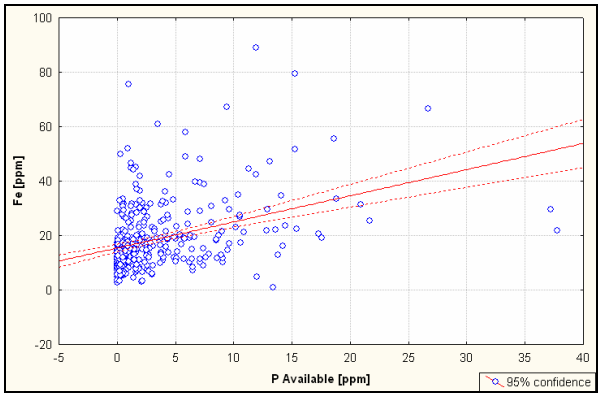

Figure 6.22. Plant-available P (ppm = mg kg^{-1}) content vs Fe content (ppm = mg kg^{-1})

Topsoil P concentrations are noticeably higher than those of the subsoil (Table 6.11; Figures 6.23 and 6.24), as also noted by Whitehead (2000), Sharpley (2000), Materechera *et al.* (1998), Kotze and Du Preez (2008) and Ellis (1988). This is most likely caused by enrichment of the topsoil by decaying plant material, and the low mobility of P in soil.

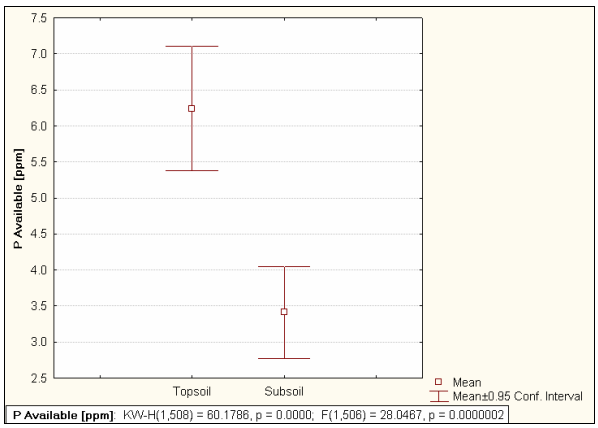

Figure 6.23. Plant-available P content (ppm = mg kg^{-1}), per topsoil and subsoil

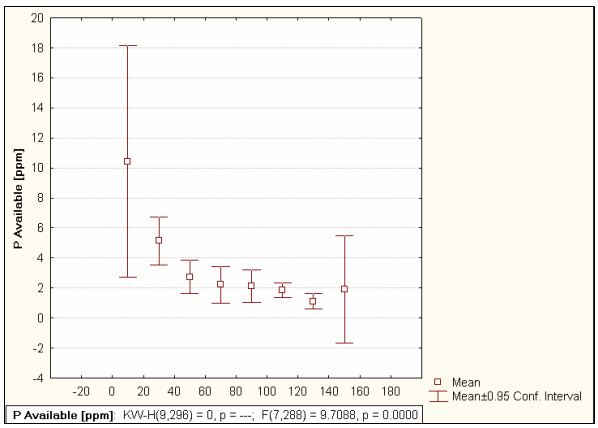

Figure 6.24. Plant-available P content (ppm = mg kg^{-1}) at various depths

Table 6.11: Plant-available P content, per topsoil (n – 208) and subsoil (n = 300).

Plant-available P	Topsoil	Subsoil
	mg kg^{-1}	mg kg^{-1}
Mean	6.24	3.41
Median	4.21	0.95
Std. Dev.	6.32	5.63
Minimum	0.00	0.00
Maximum	37.80	49.00
Range	37.80	49.00
Lower Quartile	1.70	0.26
Upper Quartile	9.02	4.00
Quartile Range	7.32	3.74
Percentile 10	0.41	0.00
Percentile 90	14.00	10.00

Deep soils seem to have less plant-available P than very shallow soils, while shallow and moderately deep soils lie between these two extremes (Figure 6.25).

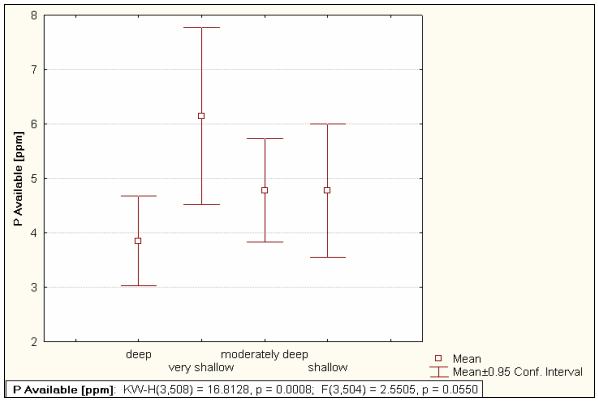

Figure 6.25. Plant-available P content (ppm = mg kg^{-1}), for soils of various depths

When disregarding clay loam and sandy clay soils, of which there are too few samples to be representative, it emerges that sandy soils have the lowest P content, followed by loamy sand and sandy loam soils, while sandy clay loam and loam soils have higher mean concentrations, but also a wide spread in the ±0.95 confidence intervals (Figure 6.26).

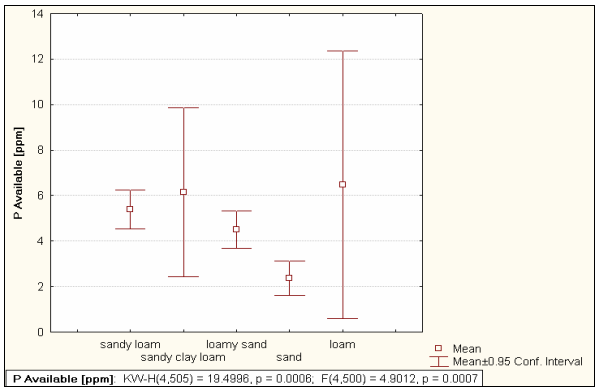

Figure 6.26. Plant-available P content (ppm = mg kg^{-1}), per textural class

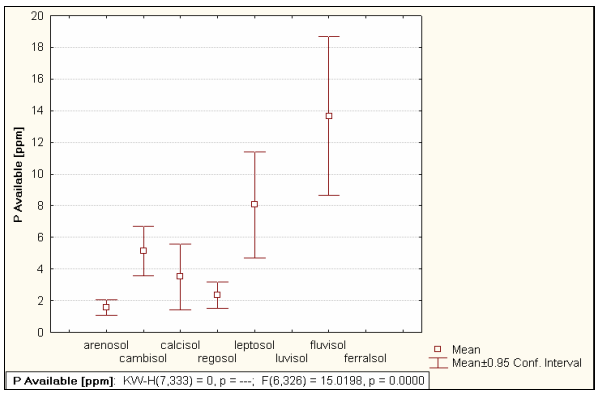

Figure 6.27. Plant-available P content (ppm = mg kg^{-1}), per WRB reference soil group

Arenosols have the lowest P concentrations, followed by Regosols, Calcisols and Cambisols. Leptosols and Fluvisols are richest in P (Table 6.12 and Figure 6.27). The enrichment of Fluvisols happens mainly through transport of particulate matter containing phosphorus by surface runoff (Whitehead, 2000).

Table 6.12: Plant-available P content, per WRB reference soil group.

P available mg kg^{-1}	**Arenosols** (n = 131)	**Calcisols** (n = 17)	**Leptosols** (n = 24)	**Fluvisols** (n = 6)	**Cambisols** (n = 66)	**Regosols** (n = 89)	**Luvisols** (n = 3)
Mean	1.57	3.51	8.06	13.67	5.13	2.34	10.46
Median	0.56	1.90	6.18	13.00	2.88	0.94	3.51
Std. Dev.	2.71	4.04	7.97	4.76	6.44	3.88	14.11
Minimum	0.00	0.00	0.43	8.00	0.00	0.00	1.18
Maximum	15.25	12.04	37.80	21.00	37.20	25.00	26.70
Range	15.25	12.04	37.37	13.00	37.20	25.00	25.52
Lower Quartile	0.16	0.57	2.77	10.00	0.69	0.31	1.18
Upper Quartile	1.70	5.49	11.30	17.00	7.06	2.29	26.70
Quartile Range	1.54	4.92	8.53	7.00	6.37	1.98	25.52
Percentile 10	0.00	0.16	0.97	8.00	0.23	0.10	1.18
Percentile 90	3.66	10.90	14.37	21.00	13.40	7.09	26.70

According to the classification of Kutuahupira and Mouton (2006), the very shallow soils of the Khomas Hochland are richest in P, while the deep, reddish sandy soils of the Kalahari plains are poorest (Figure 6.28). This agrees with above results with regard to the P content according to textural class and soil depth.

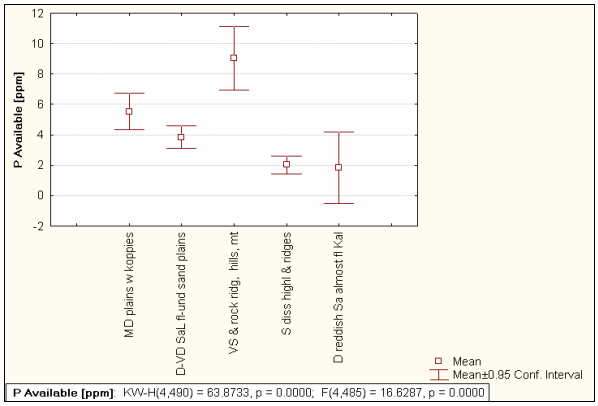

Figure 6.28. Plant-available P content (ppm = mg kg^{-1}), per broad soil group

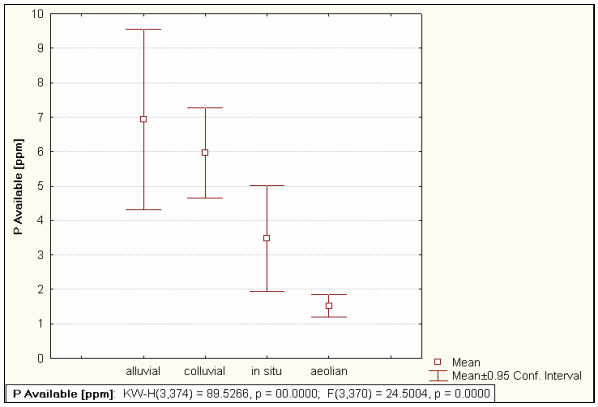

Figure 6.29. Plant-available P content (ppm = mg kg^{-1}), per origin of parent material

Soils of aeolian origin have the lowest P content, followed by those formed through *in situ* weathering, while soils from alluvial and colluvial origin have higher, comparable, P concentrations (Figure 6.29). This agrees with the results above, as the soils of aeolian origin are the sandy soils of the deep Kalahari sand plains, while alluvial soils are classified as Fluvisols, and colluvial soils as Lepto- and, in some cases, Regosols.

Soils originally formed in the Kalahari sands are poorer in plant-available P than those formed from the schist of the Khomas Hochland – a consequence of the mineral composition of the respective parent materials (Figure 6.30). The noticeable correlation between soil P and its parent material is noted in literature, e.g. by Whitehead (2000). In this analysis and all those that follow, only three lithological units were considered, namely schist, quartzite and Kalahari sand. These were the only units recorded in sufficient numbers and with complete confidence by the technicians carrying out the profile descriptions.

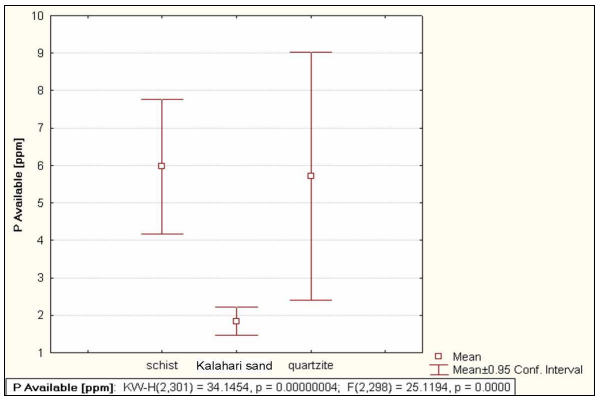

Figure 6.30. Plant-available P content (ppm = mg kg^{-1}), per type of parent material

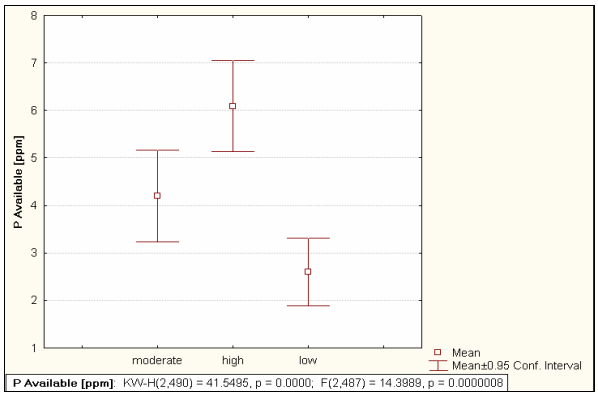

Figure 6.31. Plant-available P content (ppm = mg kg^{-1}), per degree of dissection of the landscape

P concentrations increase with the degree of dissection (Figure 6.31). One explanation is greater rates of erosion and subsequent weathering of P-containing parent material in more dissected terrain. Secondly, the highly dissected terrain of the study area occurs mainly on schist, quartzite and calcrete, whereas the less dissected areas, towards the east, are mainly covered with Kalahari sands, which are quite poor in P.

In support of above result, it is also apparent that P concentrations are lower in areas of low local relief, than in areas of high local relief (Figure 6.32).

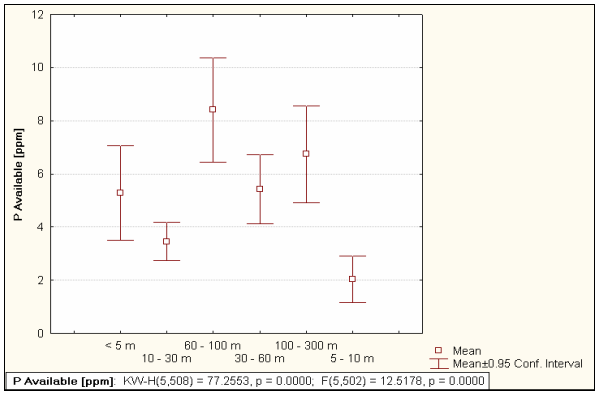

Figure 6.32. Plant-available P content (ppm = mg kg^{-1}), per local relief

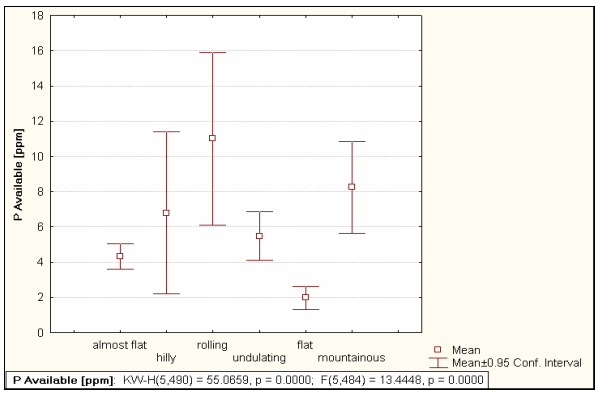

Figure 6.33. Plant-available P content (ppm = mg kg^{-1}), per topographic class

A similar result is found when considering the topographic classes: flat, almost flat and undulating land has lower P content than rolling, hilly and mountainous land (Figure 6.33).

Despite the well-known influence of pH on availability of soil P reported widely in literature, no clear-cut correlations were seen during this study: the correlation coefficient was -0.00193 at $p < 0.05$ (Figures 6.34 – 6.35). This could perhaps be explained by the choice of analytical method: the Olsen method is less sensitive at lower pH.

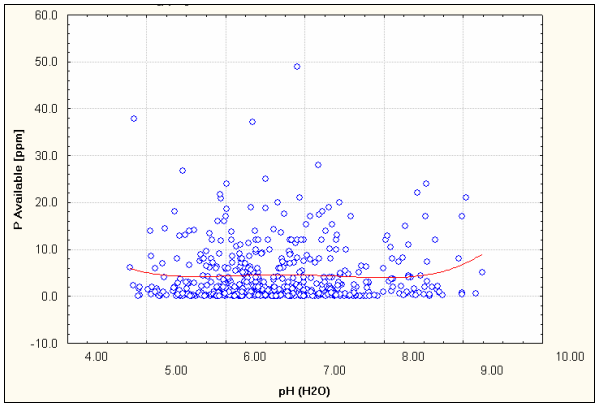

Figure 6.34. Plant-available P content (ppm = mg kg^{-1}) vs pH (H_2O)

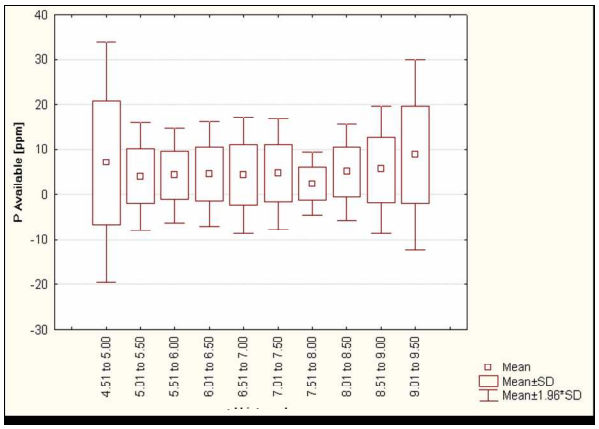

Figure 6.35. Plant-available P content (ppm = mg kg^{-1}), per pH-interval

The plant-available phosphorus levels of profiles, of topsoil and subsoil respectively, are shown in Figures 6.36 – 6.37.

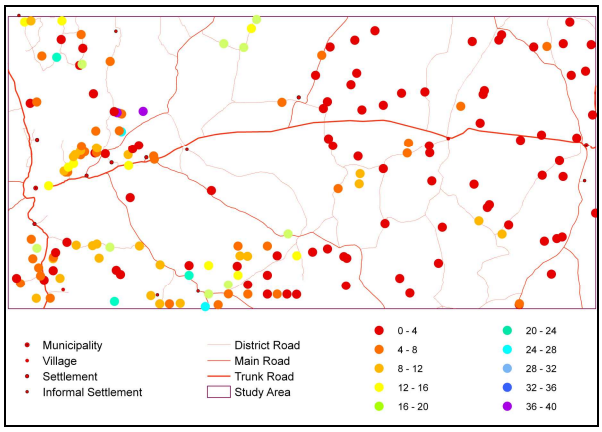

Figure 6.36. Plant-available P content (mg kg^{-1}) of topsoil

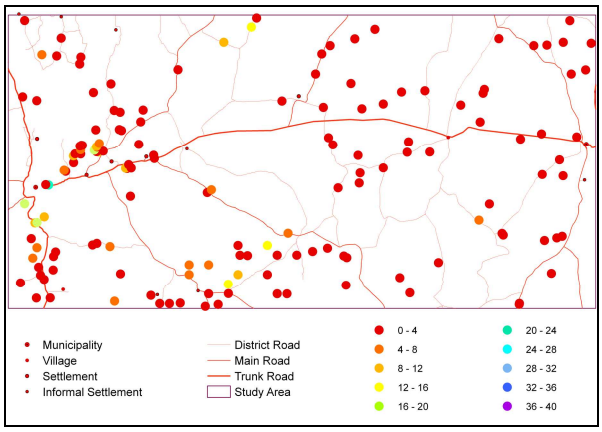

Figure 6.37. Plant-available P content (mg kg^{-1}) of subsoil

6.4 SULFUR[1]

Sulfur commonly occurs in igneous rocks as sulfides, such as pyrite [FeS_2], cinnabar [HgS], galena [PbS], sphalerite [(Zn,Fe)S], chalcopyrite [$CuFeS_2$], pentlandite [$(Fe,Ni)_9S_8$] and stibnite/antimonite [Sb_2S_3]. It also

[1] International Union of Pure and Applied Chemistry (IUPAC) adopted the spelling 'sulfur', rather than 'sulphur' in 1990 (Leigh, Favre and Metanomski, 1998).

occurs as sulfates in evaporitic settings and hydrothermal vein systems, e.g. as gypsum [$CaSO_4.2H_2O$], epsomite [$MgSO_4.7H_2O$], alunite [$KAl_3(SO_4)_2(OH)_6$] and barite [$BaSO_4$]. Sedimentary rocks which are formed under reducing conditions, e.g. shales, contain insoluble sulfides which are slowly oxidized to sulfates during weathering, on exposure to oxygen. Clay minerals and hydrous iron and aluminium oxides retain sulfate by adsorption (Whitehead, 2000).

Table 6.13: Typical sulfur concentrations (in mg kg^{-1}) found in some common rocks and soils.

SOURCE	Whitehead, 2000	Bowen, 1966	Camberato & Pan, 2000	Eriksen, Murphy & Schnug, 1998
Earth's crust				
Granite	58			
Basalt	123			
Shale	2 400			
Sandstone	240			
Limestone	1 200			
Soils from Granite	600			
Soils from Shale	1 000			
Soils from Sandstone	200			
Mineral Soils (general)	1 000 [200 – 2 000]	700 [30 – 900]	129 - 717	54 - 593

Deposition of atmospheric sulfur, in the form of sulfur dioxide [SO_2], hydrogen sulfide [H_2S], carbon disulfide [CS_2], dimethyl sulfide [$(CH_3)_2S$] and sulfate aerosols derived from sea spray, volcanic eruptions and burning of fossil fuels, contribute to soil sulfur content. Such contributions may vary from 1 – 2 kg ha^{-1} a^{-1} inland, to 8 – 10 kg ha^{-1} a^{-1} at the coast, for areas far from industrial development (such as Australia, New Zealand, South America), and 20 – 30 kg ha^{-1} a^{-1} near industrialized areas (Saggar, Hedley and Phimsarn, 1998). Fertilizers are also a source of soil sulfur in areas of intensive agriculture, but it is of no consequence in the study area.

Sulfur is relatively abundant in organic matter. In soil that has been under grassland for a long period, up to 90 % of all soil sulfur may be in organic forms. The remainder occur as sulfates in the soil solution and adsorbed on exchange sites (Whitehead, 2000). Grassland soils generally contain more sulfur than arable soils (Whitehead, 2000; Saggar *et al.*, 1998). Calcium and magnesium sulfates are precipitated under arid conditions, but are leached out under humid conditions. Typical S concentrations in saline soils of arid and semi-arid regions are more than 3 000 mg S kg^{-1} soil, humid temperate grassland soils contain between 200 and 1 000 mg S kg^{-1}, while leached sandy soils generally contain less than 200 mg S kg^{-1} (Whitehead, 2000). High Fe and Al oxide content and low pH decrease bioavailability of S from exchange sites (Saggar *et al.*, 1998). Mineralisation of organic soil S occurs at a rate of about 2 – 5 % of the organic-S (Saggar *et al.*, 1998).

Plants absorb sulfur in the form of the sulfate ion [SO_4^{2-}]. Sulfur is a component of several amino acids (e.g. cysteine, methionine), co-enzymes (e.g. biotin, thiamine), sulfonic acids, ferredoxins, sulfolipids, sulfated polysaccharides and proteins (Reuter and Robinson, 1997; Eriksen, Murphy and Schnug, 1998). The ratio of nitrogen to sulfur in plant proteins is generally around 36:1 in the number of atoms, or 15.7:1 on weight basis (Whitehead, 2000). Sulfur links adjacent polypeptide chains through the disulfide bonds of two cysteine units, thus playing an important role in the synthesis and functioning of proteins. As most enzymes are proteins,

sulfur is crucial for many physiological processes. Sulfur is found in glutathione, an antioxidant that protects plant tissues against damage from oxidation. Glutathione is a precursor of several compounds involved in detoxification of heavy metals, and it is a reservoir of reduced sulfur (Whitehead, 2000). Sulfolipids are structural elements of all biological membranes, and probably involved in regulation of ion transport across membranes (Whitehead, 2000). Methionine is a constituent of several proteins and is involved in the production of lignin, pectin, chlorophyll and flavonoids (Whitehead, 2000). Sulfur also plays a role in energy transfer and in plant structure (Reuter and Robinson, 1997).

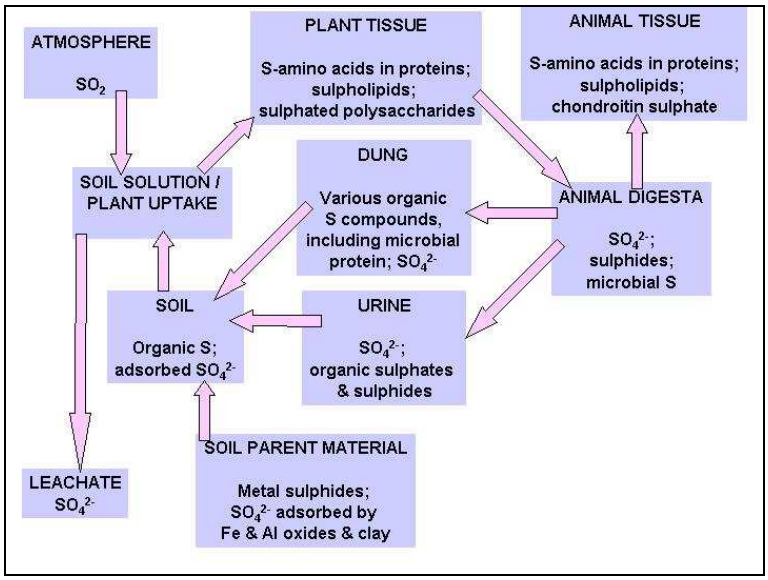

Figure 6.38. The major forms of sulfur involved in the cycling of sulfur in grassland (from Whitehead, 2000)

Table 6.14: Estimated sulfur balances (kg ha^{-1} $year^{-1}$) from an extensively managed grassland, grazed by beef cattle, in the United Kingdom (Whitehead, 2000).

	ESTIMATED S (KG HA^{-1} $YEAR^{-1}$)
INPUTS	
Deposition from atmosphere	15
ASPECT OF RECYCLING	
Uptake into herbage	6
Consumption of herbage by animals	3
Dead herbage to soil	5
Dead roots to soil	3
Excreta to soil of grazed area	2.8
OUTPUTS	
Animal products	0.16
Leaching / runoff	8
Loss through excreta off sward	0
GAIN TO SOIL	6

6.4.1 STATISTICAL ANALYSIS: SULFATE OF THE SATURATED PASTE EXTRACT

Table 6.15: Descriptive statistics – sulfate content (mg l^{-1}) of the saturated paste extract (n = 79).

	Sulfate
	mg l^{-1}
Mean	10.96
Median	9.1
Standard Deviation	6.09
Coefficient of Variation	0.56
Minimum	3.0
Maximum	29.5
Range	26.5
Lower Quartile	6.8
Upper Quartile	12.2
Quartile Range	5.4
Percentile 10	5.4
Percentile 90	20.9
Skewness	1.42
Kurtosis	1.47

Normality was rejected for sulfate by the statistical tests employed, namely the Shapiro-Wilk W test, Kolmogorov-Smirnov / Lilliefors test, and three D'Agostino tests based in skewness, on kurtosis, and on a combination of skewness and kurtosis (AnalystSoft, 2007).

Table 6.16: Distribution in terms of deciles – sulfate content (mg l^{-1}) (n = 79)

	Decile	**Sulfate**
		mg l^{-1}
minimum		3.0
	1	5.4
	2	6.3
	3	7.0
	4	8.1
median	5	9.1
	6	10.2
	7	11.8
	8	14.5
	9	20.9
maximum	10	29.5

The **sulfate** content of 79 samples from the study area ranges from 3.0 to 29.5 mg l^{-1}. The mean (10.96 mg l^{-1}) is higher than the median (9.10 mg l^{-1}), with a skewness of 1.42 and kurtosis of 1.47. The standard deviation is 6.09. Half the samples have sulfate concentrations of between 6.8 (1^{st} quartile) and 12.2 mg l^{-1} (3^{rd} quartile), for a quartile range of 5.4. In 80 % of samples, the sulfate content is between 5.4 (1^{st} decile) and 20.9 mg l^{-1} (9^{th} decile). The frequency distribution is shown in Table 6.16 and Figures 6.39 – 6.40.

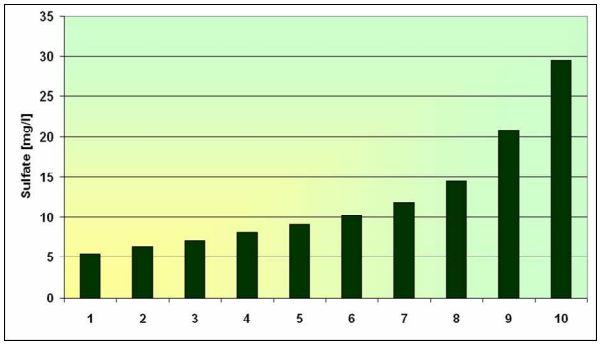

Figure 6.39. Decile distribution of sulfate content (mg l^{-1})

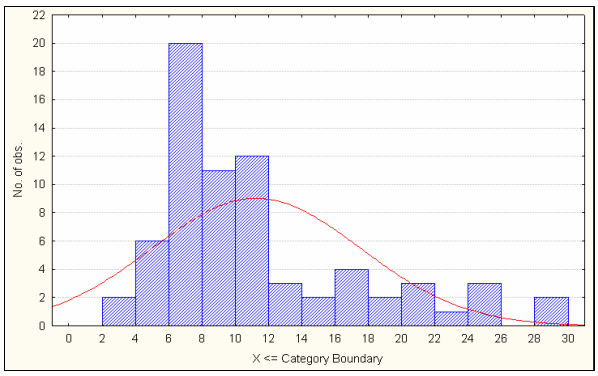

Figure 6.40. Histogram of sulfate content (mg l^{-1})

A statistically significant correlation, at $p < 0.05$, was found between sulfate content and electrical conductivity of the saturated paste extract ($r^2 = 0.36$) (Figure 6.41). Significant, but weak, correlations, at $p < 0.05$, were found with exchangeable potassium ($r^2 = 0.22$), electrical conductivity of the 2:5 soil:water suspension ($r^2 = 0.20$), chloride ($r^2 = 0.14$), coarse sand ($r^2 = 0.12$), extractable potassium ($r^2 = 0.11$), and organic matter ($r^2 = 0.10$).

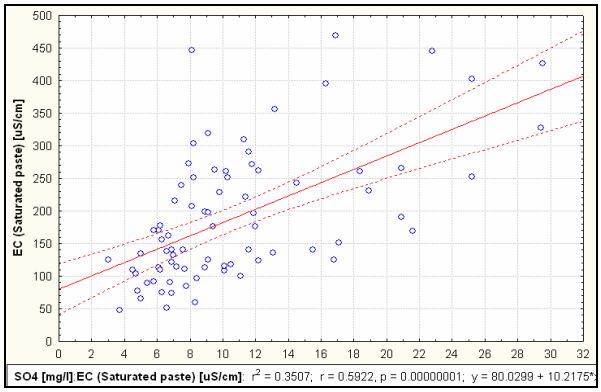

Figure 6.41. Sulfate (saturated paste) content (mg l^{-1}) vs EC (saturated paste) (uS cm^{-1})

Topsoil sulfate concentrations are virtually the same as those of the subsoil (Table 6.17; Figure 6.42). The prevailing semi-arid climate, and subsequent low organic matter content, is probably the reason why there is no significant sulfate enrichment of the topsoil.

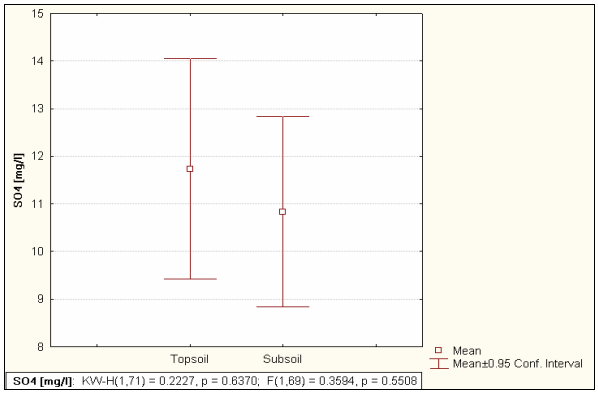

Figure 6.42. Sulfate content (mg l^{-1}), per topsoil and subsoil

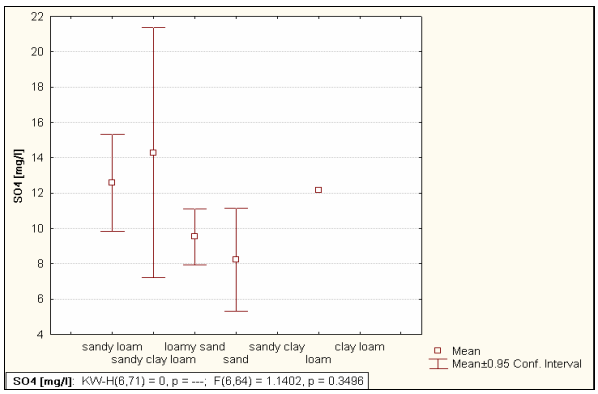

Figure 6.43. Sulfate content (mg l^{-1}), per textural class

Table 6.17: Sulfate content (mg l^{-1}), per topsoil and subsoil.

Sulfate mg l^{-1}	**Topsoil** (n = 34)	**Subsoil** (n = 37)
Mean	11.73	10.83
Median	9.12	9.54
Std. Dev.	6.64	6.00
Minimum	3.70	3.02
Maximum	29.39	29.45
Range	25.69	26.43
Lower Quartile	6.77	6.85
Upper Quartile	16.25	11.95
Quartile Range	9.48	5.10
Percentile 10	6.21	5.44
Percentile 90	22.78	20.88

Sulfate increases in the order sand → loamy sand → sandy loam → loam, though there is considerable overlap in the ±0.95 confidence limits (Figure 6.43).

Sulfate concentrations increase in the order: soils formed *in situ* → aeolian origin → alluvial origin → colluvial origin of parent material, though there is considerable overlap in the ±0.95 confidence limits (Figure 6.44).

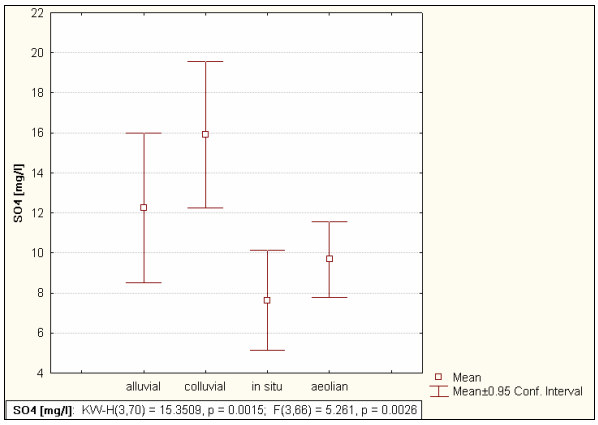

Figure 6.44. Sulfate content (mg l^{-1}), per origin of parent material

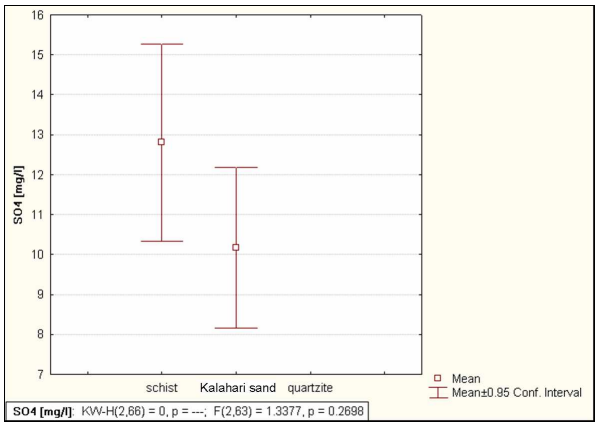

Figure 6.45. Sulfate content (mg l^{-1}), per type of parent material

Sulfate concentrations are somewhat lower in the Kalahari sands than in soils formed on the schist of the Khomas Hochland – a consequence of the mineral composition of the respective parent materials (Figure 6.45).

Arenosols and Regosols have lower SO_4^{2-} concentrations than Leptosols, Luvisols, Calcisols and, especially, Cambisols (Table 6.18; Figure 6.46).

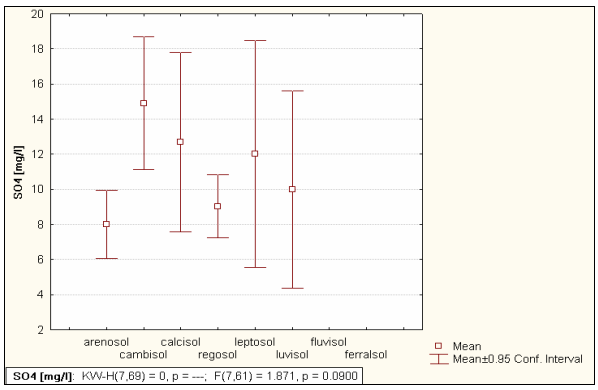

Figure 6.46. Sulfate content (mg l^{-1}), per WRB reference soil group

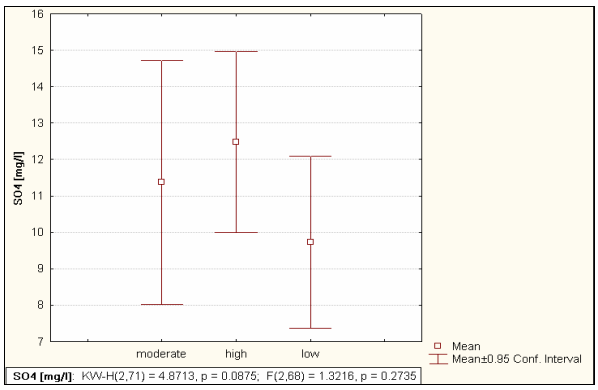

Figure 6.47. Sulfate content (mg l^{-1}), per degree of dissection of the landscape

Table 6.18: Sulfate content, per WRB reference soil group.

Sulfate mg l^{-1}	**Arenosols** (n = 9)	**Calcisols** (n = 9)	**Leptosols** (n = 9)	**Cambisols** (n = 14)	**Regosols** (n = 25)	**Luvisols** (n = 3)
Mean	8.01	12.69	12.01	14.90	9.03	9.99
Median	8.91	10.23	8.05	15.62	6.95	10.13
Std. Dev.	2.54	6.66	8.42	6.54	4.36	2.26
Minimum	4.71	5.81	3.70	6.67	3.02	7.66
Maximum	11.10	25.20	26.00	29.39	21.63	12.18
Range	6.39	19.39	22.30	22.72	18.61	4.52
Lower Quartile	4.96	9.43	6.77	7.91	6.21	7.66
Upper Quartile	10.08	11.61	16.25	18.94	11.27	12.18
Quartile Range	5.12	2.18	9.48	11.03	5.06	4.52
Percentile 10	4.71	5.81	3.70	7.21	5.78	7.66
Percentile 90	11.10	25.20	26.00	20.92	15.52	12.18

There is a slight increase in sulfate concentrations from low to high degree of dissection of the landscape, though there is considerable overlap in the ±0.95 confidence limits (Figure 6.47).

The sulfate (saturated paste extract) levels of profiles, of topsoil and subsoil respectively, are shown in Figures 6.48 – 6.49.

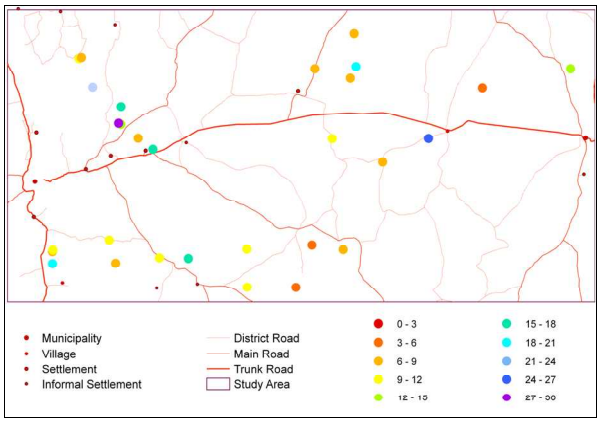

Figure 6.48. Sulfate content (mg l^{-1}) of topsoil

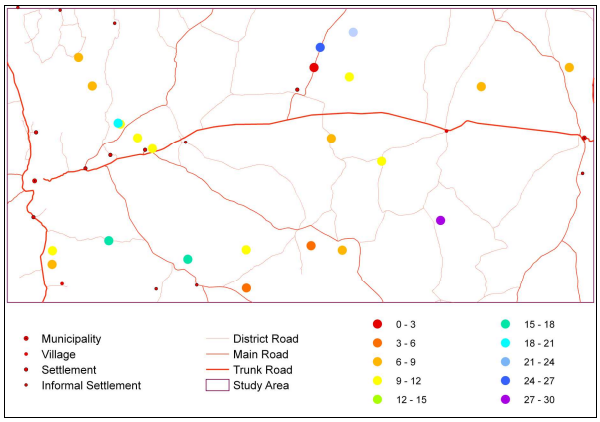

Figure 6.49. Sulfate content (mg l^{-1}) of subsoil

CHAPTER SEVEN

CHEMICAL CHARACTERISATION – BASES

7.1 INTRODUCTION

Calcium and magnesium – alkaline earth metals – and potassium and sodium – alkali metals – are known as basic cations or bases, as soils tend to be alkaline (basic) when the cation exchange complex is entirely saturated with them (Forth, 1990). Calcium, magnesium and potassium are essential plant nutrients, whereas sodium has been shown to be beneficial to some plants, without satisfying the criteria for essentiality (Whitehead, 2000).

7.2 CALCIUM

Calcium is the 5th most plentiful element in the Earth's crust. It occurs commonly in sedimentary rocks in the minerals calcite [$CaCO_3$], dolomite [$CaMg(CO_3)_2$] and gypsum [$CaSO_4 \cdot 2H_2O$], as well as in igneous and metamorphic rocks, mainly in the silicate minerals augite [$(Ca,Mg,Fe)SiO_3$], epidote [$Ca_2(Al, Fe)_3(SiO_4)_3(OH)$], hornblende [$Ca_2(Mg, Fe, Al)_5 (Al, Si)_8O_{22}(OH)_2$], plagioclase [$NaAlSi_3O_8$ to $CaAl_2Si_2O_8$], amphiboles [$Ca_2Mg_5Si_8O_{22} (OH)_2$ and $Ca_2(Fe,Mg)_5 Si_8O_{22}(OH)_2$ and $(Na,Ca)_2(Mg,Fe,Al)_5(SiAl)_8O_{22}(OH)_2$], pyroxenes [$CaMgSi_2O_6$ and $Ca(Mg,Fe,Al)Si_2O_2$] and some types of garnets [$Ca_3Y_2(SiO_4)_3$, where Y can be $Al^{3+}/Fe^{3+}/Cr^{3+}$]. There are about 159 minerals containing calcium. Relative abundance in some parent materials decreases from calcareous sedimentary rock through basic igneous rock to acid igneous rock (Jenny, 1941).

Table 7.1: Typical calcium concentrations (in mg kg^{-1}) found in the earth's crust, some common rocks and soils.

SOURCE	Whitehead, 2000	Bruce, 1999	Helmke, 2000
Earth's crust		36 000	
Granite	9 900		
Basalt	78 300		
Shale	22 100		
Sandstone	39 100		
Limestone	302 300		
Soils from Granite	3 600		
Soils from Shale	1 300		
Soils from Sandstone	5 300		
Entisol			17 600
Spodosol			19 300
Alfisol			150 000
Mollisol			11 000
Soils (general)	18 000 [10 000 – 250 000]	1 000 – 10 000 (non-calcareous); 10 000 (calcareous)	13 700 [7 000 – 500 000]

Calcium occurs in minerals, as constituents of inorganic and organic compounds, as ions on the exchange complex and in the soil solution. Bioavailability is governed by parent material, ion exchange reactions,

biological transformations, loss from the crop root zone by leaching and crop removal from the field and replenishment via atmospheric deposition, fertilizer and soil amendments (Camberato and Pan, 2000). Calcium is more tightly retained by 2:1 than by 1:1 clay minerals and organic matter. It is readily available in alkaline soil, while acidity suppresses its availability through lower cation exchange capacity and lower quantities of basic cations in the soil.

Much of the plant calcium is bound to the galacturonic acid component of pectin (Whitehead, 2000). Calcium oxalates and other calcium organic acids are found in the apoplasm or vacuoles (Camberato and Pan, 2000). It contributes to maintenance of osmotic potential, cation-anion balance and cellular pH (Reuter and Robinson, 1997). It plays a role in the structure, integrity, permeability and selectivity of membranes (Foth, 1990), with calcium being an important constituent of middle lamellae of cell walls (Whitehead, 2000). Being divalent, calcium can link adjacent polymer molecules that contain acidic groups, playing a role cell division and elongation (Reuter and Robinson, 1997), and thus in the growth of meristems and root tips (Whitehead, 2000). Calcium is required by a number of enzymes such as α-amylase and some nucleases (Clarkson and Hanson, 1980; Blevins, 1994). It functions as a messenger in environmental signals (Reuter and Robinson, 1997). Parker and Truog (1920) established that grasses contain far less calcium (~4 000 mg Ca kg^{-1}) than dicotyledons, legumes and brassicas (~12 000 – 18 000 mg Ca kg^{-1}).

7.2.1 STATISTICAL ANALYSIS: EXTRACTABLE AND EXCHANGEABLE CALCIUM CONTENT

Normality was rejected for extractable and exchangeable Ca content by the statistical tests employed, namely the Shapiro-Wilk W test, Kolmogorov-Smirnov / Lilliefors test, and three D'Agostino tests based in skewness, on kurtosis, and on a combination of skewness and kurtosis (AnalystSoft, 2007).

Table 7.2: Descriptive statistics – extractable calcium content (n = 535) and exchangeable calcium content (n = 396).

	Ca extractable		Ca exchangeable
	mg kg^{-1}	$cmol_c$ kg^{-1}	$cmol_c$ kg^{-1}
Mean	613.45	3.07	2.30
Median	412	2.06	1.32
Standard Deviation	750.08	3.75	2.99
Coefficient of Variation	1.22	1.22	1.30
Minimum	8	0.04	0.00
Maximum	6 606	33.03	19.46
Range	6 598	32.99	19.46
Lower Quartile	218	1.09	0.61
Upper Quartile	680	3.40	2.60
Quartile Range	462	2.31	1.99
Percentile 10	122	0.61	0.21
Percentile 90	1146	5.73	6.02
Skewness	3.67	3.67	2.75
Kurtosis	17.64	17.64	8.92

The **extractable calcium** content of 535 samples from the study area ranges from 0.04 to 33.03 $cmol_c$ kg^{-1}. The mean (3.07 $cmol_c$ kg^{-1}) is considerably higher than the median (2.06 $cmol_c$ kg^{-1}), with a skewness of 3.67 and kurtosis of 17.64. The standard deviation is 3.75 $cmol_c$ kg^{-1}. Half the samples have calcium

concentrations of between 1.09 (1st quartile) and 3.40 $cmol_c\ kg^{-1}$ (3rd quartile), for a quartile range of 2.32 $cmol_c\ kg^{-1}$. In 80 % of samples, the Ca content is between 0.61 (1st decile) and 5.73 $cmol_c\ kg^{-1}$ (9th decile). The lower 90 % of samples are fairly normally distributed, with the upper 10 % contributing most to the skewness. The frequency distribution is shown in Table 7.3 and Figures 7.1 – 7.2.

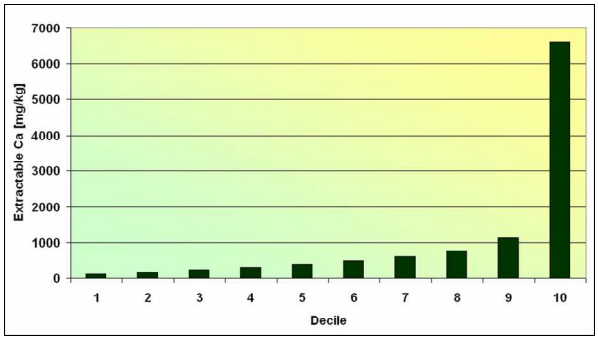

Figure 7.1. Decile distribution of extractable calcium content (mg kg^{-1})

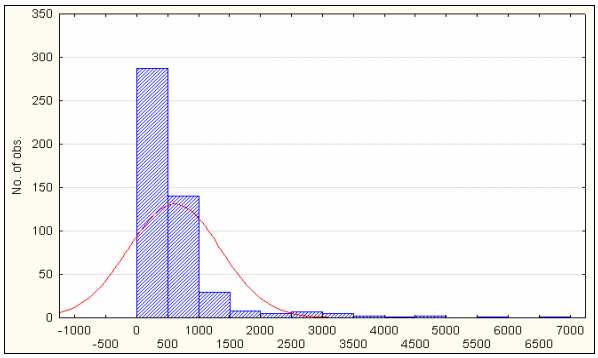

Figure 7.2. Histogram of extractable calcium content (mg kg^{-1})

Table 7.3: Distribution in terms of deciles – extractable calcium content (n = 535) and exchangeable calcium content (n = 396).

	Decile	Ca extractable		Ca exchangeable
		mg kg^{-1}	$cmol_c\ kg^{-1}$	$cmol_c\ kg^{-1}$
minimum		8	0.04	0.00
	1	122	0.61	0.21
	2	191	0.96	0.39
	3	249	1.25	0.78
	4	314	1.57	1.04
median	5	411	2.06	1.32
	6	506	2.53	1.65
	7	615	3.08	2.11
	8	781	3.91	3.09
	9	1 145	5.73	6.02
maximum	10	6 606	33.03	19.46

Statistically significant correlations, at $p < 0.05$, were found between extractable calcium content and respectively the sum of extractable bases ($r^2 = 0.95$), sum of exchangeable bases (S-value) ($r^2 = 0.64$), exchangeable calcium content ($r^2 = 0.62$), cation exchange capacity ($r^2 = 0.59$), fluoride content ($r^2 = 0.45$), and pH (H_2O) ($r^2 = 0.35$), as shown in Figures 7.3 – 7.8.

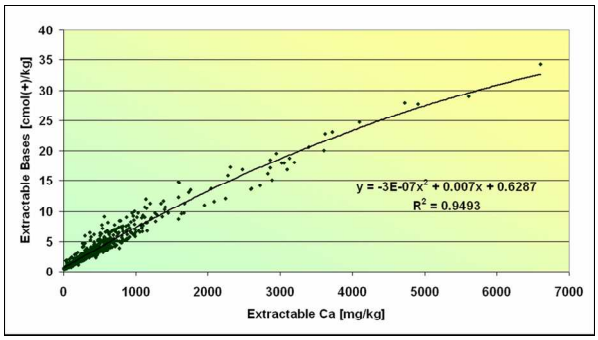

Figure 7.3. Extractable Ca content (mg kg^{-1}) vs sum of extractable bases ($cmol_c\ kg^{-1}$)

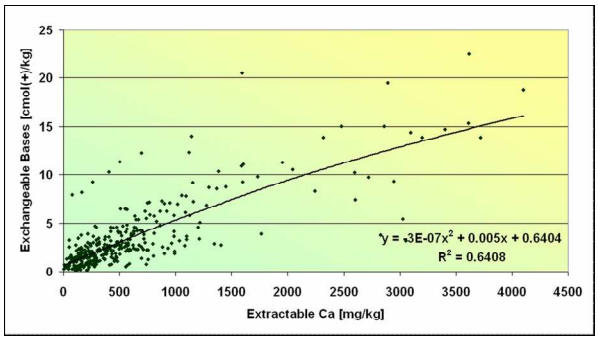

Figure 7.4. Extractable Ca content (mg kg^{-1}) vs sum of exchangeable bases ($cmol_c\ kg^{-1}$)

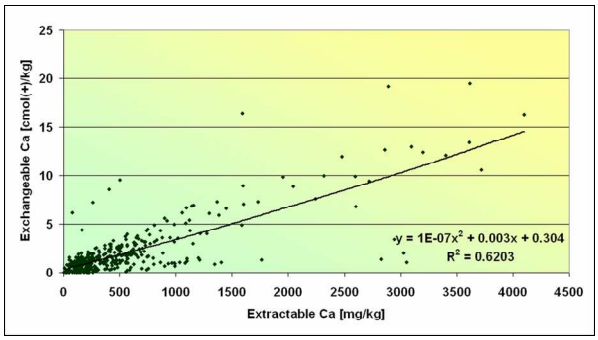

Figure 7.5. Extractable Ca content (mg kg^{-1}) vs exchangeable Ca content ($cmol_c$ kg^{-1})

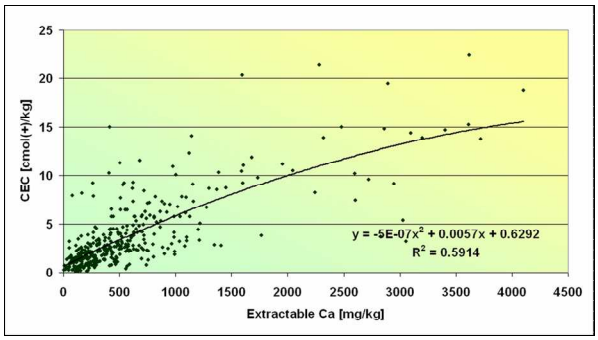

Figure 7.6. Extractable Ca (mg kg^{-1}) content vs CEC ($cmol_c$ kg^{-1})

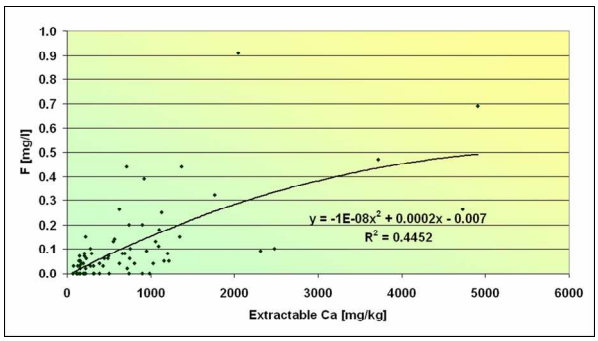

Figure 7.7. Extractable Ca content (mg kg^{-1}) vs F content (mg l^{-1})

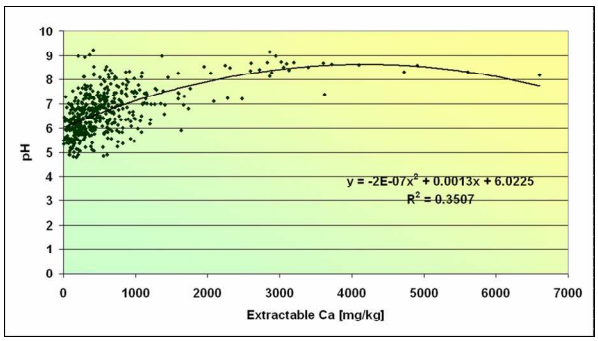

Figure 7.8. Extractable Ca content (mg kg^{-1}) vs pH (H_2O)

Significant, but weak, correlations were found with extractable magnesium content (r^2 = 0.23), electrical conductivity measured in a saturated paste (r^2 = 0.22), exchangeable magnesium content (r^2 = 0.18), clay content (r^2 = 0.13), sand content (r^2 = 0.11).

The **exchangeable calcium content** content of 396 samples from the study area ranges from 0 to 19.46 $cmol_c$ kg^{-1} (Figures 7.17 – 7.21). The mean (2.30 $cmol_c$ kg^{-1}) is considerably higher than the median (1.32 $cmol_c$ kg^{-1}), with a skewness of 2.75 and kurtosis of 8.92. The standard deviation is 2.99. Half the samples have calcium content concentrations of between 0.61 (1st quartile) and 2.60 $cmol_c$ kg^{-1} (3rd quartile), for a quartile range of 1.99. In 80 % of samples, the exchangeable Ca content is between 0.21 (1st decile) and 6.02 $cmol_c$ kg^{-1}. See Table 7.3 and Figures 7.9 – 7.10 for the frequency distribution.

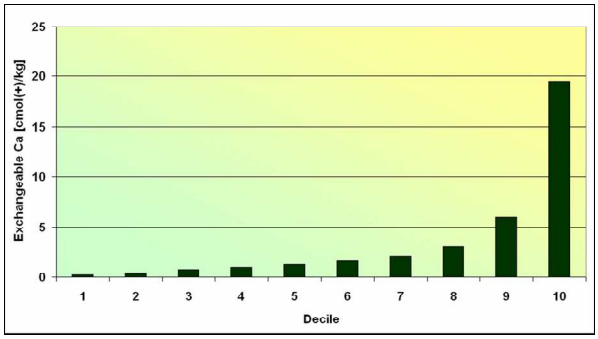

Figure 7.9. Decile distribution of exchangeable calcium content ($cmol_c$ kg^{-1})

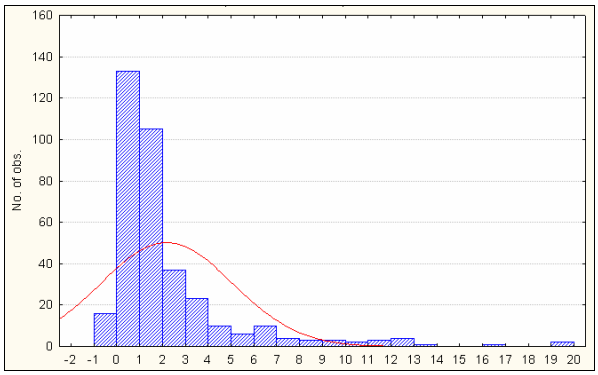

Figure 7.10. Histogram of exchangeable calcium content ($cmol_c$ kg^{-1})

The concentrations of exchangeable calcium content found in the study area are consistent with values quoted in literature, such as 30 – 40 $cmol_c\ kg^{-1}$ for neutral to alkaline Australian soils (Bruce, 1999); means of 2.4 $cmol_c\ kg^{-1}$ for acidic Australian topsoils and 0.74 $cmol_c\ kg^{-1}$ for acidic Australian subsoils, respectively (Bruce, 1999); 14.0 – 16.1 $cmol_c\ kg^{-1}$ (Forth, 1990).

Statistically significant correlations, at $p < 0.05$, were found between exchangeable calcium content and respectively the sum of exchangeable bases (S-value) ($r^2 = 0.93$), cation exchange capacity ($r^2 = 0.82$), extractable calcium content ($r^2 = 0.62$), the sum of extractable bases ($r^2 = 0.57$), and pH ($r^2 = 0.45$), as shown in Figures 7.5 and 7.11 - 7.14.

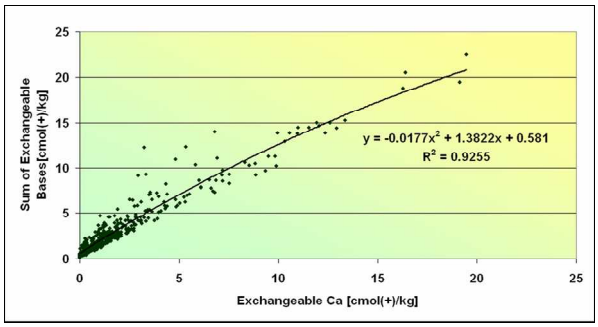

Figure 7.11. Exchangeable Ca content ($cmol_c\ kg^{-1}$) vs sum of exchangeable bases ($cmol_c\ kg^{-1}$)

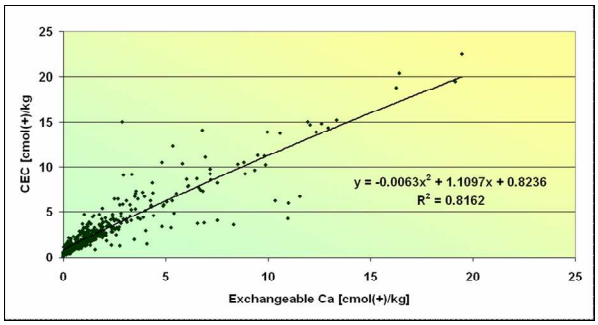

Figure 7.12. Exchangeable Ca content ($cmol_c\ kg^{-1}$) vs CEC ($cmol_c\ kg^{-1}$)

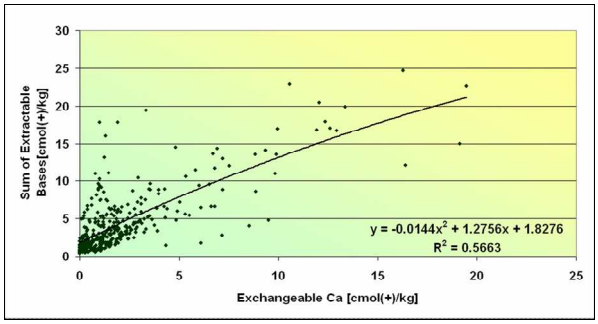

Figure 7.13. Exchangeable Ca content ($cmol_c\ kg^{-1}$) vs sum of extractable bases ($cmol_c\ kg^{-1}$)

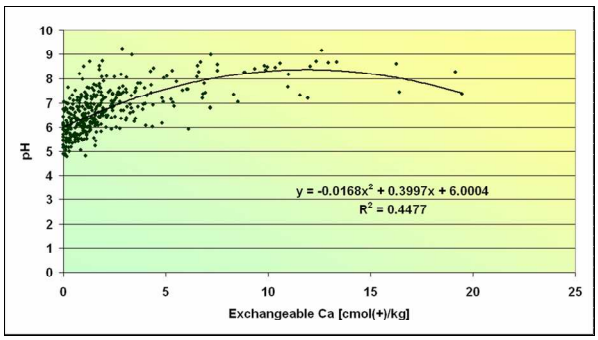

Figure 7.14. Exchangeable Ca content ($cmol_c\ kg^{-1}$) vs pH (H_2O)

Significant, but weak, correlations were found with fluoride content ($r^2 = 0.27$), exchangeable magnesium content ($r^2 = 0.17$), electrical conductivity measured in a 2:5 soil:water suspension ($r^2 = 0.16$), sand content ($r^2 = 0.15$), and extractable magnesium content ($r^2 = 0.15$).

Topsoil Ca concentrations (both extractable and exchangeable) are noticeably lower than subsoil Ca concentrations (Table 7.4; Figures 7.15 – 7.16). This is most likely caused by removal of topsoil calcium through grazing, eluviation of topsoil, accumulation of leached calcium lower down in the profile and additions through weathering of parent material. These results are consistent with literature, for example the findings of Materechera, Mandiringana and Mbokodi (1998) and Kotze and Du Preez (2008).

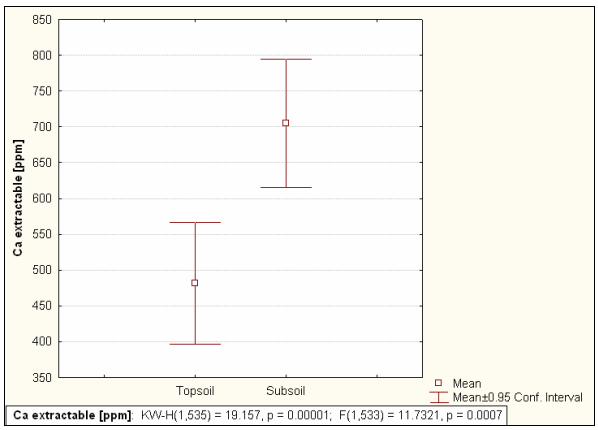

Figure 7.15. Extractable Ca content (ppm = mg kg^{-1}), per topsoil and subsoil

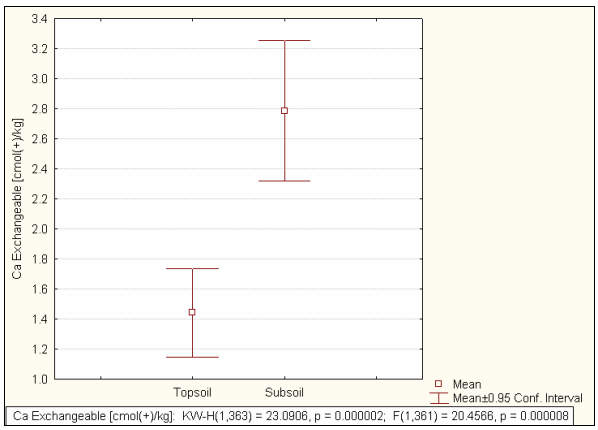

Figure 7.16. Exchangeable Ca content ($cmol_c$ kg^{-1}), per topsoil and subsoil

Table 7.4: Descriptive statistics of extractable Ca content (mg kg^{-1} and $cmol_c$ kg^{-1}) and exchangeable Ca content ($cmol_c$ kg^{-1}), per topsoil and subsoil.

	Ca extractable				Ca exchangeable	
	Topsoil (n = 199)		Subsoil (n = 289)		Topsoil (n = 161)	Subsoil (n = 202)
	mg kg^{-1}	$cmol_c$ kg^{-1}	mg kg^{-1}	$cmol_c$ kg^{-1}	$cmol_c$ kg^{-1}	$cmol_c$ kg^{-1}
Mean	483.54	2.42	697.69	3.49	1.44	2.78
Median	342.0	1.71	457.0	2.29	0.98	1.57
Std Dev	624.63	3.12	804.1	4.02	1.89	3.37
Minimum	8.0	0.04	24.0	0.12	0.00	0.00
Maximum	5610	28.05	6 606.0	33.03	12.94	19.46
Range	5602	28.01	6 582.0	32.19	12.94	19.46
Lower Quartile	182	0.91	266.0	1.33	0.34	0.80
Upper Quartile	618	3.09	780.0	3.9	1.66	3.31
Quartile Range	436	2.18	514.0	2.57	1.32	2.51
Percentile10	108	0.54	138.00	0.69	0.17	0.23
Percentile 90	823	4.12	1412.0	7.06	2.91	6.94

When disregarding clay loam and sandy clay soils (too few samples to be representative), it emerges that sandy, loamy sand and loam soils have noticeably lower concentrations of both extractable and exchangeable Ca, than those of sandy loams and sandy clay loams (Figures 7.17 – 7.18).

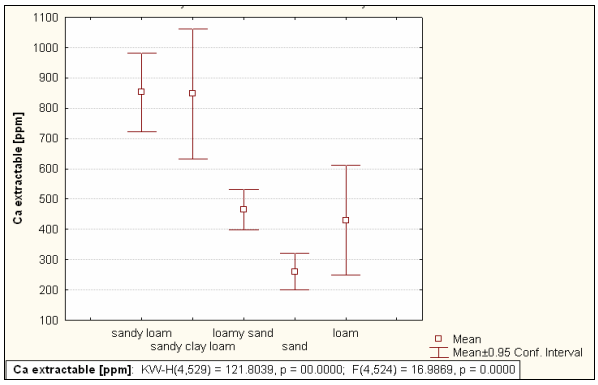

Figure 7.17. Extractable Ca content (ppm = mg kg^{-1}), per textural class

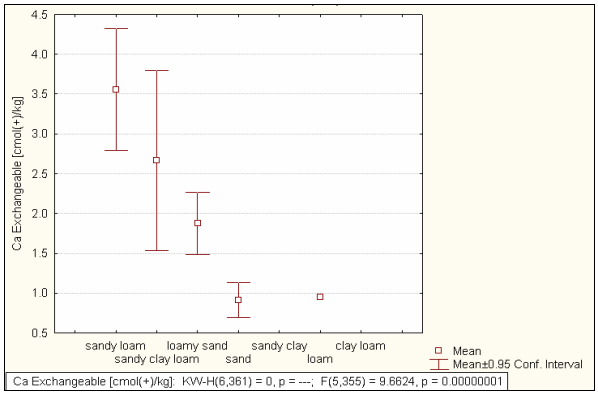

Figure 7.18. Exchangeable Ca content ($cmol_c$ kg^{-1}), per textural class

Alluvial parent material contains significantly more extractable and exchangeable Ca than those of aeolian or colluvial origin, or soils formed by weathering *in situ* (Figures 7.19 – 7.20).

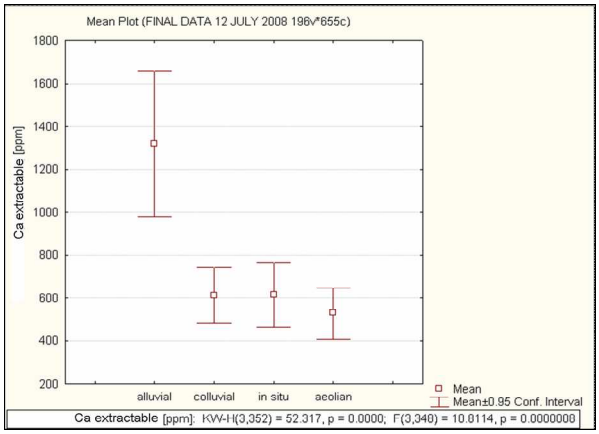

Figure 7.19. Extractable Ca content (ppm = mg kg^{-1}), per origin of parent material

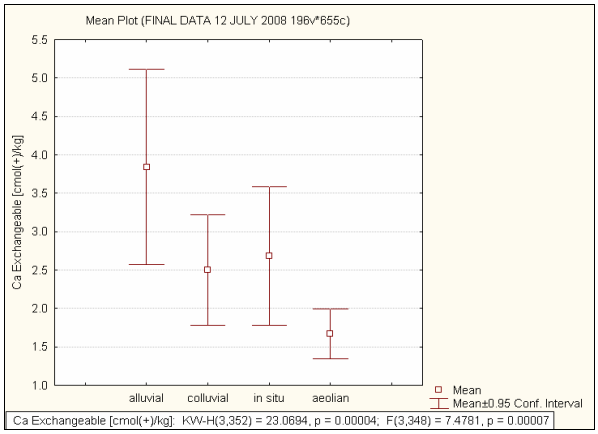

Figure 7.20. Exchangeable Ca content ($cmol_c$ kg^{-1}), per origin of parent material

Extractable Ca concentrations are significantly lower in the Kalahari sands than the soils formed on the schist of the Khomas Hochland – a direct consequence of the mineral composition of the respective parent materials (Figures 7.21 – 7.22). The means of extractable Ca content in the case of quartzite, and of exchangeable Ca content in the case of sandstone and quartzite are also lower than those of schist, though the ±0.95 confidence intervals overlap, precluding firm predictions.

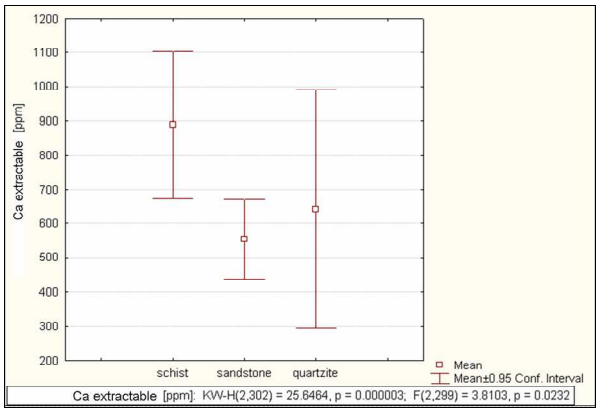

Figure 7.21. Extractable Ca content (ppm = mg kg^{-1}), per type of parent material

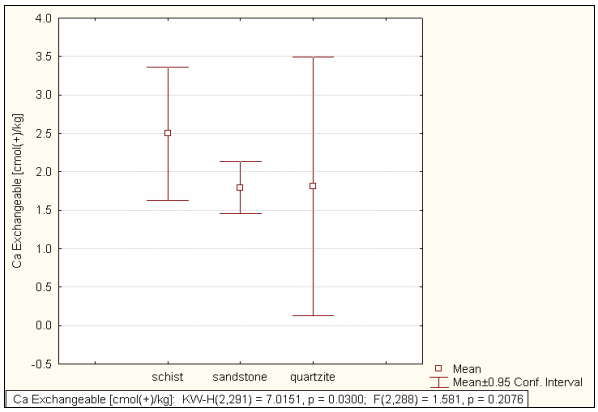

Figure 7.22. Exchangeable Ca content ($cmol_c$ kg^{-1}), per type of parent material

As expected, Calcisols from the study area contain far more extractable and exchangeable Ca than any of the other soil types (Figures 7.23 – 7.24). Cambisols and Luvisols have higher extractable Ca concentrations than Arenosols and Regosols. Cambisols have higher exchangeable Ca concentrations than Arenosols, Regosols and Luvisols. The mean exchangeable Ca content of Leptosols is considerably higher than those of Arenosols, Regosols, Cambisols and Luvisols, but there is an appreciable overlap in the ±0.95 confidence intervals.

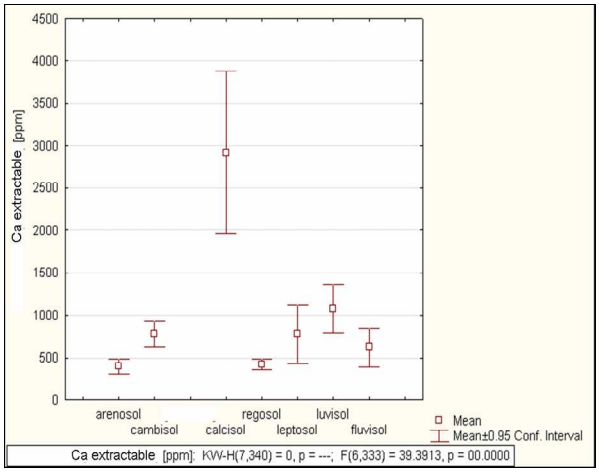

Figure 7.23. Extractable Ca content (ppm = mg kg^{-1}), per WRB reference soil group

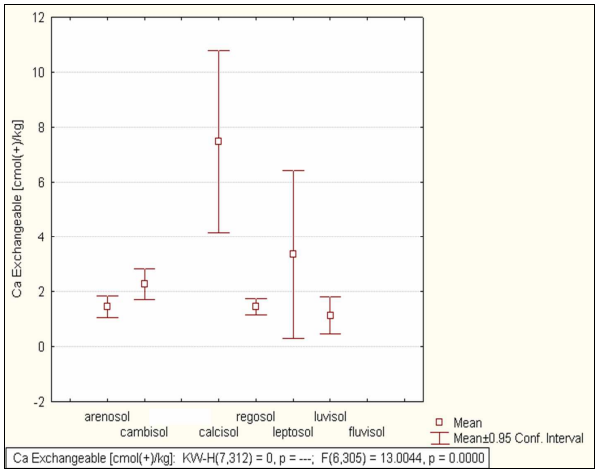

Figure 7.24. Exchangeable Ca content ($cmol_c$ kg^{-1}), per WRB reference soil group

Table 7.5: Descriptive statistics of extractable Ca content (mg kg^{-1} and $cmol_c kg^{-1}$) and exchangeable Ca content ($cmol_c kg^{-1}$), per WRB reference soil group.

Ca extractable mg kg^{-1}	**Arenosols** (n = 132)	**Calcisols** (n = 17)	**Leptosols** (n = 24)	**Fluvisols** (n = 6)	**Cambisols** (n = 66)	**Regosols** (n = 89)	**Luvisols** (n = 3)
Mean	394.7	2917.9	777.5	620.2	776.0	425.1	1 074.0
Median	220.50	3 054	534	654.5	631	328	1 034
Std.Dev.	545.9	1 859.2	816.1	217.2	637.2	303.4	113.4
Minimum	8	496	26	360	54	56	986
Maximum	2 892	6 606	3 622	872	3 202	1 406	1 202
Range	2 884	6 110	3 596	512	3 148	1 350	216
Lower Quartile	126.5	1 130	296	368	368	202	986
Upper Quartile	469.5	4104	848	812	1 022	590	1 202
Quartile Range	343	2974	552	444	654	388	216
Percentile 10	80	630	150	360	254	120	986
Percentile 90	612	5 610	1 734	872	1 386	932	1 202
Ca extractable $cmol_c$ kg^{-1}	**Arenosols** (n = 132)	**Calcisols** (n = 17)	**Leptosols** (n = 24)	**Fluvisols** (n = 6)	**Cambisols** (n = 66)	**Regosols** (n = 89)	**Luvisols** (n = 3)
Mean	1.97	14.59	3.89	3.10	3.88	2.13	5.37
Median	1.10	15.27	2.67	3.27	3.16	1.64	5.17
Std.Dev.	2.73	9.30	4.08	1.09	3.19	1.52	0.57
Minimum	0.04	2.48	0.13	1.80	0.27	0.28	4.93
Maximum	14.46	33.03	18.11	4.36	16.01	7.03	6.01
Range	14.42	30.55	17.98	2.56	15.74	6.75	1.08
Lower Quartile	0.63	5.65	1.48	1.84	1.84	1.01	4.93
Upper Quartile	2.35	20.52	4.24	4.06	5.11	2.95	6.01
Quartile Range	1.72	14.87	2.76	2.22	3.27	1.94	1.08
Percentile 10	0.40	3.15	0.75	1.80	1.27	0.60	4.93
Percentile 90	3.06	28.05	8.67	4.36	6.93	4.66	6.01
Ca exchangeable $cmol_c$ kg^{-1}	**Arenosols** (n = 129)	**Calcisols** (n = 13)	**Leptosols** (n = 15)	**Fluvisols** (n = 0)	**Cambisols** (n = 61)	**Regosols** (n = 88)	**Luvisols** (n = 3)
Mean	1.45	7.49	3.35	-	2.26	1.44	1.13
Median	0.80	7.20	1.01	-	1.58	1.06	1.00
Std.Dev.	2.34	5.48	5.54	-	2.15	1.38	0.27
Minimum	0.00	0.60	0.09	-	0.00	0.00	0.95
Maximum	19.14	16.27	19.46	-	12.35	6.81	1.45
Range	19.14	15.67	19.37	-	12.35	6.81	0.50
Lower Quartile	0.29	2.70	0.21	-	0.80	0.47	0.95
Upper Quartile	1.67	12.62	3.99	-	3.09	1.82	1.45

Quartile Range	1.38	9.92	3.78	-	2.29	1.35	0.50
Percentile 10	0.03	1.00	0.11	-	0.26	0.22	0.95
Percentile 90	2.72	13.36	11.93	-	5.05	2.94	1.45

Exchangeable Ca concentrations are highest in the lowest landscape positions (valleys and lower slopes), and lowest in the higher landscape positions (mid-slopes, upper slopes and ridges) (Figure 7.26). There is more ambiguity in the case of extractable Ca content, with upper slopes containing higher than expected Ca concentrations, and a wide ±0.95 confidence interval (Figure 7.25).

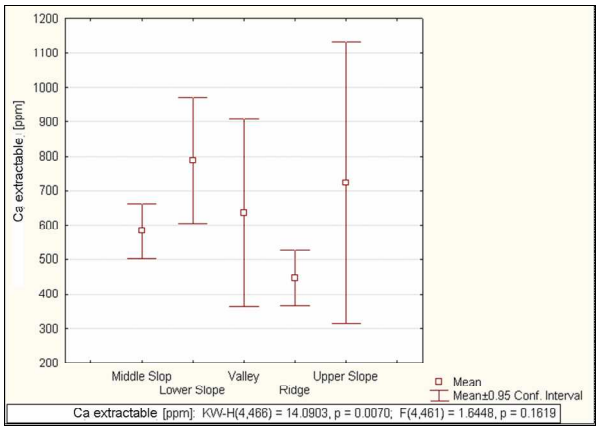

Figure 7.25. Extractable Ca content (ppm = mg kg^{-1}), per position in the landscape

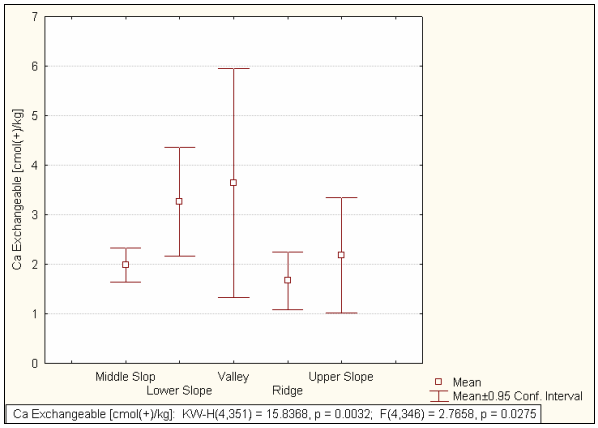

Figure 7.26. Exchangeable Ca content ($cmol_c$ kg^{-1}), per position in the landscape

Exchangeable Ca concentrations increase with the degree of dissection (Figure 7.28). The same trend, though with more overlap in the ±0.95 confidence intervals, is apparent in the case of extractable Ca content (Figure 7.27). One explanation is greater rates of erosion and subsequent weathering in more dissected terrain. Secondly, the highly dissected terrain of the study area occurs mainly on schist, quartzite and calcrete, whereas the less dissected areas, towards the east, are mainly covered with Kalahari sands.

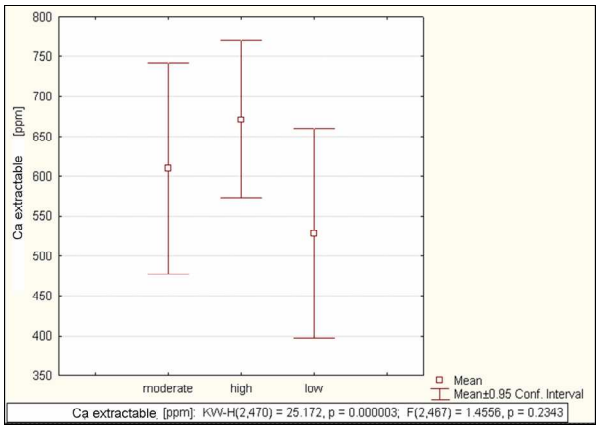

Figure 7.27. Extractable Ca content (ppm = mg kg^{-1}), per degree of dissection of the landscape

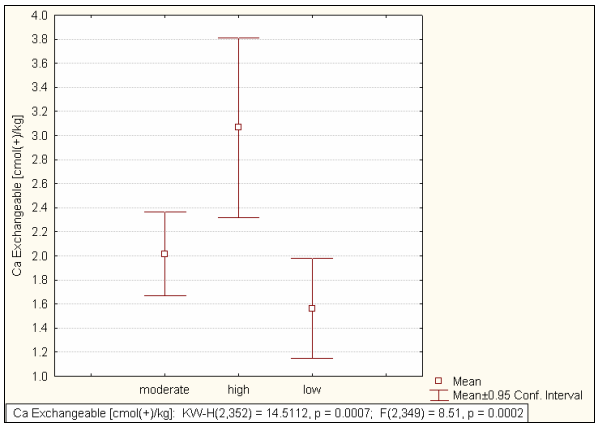

Figure 7.28. Exchangeable Ca content ($cmol_c$ kg^{-1}), per degree of dissection of the landscape

The extractable and exchangeable Ca content of profiles in the study area of topsoil and subsoil respectively, are shown in Figures 7.29 – 7.32.

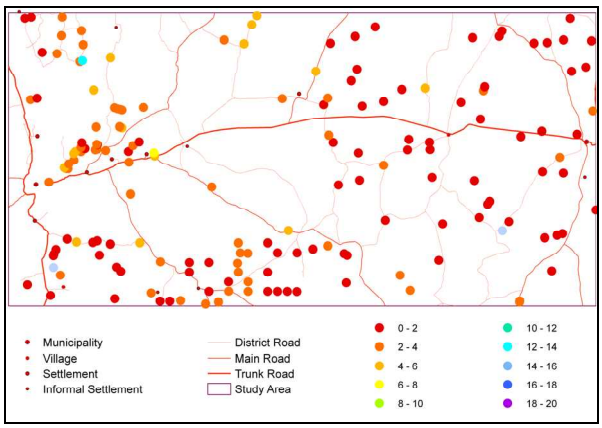

Figure 7.29. Extractable Ca content ($cmol_c\ kg^{-1}$) of topsoil

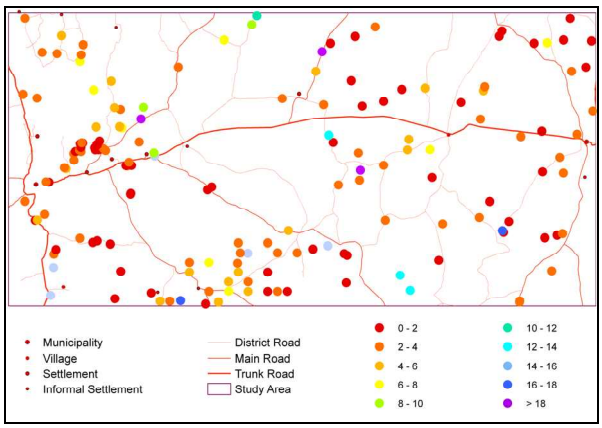

Figure 7.30. Extractable Ca content ($cmol_c\ kg^{-1}$) of subsoil

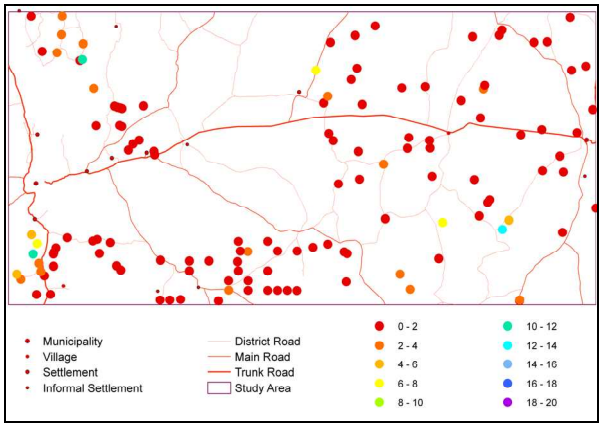

Figure 7.31. Exchangeable Ca content ($cmol_c\ kg^{-1}$) of topsoil

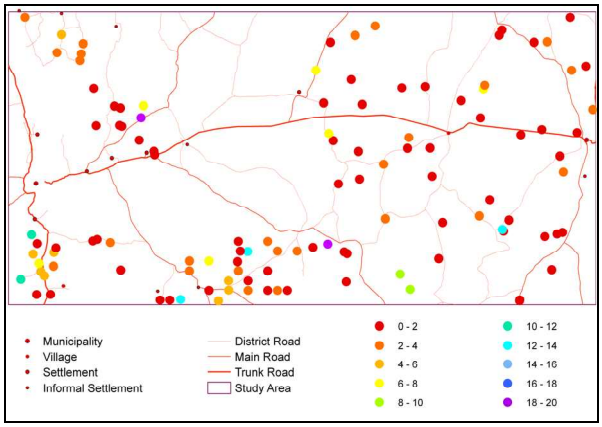

Figure 7.32. Exchangeable Ca content ($cmol_c\ kg^{-1}$) of subsoil

7.3 MAGNESIUM [Mg]

Magnesium is the ninth most abundant element in the universe by mass and the eighth most abundant element in the lithosphere (Barber, 1994). It occurs in more than 100 minerals, mainly in the primary minerals olivine [Mg_2SiO_4], pyroxene [$CaMgSi_2O_6$ and $Ca(Mg,Fe,Al)Si_2O_2$], amphibole [$Ca_2Mg_5Si_8O_{22}\ (OH)_2$ and $Ca_2(Fe,Mg)_5\ Si_8O_{22}(OH)_2$ and $(Na,Ca)_2(Mg,Fe,Al)_5(SiAl)_8O_{22}(OH)_2$], serpentine [$Mg_3Si_2O_5(OH)_4$], talc [$Mg_3Si_4O_{10}(OH)_2$] and biotite mica [$K(MgFe)_3AlSi_3O_{10}$]. It is also found in the secondary minerals magnesite [$MgCO_3$], dolomite [$CaCO_3.MgCO_3$], vermiculite [$(MgFe,Al)_3(Al,Si)_4O_{10}(OH)_2{\cdot}4H_2O$], montmorillonite [$(Na,Ca)_{0.33}(Al,Mg)_2\ (Si_4O_{10})\ (OH)_2\ {\cdot}nH_2O$] and chlorite [$(Mg,Fe)_3(Si,Al)_4O_{10}(OH)_2{\cdot}(Mg,Fe)_3(OH)_6$]. Relative abundance in some parent materials decreases from basic igneous- through acid igneous- to sedimentary rock (Metson, 1974). Soils from granite, sandstone and most shales are relatively low in magnesium, while those from mafic (ferromagnesian) igneous rocks are high in magnesium (Mayland and Wilkinson, 1989).

Table 7.6: Typical magnesium concentrations (in mg kg^{-1}) found in the earth's crust, some common rocks, and soils.

SOURCE	Whitehead, 2000	Foth, 1999	Barber, 1994	Mayland and Wilkinson, 1989	Helmke, 2000
Earth's crust		21 000	21 000	21 000	
Granite	2 400				
Basalt	29 900				
Shale	15 000				
Sandstone	7 000				
Limestone	47 000			30 000 – 120 000	
Soils from Granite	1 400				
Soils from Shale	9 600				
Soils from Sandstone	3 900				
Entisol					23 200
Spodosol					5 400
Alfisol					50 700
Mollisol					5 500
Soils (general)	8 000 [1 000 – 15 000]		5 000	5 000	600 – 6 000 [5 000]

Magnesium in soils occurs in minerals, as ions on the exchange complex, and in the soil solution. Bioavailability is governed by parent material, ion exchange reactions, biological transformations, loss from the crop root zone by leaching and crop removal from the field, and replenishment via atmospheric deposition, fertilizer and soil amendments (Camberato and Pan, 2000).

Magnesium contributes to maintenance of osmotic potential, cation-anion balance and cellular pH (Reuter and Robinson, 1997). It is the centrally coordinated atom in the chlorophyll molecule and thus plays a major role in photosynthesis (Foth, 1990). It contributes to protein synthesis by being involved in the functioning of ribosomes (Whitehead, 2000). Magnesium acts as a cofactor for many enzymes, especially those involved in the transfer of energy through substrates such as ATP (Blevins, 1994); in other words, magnesium activates various enzyme systems involved with carbohydrate and nitrogen metabolism, protein-, vitamin-, fat- and oil synthesis (Whitehead, 2000). It is involved in uptake and transportation of phosphate within the plant. It contributes, with calcium, to keeping protoplasm in a favourable colloidal condition for life processes (Whitehead, 2000).

Magnesium is readily available in alkaline soil, though the relative proportions of competing cations (Ca^{2+}, K^{+}, Na^{+}) influence magnesium activity (Mayland and Wilkinson, 1989). Acidity suppresses magnesium's availability as a result of lower CEC and lower quantities of basic cations in the soil. If magnesium comprises less than about 5 % of the exchangeable cations, deficiencies may be found in plants (Mayland and Wilkinson, 1989).

7.3.1 STATISTICAL ANALYSIS: EXTRACTABLE AND EXCHANGEABLE MAGNESIUM CONTENT

Normality was rejected for extractable and exchangeable Mg by the statistical tests employed, namely the Shapiro-Wilk W test, Kolmogorov-Smirnov / Lilliefors test, and three D'Agostino tests based in skewness, on kurtosis, and on a combination of skewness and kurtosis (AnalystSoft, 2007).

Table 7.7: Descriptive statistics – extractable magnesium content (n = 532) and exchangeable magnesium content (n = 399).

	Mg extractable		Mg exchangeable
	mg kg^{-1}	$cmol_c$ kg^{-1}	$cmol_c$ kg^{-1}
Mean	106.9	0.88	0.84
Median	65.0	0.53	0.57
Standard Deviation	114.2	0.94	0.92
Coefficient of Variation	1.1	1.07	1.09
Minimum	0.0	0.00	0.00
Maximum	627.0	5.14	6.50
Range	627.0	5.14	6.50
Lower Quartile	33.0	0.27	0.23
Upper Quartile	141.5	1.16	1.14
Quartile Range	108.5	0.89	0.91
Percentile 10	15.0	0.12	0.12
Percentile 90	278.0	2.28	2.01
Skewness	1.9	1.89	2.48
Kurtosis	3.5	3.52	8.72

The **extractable magnesium** content of 532 samples from the study area ranges from 0 to 5.14 $cmol_c$ kg^{-1}. The mean (0.88 $cmol_c$ kg^{-1}) is considerably higher than the median (0.53 $cmol_c$ kg^{-1}), with a skewness of 1.89 and kurtosis of 3.52. The standard deviation is 0.94. Half the samples have magnesium concentrations of between 0.27 (1st quartile) and 1.16 $cmol_c$ kg^{-1} (3rd quartile), for a quartile range of 0.89. In 80 % of samples, the Mg content is between 0.12 (1st decile) and 2.28 $cmol_c$ kg^{-1} (9th decile). The frequency distribution is shown in Table 7.8 and Figures 7.33 – 7.34.

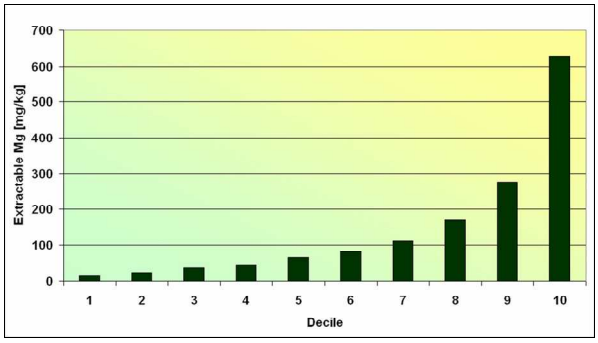

Figure 7.33. Decile distribution of extractable magnesium content (mg kg^{-1})

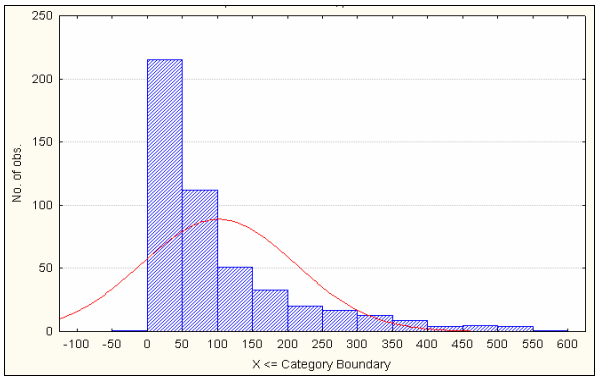

Figure 7.34. Histogram of extractable magnesium content (mg kg^{-1})

Table 7.8: Distribution in terms of deciles – extractable (n = 532) and exchangeable magnesium content (n = 399).

	Decile	Mg extractable		Mg exchangeable
		mg kg^{-1}	$cmol_c$ kg^{-1}	$cmol_c$ kg^{-1}
minimum		0	0.00	0.00
	1	15	0.12	0.12
	2	26	0.21	0.19
	3	39	0.32	0.27
	4	46	0.38	0.40
median	5	65	0.53	0.57
	6	82	0.67	0.71
	7	112	0.92	0.96
	8	172	1.41	1.30
	9	277	2.27	2.01
maximum	10	627	5.14	6.50

Statistically significant correlations, at $p<0.05$, were found between extractable magnesium content and respectively exchangeable magnesium content ($r^2 = 0.69$), the sum of extractable bases ($r^2 = 0.42$) and the sum of exchangeable bases (S-value) ($r^2 = 0.32$) (Figures 7.35 - 7.37).

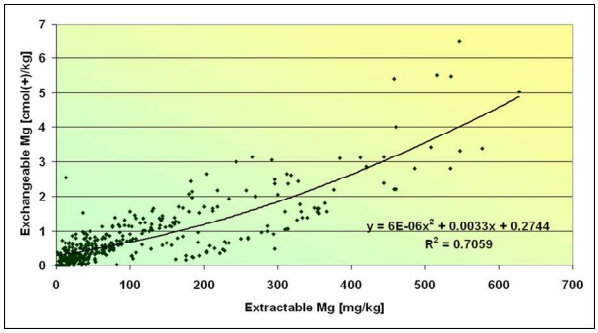

Figure 7.35. Extractable Mg content (mg kg^{-1}) vs exchangeable Mg content ($cmol_c$ kg^{-1})

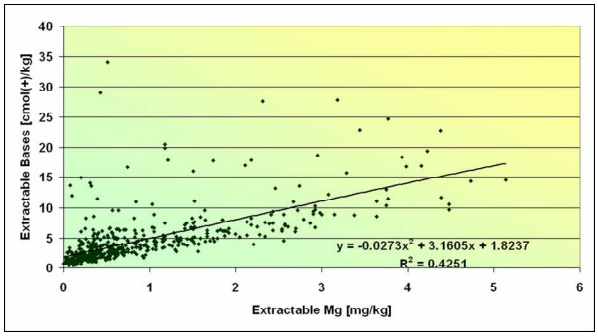

Figure 7.36. Extractable Mg content (mg kg^{-1}) vs sum of extractable bases ($cmol_c$ kg^{-1})

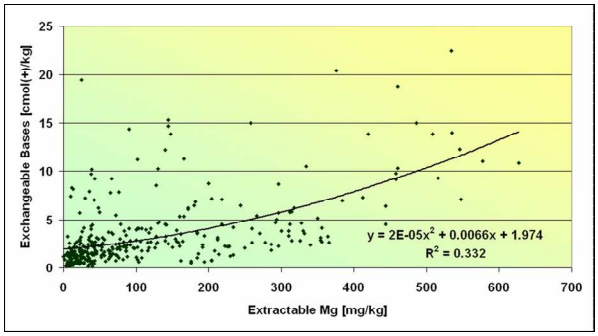

Figure 7.37. Extractable Mg content (mg kg^{-1}) vs sum of exchangeable bases ($cmol_c$ kg^{-1})

Significant, but weak, correlations were found with cation exchange capacity ($r^2 = 0.29$), extractable calcium content ($r^2 = 0.23$), clay ($r^2 = 0.23$), electrical conductivity measured in a saturated paste ($r^2 = 0.20$), manganese content ($r^2 = 0.18$), extractable potassium content ($r^2 = 0.18$), exchangeable potassium content ($r^2 = 0.17$), fluoride content ($r^2 = 0.15$), exchangeable calcium content ($r^2 = 0.15$), iron ($r^2 = 0.14$), sand content ($r^2 = 0.10$), pH ($r^2 = 0.10$), and copper content ($r^2 = 0.10$).

The **exchangeable magnesium** content of 399 samples from the study area ranges from 0 to 6.50 $cmol_c$

kg^{-1}, and is not normally distributed. The mean (0.84 $cmol_c\ kg^{-1}$) is considerably higher than the median (0.57 $cmol_c\ kg^{-1}$), with a skewness of 2.48 and kurtosis of 8.72. The standard deviation is 0.92. Half the samples have magnesium concentrations of between 0.23 (1st quartile) and 1.14 $cmol_c\ kg^{-1}$ (3rd quartile), for a quartile range of 0.91. Eighty percent of samples lies between 0.12 (1st decile) and 2.01 $cmol_c\ kg^{-1}$ (9th decile). The frequency distribution is shown in Table 7.6 and Figures 7.38 – 7.39.

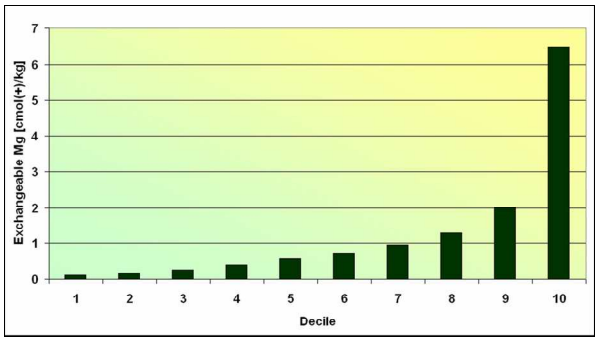

Figure 7.38. Decile distribution of exchangeable magnesium content ($cmol_c\ kg^{-1}$)

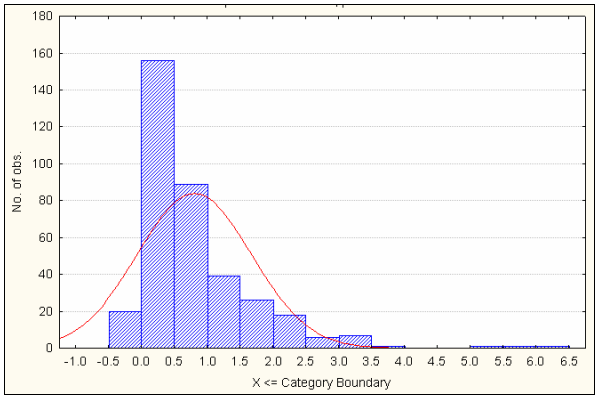

Figure 7.39. Histogram of exchangeable magnesium content ($cmol_c\ kg^{-1}$)

The range of exchangeable magnesium content (0 – 6.5 $cmol_c\ kg^{-1}$) is consistent with values quoted in literature, such as 0.5 – 14 $cmol_c\ kg^{-1}$ (Barber, 1994); 0.81 – 8.1 $cmol_c\ kg^{-1}$ (Baker, 1972); 0.21 – 14.4 $cmol_c\ kg^{-1}$ (Mokwunye and Melsted, 1972); 3.4 – 5.6 $cmol_c\ kg^{-1}$ (Forth, 1990).

Statistically significant correlations, at $p<0.05$, were found between exchangeable magnesium content and respectively extractable magnesium content ($r^2 = 0.69$), sand content ($r^2 = 0.41$), the sum of exchangeable bases (S-value) ($r^2 = 0.40$), cation exchange capacity ($r^2 = 0.38$), clay content ($r^2 = 0.37$), and the sum of extractable bases ($r^2 = 0.33$) (Figures 7.35; 7.40 – 7.44).

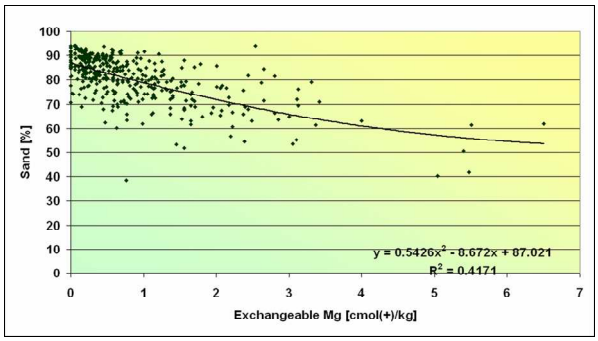

Figure 7.40. Exchangeable Mg content ($cmol_c\ kg^{-1}$) vs sand content (%)

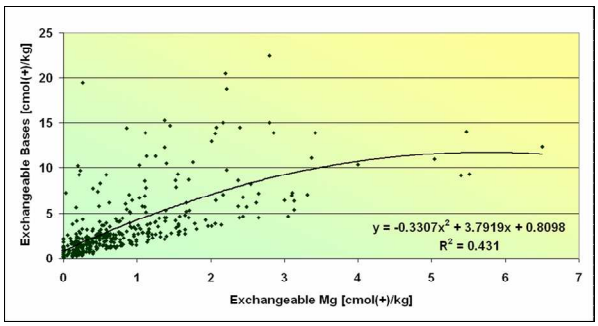

Figure 7.41. Exchangeable Mg content ($cmol_c\ kg^{-1}$) vs sum of exchangeable bases ($cmol_c\ kg^{-1}$)

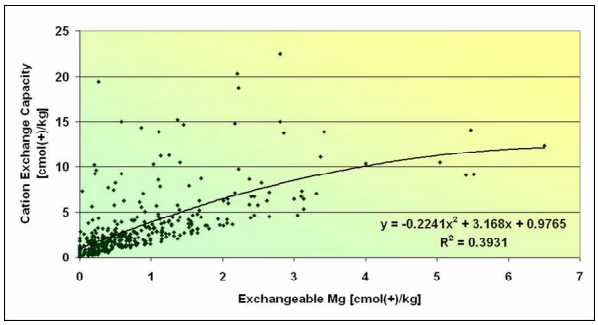

Figure 7.42 Exchangeable Mg content ($cmol_c\ kg^{-1}$) vs CEC ($cmol_c\ kg^{-1}$)

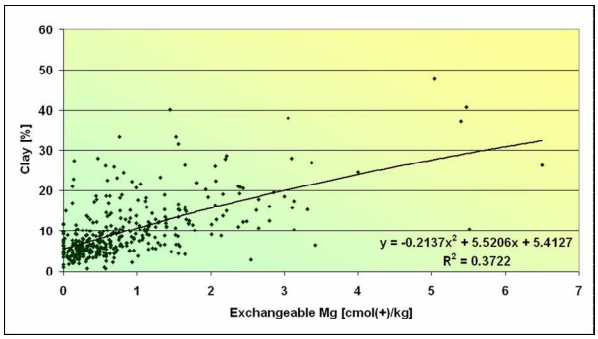

Figure 7.43. Exchangeable Mg content ($cmol_c\ kg^{-1}$) vs clay content (%)

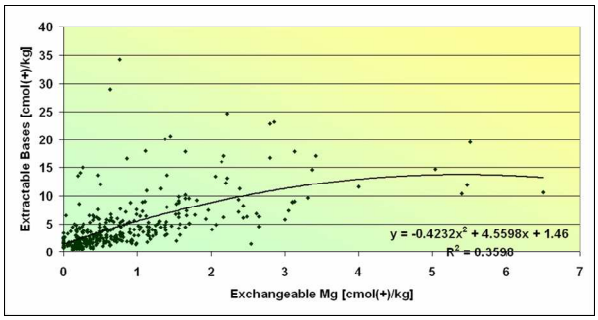

Figure 7.44. Exchangeable Mg ($cmol_c\ kg^{-1}$) content vs sum of extractable bases ($cmol_c\ kg^{-1}$)

Significant, but weak, correlations were found with manganese (r^2 = 0.24), exchangeable potassium content (r^2 = 0.23), extractable potassium content (r^2 = 0.18), pH (r^2 = 0.18), extractable calcium content (r^2 = 0.19), exchangeable calcium content (r^2 = 0.17), iron content (r^2 = 0.16), copper content (r^2 = 0.15), silt (r^2 = 0.10), medium sand content (r^2 = 0.10) and fluoride content (r^2 = 0.10).

Topsoil Mg concentrations (both extractable and exchangeable) are considerably lower than subsoil Mg concentrations (Table 7.9 and Figures 7.45 and 7.46). This is most likely caused by removal of topsoil magnesium through grazing, eluviation of topsoil magnesium, accumulation of leached magnesium lower down in the profile and additions through weathering of parent material. This trend is also found in literature, for example as noted by Troeh and Thompson (2005) and Materechera *et al.* (1998).

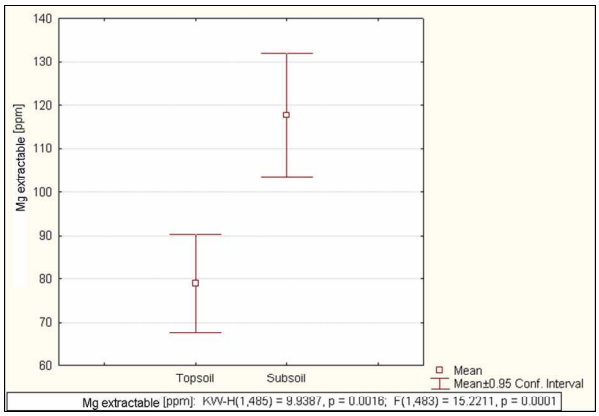

Figure 7.45. Extractable Mg content (ppm = mg kg^{-1}), per topsoil and subsoil

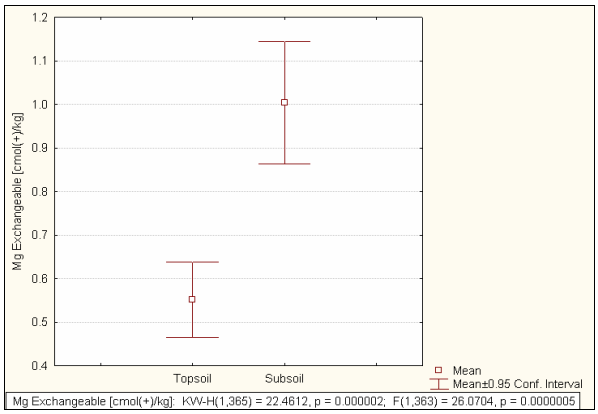

Figure 7.46. Exchangeable Mg content ($cmol_c\ kg^{-1}$), per topsoil and subsoil

Table 7.9: Extractable Mg content (mg kg^{-1} and $cmol_c$ kg^{-1}) and exchangeable Mg content ($cmol_c$ kg^{-1}), per topsoil and subsoil.

	Mg extractable				Mg exchangeable	
	Topsoil (n = 199)		Subsoil (n = 286)		Topsoil (n = 162)	Subsoil (n = 203)
	mg kg^{-1}	$cmol_c$ kg^{-1}	mg kg^{-1}	$cmol_c$ kg^{-1}	$cmol_c$ kg^{-1}	$cmol_c$ kg^{-1}
Mean	78.97	0.65	117.61	0.96	0.55	1.00
Median	52.0	0.43	68.5	0.56	0.39	0.69
Std Deviation	81.12	0.66	122.20	1.00	0.56	1.01
Minimum	2.0	0.02	0.0	0.00	0.00	0.00
Maximum	486.0	3.98	577.0	4.73	3.13	6.50
Range	484.0	3.97	577.0	4.73	3.13	6.50
Lower Quartile	26.0	0.21	35.0	0.29	0.18	0.26
Upper Quartile	100.0	0.82	166.0	1.36	0.71	1.52
Quartile Range	74.0	0.61	131.0	1.07	0.53	1.26
Percentile10	12.0	0.10	18.0	0.15	0.06	0.14
Percentile 90	194.0	1.59	300.0	2.46	1.24	2.22

When disregarding clay loam and sandy clay soils, of which there are too few samples to be representative, it emerges that sandy soils and loamy sands have considerably lower concentrations of both extractable and exchangeable Mg than sandy loams and sandy clay loams (Figures 7.47 and 7.48). This result is supported by literature (Troeh and Thompson, 2005). Mokwunye and Melsted (1972) found that the clay portion of tropical and temperate soils contain 51 – 70 % of total Mg, silt 22 – 42 % and the sand fraction only 0.1 – 1 % of the total Mg.

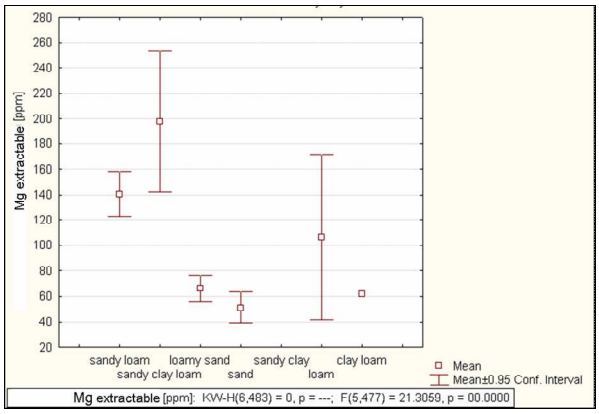

Figure 7.47. Extractable Mg content (ppm = mg kg^{-1}), per textural class

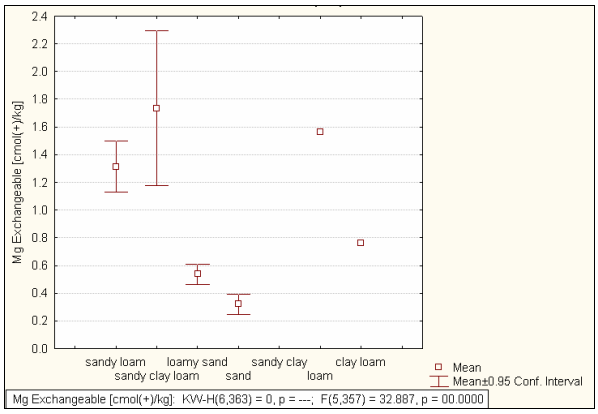

Figure 7.48. Exchangeable Mg content ($cmol_c$ kg^{-1}), per textural class

Aeolian parent material, as embodied by the Kalahari sands, contains significantly less extractable and exchangeable Mg than those of alluvial or colluvial origin (Figures 7.49 and 7.50). It also contains less extractable Mg than soils formed *in situ*, though the latter has comparable concentrations of exchangeable Mg.

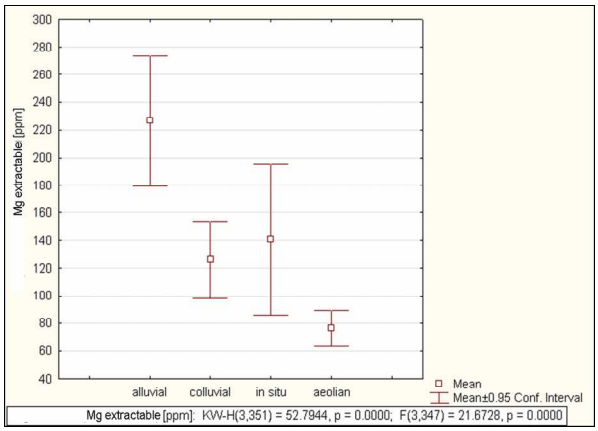

Figure 7.49. Extractable Mg content (ppm = mg kg^{-1}), per origin of parent material

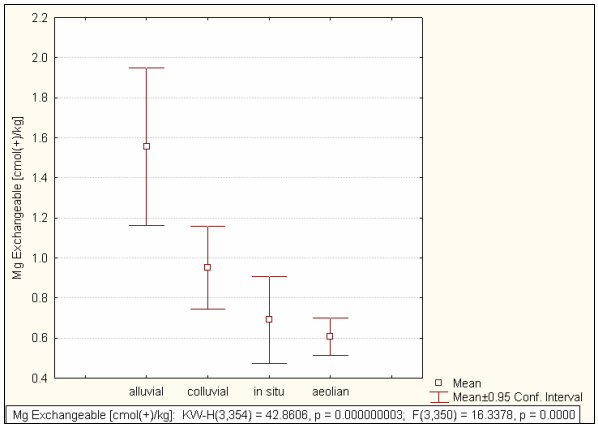

Figure 7.50. Exchangeable Mg content ($cmol_c$ kg^{-1}), per origin of parent material

Both extractable and exchangeable Mg concentrations are significantly lower in the Kalahari sands than the soils formed on the schist of the Khomas Hochland – a direct consequence of the mineral composition of the respective parent materials (Figures 7.51 and 7.52).

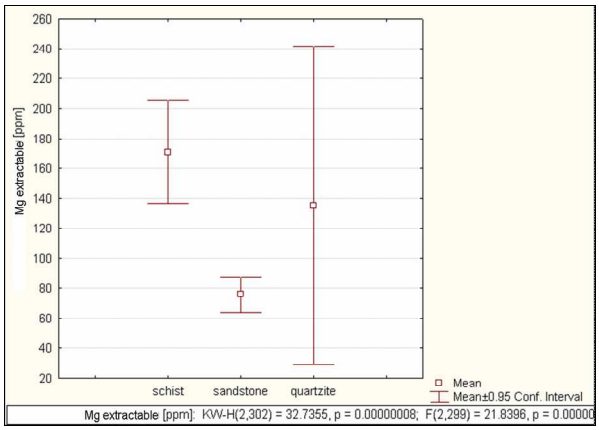

Figure 7.51. Extractable Mg content (ppm = mg kg^{-1}), per type of parent material

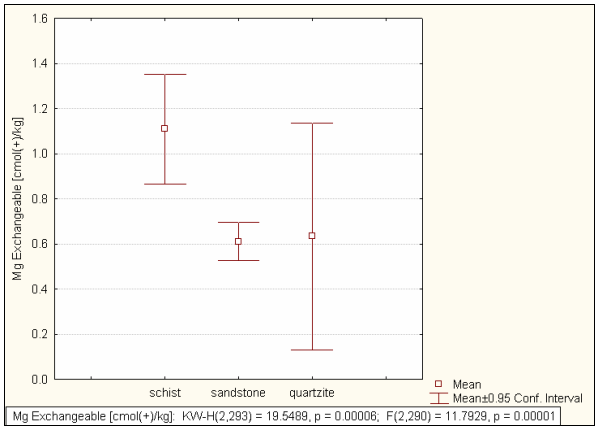

Figure 7.52. Exchangeable Mg content ($cmol_c$ kg^{-1}), per type of parent material

Arenosols and Regosols of the study area contain significantly lower concentrations of both extractable and exchangeable Mg than Cambisols, Calcisols and Luvisols. This is also the case with extractable Mg of Leptosols (Figures 7.53 and 7.54). The mean of exchangeable Mg of Leptosols is considerably higher than those of Arenosols and Regosols, but there is an appreciable overlap in the ±0.95 confidence intervals. The lower Mg concentrations in Arenosols are caused by low base concentrations in the parent material, low CEC, and greater rates of leaching due to sandy texture. Calcisols, being rich in calcium and accompanying magnesium, Cambisols, being young soils formed on schist (in the study area), and Luvisols, being soils with accumulations of fine material, all contain considerable amounts of both extractable and exchangeable Mg.

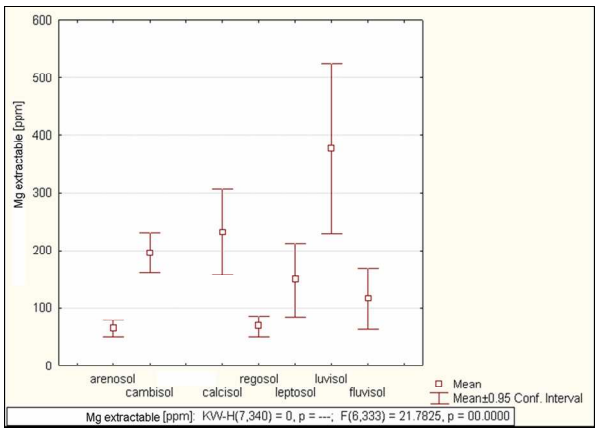

Figure 7.53. Extractable Mg content (ppm = mg kg^{-1}), per WRB reference soil group

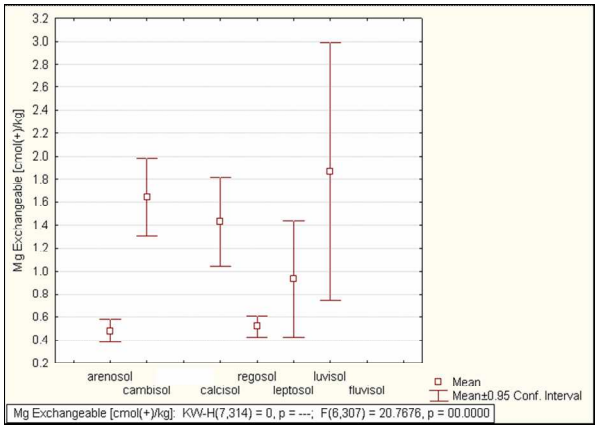

Figure 7.54. Exchangeable Mg content ($cmol_c$ kg^{-1}), per WRB reference soil group

Table 7.10: Extractable Mg content (mg kg^{-1} and $cmol_c$ kg^{-1}) and exchangeable Mg content ($cmol_c$ kg^{-1}), per WRB reference soil group.

Mg extractable mg kg^{-1}	**Arenosols** (n = 132)	**Calcisols** (n = 17)	**Leptosols** (n = 24)	**Fluvisols** (n = 6)	**Cambisols** (n = 66)	**Regosols** (n = 89)	**Luvisols** (n = 3)
Mean	61.9	232.3	148.5	116.3	195.7	68.8	376.7
Median	34.0	212.0	75.0	110.5	162.0	40.0	354.0
Std.Dev.	77.1	145.4	152.2	49.9	139.7	83.3	59.3
Minimum	0	52	8	47	7	3	332
Maximum	444	547	534	201	577	366	444
Range	444	495	526	154	570	363	112
Lower Quartile	14	126	44	101	78	19	332
Upper Quartile	69	312	215	128	296	76	444
Quartile Range	56	186	171	27	218	57	112
Percentile 10	8	62	33	47	48	10	332
Percentile 90	183	460	458	201	384	204	444
Mg extractable $cmol_c$ kg^{-1}	**Arenosols** (n = 132)	**Calcisols** (n = 17)	**Leptosols** (n = 24)	**Fluvisols** (n = 6)	**Cambisols** (n = 66)	**Regosols** (n = 89)	**Luvisols** (n = 3)
Mean	0.51	1.90	1.22	0.95	1.60	0.56	3.09
Median	0.28	1.74	0.61	0.91	1.33	0.33	2.90
Std.Dev.	0.63	1.19	1.25	0.41	1.15	0.68	0.49
Minimum	0.00	0.43	0.07	0.39	0.06	0.02	2.72
Maximum	3.64	4.48	4.38	1.65	4.73	3.00	3.64
Range	3.64	4.06	4.31	1.26	4.67	2.98	0.92
Lower Quartile	0.11	1.03	0.36	0.83	0.64	0.16	2.72
Upper Quartile	0.57	2.56	1.76	1.05	2.43	0.62	3.64
Quartile Range	0.46	1.52	1.40	0.22	1.79	0.47	0.92
Percentile 10	0.07	0.51	0.27	0.39	0.39	0.08	2.72
Percentile 90	1.50	3.77	3.75	1.65	3.15	1.67	3.64
Mg exchangeable $cmol_c$ kg^{-1}	**Arenosols** (n = 129)	**Calcisols** (n = 15)	**Leptosols** (n = 15)	**Fluvisols** (n = 0)	**Cambisols** (n = 61)	**Regosols** (n = 88)	**Luvisols** (n = 3)
Mean	0.47	1.43	0.93	-	1.64	0.51	1.87
Median	0.25	1.37	0.45	-	1.32	0.42	1.65
Std.Dev.	0.57	0.70	0.92	-	1.33	0.43	0.45
Minimum	0.00	0.63	0.15	-	0.02	0.00	1.56
Maximum	3.13	3.31	2.80	-	6.50	1.65	2.39
Range	3.13	2.68	2.65	-	6.48	1.65	0.82
Lower Quartile	0.16	0.90	0.35	-	0.77	0.17	1.56
Upper Quartile	0.58	1.65	1.15	-	2.37	0.74	2.39
Quartile Range	0.42	0.75	0.81	-	1.60	0.57	0.82

Percentile 10	0.06	0.76	0.21	-	0.36	0.00	1.56
Percentile 90	1.16	2.22	2.80	-	3.11	1.15	2.39

Both extractable and exchangeable Mg concentrations are highest in the lowest landscape positions (valleys and lower slopes), and lowest in the higher landscape positions (upper slopes and ridges) (Figures 7.55 and 7.56). This can be explained by mass movement of Mg-containing colluvial material down inclines, as well as vertical and lateral displacement of Mg by, percolating water.

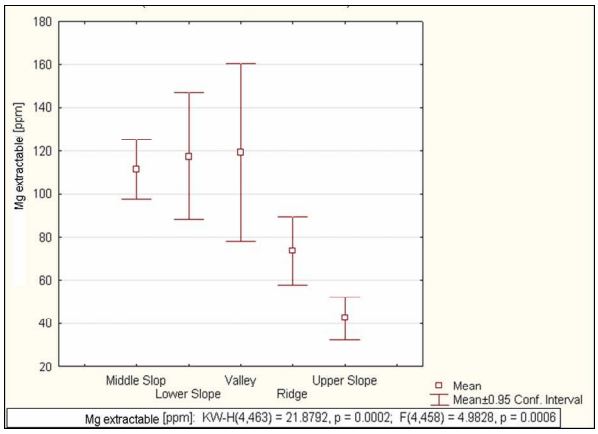

Figure 7.55. Extractable Mg content (ppm = mg kg^{-1}), per position in the landscape

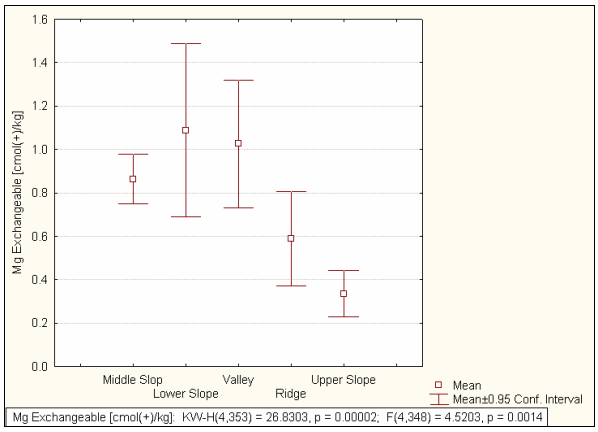

Figure 7.56. Exchangeable Mg content ($cmol_c$ kg^{-1}), per position in the landscape

Both extractable and exchangeable Mg concentrations are significantly higher in terrain with a moderate to high degree of dissection (Figures 7.57 and 7.58). One explanation is greater rates of erosion and subsequent weathering in more dissected terrain. Secondly, the highly dissected terrain of the study area occurs mainly on schist, quartzite and calcrete, whereas the less dissected areas, towards the east, are mainly covered with Kalahari sands.

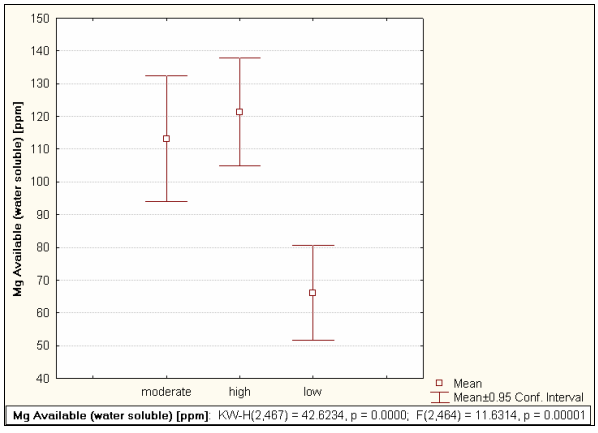

Figure 7.57. Extractable Mg content (ppm = mg kg^{-1}), per degree of dissection of the landscape

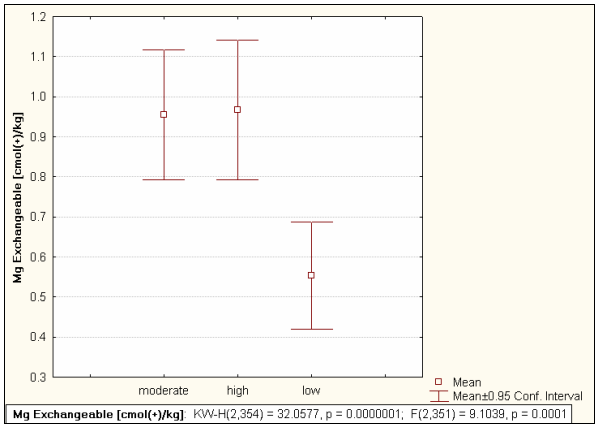

Figure 7.58. Exchangeable Mg content ($cmol_c$ kg^{-1}), per degree of dissection of the landscape

Extractable Mg concentrations of moderately deep soils on plains with koppies are significantly higher than soils in other parts of the landscape (Figure 7.59). The trend is the same for exchangeable Mg, though there is greater overlap between the ±0.95 confidence intervals (Figure 7.60).

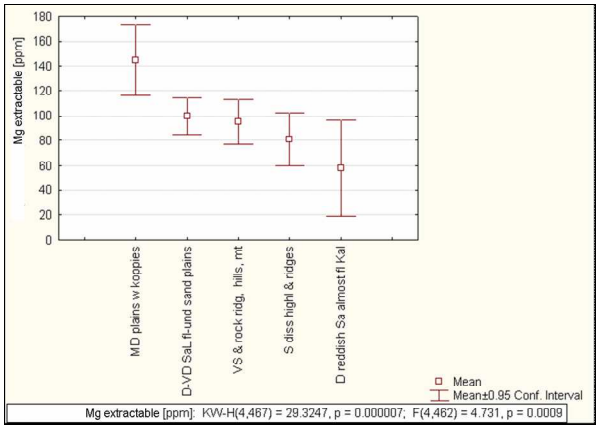

Figure 7.59. Extractable Mg content (ppm = mg kg^{-1}), per broad soil unit

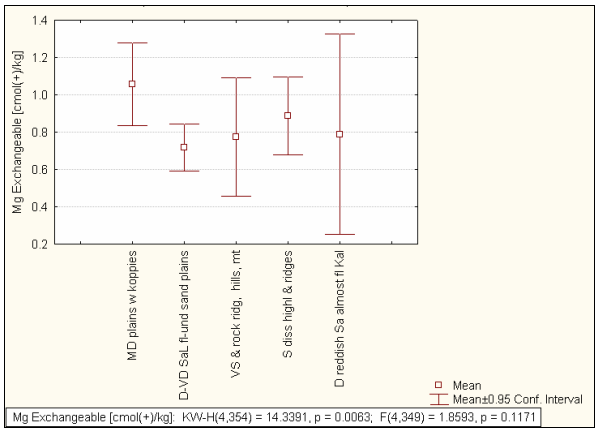

Figure 7.60. Exchangeable Mg content ($cmol_c$ kg^{-1}), per broad soil unit

The extractable and exchangeable Mg levels in profiles of the study area, of topsoil and subsoil respectively, are shown in Figures 7.61 – 7.64.

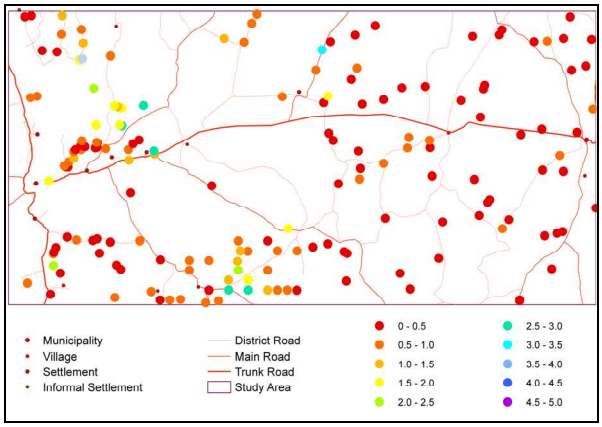

Figure 7.61. Extractable Mg content ($cmol_c$ kg^{-1}) of topsoil

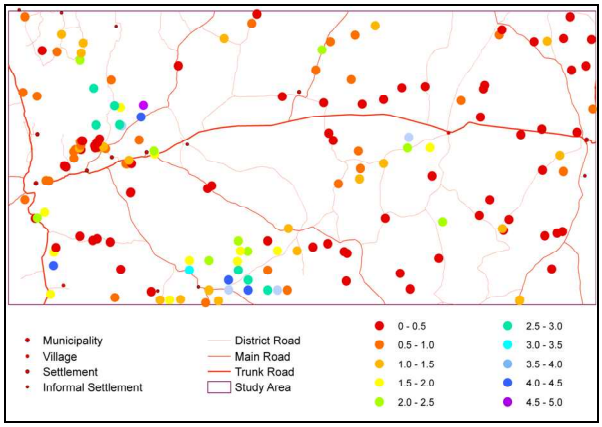

Figure 7.62. Extractable Mg content ($cmol_c$ kg^{-1}) of subsoil

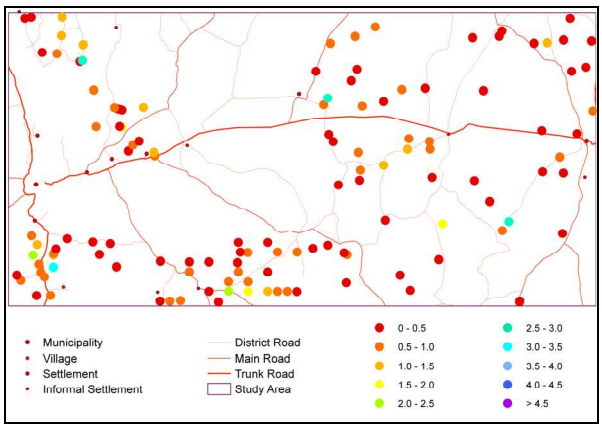

Figure 7.63. Exchangeable Mg content ($cmol_c$ kg^{-1}) of topsoil

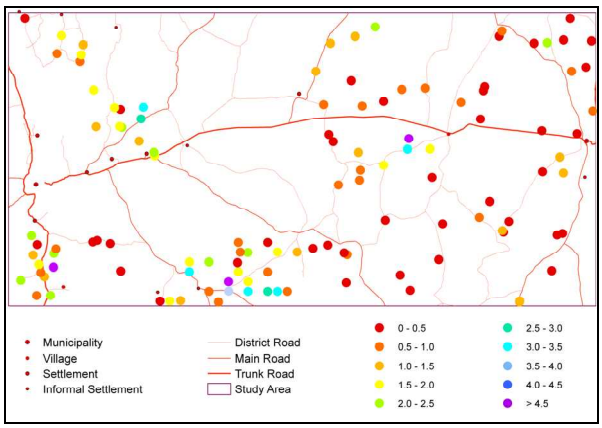

Figure 7.64. Exchangeable Mg content ($cmol_c$ kg^{-1}) of subsoil

It can be concluded that concentrations of extractable and exchangeable soil magnesium of the study area corresponds with values reported in literature. Highest concentrations are found in the subsoil, in relatively

young soils, of sandy loam and sandy clay loam texture, in moderate to highly dissected terrain, in parent material of alluvial and colluvial origin, particularly those derived from schist, in lower positions in the landscape and in association with carbonates.

7.4 POTASSIUM [K]

Potassium is the 7th most abundant element in the Earth's crust, with a concentration of approximately 2.4 - 2.6 %. Locally it varies according to parent material, the degree of weathering and leaching, and removal by crops (or grazing of grass, in the case of the study area). Granites contain about 4.6 %, syenites 5.4 %, basalts 0.7%, peridotes 0.2 %, clayey shales 3.0 % and limestones on average 0.6 % potassium (Malavolta, 1985). Potassium is found in more than 50 minerals, including potassium feldspars such as orthoclase and microcline [$KAlSi_3O_8$] – occurring mainly in sand and silt fractions of poorly weathered soil. It is also found in the primary mica clay minerals biotite [$K(MgFe)_3AlSi_3O_{10}$] and muscovite [$KAl_2AlSi_3O_{10}(OH)_2$] – in the finer sand and silt fractions – and in vermiculite [$(K,Ca,Mg)(MgFe)_3AlSi_3O_{10}(OH)_2$], which is common in fine sand, silt and clay fractions. The secondary clay mineral illite [$(K)Al_2(Al,Si)_4O_{10}(OH)_2$] contains less potassium. Potassium is released more readily from biotite than from muscovite, and more readily from muscovite than from orthoclase or microcline (Whitehead, 2000).

Table 7.11: Typical potassium concentrations (in mg kg-^{1}) found in the earth's crust, some common rocks and soils.

SOURCE	Whitehead, 2000	Foth, 1999	Helmke, 2000	Troeh and Thompson, 2005
Earth's crust		26 000		
Granite	45 100			
Basalt	5 300			
Shale	26 600			
Sandstone	10 700			
Limestone	2 700			
Soils from Granite	39 000			
Soils from Shale	15 000			
Soils from Sandstone	17 000			
Entisol			26 300	
Spodosol			24 400	17 000 [a] 29 000 [b] 31 000 [c]
Alfisol			11 700	14 000 – 17 000 [a] 16 000 – 19 000 [b] 15 000 – 19 000 [c]
Mollisol			17 200	16 000 – 18 000 [a] 17 000 [b] 13 000 – 16 000 [c]
Inceptisol				17 000 – 21 000 [a] 18 000 – 25 000 [b] 24 000 – 26 000 [c]
Oxisol				1 100 [a] 1 000 [b] 1 000 [c]
Aridisol				23 000 [a] 15 000 [b] 18 000 [c]
Ultisol				1 000 – 13 000 [a] 1 000 – 19 000 [b] 2 000 – 35 000 [c]

Soils (general)	3 000 – 25 000 [15 000]		400 – 30 000 [14 000]	

[a] A-horizon; [b] B-horizon; [c] C-horizon

Potassium occurs in four forms in soils: soluble, exchangeable, fixed / non-exchangeable and structural / mineral (Sparks, 2000). Hydrated potassium ions in the soil solution (about 0.01 % of the total) and adsorbed on the exchange complex (about 1 % of the total) are readily available to plants, but the major portion (98 - 99 % of the total) is locked up in minerals, and thus unavailable to plants in the short term (Sparks, 2000; Troeh and Thompson, 2005). Potassium is readily available in alkaline soil, while acidity suppresses its availability as a result of lower CEC and lower quantities of basic cations in the soil.

Potassium contributes to regulation of osmotic potential, cation-anion balance and cellular pH (Reuter and Robinson, 1997). It is involved in opening and closing of stomata, through its influence on the osmotic potential and turgor of the guard cells (Whitehead, 2000). Plants deficient in potassium are more susceptible to drought. It also contributes to transport of photosynthate from the leaves. Potassium is an activator of many enzymes, including some involved in protein synthesis (Blevins, 1994). According to Foth (1990), potassium has some functions in photosynthesis, carbohydrate translocation and protein synthesis.

7.4.1 STATISTICAL ANALYSIS: EXTRACTABLE AND EXCHANGEABLE POTASSIUM CONTENT

Normality was rejected for extractable and exchangeable K by the statistical tests employed, namely the Shapiro-Wilk W test, Kolmogorov-Smirnov / Lilliefors test, and three D'Agostino tests based in skewness, on kurtosis, and on a combination of skewness and kurtosis (AnalystSoft, 2007).

Table 7.12: Descriptive statistics – extractable potassium content (n = 532) and exchangeable potassium content (n = 399).

	K extractable		K exchangeable
	mg kg^{-1}	$cmol_c$ kg^{-1}	$cmol_c$ kg^{-1}
Mean	137.36	0.35	0.30
Median	114	0.29	0.26
Standard Deviation	93.79	0.24	0.21
Coefficient of Variation	0.68	0.68	0.71
Minimum	4	0.01	0.03
Maximum	756	1.93	1.74
Range	752	1.92	1.71
Lower Quartile	82	0.21	0.17
Upper Quartile	169	0.43	0.36
Quartile Range	87	0.22	0.19
Percentile 10	51	0.13	0.12
Percentile 90	213	0.54	0.49
Skewness	2.55	2.55	3.03
Kurtosis	9.44	9.44	13.95

The **extractable potassium** content of 532 samples from the study area ranges from 0.01 to 1.93 $cmol_c$ kg^{-1}. The lower 90 % of samples are fairly normally distributed, but the upper 10 % skews the distribution (Table

7.13; Figures 7.65 – 7.66). The mean (0.35 $cmol_c\ kg^{-1}$) is higher than the median (0.29 $cmol_c\ kg^{-1}$), with a skewness of 2.55 and kurtosis of 9.44. The standard deviation is 0.24. Half the samples have concentrations of between 0.21 (1st quartile) and 0.43 $cmol_c\ kg^{-1}$ (3rd quartile), for a quartile range of 0.22. In 80 % of samples, the K content is between 0.13 (1st decile) and 0.54 $cmol_c\ kg^{-1}$ (9th decile).

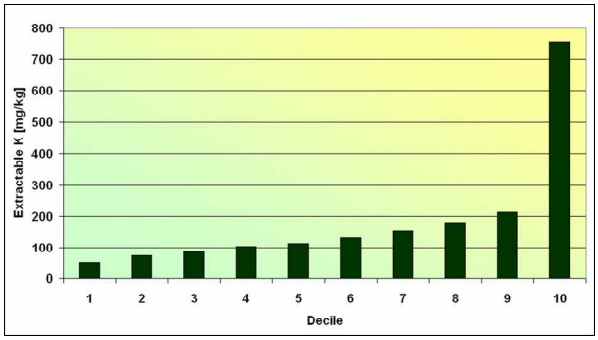

Figure 7.65. Decile distribution of extractable K content (mg kg^{-1})

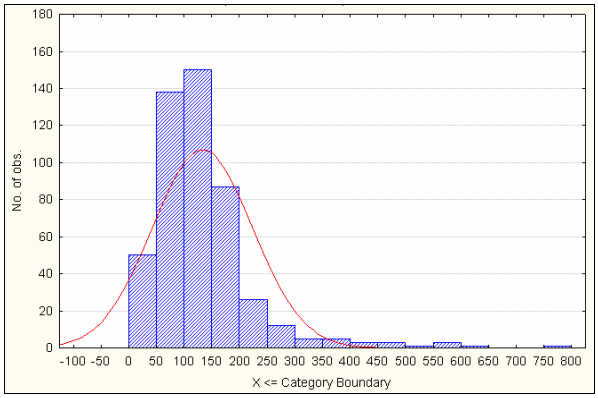

Figure 7.66. Histogram of extractable K content (mg kg^{-1})

Table 7.13: Distribution in terms of deciles – extractable potassium content (n = 532) and exchangeable potassium content (n = 399).

	Decile	K extractable		K exchangeable
		mg kg^{-1}	$cmol_c\ kg^{-1}$	$cmol_c\ kg^{-1}$
minimum		4	0.01	0.03
	1	51	0.13	0.12
	2	74	0.19	0.15
	3	88	0.23	0.19
	4	104	0.27	0.23
median	5	114	0.29	0.26
	6	132	0.34	0.29
	7	154	0.39	0.33
	8	181	0.46	0.39
	9	213	0.54	0.49
maximum	10	756	1.93	1.74

A statistically significant correlation, at $p < 0.05$, was found between extractable potassium content and exchangeable potassium content ($r^2 = 0.55$), as shown in Figure 7.67.

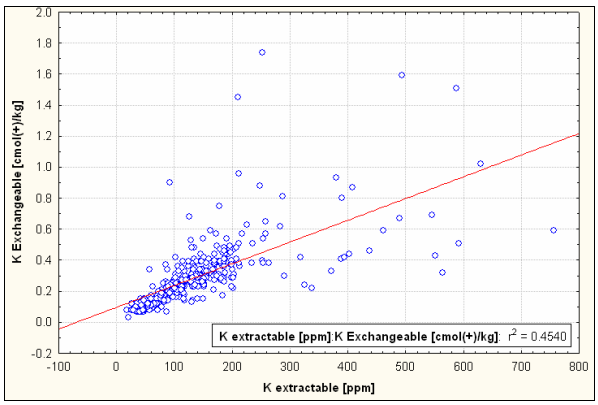

Figure 7.67. Extractable K content (ppm = mg kg^{-1}) vs exchangeable K ($cmol_c\ kg^{-1}$) content

Significant, but weak, correlations were found with extractable magnesium content (r^2 = 0.16), iron (r^2 = 0.13), exchangeable magnesium content (r^2 = 0.12), electrical conductivity of the saturated paste (r^2 = 0.11), clay content (r^2 = 0.11), sulfate content (r^2 = 0.11) and manganese content (r^2 = 0.10), respectively.

The **exchangeable potassium** content of 399 samples from the study area ranges from 0.03 to 1.74 $cmol_c$ kg^{-1}. The lower 90 % of samples are normally distributed, but the upper 10 % skews the distribution (Table 7.13; Figures 7.68 – 7.69).The mean (0.30 $cmol_c$ kg^{-1}) is thus higher than the median (0.26 $cmol_c$ kg^{-1}), with a skewness of 3.03 and kurtosis of 13.95. The standard deviation is 0.21. Half the samples have potassium concentrations of between 0.17 (1st quartile) and 0.36 $cmol_c$ kg^{-1} (3rd quartile), for a quartile range of 0.19. In 80 % of samples, the K content is between 0.12 (1st decile) and 0.49 $cmol_c$ kg^{-1} (9th decile).

These values correspond to exchangeable K concentrations reported in literature, such as 0.3 – 0.5 $cmol_c$ kg^{-1} (Forth, 1990); 0.40 – 0.46 $cmol_c$ kg^{-1} (Alfisols), 0.20 – 0.40 $cmol_c$ kg^{-1} (Inceptisols) and 0.11 – 0.33 $cmol_c$ kg^{-1} (Ultisols) of the United States of America and West Africa (Sparks, 2000).

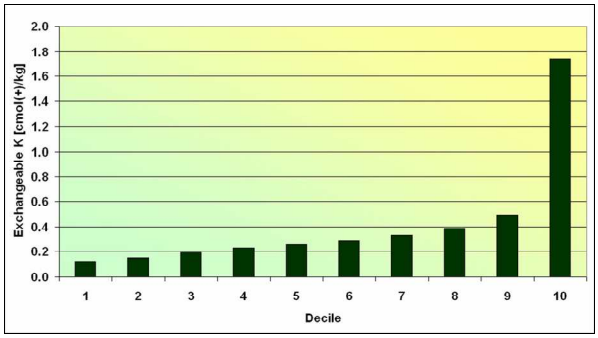

Figure 7.68. Decile distribution of exchangeable K content ($cmol_c$ kg^{-1})

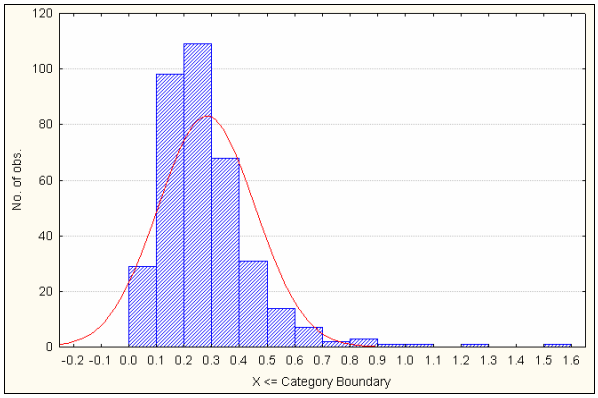

Figure 7.69. Histogram of exchangeable K content ($cmol_c$ kg^{-1})

A statistically significant correlation, at $p < 0.05$, was found between exchangeable potassium content and extractable potassium content (r^2 = 0.55) (Figure 7.67).

Significant, but weak, correlations were found with sulphate content (r^2 = 0.22), exchangeable magnesium content (r^2 = 0.18), sand content (r^2 = 0.17), iron (r^2 = 0.15), manganese content (r^2 = 0.14), electrical conductivity of the 2:5 soil:water suspension (r^2 = 0.14), electrical conductivity of the saturated paste (r^2 = 0.14), extractable magnesium content (r^2 = 0.13), clay content (r^2 = 0.13), zinc content (r^2 = 0.13), sum of extractable bases (r^2 = 0.11) and sum of exchangeable bases (S-value) (r^2 = 0.10).

Topsoil and subsoil K concentrations (both extractable and exchangeable) do not differ significantly (Table 7.14; Figures 7.70 and 7.71), in accord with most reports in literature (Troeh and Thompson, 2005). The exchangeable potassium percentage also remains constant with increase in depth (Table 7.15). Other sources, however, report a decrease in K with depth (Materechera *et al*., 1998; Kotze and Du Preez, 2008).

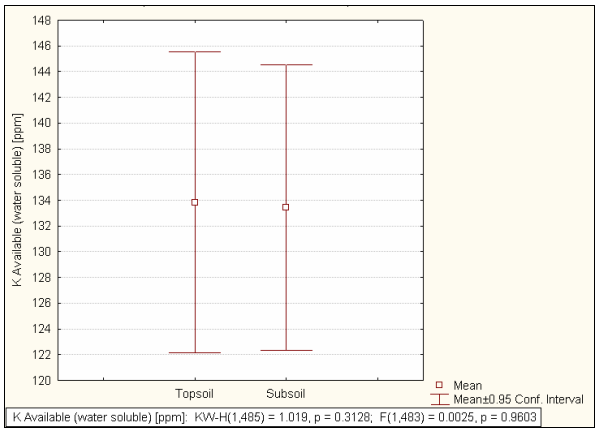

Figure 7.70. Extractable K content (ppm = mg kg^{-1}), per topsoil and subsoil

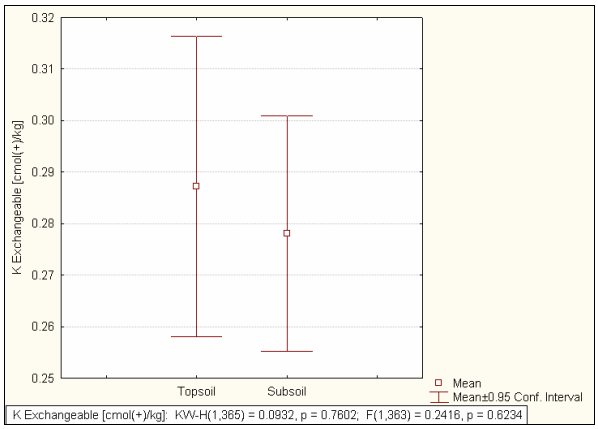

Figure 7.71. Exchangeable K content ($cmol_c$ kg^{-1}), per topsoil and subsoil

Table 7.14: Extractable K content (mg kg^{-1} and $cmol_c$ kg^{-1}) and exchangeable K content ($cmol_c$ kg^{-1}), per topsoil and subsoil.

	K extractable				K exchangeable	
	Topsoil (n = 199)		Subsoil (n = 286)		Topsoil (n = 161)	Subsoil (n = 204)
	mg kg^{-1}	$cmol_c$ kg^{-1}	mg kg^{-1}	$cmol_c$ kg^{-1}	$cmol_c$ kg^{-1}	$cmol_c$ kg^{-1}
Mean	133.84		133.43		0.29	0.28
Median	118.00		109.00		0.26	0.24
Std.Dev.	83.62		95.45		0.19	0.17
Minimum	24.00		17.00		0.07	0.03
Maximum	630.00		756.00		1.51	1.26
Range	606.00		739.00		1.44	1.23
Lower Quartile	85.00		76.00		0.17	0.15
Upper Quartile	166.00		166.00		0.34	0.36
Quartile Range	81.00		90.00		0.17	0.21
Percentile 10	58.00		47.00		0.12	0.11
Percercentile 90	199.00		221.00		0.44	0.48

Table 7.15: Exchangeable K calculated as a percentage of CEC, at various depths.

Depth	Exchangeable potassium percentage			
	0 – 10 cm (n = 35)	11 – 20 cm (n = 91)	21 – 30 cm (n = 201)	> 30 cm (n = 33)
Mean	17.41	18.71	14.18	15.19
Median	13.82	16.53	11.48	12.79
Standard. Deviation	12.92	13.31	14.28	9.65
Minimum	0.00	1.38	0.41	1.07
Maximum	61.15	89.44	100.00	40.56
Range	61.15	88.06	99.59	39.48
Lower Quartile	9.18	10.00	5.76	9.48
Upper Quartile	22.37	23.42	16.22	17.06
Quartile Range	13.19	13.42	10.47	7.58
Percentile 10	5.88	7.17	3.21	5.97
Percentile 90	36.56	34.76	29.33	29.78

When disregarding clay loam and sandy clay soils, of which there are too few samples to be representative, extractable K concentrations decrease in the order sandy clay loam > sandy loam > loamy sand > sand (Figure 7.72). Exchangeable K concentrations decrease in the same order (Figure 7.73).

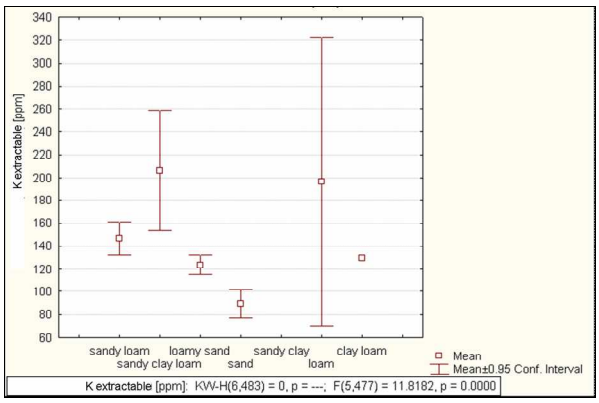

Figure 7.72. Extractable K content (ppm = mg kg^{-1}), per textural class

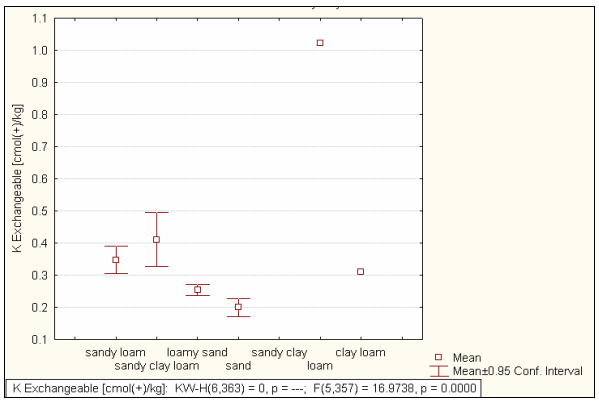

Figure 7.73. Exchangeable K content ($cmol_c$ kg^{-1}), per textural class

Aeolian parent material, as embodied by the Kalahari sands, contains significantly less extractable and exchangeable K than those of alluvial or colluvial origin (Figures 7.74 and 7.75). It also contains less extractable K than soils formed *in situ*.

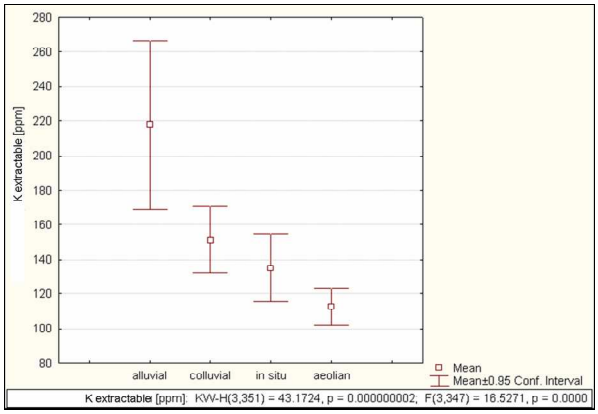

Figure 7.74. Extractable K content (ppm = mg kg^{-1}), per origin of parent material

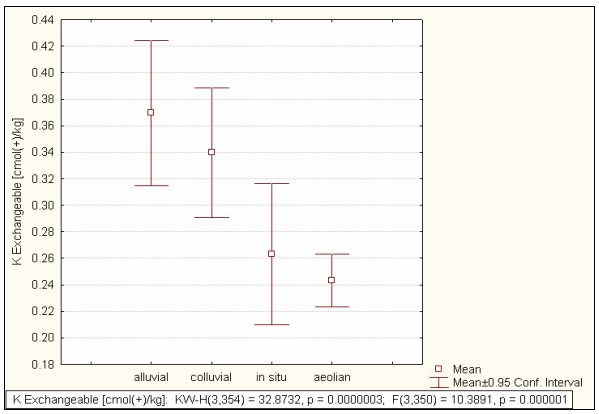

Figure 7.75. Exchangeable K content ($cmol_c$ kg^{-1}), per origin of parent material

Both extractable and exchangeable K concentrations are significantly lower in the Kalahari sands than the soils formed on the Khomas Hochland schist, due to the mineral composition of the parent materials (Figures 7.76 – 7.77).

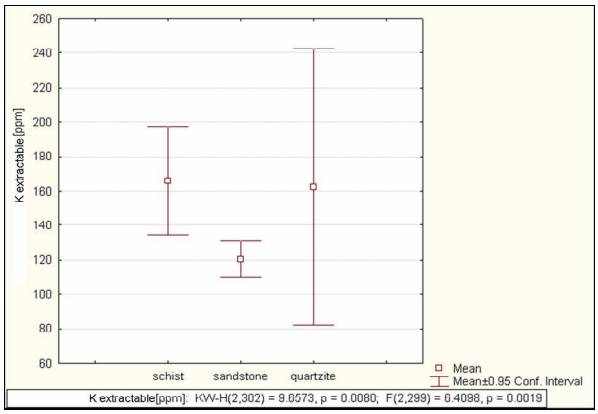

Figure 7.76. Extractable K content (ppm = mg kg^{-1}), per type of parent material

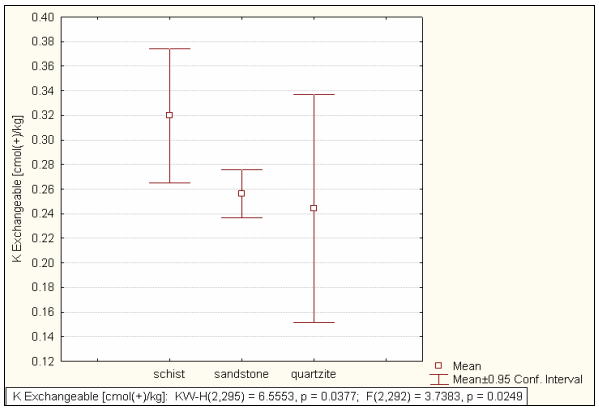

Figure 7.77. Exchangeable K content ($cmol_c$ kg^{-1}), per type of parent material

Arenosols, Regosols and Leptosols of the study area contain significantly lower concentrations of extractable and exchangeable K than Cambisols and Calcisols (Figures 7.80 – 7.81). The ±0.95 confidence interval of Luvisols is too large to allow predictions of this class (Figures 7.78 – 7.79). The lower K concentrations in Arenosols are caused by low base concentrations in the parent material, low CEC, and greater rates of leaching due to sandy texture. Calcisols, being rich in calcium and accompanying bases, and Cambisols, being young soils formed on schist, contain considerable amounts of both extractable and exchangeable K.

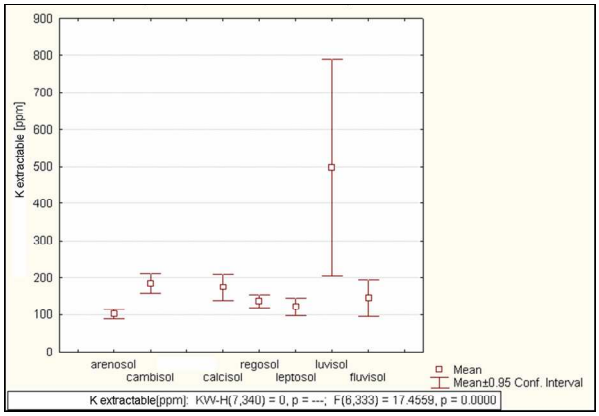

Figure 7.78. Extractable K content (ppm = mg kg^{-1}), per WRB reference soil group

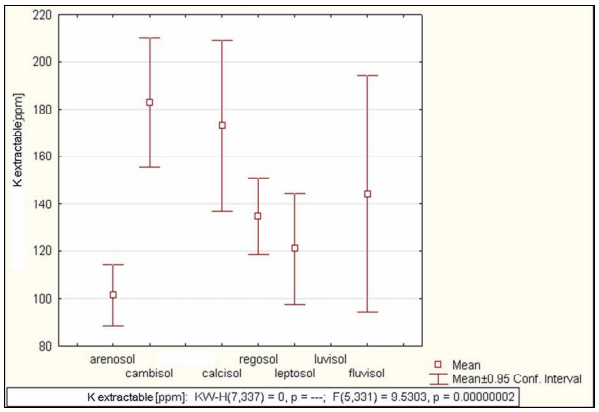

Figure 7.79. Extractable K content (ppm = mg kg^{-1}), per WRB reference soil group, excluding Luvisols

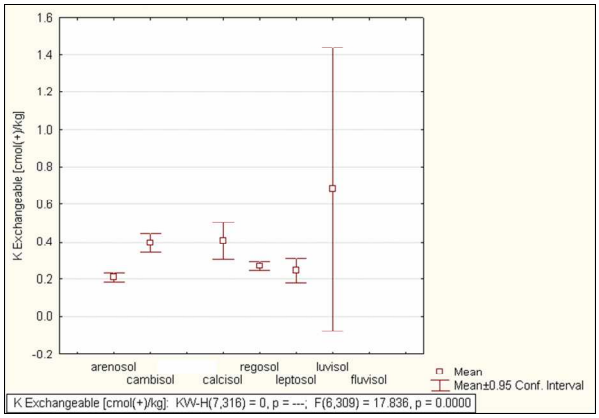

Figure 7.80. Exchangeable K content ($cmol_c$ kg^{-1}), per WRB reference soil group

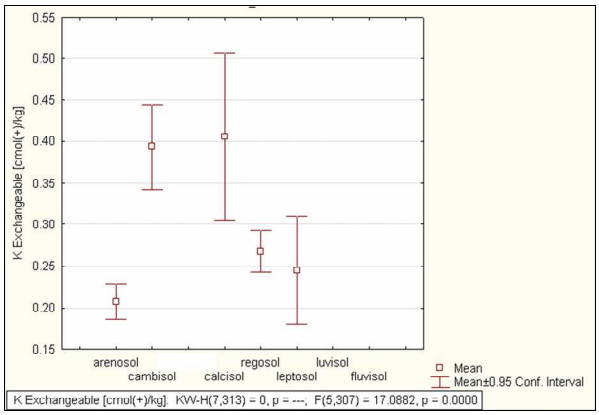

Figure 7.81. Exchangeable K content ($cmol_c$ kg^{-1}), per WRB reference soil group, excluding Luvisols

Table 7.16: Extractable K content (mg kg^{-1} and $cmol_c$ kg^{-1}) and exchangeable K content ($cmol_c$ kg^{-1}), per WRB reference soil group.

K extractable mg kg^{-1}	**Arenosols** (n = 132)	**Calcisols** (n = 17)	**Leptosols** (n = 24)	**Fluvisols** (n = 6)	**Cambisols** (n = 66)	**Regosols** (n = 89)	**Luvisols** (n = 3)
Mean	101.2	173.2	121.0	144.2	182.8	134.9	498.0
Median	84.5	178.0	112.5	125.5	166.0	117.0	462.0
Std.Dev.	77.9	70.0	55.4	47.6	111.1	77.3	118.2
Minimum	18	58	27	104	57	35	402
Maximum	756	326	268	212	592	564	630
Range	738	268	241	108	535	529	228
Lower Quartile	52	130	81	106	114	96	402
Upper Quartile	130	213	154	192	196	152	630
Quartile Range	78	83	73	86	82	56	228
Percentile 10	43	72	58	104	96	70	402

Percentile 90	170	248	188	212	258	188	630
K extractable $cmol_c\ kg^{-1}$	**Arenosols** (n = 132)	**Calcisols** (n = 17)	**Leptosols** (n = 24)	**Fluvisols** (n = 6)	**Cambisols** (n = 66)	**Regosols** (n = 89)	**Luvisols** (n = 3)
Mean	0.26	0.44	0.31	0.37	0.47	0.35	1.27
Median	0.22	0.46	0.29	0.32	0.42	0.30	1.18
Std.Dev.	0.20	0.18	0.14	0.12	0.28	0.20	0.30
Minimum	0.05	0.15	0.07	0.27	0.15	0.09	1.03
Maximum	1.93	0.83	0.69	0.54	1.51	1.44	1.61
Range	1.89	0.69	0.62	0.28	1.37	1.35	0.58
Lower Quartile	0.13	0.33	0.21	0.27	0.29	0.25	1.03
Upper Quartile	0.33	0.54	0.39	0.49	0.50	0.39	1.61
Quartile Range	0.20	0.21	0.19	0.22	0.21	0.14	0.58
Percentile 10	0.11	0.18	0.15	0.27	0.25	0.18	1.03
Percentile 90	0.43	0.63	0.48	0.54	0.66	0.48	1.61
K exchangeable $cmol_c\ kg^{-1}$	**Arenosols** (n = 129)	**Calcisols** (n = 11)	**Leptosols** (n = 15)	**Fluvisols** (n = 0)	**Cambisols** (n = 61)	**Regosols** (n = 88)	**Luvisols** (n = 3)
Mean	0.21	0.41	0.25	-	0.39	0.27	0.68
Median	0.16	0.34	0.23	-	0.36	0.25	0.59
Std.Dev.	0.13	0.20	0.12	-	0.20	0.12	0.31
Minimum	0.03	0.20	0.12	-	0.14	0.07	0.44
Maximum	0.90	0.88	0.45	-	1.51	0.87	1.02
Range	0.87	0.68	0.34	-	1.37	0.80	0.59
Lower Quartile	0.12	0.24	0.13	-	0.27	0.20	0.44
Upper Quartile	0.27	0.51	0.36	-	0.47	0.33	1.02
Quartile Range	0.15	0.27	0.23	-	0.20	0.13	0.59
Percentile 10	0.08	0.21	0.12	-	0.24	0.14	0.44
Percentile 90	0.38	0.75	0.44	-	0.59	0.39	1.02

Both extractable and exchangeable K concentrations tend to be highest in the lowest landscape positions (valleys and lower slopes), and lowest in the higher landscape positions (upper slopes and ridges) (Figures 7.82 – 7.83). This can be explained by mass movement of K-containing colluvial material down inclines, as well as vertical and lateral displacement of K by, percolating water.

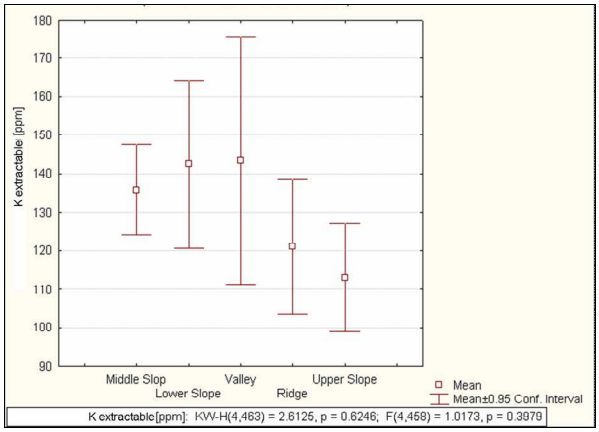

Figure 7.82. Extractable K content (ppm = mg kg^{-1}), per position in the landscape

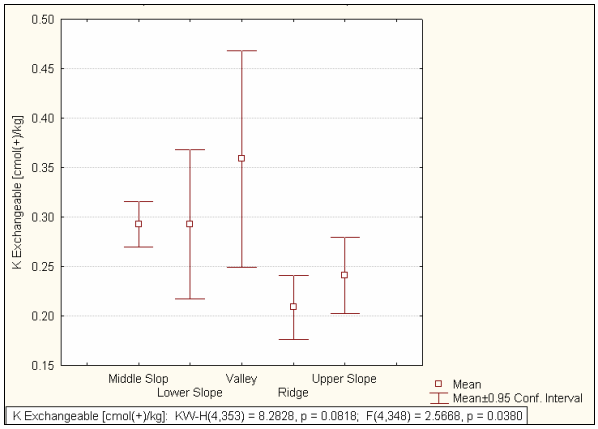

Figure 7.83. Extractable K content (ppm = mg kg^{-1}), per position in the landscape

Both extractable and exchangeable K concentrations are significantly higher in terrain with a moderate to high degree of dissection (Figures 7.84 – 7.85). One explanation is greater rates of erosion and subsequent weathering in more dissected terrain. Secondly, the highly dissected terrain of the study area occurs mainly

on schist, quartzite and calcrete, whereas the less dissected areas, towards the east, are mainly covered with Kalahari sands.

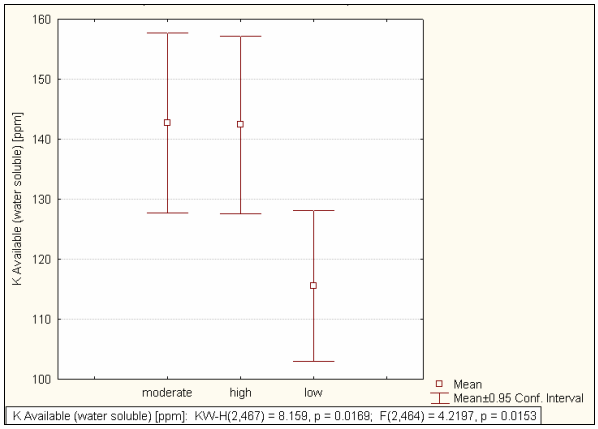

Figure 7.84. Extractable K content (ppm = mg kg^{-1}), per degree of dissection of the landscape

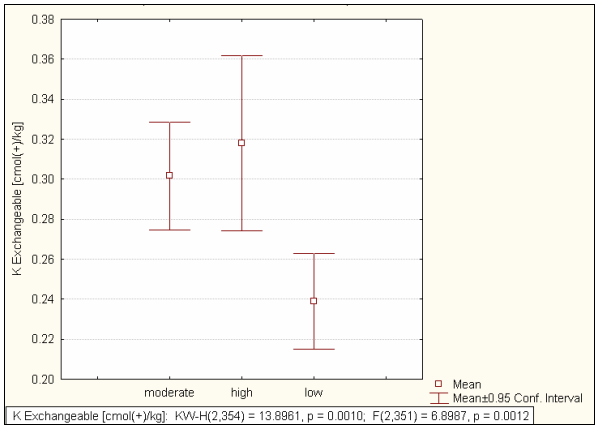

Figure 7.85. Exchangeable K content ($cmol_c$ kg^{-1}), per degree of dissection of the landscape

The extractable and exchangeable K levels of profiles from the study area, of topsoil and subsoil respectively, are shown in Figures 7.86 – 7.89.

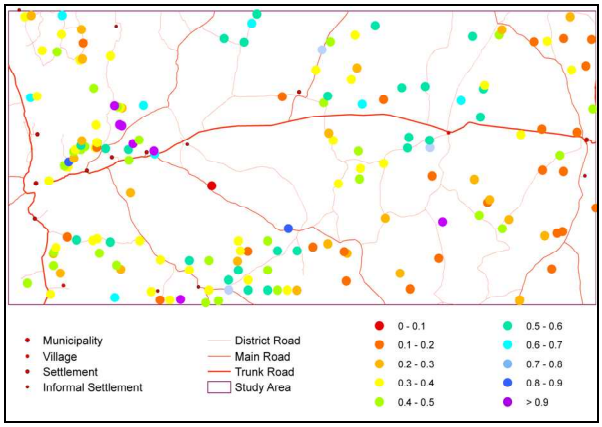

Figure 7.86. Extractable K content ($cmol_c$ kg^{-1}) of topsoil

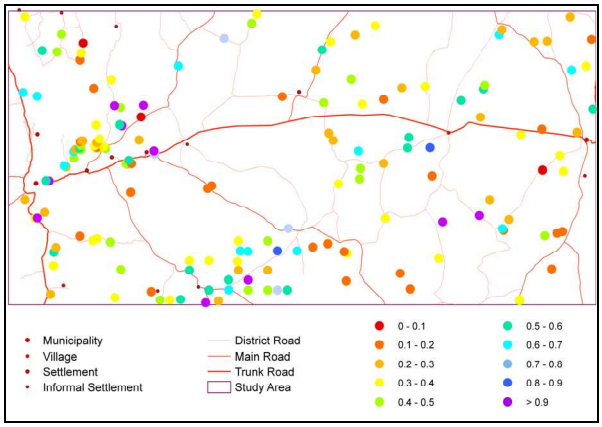

Figure 7.87. Extractable K content ($cmol_c$ kg^{-1}) of subsoil

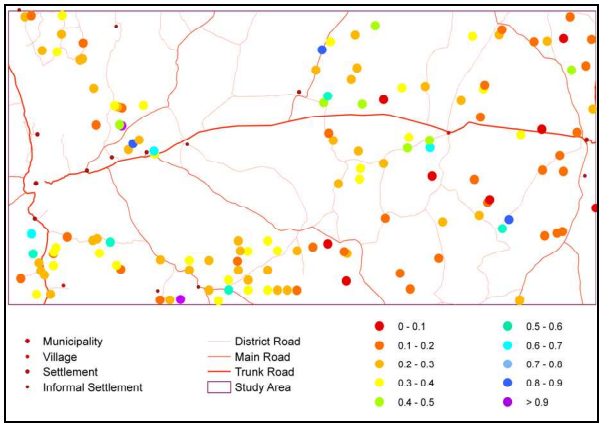

Figure 7.88. Exchangeable K content ($cmol_c$ kg^{-1}) of topsoil

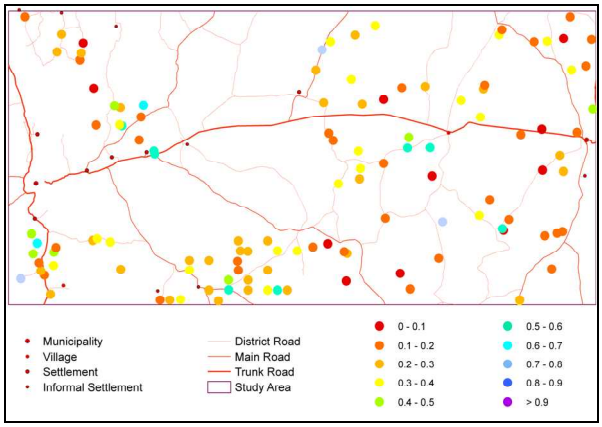

Figure 7.89. Exchangeable K content ($cmol_c$ kg^{-1}) of subsoil

7.5 SODIUM [Na]

Sodium is the 6th most abundant element in the Earth's crust. It occurs in more than 100 minerals, such as the primary minerals plagioclase feldspars [$NaAlSi_3O_8$], amphiboles [$(Na,Ca)_2(Mg,Fe,Al)_5(SiAl)_8\ O_{22}(OH)_2$] and halite (rock salt) [NaCl] , and secondary minerals such as montmorillonite [$(Na,Ca)_{0.33}(Al,Mg)_2(Si_4O_{10})(OH)_2 \cdot nH_2O$]. It occurs in simple compounds such as sulphate [Na_2SO_4], carbonate [Na_2CO_3], bicarbonate [$NaHCO_3$] and phosphate [Na_3PO_4] (Whitehead, 2000).

Table 7.17: Typical sodium concentrations (in mg kg^{-1}) found in the earth's crust, some common rocks, and soils.

SOURCE	Whitehead, 2000	Foth, 1999	Helmke, 2000
Earth's crust		28 000	
Granite	24 600		
Basalt	16 000		
Shale	9 600		
Sandstone	3 300		
Limestone	400		
Soils from Granite	16 000		
Soils from Shale	12 000		
Soils from Sandstone	7 100		
Entisol			20 100
Spodosol			18 600
Alfisol			7 500
Mollisol			10 000
Soils (general)	200-10 000		750 – 7 500 [6 300]

Sodium in soils occurs in minerals, as ions on the exchange complex, and as the mobile Na^+ ion in the soil solution. It moves within the soil mainly by diffusion. Sodium is easily lost through leaching, especially from sandy soils, removal of herbage through grazing, and surface runoff. Replenishment is from weathering of parent materials, livestock excreta and atmospheric input, particularly in coastal areas. Atmospheric inputs of between 2 and 70 kg ha^{-1} a^{-1} had been reported in literature, with the more usual range between 21 and 41 kg ha^{-1} a^{-1} (Whitehead, 2000).

Table 7.18: Estimated sodium balances (g ha^{-1} $year^{-1}$) from an extensively managed clover-grassland, grazed by cattle (Whitehead, 2000).

	Estimated Na (g ha^{-1} $year^{-1}$)
Inputs	
Deposition from atmosphere	20
Aspect of recycling	
Uptake into herbage	3.7
Consumption of herbage by animals	2.2
Dead herbage to soil	4.5
Dead roots to soil	7
Excreta to soil of grazed area	1.7
Outputs	
Milk / live-weight gain	0.5
Leaching / runoff	2.0
Loss through excreta off sward	0
Gain to soil	0

Sodium is not generally considered to be an essential plant nutrient, though it is found in plants and can apparently substitute for potassium in some non-specific functions, such as maintenance of osmotic potential and pH (Whitehead, 2000). It activates some enzyme systems and may be involved in carbon assimilation

(Foth, 1990). It apparently protects mesophyll chloroplasts (Mengel *et al.*, 2001). Positive yield responses had been recorded for additions of sodium in cases of slight to moderate potassium deficiency (Mundy, 1984; Webb *et al*., 1990). *Atriplex* species (old man's salt bush) need sodium, while beetroot, sugar, celery, spinach and turnips react well to sodium, provided that sufficient potassium is also available. Herbage concentrations of sodium may vary from traces to more than 2 % (Whitehead, 2000), though it is most often around 0.1 – 0.2 %. It is an essential nutrient for animals, where it contributes to maintenance of osmotic potential and cellular pH, and is involved in muscle contraction, the active transport of amino acids and glucose, the absorption and transport of calcium, and milk production (Whitehead, 2000). The main reason for sodium analysis is to diagnose sodicity problems.

7.5.1 STATISTICAL ANALYSIS: EXTRACTABLE AND EXCHANGEABLE SODIUM CONTENT

Normality was rejected for extractable and exchangeable Na content by the statistical tests employed, namely the Shapiro-Wilk W test, Kolmogorov-Smirnov / Lilliefors test, and three D'Agostino tests based in skewness, on kurtosis, and on a combination of skewness and kurtosis (AnalystSoft, 2007).

Table 7.19: Descriptive statistics – extractable sodium content (n = 529) and exchangeable sodium content (n = 400).

	Na extractable		**Na exchangeable**
	mg kg^{-1}	$cmol_c$ kg^{-1}	$cmol_c$ kg^{-1}
Mean	57.43	0.25	0.05
Median	31	0.13	0.02
Standard Deviation	105.27	0.46	0.10
Coefficient of Variation	1.83	1.83	1.98
Minimum	0	0.00	0.00
Maximum	820	3.57	0.79
Range	820	3.57	0.79
Lower Quartile	19	0.08	0.00
Upper Quartile	55	0.24	0.05
Quartile Range	36	0.16	0.05
Percentile 10	11	0.05	0.00
Percentile 90	87	0.38	0.13
Skewness	5.20	5.20	3.50
Kurtosis	29.34	29.34	14.56

The **extractable sodium** content of 529 samples from the study area ranges from 0 to 3.57 $cmol_c$ kg^{-1}. The lower 90 % of samples are fairly normally distributed, but the upper 10 % skews the distribution (Table 7.20; Figures 7.90 – 7.91). The mean (0.25 $cmol_c$ kg^{-1}) is higher than the median (0.13 $cmol_c$ kg^{-1}), with a skewness of 5.20 and kurtosis of 29.34. The standard deviation is 0.46. Half the samples have concentrations of between 0.08 (1^{st} quartile) and 0.24 $cmol_c$ kg^{-1} (3^{rd} quartile), for a quartile range of 0.16. In 80 % of samples, the Na content is between 0.05 (1^{st} decile) and 0.38 $cmol_c$ kg^{-1} (9^{th} decile).

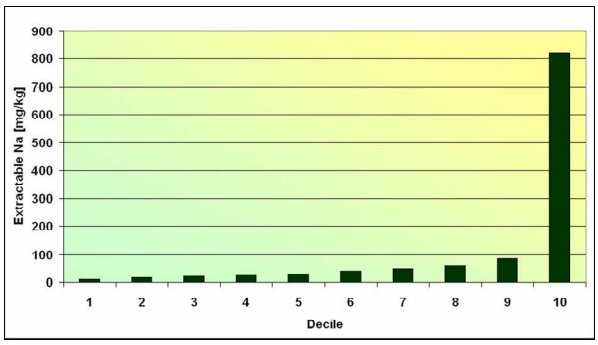

Figure 7.90. Decile distribution of extractable sodium content (mg kg^{-1})

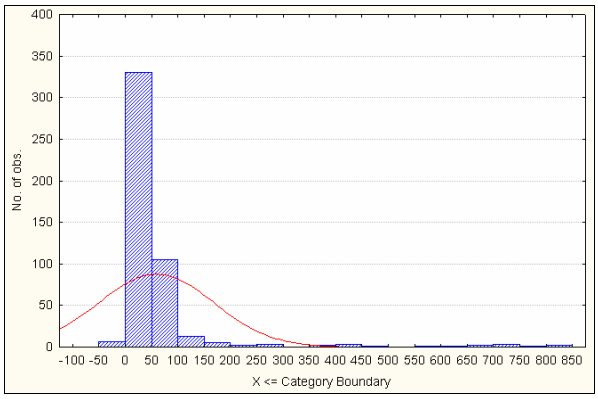

Figure 7.91. Histogram of extractable sodium content (mg kg^{-1})

Table 7.20: Distribution in terms of deciles – extractable sodium content (n = 529) and exchangeable sodium content (n = 400).

	Decile	Na extractable		Na exchangeable
		mg kg^{-1}	$cmol_c$ kg^{-1}	$cmol_c$ kg^{-1}
minimum		0	0.00	0.00
	1	11	0.05	0.00
	2	17	0.07	0.00
	3	21	0.09	0.00
	4	27	0.12	0.01
median	5	31	0.13	0.02
	6	41	0.18	0.02
	7	50	0.22	0.04
	8	60	0.26	0.06
	9	87	0.38	0.12
maximum	10	820	3.57	0.79

A statistically significant correlation, at $p < 0.05$, was found between extractable sodium content and the electrical conductivity of the 2:5 soil:water suspension ($r^2 = 0.43$). Significant, but weak, correlations were found with exchangeable sodium content ($r^2 = 0.18$), available phosphorus ($r^2 = 0.13$) and exchangeable potassium content ($r^2 = 0.10$).

The **exchangeable sodium** content of 400 samples from the study area ranges from 0.00 to 0.79 $cmol_c$ kg^{-1}. The lower 90 % of samples is normally distributed, but the upper 10 % skews the distribution (Table 7.20; Figures 7.92 – 7.93).The mean (0.05 $cmol_c$ kg^{-1}) is thus higher than the median (0.02 $cmol_c$ kg^{-1}), with a skewness of 3.50 and kurtosis of 14.56. The standard deviation is 0.10. Half the samples have sodium concentrations of between 0.00 (1^{st} quartile) and 0.05 $cmol_c$ kg^{-1} (3^{rd} quartile), for a quartile range of 0.05. In 80 % of samples, the Na content is between 0.00 (1^{st} decile) and 0.13 $cmol_c.kg^{-1}$ (9^{th} decile). These values correspond to exchangeable Na concentrations reported in literature, such as 0.1 – 0.2 $cmol_c$ kg^{-1} (Forth, 1990) and 0.0 – 0.02 $cmol_c$ kg^{-1} for Kalahari soils (Dougill and Cox, 1995)

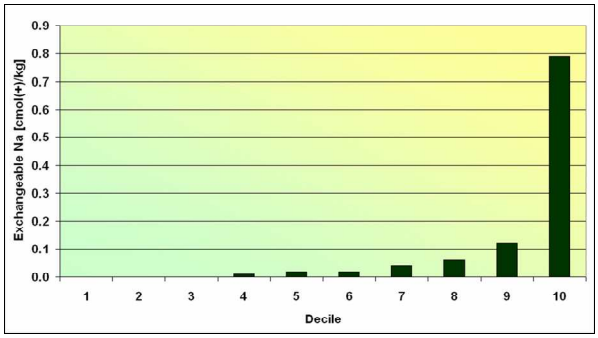

Figure 7.92. Decile distribution of exchangeable sodium content ($cmol_c kg^{-1}$)

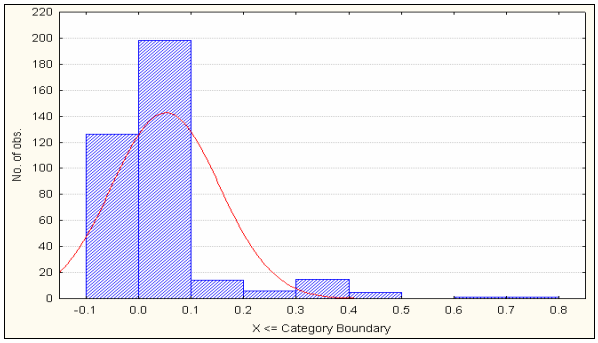

Figure 7.93. Histogram of exchangeable sodium content ($cmol_c kg^{-1}$)

Topsoil and subsoil concentrations of exchangeable Na do not differ significantly (Table 7.21; Figure 7.95). The mean of extractable Na content is higher in the subsoil than the topsoil. There is, however, a large overlap of the ±0.95 confidence intervals (Table 7.21; Figure 7.94).

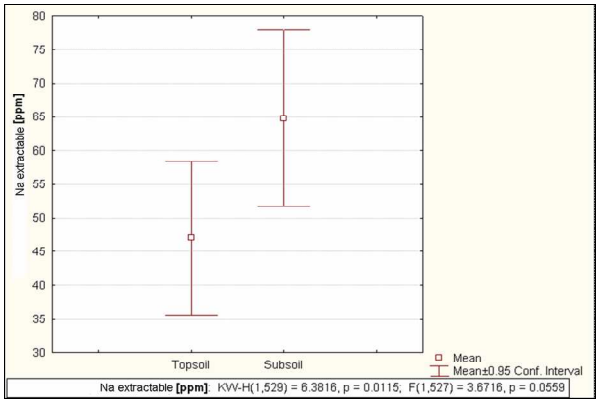

Figure 7.94. Extractable Na content (ppm = mg kg^{-1}), per topsoil and subsoil

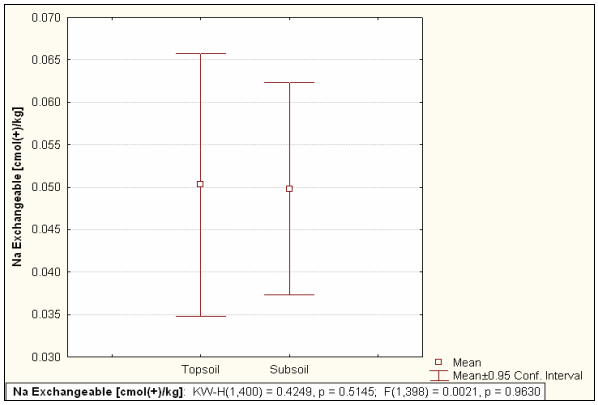

Figure 7.95. Exchangeable Na content ($cmol_c kg^{-1}$), per topsoil and subsoil

Table 7.21. Extractable Na content (mg kg^{-1} and $cmol_c kg^{-1}$) and exchangeable Na content ($cmol_c kg^{-1}$), per topsoil and subsoil.

	Na extractable				Na exchangeable	
	Topsoil (n = 199)		Subsoil (n = 283)		Topsoil (n = 163)	Subsoil (n = 203)
	mg kg^{-1}	$cmol_c$ kg^{-1}	mg kg^{-1}	$cmol_c$ kg^{-1}	$cmol_c$ kg^{-1}	$cmol_c$ kg^{-1}
Mean	48.46	0.21	66.40	0.29	0.05	0.05
Median	29.00	0.13	33.00	0.14	0.02	0.02
Std Dev	89.97	0.39	121.43	0.53	0.11	0.10
Minimum	0.00	0.00	0.00	0.00	0.00	0.00
Maximum	721.00	3.13	820.00	3.57	0.79	0.61
Range	721.00	3.13	820.00	3.57	0.79	0.61
Lower Quartile	18.00	0.08	19.00	0.08	0.00	0.00
Upper Quartile	51.00	0.22	60.00	0.26	0.05	0.05
Quartile Range	33.00	0.14	41.00	0.18	0.05	0.05
Percentile10	10.00	0.04	12.00	0.05	0.00	0.00
Percentile 90	69.00	0.30	103.00	0.45	0.15	0.12

Arenosols of the study area contain significantly lower concentrations of extractable Na than Cambisols and Regosols. The ±0.95 confidence intervals of Fluvisols, Calcisols and Luvisols are too large to allow

predictions of these classes (Table 7.22; Figures 7.96 – 7.97). Furthermore, Arenosols and Leptosols of the study area contain significantly lower concentrations of exchangeable Na than Cambisols, Regosols and Luvisols. The ±0.95 confidence interval of Calcisols is too large to allow predictions of this class (Figure 7.98).

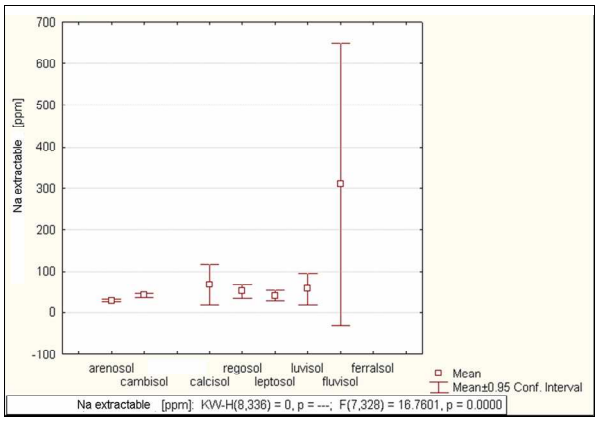

Figure 7.96. Extractable Na content (ppm = mg kg^{-1}), per WRB reference soil group

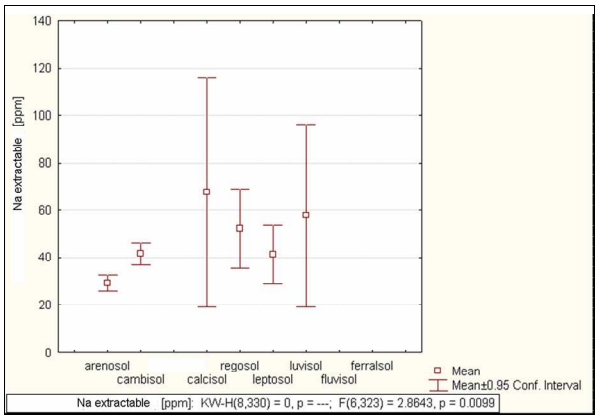

Figure 7.97. Extractable Na content (ppm = mg kg^{-1}), per WRB reference soil group, excluding Fluvisols

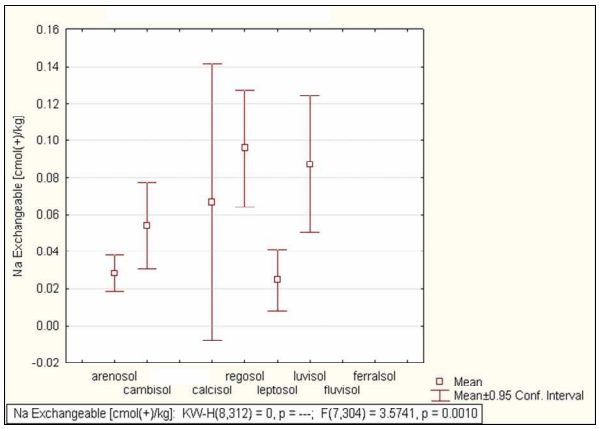

Figure 7.98. Exchangeable Na content ($cmol_c$ kg^{-1}), per WRB reference soil group, excluding Fluvisols

Table 7.22. Extractable Na content (mg kg^{-1} and $cmol_c$ kg^{-1}) and exchangeable Na content ($cmol_c$ kg^{-1}), per WRB reference soil group.

Na extr mg kg^{-1}	**Arenosols** (n = 132)	**Calcisols** (n = 17)	**Leptosols** (n = 24)	**Fluvisols** (n = 6)	**Cambisols** (n = 66)	**Regosols** (n = 88)	**Luvisols** (n = 3)
Mean	29.5	67.7	41.4	309.7	41.6	52.2	57.7
Median	28.0	43.0	37.5	219.0	41.5	46.0	64.0
Std.Dev.	20.1	94.4	29.0	324.0	19.0	78.9	15.5
Minimum	0	10	17	14	3	2	40
Maximum	86	407	156	698	92	721	69
Range	86	397	139	684	89	719	29
Lower Quartile	14	26	21	27	27	26	40
Upper Quartile	40	60	50	681	52	58	69
Quartile Range	26	34	29	654	25	33	29
Percentile 10	6	12	18	14	18	15	40
Percentile 90	63	164	61	698	67	73	69

Na extr $cmol_c\ kg^{-1}$	**Arenosols** (n = 132)	**Calcisols** (n = 17)	**Leptosols** (n = 24)	**Fluvisols** (n = 6)	**Cambisols** (n = 66)	**Regosols** (n = 88)	**Luvisols** (n = 3)
Mean	0.13	0.29	0.18	1.35	0.18	0.23	0.25
Median	0.12	0.19	0.16	0.95	0.18	0.20	0.28
Std.Dev.	0.09	0.41	0.13	1.41	0.08	0.34	0.07
Minimum	0.00	0.04	0.07	0.06	0.01	0.01	0.17
Maximum	0.37	1.77	0.68	3.03	0.40	3.13	0.30
Range	0.37	1.73	0.60	2.97	0.39	3.13	0.13
Lower Quartile	0.06	0.11	0.09	0.12	0.12	0.11	0.17
Upper Quartile	0.17	0.26	0.22	2.96	0.23	0.25	0.30
Quartile Range	0.11	0.15	0.13	2.84	0.11	0.14	0.13
Percentile 10	0.03	0.05	0.08	0.06	0.08	0.07	0.17
Percentile 90	0.27	0.71	0.27	3.03	0.29	0.32	0.30
Na exch $cmol_c\ kg^{-1}$	**Arenosols** (n = 129)	**Calcisols** (n = 17)	**Leptosols** (n = 15)	**Fluvisols** (n = 0)	**Cambisols** (n = 61)	**Regosols** (n = 87)	**Luvisols** (n = 3)
Mean	0.03	0.07	0.02	-	0.05	0.10	0.09
Median	0.02	0.02	0.00	-	0.00	0.02	0.10
Std.Dev.	0.05	0.15	0.03	-	0.09	0.15	0.02
Minimum	0.00	0.00	0.00	-	0.00	0.00	0.07
Maximum	0.44	0.61	0.09	-	0.42	0.79	0.10
Range	0.44	0.61	0.09	-	0.42	0.79	0.03
Lower Quartile	0.00	0.00	0.00	-	0.00	0.01	0.07
Upper Quartile	0.04	0.06	0.04	-	0.06	0.12	0.10
Quartile Range	0.04	0.06	0.04	-	0.06	0.11	0.03
Percentile 10	0.00	0.00	0.00	-	0.00	0.00	0.07
Percentile 90	0.06	0.14	0.06	-	0.16	0.34	0.10

There are no clear relationships between extractable or exchangeable Na concentrations and positions in the landscape (Figures 7.99 – 7.100).

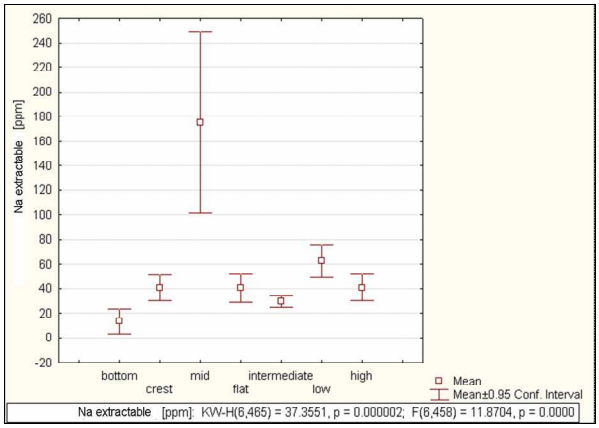

Figure 7.99. Extractable Na content (ppm = mg kg^{-1}), per position in the landscape

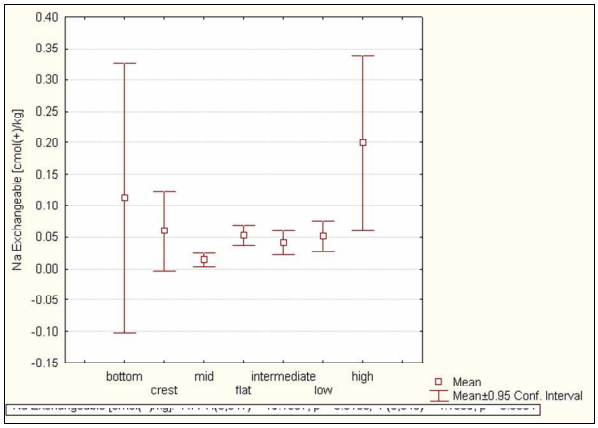

Figure 7.100. Exchangeable Na content ($cmol_c\ kg^{-1}$), per position in the landscape

Extractable Na concentrations are significantly higher in terrain with a moderate to high degree of dissection (Figure 7.101), but there is no discernable relationship for exchangeable Na (Figure 7.102).

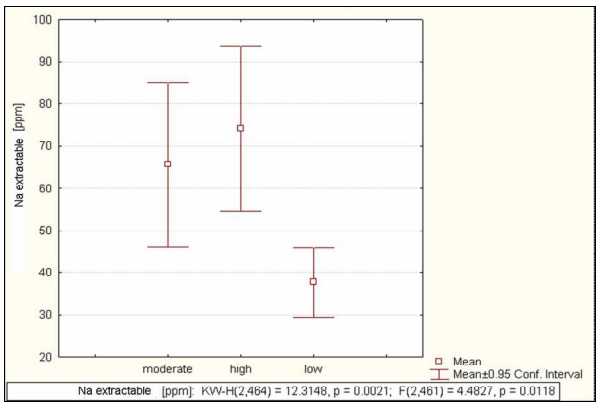

Figure 7.101. Extractable Na content (ppm = mg kg^{-1}), per degree of dissection of the landscape

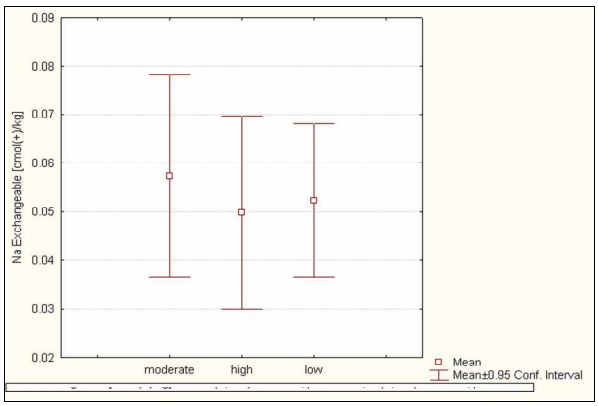

Figure 7.102. Exchangeable Na content ($cmol_c$ kg^{-1}), per degree of dissection of the landscape

The extractable and exchangeable Na levels, of topsoil and subsoil respectively, are shown in Figures 7.103 – 7.106, while Figures 7.107 and 7.108 depicts exchangeable sodium percentage.

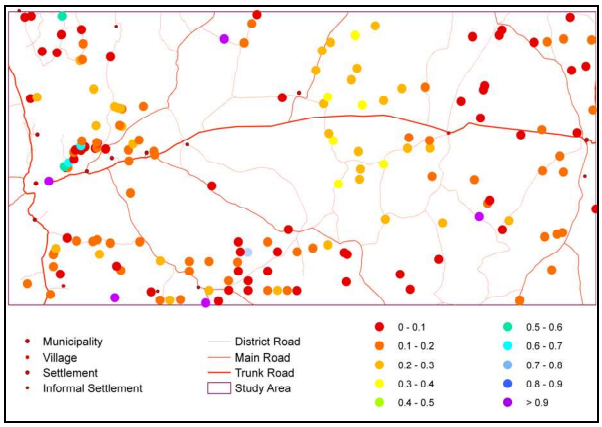

Figure 7.103. Extractable Na content ($cmol_c$ kg^{-1}) of topsoil

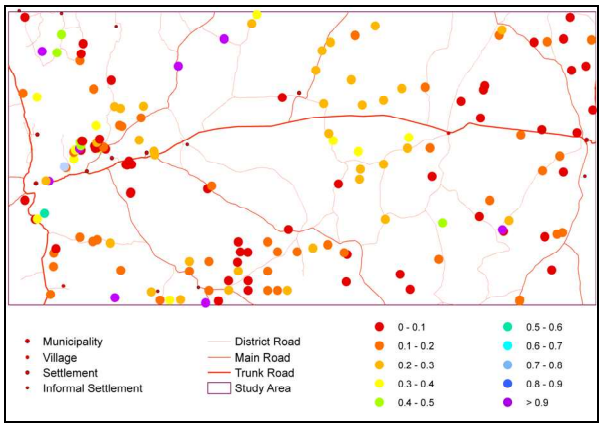

Figure 7.104. Extractable Na content ($cmol_c$ kg^{-1}) of subsoil

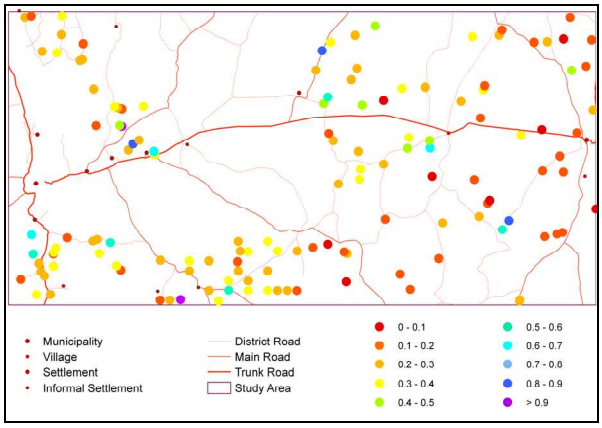

Figure 7.105. Exchangeable Na content ($cmol_c$ kg^{-1}) of topsoil

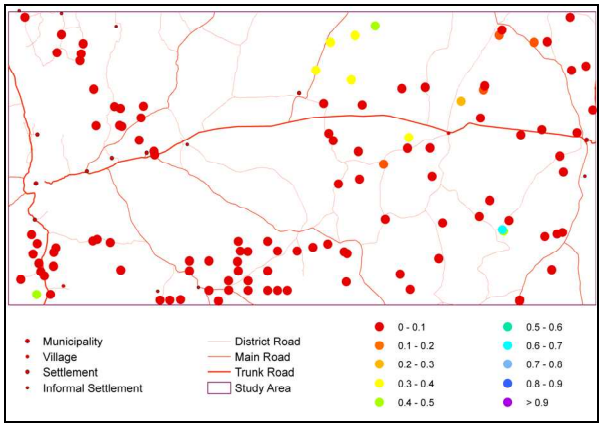

Figure 7.106. Exchangeable Na content ($cmol_c$ kg^{-1}) of subsoil

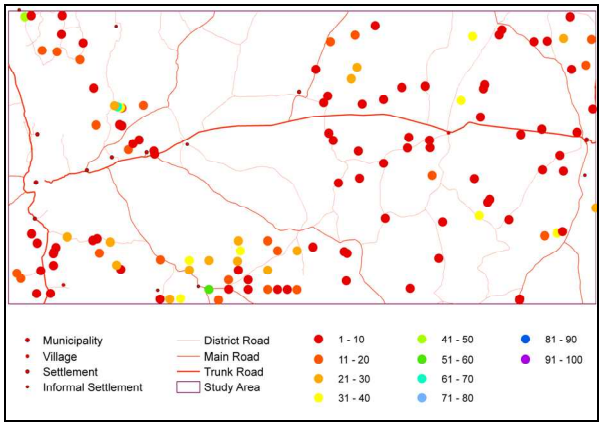

Figure 7.107. Exchangeable Na as a percentage of CEC, in topsoil

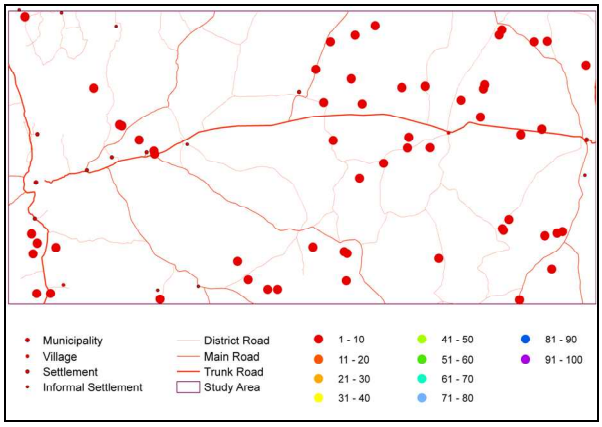

Figure 7.108. Exchangeable Na as a percentage of CEC, in subsoil

CHAPTER EIGHT

CHEMICAL CHARACTERISATION – CEC, BASE SATURATION AND SALINITY

8.1 CATION EXCHANGE CAPACITY, SUM OF EXCHANGEABLE BASES, SUM OF EXTRACTABLE BASES

The **cation exchange capacity** (CEC) is the sum total of exchangeable cations that a soil can adsorb, due to the negative electrical charge of the colloidal fraction of soil (Van der Watt and Van Rooyen, 1995). It is expressed in $cmol_c\ kg^{-1}$ (or $cmol(+)\ kg^{-1}$) of soil or clay, and is associated with phyllosilicates and soil organic matter, and under alkaline conditions also with secondary iron and aluminium phases (Bühmann, Beukes and Turner, 2006). These colloids all carry negative charges that are balanced through the adsorption of cations from the soil solution. In the case of phyllosilicates, the charges are partly the result of isomorphous replacement and partly due to the displacement of H^+ from the edges of the lattice structure. The number of adsoption sites, and thus the cation exchange capacity, determines the nutrient storage capacity of the soil. Adsorbed cations are potentially available to plants, but not readily susceptible to leaching. The more strongly a cation is bound to an exchange site, the less susceptible it is to leaching. CEC of organic matter is entirely pH dependent (increasing with pH), through dissociation of H^+ ions from carboxyl and phenolic hydroxyl groups of organic matter (Foth, 1990; Whitehead, 2000), while the CEC of a small component of inorganic matter is also pH dependent through dissociation of H^+ from functional groups of clay minerals and amorphous compounds (Van der Watt and Van Rooyen, 1995).

Exchange of cations depends on their relative concentrations and strength of ionic bonding, with trivalent cations generally bound more strongly than divalent cations, which are, in turn, bound more strongly than monovalent cations. This in not always straightforward, as the degree of hydration of a cation, and thus the diameter of the hydrated cation determines how close it can come to exchange sites. When unhydrated, Na^+ is smaller than K^+, while Mg^{2+} is smaller than Ca^{2+}. When hydrated, however, K^+ is smaller than Na^+, while Ca^{2+} is smaller than Mg^{2+} (Mengel and Kirby, 1987).

In non-acidic soils, Ca^{2+} and Mg^{2+} dominate the exchange sites, accounting for up to 90% of cations, while K^+ accounts for around 5%. Na^+ content is generally very low, except in arid saline soils. In acid soils the ratios of nutrient cations are completely different, with H^+ and Al^{3+}, released from clay minerals and hydrous oxides, forming up to 90% of exchangeable cations, and Ca^{2+} and Mg^{2+} accounting for less than 10% (Whitehead, 2000).

8.1.1 STATISTICAL ANALYSIS: CEC, SUM OF EXCHANGEABLE BASES, SUM OF EXTRACTABLE BASES

Normality was rejected for cation exchange capacity, sum of extractable bases and sum of exchangeable bases by the statistical tests employed, namely the Shapiro-Wilk W test, Kolmogorov-Smirnov / Lilliefors test, and three D'Agostino tests based on skewness, on kurtosis, and on a combination of skewness and kurtosis

(AnalystSoft, 2007).

Table 8.1: Descriptive statistics – Cation exchange capacity (n = 426), sum of exchangeable bases (n = 535) and sum of extractable bases (n = 391).

	CEC	∑ Exchangeable Bases	∑ Extractable Bases
	$cmol_c\ kg^{-1}$	$cmol_c\ kg^{-1}$	$cmol_c\ kg^{-1}$
Mean	3.57	3.48	4.53
Median	2.39	2.30	3.21
Std. Dev.	3.57	3.61	4.39
CV	1.00	1.04	0.97
Minimum	0.10	0.11	0.37
Maximum	22.47	22.47	34.12
Range	22.37	22.36	33.75
Skewness	2.27	2.26	2.83
Kurtosis	6.31	5.74	10.60

The **cation exchange capacity** of 426 samples from the study area ranges from 0.10 to 22.47 $cmol_c\ kg^{-1}$ (Table 8.1; Figures 8.1 – 8.2). The mean (3.57 $cmol_c\ kg^{-1}$) is higher than the median (2.39 $cmol_c\ kg^{-1}$), with a skewness of 2.27 and kurtosis of 6.31. The standard deviation is 3.57. Most soils have a low ability to retain nutrients against leaching, as shown by the 345 samples with CEC < 7 $cmol_c\ kg^{-1}$ soil, which is considered the threshold for low nutrient retention properties by FAO (1989b).

The **sum of exchangeable bases (S-value)** of 391 samples from the study area ranges from 0.11 to 22.47 $cmol_c\ kg^{-1}$ (Table 8.1; Figures 8.3 – 8.4). The mean (3.48 $cmol_c\ kg^{-1}$) is higher than the median (2.30 $cmol_c\ kg^{-1}$), with a skewness of 2.26 and kurtosis of 5.74. The standard deviation is 3.61. Tucker (1983) found the mean sum of exchangeable bases of 75 Australian soil profiles to be 10 $cmol_c\ kg^{-1}$, and the median 8.4 $cmol_c\ kg^{-1}$. These values are lower in the study area, namely 3.48 and 2.30 $cmol_c\ kg^{-1}$ respectively.

The CEC and the sum of exchangeable bases (S-value) are virtually identical (Table 8.1; Figures 8.1 – 8.4; 8.7), which indicate the almost complete absence of exchangeable H^+ and Al^{3+} in the soil of the study area. This is as expected from a semi-arid climate.

The **sum of extractable bases** of 535 samples from the study area ranges from 0.37 to 34.12 $cmol_c\ kg^{-1}$ (Table 8.1; Figures 8.5 – 8.6). The mean (4.53 $cmol_c\ kg^{-1}$) is higher than the median (3.21 $cmol_c\ kg^{-1}$), with a skewness of 2.83 and kurtosis of 10.60. The standard deviation is 4.39.

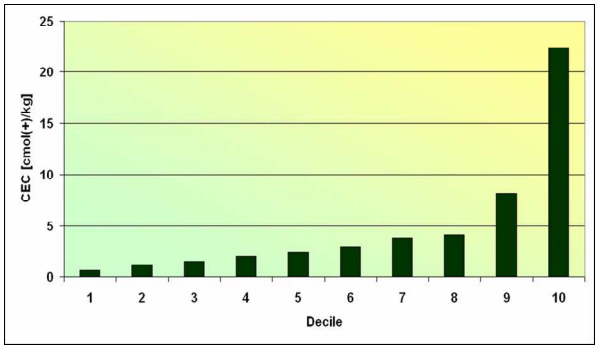

Figure 8.1. Decile distribution of CEC ($cmol_c\ kg^{-1}$)

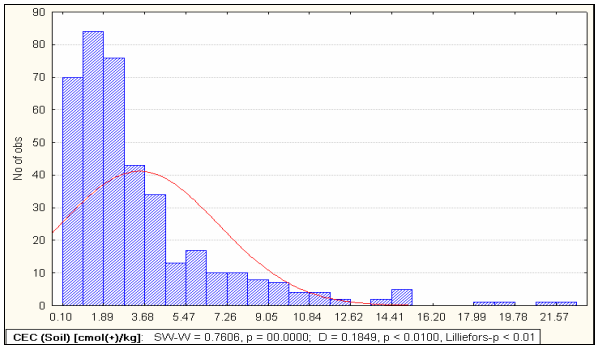

Figure 8.2. Histogram of CEC ($cmol_c\ kg^{-1}$)

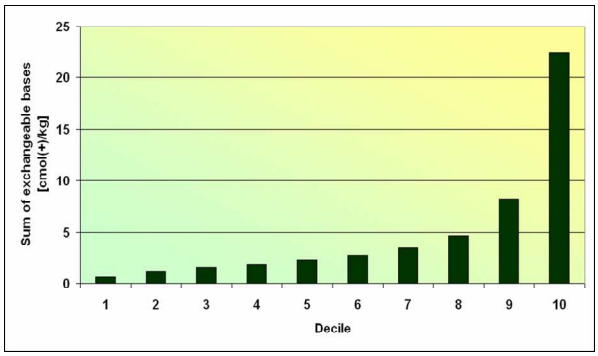

Figure 8.3. Decile distribution of sum of exchangeable bases ($cmol_c\ kg^{-1}$)

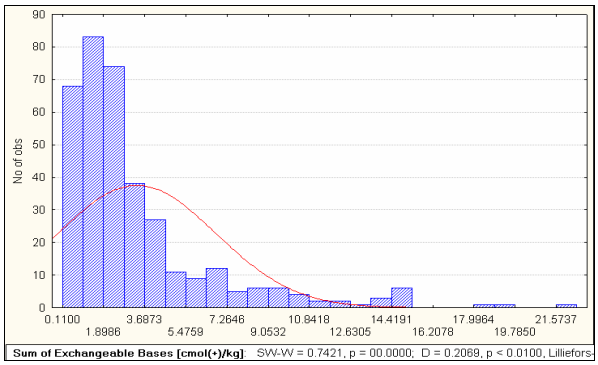

Figure 8.4. Histogram of sum of exchangeable bases ($cmol_c\ kg^{-1}$)

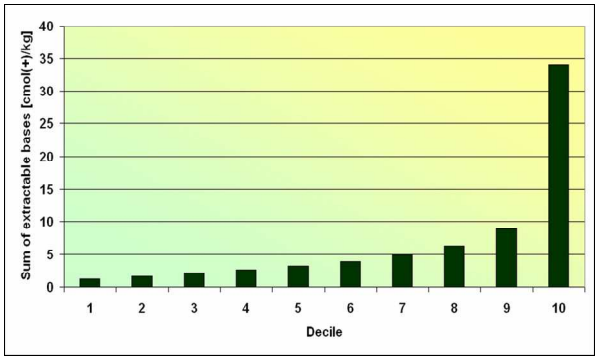

Figure 8.5. Decile distribution of sum of extractable bases ($cmol_c\ kg^{-1}$)

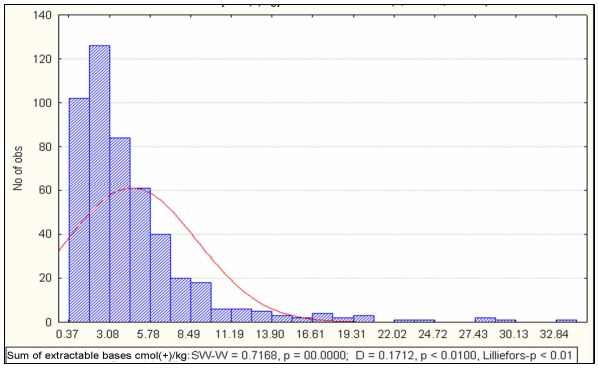

Figure 8.6. Histogram of sum of extractable bases ($cmol_c\ kg^{-1}$)

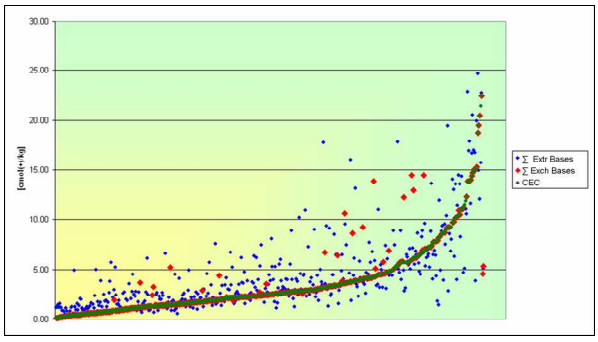

Figure 8.7. Distribution of CEC ($cmol_c\ kg^{-1}$), sum of extractable bases ($cmol_c\ kg^{-1}$) and sum of exchangeable bases ($cmol_c\ kg^{-1}$)

Topsoil CEC, sum of exchangeable bases and sum of extractable bases are lower than those of subsoil (Table 8.2; Figure 8.8). The prevailing hot semi-arid climate of the study area leads to low levels of biomass production and subsequent low levels of organic matter in the soil, combined with high rates of mineralization of organic matter. Exchange sites are thus provided to a relatively larger extent by clay than organic matter, when compared to temperate climate soils. The illuviation of clay in subsoil thus contributes more to the CEC (and exchangeable bases) than organic matter accumulation in the topsoil. Although leaching is lower than in tropical and temperate climates, there is some displacement of soluble bases towards deeper soil layers.

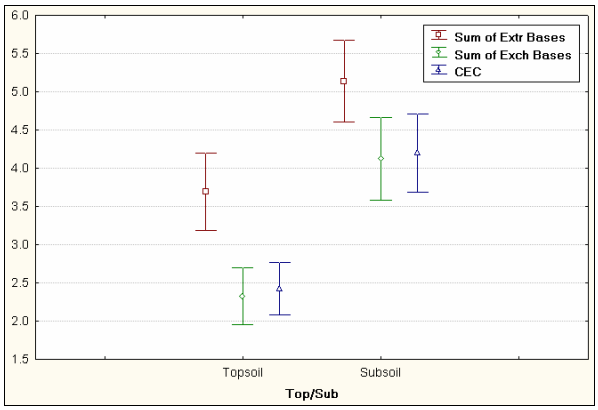

Figure 8.8. CEC ($cmol_c\ kg^{-1}$), sum of exchangeable bases ($cmol_c\ kg^{-1}$) and sum of extractable bases ($cmol_c\ kg^{-1}$), per topsoil and subsoil

Table 8.2: CEC, sum of exchangeable bases, sum of extractable bases, per topsoil and subsoil.

	CEC (Soil) $cmol_c\ kg^{-1}$		**∑ Exchangeable Bases** $cmol_c\ kg^{-1}$		**∑ Extractable Bases** $cmol_c\ kg^{-1}$	
	Topsoil (n = 184)	**Subsoil** (n = 242)	**Topsoil** (n = 172)	**Subsoil** (n = 221)	**Topsoil** (n = 184)	**Subsoil** (n = 242)
Mean	2.54	4.35	2.45	4.30	2.54	4.35
Median	1.90	3.02	1.76	2.90	1.90	3.02
Std Dev	2.43	4.07	2.53	4.08	2.43	4.07
CV	0.96	0.93	1.03	0.95	0.96	0.93
Minimum	0.15	0.10	0.15	0.11	0.15	0.10
Maximum	14.97	22.47	14.97	22.47	14.97	22.47
Range	14.82	22.37	14.82	22.36	14.82	22.37
Lower Quartile	1.10	1.57	1.03	1.55	1.10	1.57
Upper Quartile	2.72	5.30	2.55	5.18	2.72	5.30
Quartile Range	1.62	3.73	1.52	3.63	1.62	3.73
Percentile 10	0.59	0.69	0.55	0.61	0.59	0.69
Percentile 90	5.70	9.16	4.13	9.24	5.70	9.16

Tucker (1983) found the mean sum of exchangeable bases of 102 Australian topsoil samples to be 14 $cmol_c\ kg^{-1}$ and the median 10 $cmol_c\ kg^{-1}$. These values are lower in the study area, namely 2.45 and 1.76 $cmol_c\ kg^{-1}$ respectively.

No clear pattern could be discerned for CEC or sum of exchangeable bases with depth (Table 8.3).

Table 8.3: CEC and sum of exchangeable bases at various depths.

Depth cm	**CEC (Soil)** $cmol_c\ kg^{-1}$			
	0 – 10 (n = 7)	**10 – 20** (n = 29)	**20 – 30** (n = 5)	**>30** (n = 88)
Mean	1.67	1.48	1.42	2.43
Std.Dev.	1.10	1.47	1.05	2.85
Minimum	0.54	0.18	0.36	0.10
Maximum	3.41	8.17	2.71	19.46
Range	2.87	7.99	2.35	19.36
Percentile 10	0.54	0.26	0.36	0.37
Percentile 90	3.41	2.29	2.71	4.55

Depth cm	∑ Exchangeable Bases $cmol_c\ kg^{-1}$			
	0 – 10 (n = 7)	**10 – 20** (n = 29)	**20 – 30** (n = 5)	**>30** (n = 88)
Mean	1.69	1.49	1.46	2.46
Std.Dev.	1.10	1.47	1.05	2.85
Minimum	0.58	0.18	0.41	0.11
Maximum	3.45	8.17	2.75	19.48
Range	2.87	7.99	2.34	19.37
Percentile 10	0.58	0.27	0.41	0.38
Percentile 90	3.45	2.29	2.75	4.56

When disregarding sandy clay and clay loam soils, of which there are too few samples to be statistically meaningful, the CEC, sum of exchangeable bases and sum of extractable bases increase in the order sand → loamy sand → sandy loam ≈ sandy clay loam ≈ loam (Figure 8.9).

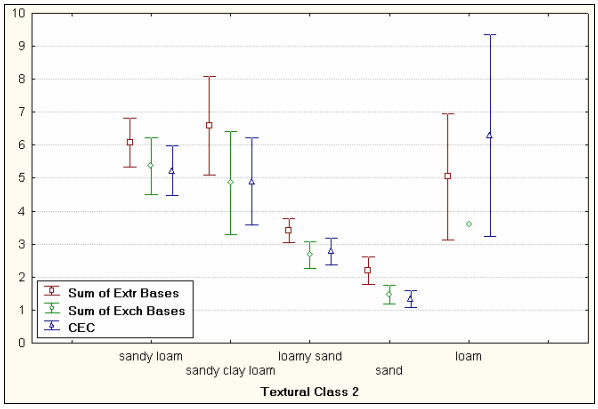

Figure 8.9. CEC ($cmol_c\ kg^{-1}$), sum of exchangeable bases ($cmol_c\ kg^{-1}$) and sum of extractable bases ($cmol_c\ kg^{-1}$), per textural class

When disregarding the pH interval 9.01 – 9.50, which has too large a ±0.95 confidence interval to be of any predictive value (Figure 8.10), the CEC, sum of exchangeable bases and sum of extractable bases increase with increasing pH (Figure 8.11).

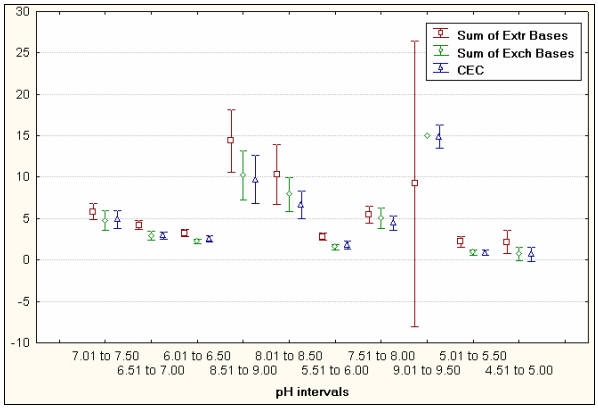

Figure 8.10. CEC ($cmol_c\ kg^{-1}$), sum of exchangeable bases ($cmol_c\ kg^{-1}$) and sum of extractable bases ($cmol_c\ kg^{-1}$), with increasing pH

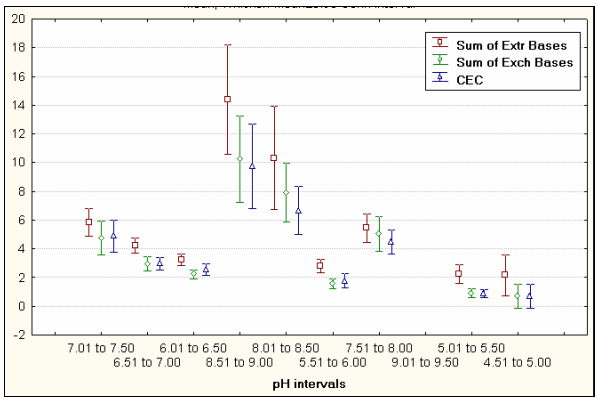

Figure 8.11. CEC ($cmol_c\ kg^{-1}$), sum of exchangeable bases ($cmol_c\ kg^{-1}$) and sum of extractable bases ($cmol_c\ kg^{-1}$), with increasing pH, excluding pH interval 9.01 – 9.50

CEC, sum of exchangeable bases and sum of extractable bases increase in the order aeolian origin (as embodied by the Kalahari sands) → formed *in situ* → colluvial origin → alluvial origin (Figure 8.12).

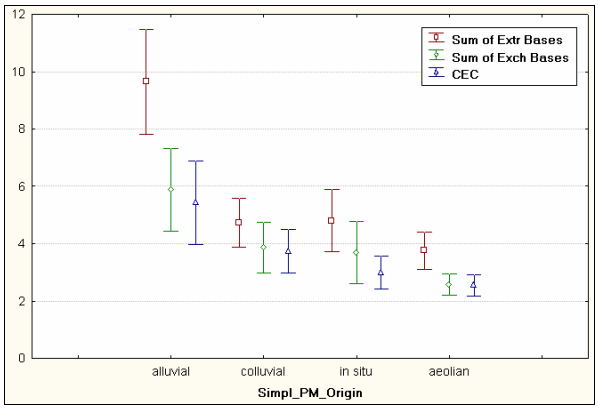

Figure 8.12. CEC ($cmol_c\ kg^{-1}$), sum of exchangeable bases ($cmol_c\ kg^{-1}$) and sum of extractable bases ($cmol_c\ kg^{-1}$), per origin of parent material

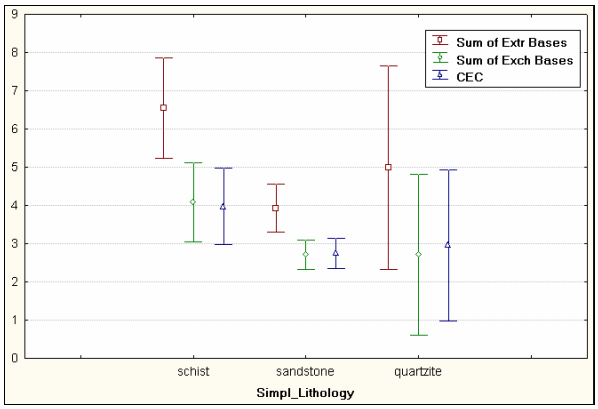

Figure 8.13. CEC ($cmol_c\ kg^{-1}$), sum of exchangeable bases ($cmol_c\ kg^{-1}$) and sum of extractable bases ($cmol_c\ kg^{-1}$), per type of parent material

CEC, sum of exchangeable bases and sum of extractable bases are significantly lower in the Kalahari sands than the soils formed on the schist of the Khomas Hochland – a consequence of the mineral composition of the respective parent materials (Figure 8.13).

Arenosols, Cambisols, Regosols and Luvisols of the study area contain significantly lower CEC, sum of exchangeable bases and sum of extractable bases than Calcisols (Table 8.4 and Figure 8.14). The spread in ±0.95 confidence intervals of Leptosols and Fluvisols are too large to allow predictions of these classes.

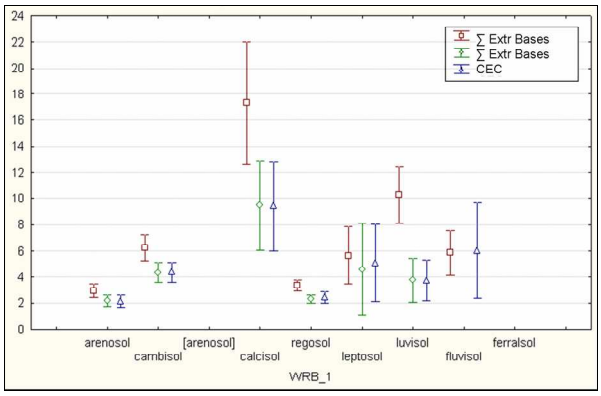

Figure 8.14. CEC ($cmol_c\ kg^{-1}$), sum of exchangeable bases ($cmol_c\ kg^{-1}$) and sum of extractable bases ($cmol_c\ kg^{-1}$), per WRB reference soil group

Table 8.4: CEC, sum of exchangeable bases and sum of extractable bases, per WRB Reference Soil Group.

CEC $cmol_c kg^{-1}$	**Arenosols** (n = 129)	**Calcisols** (n = 13)	**Leptosols** (n = 18)	**Fluvisols** (n = 4)	**Cambisols** (n = 62)	**Regosols** (n = 88)	**Luvisols** (n = 3)
Mean	2.13	9.42	5.08	6.02	4.39	2.42	3.73
Median	1.43	8.53	2.20	5.50	3.72	2.05	3.61
Std Dev	2.50	5.61	5.97	2.30	3.04	2.04	0.63
Minimum	0.10	2.09	0.38	3.84	0.44	0.20	3.18

Maximum	19.46	18.78	22.47	9.25	13.85	15.00	4.42
Range	19.36	16.69	22.08	5.41	13.41	14.81	3.18
Lower Quartile	0.66	3.94	1.16	4.55	2.06	1.27	3.18
Upper Quartile	2.54	14.68	7.65	7.49	6.09	2.75	4.42
Quartile Range	1.88	10.74	6.49	2.94	4.03	1.48	1.25
Percentile 10	0.37	3.16	0.56	3.84	1.32	0.79	4.42
Percentile 90	4.13	15.21	14.97	9.25	8.70	4.11	1.25
∑Exch Bases $cmol_c kg^{-1}$	**Arenosols** (n = 129)	**Calcisols** (n = 13)	**Leptosols** (n = 15)	**Fluvisols** (n = 0)	**Cambisols** (n = 61)	**Regosols** (n = 87)	**Luvisols** (n = 3)
Mean	2.16	9.47	4.55	-	4.35	2.30	3.77
Median	1.45	8.54	2.08	-	3.63	2.06	3.61
Std Dev	2.51	5.63	6.37	-	3.02	1.54	0.69
Minimum	0.11	2.09	0.47	-	0.45	0.21	3.18
Maximum	19.48	18.78	22.47	-	13.85	7.82	4.52
Range	19.37	16.69	22.00	-	13.40	7.61	1.34
Lower Quartile	0.66	3.95	0.76	-	2.12	1.25	3.18
Upper Quartile	2.65	14.70	5.06	-	5.82	2.76	4.52
Quartile Range	1.99	10.75	4.30	-	3.71	1.51	1.34
Percentile 10	0.38	3.20	0.55	-	1.33	0.77	3.18
Percentile 90	4.15	15.28	14.97	-	8.70	3.88	4.52
∑Extr Bases $cmol_c kg^{-1}$	**Arenosols** (n = 132)	**Calcisols** (n = 17)	**Leptosols** (n = 24)	**Fluvisols** (n = 6)	**Cambisols** (n = 66)	**Regosols** (n = 89)	**Luvisols** (n = 3)
Mean	2.93	17.33	5.66	5.85	6.24	3.34	10.27
Median	1.88	17.15	4.30	5.96	5.50	2.50	9.93
Std Dev	2.97	9.11	5.19	1.63	4.06	2.13	0.88
Minimum	0.37	4.19	0.59	3.27	0.98	0.82	9.61
Maximum	16.08	34.19	22.78	8.05	19.50	10.24	11.27
Range	15.71	30.00	22.18	4.79	18.52	9.43	1.66
Lower Quartile	1.17	9.02	2.61	5.13	3.05	1.83	9.61
Upper Quartile	3.74	24.67	6.26	6.74	7.70	4.52	11.27
Quartile Range	2.57	15.65	3.66	1.61	4.65	2.69	1.66
Percentile 10	0.82	6.26	1.65	3.27	2.48	1.17	9.61
Percentile 90	5.44	29.00	13.07	8.05	11.27	6.59	11.27

The CEC values of Arenosols in 10 cm depth intervals from the study area are comparable to those found in Zimbabwe and somewhat lower than those of other southern African countries, recorded by Hartemink and Hunting (2008), as shown in Table 8.5.

Table 8.5. CEC of Arenosols in southern Africa (mean ± 1 SD).

Depth cm	**CEC** $cmol_c\ kg^{-1}$				
	n	**0 – 10**	**10 – 20**	**20 – 30**	**> 30**
Present study	7, 29, 5, 88	1.67 ± 1.10	1.48 ± 1.47	1.42 ± 1.05	2.43 ± 2.85
Angola [a]	60	3.4 ± 1.5	2.9 ± 1.3	2.5 ±1.2	-
Botswana [a]	6	3.3 ±2.0	3.2 ± 2.0	3.1 ± 1.9	-
Mozambique [a]	30	4.1 ± 2.9	3.8 ± 3.1	3.8 ± 3.1	-
Namibia [a]	3	1.5 ± 1.3	1.6 ± 1.4	1.6 ± 1.9	-
South Africa [a]	39	3.0 ± 2.0	3.0 ± 2.1	2.9 ± 2.0	-
Zimbabwe [a]	12	1.7 ± 0.8	1.5 ± 0.7	1.4 ± 1.0	-

([a] Hartemink and Hunting, 2008)

CEC, sum of exchangeable bases and sum of extractable bases increase in the order low → moderate →

high degree of dissection of the terrain (Figure 8.15). One explanation is greater rates of erosion and subsequent exposure of fresh parent material in more dissected terrain. Secondly, the highly dissected terrain of the study area occurs mainly on schist, quartzite and calcrete, whereas the less dissected areas, towards the east, are mainly covered with Kalahari sands.

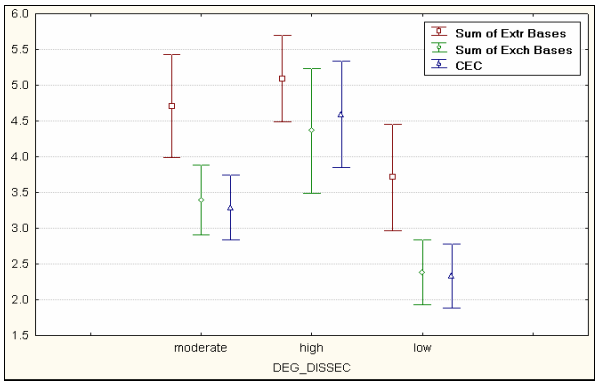

Figure 8.15. CEC ($cmol_c\ kg^{-1}$), sum of exchangeable bases ($cmol_c\ kg^{-1}$)and sum of extractable bases ($cmol_c\ kg^{-1}$), per degree of dissection of the landscape

The CEC, sum of exchangeable bases and sum of extractable bases levels, of topsoil and subsoil respectively, are shown in Figures 8.16 – 8.21.

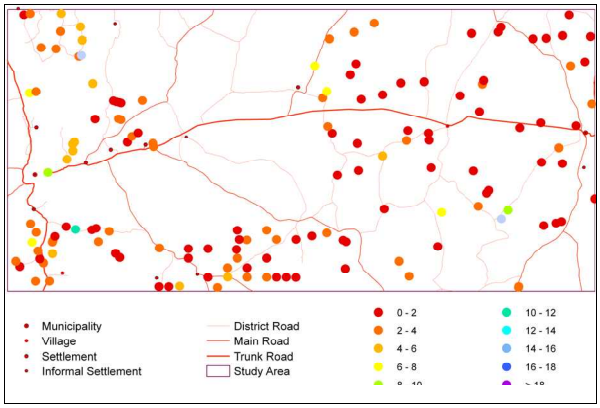

Figure 8.16. CEC ($cmol_c\ kg^{-1}$) of topsoil

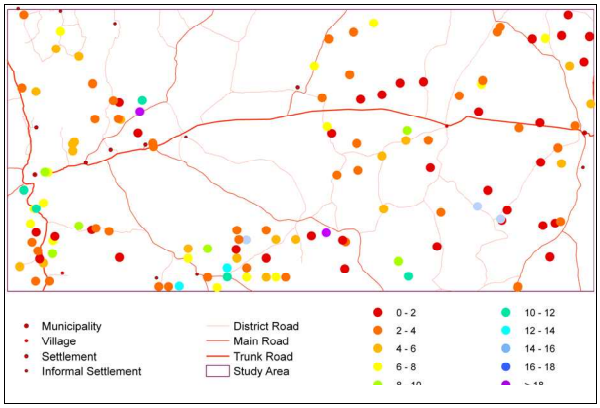

Figure 8.17. CEC ($cmol_c\ kg^{-1}$) of subsoil

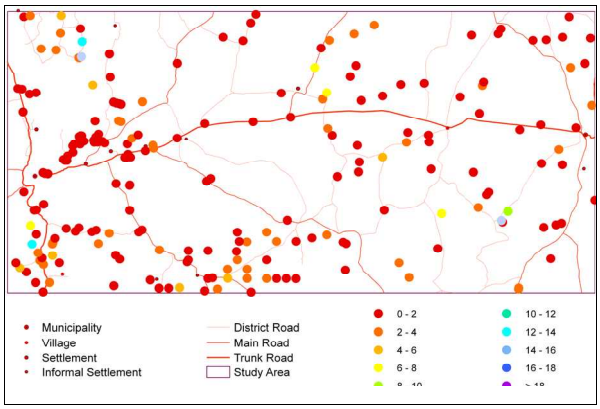

Figure 8.18. Sum of exchangeable bases ($cmol_c\ kg^{-1}$) of topsoil

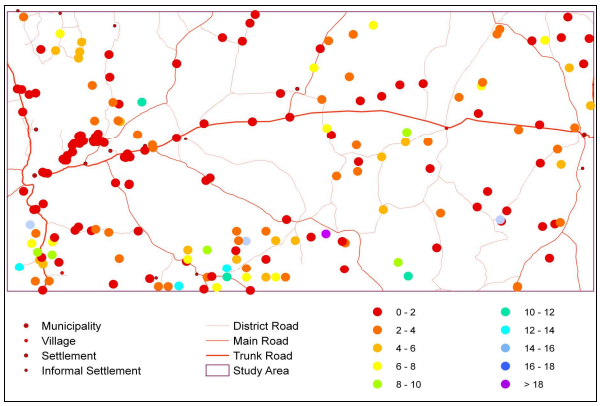

Figure 8.19. Sum of exchangeable bases ($cmol_c\ kg^{-1}$) of subsoil

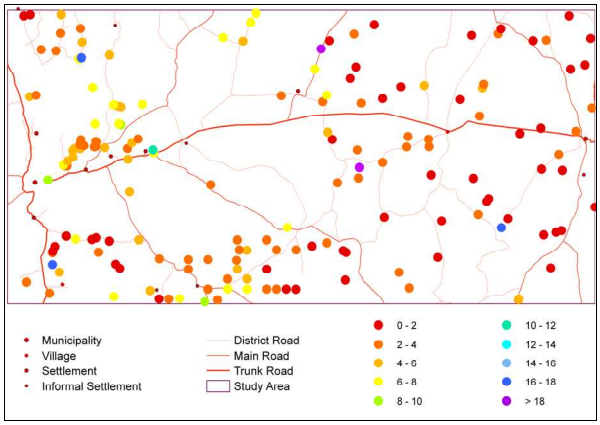

Figure 8.20. Sum of extractable bases ($cmol_c\ kg^{-1}$) of topsoil

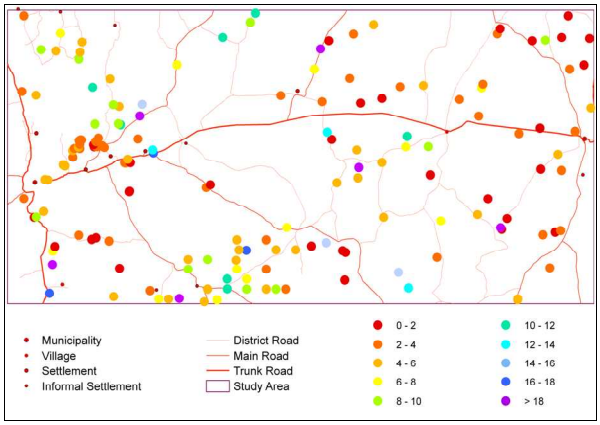

Figure 8.21. Sum of extractable bases ($cmol_c\ kg^{-1}$) of subsoil

8.2 CA-, MG-, K-, NA SATURATION, BASE STATUS AND BASE SATURATION

Calcium-, magnesium-, potassium and sodium saturation refers to the proportion of the cation exchange sites in the soil that are occupied by the respective cations (Table 8.6; Figures 8.22 – 8.23). It is calculated as follows for Na (and similarly for Ca, Mg and K):

$$\text{Exchangeable sodium percentage (ESP)} = \frac{\text{exchangeable Na}}{\text{CEC}} \times 100$$

Base status is a qualitative expression of base saturation (Van der Watt and Van Rooyen, 1995). An eutrophic soil has undergone little or no leaching, so that the sum of exchangeable Ca, Mg, K and Na (S_{clay}), expressed in $cmol_c kg^{-1}$ *clay*, is more than 15. This value is less than 5 in dystrophic soil, which has undergone marked leaching, and between 5 and 15 in mesotrophic soil, which has undergone moderate leaching (Van der Watt and Van Rooyen, 1995).

Base saturation is the sum of exchangeable Ca, Mg, K and Na (known as the *S-value*, in $cmol_c\ kg^{-1}$ *soil*), expressed as a percentage of the total cation exchange capacity of the soil at a specific pH (Van der Watt and Van Rooyen, 1995; McVicar *et al*., 1977; Soil Classification Working Group, 1991).

$$\text{Base Saturation [\%]} = \frac{S\ [cmol_c\ kg^{-1}\ soil]}{CEC\ [cmol_c\ kg^{-1}\ soil]} \times 100$$

$$S\ [cmol_c\ kg^{-1}\ soil] = Ca^{2+}_{exch} + Mg^{2+}_{exch} + K^{+}_{exch} + Na^{+}_{exch}$$

8.2.1 STATISTICAL ANALYSIS: CA, MG, K AND NA SATURATION; BASE STATUS; BASE SATURATION

Ca, Mg, K, Na saturation

Table 8.6: Calcium saturation (n = 361), magnesium saturation (n = 361), potassium saturation (n = 360) and sodium saturation (n = 360).

	Ca saturation	Mg saturation	K saturation	Na saturation
	%	%	%	%
Mean	60.9	28.6	15.7	2.9
Median	58.8	26.6	12.6	0.8
SD	38.7	18.1	13.6	5.8

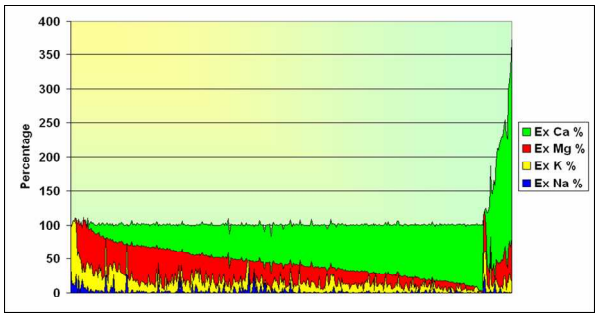

Figure 8.22. Cumulative Ca-, Mg-, K- and Na saturation (%), including outliers

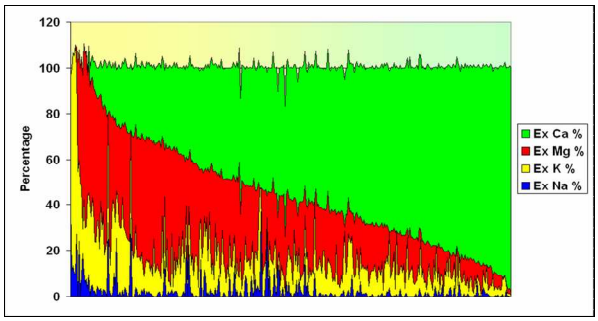

Figure 8.23. Cumulative Ca-, Mg-, K- and Na saturation (%), excluding outliers

No consistent pattern could be discerned for exchangeable sodium percentage with increase in depth (Table 8.7).

Table 8.7: Exchangeable sodium percentage (ESP) at various depths.

Depth cm	ESP %				
	All (n = 393)	0 – 10 (n = 35)	10 – 20 (n = 92)	20 – 30 (n = 201)	> 30 (n = 32)
Mean	2.8	5.83	2.92	2.37	3.30
Median	0.7	1.17	0.74	0.88	0.02
SD	5.6	9.53	5.63	4.72	6.68
Minimum	0.0	0.00	0.00	0.00	0.00
Maximum	38.5	36.84	40.23	31.54	25.41
Range	38.5	36.84	40.23	31.54	25.41

No consistent pattern could be discerned for exchangeable sodium percentage of Arenosols, with increase in depth (Table 8.8). Values are somewhat higher than those found in Angola, Botswana, Mozambique and elsewhere in Namibia, but similar to values recorded in South Africa and Zimbabwe (Hartemink and Hunting, 2008).

Table 8.8 Exchangeable sodium percentage (ESP) of Arenosols in southern Africa (mean ± 1 SD).

Depth cm	ESP %				
	Valid N	0 – 10	10 – 20	20 – 30	> 30
Present study	35; 92; 201; 32	6 ± 10	3 ± 6	2 ± 5	3 ± 7
Angola [a]	60	1 ± 1	2 ± 1	2 ± 1	-
Botswana [a]	6	1 ± 2	2 ± 2	2 ± 3	-
Mozambique [a]	30	2 ± 4	2 ± 4	3 ± 3	-
Namibia [a]	3	3 ± 1	2 ± 1	2 ± 0.2	-
South Africa [a]	39	5 ± 7	5 ± 6	5 ± 8	-
Zimbabwe [a]	12	5 ± 8	5 ± 8	3 ± 4	-

([a] Hartemink and Hunting, 2008)

One third of the samples (120) exhibit low potassium reserves properties, as defined by FAO (1989b), namely < 0.20 $cmol_c\ kg^{-1}$ exchangeable K, or K less than 2 % of sum of bases, if bases < 10 $cmol_c\ kg^{-1}$.

Base status: Of 360 samples, 10 (2.8 % of samples) were found to be **dystrophic** (S_{clay} ≤ 5 $cmol_c\ kg^{-1}$ clay), 60 (16.7 %) **mesotrophic** (5 < S_{clay} < 15 $cmol_c\ kg^{-1}$clay) and 290 (77,8 %) **eutrophic** (S_{clay} ≥ 15 $cmol_c\ kg^{-1}$ clay).

The S_{clay} normally decreases with depth up to a point, when primary minerals present in deeper horizons start contributing to the value. This trend is discernable in the study area (Table 8.9 and Figures 8.24 – 8.26).

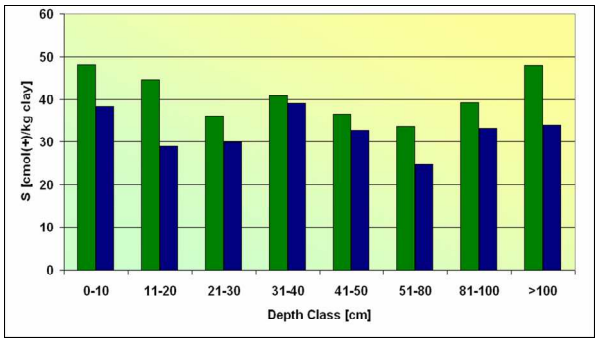

Figure 8.24. Mean (green) and median (blue) S_{clay} ($cmol_c\ kg^{-1}$ clay) at various depths

Table 8.9: Descriptive statistics – Sclay ($cmol_c\ kg^{-1}$ clay) at various depths.

Depth Class cm	S_{clay} $cmol_c\ kg^{-1}$ clay							
	0 – 10 (n = 33)	**11 – 20** (n = 91)	**21 – 30** (n = 32)	**31 – 40** (n = 25)	**41 – 50** (n = 43)	**51 – 80** (n = 63)	**81 – 100** (n = 13)	**>100** (n = 53)
Mean	48.2	44.5	36.1	40.9	36.6	33.6	39.3	48.0
Median	38.4	29.0	29.8	39.2	32.7	24.8	33.2	33.9
Std Dev	43.9	52.8	27.9	23.4	28.0	28.0	31.0	48.3
Minimum	1.7	1.0	7.5	5.2	1.4	1.4	2.7	1.8
Maximum	211.5	294.8	121.3	92.2	141.3	172.1	126.3	215.6
Range	209.8	293.7	113.8	86.9	139.9	170.7	123.6	213.7

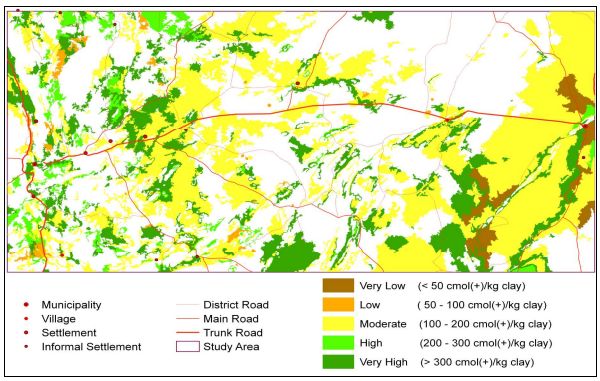

Figure 8.25. S_{clay} ($cmol_c$ kg^{-1} clay) of topsoil [1]

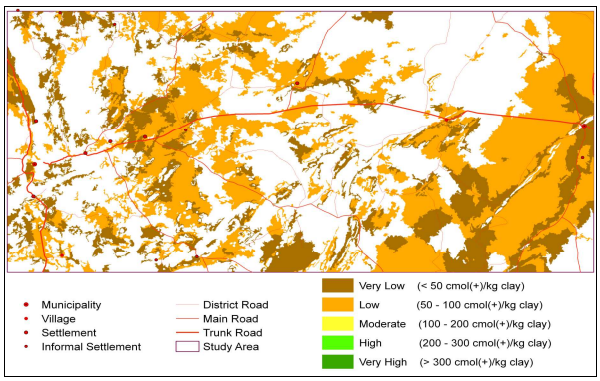

Figure 8.26. S_{clay} ($cmol_c$ kg^{-1} clay) of subsoil

The **base saturation** of 358 samples from the study area ranges from 88.19 to 372.14 % (Table 8.8; Figures 8.27 – 8.28).The mean (108.22 %) is higher than the median (100.46 %), with a skewness of 5.38 and kurtosis of 31.46. The standard deviation is 32.56. Free lime (calcium carbonate) is the most likely explanation for base saturation, percentages higher than 100.

Table 8.10: Descriptive statistics – base saturation (Ca + Mg + K + Na) (n = 358) and S_{clay} (n = 360).

	Base Saturation	**S_{clay}**
	%	$cmol_c$ kg^{-1} clay
Mean	108.22	40.81
Median	100.45	30.67
Std. Dev.	32.56	40.09
Minimum	86.19	1.01
Maximum	372.14	294.75
Range	285.95	293.74
Skewness	5.38	3.02
Kurtosis	31.46	12.59

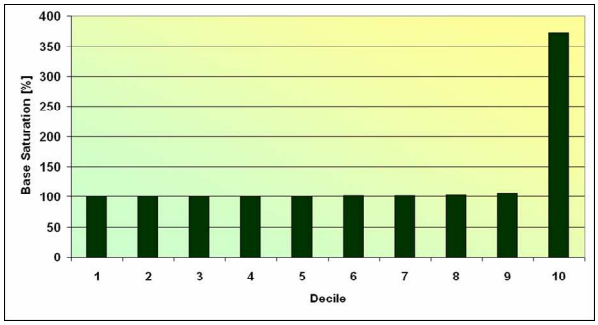

Figure 8.27. Decile distribution of total base saturation (%)

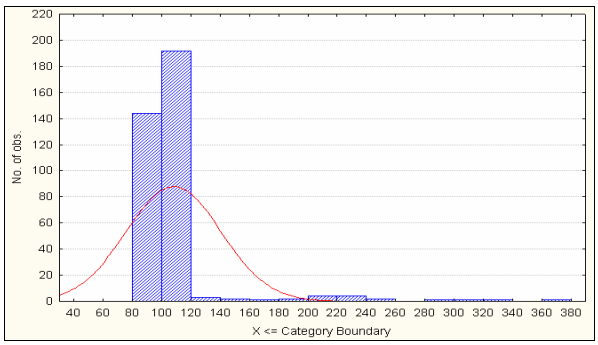

Figure 8.28. Histogram of total base saturation (%)

The base saturation of Arenosols at 10 cm depth intervals from the study area are higher than those in all other southern African countries, recorded by Hartemink and Hunting (2008), as shown in Table 8.11. This can probably be ascribed to the more arid climate of the study area.

[1] Blank areas indicate either the absence of sufficient analytical data to extrapolate to the respective terrain units, or contradictory data from different profiles within a terrain unit.

Table 8.11. Base Saturation of Arenosols in southern Africa (mean ± 1 SD).

Depth cm	Base Saturation %				
	n	0 – 10	10 – 20	20 – 30	> 30
Present study	34; 91; 32; 200	113 ± 38	103 ± 15	102 ± 9	109 ± 34
Angola [a]	60	40 ± 30	35 ± 31	32 ± 31	-
Botswana [a]	6	80 ± 19	79 ± 19	75 ± 25	-
Mozambique [a]	30	86 ± 71	77 ± 80	68 ± 81	-
Namibia [a]	3	100 ± 0	100 ± 0	100 ± 0	-
South Africa [a]	39	80 ± 27	80 ± 27	96 ± 48	-
Zimbabwe [a]	12	80 ± 22	80 ± 24	100 ± 15	-

([a] Hartemink and Hunting, 2008)

8.3 ELECTRICAL CONDUCTIVITY [EC]

The exchangeable sodium percentage (ESP) and electrical conductivity of the saturated paste give an indication of salinity and/or sodicity of soils (Van der Watt and Van Rooyen, (1995).

8.3.1 STATISTICAL ANALYSIS: ELECTRICAL CONDUCTIVITY OF THE SATURATED PASTE EXTRACT; ELECTRICAL CONDUCTIVITY OF THE 2:5 SOIL:WATER SUSPENSION

Table 8.12: Descriptive statistics – EC (2:5) (n = 524) and EC (saturated paste extract) (n = 79)

	EC (2:5)		EC (saturated paste)	
	uS cm^{-1}	mS m^{-1}	uS cm^{-1}	mS m^{-1}
Mean	61.02	6.10	192.47	19.25
Median	25	2.5	169	16.9
Std Dev	118.31	11.83	103.09	10.31
Minimum	5	0.5	48	4.8
Maximum	924	92.4	469	46.9
Range	919	91.9	421	42.1
Skewness	4.89	0.49	0.93	0.09
Kurtosis	26.61	2.66	0.21	0.02

1 mS cm^{-1} = 100 mS m^{-1} = 1 dS m^{-1} = 1 000 µS cm^{-1}; 10 µS cm^{-1} = 1 mS m^{-1}

Table 8.12 contains the descriptive statistics of the EC, as measured in the supernatant of a 2:5 soil:water suspension, and in the saturated extract (Figures 8.29 – 8.30). Of 79 samples, none had EC (saturated paste) above 400 mS m^{-1}. In fact, the maximum was 46.9 mS m^{-1}. There were, thus, no profiles with saline soils in the study area. Of 393 samples, 17 had ESP > 15, so they are sodic (Van der Watt and Van Rooyen, 1995).

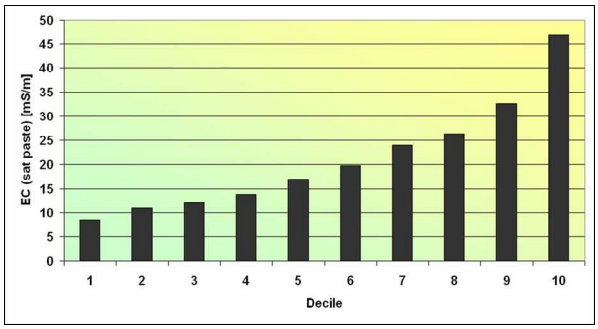

Figure 8.29. Deciles of EC (saturated paste) (mS m^{-1})

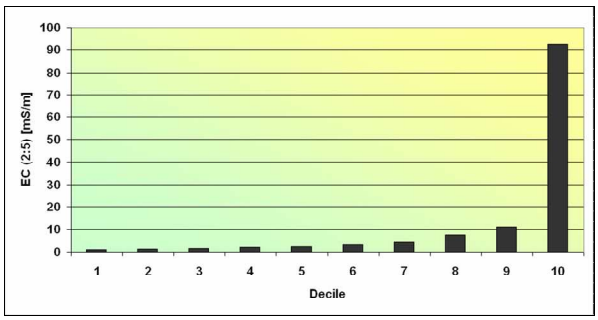

Figure 8.30. Deciles of EC (2:5) (mS m^{-1})

EC (2:5) was highest in Calci- and Leptosols, and lowest in Luvisols, Arenosols, Regosols and Fluvisols (Table 8.11). EC (saturated paste) was highest in Calcisols, Cambisols and Leptosols, and lowest in Luvisols and Arenosols (Table 8.13).

Table 8.13: Electrical conductivity, per WRB reference soil group.

EC 2:5 uS/cm	**Arenosols** (n = 141)	**Calcisols** (n = 20)	**Leptosols** (n = 21)	**Fluvisols** (n = 8)	**Cambisols** (n = 72)	**Regosols** (n = 99)	**Luvisols** (n = 3)
Mean	23.3	114.1	67.1	102.6	52.6	27.2	32.7
Median	17	78	68	21	33.5	19	13
Std.Dev.	26.9	146.1	45.8	207.7	60.1	26.7	35.8
Minimum	5	15	7	12	8	7	11
Maximum	281	710	166	612	310	180	74
Range	276	695	159	600	302	173	63
Lower Quartile	12	64	21	17	22	13	11
Upper Quartile	24	98.5	100	60.5	59	29	74
Quartile Range	12	34.5	79	43.5	37	16	63
Percentile 10	9	39	12	12	15	9	11
Percentile 90	42	174.5	116	612	94	53	74
EC sat uS cm^{-1}	**Arenosols** (n = 9)	**Calcisols** (n = 9)	**Leptosols** (n = 8)	**Fluvisols** (n = 0)	**Cambisols** (n = 14)	**Regosols** (n = 25)	**Luvisols** (n = 3)
Mean	106.7	266.8	212.4	-	218.8	156.3	160.1
Median	113.0	261.0	171.1	-	193.8	141.1	110.6
Std.Dev.	21.2	107.0	160.8	-	94.9	59.8	88.3
Minimum	65.30	92.2	47.5	-	114.0	51.2	107.6
Maximum	135.0	445.0	446.0	-	469.0	309.0	262.0
Range	69.7	352.8	398.5	-	355.0	257.8	154.4
Lower Quartile	99.5	221.0	74.65	-	150.7	123.9	107.6
Upper Quartile	118.2	290.0	357.0	-	265.0	177.9	262.0
Quartile Range	18.7	69.0	282.4	-	114.3	54.0	154.4
Percentile 10	65.3	92.2	47.5	-	124.8	88.5	107.6
Percentile 90	135.0	445.0	446.0	-	327.0	239.0	262.0

The EC (saturated paste) and EC (2:5) levels, of topsoil and subsoil respectively, are shown in Figures 8.31 – 8.34.

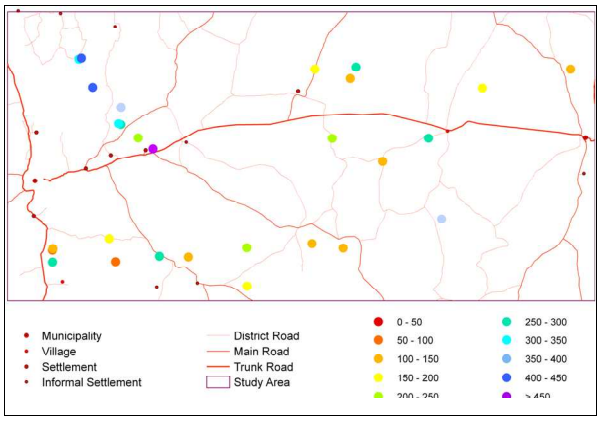

Figure 8.31. EC (sat paste) (uS cm^{-1}) of topsoil

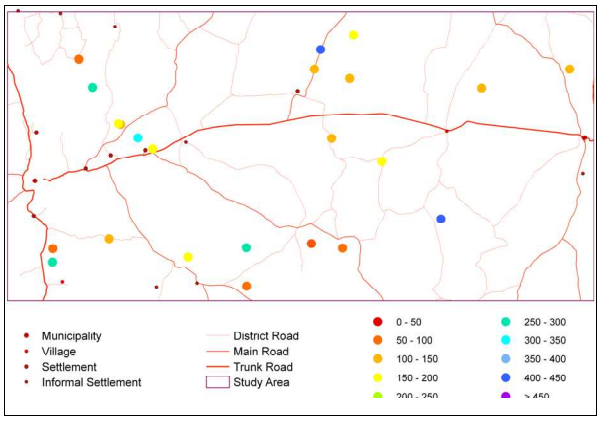

Figure 8.32. EC (sat paste) (uS cm^{-1}) of subsoil

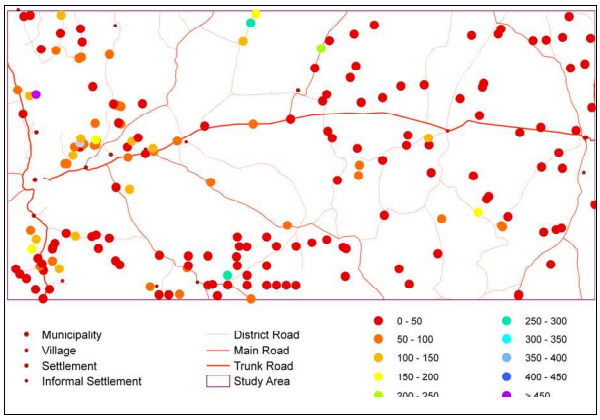

Figure 8.33. EC (2:5) (uS cm^{-1}) of topsoil

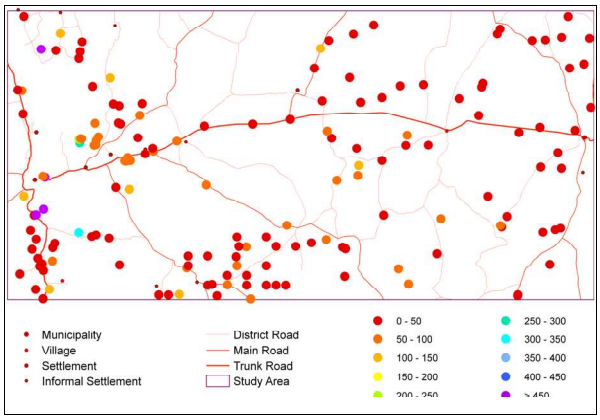

Figure 8.34. EC (2:5) (uS cm^{-1}) of subsoil

CHAPTER NINE

CHEMICAL CHARACTERISATION - IRON, MANGANESE, ZINC, COPPER

9.1 INTRODUCTION

Micronutrients (B, Cu, Fe, Mn, Mo, Zn, Cl) are elements which are essential for plant growth, but are required in much smaller quantities than the major nutrients (N, P, K, Mg, Ca, S) (Mortvedt, 2000). This chapter deals with the plant-available iron, manganese, zinc and copper concentrations in the soils of the study area.

9.2 IRON [Fe]

Iron is the 6th most abundant element in the universe, the most abundant element on Earth – when taking Earth's core into consideration – and the 4th most plentiful element in the Earth's crust. It occurs in both the ferrous [Fe^{2+}] and ferric [Fe^{3+}] forms as oxides, silicates, sulphates and carbonates in igneous rocks. It is common in primary minerals such as biotite [$K(Si_3Al)(MgFe)_3O_{10}(OH)_2$], augite [$Ca(Mg,Fe,Al)\ (Si,Al)_2O_6$], and hornblende [$(Ca,Na)_2(Mg,Fe,Al)_5(Si,Al)_8O_{22}(OH)_2$] (Whitehead, 2000). During weathering, iron is largely retained in clay minerals by substituting for aluminium in the lattice structure. it is found *inter alia* in the clay minerals montmorillonite [$(Na,Ca)_{0.33}(Al,Mg)_2(Si_4O_{10})(OH)_2{\cdot}nH_2O$] and vermiculite [$(Mg,Fe,Al)_3(Al,Si)_4\ O_{10}(OH)_2{\cdot}4H_2O$], in the yellow hydroxide goethite [FeOOH] and red oxide haematite [Fe_2O_3], the sulphur-containing pyrite [FeS_2], siderite [$FeCO_3$], magnetite [Fe_3O_4], pyrrhotite [$Fe_{1-x}S$] and jarosite [$KFe_3(OH)_6\ (SO_4)_4$] (Vlek and Harmsen, 1985; Mortvedt, 2000; mindat website, 2008; webmineral website, 2008). Soil iron is derived almost entirely from the parent material, though there is some contribution from atmospheric deposition: in Europe, the United Kingdom and North America atmospheric deposition contributes between 1 400 and 7 700 g ha^{-1} year^{-1} (Whitehead, 2000).

Table 9.1: Typical iron concentrations (in mg kg^{-1}) found in the earth's crust, some common rocks and soils.

SOURCE	Whitehead, 2000	Helmke, 2000	Bradford *et al*., 1967	Haynes & Swift, 1984	Vlek & Harmsen, 1985
EARTH'S CRUST	50 000				50 000
GRANITE	13 700				27 000
BASALT	77 600				86 000
SHALE	47 200				47 000
SANDSTONE	9 800				9 800
LIMESTONE	3 800				3 800
SOILS FROM GRANITE	10 000				
SOILS FROM SHALE	35 000				
SOILS FROM SANDSTONE	20 000				
ENTISOL		59 900			
SPODOSOL		55 700			
ALFISOL		15 500			
MOLLISOL		23 700			
SOILS (GENERAL)	5 000 – 50 000 [35 000]	7 000 – 550 000 [38 000]	12 000 – 100 000	27 500 – 30 500	10 000 – 100 000 [38 000]

The ability of iron to change oxidation state and to form complexes with organic molecules influences its activity and movement in soil and plants (Whitehead, 2000). Under reducing conditions Fe^{3+} is reduced to Fe^{2+}, which is more soluble and is thus more mobile. Microbial respiration and organic matter composition induces chemically reducing conditions, thereby increasing iron solubility. A great deal of soil iron is in the form of hydrous ferric oxides and hydroxides. Haematite [Fe_2O_3] and goethite [FeOOH] are less soluble than lepidocrocite [FeOOH] and amorphous iron [$Fe(OH)_3$] (Whitehead, 2000). In neutral and alkaline well-drained soils iron bio-availability is usually very low, as most iron occurs as immobile hydrous ferric oxides. According to Lindsey (1979, quoted by Mortvedt, 2000), solubility of Fe decreases a thousand fold for each unit increase in pH within the range 4 to 9. Free lime, in particular, suppresses iron availability. Fe^{3+} exist almost entirely in complexed form in the soil solution, as it is complexed more easily than Fe^{2+} and binds strongly to organic groups that contain oxygen, such as carboxyl and phenolic groups (Whitehead, 2000).

Iron can be lost beyond the root zone in acidic conditions, when hydrous ferric oxides become soluble, or through unusually high production of soluble organic chelates. Bicarbonate ions can mobilise phosphorus in poorly aerated soils, and thus can suppress iron availability to plants (Whitehead, 2000). High concentrations of copper and manganese both act antagonistically towards the uptake of iron (US, 2002). Iron concentrations are generally lower in sandy soils than in loams and clays, and lower in soils from acid than from basic rocks (Vlek and Harmsen, 1985; Whitehead, 2000). Acid sandy soils and highly calcareous soils often have a low total content of Fe (Whitehead, 2000). Losses through volatilisation, leaching, surface runoff and crop removal or grazing are negligible (Whitehead, 2000).

Iron is a component of porphyrins in leaves and of ferredoxins (Reuter and Robinson, 1997). It is an essential constituent of cytochromes and Fe-S proteins, where it enables transfer of electrons to and from a variety of molecules, including several involved in the process of photosynthesis and nitrogen fixation. Iron activates a number of enzymes and is involved in the synthesis of ribonucleic acid (Whitehead, 2000). It is a constituent of leghaemoglobin in legumes – which is essential for nitrogen fixation – and in enzymes of the nitrogenase complex. Concentrations of iron are generally higher in legumes than in grasses (Whitehead, 2000).

Table 9.2: Estimated iron balances (g ha^{-1} $year^{-1}$) from an extensively managed clover-grassland, grazed by cattle (Whitehead, 2000).

	ESTIMATED FE (G HA^{-1} $YEAR^{-1}$)
INPUTS	
Deposition from atmosphere	3 500
ASPECT OF RECYCLING	
Uptake into herbage	150
Consumption of herbage by animals	75
Dead herbage to soil	225
Dead roots to soil	150
Excreta to soil of grazed area	1 175

OUTPUTS	
Milk / live-weight gain	0.13
Leaching / runoff	0
Loss through excreta off sward	0
GAIN TO SOIL	3 500

9.3 MANGANESE [Mn]

Manganese occurs in more than 100 minerals (Howe *et al.*, 2004), *inter alia* pyrolusite [MnO_2], haussmannite [Mn_3O_4], manganite [MnOOH], braunite (Mn_2O_3)3·$MnSiO_3$], rhodochrosite [$MnCO_3$], psilomelane [$Ba(Mn^{2+})(Mn^{4+})_8O_{16}(OH)_4$] and rhodonite [(Mn,Fe,Mg,Ca)SiO_3] (Vlek and Harmsen, 1985; Mortvedt, 2000; mindat website, 2008; webmineral website, 2008). It is often associated with iron as a minor constituent of ferromagnesian minerals, such as biotite mica and amphiboles (Howe *et al.*, 2004).

Table 9.3: Typical manganese concentrations (in mg kg^{-1}) found in the earth's crust, some common rocks and soils.

SOURCE	Whitehead, 2000	Foth, 1999	Helmke, 2000	Vlek & Harmsen, 1985	Han & Singer, 2007
EARTH'S CRUST		950		1 000	900 – 1 000
GRANITE	195	400		400	
BASALT	1 280	1 500		1 500	1 000 – 2 000
SHALE	850	850		800	
SANDSTONE	10 – 100	10 – 100		10 – 100	
LIMESTONE	1 100	1 100		1 100	
SOILS FROM GRANITE	450				
SOILS FROM SHALE	920				
SOILS FROM SANDSTONE	440				
ENTISOL			890		
SPODOSOL			716		
ALFISOL			535		
MOLLISOL			595		
SOILS (GENERAL)	50 – 3 000 [1 600]	10 – 3 000	20 – 6 000 [600]	20 – 3 000 [600]	200 – 3 000 [850 – 1 000]
ARID SOILS					Trace – 10 000

Due to the high mobility of Mn there is no correlation between soil Mn (total and exchangeable) and total Mn in bedrock (Mortvedt, 2000). Soil Mn is found in residual primary minerals, in clay minerals such as smectite, adsorbed onto various mineral surfaces, precipitated as oxides and hydroxides such as MnO_2, or sometime substituting for Fe^{3+} in secondary minerals such as goethite. Manganese has three possible oxidation states in soils, *viz.* Mn^{2+}, which is stable in solution, Mn^{3+} and Mn^{4+} (Whitehead, 2000). Mn^{3+} and Mn^{4+} form insoluble oxides and hydroxides. Mn^{2+} is easily adsorbed by organic matter, iron oxides and silicates, especially under neutral and alkaline conditions (Whitehead, 2000). Under acidic conditions, a high proportion of manganese is in exchangeable and soluble forms. Under alkaline and well-drained conditions, Mn^{2+} becomes less soluble. It precipitates as oxides and hydroxides in the form of MnO_2 nodules or, in association with iron, forms amorphous coatings on soil particles (Whitehead, 2000). Manganese solubility is increased through microbial respiration and organic matter decomposition, which induces chemically

reducing conditions for forming the mobile manganous ion, Mn^{2+} (Whitehead, 2000). Most of the complexed manganese in soils is bound to inorganic rather than organic ligands (Laurie and Manthey, 1994, as quoted by Whitehead, 2000).

The correlation between total manganese content of soil and its bioavailability is very poor. Low bioavailability is caused by neutral to high pH, aeration and oxidation, low soil temperature and sandy texture of the soil (Mortvedt, 2000). According to Lindsey (1979, quoted by Mortvedt, 2000), the activity and bioavailability of Mn decrease a hundredfold for each unit increase in pH within the range 4 to 9. Manganese concentrations are generally lower in sandy soils than in loams and clays, and lower in soils from acid than from basic rocks. (Vlek and Harmsen, 1985; Whitehead, 2000). It is retained in soil mainly by precipitation and complexation. No losses occur through volatilisation, while leaching is negligible unless conditions are highly acidic or unusually high concentrations of soluble organic chelates are produced (Whitehead, 2000). Manganese toxicity only occurs on very acid or waterlogged soils (Mortvedt, 2000).

The ability of manganese to change oxidation state and to form complexes with organic molecules rules its activity and movement in soil and plants (Whitehead, 2000). Manganese is involved in several redox processes (and thus the transfer of electrons) in photosynthesis and activation of enzymes. It is found in manganese superoxide dismutase, which is involved in the detoxification of free-radical oxidants (Reuter and Robinson, 1997). It plays a role in respiration and the synthesis of amino acids, phenolic acids and lignin through participation in phosphorylation, decarboxylation, reduction and hydrolysis reactions (Whitehead, 2000). Manganese is involved with carbohydrate metabolism and the citric acid cycle and it is a component of chloroplasts (US, 2002).

Table 9.4: Estimated manganese balances (g ha^{-1} $year^{-1}$) from an extensively managed clover-grassland, grazed by cattle (Whitehead, 2000).

	ESTIMATED MN (G HA^{-1} $YEAR^{-1}$)
INPUTS	
Deposition from atmosphere	100
ASPECT OF RECYCLING	
Uptake into herbage	60
Consumption of herbage by animals	30
Dead herbage to soil	90
Dead roots to soil	60
Excreta to soil of grazed area	30
OUTPUTS	
Milk / live-weight gain	0.013
Leaching / runoff	0
Loss through excreta off sward	0
GAIN TO SOIL	100

9.4 ZINC [Zn]

Zinc is the 23rd most abundant element in Earth's crust (Han and Singer, 2007). It occurs in igneous rocks as a minor constituent of pyroxenes, amphiboles, biotite and iron oxides. It also occurs in the form of sulfides (e.g. sphalerite [ZnS]), oxides (e.g. franklinite $[Fe,Mn,Zn)(Fe,Mn)_2O_4]$), carbonates (e.g. smithsonite $[ZnCO_3]$), phosphates (e.g. hopeite $[Zn_3(PO_4)_2 \cdot 4H_2O]$) and silicates (e.g. hemimorphite $[Zn(OH)_2Si_2O_7.H_2O]$) (Vlek and Harmsen, 1985; Mortvedt, 2000; mindat website, 2008; webmineral website, 2008).

Table 9.5: Typical zinc concentrations (in mg kg^{-1}) found in the earth's crust, some common rocks and soils.

SOURCE	Whitehead, 2000	US, 2002	Helmke, 2000	Vlek & Harmsen, 1985	Han & Singer, 2007
EARTH'S CRUST		70		80	50 – 70
GRANITE	45	40		40	
BASALT	86	100		100	70 – 130
SHALE	95	95		95	
SANDSTONE	16	16		16	
LIMESTONE	20	20		20	16 – 20
METAMORPHIC ROCKS					80
SEDIMENTARY ROCKS					80
SOILS FROM GRANITE	36				
SOILS FROM SHALE	47				
SOILS FROM SANDSTONE	57				
ENTISOL			146		
SPODOSOL			124		
ALFISOL			52		
MOLLISOL			94		
SOILS (GENERAL)	20 – 300 [150]	10 - 300	10 – 300 [50]	10 – 300 [50]	10 – 300 [50 – 100]
ARID SOILS					Trace – 900

Zn^{2+} may substitute for Fe^{2+} and Mg^{2+} in clay minerals. It occurs in soil only in one valence state, Zn^{2+}, and does not undergo reduction in nature (Mortvedt, 2000). It is the most mobile of the heavy metals and sorbed less strongly than Cu. Zinc is readily adsorbed by hydrous oxides, carbonates, clays and soil organic matter. The more hydroxyl groups on the surface of a clay or an oxide, the higher the adsorption of zinc. The zinc adsorbed by clay and organic matter under acid conditions is readily exchangeable. Under progressively more alkaline conditions the availability drops radically, as the result of strong complexing by organic matter and adsorption by iron- and manganese oxides (Whitehead, 2000). Above a pH of 7.7, $Zn(OH)_2$ is the common form of zinc in the soil solution (Mortvedt, 2000). Half the zinc present in the soil solution is complexed by organic or inorganic ligands, while the remainder exists as the free hydrated cation.

The correlation between total zinc content of soil and its availability to plants is very poor. Low bioavailability is caused by high pH, strong adsorption (especially in calcaric soils), immobilising by soil microbes, high phosphate concentration, sandy soil texture and reducing (waterlogged) conditions (Mortvedt, 2000). Zinc concentrations are generally lower in sandy soils than in loams and clays, and lower in soils from acid than from basic rocks (Vlek and Harmsen, 1985; Whitehead, 2000). No losses occur through volatilisation and leaching is negligible unless conditions are highly acidic or unusually high concentrations of soluble organic

chelates are produced (Whitehead, 2000). According to Lindsey (1979, quoted by Mortvedt, 2000), the activity and bioavailability of Zn decreases a hundredfold for each unit increase in pH within the range 4 to 9. Zinc toxicity only occurs when soil had been polluted by mining or gross over-application of zinc-containing fertilizers (US, 2002).

Zinc exists in plants in only one oxidation state, namely Zn^{2+}. It helps to stabilize the structures of RNA and DNA and to regulate enzymes that control their synthesis and degradation (Whitehead, 2000). It ensures the stability and structural orientation of membrane proteins and cytoplasmic ribosomes. Zinc is a component and/or activator of various enzymes, such as dehydrogenase, proteinase, CuZn superoxide dismutase, carbonic anhydrase, RNA polymerase, alkaline phosphatase, phospholipase and carboxypeptidase, by linking the enzyme to the corresponding substrate or by modifying the conformation of the enzyme or substrate (Whitehead, 2000). It is also thought to be necessary for the production of growth regulators, such as the auxin indole-3-acetic acid (Reuter and Robinson, 1997; Whitehead, 2000; US, 2002).

Table 9.6: Estimated zinc balances (g ha^{-1} $year^{-1}$) from an extensively managed clover-grassland, grazed by cattle (Whitehead, 2000).

	ESTIMATED ZN (G HA^{-1} $YEAR^{-1}$)
INPUTS	
Deposition from atmosphere	700
ASPECT OF RECYCLING	
Uptake into herbage	45
Consumption of herbage by animals	23
Dead herbage to soil	66
Dead roots to soil	44
Excreta to soil of grazed area	21
OUTPUTS	
Milk / live-weight gain	0.12
Leaching / runoff	0
Loss through excreta off sward	0
GAIN TO SOIL	700

9.5 COPPER [Cu]

Copper, the 26th most abundant element in the Earth's crust (Han and Singer, 2007), occurs in igneous rocks as sulphides (such as chalcopyrite [$CuFeS_2$], bornite [Cu_5FeS_4], covellite [CuS] and chalcosite [Cu_2S]), oxides (such as cuprite [Cu_2O] and tenorite [CuO]), and carbonates (such as malachite [$Cu_2(OH)_2CO_3$] and azurite [$Cu_3(OH)_2(CO_3)_2$]) (Vlek and Harmsen, 1985; Mortvedt, 2000; mindat website, 2008; webmineral website, 2008). Shale that contains large amounts of organic matter is usually rich in copper.

Table 9.7: Typical copper concentrations (in mg kg^{-1}) found in the earth's crust, some common rocks and soils.

SOURCE	Whitehead, 2000	US, 2002	Helmke, 2000	Han & Singer 2007	Vlek & Harmsen, 1985
EARTH'S CRUST		55		100	70
GRANITE	13	10		10 - 20	10
BASALT	110	100		100 - 200	100
SHALE	45	10 – 80			45
SANDSTONE	1 - 10	45		3 – 15	30
LIMESTONE	4			3 – 15	20
METAMORPHIC ROCKS				30 – 40	
SEDIMENTARY ROCKS				30 – 40	
SOILS FROM GRANITE	7				
SOILS FROM SHALE	6				
SOILS FROM SANDSTONE	8.5				
SANDS				3 - 15	
ENTISOL			61		
SPODOSOL			6.6		
ALFISOL			16		
MOLLISOL			21.0		
SOILS (GENERAL)	2 – 50 [30]		2 – 100 [30]	Trace – 250 [15 – 40]	2 – 100 [30]

Copper is released through weathering as the cuprous ion [Cu^{+}] or cupric ion [Cu^{2+}]. Cu^{+} is unstable, unless in the form of anionic complexes. Below pH 7.3, Cu^{2+} is the dominant ion species in the soil solution, while $CuOH^{-}$ is most common above that pH (Mortvedt, 2000). Cu^{2+} tends to be adsorbed and occluded by iron and manganese hydrous oxides, especially under alkaline conditions. Cu^{2+} forms very stable complexes with organic matter, particularly with carboxyl and phenolic groups, as well as groups that contain nitrogen, such as amino groups and porphyrins (Mortvedt, 2000; Whitehead, 2000). The complexing bonds of copper with organic matter are strongest of all the divalent micronutrient cations. Almost all copper in the soil solution is in the divalent form and is complexed. Only in waterlogged soils does copper occur in the monovalent form, where it tends to form insoluble CuS.

The correlation between total copper content of soil and its availability to plants is very poor. Low availability is caused by high pH, high organic matter content, sandy texture and antagonisms with phosphorus, iron, molybdenum, zinc and aluminium (Mortvedt, 2000). Copper concentrations are generally lower in sandy soils than in loams and clays, and lower in soils from acid than from basic rocks (Vlek and Harmsen, 1985; Whitehead, 2000). No losses occur through volatilisation and leaching is negligible unless conditions are highly acidic or unusually high concentrations of soluble organic chelates are produced (Whitehead, 2000). According to Lindsey (1979, quoted by Mortvedt, 2000), the activity and bioavailability of Cu decrease a hundredfold for each unit increase in pH within the range 4 to 9. According to Lal (2006), free Cu^{2+} in soil solution decreases with increasing pH, with a minimum above pH 10.

The functions of copper in plants are linked to its ability to change oxidation state. It is an essential constituent of several enzymes that catalyse oxidation reactions involving molecular oxygen, such as cytochrome oxidase, amine oxidase, ascorbic acid oxidase, laccase and phenol oxidase (Reuter and Robinson, 1997). It is involved in lignin synthesis through polyphenol oxidase (Lal, 2006). It is found in CuZn

superoxide dismutase (involved in detoxification of superoxide radicals) and plays a role in pollen formation and fertilization (Reuter and Robinson, 1997). Copper is a constituent of the protein plastocyanin, which is involved in transfer of electrons during photosynthesis (Lal, 2006). It serves as a catalyst in the process of respiration. Legumes need copper for nodulation and nitrogen fixation (Whitehead, 2000).

Table 9.8: Estimated copper balances (g ha^{-1} $year^{-1}$) from an extensively managed clover-grassland, grazed by cattle (Whitehead, 2000).

	ESTIMATED CU (G HA^{-1} $YEAR^{-1}$)
INPUTS	
Deposition from atmosphere	210
ASPECT OF RECYCLING	
Uptake into herbage	15
Consumption of herbage by animals	8
Dead herbage to soil	21
Dead roots to soil	14
Excreta to soil of grazed area	8
OUTPUTS	
Milk / live-weight gain	0.04
Leaching / runoff	0
Loss through excreta off sward	0
GAIN TO SOIL	210

Figure 9.1 shows the various forms and pathways of Fe, Mn, Zn and Cu in grassland, which would also be applicable to the present study area.

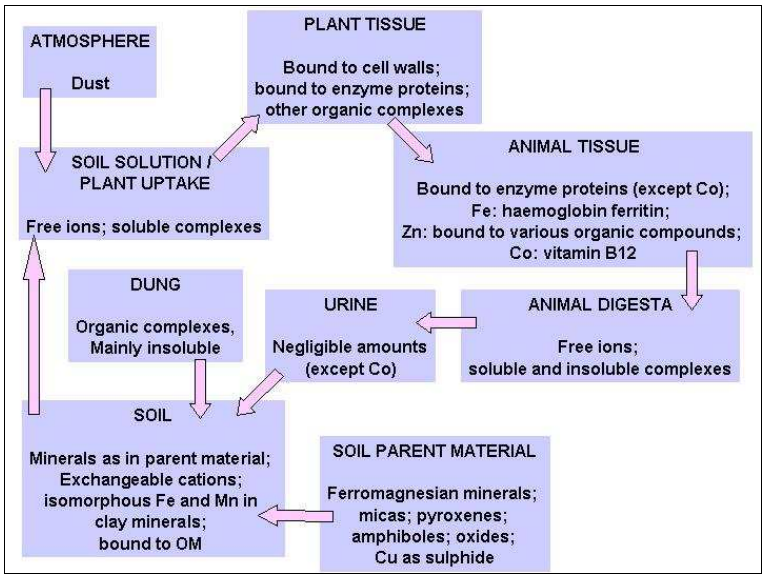

Figure 9.1. The main forms of Fe, Mn, Cu, Zn and Co involved in nutrient cycling in grassland (from Whitehead, 2000)

9.6.1 STATISTICAL ANALYSIS: IRON, MANGANESE, ZINC AND COPPER CONTENT

Table 9.9: Descriptive statistics – plant-available iron (n = 369), manganese (n = 368), zinc (n = 368) and copper (n = 367) content.

	Fe	Mn	Zn	Cu
	mg kg^{-1}	mg kg^{-1}	mg kg^{-1}	mg kg^{-1}
Mean	18.50	88.74	0.61	1.70
Median	15.10	60.35	0.30	1.30
Standard Deviation	12.43	81.36	0.79	1.69
Coefficient of Variation	0.67	0.92	1.30	0.99
Minimum	1.00	1.60	0.00	0.00
Maximum	88.90	389.00	3.90	8.70
Range	87.90	387.40	3.90	8.70
Lower Quartile	10.40	27.00	0.10	0.50
Upper Quartile	22.20	126.40	0.85	2.20
Quartile Range	11.80	99.4	0.75	1.70
Percentile 10	7.20	13.60	0.00	0.00
Percentile 90	32.80	207.50	1.80	4.00
Skewness	2.09	1.42	1.87	1.61
Kurtosis	6.28	1.70	3.46	2.79

Normality was rejected for Fe, Mn, Zn and Cu content by the statistical tests employed, namely the Shapiro-Wilk W test, Kolmogorov-Smirnov / Lilliefors test, and three D'Agostino tests based on skewness, on kurtosis, and on a combination of skewness and kurtosis (AnalystSoft, 2007).

Table 9.10: Distribution in terms of deciles – plant-available iron (n = 369), manganese (n = 368), zinc (n = 368) and copper (n = 367) content.

	Decile	Fe	Mn	Zn	Cu
		mg kg^{-1}	mg kg^{-1}	mg kg^{-1}	mg kg^{-1}
minimum		1.0	1.6	0.0	0.0
	1	7.1	13.6	0.0	0.0
	2	9.3	22.5	0.0	0.3
	3	11.1	32.0	0.1	0.6
	4	13.2	45.4	0.2	1.0
median	5	15.1	60.0	0.3	1.3
	6	17.6	84.0	0.4	1.6
	7	19.8	108.0	0.7	2.0
	8	25.2	142.3	1.0	2.7
	9	32.0	201.5	1.7	4.0
maximum	10	88.9	389.0	3.9	8.7

The **plant-available iron** content of 369 samples from the study area ranges from 1.0 to 88.9 mg kg^{-1}. The mean (18.5 mg kg^{-1}) is higher than the median (15.1 mg kg^{-1}), with a skewness of 2.09 and kurtosis of 6.28. The standard deviation is 12.43. Half the samples have iron concentrations of between 10.4 (1^{st} quartile) and 22.2 mg kg^{-1} (3^{rd} quartile), for a quartile range of 11.8. In 80 % of samples, the Fe content is between 7.2 (1^{st} decile) and 32.8 mg kg^{-1} (9^{th} decile). The frequency distribution is shown in Table 9.10 and Figures 9.2 – 9.3.

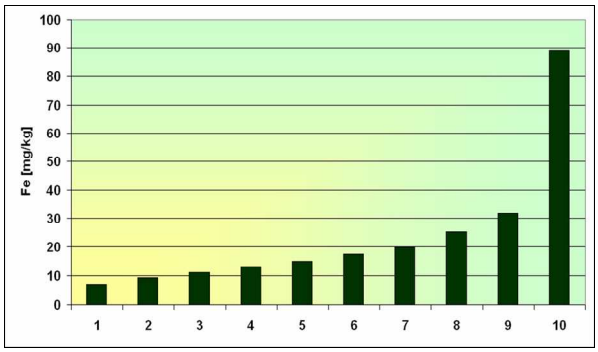

Figure 9.2. Decile distribution of plant-available Fe content (mg kg^{-1})

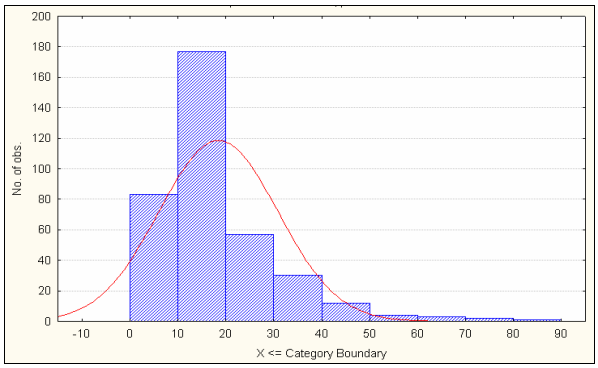

Figure 9.3. Histogram of plant-available Fe content (mg kg^{-1})

A statistically significant correlation, at $p < 0.01$, was found between iron content and manganese content ($r^2 = 0.35$), as shown in Figure 9.4. Significant, but weak, correlations were found with sand content ($r^2 = 0.24$), exchangeable potassium content ($r^2 = 0.17$), zinc content ($r^2 = 0.17$), exchangeable magnesium content ($r^2 = 0.16$), silt content ($r^2 = 0.15$), plant-available phosphorus content ($r^2 = 0.14$), extractable magnesium content ($r^2 = 0.143$), extractable potassium content ($r^2 = 0.14$), clay content ($r^2 = 0.12$), medium sand content ($r^2 = 0.11$) and copper content ($r^2 = 0.10$).

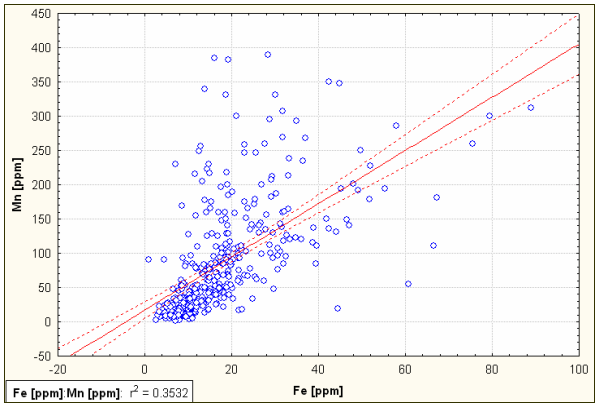

Figure 9.4. Plant-available Fe content vs plant-available Mn content (ppm = mg kg^{-1})

The **plant-available manganese** content of 368 samples from the study area ranges from 1.6 to 389.0 mg kg^{-1}. The mean (88.74 mg kg^{-1}) is considerably higher than the median (60.35 mg kg^{-1}), with a skewness of 1.42 and kurtosis of 1.70. The standard deviation is 81.36. Half the samples have manganese concentrations of between 27.0 (1^{st} quartile) and 126.4 mg kg^{-1} (3^{rd} quartile), for a quartile range of 99.4. In 80 % of samples, the Mn content is between 13.6 (1^{st} decile) and 207.5 mg kg^{-1} (9^{th} decile). The frequency distribution is shown in Table 9.10 and Figures 9.5 – 9.6.

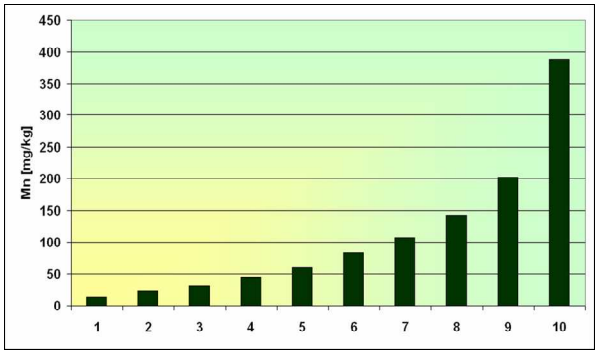

Figure 9.5. Decile distribution of plant-available Mn content (mg kg^{-1})

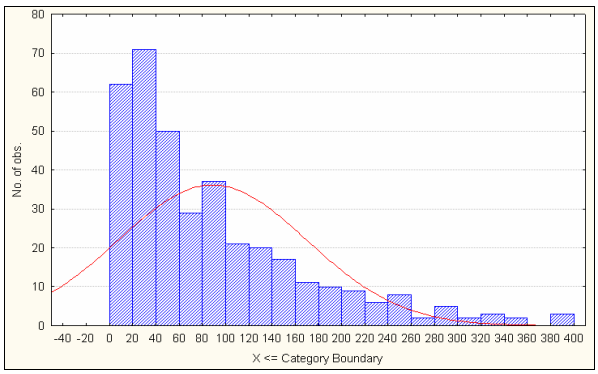

Figure 9.6. Histogram of plant-available Mn content (mg kg^{-1})

The concentrations of Mn found in the study area are consistent with the findings of Ellis (1988) in comparable areas in southern Africa: median 84 mg kg^{-1} and range 324 mg kg^{-1} for A horizons, median 57 mg kg^{-1} and range 459 mg kg^{-1} for B horizons in the eastern Boesmanland; median 100 mg kg^{-1} and range 600 mg kg^{-1} for A horizons, median 61 mg kg^{-1} and range 280 mg kg^{-1} for B horizons in western Boesmanland.

A statistically significant correlation, at $p < 0.01$, was found between manganese content and iron content ($r^2 = 0.35$), as shown in Figure 9.4. Significant, but weak, correlations were found with exchangeable magnesium content ($r^2 = 0.24$), copper content ($r^2 = 0.23$), zinc content ($r^2 = 0.21$), sand content ($r^2 = 0.20$), extractable magnesium content ($r^2 = 0.18$), clay content ($r^2 = 0.166$), exchangeable potassium content ($r^2 = 0.14$), medium sand content ($r^2 = 0.12$) and extractable potassium content ($r^2 = 0.10$).

The **plant-available zinc** content of 368 samples from the study area ranges from 0 to 3.90 mg kg^{-1}. The mean (0.61 mg kg^{-1}) is considerably higher than the median (0.30 mg kg^{-1}), with a skewness of 1.87 and kurtosis of 3.46. The standard deviation is 0.79. Half the samples have zinc concentrations of between 0.10 (1^{st} quartile) and 0.82 mg kg^{-1} (3^{rd} quartile), for a quartile range of 0.75. In 80 % of samples, the Zn content is between 0 (1^{st} decile) and 1.80 mg kg^{-1} (9^{th} decile). The frequency distribution is shown in Table 9.10 and Figures 9.7 – 9.8.

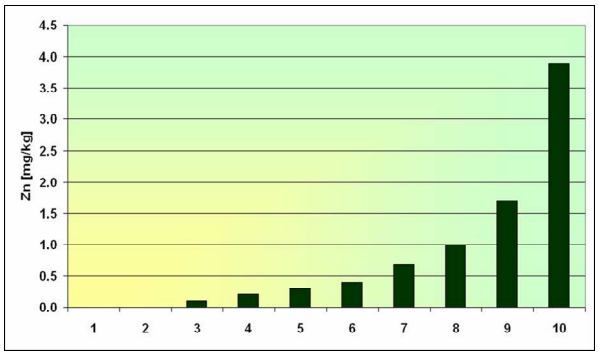

Figure 9.7. Decile distribution of plant-available Zn content (mg kg^{-1})

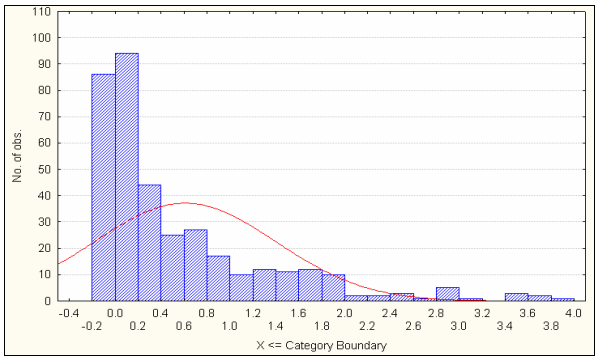

Figure 9.8. Histogram of plant-available Zn content (mg kg^{-1})

The concentrations of Zn found in the study area are consistent with the findings of Ellis (1988) in

comparable areas in southern Africa: median 0.9 mg kg^{-1} and range 3.4 mg kg^{-1} for A horizons, median 0.5 mg kg^{-1} and range 2.2 mg kg^{-1} for B horizons in the eastern Boesmanland; median 0.4 mg kg^{-1} and range 6.2 mg kg^{-1} for A horizons, median 0.2 mg kg^{-1} and range 0.6 mg kg^{-1} for B horizons in western Boesmanland. Han and Singer (2007) mentions Zn concentrations of 15.7 – 62.3 mg kg^{-1} in Nakuru District, Kenya.

Statistically significant, but weak, correlations, at $p < 0.01$, were found between zinc content and copper content ($r^2 = 0.22$), manganese content ($r^2 = 0.21$), plant-available phosphorus content ($r^2 = 0.17$), and iron content ($r^2 = 0.17$).

The **plant-available copper** content of 367 samples from the study area ranges from 0 to 8.70 mg kg^{-1}. The mean (1.70 mg kg^{-1}) is considerably higher than the median (1.30 mg kg^{-1}), with a skewness of 1.61 and kurtosis of 2.79. The standard deviation is 1.69. Half the samples have copper concentrations of between 0.50 (1st quartile) and 2.20 mg kg^{-1} (3rd quartile), for a quartile range of 1.70. In 80 % of samples, the Cu content is between 0 (1st decile) and 4.00 mg kg^{-1} (9th decile). The frequency distribution is shown in Table 9.10 and Figures 9.9 – 9.10.

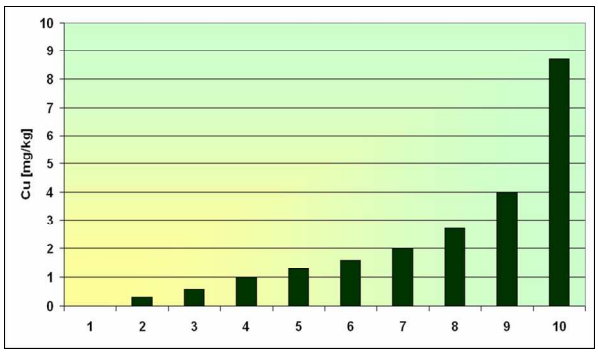

Figure 9.9. Decile distribution of plant-available Cu content (mg kg^{-1})

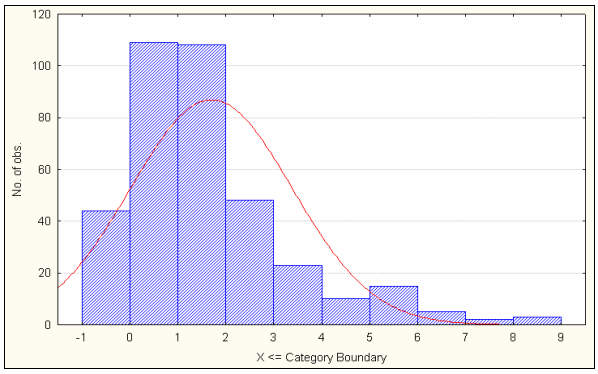

Figure 9.10. Histogram of plant-available Cu content (mg kg^{-1})

The concentrations of Cu found in the study area are consistent with the findings of Ellis (1988) in comparable areas in southern Africa: median 1.1 mg kg^{-1} and range 13.3 mg kg^{-1} for A horizons, median 1.0 mg kg^{-1} and range 18.4 mg kg^{-1} for B horizons in the eastern Boesmanland; median 0.6 mg kg^{-1} and range 2.7 mg kg^{-1} for A horizons, median 0.6 mg kg^{-1} and range 1.7 mg kg^{-1} for B horizons in western Boesmanland. Han and Singer (2007) reported Cu concentrations of 2.2 – 4.2 mg kg^{-1} in Kenyan soils of the Nakuru District.

Significant, but weak, correlations, at $p < 0.01$, were found between copper content and manganese content ($r^2 = 0.23$), zinc content ($r^2 = 0.22$), sand content ($r^2 = 0.18$), exchangeable magnesium content ($r^2 = 0.15$), pH ($r^2 = 0.12$), fluoride content ($r^2 = 0.12$), iron content ($r^2 = 0.11$), sum of exchangeable bases ($r^2 = 0.11$), clay content ($r^2 = 0.10$), sum of extractable bases ($r^2 = 0.10$), extractable magnesium content ($r^2 = 0.10$), and silt content ($r^2 = 0.10$).

Mn and Cu concentrations are slightly higher in sub- than topsoil (Table 9.11; Figures 9.12 and 9.14), while the opposite is true for Zn (Table 9.11; Figure 9.13). There is no discernible difference between Fe

concentrations in subsoil and topsoil (Table 9.11; Figure 9.11). Ellis (1988) found slightly higher concentrations of zinc and manganese in topsoil, relative to subsoil, in the eastern and western Boesmanland.

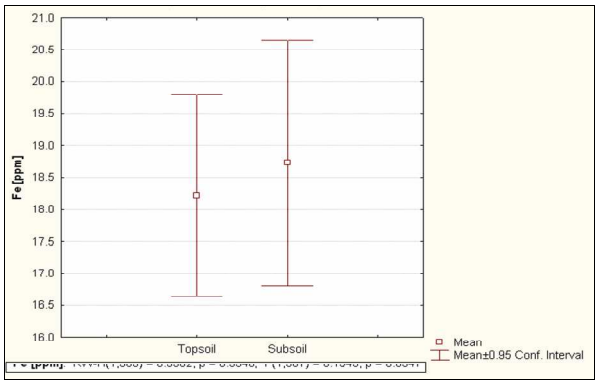

Figure 9.11. Fe content (ppm = mg kg^{-1}), per topsoil and subsoil

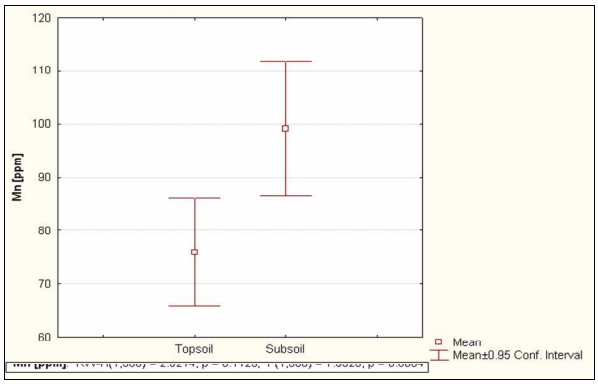

Figure 9.12. Mn content, per topsoil and subsoil

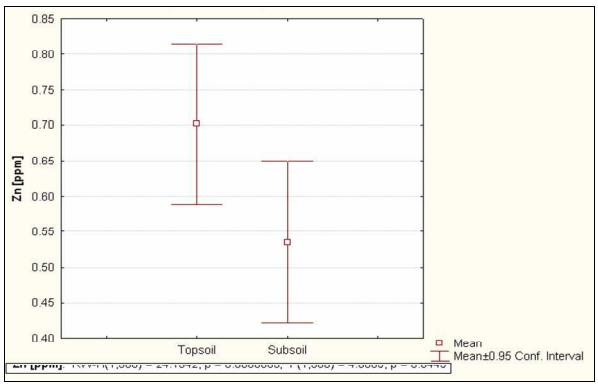

Figure 9.13. Zn content, per topsoil and subsoil

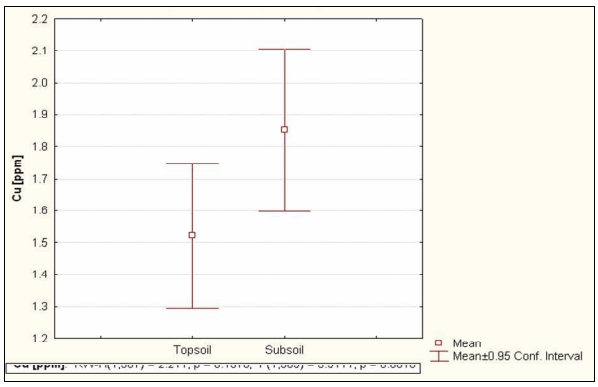

Figure 9.14. Cu content , per topsoil and subsoil

Table 9.11: Plant-available iron, manganese, zinc and copper content, per topsoil and subsoil

	Fe mg kg^{-1}		**Mn** mg kg^{-1}		**Zn** mg kg^{-1}		**Cu** mg kg^{-1}	
	Topsoil (n = 152)	**Subsoil** (n = 183)	**Topsoil** (n = 152)	**Subsoil** (n = 183)	**Topsoil** (n = 152)	**Subsoil** (n = 183)	**Topsoil** (n = 152)	**Subsoil** (n = 181)
Mean	18.13	18.34	71.91	95.96	0.70	0.49	1.48	1.82
Median	15.65	14.70	53.85	65.00	0.40	0.10	1.15	1.30
Std.Dev.	10.48	14.18	60.43	89.37	0.73	0.78	1.43	1.87
Minimum	1.00	2.70	2.90	1.60	0.00	0.00	0.00	0.00
Maximum	66.60	88.90	331.50	389.00	3.65	3.85	6.50	8.65
Range	65.60	86.20	328.60	387.40	3.65	3.85	6.50	8.65
Lower Quartile	11.10	9.40	27.00	24.20	0.20	0.00	0.40	0.50
Upper Quartile	21.95	21.50	99.75	155.00	0.94	0.65	2.15	2.20
Quartile Range	10.85	12.10	72.75	130.80	0.74	0.65	1.75	1.70
Percentile 10	8.10	6.40	13.70	10.50	0.10	0.00	0.00	0.00
Percentile 90	31.30	33.10	150.00	230.00	1.70	1.50	3.30	4.50

When disregarding clay loam and sandy clay soils, of which there are too few samples to be representative, it emerges that sand and loamy sand have noticeably lower concentrations of plant-available Fe than sandy loam, sandy clay loam, loam and clay loam soils (Figure 9.15). This result agrees with the statement by

Whitehead (2000), that “iron concentrations are generally lower in sandy soils than in loams and clays”. The same pattern is followed by Zn, though the Zn concentrations in loamy sand, sandy loam and sandy clay loam are comparable (Figure 9.17). In the case of Mn and Cu, concentrations increase in the order sand → loamy sand → sandy loam → loam → sandy clay loam soils (Figures 9.16 and 9.18).

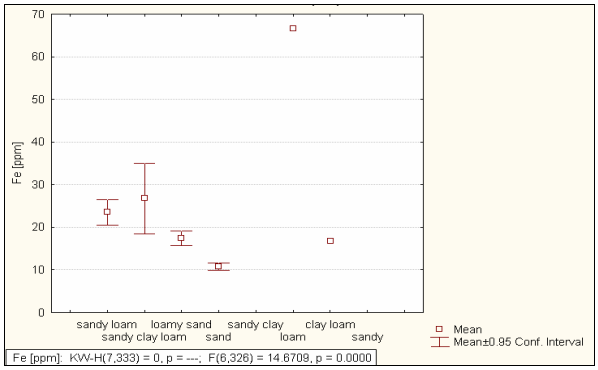

Figure 9.15. Fe content (ppm = mg kg^{-1}), per textural class

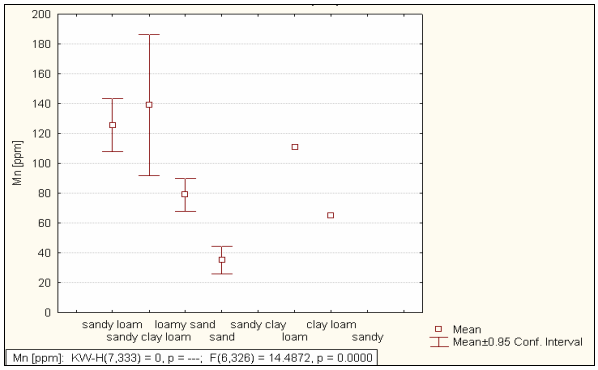

Figure 9.16. Mn content, per textural class

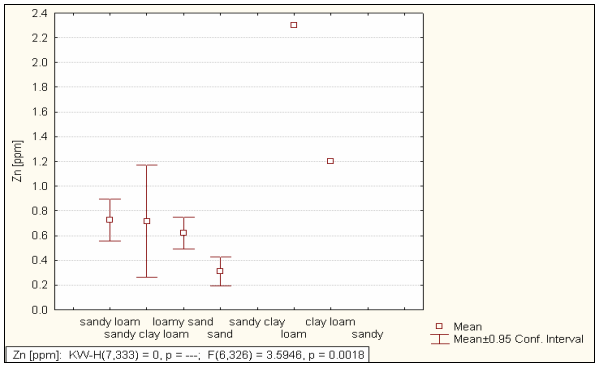

Figure 9.17. Zn content, per textural class

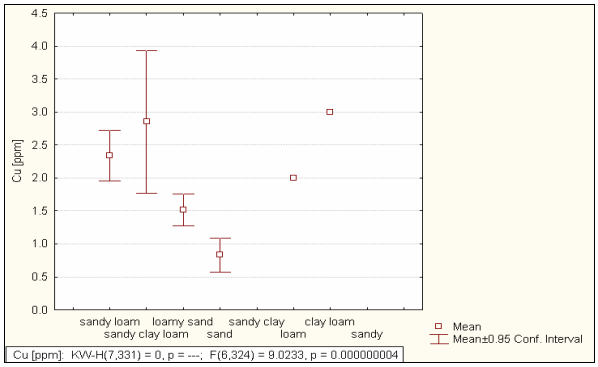

Figure 9.18. Cu content, per textural class

Fe, Mn, Zn and Cu concentrations increase in the order aeolian → weathered in situ → colluvial → alluvial origin of parent material (Figures 9.19 – 9.22). The low concentrations in aeolian material are especially noticeable in the cases of Fe and Cu.

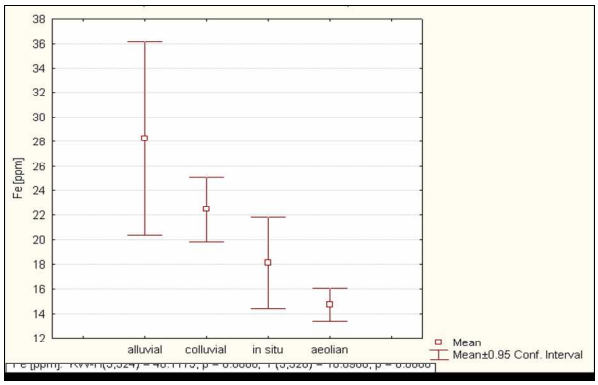

Figure 9.19. Fe content (ppm = mg kg^{-1}), per origin of parent material

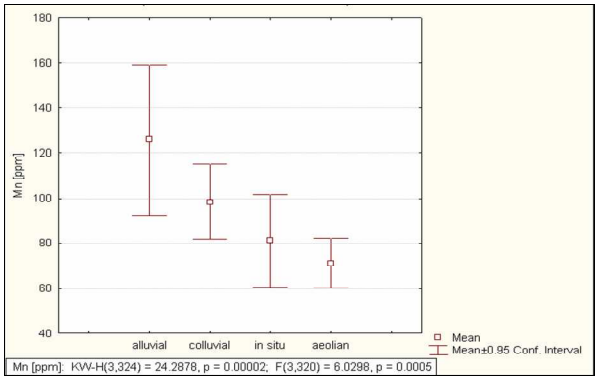

Figure 9.20. Mn content, per origin of parent material

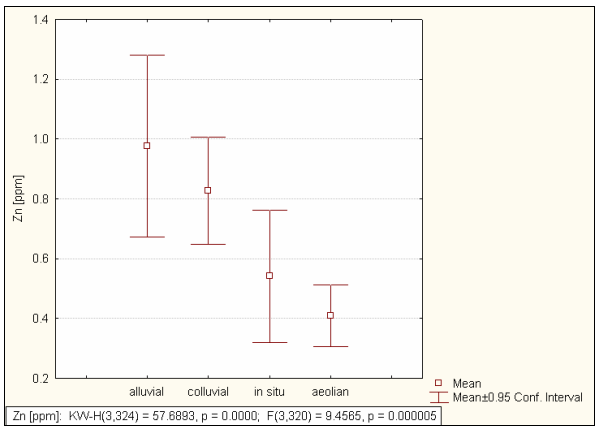

Figure 9.21. Zn content, per origin of parent material

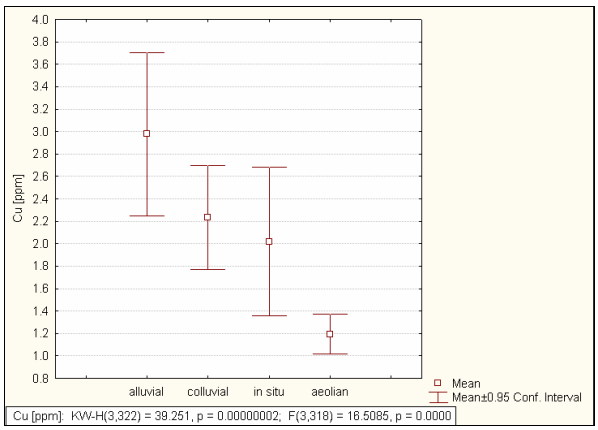

Figure 9.22. Cu content, per origin of parent material

Fe, Mn, Zn and Cu concentrations are significantly lower in the Kalahari sands than the soils formed on the schist of the Khomas Hochland – a direct consequence of the mineral composition of the respective parent materials (Figures 9.23 – 9.26), and in agreement literature, for example Vlek and Harmsen (1985) and Whitehead (2000).

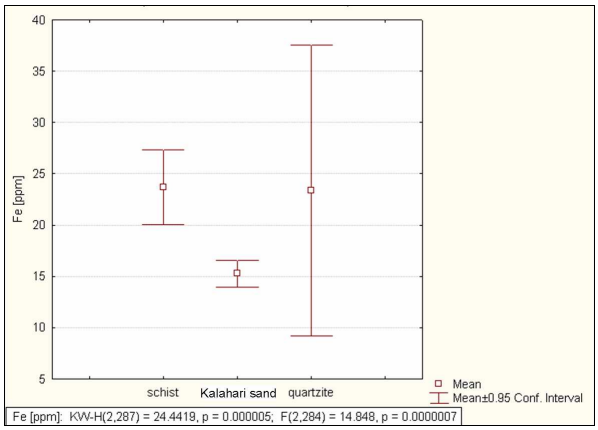

Figure 9.23. Fe content (ppm = mg kg^{-1}), per type of parent material

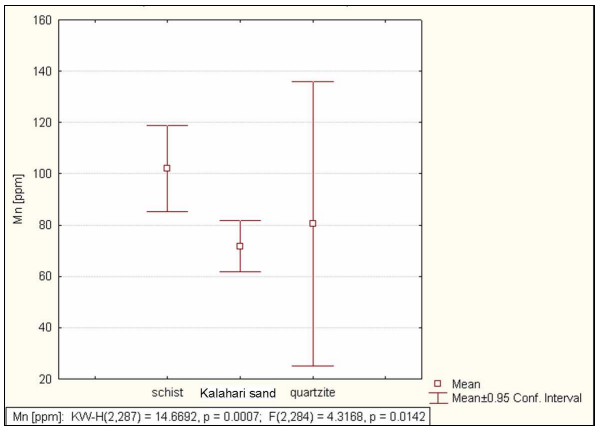

Figure 9.24. Mn content, per type of parent material

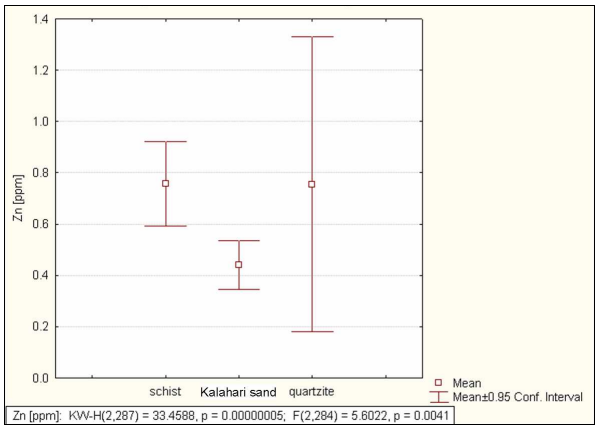

Figure 9.25. Zn content, per type of parent material

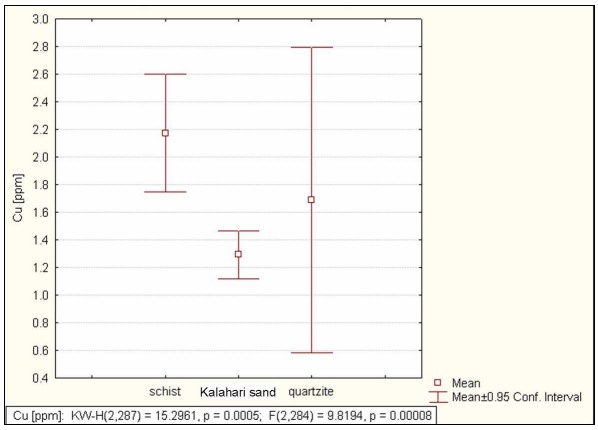

Figure 9.26. Cu content, per type of parent material

Fe concentrations increase in the order Arenosols → Calcisols → Regosols → Leptosols → Cambisols → Luvisols (Figure 9.27). Arenosols have the lowest Mn concentrations and Cambisols the highest. Mn

concentrations in Leptosols, Regosols, Calcisols and Luvisols are intermediate between these two groups, while Luvisols show a large spread in the ±0.95 confidence interval (Figure 9.28). Arenosols and Regosols have the lowest Zn concentrations, and Cambisols and Calcisols noticeably higher concentrations. Zn concentrations in Leptosols are intermediate between these two groups, while Luvisols show a large spread in the ±0.95 confidence interval (Figure 9.29). Cu concentrations increase in the order Arenosols → Leptosols → Regosols → Luvisols → Calcisols → Cambisols, but with large overlaps in the ±0.95 confidence intervals, especially in the case of Luvisols (Figure 9.30).

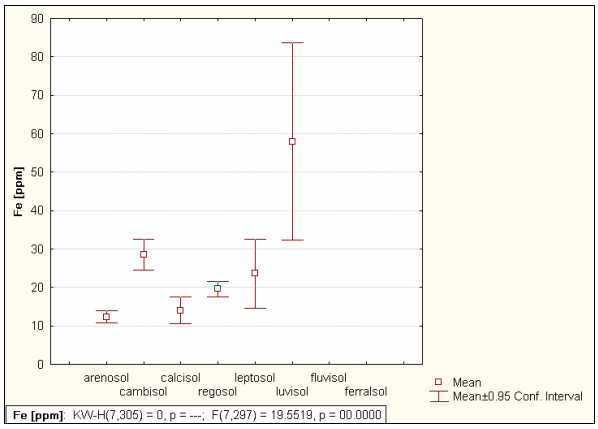

Figure 9.27. Fe content (ppm = mg kg^{-1}), per WRB reference soil group

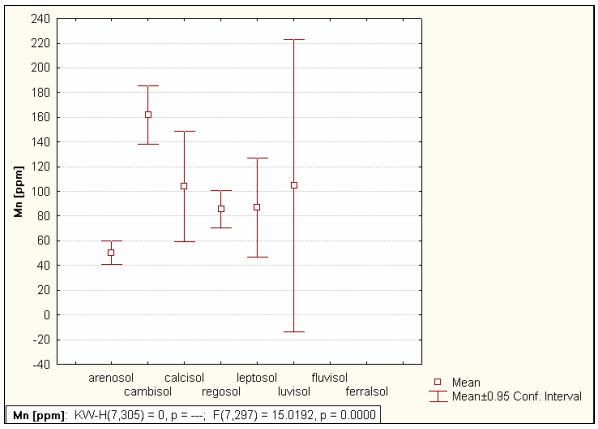

Figure 9.28. Mn content, per WRB reference soil group

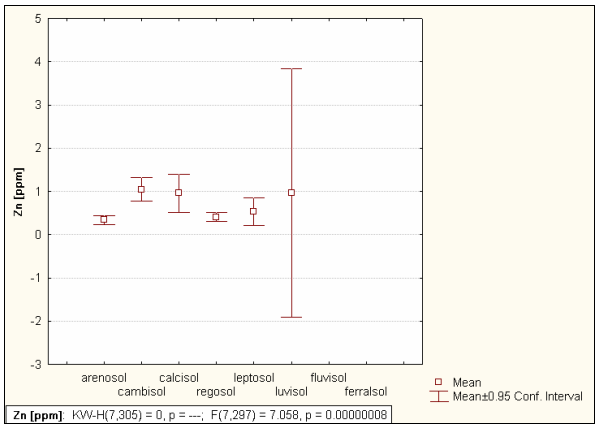

Figure 9.29. Zn content, per WRB reference soil group

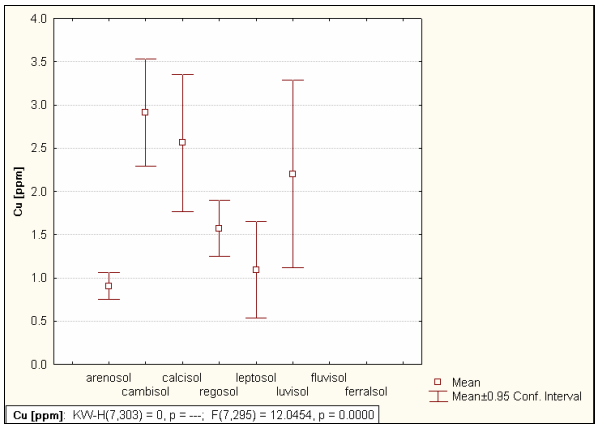

Figure 9.30. Cu content, per WRB reference soil group

Table 9.12: Iron, manganese, zinc and copper content, per WRB reference soil group.

Fe mg kg^{-1}	**Arenosols** (n = 130)	**Calcisols** (n = 17)	**Leptosols** (n = 15)	**Cambisols** (n = 59)	**Regosols** (n = 81)	**Luvisols** (n = 3)
Mean	12.34	14.05	23.62	28.52	19.61	57.97
Median	10.20	15.00	20.60	26.80	18.10	60.80
Std.Dev.	8.80	6.95	16.16	15.57	9.24	10.35
Minimum	2.7	3.0	7.9	1.0	3.5	46.5
Maximum	67.2	24.7	75.6	88.9	51.9	66.6
Range	64.5	21.7	67.7	87.9	48.4	20.1
Lower Quartile	7.4	9.5	14.2	19.2	13.3	46.5
Upper Quartile	14.7	18.9	29.3	33.1	23.7	66.6
Quartile Range	7.3	9.4	15.1	14.0	10.4	20.1

Percentile 10	5.9	4.6	10.8	12.8	10.5	46.5
Percentile 90	19.2	24.3	30.7	49.1	30.7	66.6
Mn mg kg^{-1}	**Arenosols** (n = 130)	**Calcisols** (n = 17)	**Leptosols** (n = 15)	**Cambisols** (n = 59)	**Regosols** (n = 81)	**Luvisols** (n = 3)
Mean	50.40	103.82	87.11	161.64	85.75	104.67
Median	27.35	85.00	71.40	143.90	67.80	110.60
Std.Dev.	54.50	87.07	72.55	90.68	68.66	47.58
Minimum	1.6	9.6	17.0	14.0	2.9	54.4
Maximum	230.0	300.0	260.0	389.0	331.5	149.0
Range	228.4	290.4	243.0	375.0	328.6	94.6
Lower Quartile	15.6	34.5	32.4	92.5	33.5	54.4
Upper Quartile	63.9	142.3	105.8	213.0	125.8	149.0
Quartile Range	48.3	107.8	73.4	120.5	92.3	94.6
Percentile 10	7.7	13.7	23.4	50.7	19.6	54.4
Percentile 90	135.0	258.0	211.9	300.0	178.5	149.0
Zn mg kg^{-1}	**Arenosols** (n = 130)	**Calcisols** (n = 17)	**Leptosols** (n = 15)	**Cambisols** (n = 59)	**Regosols** (n = 81)	**Luvisols** (n = 3)
Mean	0.34	0.96	0.53	1.05	0.41	0.97
Median	0.10	0.70	0.40	0.60	0.20	0.40
Std.Dev.	0.62	0.86	0.58	1.06	0.48	1.16
Minimum	0.0	0.0	0.0	0.0	0.0	0.2
Maximum	3.7	3.0	2.0	3.9	3.0	2.3
Range	3.7	3.0	2.0	3.9	3.0	2.1
Lower Quartile	0.0	0.3	0.2	0.2	0.1	0.2
Upper Quartile	0.3	1.5	0.4	1.8	0.6	2.3
Quartile Range	0.3	1.2	0.2	1.6	0.5	2.1
Percentile 10	0.0	0.0	0.1	0.0	0.0	0.2
Percentile 90	0.9	2.0	1.8	2.7	0.8	2.3
Cu mg kg^{-1}	**Arenosols** (n = 130)	**Calcisols** (n = 17)	**Leptosols** (n = 15)	**Cambisols** (n = 57)	**Regosols** (n = 81)	**Luvisols** (n = 3)
Mean	0.91	2.56	1.09	2.91	1.57	2.20
Median	0.80	2.10	0.60	2.40	1.30	2.00
Std.Dev.	0.90	1.54	1.01	2.33	1.48	0.44
Minimum	0.0	0.3	0.0	0.0	0.0	1.9
Maximum	6.5	5.9	2.9	8.7	7.9	2.7
Range	6.5	5.6	2.9	8.7	7.9	0.8
Lower Quartile	0.1	1.5	0.3	1.2	0.5	1.9
Upper Quartile	1.4	3.3	2.1	4.2	2.1	2.7
Quartile Range	1.3	1.8	1.8	3.0	1.6	0.8
Percentile 10	0.0	1.0	0.0	0.4	0.1	1.9
Percentile 90	1.9	5.6	2.6	6.6	3.4	2.7

Fe, Mn, Zn and Cu concentrations tend to increase with the degree of dissection of the landscape (Figures 9.31 – 9.34). One possible explanation is greater rates of erosion and subsequent weathering in more dissected terrain. Secondly, the highly dissected terrain of the study area occurs mainly on schist, quartzite and calcrete – all of them richer in minerals than the windblown, quartz-rich Kalahari sands, which covers the less dissected areas towards the east.

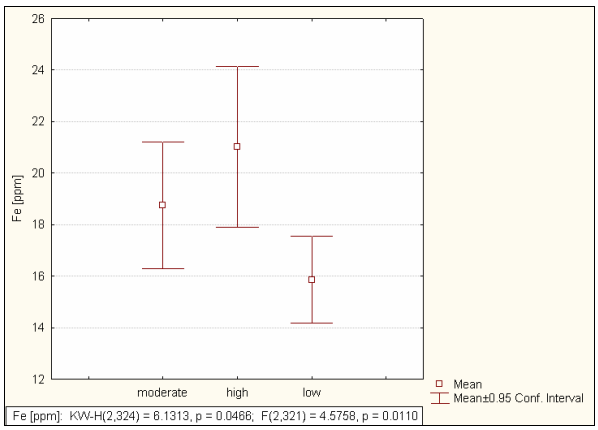

Figure 9.31. Fe content (ppm = mg kg^{-1}), per degree of dissection of the landscape

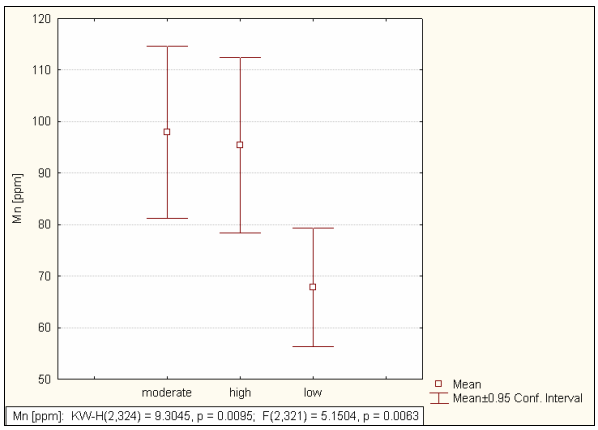

Figure 9.32. Mn content, per degree of dissection of the landscape

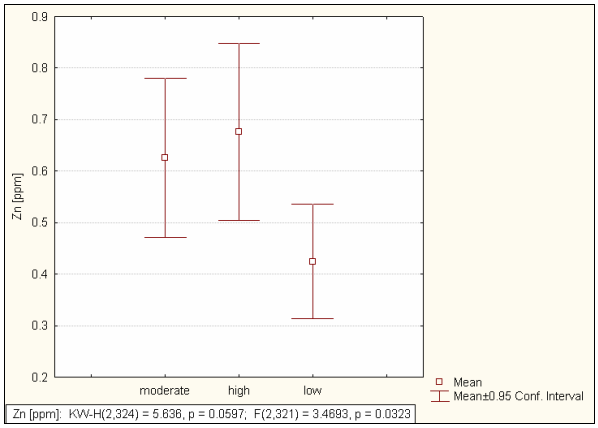

Figure 9.33. Zn content, per degree of dissection of the landscape

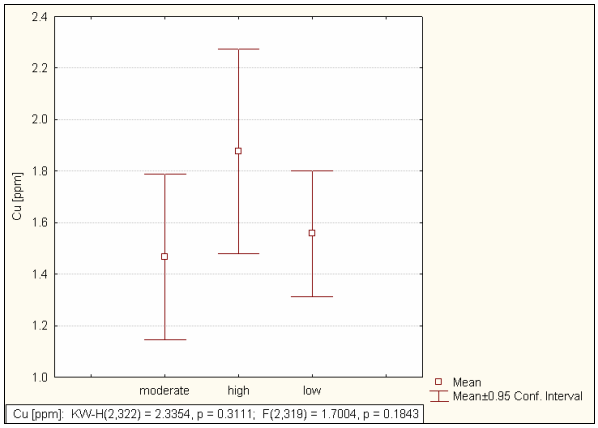

Figure 9.34. Cu content, per degree of dissection of the landscape

Fe concentration slightly increases from pH 5.0 to 6.5, where after it gradually decreases to a minimum around pH 9.0 (Figures 9.35 – 9.36). This agrees with the 'traditional' micronutrient availability diagrams.

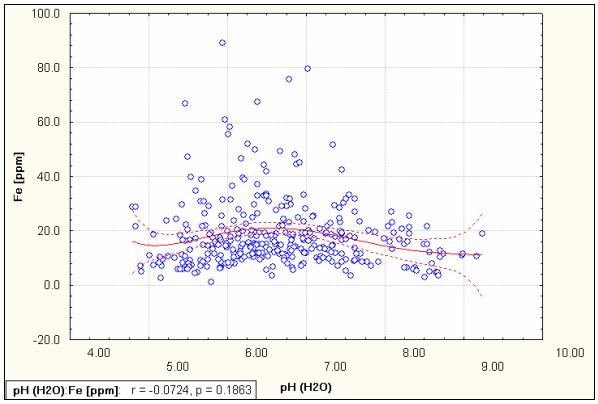

Figure 9.35. Fe content (ppm = mg kg^{-1}) vs pH

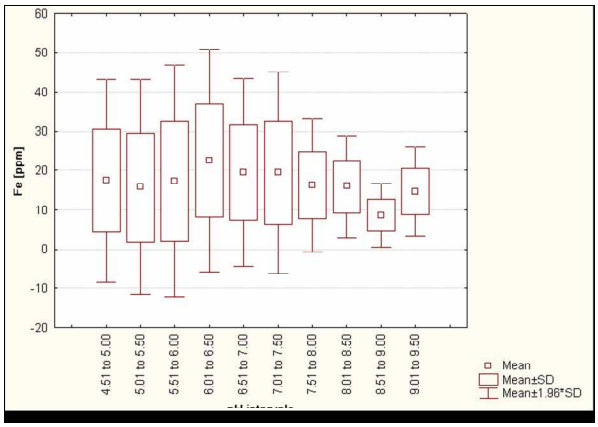

Figure 9.36. Fe content, per pH interval

Mn concentration increases gradually from pH 5.0 to 8.0, where after it decreases (Figures 9.37 – 9.38). This differs from the 'traditional' micronutrient availability diagrams found in general soil literature.

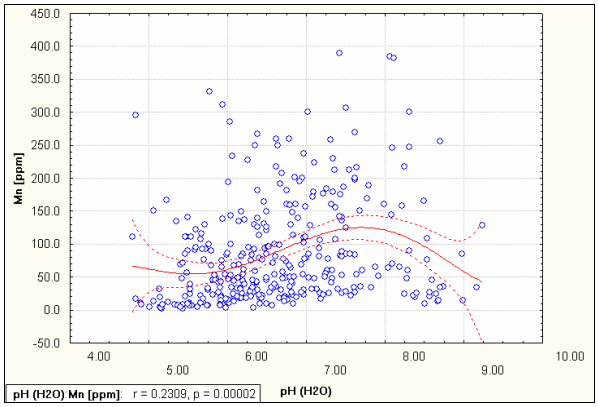

Figure 9.37. Mn content (ppm = mg kg^{-1}) vs pH

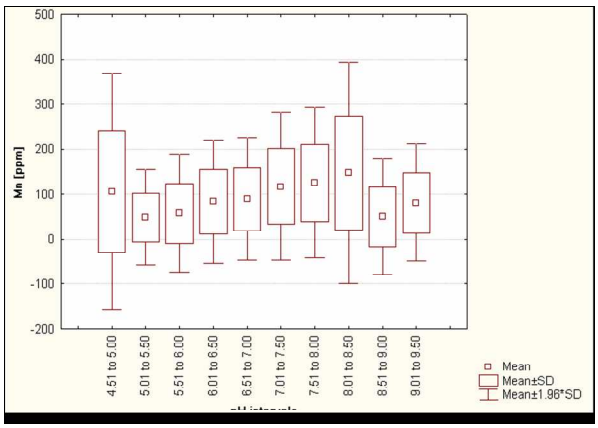

Figure 9.38. Mn content, per pH interval

Zn concentration increases with pH up to pH 8, where after it drops (Figures 9.39 – 9.40). This differs from the 'traditional' micronutrient availability diagrams found in general soil literature.

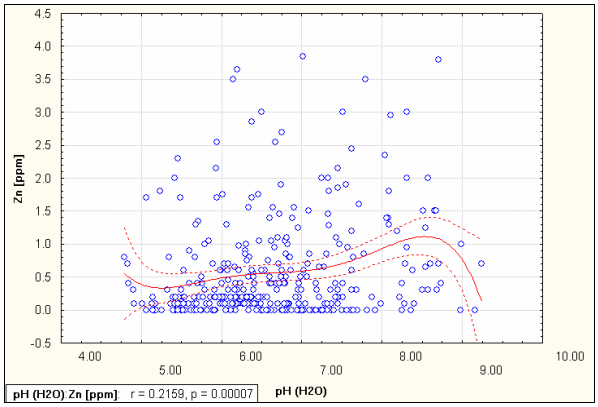

Figure 9.39. Zn content (ppm = mg kg^{-1}) vs pH

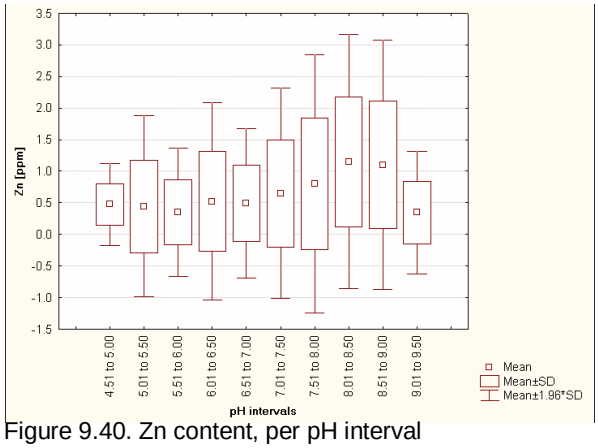

Figure 9.40. Zn content, per pH interval

Cu concentrations increase gradually with pH (Figures 9.41 – 9.42). This differs from the 'traditional' micronutrient availability diagrams in general soil literature.

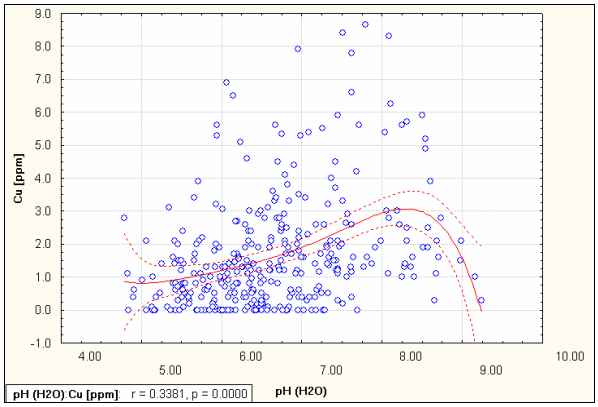

Figure 9.41. Cu content (ppm = mg kg^{-1}) vs pH

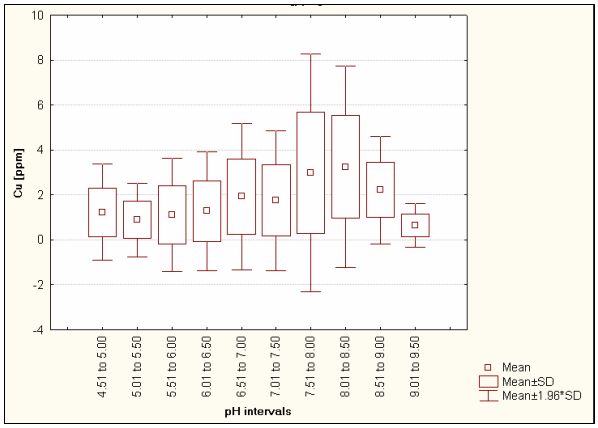

Figure 9.42. Cu content, per pH interval

In flat, almost flat and slightly undulating landscapes, plant-available Fe, Mn, Zn and Cu concentrations are highest in low landscape positions, lowest in high landscape positions and intermediate (relatively high) in flat and intermediate landscape positions (Figures 9.43 – 9.46). It is probably caused by loss of finer soil

particles from higher positions and accumulation of the same on flat and in low areas.

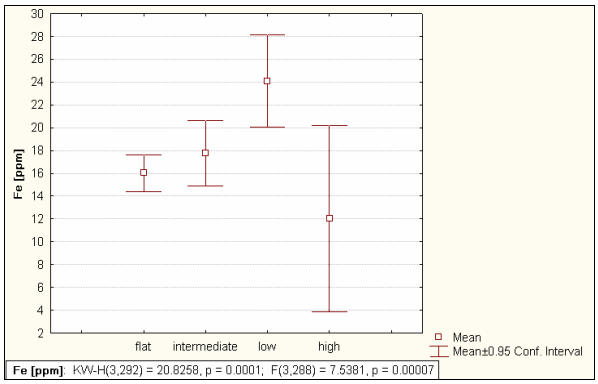

Figure 9.43. Fe content (ppm = mg kg^{-1}), per landscape position in flat to slightly undulating landscapes

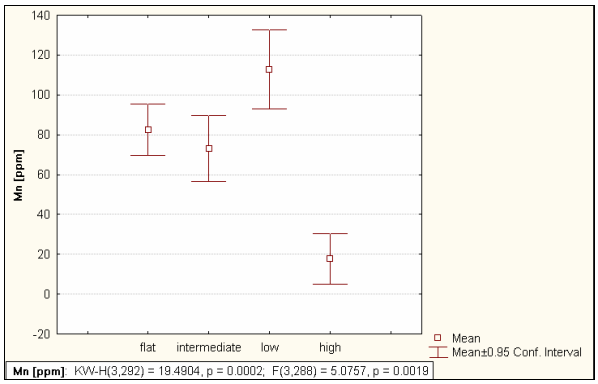

Figure 9.44. Mn content, per landscape position in flat to slightly undulating landscapes

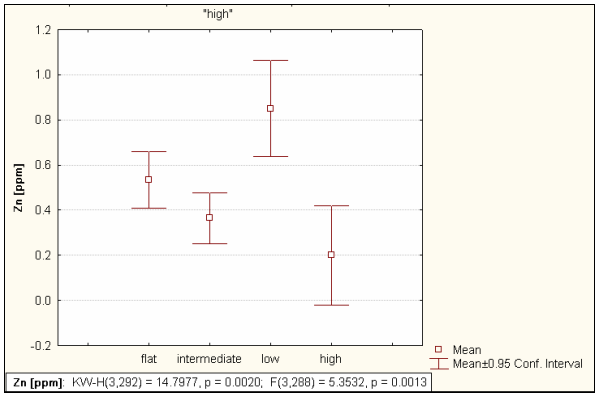

Figure 9.45. Zn content, per landscape position in flat to slightly undulating landscapes

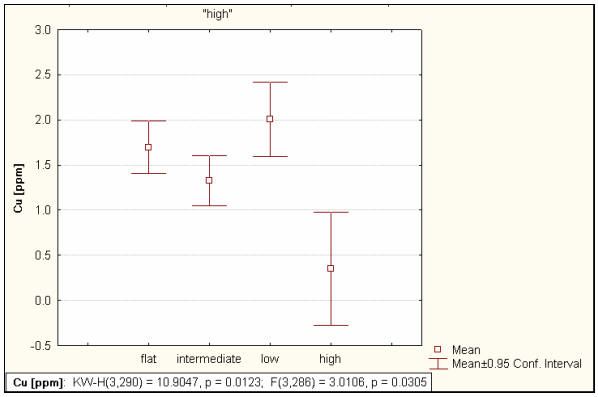

Figure 9.46. Cu content, per landscape position in flat to slightly undulating landscapes

In undulating to mountainous landscapes, there are no discernable differences in Fe, Mn, Zn and Cu concentrations from crests and mid-slopes, and no data are available from bottom positions (Figure 9.47 – 9. 50).

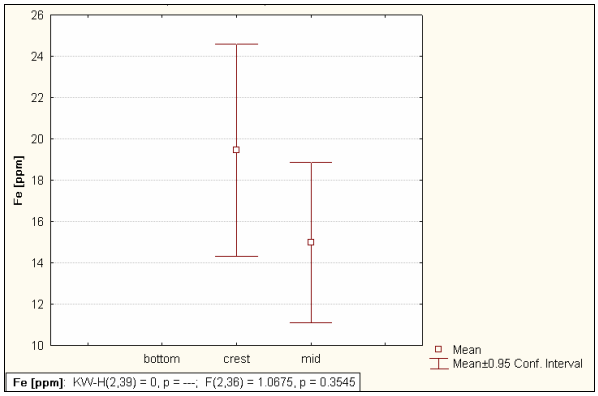

Figure 9.47. Fe content (ppm = mg kg^{-1}), per landscape position in undulating to mountainous landscapes

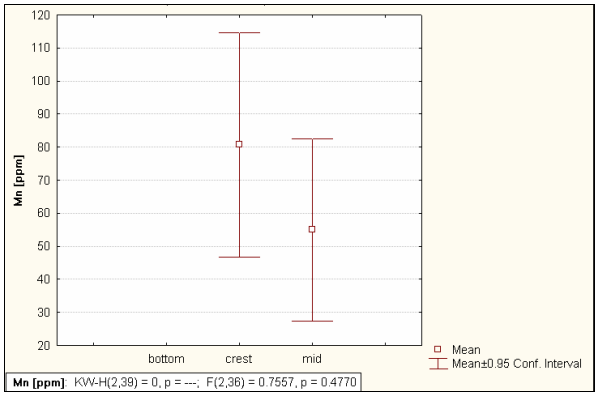

Figure 9.48. Mn content, per landscape position in undulating to mountainous landscapes

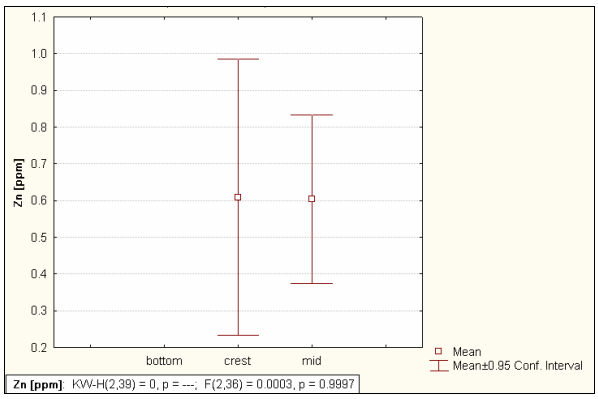

Figure 9.49. Zn content, per landscape position in undulating to mountainous landscapes

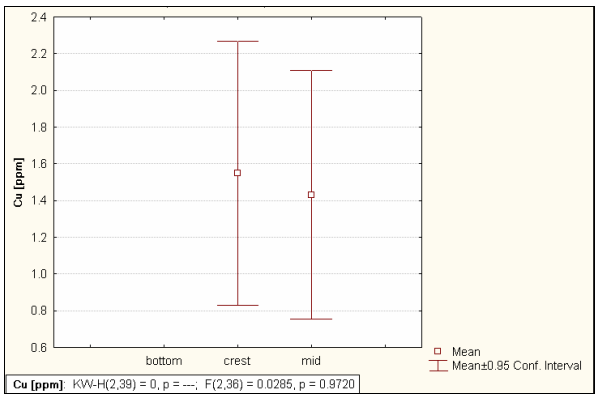

Figure 9.50. Cu content, per landscape position in undulating to mountainous landscapes

The plant-available Fe, Mn, Zn and Cu levels, of topsoil and subsoil respectively, are shown in Figures 9.51 – 9.58.

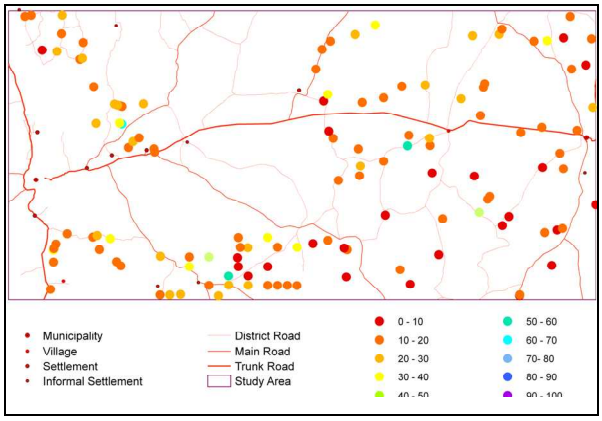

Figure 9.51. Fe content (mg kg^{-1}) of topsoil

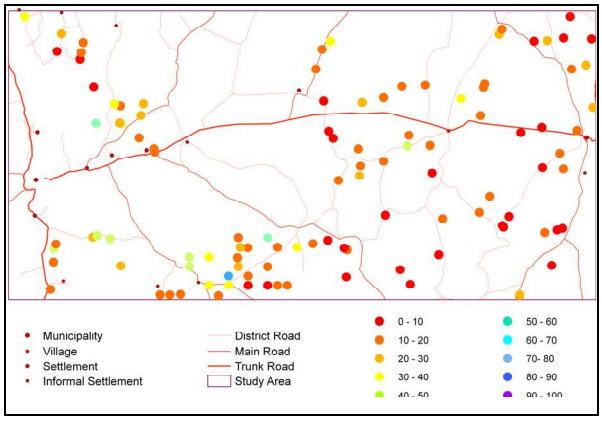

Figure 9.52. Fe content (mg kg^{-1}) of subsoil

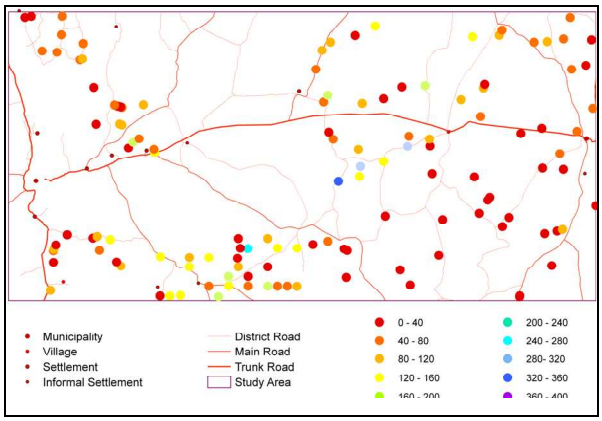

Figure 9.53. Mn content (mg kg^{-1}) of topsoil

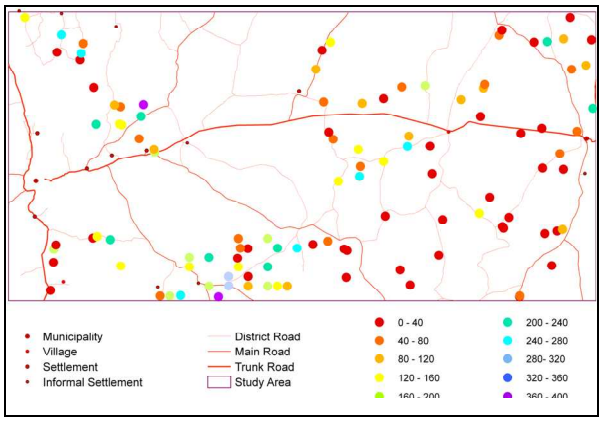

Figure 9.54. Mn content (mg kg^{-1}) of subsoil

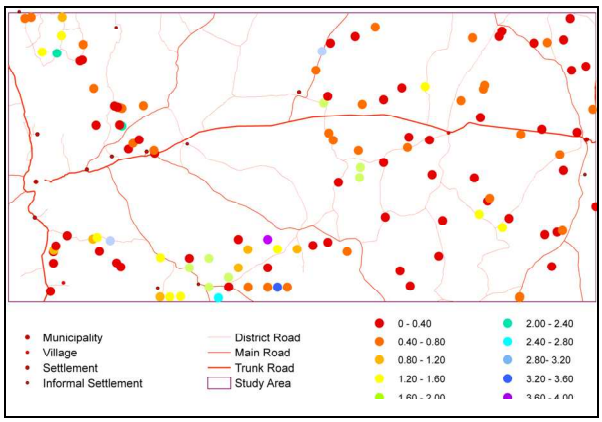

Figure 9.55. Zn content (mg kg^{-1}) of topsoil

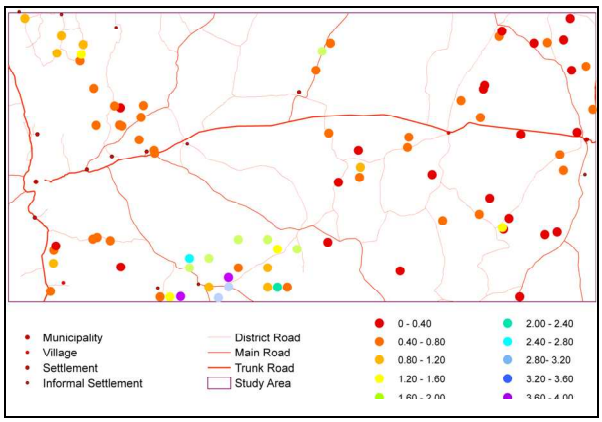

Figure 9.56. Zn content (mg kg^{-1}) of subsoil

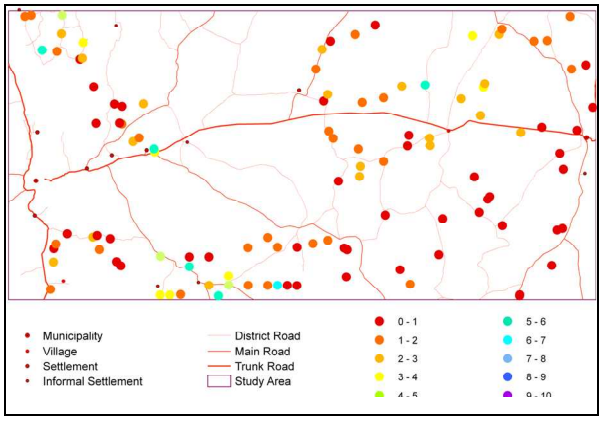

Figure 9.57. Cu content (mg kg^{-1}) of topsoil

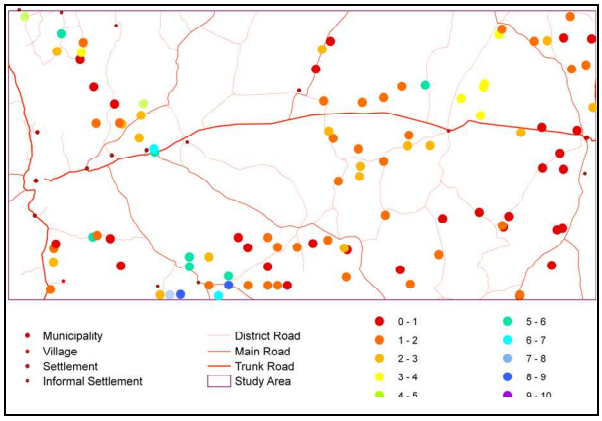

Figure 9.58. Cu content (mg kg^{-1}) of subsoil

CHAPTER TEN

CHARACTERISATION – SOIL ORGANIC MATTER, pH, PARTICLE SIZE, CRUSTING AND SEALING

10.1 SOIL ORGANIC MATTER [SOM]

Soil organic matter is a key characteristic of soil fertility. It is composed of plant and animal debris, living and dead microbial cells, which are or have been involved in the degradation of debris, intermediate products and humic substances (Foth, 1999). Humic substances are usually categorised into three fractions: fulvic acids, humic acids and humin. *Fulvic acids* are light yellow to yellow-brown in colour, and soluble in water under all pH conditions (Stevenson, 1994). *Humic acids* are dark brown to black, and are soluble in water under neutral and alkaline conditions, but insoluble under highly acidic conditions (pH < 2). They are complex aromatic macromolecules with amino acid-, amino sugar-, peptide- and aliphatic compounds linked to the aromatic groups. They may contain free and bound phenolic OH-groups, quinone structures, nitrogen and oxygen as bridge units, and a variety of COOH groups (Stevenson, 1994). *Humin* is the black fraction of humic substances that is water-insoluble under all pH conditions (Stevenson, 1994).

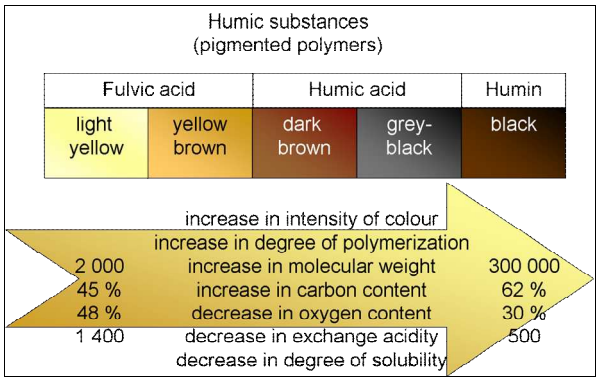

Figure 10.1. Characteristics of humic substances (adapted from Stevenson, 1994)

The humic substances in grassland soils are composed of roughly 70 % humic acids and 30 % fulvic acids, while the ratio is inverted in forests soils (Stevenson, 1994). The comparative properties of humic substances are summarised in Figure 10.1. Labile soil organic matter, such as cellulose and hemicellulose, comprises around 10 – 20 % of soil organic matter and serves as the reservoir of readily available nutrients, especially nitrogen (Foth, 1999).

Soil micobes produce organic acids – such as citric, tartaric, malic and α-ketogluconic acid (Stevenson, 1991) – and other complexing (chelating) agents. Almost all of the nitrogen and much of the phosphorus and sulphur needed by plants are released by microbial enzymes from soil organic matter into plant-available forms, namely as NH_4^+, $H_2PO_4^-$ and SO_4^{2-}. The ratio of C:N:P:S in humus is approximately 100:10:1:1 (Foth, 1999). Though soil organic matter does not directly supply much Ca, Mg, K and Na, it assists in the effective release and mobilisation of divalent and trivalent cations from insoluble inorganic matter by complexing (Whitehead, 2000). These cations are re-precipitated or sorbed in a different position, usually at greater

depth, when the complex breaks down. The interaction between soil organic matter and micronutrients is complicated, e.g. through formation of complexes of varying mobility between micronutrients and carboxyl-, phenolic- and other organic groups, occupation of exchange sites by micronutrients, and interactions with hydrous Fe, Al and Mn oxides (Whitehead, 2000). Humus, with its large specific surface area, contributes (together with clay) to the colloidal fraction of soil (Foth, 1999), to the extent of 20 – 70 % of the cation exchange capacity (Stevenson, 1994). Soil organic matter plays an important role in regulating soil pH. The negatively charged sites formed by dissociation of phenolic- and carboxyl groups, at pH higher than 7, contribute to the cation exchange capacity of the soil by allowing adsorption of cations, including H^+, from the soil solution (Whitehead, 2000).

Soil organic matter contributes significantly to soil structure formation, water adsorption and nutrient adsorpsion, and as a consequence, to favourable soil conditions for high levels of biological activity (Foth, 1999). It also reduces erodibility.

10.1.1 STATISTICAL ANALYSIS: SOIL ORGANIC MATTER CONTENT [SOM]

Normality was the rejected for soil organic matter content by most of the statistical tests employed, namely the Shapiro-Wilk W test and three D'Agostino tests based on skewness, on kurtosis, and on a combination of skewness and kurtosis, but no evidence against normality was found by the Kolmogorov-Smirnov / Lilliefors test (AnalystSoft, 2007).

Table 10.1: Descriptive statistics – soil organic carbon and soil organic matter content (n = 505). (SOM = 1.74 x SOC)

	Soil Organic Carbon %	Soil Organic Matter %
Mean	0.39	0.67
Median	0.33	0.58
Standard Deviation	0.23	0.40
Coefficient of Variation	0.59	0.59
Minimum	0.03	0.05
Maximum	1.15	2.00
Range	1.12	1.95
Lower Quartile	0.22	0.39
Upper Quartile	0.51	0.89
Quartile Range	0.29	0.50
Percentile 10	0.14	0.25
Percentile 90	0.69	1.20
Skewness	1.15	1.15
Kurtosis	1.14	1.14

The **soil organic matter** content of 505 samples from the study area ranges from 0.05 to 2.00 %. The mean (0.67 %) is higher than the median (0.58 %), with a skewness of 1.15 and kurtosis of 1.14. The standard deviation is 0.40. Half the samples have SOM content of between 0.38 (1^{st} quartile) and 0.89 % (3^{rd} quartile), for a quartile range of 0.50. In 80 % of samples, the SOM content is between 0.25 (1^{st} decile) and 1.20 % (9^{th} decile). The frequency distribution is shown in Table 10.2 and Figures 10.2 – 10.3.

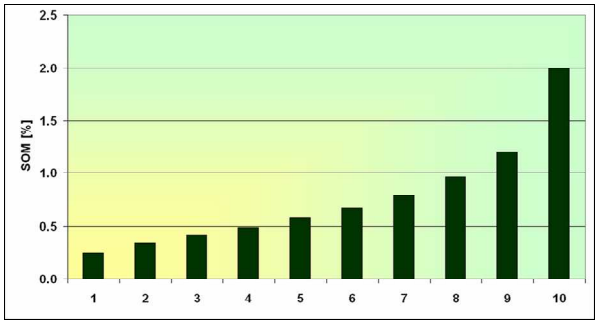

Figure 10.2. Decile distribution of soil organic matter content (%)

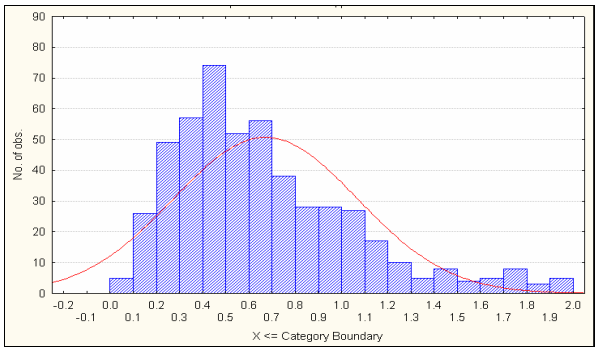

Figure 10.3. Histogram of soil organic matter content (%)

Table 10.2: Distribution in terms of deciles – soil organic matter content (n = 505).

	Decile	SOM
		%
minimum		0.05
	1	0.25
	2	0.34
	3	0.42
	4	0.49
median	5	0.58
	6	0.68
	7	0.80
	8	0.96
	9	1.20
maximum	10	2.00

The soil organic carbon (and thus soil organic matter) of the study area is far lower than values reported for other southern African locations (Table 10.3).

It does, however, agree with concentrations recorded elsewhere in Namibia (Petersen, 2008; Coetzee, Beernaert and Calitz, 1999; Kempf, 1999c; Coetzee, 2001b; Kutuahupira, Mouton and Coetzee, 2001a, 2001b; Kutuahupira, Mouton and Beukes, 2003; ICC, MAWRD and AECI, 2000). Ellis (1988) also recorded low concentrations of organic carbon in western Boesmanland: median 0.1 %, range 0.5 %; and eastern Boesmanland, South Africa: median 0.2 %, range 0.6 %. The extremely low organic matter content can be linked directly to the low rainfall and subsequent low plant biomass production of the study area, as compared to other southern African locations, as well as high rates of mineralisation due to relatively high temperatures.

Table 10.3: Organic carbon content of some southern Africa soils at different depths.

	Organic Carbon (mean ± SD) %							
Depth (cm)	0 – 5	5 – 10	10 – 15	15 – 20	20 – 25	25 – 30	30 – 35	35 – 45
[a] Present study	0.55 ± 0.20		0.43 ± 0.21		0.46 ± 0.21		0.42 ± 0.18	
[b1] Angola	6.2 ± 4.2		4.4 ± 4.0		3.1 ± 2.4			
[b2] Botswana	2.9 ± 1.1		2.8 ± 0.9		2.2 ± 1.0			
[b3] Mozambique	7.0 ± 4.1		5.9 ± 4.2		4.1 ± 3.2			
[b4] Namibia	2.6 ± 0.7		2.5 ± 0.7		1.7 ± 0.6			
[b5] South Africa	3.3 ± 4.6		3.1 ± 4.7		2.9 ± 4.8			

Depth (cm)	Organic Carbon (mean ± SD) %							
	0 – 5	5 – 10	10 – 15	15 – 20	20 – 25	25 – 30	30 – 35	35 – 45
[b6] Zimbabwe	3.6 ± 0.4		2.2 ± 0.5		3.2 ± 0.8			
[c] Eastern Cape, South Africa	1.12 ± 0.19	0.89 ± 0.08	0.17 ± 0.14		0.56 ± 0.11		0.46 ± 0.09	
[d] Eastern Free State, South Africa	0.78	0.64	0.68	0.67		0.64		0.59
[e1] Okamboro, Namibia	~0.4		~0.35				~0.3	
[e2] Nareis, Namibia	~0.8		~0.7				~0.6	
[e3] Duruchaus, Namibia	~0.8		~0. 7				~0.6	

[a] present study (n = 63; 87; 42; 54)

[b] Hartemink and Hunting (2008) (n^{b1} = 60; n^{b2} = 6; n^{b3} = 30; n^{b4} = 3; n^{b5} = 30; n^{b6} = 12)

[c] Materechera, Mandiringana and Mbokodi (1998) (n = 10)

[d] Kotze and Du Preez (2008) (n = 1)

[e] Petersen (2008) (n^{e1} = 25, 23, 20; n^{e2} = 25, 22, 9; n^{e3} = 25, 16, 7)

Statistically significant, but weak, correlations were found with plant-available phosphorus (r^2 = 0.15), electrical conductivity of the saturated paste extract (r^2 = 0.12), horizon depth (r^2 = 0.11) and sulfate of the saturated paste extract (r^2 = 0.10).

Topsoil SOM concentrations are noticeably higher than those of the subsoil (Figures 10.4 – 10.5). This is caused by enrichment of the topsoil by decaying plant material and addition of animal excreta, and agrees with the findings of other researchers in southern Africa (Table 10.3).

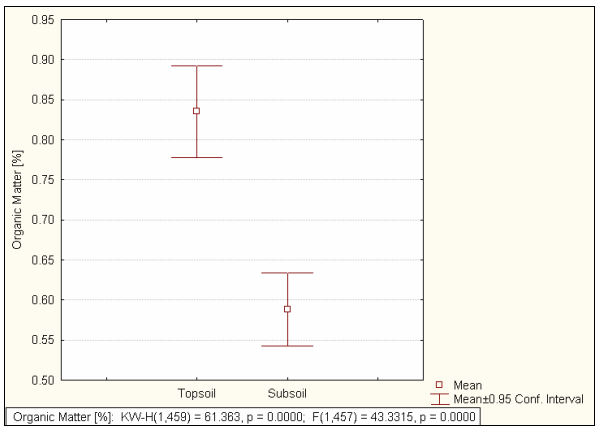

Figure 10.4. SOM content, per topsoil and subsoil

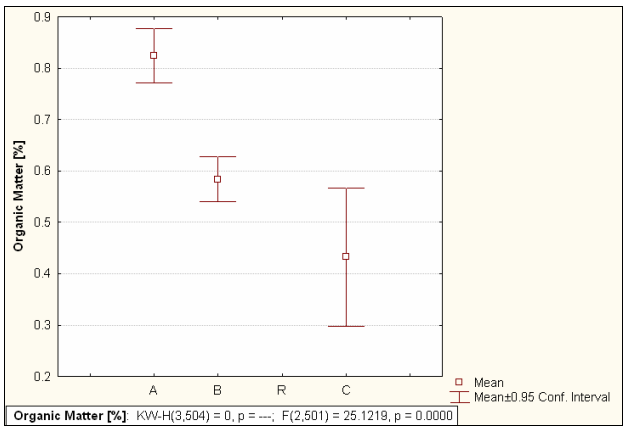

Figure 10.5. SOM content, per soil horizon

Arenosols have the lowest SOM concentrations, followed by Cambi- and Regosols. Fluvisols are richest in SOM (Table 10.4; Figure 10.6). The enrichment of Fluvisols probably happens through transport of particulate material containing organic matter by surface runoff.

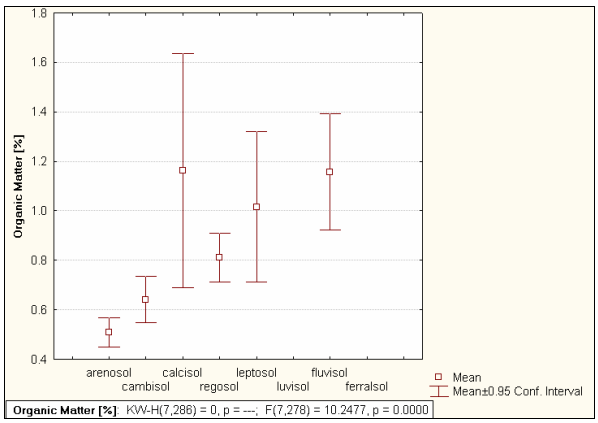

Figure 10.6. SOM content, per WRB reference soil group

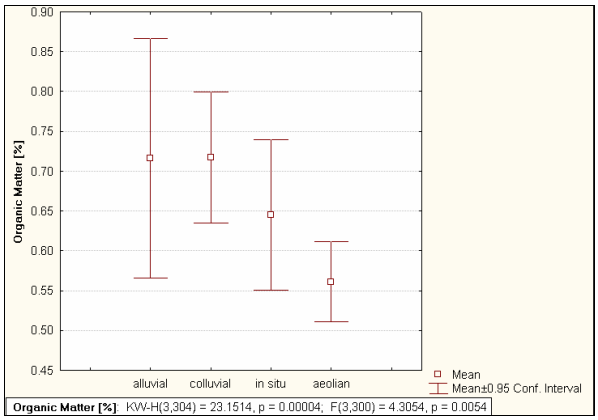

Figure 10.7. SOM content, per origin of parent material

Table 10.4: SOM content, per WRB reference soil group.

SOM %	Arenosols (n = 127)	Calcisols (n = 10)	Leptosols (n = 11)	Fluvisols (n = 9)	Cambisols (n = 58)	Regosols (n = 71)
Mean	0.51	1.16	1.02	1.16	0.64	0.81
Median	0.40	1.02	1.05	1.20	0.57	0.72
Std. Dev.	0.35	0.66	0.45	0.30	0.36	0.42
Minimum	0.17	0.25	0.44	0.61	0.05	0.23
Maximum	2.00	1.96	1.80	1.60	2.00	2.00
Range	1.83	1.71	1.36	0.99	1.95	1.77
Lower Quartile	0.30	0.68	0.58	1.01	0.41	0.51
Upper Quartile	0.58	1.81	1.28	1.30	0.79	0.99
Quartile Range	0.28	1.13	0.70	0.29	0.38	0.48
Percentile 10	0.20	0.28	0.48	0.61	0.25	0.42
Percentile 90	0.96	1.93	1.68	1.60	1.17	1.60

Soils of aeolian origin have the lowest SOM content, followed by those formed through *in situ* weathering, while soils from alluvial and colluvial origin have higher, comparable SOM concentrations (Figure 10.7). This agrees with the results above, as the soils of aeolian origin are the sandy soils of the deep Kalahari sand plains, while Fluvisols are of alluvial origin.

The soil organic matter levels, of topsoil and subsoil respectively, are shown in Figures 10.8 – 10.9.

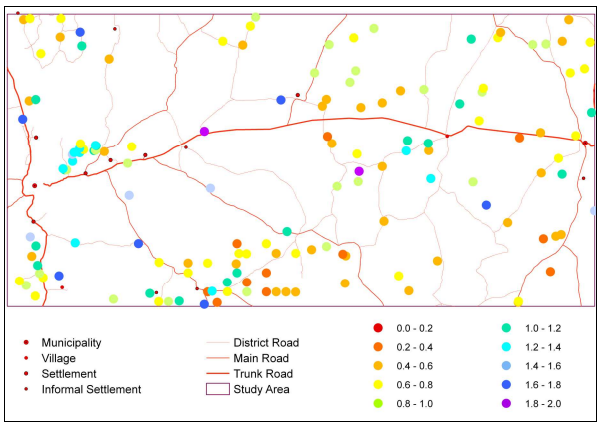

Figure 10.8. SOM content (%) of topsoil

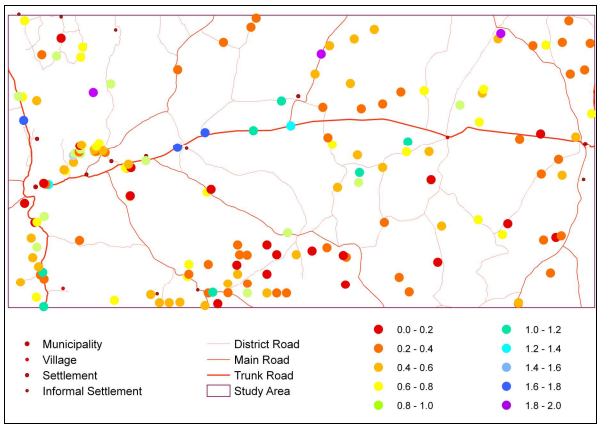

Figure 10.9. SOM content (%) of subsoil

10.2 PH

The pH of a solution is the negative logarithm to the base ten of the hydrogen ion activity in the solution: $pH = -\log_{10} a_H$ (Van der Watt and Van Rooyen, 1995; Bloom, 2000). In soil the pH indicates the degree of acidity or alkalinity, as measured on the pH scale from 1 to 14.

There are several sources of soil acidity:

- Weak carbonic acid [H_2CO_3] is formed when water reacts with the carbon dioxide produced by soil organisms and roots during the process of respiration (Foth, 1990; Bloom, 2000; Whitehead, 2000). On dissociation, the carbonic acid contributes hydrogen ions [H^+] to the soil solution.
- Carbonic acid is also formed by rainwater dissolving atmospheric carbon dioxide (Foth, 1990; Whitehead, 2000).
- When organic matter is mineralised, organic acids such as fulvic and humic acid are formed and the liberated nitrogen and sulphur are oxidised to nitric and sulphuric acid (Foth, 1990; Stevenson, 1994; Bloom, 2000; Whitehead, 2000). Accumulation of organic matter is higher in grassland systems with grazing animals where grazed vegetation is returned in the form of dung and urine, than in cropping systems where much of the organic material is removed during harvest (Whitehead, 2000). Consequently, mineralization of organic matter contributes more to soil acidity in grassland systems than in cropping systems.
- Nitrification, especially of ammonium from urea in animal urine in grassland systems, contributes to soil acidity (Whitehead, 2000).
- Basic cations are replaced by H^+ from various sources and these displaced cations are subsequently lost through leaching. Once leaching has removed the basic cations in the soil solution, those adsorbed on the exchange complex are also progressively lost, together with anions such as nitrate. The H^+ ions associated with the anions remains behind and are in turn adsorbed onto the exchange complex, where they induce instability and the release of Al^{3+}. The latter is subsequently hydrolysed, with production of more H^+.

  $$Al^{3+}\text{(from lattice)} + H_2O \leftrightarrows Al(OH)^{2+} + H^+$$
  $$Al(OH)^{2+} + H_2O \leftrightarrows Al(OH)_3 + 2H^+$$

  A positive feedback develops, with acidity promoting more acidity through aluminium hydrolysis. $Al(OH)^{2+}$ is so strongly adsorbed on the soil complex that it in effect becomes non-exchangeable and reduces the CEC of the soil (Foth, 1990).

There are a number of sources of soil alkalinity:

- Many primary minerals contribute to alkalinity on weathering, by consuming H^+ and producing OH^- during hydrolysis. In general,

  $$\text{M-silicate mineral} + H_2O \rightarrow \text{H-silicate mineral} + M^+ + OH^-$$

  where M represents metal ions such as calcium, magnesium, potassium or sodium (Foth, 1990).
- The hydrolysis of calcium carbonate contributes OH^- to soils, controlling soil pH in calcareous soils. An equilibrium is reached with atmospheric carbon dioxide, with a soil pH of 8.3 as the maximum that can be attained through this reaction (Foth, 1990).

  $$CaCO_3 + H_2O \leftrightarrows Ca^{2+} + HCO_3^- + OH^-$$
- The hydrolysis of sodium carbonate can result in a pH of 10 or more, as sodium carbonate is more

soluble than calcium carbonate (Foth, 1990).

$$Na_2CO_3 + H_2O \leftrightarrows 2Na^+ + HCO_3^- + OH^-$$

pH of most soils is maintained between 4.0 and 8.5 by various buffering reactions such as cation exchange, dissociation of H^+ and OH^- and the equilibrium between $CaCO_3$ and CO_2 (Foth, 1990; Bloom, 2000). Free calcium carbonate is a very effective buffer, as it dissolves in the presence of acids, neutralising them and releasing CO_2. In basic non-calcareous soils, buffering is affected by dissociation of H^+ and OH^- from clay minerals, organic matter and the hydrous oxides of iron and aluminium. In acid soils (pH<5), Al^{3+} ions dissolve from clay minerals, occupy the cation exchange sites and occur in the soil solution where they are toxic to plants. Liming precipitates the aluminium as $Al(OH)_3$, with Ca occupying the vacated exchange sites. Manganese can have a similar toxic effect on plants at low pH (Foth, 1990).

In arid regions, soils tend to be neutral to alkaline. Where rates of evaporation exceed that of precipitation, capillary rise causes basic cations to accumulate near the soil surface. As long as a soil remains calcareous, carbonate hydrolysis dominates the system, maintaining pH between 7.5 and 8.3. Under these circumstances, mineral weathering is severely curtailed. In humid regions, soils tend to become acidic over time as basic cations are leached out and H^+ is released by hydroxy-aluminium hydrolyses and exchangeable aluminium hydrolysis. Intensively weathered soils have low CEC, high aluminium saturation of the exchange complex and very low base saturation (Foth, 1990).

The availability of most nutrients is pH dependent, as expressed in the well-known diagrams (Figure 10.10):

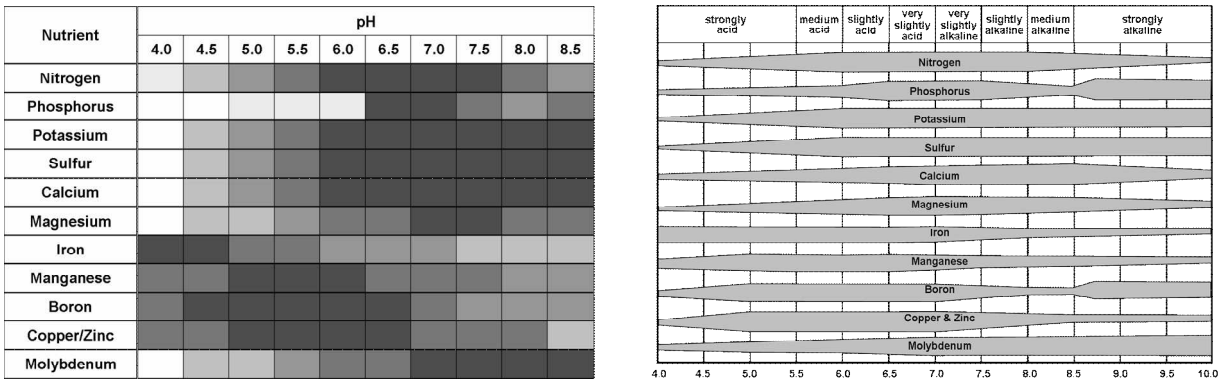

Figure 10.10. pH and nutrient availability diagrams (Forth, 1990)

Iron, manganese and aluminium is readily availability to plants at high levels of acidity, while potassium, sulphur, molybdenum, nitrogen, iodine, calcium, magnesium, phosphorus, boron copper, zinc, cobalt and selenium availability is limited by acidity. Biological activity and root growth are suppressed by high acidity. At the other end of the spectrum, high pH depresses uptake of iron, manganese, aluminium, copper, zinc, cobalt, nitrogen and iodine.

10.2.1 STATISTICAL ANALYSIS: PH IN 2:5 SOIL:WATER SUSPENSION

Normality was accepted for pH (H_2O) by the Kolmogorov-Smirnov / Lilliefors test, but rejected by the

Shapiro-Wilk W test and three D'Agostino tests based on skewness, on kurtosis, and on a combination of skewness and kurtosis (AnalystSoft, 2007). The distribution is almost, but not quite, normal (Figure 10.12).

Table 10.5: Descriptive statistics – pH (H_2O) (n = 578).

	pH (H_2O)
Mean	6.74
Median	6.63
Standard Deviation	0.94
Coefficient of Variation	0.14
Minimum	4.79
Maximum	9.24
Range	4.45
Lower Quartile	6.02
Upper Quartile	7.32
Quartile Range	1.30
Percentile 10	5.54
Percentile 90	8.18
Skewness	0.37
Kurtosis	-0.41

The **pH** (H_2O) of 578 samples from the study area ranges from 4.79 to 9.24. The mean (6.74) is somewhat higher than the median (6.63), with a skewness of 0.37 and kurtosis of -0.41. The standard deviation is 0.94. Half the samples have pH of between 6.02 (1st quartile) and 7.32 (3rd quartile), for a quartile range of 1.30. In 80 % of samples, the pH is between 5.54 (1st decile) and 8.18 (9th decile). The frequency distribution is shown in Table 10.6 and Figures 10.11 – 10.12.

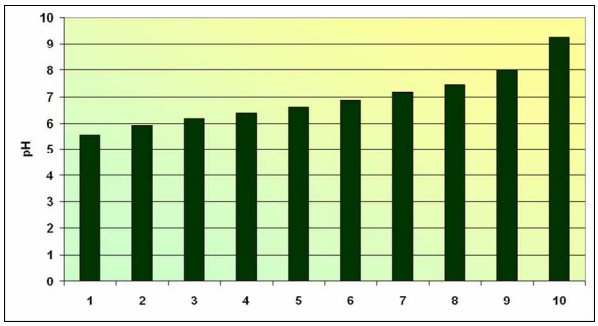

Figure 10.11. Decile distribution of pH (H_2O)

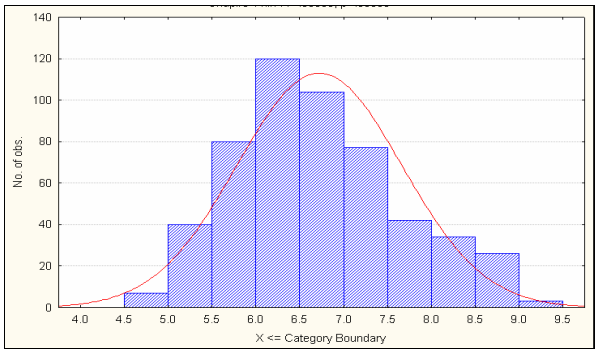

Figure 10.12. Histogram of pH (H_2O)

Table 10.6: Distribution in terms of deciles – pH (H_2O) (n = 578).

	Decile	**pH (H2O)**
minimum		4.79
	1	5.53
	2	5.92
	3	6.18
	4	6.38
median	5	6.63
	6	6.87
	7	7.17
	8	7.47
	9	8.00
maximum	10	9.24

If the descriptive terminology of Van der Watt and Van Rooyen (1995) is used, 85 % of all soil samples have

a pH from moderately acid (> 5.5) to moderately alkaline (< 8.5), as elaborated in Table 10.7 and in Figure 10.13. Only seven samples (1.2 % of samples) presented very strong acidity (pH < 5.0) and another 42 (7.3 %) strong acidity (pH < 5.5), while three (0.5 %) presented very strong alkalinity (pH > 9.0) and 36 (6.2 %) strong alkalinity (pH > 8.5).

Table 10.7: pH (H_2O) distribution according to the classes of Van der Watt and Van Rooyen (1995) (n = 578).

Description	pH range	No of samples	% of samples
Extremely acid	< 4.5	0	0.0
Very strongly acid	4.5 – 5.0	7	1.2
Strongly acid	5.1 – 5.5	42	7.3
Moderately acid	5.6 – 6.0	87	15.1
Mildly acid	6.1 – 6.5	127	22.0
Neutral	6.6 – 7.3	165	28.5
Mildly alkaline	7.4 – 7.8	69	11.9
Moderately alkaline	7.9 – 8.4	42	7.3
Strongly alkaline	8.5 – 9.0	36	6.2
Very strongly alkaline	> 9.0	3	0.5

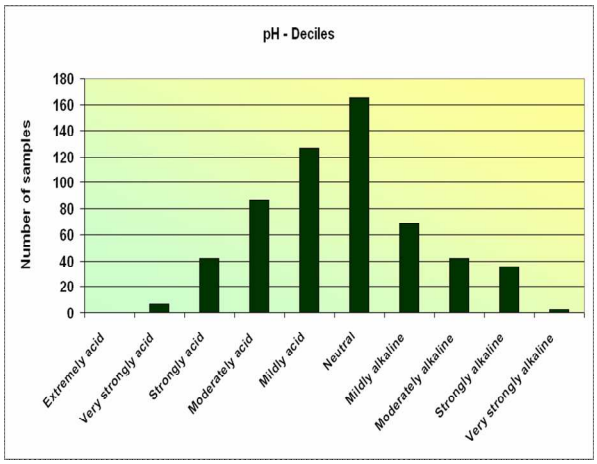

Figure 10.13. Histogram of pH (H_2O), according to the classes of Van der Watt and Van Rooyen (1995)

The pH (H_2O) values found in the study area agree with those recorded elsewhere in Namibia (Coetzee, Beernaert and Calitz, 1999; Kempf, 1999; Coetzee, 2001b; Kutuahupira, Mouton and Coetzee, 2001a, 2001b; Kutuahupira, Mouton and Beukes, 2003; ICC, MAWRD and AECI, 2000). Petersen (2008) recorded pH (H_2O) values of 7.0 – 8.9 at Duruchaus, 7.5 – 9.5 at Narais and 5.6 – 8.7 at Okamboro (locations on the edge of the study area). Ellis (1988) recorded topsoil pH (H_2O) values of median 8.3 and range 2.9 in western Boesmanland, and median 8.6 and range 1.4 eastern Boesmanland.

Statistically significant correlations, at $p < 0.05$, were found between pH (H_2O) and fluoride content ($r^2 = 0.57$), the sum of exchangeable bases (S-value) ($r^2 = 0.49$), exchangeable calcium content ($r^2 = 0.40$), cation exchange capacity ($r^2 = 0.44$), and the sum of extractable bases ($r^2 = 0.34$), as shown in Figures 10.14 – 10.18.

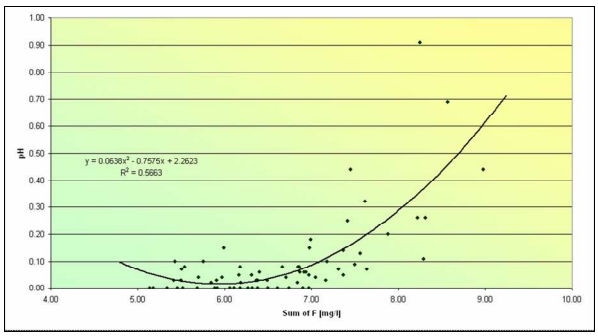

Figure 10.14. pH (H_2O) vs F content

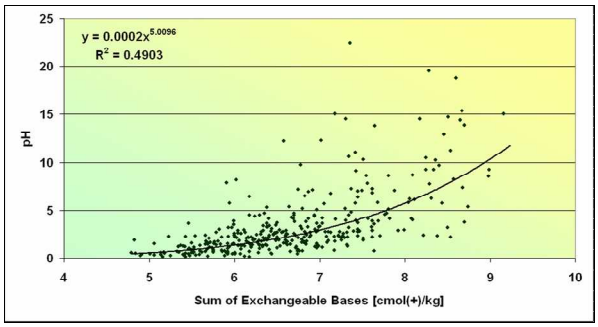

Figure 10.15. pH (H_2O) vs sum of exchangeable bases

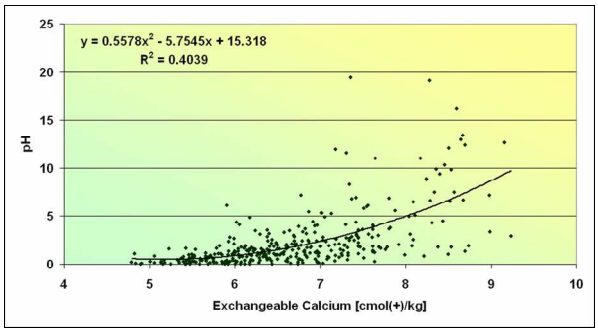

Figure 10.16. pH (H_2O) vs exchangeable Ca content

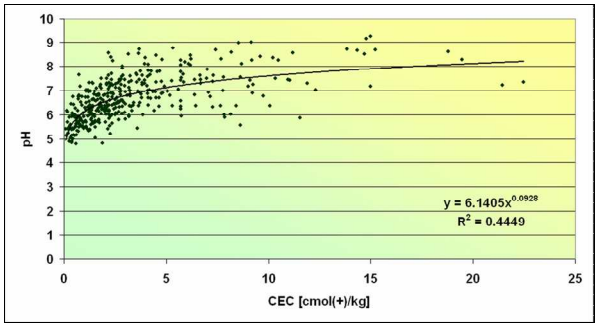

Figure 10.17. pH (H_2O) vs CEC

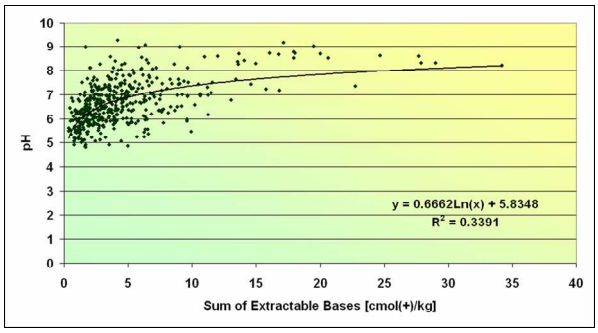

Figure 10.18. pH (H_2O) vs sum of extractable bases

There is a very small increase of pH with depth (Table 10.8; Figures 10.19 – 10.20). This is most likely caused by leaching of the topsoil and accumulation of bases lower down in the profile. Ellis (1988) reported a slight decrease in pH (H_2O) with depth, from 8.3 to 8.2 in western Boesmanland, and 8.6 to 8.3 in eastern Boesmanland, South Africa.

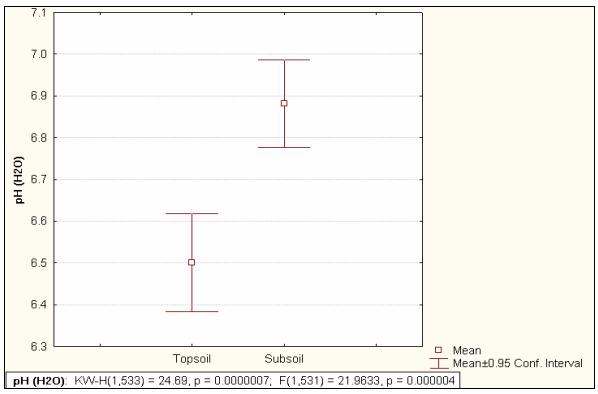

Figure 10.19. pH (H_2O), per topsoil and subsoil

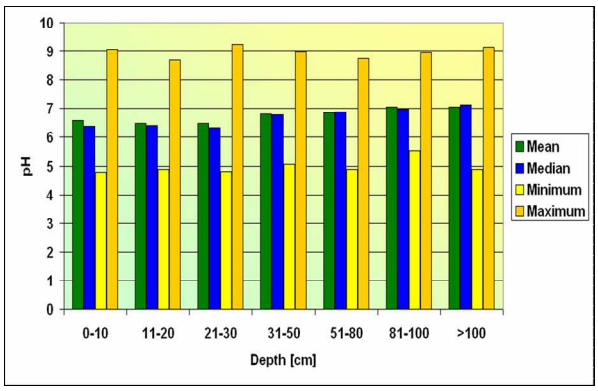

Figure 10.20. pH (H_2O), at various depths (cm)

Table 10.8: pH (H_2O), at various depths.

Depth (cm)	pH (H_2O)						
	0 – 10 (n = 69)	**11 – 20** (n = 117)	**21 – 30** (n = 56)	**31 – 50** (n = 95)	**51 – 80** (n = 87)	**81 – 100** (n = 25)	**> 100** (n = 83)
Mean	6.59	6.47	6.47	6.81	6.84	7.05	7.05
Median	6.37	6.40	6.33	6.78	6.87	6.97	7.13
Std. Dev.	1.04	0.78	0.91	0.85	0.92	0.88	1.07
CV	0.16	0.12	0.14	0.12	0.13	0.12	0.15
Minimum	4.79	4.90	4.83	5.07	4.89	5.55	4.91
Maximum	9.04	8.69	9.24	8.98	8.74	8.94	9.16
Range	4.25	3.79	4.41	3.91	3.85	3.39	4.25
Lower Quartile	5.94	5.92	5.96	6.18	6.29	6.43	6.09
Upper Quartile	7.22	6.85	6.83	7.41	7.45	7.56	7.82
Quartile Range	1.28	0.93	0.87	1.23	1.16	1.13	1.73
Percentile 10	5.35	5.53	5.34	5.82	5.47	5.89	5.59
Percentile 90	8.31	7.42	7.80	8.09	7.99	8.25	8.60

When disregarding clay loam and sandy clay soils (too few samples to be representative), it emerges that sandy soils have the lowest pH, and loamy soils the greatest spread in the ±0.95 confidence limits (Table 10.9; Figure 10.21).

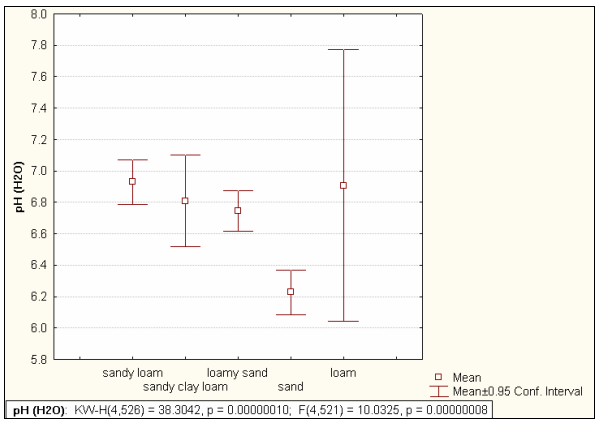

Figure 10.21. pH (H_2O), per textural class

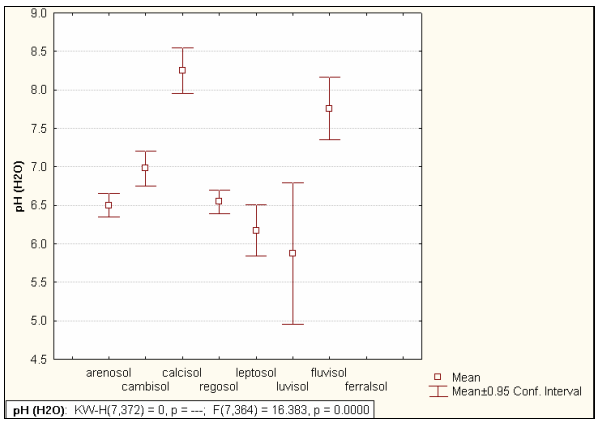

Figure 10.22. pH (H_2O), per WRB reference soil group

Table 10.9. pH (H_2O), per textural class.

Textural Class	pH (H_2O)				
	Sand (n = 100)	**Loamy Sand** (n = 195)	**Sandy Loam** (n = 185)	**Loam** (n = 8)	**Sandy Clay Loam** (n = 38)
Mean	6.23	6.75	6.93	6.91	6.81
Median	6.19	6.62	6.87	6.89	6.87
Std Dev.	0.73	0.92	0.99	1.03	0.89
CV	0.12	0.14	0.14	0.15	0.13
Minimum	4.90	4.83	4.79	5.46	4.84
Maximum	8.68	9.04	9.24	8.94	8.79
Range	3.78	4.21	4.45	3.48	3.95
Lower Quartile	5.69	6.11	6.21	6.25	6.19
Upper Quartile	6.70	7.31	7.56	7.30	7.32
Quartile Range	1.01	1.20	1.35	1.06	1.13
Percentile 10	5.35	5.60	5.73	5.46	5.55
Percentile 90	7.26	8.22	8.38	8.94	7.62

Calcisols from the study area have the highest mean and median pH of all soil types, followed by Fluvisols,

with Luvisols having the lowest mean and median (Table 10.10; Figure 10.22). Areno-, Rego- and Leptosols also have noticeably lower pH than Fluvi- and Calcisols.

Table 10.10: pH (H_2O), per WRB reference soil group

pH	Arenosol (n = 140)	Calcisol (n = 20)	Leptosol (n = 24)	Fluvisol (n = 12)	Cambisol (n = 72)	Regosol (n = 101)	Luvisol (n = 3)
Mean	6.50	8.25	6.18	7.76	6.98	6.55	5.87
Median	6.42	8.47	6.18	7.56	6.82	6.50	5.97
Std.Dev.	0.91	0.63	0.79	0.64	0.96	0.76	0.37
CV	0.14	0.08	0.13	0.08	0.14	0.12	0.06
Minimum	4.90	6.71	4.84	7.07	5.40	4.79	5.46
Maximum	8.70	9.16	7.99	9.04	8.99	9.24	6.18
Range	3.80	2.45	3.15	1.97	3.59	4.45	0.72
Lower Quartile	5.75	7.85	5.57	7.29	6.31	6.08	5.46
Upper Quartile	7.18	8.66	6.58	8.20	7.62	6.95	6.18
Quartile Range	1.43	0.81	1.02	0.91	1.32	0.87	0.72
Percentile 10	5.43	7.37	5.23	7.11	5.79	5.66	5.46
Percentile 90	7.67	8.85	7.31	8.57	8.46	7.51	6.18

The pH of Arenosols from the study area compares favourably with those recorded by Hartemink and Hunting (2008) elsewhere in southern Africa, as shown in Table 10.11.

Table 10.11. pH of Arenosols in southern Africa (mean ± 1 SD).

pH (2:5 soil:water)				
	n	0 – 10 cm	10 – 20 cm	20 – 30 cm
Present study	7; 34; 6	6.4 ± 0.6	6.2 ± 0.7	7.0 ± 1.3
Angola [a]	60	5.8 ± 0.7	5.7 ± 0.8	5.7 ± 0.8
Botswana [a]	6	6.6 ± 1.5	6.6 ± 1.5	6.6 ± 1.6
Mozambique [a]	30	6.0 ± 0.6	5.9 ± 0.5	6.0 ± 0.5
Namibia [a]	3	7.9 ± 0.4	7.9 ± 0.3	7.5 ± 0.6
South Africa [a]	39	7.1 ± 1.1	7.1 ± 1.2	6.8 ± 1.8

[a] Hartemink and Hunting (2008)

Parent material of alluvial origin has the highest pH (Figure 10.23), confirming the finding above, namely that Fluvisols have relatively high pH. Soils formed in the Kalahari sands have lower pH than those formed on schist (Figure 10.24).

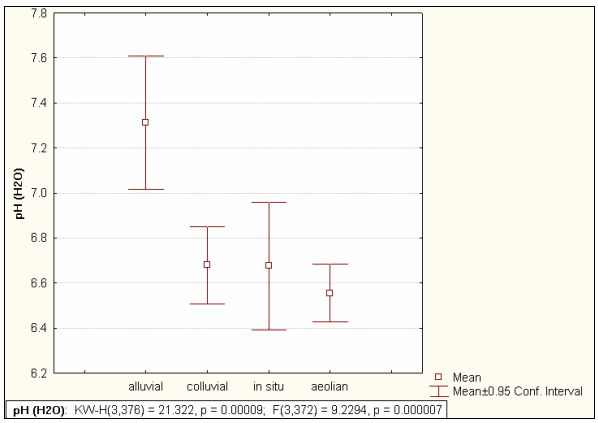

Figure 10.23. pH (H_2O), per origin of parent material

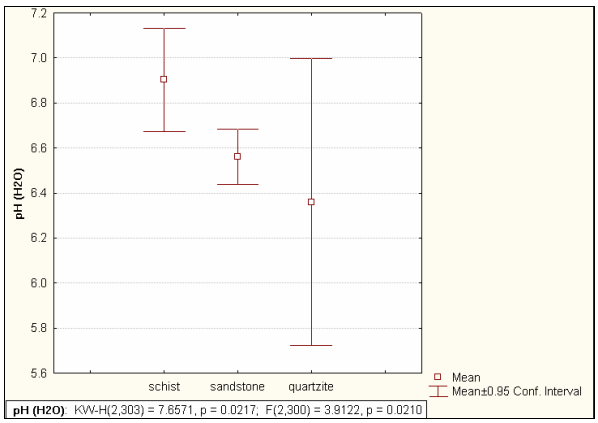

Figure 10.24. pH (H_2O), per type of parent material

pH increases with the degree of dissection (Figure 10.25) of the terrain. The highly dissected terrain of the study area occurs mainly on schist, quartzite and calcrete, whereas the less dissected areas, towards the east, are mainly covered with Kalahari sands.

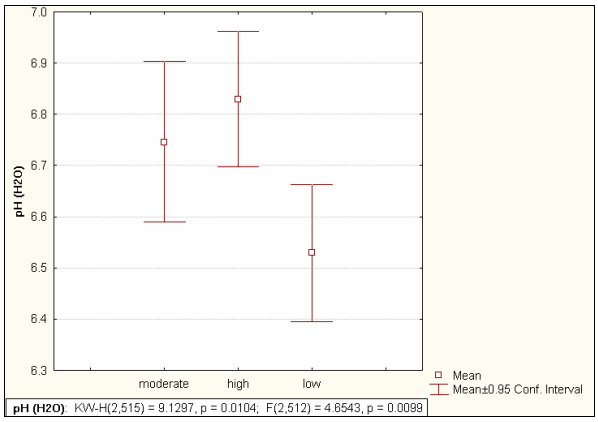

Figure 10.25. pH (H_2O), per degree of dissection of the landscape

The pH (H_2O), of topsoil and subsoil are shown in Figures 10.26 – 10.27.

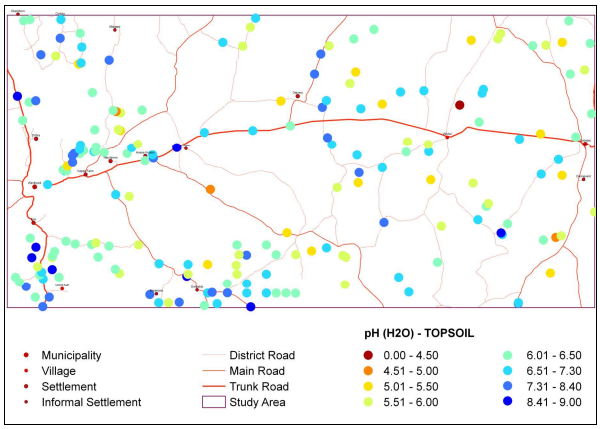

Figure 10.26. pH (H_2O) of topsoil

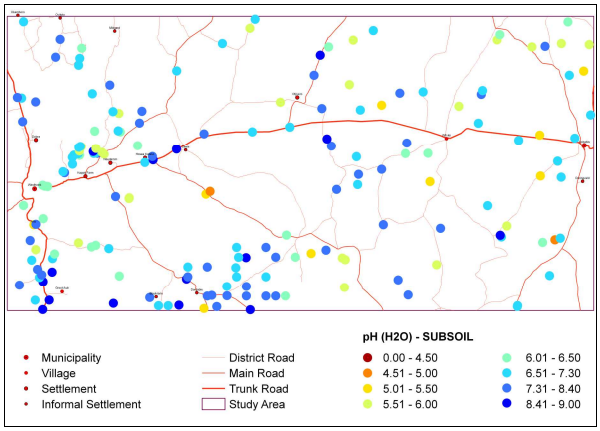

Figure 10.27. pH (H_2O) of subsoil

10.3 PARTICLE SIZE

Particle size distribution is a fundamental soil property that influences most physical properties (Skopp, 2000). The fine earth fraction, all particles less than 2 mm in diameter, is subdivided as follows:

Table 10.12: Soil separates (South African standard, Van der Watt and Van Rooyen, 1995).

	Ø in mm	Ø in µm
Very coarse sand	2.0 – 1.0	2 000 – 1 000
Coarse sand	1.0 – 0.5	1 000 – 500
Medium sand	0.5 – 0.25	500 – 250
Fine sand	0.25 – 0.1	250 – 100
Very fine sand	0.1 – 0.05	100 – 50

Coarse silt	0.05 – 0.02	50 – 20
Fine silt	0.02 – 0.002	20 – 2
Clay	< 0.002	< 2

Soil textural classes summarise particle size properties in a single phrase, based on relative abundance of sand, silt and clay, through the use of a textural triangle, as shown in Figure 10.28 (Van der Watt and Van Rooyen, 1995). A textural class, e.g. clay, describes a specific distribution of sand, silt and clay sized particles, whereas a soil separate contains only the particles in a specific size range, e.g. < 2 µm in the case of clay (Skopp, 2000).

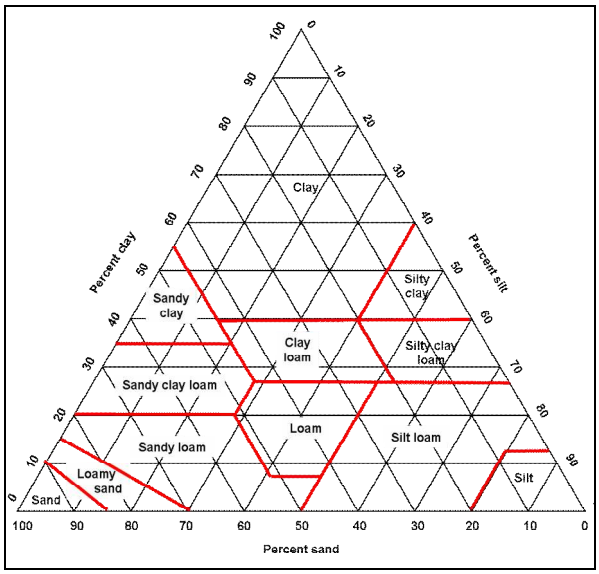

Figure 10.28. Textural triangle (South African standard, Van der Watt and Van Rooyen, 1995)

The relative proportions of sand, silt and clay fractions, as measured by particle size analysis and described by the classes of soil texture, are closely linked with plant available water holding capacity, hydraulic conductivity, infiltration, workability, aeration, soil fertility, chemical activity, erodibility, surface crusting and sealing, capillary rise, Atterberg limits, compaction, swell and shrink characteristics, compressibility and shear strength (Le Roux, *et al.*, 1999; Rowell, 2000a). Table 10.13 summarises some general relationships between soil properties and texture.

Table 10.13: Some general relationships between soil properties and texture (Brady and Weil, 2008).

Property / Behaviour	**Sand content**	**Silt content**	**Clay content**
Surface area to volume ratio	Low	Medium	High
Water-holding capacity	Low	Medium to high	High
Ability to store plant nutrients	Poor	Medium to high	High
Nutrient supplying capacity	Low	Medium to high	High
Aeration	Good	Medium	Poor
Internal drainage	High	Slow to medium	Very slow
Organic matter levels	Low	Medium to high	High to medium
Compactability	Low	Medium	High
Susceptibility to wind erosion	Moderate	High	Low
Susceptibility to water erosion	Low	High	Low if aggregated, high if not
Sealing of ponds and dams	Poor	Poor	Good
Pollutant leaching	Poor	Medium	Good

Sand and silt fractions are dominated by residual primary minerals such as quartz, feldspars and micas (Foth, 1990; Schaetzl and Anderson, 2005). The silt fraction may also contain some secondary minerals. The clay fraction consists almost exclusively of secondary minerals (Schaetzl and Anderson, 2005; Paul and Huang, 1980).

10.3.1 STATISTICAL ANALYSIS: SAND, SILT AND CLAY CONTENT

Normality was accepted for sand and silt content by some of the statistical tests for normality (D'Agostino Skewness, Kurtosis and Omnibus tests), but rejected by the other (Shapiro-Wilk W test, Kolmogorov-Smirnov / Lilliefors test), as summarised in Table 10.14 (AnalystSoft, 2007).

Table 10.14: Summary of five normality tests – sand, silt and clay content.

	Sand	Silt	Clay
	%	%	%
Kolmogorov-Smirnov / Lilliefors	Reject Normality	Reject Normality	Reject Normality
Shapiro-Wilk W	Reject Normality	Reject Normality	Reject Normality
D'Agostino Skewness	Reject Normality	Reject Normality	Reject Normality
D'Agostino Kurtosis	Accept Normality	Accept Normality	Reject Normality
D'Agostino Omnibus	Reject Normality	Reject Normality	Reject Normality

Table 10.15: Descriptive statistics – sand (n = 594), silt (n = 594) and clay (n = 594) content.

	Sand	Silt	Clay
	%	%	%
Mean	77.1	12.9	10.0
Median	79.8	11.3	8.0
Standard Deviation	11.5	7.9	6.8
Coefficient of Variation	0.1	0.6	0.7
Minimum	38.5	0.8	0.7
Maximum	94.1	39.9	47.7
Range	55.6	39.1	47.0
Lower Quartile	69.9	6.5	5.2
Upper Quartile	85.9	17.1	12.9
Quartile Range	16.0	10.6	7.7
Percentile 10	60.3	4.6	3.5
Percentile 90	89.7	25.2	19.1
Skewness	-0.8	1.0	1.6
Kurtosis	0.1	0.5	3.6

The **sand** content of 594 samples from the study area ranges from 38.5 to 94.1 %. The mean (77.1 %) is slightly lower than the median (79.8 %), with a skewness of -0.8 and kurtosis of 0.1. The standard deviation is 11.5. Half the samples have sand content of between 69.9 (1^{st} quartile) and 85.9 % (3^{rd} quartile), for a quartile range of 16.0. In 80 % of samples, the sand content is between 60.3 (1^{st} decile) and 89.7 % (9^{th} decile). The frequency distribution is shown in Table 10.16; Figures 10.29 – 10.30.

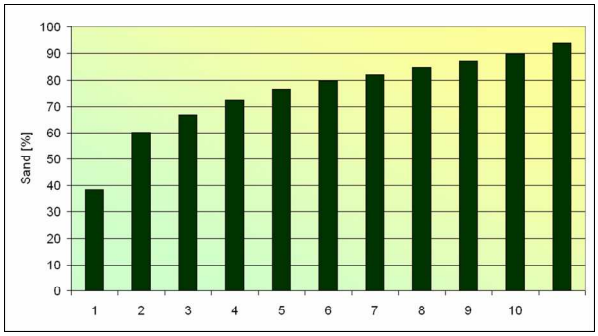

Figure 10.29. Decile distribution of sand percentage

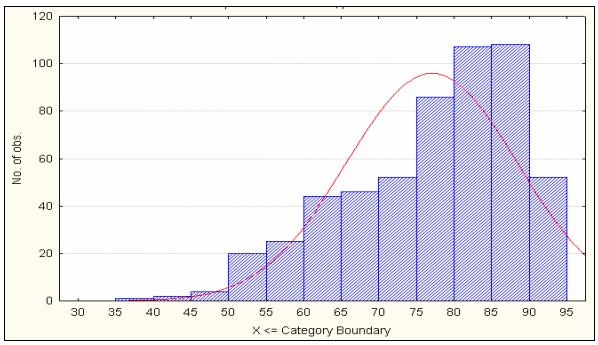

Figure 10.30. Histogram of sand percentage

Table 10.16: Distribution in terms of deciles – sand (n = 594), silt (n = 594), clay (n = 594) content.

	Decile	Sand	Silt	Clay
		%	%	%
minimum		38.5	0.8	0.7
	1	60.2	4.6	3.5
	2	66.6	5.9	4.6
	3	72.5	7.0	5.6
	4	76.7	9.2	6.5
median	5	79.8	11.3	8.0
	6	82.0	13.3	9.8
	7	85.0	15.9	11.8
	8	87.3	18.5	14.7
	9	89.7	25.2	19.1
maximum	10	94.1	39.9	47.7

Sand concentrations of 61.5 to 79.0 % were reported on Claratal (Medinski, 2007), 63.0 to 79.5 % on Duruchaus (Petersen, 2008), and 63.5 to 79.5 % on Okamboro (Petersen, 2008) – all of these located on the edge of the study area.

The **silt** content of 594 samples from the study area ranges from 0.8 to 39.9 %. The mean (12.9 %) is slightly higher than the median (11.3 %), with a skewness of 1.0 and kurtosis of 0.5. The standard deviation is 7.9. Half the samples have silt content of between 6.5 (1st quartile) and 17.1 % (3rd quartile), for a quartile range of 10.6. In 80 % of samples, the silt content is between 4.6 (1st decile) and 25.2 % (9th decile). The frequency distribution is shown in Table 10.16 (above) and Figures 10.31 – 10.32.

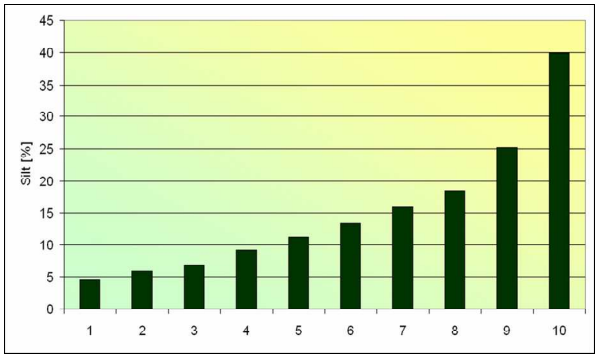

Figure 10.31. Decile distribution of silt percentage

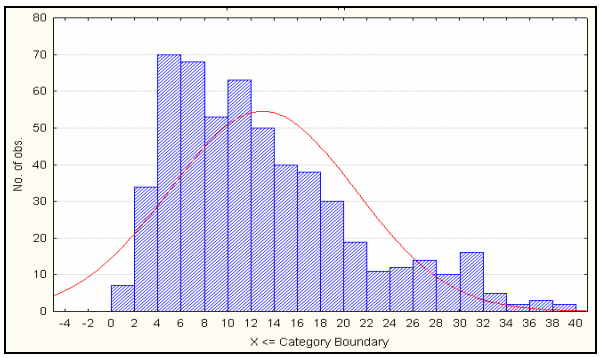

Figure 10.32. Histogram of silt percentage

Silt concentrations of 19.9 to 37.2 % were reported on Claratal (Medinski, 2007), 16.5 to 31.5 % on Duruchaus (Petersen, 2008), and 17.2 to 22.2 % on Okamboro (Petersen, 2008) – all of these located on the

edge of the study area.

The **clay** content of 594 samples from the study area ranges from 0.7 to 47.7 %. The mean (10.0 %) is slightly higher than the median (8.0 %), with a skewness of 1.6 and kurtosis of 3.6. The standard deviation is 6.8. Half the samples have clay content of between 5.2 (1st quartile) and 12.9 % (3rd quartile), for a quartile range of 7.7. In 80 % of samples, the clay content is between 3.5 (1st decile) and 19.1 % (9th decile). The frequency distribution is shown in Table 10.16 and Figures 10.33 – 10.34.

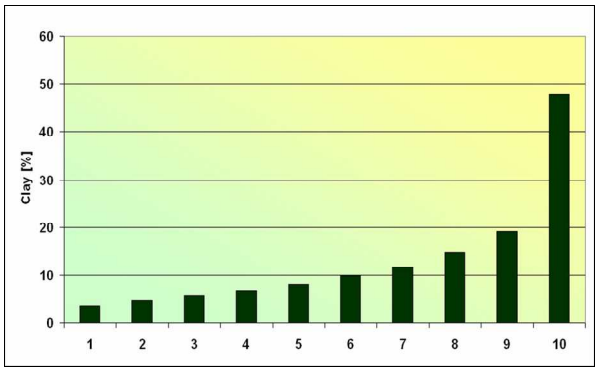

Figure 10.33. Decile distribution of clay percentage

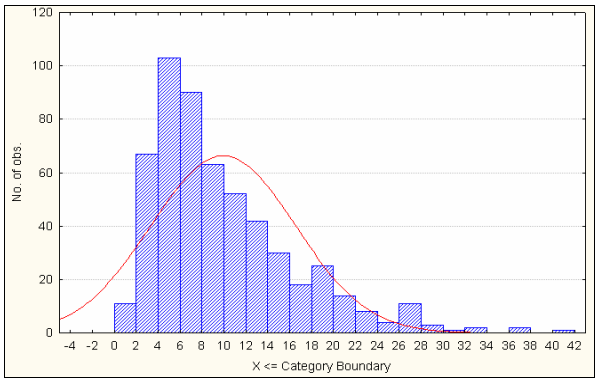

Figure 10.34. Histogram of clay percentage

Clay concentrations of 1.0 to 2.1 % were reported on Claratal (Medinski, 2007), 4.0 to 6.5 % on Duruchaus (Petersen, 2008), and 3.2 to 15.7 % on Okamboro (Petersen, 2008) – all of these located on the edge of the study area.

Statistically significant negative correlations, at $p < 0.05$, were found between **sand** content and respectively silt content ($r^2 = 0.67$), clay content ($r^2 = 0.54$) and exchangeable magnesium content ($r^2 = 0.41$), as shown in Figures 10.35 – 10.37. Significant, but weak, correlations were also found between sand content and the cation exchange capacity ($r^2 = 0.29$), sum of exchangeable bases (S-value) ($r^2 = 0.28$), iron content ($r^2 = 0.24$), exchangeable potassium content ($r^2 = 0.23$), manganese content ($r^2 = 0.20$), copper content ($r^2 = 0.18$), sum of the extractable bases ($r^2 = 0.16$), coarse sand content ($r^2 = 0.16$), exchangeable calcium content ($r^2 = 0.15$), extractable magnesium content ($r^2 = 0.13$), very fine sand content ($r^2 = 0.13$), extractable calcium content ($r^2 = 0.11$) and sulfate content ($r^2 = 0.11$).

A statistically significant correlation, at $p < 0.05$, was found between **silt** content and sand content ($r^2 = 0.67$), as shown in Figure 10.35. Significant, but weak, correlations were found between silt content and the very fine sand fraction ($r^2 = 0.29$), coarse sand fraction ($r^2 = 0.27$), fine sand fraction ($r^2 = 0.17$), iron content ($r^2 = 0.15$), cation exchange capacity ($r^2 = 0.13$), sum of exchangeable bases (S-value) ($r^2 = 0.10$), exchangeable magnesium content ($r^2 = 0.10$) and copper content ($r^2 = 0.10$).

Statistically significant correlations, at $p < 0.05$, were found between **clay** content and respectively the sand fraction ($r^2 = 0.54$) (Figure 10.36) and exchangeable magnesium content ($r^2 = 0.37$) (Figure 10.38). Significant, but weak, correlations were found with extractable magnesium content ($r^2 = 0.23$), cation exchange capacity ($r^2 = 0.22$), sum of exchangeable bases (S-value) ($r^2 = 0.20$), sum of extractable bases ($r^2 = 0.20$), exchangeable potassium content ($r^2 = 0.18$), manganese content ($r^2 = 0.16$), extractable potassium

content (r^2 = 0.13), extractable calcium content (r^2 = 0.13), iron (r^2 = 0.12), fluoride content (r^2 = 0.11) and copper content (r^2 = 0.10).

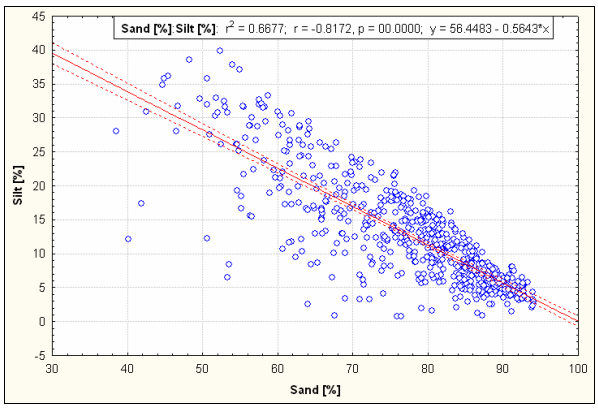

Figure 10.35. Sand content vs silt content

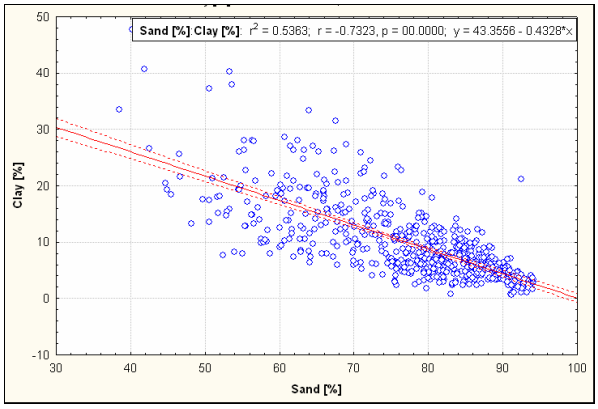

Figure 10.36. Sand content vs clay content

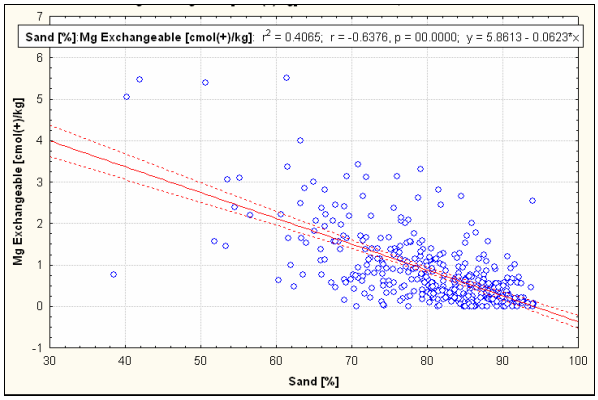

Figure 10.37. Sand content vs exchangeable Mg

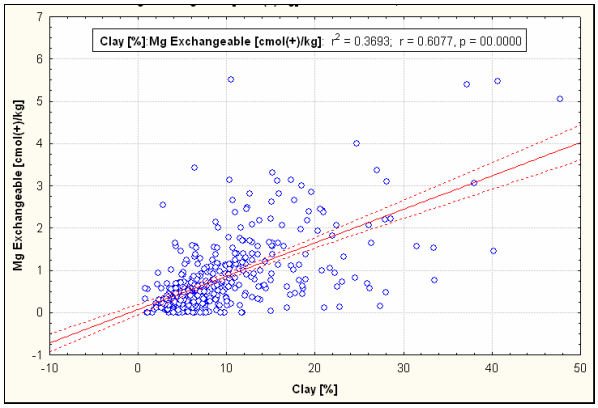

Figure 10.38. Clay content vs exchangeable Mg content

Topsoil contains significantly more sand, less silt and less clay than subsoil (Table 10.17 and Figures 10.39 – 10.41), as a result of eluviation of the finer material.

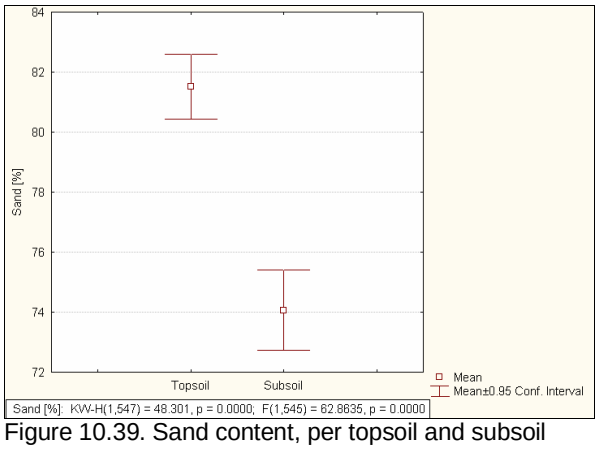

Figure 10.39. Sand content, per topsoil and subsoil

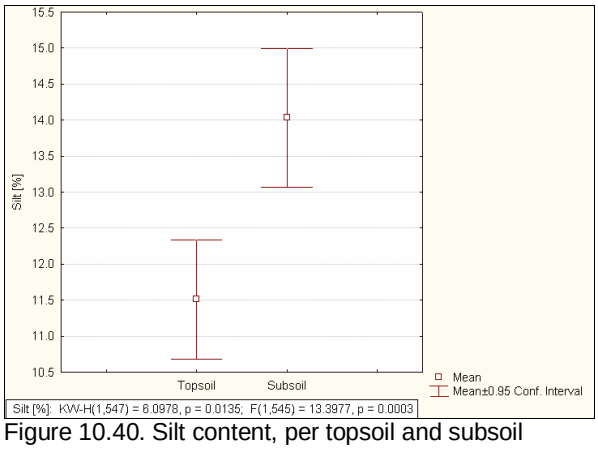

Figure 10.40. Silt content, per topsoil and subsoil

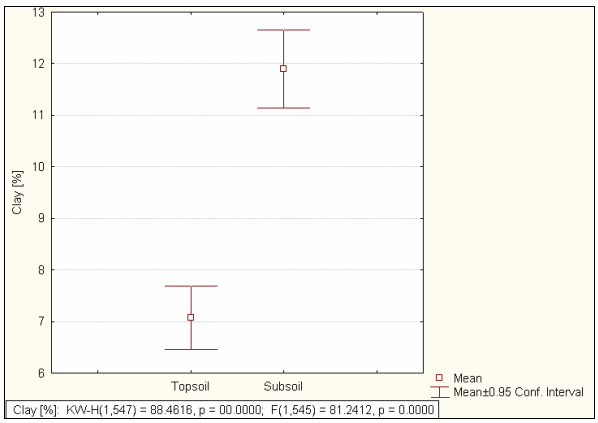

Figure 10.41. Clay content, per topsoil and subsoil

Table 10.17. Percentage sand, silt and clay of topsoil and subsoil.

	Sand %		Silt %		Clay %	
	Topsoil (n = 221)	**Subsoil** (n = 326)	**Topsoil** (n = 221)	**Subsoil** (n = 326)	**Topsoil** (n = 221)	**Subsoil** (n = 326)
Mean	81.5	74.1	11.5	14.0	7.1	11.9
Median	82.1	75.7	10.8	12.1	5.9	10.3
Std.Dev.	8.2	12.2	6.27	8.9	4.7	7.0
Minimum	51.7	38.5	0.8	0.8	0.7	1.1
Maximum	94.1	94.0	32.9	39.9	27.4	40.2
Range	42.4	55.5	32.1	39.1	26.7	39.1
Lower Quartile	77.1	64.2	6.9	6.6	4.0	6.5
Upper Quartile	88.0	84.5	15.0	19.1	8.4	15.7
Quartile Range	10.9	20.3	8.1	12.5	4.4	9.2
Percentile 10	70.3	56.3	4.7	4.6	3.0	4.6
Percentile 90	91.2	88.9	19.7	28.1	12.9	21.3

Arenosols have the highest sand content, as expected from the way this WRB reference soil group is defined, followed by Rego-, Lepto-, Fluvi- Cambi- and Calcisols. Luvisols have the least sand and also the greatest spread in ±0.95 confidence intervals, due to the small number of samples (Table 10.18; Figure 10.42). Arenosols have the lowest silt content, followed by Rego-, Lepto-, Cambi- and Calcisols. Luvisols have the highest silt content and also the greatest spread in ±0.95 confidence intervals, followed by Fluvisols (Table 10.18; Figure 10.43). Areno- and Fluvisols are low in clay, with Luvi-, Calci- and Cambisols relatively rich in clay. Rego- and Leptosols have intermediate clay content (Table 10.18; Figure 10.44).

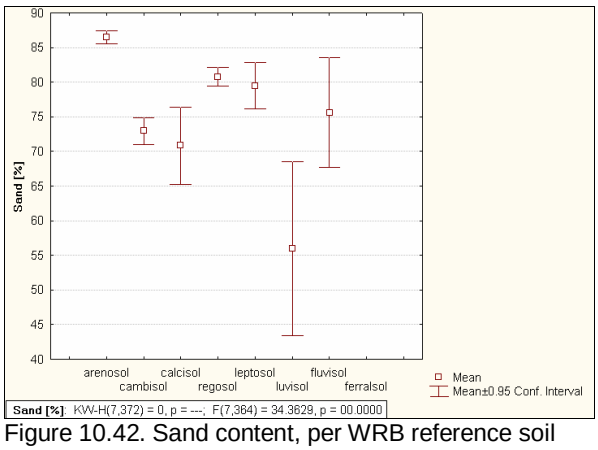

Figure 10.42. Sand content, per WRB reference soil group

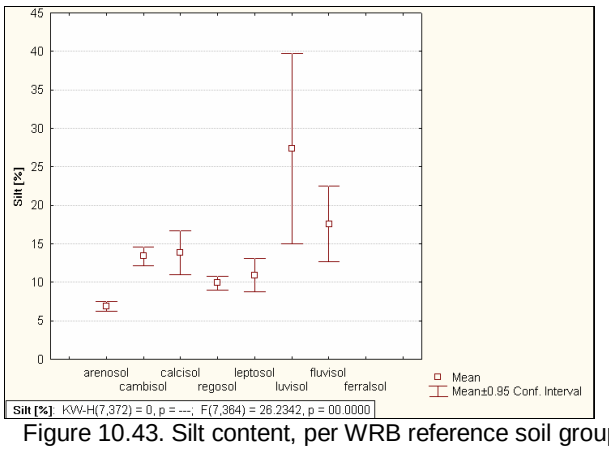

Figure 10.43. Silt content, per WRB reference soil group

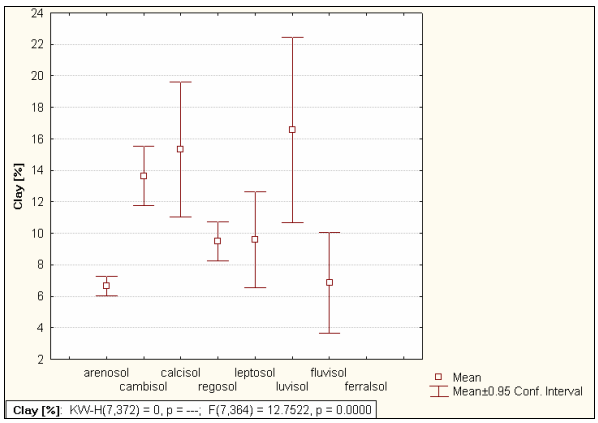

Figure 10.44. Clay content, per WRB reference soil group

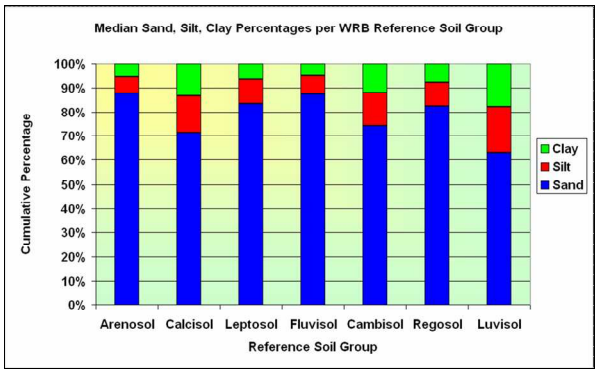

Figure 10.45. Median sand, silt and clay contribution to each WRB reference soil group

Table 10.18: Sand, silt and clay fractions of the WRB reference soil groups.

Sand	**Arenosol** (n = 140)	**Calcisol** (n = 20)	**Leptosol** (n = 24)	**Fluvisol** (n = 12)	**Cambisol** (n = 72)	**Regosol** (n = 101)	**Luvisol** (n = 3)
Mean	86.47	70.83	79.47	75.59	72.96	80.76	55.97
Median	88.10	71.20	81.35	80.85	74.20	81.50	54.50
Std.Dev.	5.66	12.00	7.97	12.43	8.17	6.82	5.06
Minimum	61.90	38.50	60.70	51.70	50.60	63.50	51.80
Maximum	94.10	88.10	90.60	87.20	85.40	93.30	61.60
Range	32.20	49.60	29.90	35.50	34.80	29.80	9.80
Lower Quartile	83.90	64.60	74.80	67.00	67.70	75.50	51.80
Upper Quartile	90.30	79.70	86.15	85.65	79.50	85.60	61.60
Quartile Range	6.40	15.10	11.35	18.65	11.80	10.10	9.80
Percentile 10	77.55	56.80	69.00	55.50	61.90	71.40	51.80
Percentile 90	92.45	84.75	88.20	86.50	82.50	89.00	61.60
Silt	**Arenosol** (n = 140)	**Calcisol** (n = 20)	**Leptosol** (n = 24)	**Fluvisol** (n = 12)	**Cambisol** (n = 72)	**Regosol** (n = 101)	**Luvisol** (n = 3)
Mean	6.85	13.86	10.89	17.58	13.39	9.92	27.40
Median	5.90	14.10	10.80	15.45	12.95	9.50	26.10
Std.Dev.	3.96	6.13	5.13	7.76	5.05	4.64	4.98
Minimum	0.80	5.40	1.20	10.20	0.80	0.90	23.20
Maximum	22.90	28.00	22.00	31.60	28.10	26.30	32.90
Range	22.10	22.60	20.80	21.40	27.30	25.40	9.70
Lower Quartile	4.50	9.05	7.80	10.75	10.85	6.70	23.20
Upper Quartile	8.05	17.60	14.80	23.15	16.55	12.20	32.90
Quartile Range	3.55	8.55	7.00	12.40	5.70	5.50	9.70
Percentile 10	3.35	5.80	3.40	10.20	7.00	4.60	23.20
Percentile 90	12.05	21.40	17.60	30.30	19.30	15.40	32.90
Clay	**Arenosol** (n = 140)	**Calcisol** (n = 20)	**Leptosol** (n = 24)	**Fluvisol** (n = 12)	**Cambisol** (n = 72)	**Regosol** (n = 101)	**Luvisol** (n = 3)
Mean	6.65	15.34	9.61	6.84	13.64	9.50	16.57
Median	5.60	13.30	6.35	4.60	11.90	7.60	15.20
Std.Dev.	3.66	9.17	7.21	5.05	8.07	6.21	2.37
Minimum	1.10	4.90	3.30	2.40	1.80	0.70	15.20
Maximum	22.80	40.20	28.60	18.00	38.00	31.50	19.30
Range	21.70	35.30	25.30	15.60	36.20	30.80	4.10
Lower Quartile	4.30	9.35	4.30	2.85	7.85	5.10	15.20
Upper Quartile	8.50	18.75	12.85	10.00	18.05	11.80	19.30
Quartile Range	4.20	9.40	8.55	7.15	10.20	6.70	4.10
Percentile 10	3.30	6.30	3.60	2.60	5.90	3.50	15.20
Percentile 90	10.25	29.95	17.20	12.90	26.10	18.20	19.30

The silt and clay contents increase with an increase in the degree of dissection of the landscape (Figures 10.47 – 10.48), while the opposite is true for sand (Figure 10.46). Highly dissected areas are prone to higher rates of erosion, exposing fresh parent material to weathering agents. The highly dissected areas of the present study area are located towards the west, in the Khomas Hochland, and mainly occur on schist. The areas of low dissection are towards the east and are mainly covered in quartz-rich Kalahari sand.

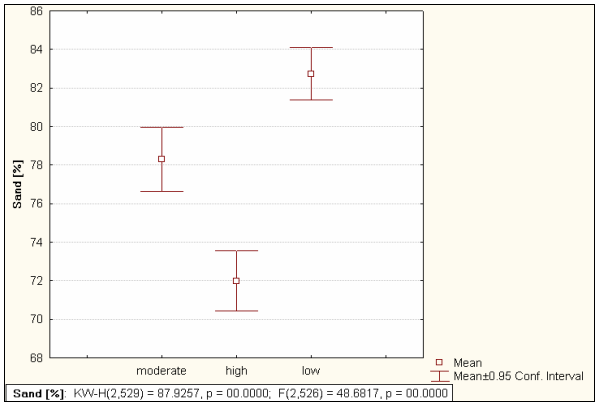

Figure 10.46. Sand content, per degree of dissection of the landscape

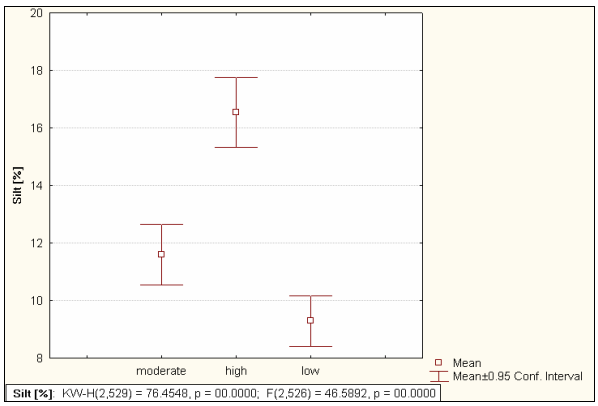

Figure 10.47. Silt content, per degree of dissection of the landscape

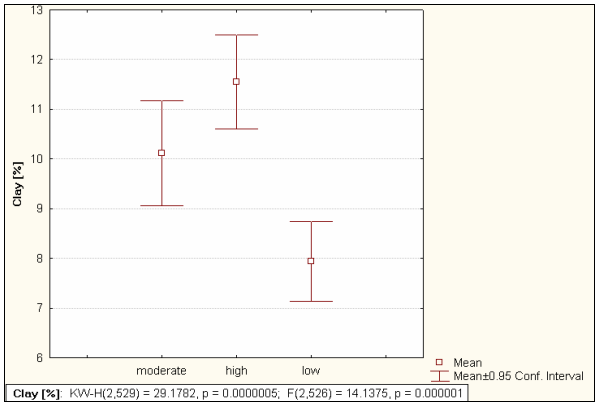

Figure 10.48. Clay content, per degree of dissection of the landscape

Flat and almost flat areas have the highest sand content (Figure 10.49) and lowest silt content (Figure 10.50) of the different topographic classes. Undulating, rolling, hilly and mountainous areas are relatively low in sand content and high in silt content. The clay content, per topographical class is more ambiguous (Figure 10.51).

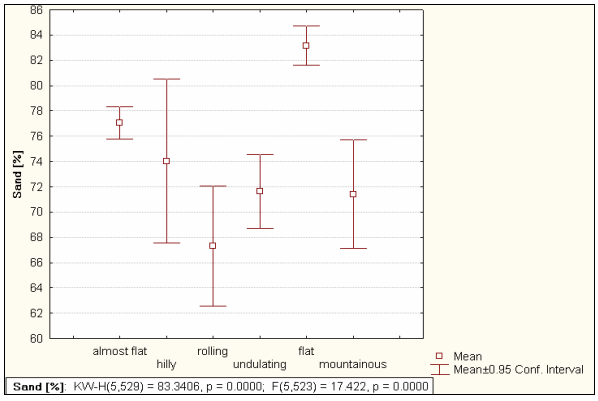

Figure 10.49. Sand content, per topographic class

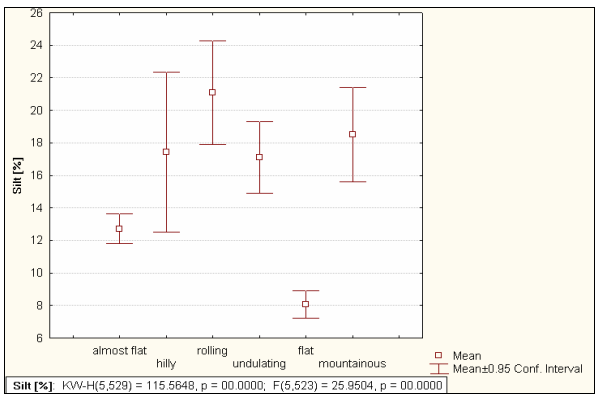

Figure 10.50. Silt content, per topographic class

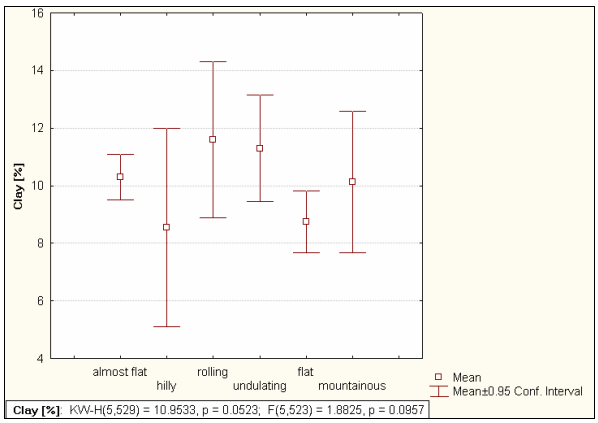

Figure 10.51. Clay content, per topographic class

Parent material of aeolian origin has the highest sand content, lowest silt content and lowest clay content. (Figures 10.52 – 10.54).

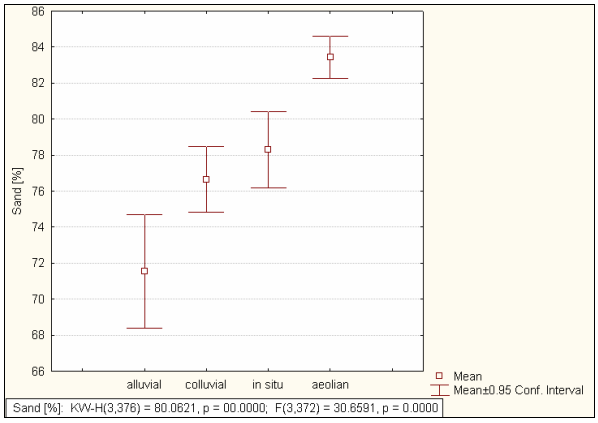

Figure 10.52. Sand content, per origin of parent material

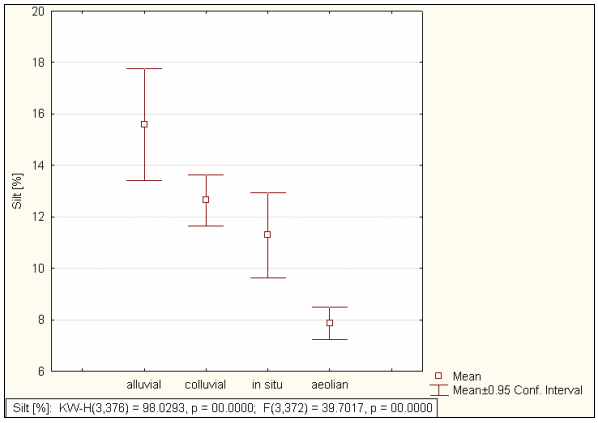

Figure 10.53. Silt content, per origin of parent material

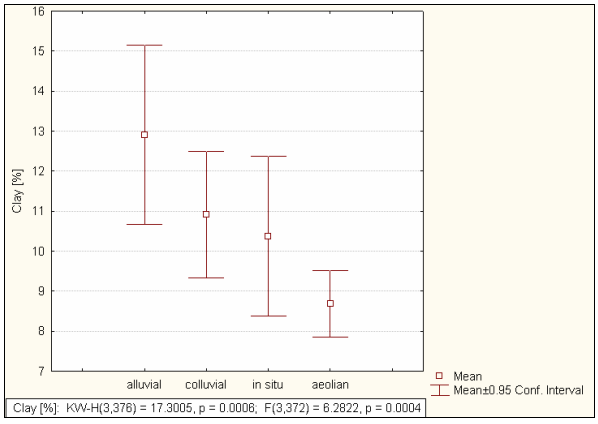

Figure 10.54. Clay content, per origin of parent material

The quartz-rich Kalahari sand contain high percentages of sand-sized particles and low concentrations of silt and clay, whereas soils formed from schist are rich in silt and poor in sand (Figures 10.55 – 10.56). Soils from quartzite show a great spread in sand, silt and clay concentrations.

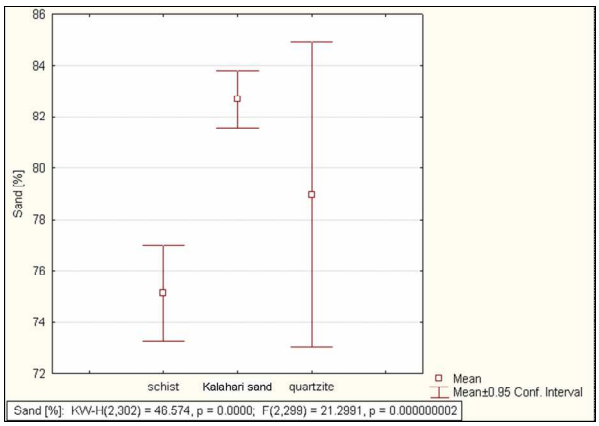

Figure 10.55. Sand content, per type of parent material

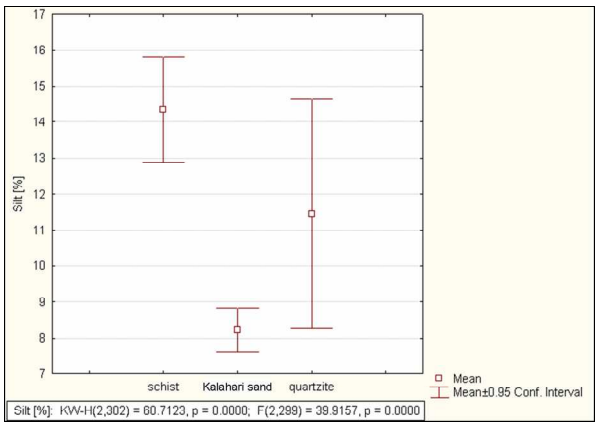

Figure 10.56. Silt content, per, per type of parent material

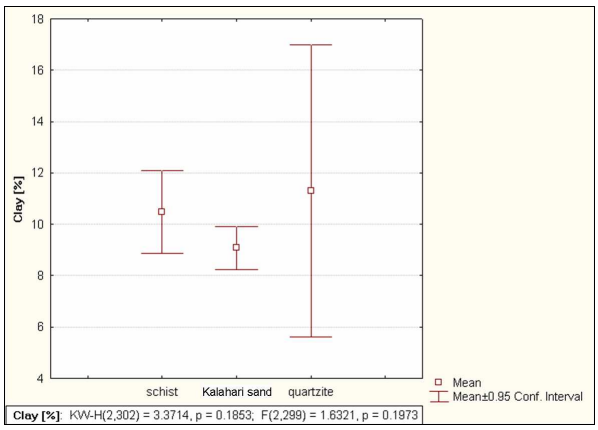

Figure 10.57. Clay content, per type of parent material

The sand, silt and clay levels of topsoil and subsoil are shown in Figures 10.58 – 10.63.

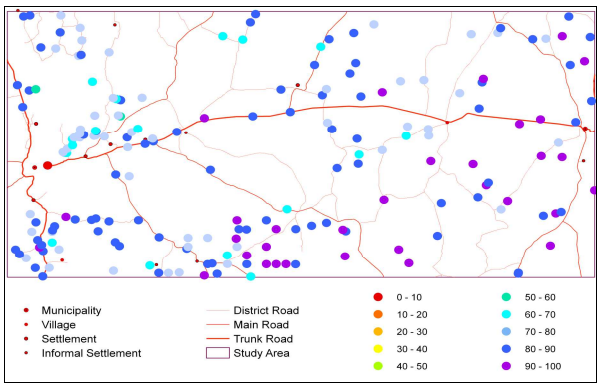

Figure 10.58. Sand content (%) of topsoil

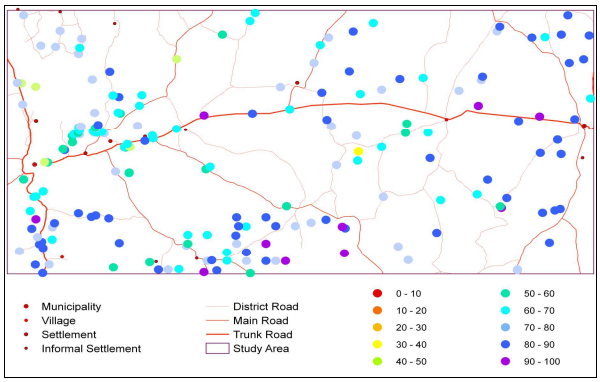

Figure 10.59. Sand content (%) of subsoil

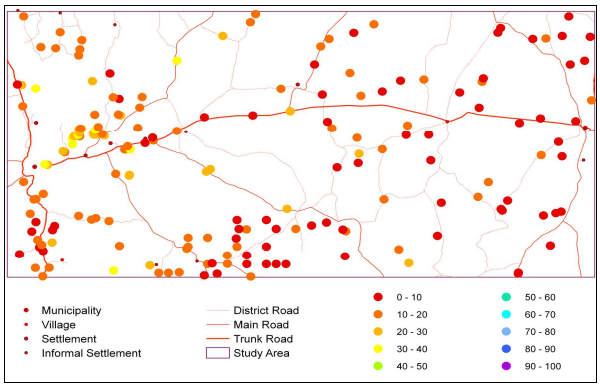

Figure 10.60. Silt content (%) of topsoil

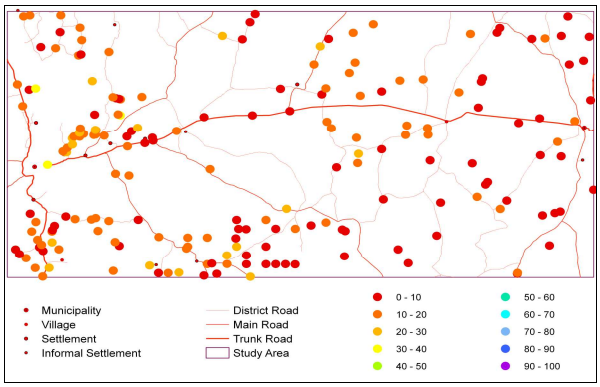

Figure 10.61. Silt content (%) of subsoil

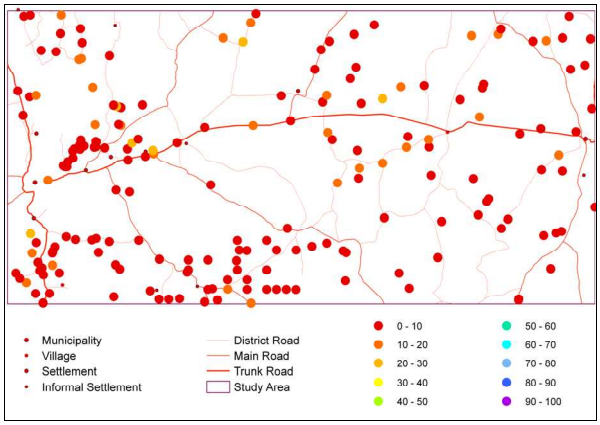

Figure 10.62. Clay content (%) of topsoil

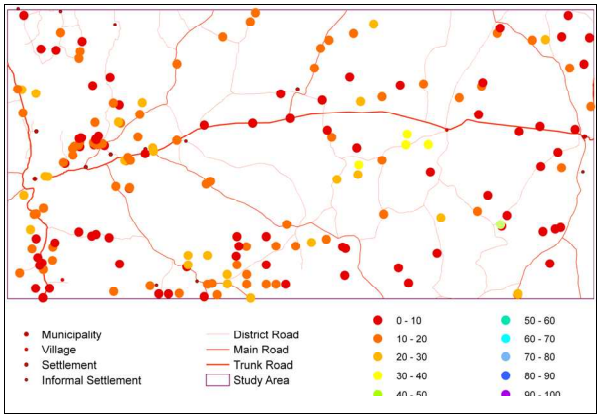

Figure 10.63. Clay content (%) of subsoil

10.3.2 STATISTICAL ANALYSIS: SAND FRACTIONS

Normality was accepted for fine sand and very fine sand content by some of the statistical tests for normality (D'Agostino Skewness, Kurtosis and Omnibus tests), but rejected by the other (Shapiro-Wilk W test, Kolmogorov-Smirnov / Lilliefors test), as summarised in Table 19 (AnalystSoft, 2007).

Table 10.19: Summary of five normality tests – coarse sand, medium sand, fine sand, very fine sand content.

Normality test	Coarse Sand %	Medium Sand %	Fine Sand %	Very Fine Sand %
Kolmogorov-Smirnov / Lilliefors	No evidence against normality	No evidence against normality	Suggestive evidence against normality	No evidence against normality
Shapiro-Wilk W	Reject Normality	Reject Normality	Reject Normality	Reject Normality
D'Agostino Skewness	Reject Normality	Reject Normality	Accept Normality	Accept Normality
D'Agostino Kurtosis	Reject Normality	Reject Normality	Accept Normality	Reject Normality
D'Agostino Omnibus	Reject Normality	Reject Normality	Accept Normality	Reject Normality

Table 10.20: Descriptive statistics – sand fractions (n = 345).

	Coarse Sand %	Medium Sand %	Fine Sand %	Very Fine Sand %
Mean	17.2	28.8	47.3	6.7
Median	14.4	28.6	48.5	7.6
Std.Dev.	11.7	6.8	10.3	5.2
CV	0.68	0.23	0.22	0.78
Minimum	1.4	8.0	9.0	0.0
Maximum	53.9	70.3	75.1	19.7
Range	52.5	62.3	66.1	19.7
Lower Quartile	7.6	24.4	38.7	0.0
Upper Quartile	26.3	33.3	54.5	10.6
Quartile Range	18.7	8.9	15.8	10.6
Percentile 10	3.5	20.5	34.0	0.0
Percentile 90	34.5	37.3	60.1	12.9
Skewness	0.6	0.6	-0.2	0.0
Kurtosis	-0.5	3.5	-0.1	-1.1

Table 10.21: Decile distribution – sand fractions (n = 345).

	Decile	Coarse Sand %	Medium Sand %	Fine Sand %	Very Fine Sand %
minimum		1.4	8.0	9.0	0.0
	1	3.5	20.5	34.0	0.0
	2	6.3	23.2	36.5	0.0
	3	8.8	25.3	40.8	0.0
	4	11.5	27.0	45.2	6.6
median	5	14.4	28.6	48.5	7.6
	6	17.5	30.4	51.0	8.7
	7	23.4	32.1	53.5	9.9
	8	29.3	34.1	55.9	11.2
	9	34.5	37.3	60.1	12.9
maximum	10	53.9	70.3	75.1	19.7

The **coarse sand** content of 345 samples from the study area ranges from 1.4 to 53.9 % (Table 10.21; Figures 10.64 – 10.65). The mean (17.2 %) is slightly higher than the median (14.4 %), with a skewness of 0.6 and kurtosis of -0.5. The standard deviation is 11.7. Half the samples have coarse sand content of between 7.6 (1st quartile) and 26.3 % (3rd quartile), for a quartile range of 18.7 %. In 80 % of samples, the coarse sand content is between 3.5 (1st decile) and 34.5 % (9th decile).

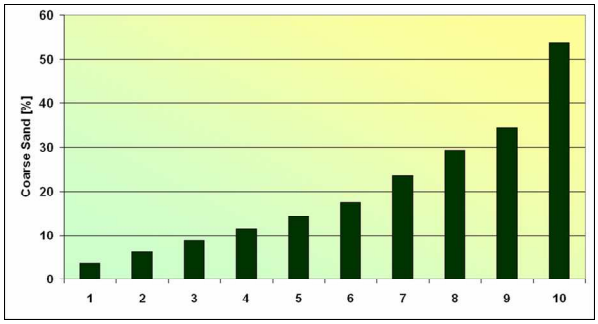

Figure 10.64. Decile distribution of coarse sand content (%)

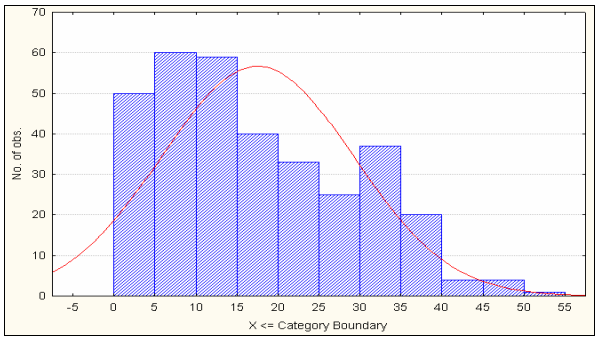

Figure 10.65. Histogram of coarse sand content (%)

The **medium sand** content of 345 samples from the study area ranges from 8.0 to 70.3 % (Table 10.21 and

Figures 10.66 – 10.67). The mean (28.8 %) is virtually the same as the median (28.6 %), with a skewness of 0.6 and kurtosis of 3.5. The standard deviation is 6.8. Half the samples have medium sand content of between 24.4 (1st quartile) and 33.3 % (3rd quartile), for a quartile range of 8.9 %. In 80 % of samples, the medium sand content is between 20.5 (1st decile) and 37.3 % (9th decile).

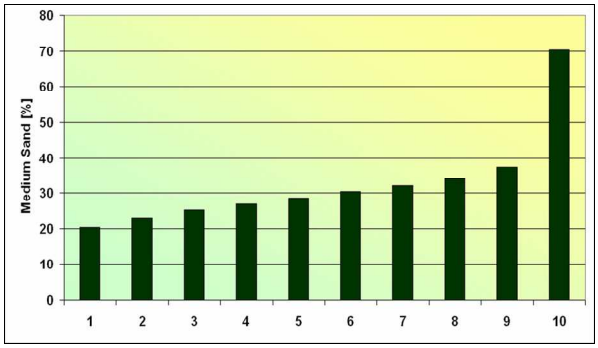

Figure 10.66. Decile distribution of medium sand content (%)

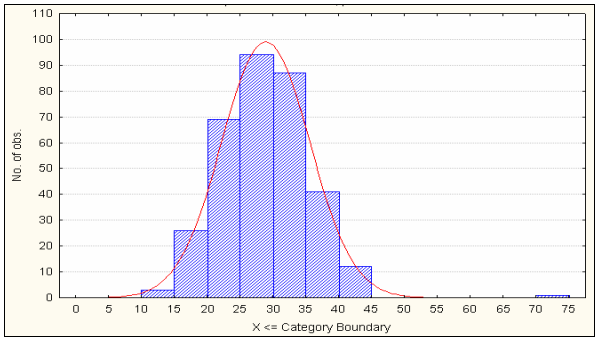

Figure 10.67. Histogram of medium sand content (%)

The **fine sand** content of 345 samples from the study area ranges from 9.0 to 75.1 % (Table 10.21; Figures 10.68 – 10.69). The mean (47.3 %) is slightly lower than the median (48.5 %), with a skewness of -0.2 and kurtosis of -0.1. The standard deviation is 10.3. Half the samples have fine sand content of between 38.7 (1st quartile) and 54.5 % (3rd quartile), for a quartile range of 15.8 %. In 80 % of samples, the fine sand content is between 34.0 (1st decile) and 60.1 % (9th decile).

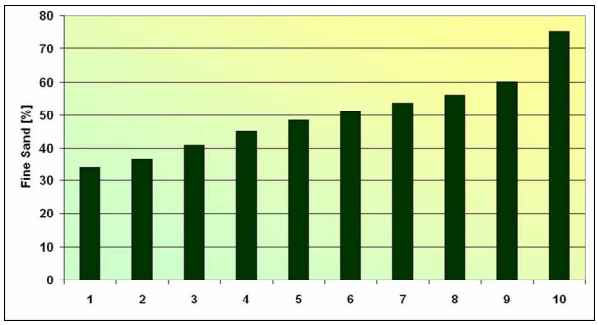

Figure 10.68. Decile distribution of fine sand content (%)

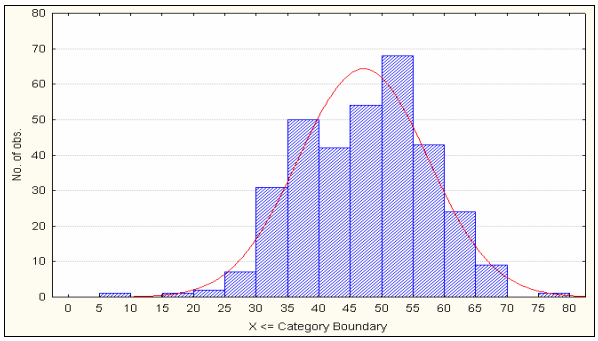

Figure 10.69. Histogram of fine sand content (%)

The **very fine sand** content of 345 samples from the study area ranges from 0 to 19.7 % (Table 10.21; Figures 10.70 – 10.71). The mean (6.7 %) is slightly lower than the median (7.6 %), with a skewness of 0.0 and kurtosis of -1.1. The standard deviation is 5.2. Half the samples have very fine sand content of between 0.0 (1st quartile) and 10.6 % (3rd quartile), for a quartile range of 10.6 %. In 80 % of samples, the very fine sand content is between 0.0 (1st decile) and 12.9 % (9th decile).

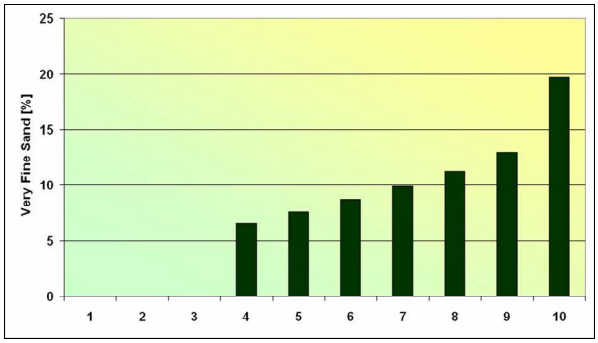

Figure 10.70. Decile distribution of very fine sand content (%)

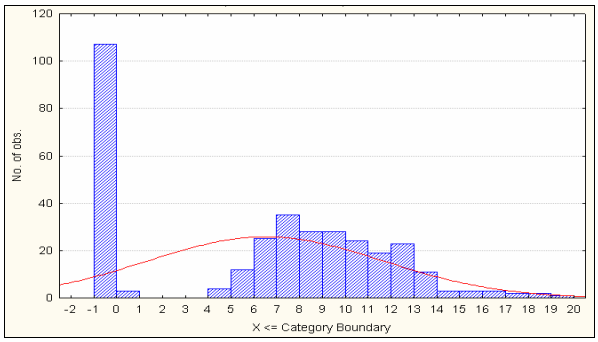

Figure 10.71. Histogram of very fine sand content (%)

From Figure 10.72 it can be deduced that the fine sand fraction is most abundant in the majority of soils from the study area, and the very fine sand fraction is relatively scarce. This supports the proposed aeolian origin of much of the study area soils.

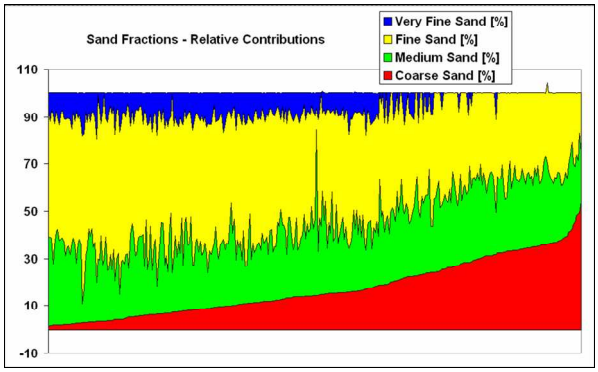

Figure 10.72. Relative contributions of various sand fractions

Topsoil contains somewhat less coarse sand and more very fine sand than subsoil (Table 10.22 and Figures 10.73 – 10.76), most probably caused by eluviation of the finer material. The overlaps in the ±0.95 confidence intervals are too large to make predictions in the cases of medium and fine sand content.

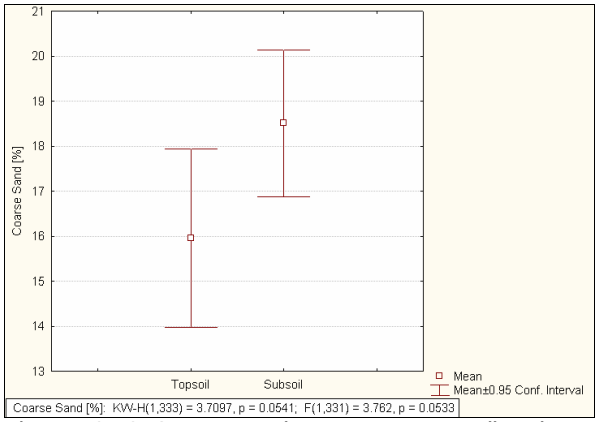

Figure 10.73. Coarse sand content, per topsoil and subsoil

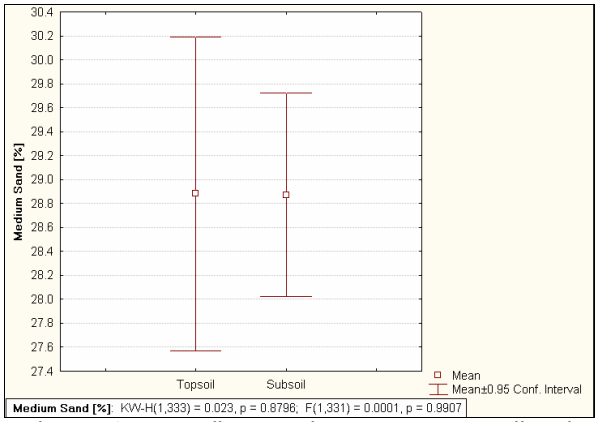

Figure 10.74. Medium sand content, per topsoil and subsoil

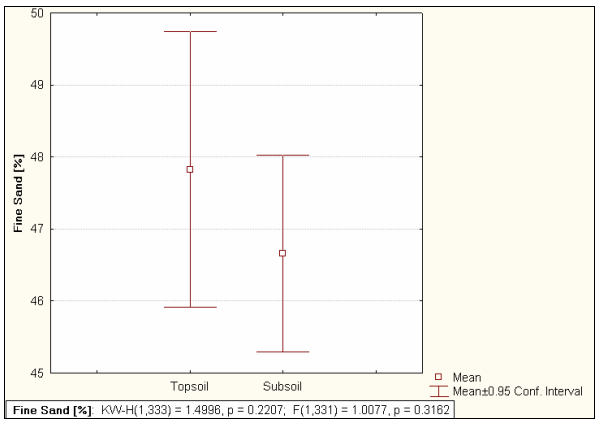

Figure 10.75. Fine sand content, per topsoil and subsoil

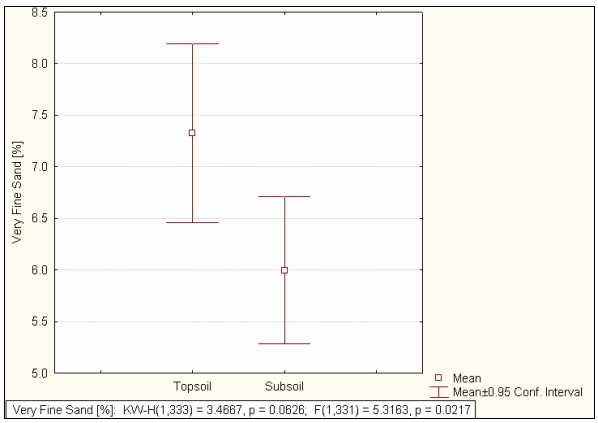

Figure 10.76. Very fine sand content, per topsoil and subsoil

Table 10.22: Percentage coarse-, medium-, fine- and very fine sand, per topsoil and subsoil.

	Coarse Sand %		Medium Sand %		Fine Sand %		Very Fine Sand %	
	Topsoil n = 128	Subsoil n = 205	Topsoil n = 128	Subsoil n = 205	Topsoil n = 128	Subsoil n = 205	Topsoil n = 128	Subsoil n = 205
Mean	16.0	18.5	28.9	28.9	47.8	46.7	7.3	6.0
Median	12.65	16.1	28.7	28.6	49.5	46.5	7.8	7.3
Std.Dev.	11.36	11.87	7.5	6.18	10.94	9.93	4.96	5.2
Minimum	1.7	1.4	10.7	12.1	9.00	25.00	0.00	0.00
Maximum	49.3	53.9	70.3	44.6	75.1	69.7	19.7	18.2
Range	47.6	52.5	59.6	32.5	66.1	44.7	19.7	18.2
Lower Quartile	7.4	8.2	24.3	24.4	38.9	38.2	4.85	0.00
Upper Quartile	24.1	28.4	33.3	33.3	55.1	54.00	10.6	10.1
Quartile Range	16.7	20.2	9.00	8.9	16.2	15.8	5.75	10.1
Percentile 10	3.1	3.7	19.3	21.2	33.9	33.8	0.00	0.00
Percentile 90	34.6	34.9	37.9	37.2	60.2	59.6	13.1	12.6

Fluvisols have a relatively high percentage of coarse and medium sand compared to the other soil groups, low fine sand percentage and no measurable very fine sand fraction (Table 10.23; Figures 10.77 – 10.81). Areno-, Cambi-, Rego and Luvisols are rich in fine and very fine sand fractions and poor in coarse sand fractions. Calcisols have a relatively high percentage of very fine sand and low percentage of coarse sand, but a wide range of values for medium and fine sand content. The ±0.95 confidence intervals of all Leptosol sand fractions are quite wide.

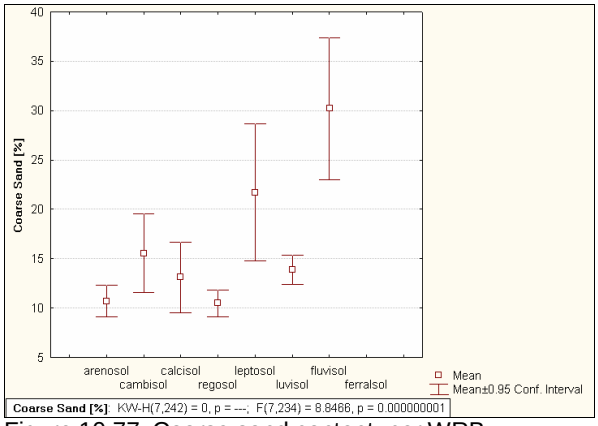

Figure 10.77. Coarse sand content, per WRB reference soil group

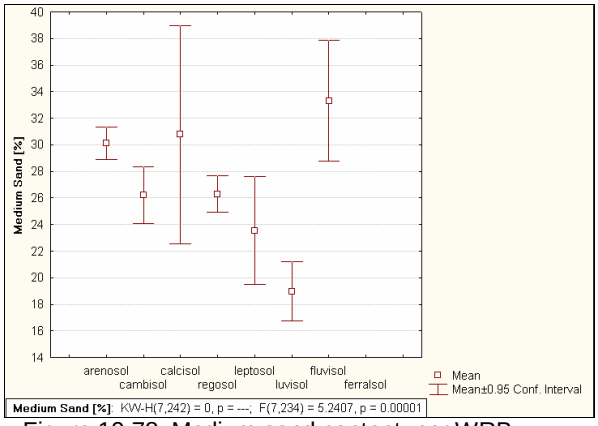

Figure 10.78. Medium sand content, per WRB reference soil group

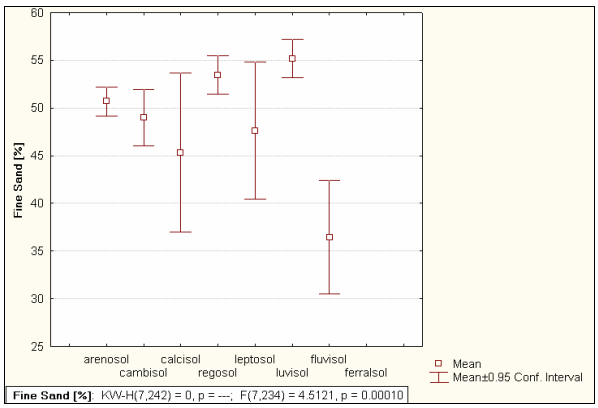

Figure 10.79. Fine sand content, per WRB reference soil group

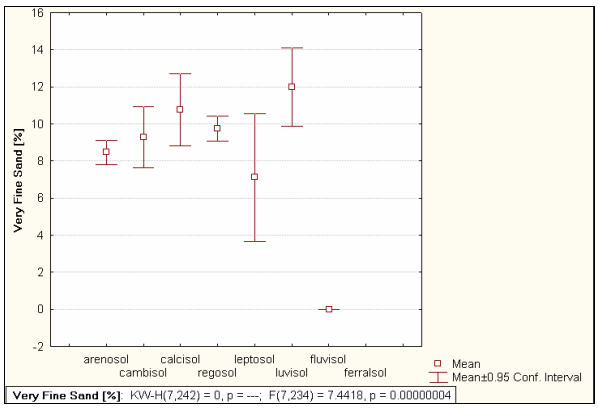

Figure 10.80. Very fine sand content, per WRB reference soil group

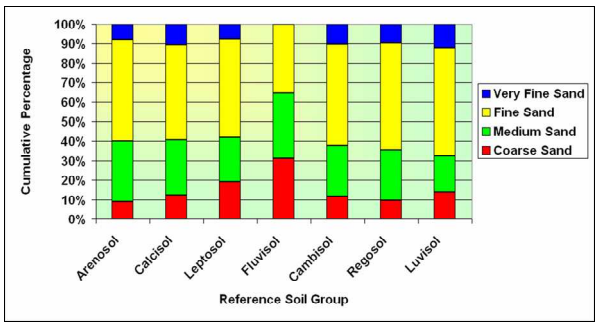

Figure 10.81. Median coarse, medium, fine and very fine sand contributions to each WRB reference soil group

Table 10.23: Sand fractions of the WRB reference soil groups.

Coarse Sand	**Arenosol** (n = 95)	**Calcisol** (n = 12)	**Leptosol** (n = 16)	**Fluvisol** (n = 6)	**Cambisol** (n = 32)	**Regosol** (n = 78)	**Luvisol** (n = 3)
Mean	10.72	13.11	21.71	30.22	15.54	10.48	13.87
Median	8.70	12.65	19.10	31.15	11.45	9.70	13.80
Std.Dev.	7.94	5.64	13.03	6.85	11.03	6.13	0.60
Minimum	1.4	6.3	4.3	20.7	3.1	2.2	13.3
Maximum	37.4	27.2	49.3	39.0	53.9	28.5	14.5
Range	36.0	20.9	45.0	18.3	50.8	26.3	1.2
Lower Quartile	3.3	9.5	12.4	24.3	9.4	5.5	13.3
Upper Quartile	15.5	15.3	30.8	35.0	18.8	14.0	14.5
Quartile Range	12.2	5.8	18.5	10.7	9.4	8.5	1.2
Percentile 10	2.0	7.5	4.3	20.7	5.5	3.6	13.3
Percentile 90	22.6	17.7	38.2	39.0	34.3	18.9	14.5
Medium Sand	**Arenosol** (n = 95)	**Calcisol** (n = 12)	**Leptosol** (n = 16)	**Fluvisol** (n = 6)	**Cambisol** (n = 32)	**Regosol** (n = 78)	**Luvisol** (n = 3)
Mean	30.14	30.76	23.55	33.32	26.20	26.30	18.97
Median	30.90	28.50	22.70	33.10	25.40	25.85	18.50
Std.Dev.	6.02	12.93	7.65	4.31	5.90	6.03	0.90
Minimum	16.8	21.0	10.7	27.6	16.4	14.1	18.4
Maximum	42.4	70.3	35.1	38.1	39.2	43.7	20.0
Range	25.6	49.3	24.4	10.5	22.8	29.6	1.6
Lower Quartile	26.1	24.3	18.7	30.1	21.9	22.3	18.4
Upper Quartile	34.8	29.6	31.5	37.9	29.4	29.7	20.0
Quartile Range	8.7	5.3	12.8	7.8	7.5	7.4	1.6
Percentile 10	20.8	23.3	12.1	27.6	19.3	19.0	18.4
Percentile 90	37.6	33.9	33.7	38.1	33.3	34.0	20.0

Fine Sand	Arenosol (n = 95)	Calcisol (n = 12)	Leptosol (n = 16)	Fluvisol (n = 6)	Cambisol (n = 32)	Regosol (n = 78)	Luvisol (n = 3)
Mean	50.69	45.33	47.61	36.47	48.98	53.47	55.20
Median	51.10	49.00	50.20	35.45	50.25	54.80	55.40
Std.Dev.	7.54	13.10	13.52	5.65	8.15	8.88	0.82
Minimum	33.4	9.0	17.0	28.7	25.0	30.9	54.3
Maximum	75.1	58.6	68.5	44.4	59.2	67.9	55.9
Range	41.7	49.6	51.5	15.7	34.2	37.0	1.6
Lower Quartile	46.8	42.5	38.5	33.4	45.8	49.8	54.3
Upper Quartile	54.4	53.1	58.7	41.4	55.1	60.2	55.9
Quartile Range	7.6	10.7	20.2	8.0	9.3	10.4	1.6
Percentile 10	40.8	36.1	34.2	28.7	37.6	38.8	54.3
Percentile 90	59.6	55.6	63.3	44.4	58.3	63.8	55.9
Very Fine Sand	**Arenosol** (n = 95)	**Calcisol** (n = 12)	**Leptosol** (n = 16)	**Fluvisol** (n = 0)	**Cambisol** (n = 32)	**Regosol** (n = 78)	**Luvisol** (n = 3)
Mean	8.46	10.78	7.11	-	9.28	9.76	12.00
Median	8.00	10.65	7.45	-	9.85	9.55	11.90
Std.Dev.	3.21	3.06	6.45	-	4.53	3.02	0.85
Minimum	0.0	6.3	0.0	-	0.0	0.0	11.2
Maximum	15.2	16.8	18.2	-	18.4	19.7	12.9
Range	15.2	10.5	18.2	-	18.4	19.7	1.7
Lower Quartile	6.7	8.9	0.0	-	7.6	7.7	11.2
Upper Quartile	10.6	12.9	11.9	-	11.5	12.0	12.9
Quartile Range	3.9	4.0	11.9	-	3.9	4.3	1.7
Percentile 10	5.4	7.0	0.0	-	0.0	6.7	11.2
Percentile 90	13.0	14.2	16.5	-	13.4	12.9	12.9

Aeolian material is poor in coarse sand, rich in medium and fine sand (Figures 10.82 – 10.85). Alluvial parent material is rich in coarse sand and poor in fine sand. Colluvium and material weathered *in situ* are both rich in the fine sand fraction. The very fine sand fraction is best represented in alluvium and material weathered *in situ.*

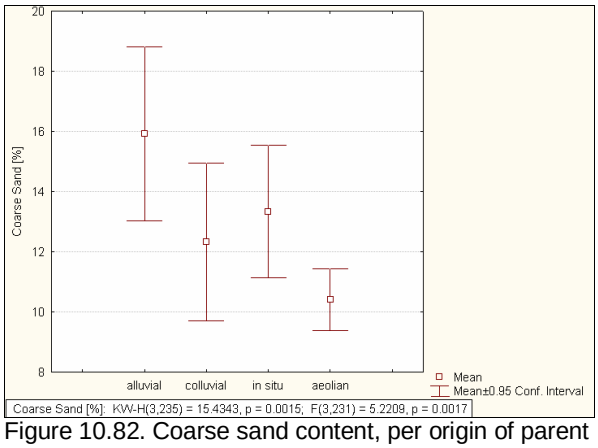

Figure 10.82. Coarse sand content, per origin of parent material

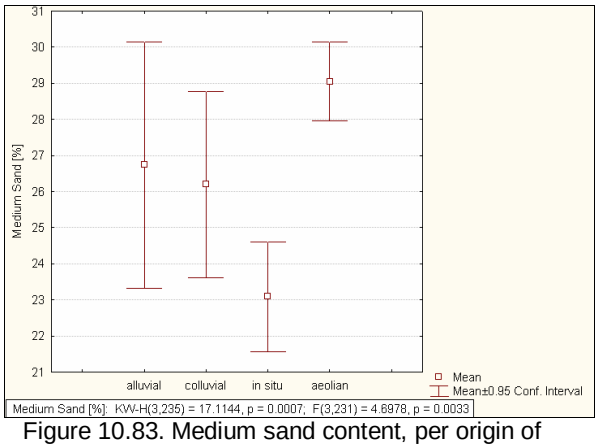

Figure 10.83. Medium sand content, per origin of parent material

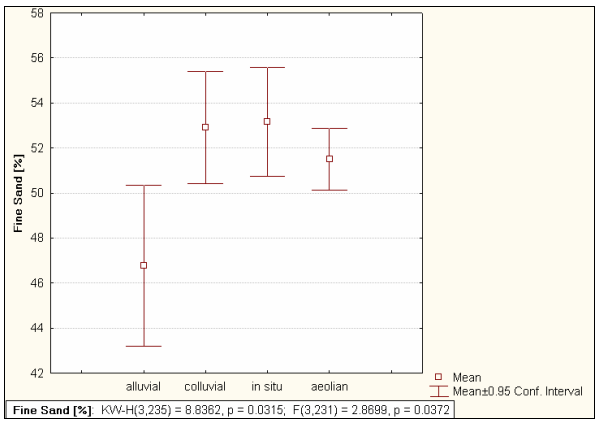

Figure 10.84. Fine sand content, per origin of parent material

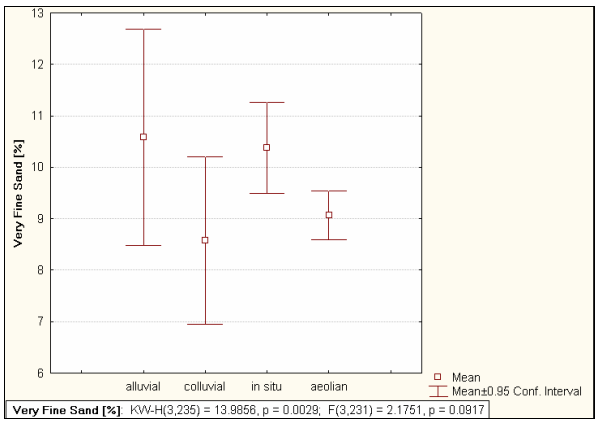

Figure 10.85. Very fine sand content, per origin of parent material

Soils formed from schist contain more coarse sand, fine sand and very fine sand, and less medium sand than those formed from Kalahari sand (Figures 10.86 – 10.89). Soils formed from quartzite show large spreads in ±0.95 confidence intervals for all sand fractions.

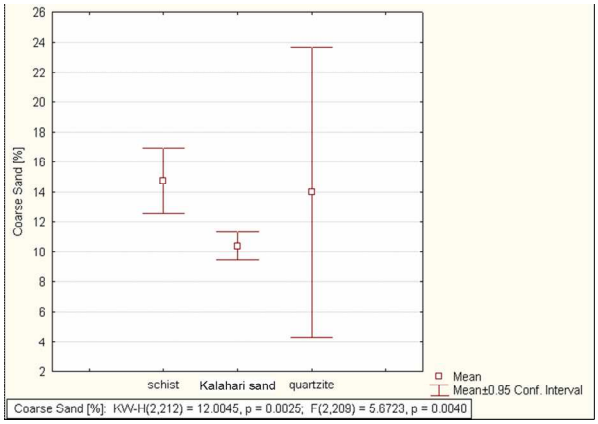

Figure 10.86. Coarse sand content, per type of parent material

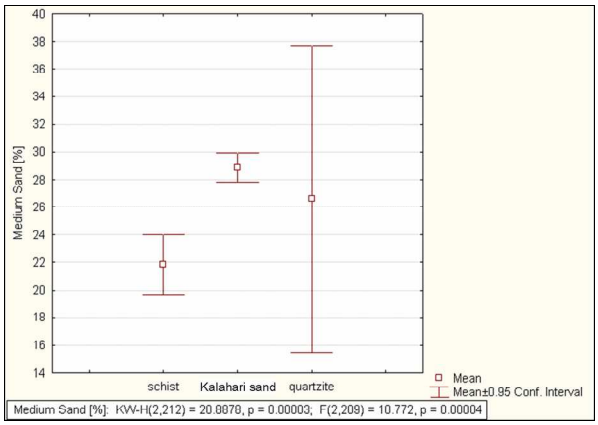

Figure 10.87. Medium sand content, per type of parent material

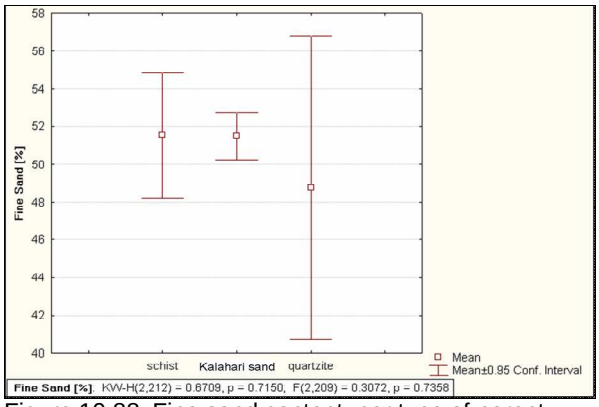

Figure 10.88. Fine sand content, per type of parent material

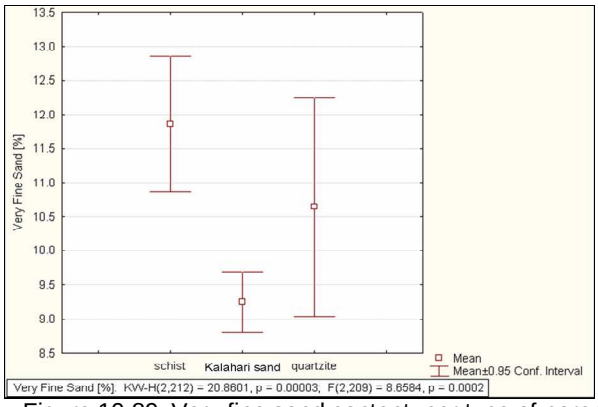

Figure 10.89. Very fine sand content, per type of parent material

The coarse sand content increases, while fine and very fine sand content decreases with degree of dissection of the landscape (Figures 10.90, 10.92, 10.93). The case of medium sand content is ambiguous (Figure 10.91).

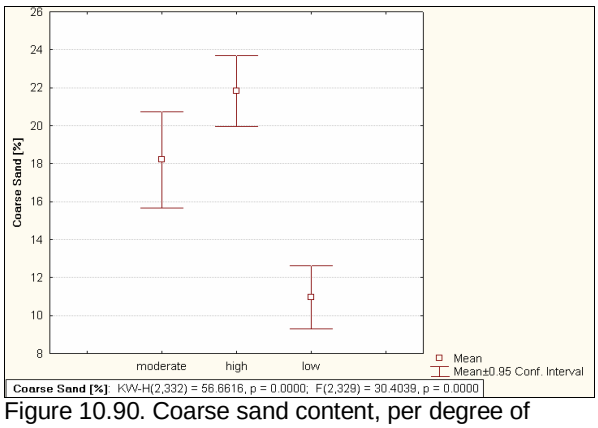

Figure 10.90. Coarse sand content, per degree of dissection of the landscape

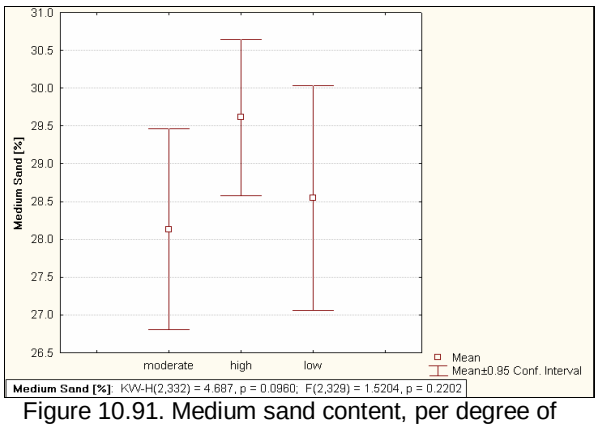

Figure 10.91. Medium sand content, per degree of dissection of the landscape

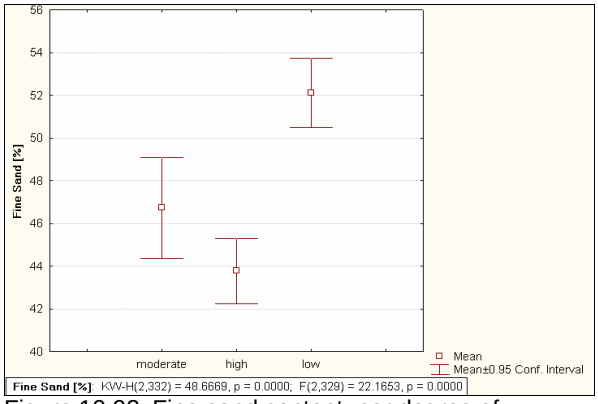

Figure 10.92. Fine sand content, per degree of dissection of the landscape

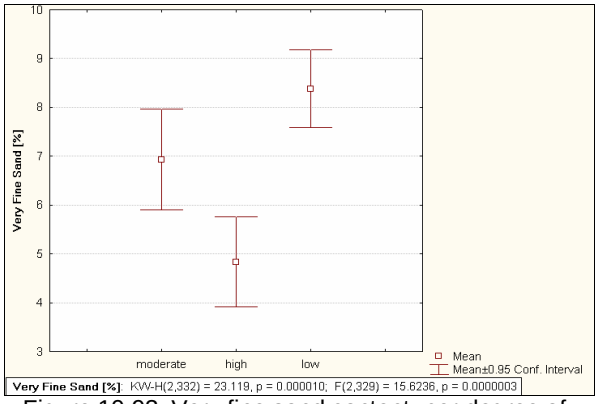

Figure 10.93. Very fine sand content, per degree of dissection of the landscape

Coarse sand content is lowest when the landscape is flat or almost flat, while the opposite is true for fine and very fine sand content (Figures 10.94 – 10.97).

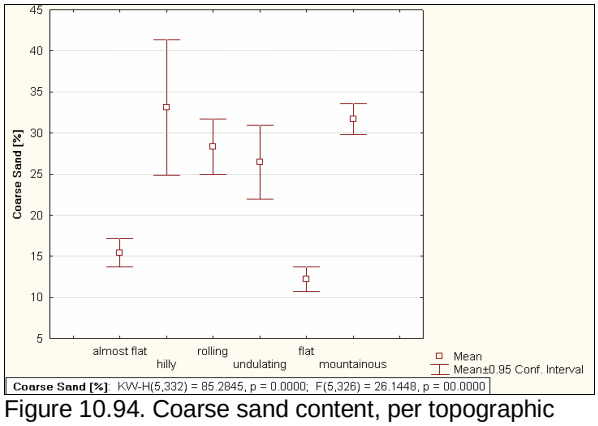

Figure 10.94. Coarse sand content, per topographic class

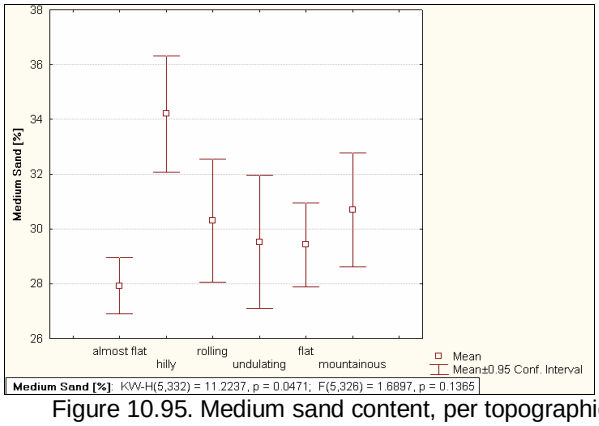

Figure 10.95. Medium sand content, per topographic class

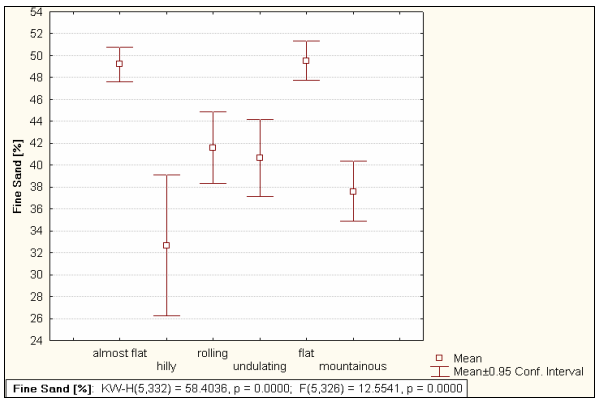

Figure 10.96. Fine sand content, per topographic class

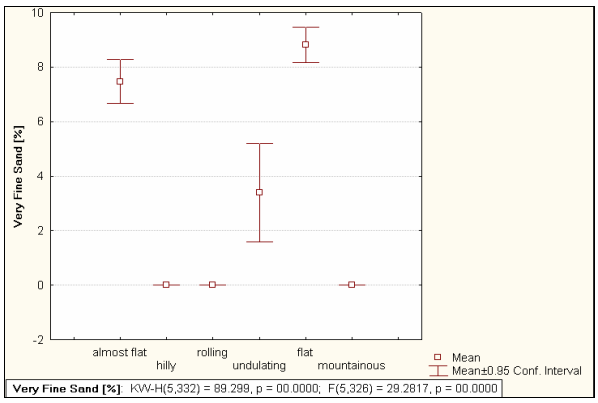

Figure 10.97. Very fine sand content, per topographic class

The coarse-, medium-, fine- and very fine sand fractions of topsoil and subsoil are shown in Figures 10.98 – 10.105.

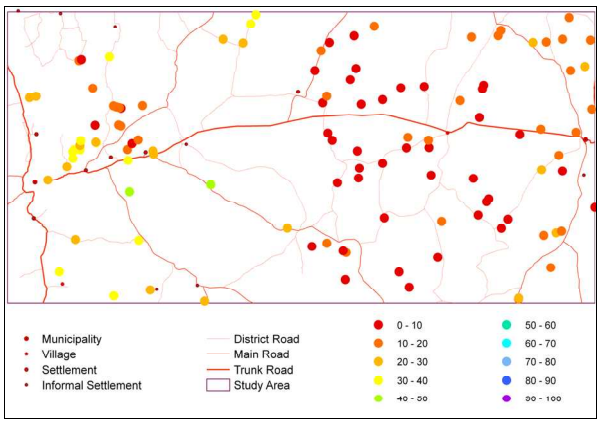

Figure 10.98. Coarse sand content (%) of topsoil

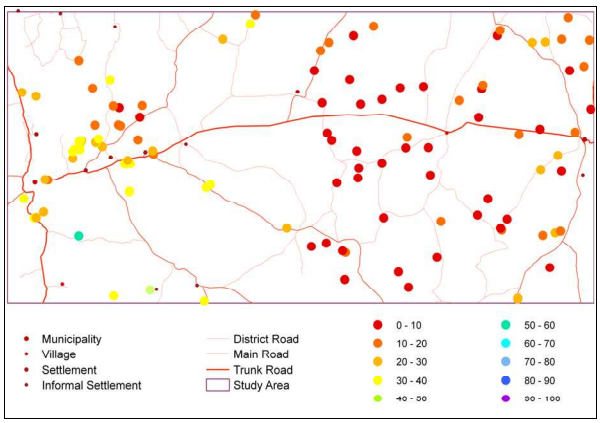

Figure 10.99. Coarse sand content (%) of subsoil

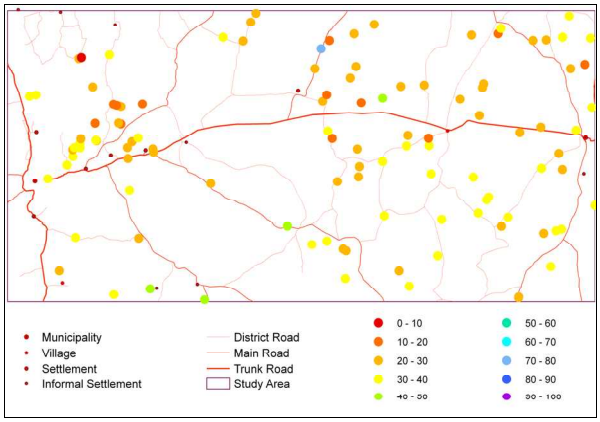

Figure 10.100. Medium sand content (%) of topsoil

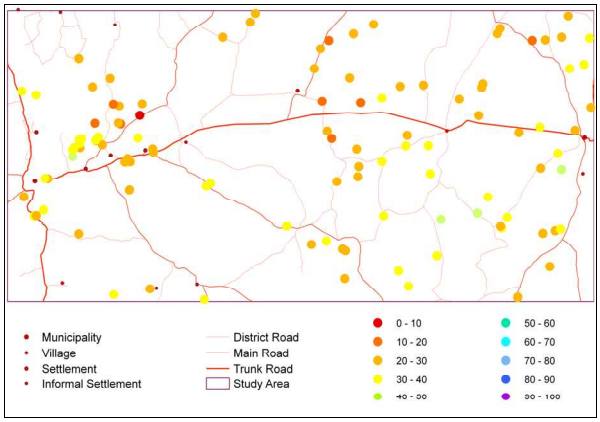

Figure 10.101. Medium sand content (%) of subsoil

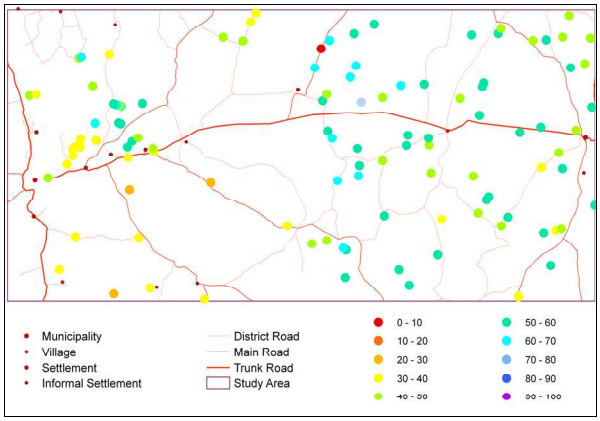

Figure 10.102. Fine sand content (%) of topsoil

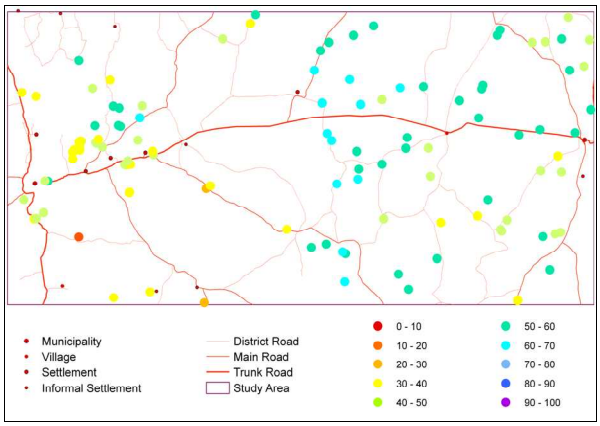

Figure 10.103. Fine sand content (%) of subsoil

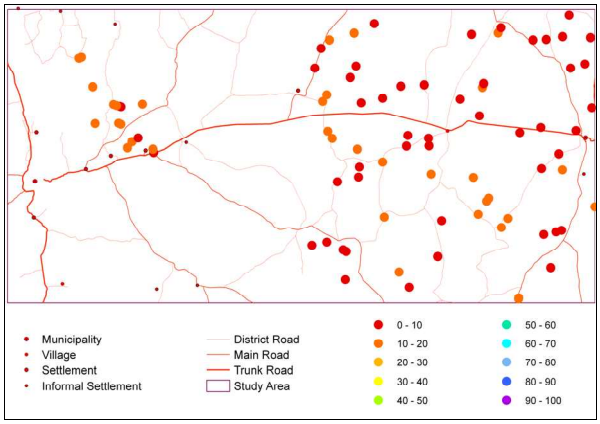

Figure 10.104. Very fine sand content (%) of topsoil

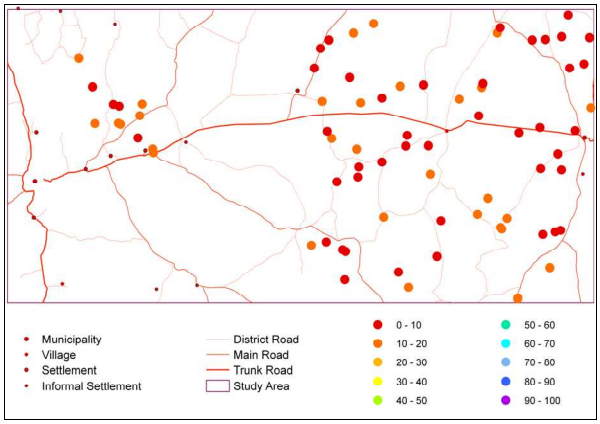

Figure 10.105. Very fine sand content (%) of subsoil

10.4 CRUSTING AND SEALING

Instances of sealing, crusting and hardening occur in the study area. Cracking is only found in pans, while self-mulching is not evident. Sealing occurs in poorly aggregated topsoils with high silt content, as a result of dry-wet cycles. On drying these seals develop into crusts. Soil crusts have higher density, higher shear strength, finer pores and lower saturated hydraulic conductivity than the underlying soil. They reduce infiltration, increase runoff and interfere with seedling development. Casenave and Valentin (1989), as quoted by FAO (1998b), described the principal soil parameters that determine vulnerability to crusting as being textural differentiation, type of clay minerals, chemical composition, quantity and type of organic matter and, to a lesser extent, hydrophobia and aptitude to cracking. According to them the highest aggregate instability is reached when silt content exceeds 25 %, with less than 35 % sand content. No such highly instable soils were encountered in the study area.

Smectites are more sensitive to dispersion than kaolinites. Iron and aluminium give high stability. Gypsum gives more stability than lime. Magnesium contributes strongly to instability if it exceeds 50 % base saturation, while an exchangeable sodium percentage (ESP) of 15 – 20 % strongly promotes dispersion (Casenave and Valentin, 1989). Twenty-eight topsoil samples with exchangeable magnesium percentage above 50 % and exchangeable potassium percentage above 15 % were encountered, but the relationship with surface sealing and crusting and erosion, as observed in the field, was ambiguous.

FAO (1998b) suggested two further subdivisions to distinguish between surface sealing properties – orientation and packing of dispersed soil particles which have disintegrated from soil aggregates due to impact of rain drops; formed at the soil surface – and depositional crust properties – crusts constructed when soil particles from externally derived materials, suspended in water, are deposited on the soil surface as water infiltrates or evaporates. FAO (1998b) also recognized topsoils with compacted properties, i.e. a bulk density of ≥ 1.7 g cm^{-3}. In the study area, three such naturally occurring compacted soils were found among those with highly soluble components: carbonates, sulfates and salts. Structural crusts, caused by livestock trampling, are included under these soils.

Water harvesting, where rainfall is actively concentrated by encouraging sealing on poor soils on slight slopes, to channel water towards better soils, is not actively practiced in the study area. It is an unintentional by-product of urban development, where roofs, concrete and bitumen surfaces concentrate rainwater towards reservoirs for later consumption.

CHAPTER ELEVEN

SUMMARY AND CONCLUSIONS

11.1 SOIL-FORMING FACTORS IN THE STUDY AREA

Soil characteristics are the end result of a number of interdependent soil forming factors, namely climate, vegetation, organic matter, topography and physiography, mineralogical soil constituents, surface processes, biological activity and human activity (FAO, 1998b). The imprint of the respective soil-forming factors originally recognised by Jenny in 1941 (as reprinted in 1994) can be recognised in the study area.

11.1.1 CLIMATE

Climate both directly controls soil formation and indirectly influences it through vegetation production, shaping the landscape and determining the biological and human activity of the area. In the semi-arid study area climate-related surface processes act on topsoil in the form of heating, wind- and water erosion. Splash erosion, the process of physical breakdown of soil aggregates by raindrop impact, as well as sheet-, rill- and gully erosion are worsened in the absence of vegetation, which is often the case during the latter part of the dry season. At the same time, dry bare soil with low surface aggregation is susceptible to wind erosion. Whirlwinds, developed through differential heating, are visible agents of wind erosion in the study area. Soil temperatures are very high, often exceeding 50 ^{o}C in the dry hot season (September to December), resulting in extreme desiccation and lowering biological activity in the topsoil. Relatively low rainfall means that there is some leaching of topsoil with subsequent accumulation of bases in deeper horizons. High rates of evaporation causes capillary rise of groundwater with concomitant accumulation of carbonates and silicates, sometimes to the extent of forming indurated layers.

11.1.2 PARENT MATERIAL

Parent material determines the type of mineral soil particles found. In the study area no volcanic material and very little shrinking-swelling clay occur. The western third of the area is dominated by schist, with the attendant abundance of primary minerals rich in nutrients. The eastern half is dominated by quartz-rich sandy soils formed in the Kalahari sands, with the associated low levels of clay minerals, low coherence, poor soil structure, high infiltration rates and low cation exchange capacity.

11.1.3 VEGETATION

Vegetation improves porosity and aeration through loosening of soil by root penetration. Vegetation cover protects the surface against wind and raindrop impact and slows overland flow of water, thereby lowering erosion risk and downstream sedimentation and allowing better infiltration of rainwater. The low amount of

vegetation present during the latter part of the dry season renders the study area vulnerable to erosion. Nutrients are extracted from deeper within the soil by plants and are accumulated in the surface layers when the plants die and decompose. Organic matter enhances aggregation, increases structural stability, increases water holding capacity, contributes to nutrient holding capacity, buffers against potential acidification, binds toxic substances and provides the soil with nutrients captured from the atmosphere by vegetation (FAO, 1998b). Organic matter is central to maintenance of soil fertility through mineralisation of nitrogen, phosphor and sulfur, improving soil nutrient- and water holding capacity, structural ability and promoting soil fauna. The study area has no organic topsoils. The percentage of organic matter found in topsoils of the area is very low – the result of the dry and hot climate, with low biomass production rate by relatively sparse vegetation and a high rate of mineralisation. The organic matter is not as intimately mixed with mineral particles as would be the case in temperate regions with a wetter moisture regime and more earthworm activity. In consequence, poorer aggregation and structure development are found. Most topsoils in the study area display *arescic* properties, which are defined by FAO (1998b) as having less than 3 % organic matter and biological activity being restricted to a well-defined rainy season, resulting in a surface layer enriched in humus of no more than 10 cm thick. These soils are dry for more than three consecutive months during each year and frequently have hard-setting properties.

11.1.4 SOIL FAUNA

Soil fauna help with physical mixing of organic matter in the soil profile, inoculation of plant litter with decomposer populations, improvement of soil physical properties, physical disintegration of organic matter, direct metabolism of organic components and stimulation of decomposer populations (Tate, 1987). Soil microbes, such as fungi, yeasts and bacteria, biochemically free plant nutrients and manufacture humus compounds from plant litter. The study area shows abundant features of mesofaunal activity, particularly by termites and to a lesser extent by earthworms and ants. Termites enrich the subsoil in the proximity of termitaria in clay, organic materials and subsequently in nutrients. They create mounds above and chambers below the surface. They effect rapid physical disintegration of vegetation residues and convert cellulose, hemi-cellulose and lignin into products that other meso- and microfauna can digest more easily. Other burrowing animals, particularly ground squirrels, suricates, mongooses, aardvarks and porcupines contribute to mixing of soil layers, aeration and introduction of plant litter and animal excreta into deeper horizons.

11.1.5 HUMAN ACTIVITY AND MANAGEMENT

Extensive livestock farming dominates human activity in the study area. Ranching has a less radical influence on topsoil than cultivation, but can still degrade land through overgrazing and trampling by livestock. The former will denude vegetation, increase wind erosion, runoff and sealing, decrease infiltration, and lead to sheet-, rill- and eventual gully erosion. Trampling can have the same end result by destroying soil structure. In the study area, incipient bush encroachment is changing the vegetation dynamics. Undesirable bush is replacing grass and forbs, with a lowering in both production potential and biodiversity. The causes of bush encroachment are complex, but poor management (grazing) practices are major contributors.

11.1.6 TOPOGRAPHY AND PHYSIOGRAPHY

The western third of the study area is dominated by the high, deeply incised Khomas Hochland and its transition towards the lower, relatively flat Kalahari. Leptosols and bare rocky outcrops are abundant in the Khomas Hochland, while the Kalahari is generally covered by deep soils, only occasionally interrupted by shallow calcretes in the lower landscape positions.

Topography and physiography largely determine soil depth (Figure 5.21) and stability of the topsoil, with thin topsoil overlying hard rock found in upper slope positions in steep topographical settings. Higher rates of leaching occur in upper and mid-slopes, with accumulation of soluble constituents such as calcium carbonate lower in the landscape, where they may form indurated layers that constrain topsoil thickness.

Drainage features, such as water saturation, are largely determined by physiography. The study area does not feature topsoils with reductive properties (FAO, 1998b) associated with permanently saturated with groundwater, but it has some soils with redoxic properties associated with periodic saturation.

11.1.7 TIME

Soil aging is marked by a decrease in the silt/clay ratio (Figures 11.1 – 11.2), a progressive increase in clay content (Figures 11.37 – 11.38), and a slight reduction in the CEC of clay (Ellis, 1988; Constantini, Angelone and Damiani, 2002). From Figures 11.1 and 11.2 it can be concluded that most pedological development seems to have taken place in the central part of the study area. Towards the west the pronounced topography probably caused rapid removed of soil by water erosion and mass movement, while the high quartz content of the Kalahari sands towards the east probably inhibited weathering of silt to clay particles, as quartz is quite resistant to weathering.

No highly weathered soils (silt/clay < 0.02) were found in the study area, and it can be concluded that the soils currently at the surface are pedogenically young. Remnants of old, buried soils were found sporadically, such as deeply weathered Ferralsols in the highlands east of Windhoek which were covered and preserved by colluvium. Kempf (2008) postulated that Quaternary pedogenesis, soil dynamics and morphological development of central Namibia are characterised by peneplanation and deep weathered (suggested by existence of fossil ferralitic and fersialitic paleosoils), probably until the Miocene and discrete erosive periods with temporary re-deposition. During the Quaternary physical weathering intensified and topography became more pronounced.

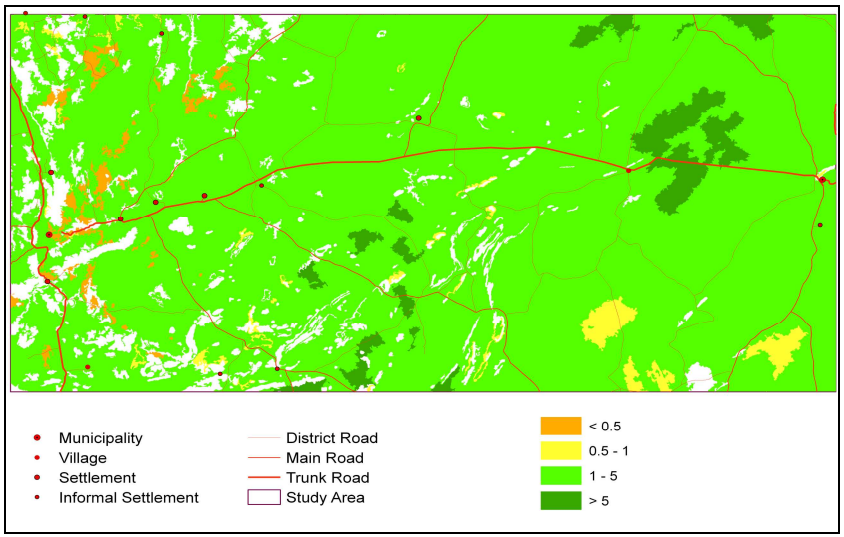

Figure 11.1 Silt : clay ratio of topsoil, indicating relative stage of weathering and eluviation

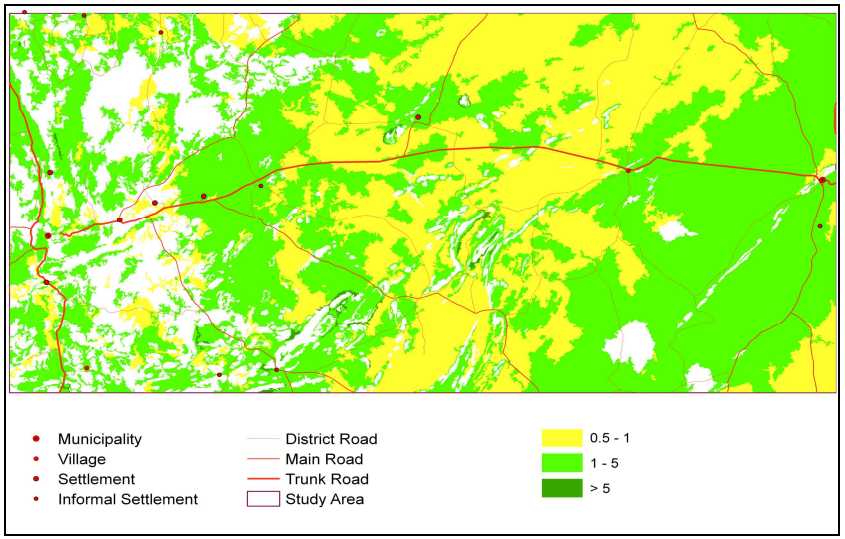

Figure 11.2. Silt : clay ratio of subsoil, indicating relative stage of weathering and illuviation

NOTE: In these maps, and those that follow, blank areas indicate either the absence of sufficient analytical data to extrapolate to the respective terrain units, or contradictory data from different profiles within a terrain unit.

11.2 SUMMARY OF ANALYTICAL RESULTS

11.2.1 NITROGEN

In 80 % of samples, the nitrate content of the saturated paste extract is between 0 and 54.6 mg l^{-1}, while the nitrite content is between 0 and 24.7 mg l^{-1}. Weak positive correlations were found between nitrate and the electrical conductivity and sulphate of the saturated paste extract, as well as electrical conductivity of the 2:5 soil:water suspension. A weak positive correlation was also found between nitrite and the electrical conductivity of the saturated paste extract. Nitrate and nitrite are more abundant in topsoil than subsoil, most likely due to the contribution of leaf litter and animal excreta to the topsoil. Sandy soils are extremely poor in nitrite, as they are highly prone to leaching of these very mobile ions.

11.2.2 PHOSPHORUS

In 90 % of samples, the plant-available phosphorus content is below 12 mg kg^{-1}, which is low for a soil under natural grassland, but can be explained by the prevailing semi-arid climate and low biomass production. It is generally lower than values recorded in southern Africa, but comparable with findings elsewhere within Namibia. Weak positive correlations were found with electrical conductivity (2:5 soil:water suspension and saturated paste extract), zinc, iron, organic matter and extractable sodium. Phosphorus content decreases with horizon depth (Figures 11.3 – 11.4), so that the topsoil has noticeably more phosphorus than the subsoil, most likely as a result of topsoil enrichment by decaying plant material and animal excreta, augmented by the low mobility of phosphorus in soil. Sandy soils, and thus Arenosols, are poorest in phosphorus. Leptosols and Fluvisols are richest in phosphorus. Enrichment of Fluvisols may be ascribed to transport of phosphorus-containing particulate matter by surface runoff. The quartz-rich Kalahari sands are poorer in phosphorus than soils formed on schist, as a consequence of the mineral composition. Phosphorus concentrations increase with the degree of dissection, probably due to greater rates of erosion and subsequent weathering of phosphorus-containing parent material in more dissected terrain, and the schist, quartzite and calcrete found in the highly dissected terrain of the study area, whereas the less dissected areas towards the east are mainly covered with Kalahari sands. Flat, almost flat and undulating land has lower phosphorus content than rolling, hilly and mountainous land. The relationship with pH was ambiguous.

11.2.3 SULFATE

In 80 % of samples, the sulfate content of the saturated paste extract is between 5.4 and 20.9 mg l^{-1}. Sulfate is strongly positively correlated with electrical conductivity of the saturated paste extract, and weakly positively correlated with both extractable and exchangeable potassium content, with chloride content, organic matter, electrical conductivity of the 2:5 soil:water suspension and coarse sand content. There is no sulfate enrichment of topsoil in evidence, probably due to the low organic matter content. Sandy soil tends to be poorest in sulfate, as a result of leaching Sulfate concentrations are somewhat lower in the Kalahari sands than in soils formed on the schist of the Khomas Hochland – a consequence of the mineral composition of the respective parent materials.

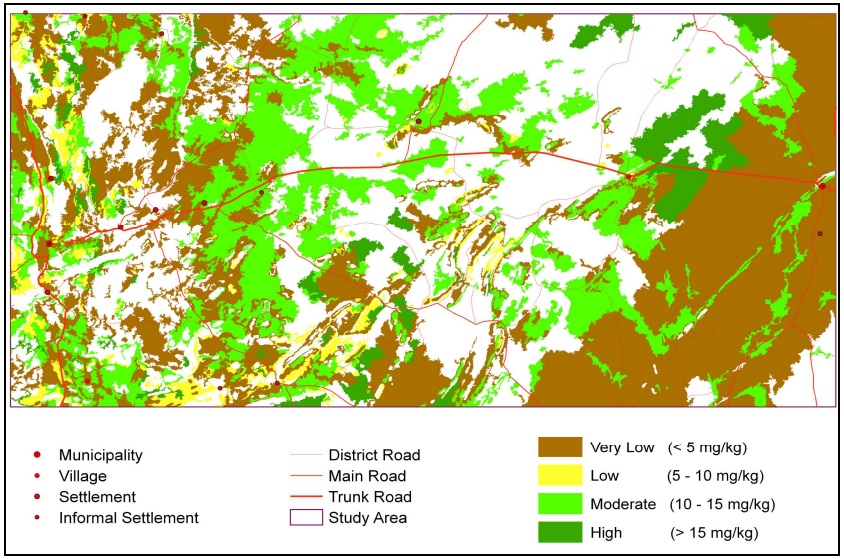

Figure 11.3. Spatial distribution of phosphorus content (mg kg^{-1}) of topsoil

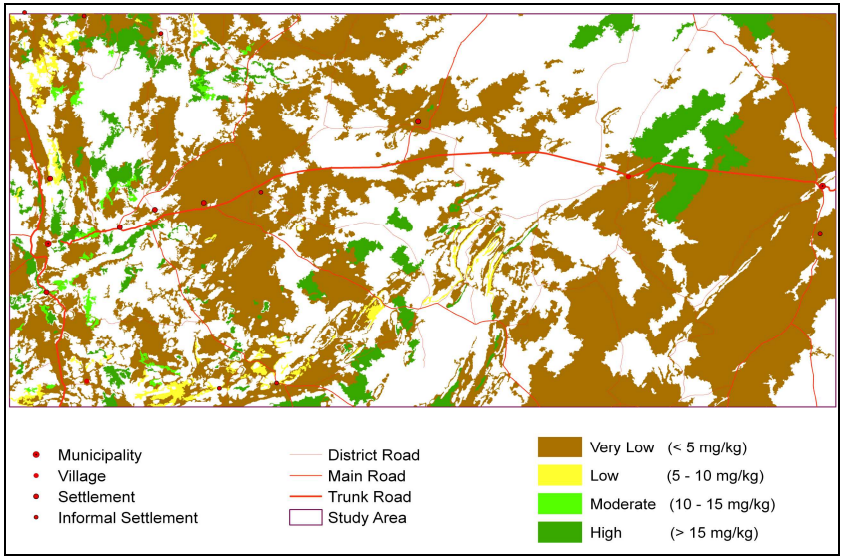

Figure 11.4 Spatial distribution of phosphorus content (mg kg^{-1}) of subsoil

11.2.4 CALCIUM

In 80 % of samples, the extractable calcium content is between 0.61 and 5.73 $cmol_c kg^{-1}$ (122 and 1 146 mg kg^{-1}), and exchangeable calcium is between 0.21 and 6.02 $cmol_c kg^{-1}$. Extractable calcium content is strongly positively correlated with exchangeable calcium content, cation exchange capacity, fluoride, pH and the sums of both extractable and exchangeable bases. It is weakly positively correlated with extractable and exchangeable magnesium content, electrical conductivity (saturated paste extract), and lay, and weakly negatively correlated with sand content. Exchangeable calcium content is strongly positively correlated with extractable calcium content, pH, cation exchange capacity and the sums of both exchangeable and extractable bases. It is weakly positively correlated with fluoride content, exchangeable and extractable magnesium content and electrical conductivity (2:5 soil:water suspension). It is weakly negatively correlated with sand content. Both extractable and exchangeable calcium concentrations are higher in subsoil than in topsoil, most likely as a result of leaching, as well as depletion by plants and subsequent removal of plants by grazing. Soil water movement in the vadose zone, coupled with seasonality of rainfall and high evapotranspiration rates, tend to concentrate calcium in subsurface layers. Sandy, loamy sand and loamy soils have noticeably lower concentrations of both extractable and exchangeable calcium than sandy loams and sandy clay loams. Alluvial material is richest in calcium. Soils formed on the schist of the Khomas Hochland are richer in calcium than the Kalahari sands, as a consequence of the respective mineral compositions. Calcisols are, as per definition, richest in calcium, followed by Cambisols, with Arenosols being poorest. Exchangeable calcium concentrations are highest in the lowest landscape positions (valleys and lower slopes), and lowest in the higher landscape positions (mid-slopes, upper slopes and ridges), in parallel with accumulation of finer soil fractions lower in the landscape. It increases with degree of dissection of the landscape, which can probably be ascribed to greater rates of erosion and subsequent weathering of mineral-rich parent material in the more dissected terrain. Furthermore, the highly dissected terrain of the study area occurs mainly on schist, quartzite and calcrete, whereas the less dissected areas, towards the east, are mainly covered with Kalahari sands (Figures 11.5 – 11.8).

11.2.5 MAGNESIUM

In 80 % of samples, the extractable magnesium content is between 0.12 and 2.28 $cmol_c kg^{-1}$ (15 and 278 mg kg^{-1}), and exchangeable magnesium content is between 0.12 and 2.01 $cmol_c kg^{-1}$, which is consistent with reports in literature. Extractable magnesium content is strongly positively correlated with exchangeable magnesium content and the sums of both extractable and exchangeable bases. It is weakly positively correlated with extractable and exchangeable calcium content and potassium content, electrical conductivity (saturated paste extract), cation exchange capacity, manganese content, iron content, copper content, fluoride content, pH, and clay content, and weakly negatively correlated with sand content. Exchangeable magnesium content is strongly positively correlated with extractable magnesium content, clay content, cation exchange capacity and the sums of both extractable and exchangeable bases, while it is strongly negatively correlated with sand content. It is weakly positively correlated with both extractable and exchangeable calcium content and potassium content, pH, manganese content, iron content, copper content, fluoride content, and silt content, while it is weakly negatively correlated with medium sand content. Both extractable and exchangeable magnesium concentrations are higher in subsoil than in topsoil, most likely as a result of

leaching, depletion by plants and subsequent removal of plants by grazing, and additions from weathering of primary minerals from parent materials. Sandy soils and loamy sands have considerably lower concentrations of both extractable and exchangeable magnesium than sandy loams and sandy clay loams, which is consistent with literature. The sandy, quartz-rich Arenosols of the Kalahari contain less magnesium than the soils formed on schist in the Khomas Hochland. Cambisols, Calcisols and Luvisols are relatively rich in magnesium. Magnesium concentrations are highest in the lowest landscape positions (valleys and lower slopes), and lowest in the higher landscape positions (mid-slopes, upper slopes and ridges), most probably as a result of mass movement of magnesium-containing colluvial material down inclines, as well as vertical and lateral displacement of magnesium by percolating water. Moderately to highly dissected terrain is richer in magnesium (Figures 11.9 – 11.12), for the same reasons explained above in the case of calcium.

11.2.6 POTASSIUM

In 80 % of samples, the extractable potassium content is between 0.13 and 0.54 $cmol_c kg^{-1}$ (51 and 213 mg kg^{-1}), and exchangeable potassium content is between 0.12 and 0.49 $cmol_c kg^{-1}$. Extractable potassium content is strongly positively correlated with exchangeable potassium content and weakly positively correlated with extractable and exchangeable magnesium content, electrical conductivity (saturated paste extract), manganese content, iron content, clay content and sulfate content. Exchangeable potassium content is strongly positively correlated with extractable potassium content, and weakly positively correlated with both exchangeable and extractable magnesium content, electrical conductivity (2:5 soil:water suspension and saturated paste extract), sums of both extractable and exchangeable bases, iron content, manganese content, zinc content, sulfate content, and clay content. It is weakly negatively correlated with sand content. Topsoil and subsoil potassium concentrations do not differ significantly, in accord with most reports in literature. Potassium content increases from sandy soils, through loamy sand and sandy loam, to sandy clay loam, as increasing clay content provide more exchange sites as well as more potassium-containing secondary minerals. The sandy, quartz-rich Arenosols of the Kalahari contain less potassium than the soils formed on schist in the Khomas Hochland, as a consequence of both texture and mineral composition of parent material. Cambisols and Calcisols are relatively rich in potassium, with Arenosols, Regosols and Leptosols being poor in potassium. Potassium concentrations are highest in the lowest landscape positions (valleys and lower slopes) and lowest in the higher landscape positions (mid-slopes, upper slopes and ridges), most probably as a result of mass movement of potassium-containing colluvial material down inclines, as well as vertical and lateral displacement of potassium by percolating water. Moderately to highly dissected terrain is richer in potassium (Figures 11.13 – 11.16), for the same reasons explained above, in the case of calcium and magnesium.

11.2.7 SODIUM

In 80 % of samples, the extractable sodium content is between 0.05 and 0.38 $cmol_c kg^{-1}$ (11 and 87 mg kg^{-1}), and exchangeable sodium content is between 0 and 0.13 $cmol_c kg^{-1}$, which corresponds to values reported in literature. Extractable sodium content is strongly positively correlated with the electrical conductivity of the 2:5 soil:water suspension, and weakly positively correlated with exchangeable potassium content and exchangeable sodium content. Exchangeable sodium content is only correlated with extractable sodium

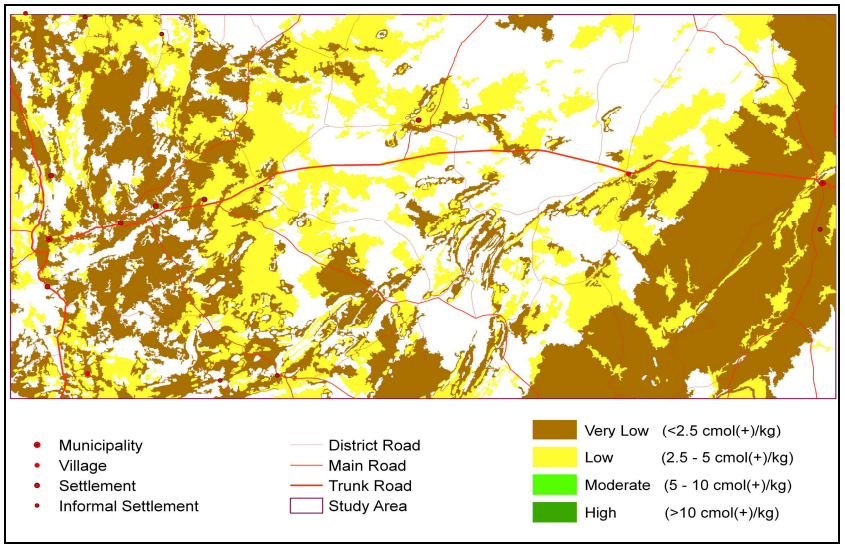

Figure 11.5. Spatial distribution of extractable calcium content ($cmol_c\ kg^{-1}$) of topsoil

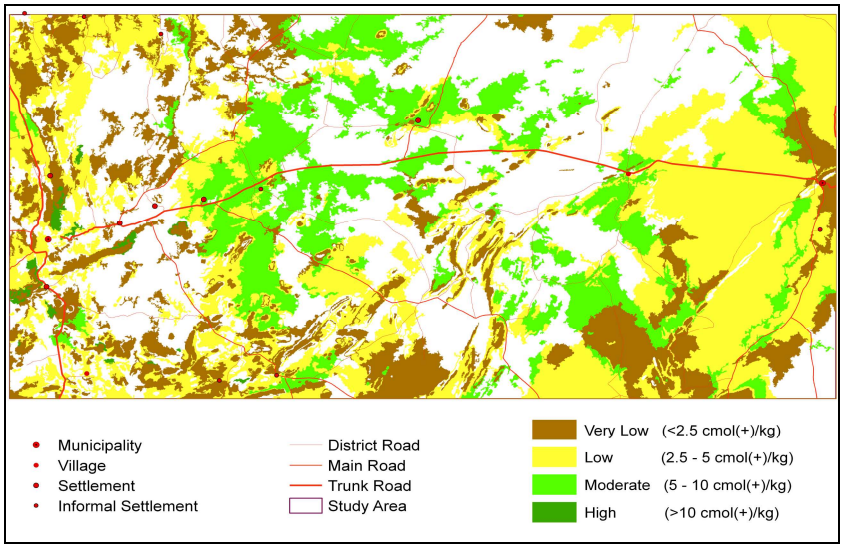

Figure 11.6 Spatial distribution of extractable calcium content ($cmol_c\ kg^{-1}$) of subsoil

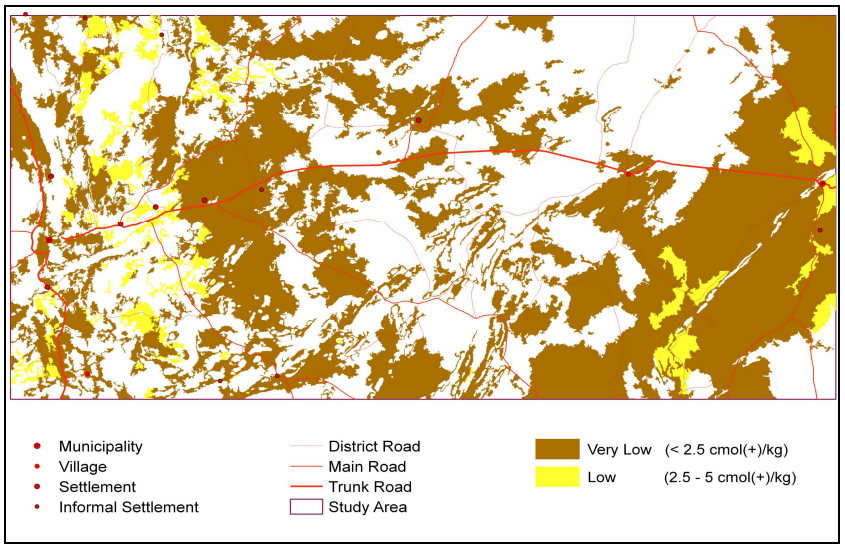

Figure 11.7. Spatial distribution of exchangeable calcium content ($cmol_c\ kg^{-1}$) of topsoil

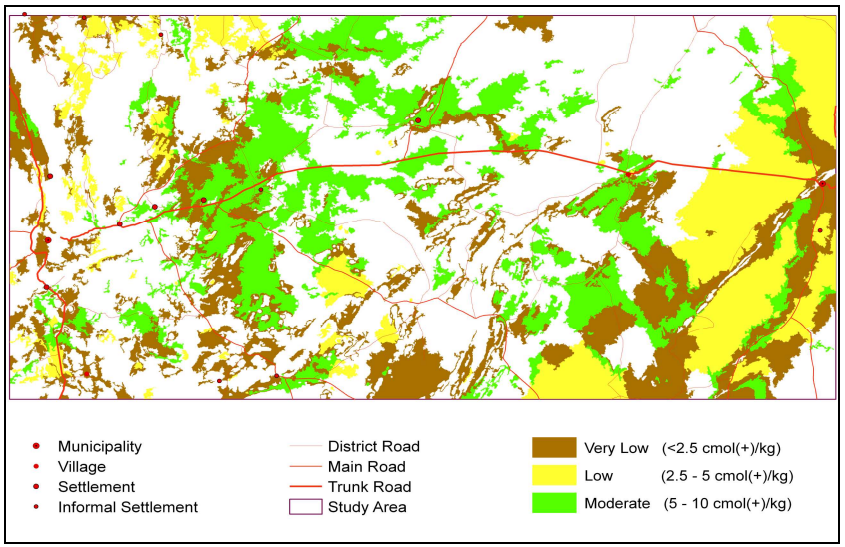

Figure 11.8 Spatial distribution of exchangeable calcium content ($cmol_c\ kg^{-1}$) of subsoil

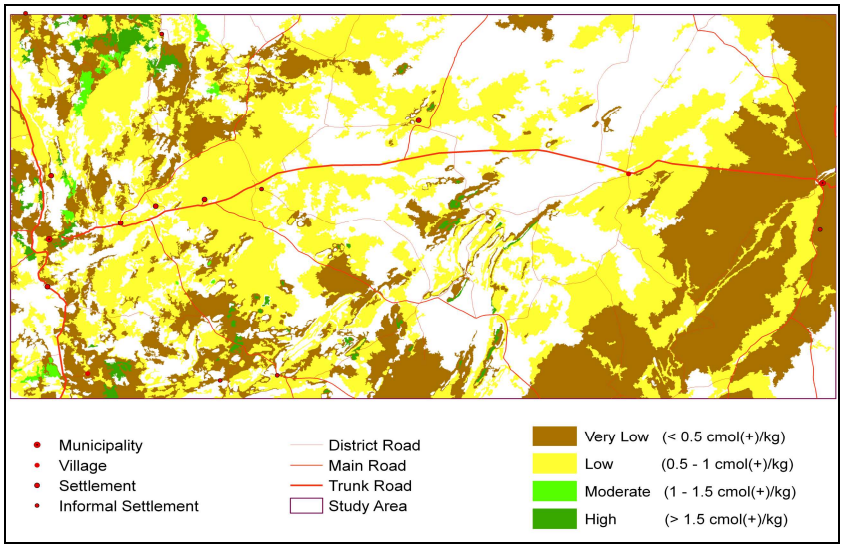

Figure 11.9. Spatial distribution of extractable magnesium content ($cmol_c\ kg^{-1}$) of topsoil

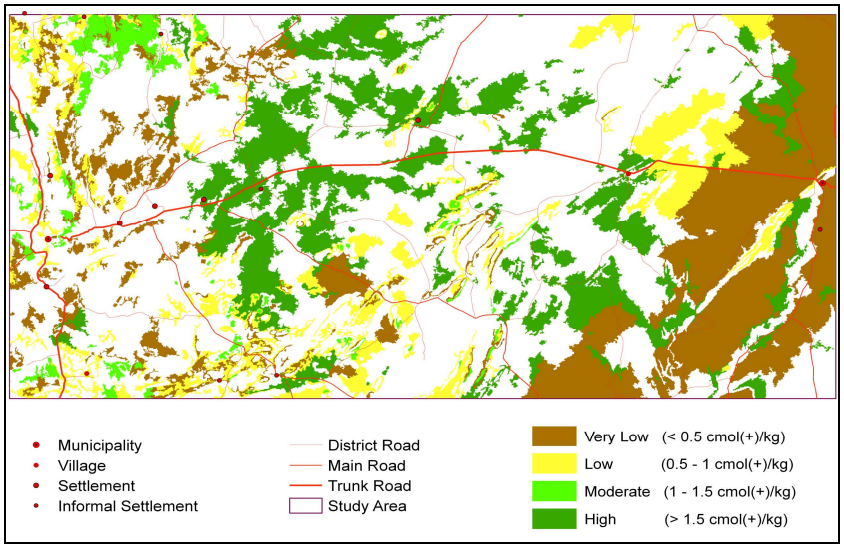

Figure 11.10 Spatial distribution of extractable magnesium content ($cmol_c\ kg^{-1}$) of subsoil

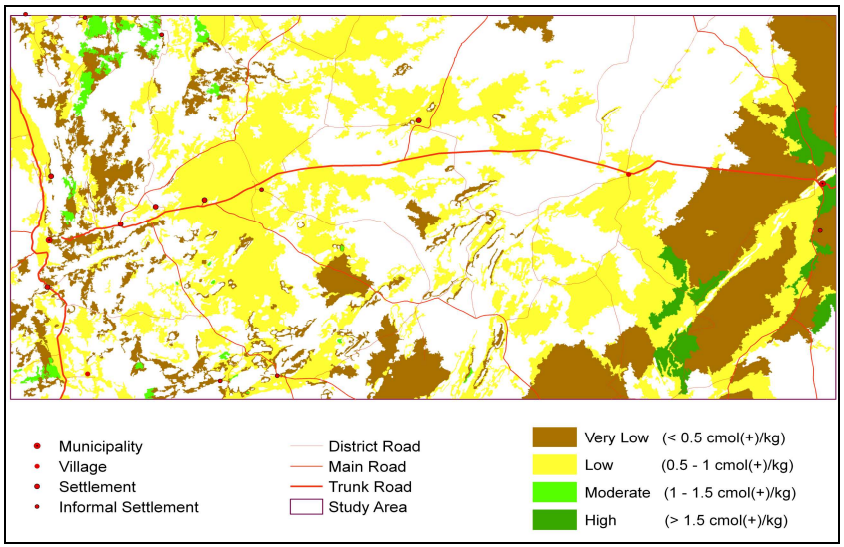

Figure 11.11. Spatial distribution of exchangeable magnesium content ($cmol_c\ kg^{-1}$) of topsoil

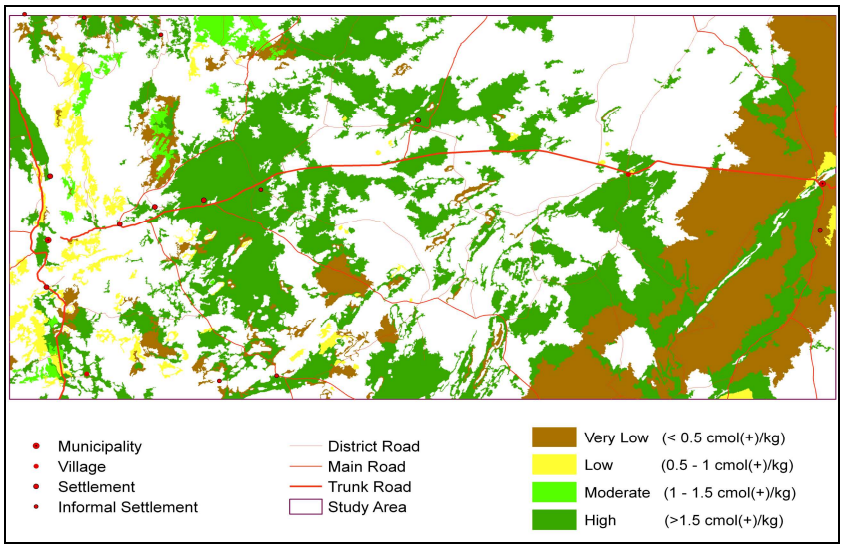

Figure 11.12. Spatial distribution of exchangeable magnesium content ($cmol_c\ kg^{-1}$) of subsoil

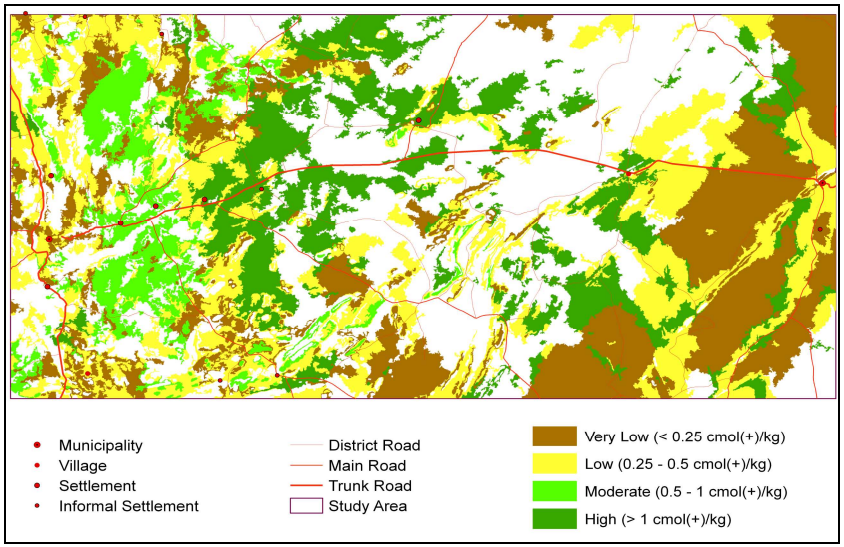

Figure 11.13. Spatial distribution of extractable potassium content ($cmol_c\ kg^{-1}$) of topsoil

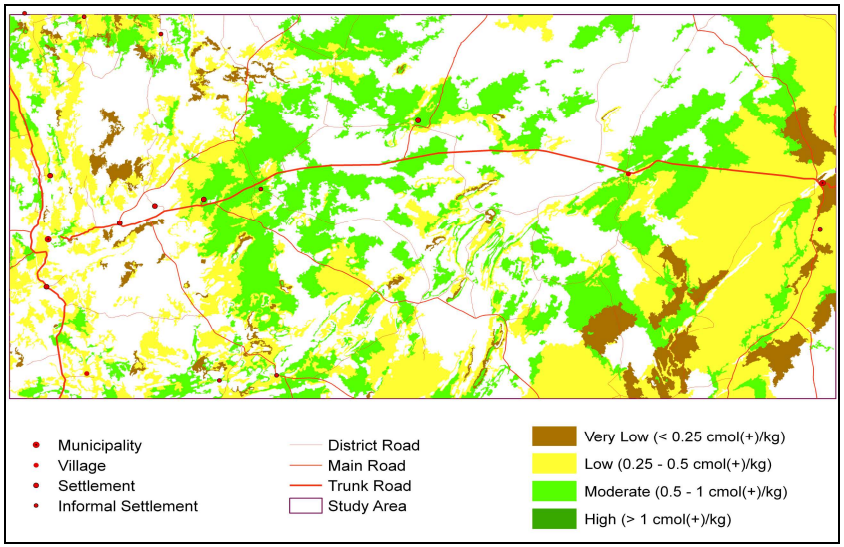

Figure 11.14 Spatial distribution of extractable potassium content ($cmol_c\ kg^{-1}$) of subsoil

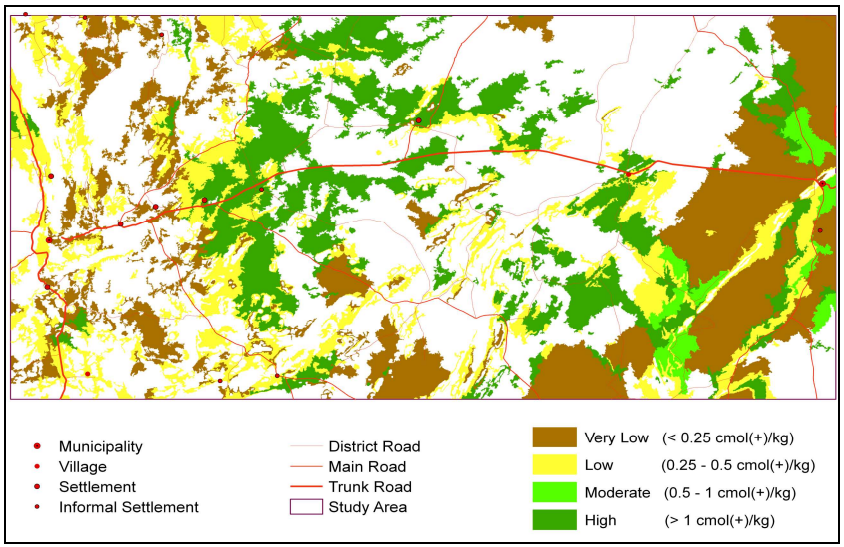

Figure 11.15. Spatial distribution of exchangeable potassium content ($cmol_c\ kg^{-1}$) of topsoil

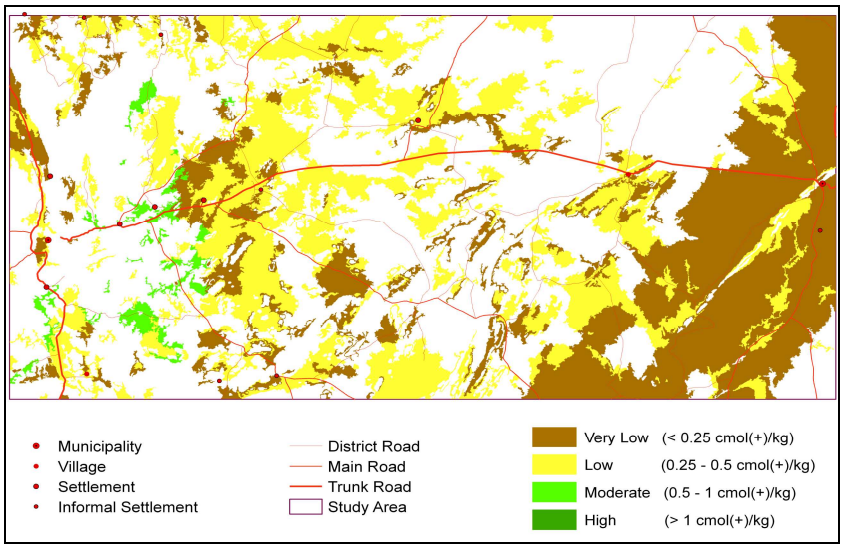

Figure 11.16 Spatial distribution of exchangeable potassium content ($cmol_c\ kg^{-1}$) of subsoil

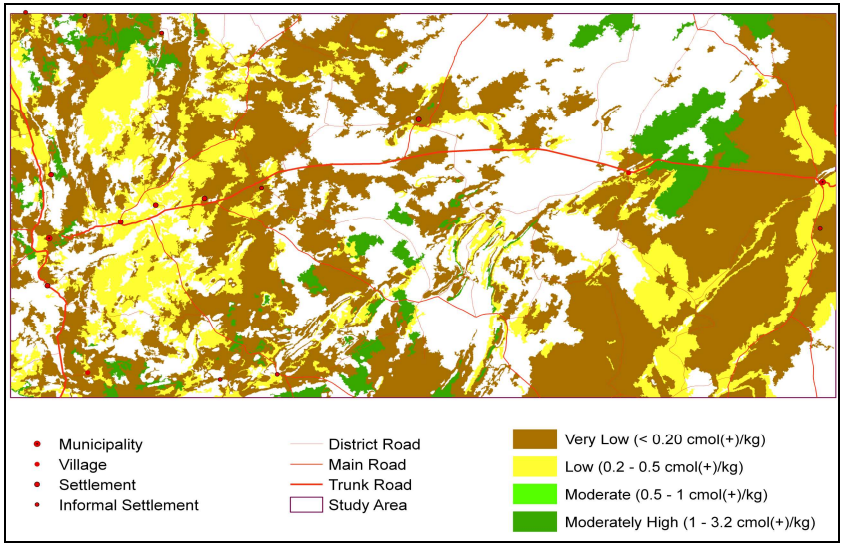

Figure 11.17. Spatial distribution of extractable sodium content ($cmol_c\ kg^{-1}$) of topsoil

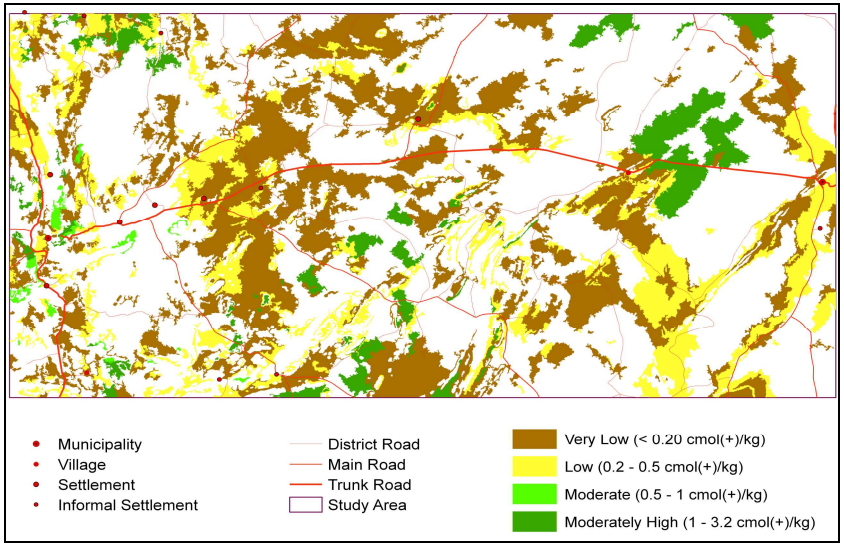

Figure 11.18 Spatial distribution of extractable sodium content ($cmol_c\ kg^{-1}$) of subsoil

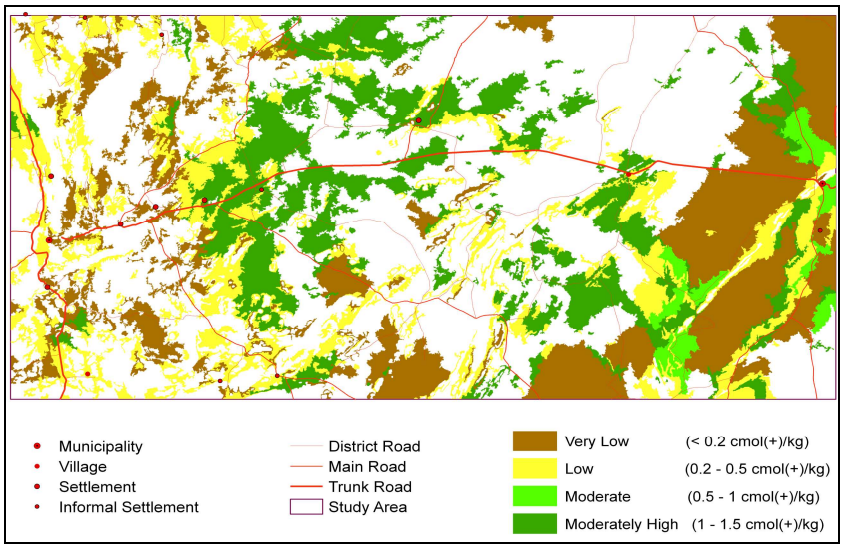

Figure 11.19. Spatial distribution of exchangeable sodium content ($cmol_c\ kg^{-1}$) of topsoil

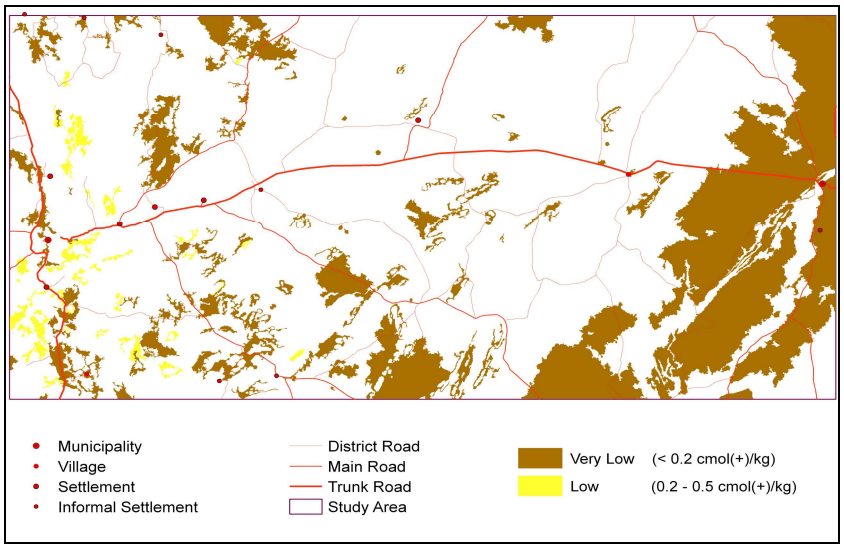

Figure 11.20 Spatial distribution of exchangeable sodium content ($cmol_c\ kg^{-1}$) of subsoil

content. Topsoil sodium content does not differ significantly from that of the subsoil, and no consistent pattern could be discerned for exchangeable sodium percentage with increase in depth. Extractable sodium content is lowest in Arenosols, and exchangeable sodium content lowest in Arenosols and Leptosols. The spread in values is so large for all the other soil types that no firm conclusions could be drawn. No clear relationships could be established between sodium concentrations and positions in the landscape. Extractable sodium is more abundant in moderately to highly dissected terrain, but there does not seem to be any pattern to exchangeable sodium content and degree of dissection of the landscape (Figures 11.17 – 11.20).

11.2.8 CATION EXCHANGE CAPACITY; SUM OF EXCHANGEABLE BASES; SUM OF EXTRACTABLE BASES

The mean ± 1 standard deviation is 3.57 ± 3.57 $cmol_c kg^{-1}$ for cation exchange capacity, 3.48 ± 3.61 for sum of exchangeable bases, and 4.53 ± 4.39 for sum of extractable bases. The CEC and the ∑ exchangeable bases (S-value) are virtually identical, which indicate the almost complete absence of exchangeable H^+ and Al^{3+} in the soil of the study area, as expected from a semi-arid climate. Topsoil CEC, ∑ exchangeable bases and ∑ extractable bases are lower than those of subsoil. The illuviation of clay in subsoil contributes more to the CEC (and exchangeable bases) than organic matter accumulation in the topsoil, due to the hot semi-arid climate of the study area. Low levels of biomass production and, subsequently, leaf litter and organic matter in the soil, combined with high rates of mineralisation of organic matter, means that exchange sites are provided to a relatively larger extent by clay than organic matter, when compared to temperate climate soils. Although leaching is lower than in tropical and temperate climates, there is some displacement of soluble bases towards deeper soil layers. As expected, CEC and the sums of extractable and exchangeable bases are lowest in sandy soils (and thus the Arenosols of the Kalahari), while being highest in loam and sandy clay loam. CEC, ∑ exchangeable bases and ∑ extractable bases increase with increasing pH. They are higher in the phyllosilicate-rich soils formed on schist of the Khomas Hochland than in the quartz-rich Kalahari sands and also higher in highly dissected terrain, relative to terrain with low degrees of dissection (Figures 11.21 – 11.22).

11.2.9 CA-, MG-, K AND NA SATURATION; BASE STATUS; BASE SATURATION

The majority of samples, namely 77.8 %, are eutrophic, with 16.7 % being mesotrophic and only 2.8 % being dystrophic. Calcium is the dominant cation in most soils, although there is a significant portion of soils in which magnesium is most abundant. The generalised ratio of Ca : Mg : K : Na for the whole study area is 61 : 29 : 16 : 3. Free calcium carbonate is abundant.

11.2.10 ELECTRICAL CONDUCTIVITY

None of the profiles were classified as saline. EC (2:5) is highest in Calci- and Leptosols, and lowest in Luvi-, Areno-, Rego- and Fluvisols. EC (saturated paste) is highest in Calci-, Cambi- and Leptosols, and lowest in Luvi- and Arenosols (Figures 11.23 – 11.24).

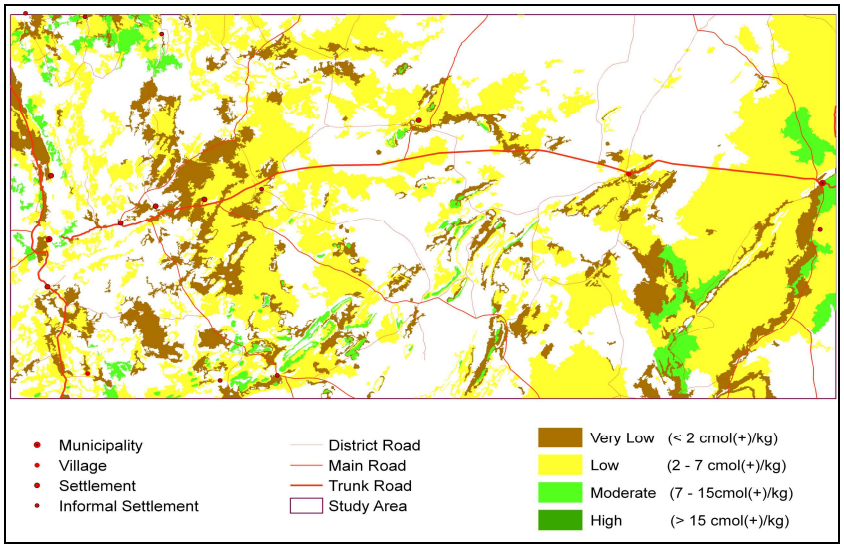

Figure 11.21. Spatial distribution of cation exchange capacity ($cmol_c\ kg^{-1}$) of topsoil

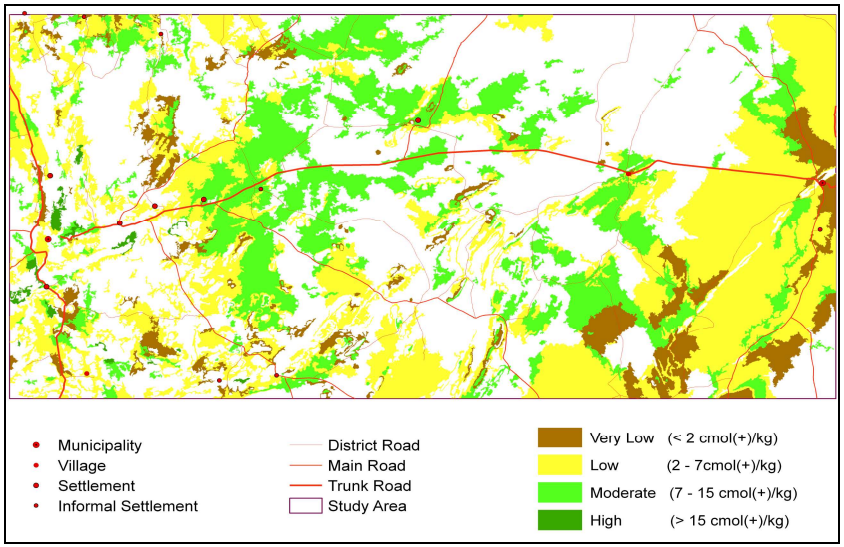

Figure 11.22. Spatial distribution of cation exchange capacity ($cmol_c\ kg^{-1}$) of subsoil

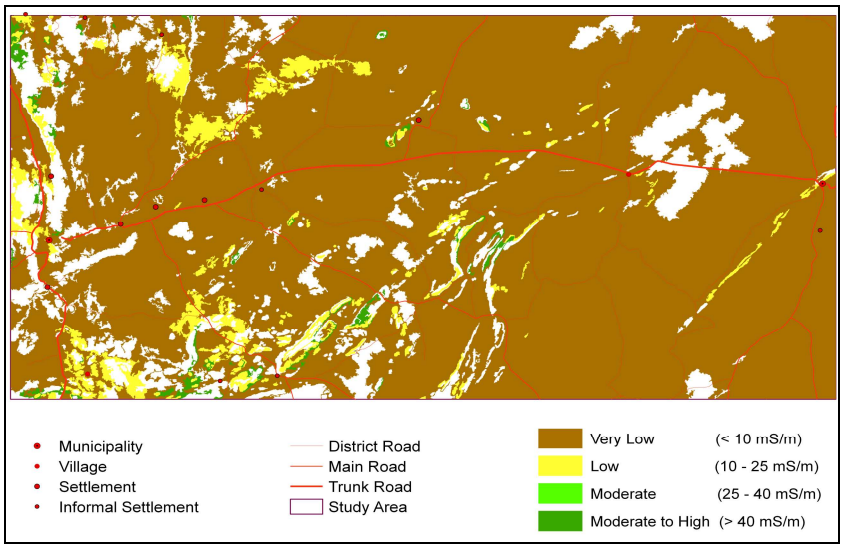

Figure 11.23. Spatial distribution of electrical conductivity (2:5) ($mS\ m^{-1}$) of topsoil

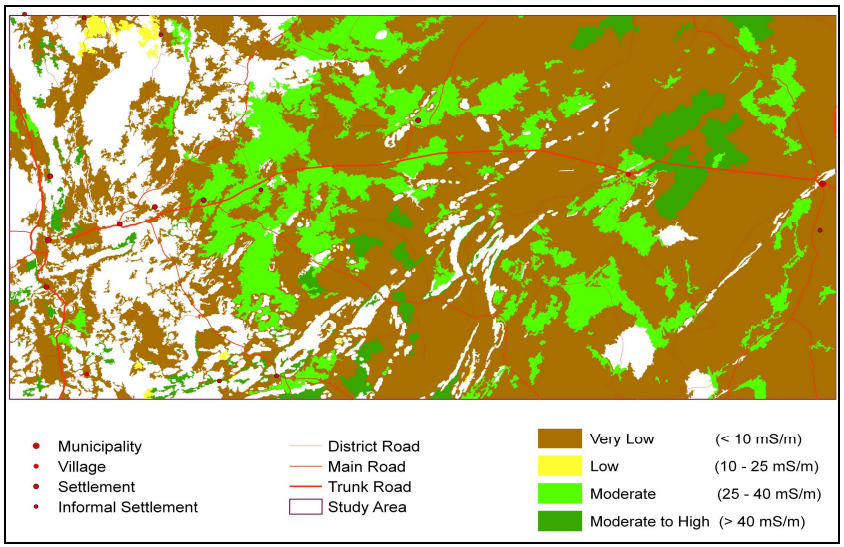

Figure 11.24. Spatial distribution of electrical conductivity (2:5) ($mS\ m^{-1}$) of subsoil

11.2.11 IRON

In 80 % of samples, the plant-available iron content is between 7.2 and 32.8 mg kg^{-1}. Iron is strongly positively correlated with manganese content and weakly positively correlated with both exchangeable and extractable magnesium and potassium content, phosphorus content, zinc content, copper content, silt content, clay content, available water, field capacity and saturation. It is negatively correlated with sand content, medium sand content and bulk density. There is no significant difference between iron concentrations in subsoil and topsoil (Figures 11.25 – 11.26). Iron is lowest in sand and loamy sand, in agreement with literature. Alluvial material is richest in iron, followed by colluvial material, while aeolian material is poorest. This goes together with the lithology and texture of the aeolian material, namely quartz-rich Kalahari sand. Young soils in the early stages of pedogenesis, Cambisols, and those showing signs of clay eluviation, Luvisols, are richer in iron than the sandy Arenosols and the Calcisols. Highly dissected terrain is richest in iron. In flat, almost flat and undulating landscapes, most iron is found in relatively lower landscape positions, where finer soil particles accumulate. Iron concentration slightly increases from pH 5.0 to 6.5, where after it gradually decreases to a minimum around pH 9.0

11.2.12 MANGANESE

In 80 % of samples, the plant-available manganese content is between 13.6 and 207.5 mg kg^{-1}, which is similar to literature reports from elsewhere in southern Africa. Manganese content is strongly positively correlated with iron content and weakly positively correlated with both exchangeable and extractable magnesium and potassium content, zinc content, copper content, clay content, field capacity, wilting point and saturation. It is weakly negatively correlated with sand content, medium sand content, saturated hydraulic conductivity and bulk density. Manganese concentrations are higher in subsoil than topsoil. It is lowest in sandy soils and highest in sandy clay loams. Alluvial material is richest in manganese, followed by colluvial material, while aeolian material is poorest. The latter goes together with the lithology and texture of the aeolian material, namely quartz-rich Kalahari sand. Cambisols are richest in manganese and Arenosols are poorest. Highly dissected terrain is richest in manganese. Manganese concentration increases gradually from pH 5.0 to 8.0, where after it decreases. In flat, almost flat and undulating landscapes, most manganese is found in relatively lower landscape positions, where finer soil particles accumulate (Figures 11.27 – 11.28).

11.2.13 ZINC

In 80 % of samples, the plant-available zinc content is between 0 and 1.80 mg kg^{-1}, which is similar to literature reports from other parts of southern Africa. Zinc is weakly positively correlated with copper, manganese, phosphorus and iron. Zinc concentrations are slightly higher in topsoil than subsoil. It is lowest in sandy soil. Alluvial material is richest in zinc, followed by colluvial material, while aeolian material is poorest. The latter goes together with the lithology and texture of the aeolian material, namely quartz-rich Kalahari sand. Cambisols and Calcisols are richer in zinc than Arenosols and Regosols. Highly dissected terrain is richest in zinc. Zinc concentration increases with pH up to pH 8, where after it drops. In flat, almost flat and undulating landscapes, most zinc is found in relatively lower landscape positions, where finer soil

particles accumulate (Figures 11.29 – 11.30).

11.2.14 COPPER

In 80 % of samples, the plant-available copper content is between 0 and 4.0 mg kg^{-1}, which is similar to literature reports from other parts of southern Africa. Copper is weakly positively correlated with pH, exchangeable and extractable magnesium content, sum of exchangeable and extractable bases, iron content, zinc content, manganese content, fluoride content, silt content, clay content, field capacity, saturation, available water and saturated hydraulic conductivity. It is weakly negatively correlated with sand content and bulk density. Copper concentrations are slightly higher in subsoil than topsoil. It is lowest in sandy soils and highest in sandy clay loams. Alluvial material is richest in copper, followed by colluvial material, while aeolian material is poorest. The latter goes together with the lithology and texture of the aeolian material, namely quartz-rich Kalahari sand. Cambisols are relatively rich in copper, while Arenosols are the poorest. Highly dissected terrain is richest in copper. Copper concentrations increase gradually with pH. In flat, almost flat and undulating landscapes, most copper is found in relatively lower landscape positions, where finer soil particles accumulate (Figures 11.31 – 11.32).

11.2.15 SOIL ORGANIC MATTER

Organic matter content of the study area soils ranges between 0.05 and 2.00 %, with 80 % of samples ranging between 0.25 and 1.20 %. This is considerably lower than values reported in literature, even for other southern African countries. It can be explained by the hot, semi-arid climate. Relatively low rainfall causes low plant biomass production, with subsequent low levels of plant litter. In the hot dry season, when vegetation cover is at its lowest, soil temperature regularly exceeds 50 oC in the study area. The consequence is a high rate of mineralisation. This is probably also the reason why only poor correlations were found with plant-available phosphorus content and sulfate, and none with nitrate and nitrite content. Weak positive correlations were found with plant-available phosphorus content, sulfate content and electrical conductivity, and a weak negative correlation with horizon depth. As expected, topsoil contained more soil organic matter than subsoil, due to topsoil enrichment by decaying plant material and animal excreta (Figures 11.33 – 11.34). Fluvisols, being soils that accumulate along drainage lines, are richest in SOM, most likely through transport and accumulation of organic particles by surface runoff from the surrounding slopes. Colluvial material also has relatively higher soil organic matter content than other parent materials, probably through the same mechanism.

11.2.16 PH

The pH distribution is close to normal, with 80 % of samples having pH (H_2O) of between 5.54 and 8.18, namely moderately acid to moderately alkaline (Figures 11.35 – 11.36). Strong positive correlations were found with fluoride content, sum of extractable and of exchangeable bases, exchangeable calcium content and cation exchange capacity. Weak positive correlations also exist with extractable calcium content, exchangeable magnesium content, copper content, presence of carbonates and the ratio of CEC to clay and

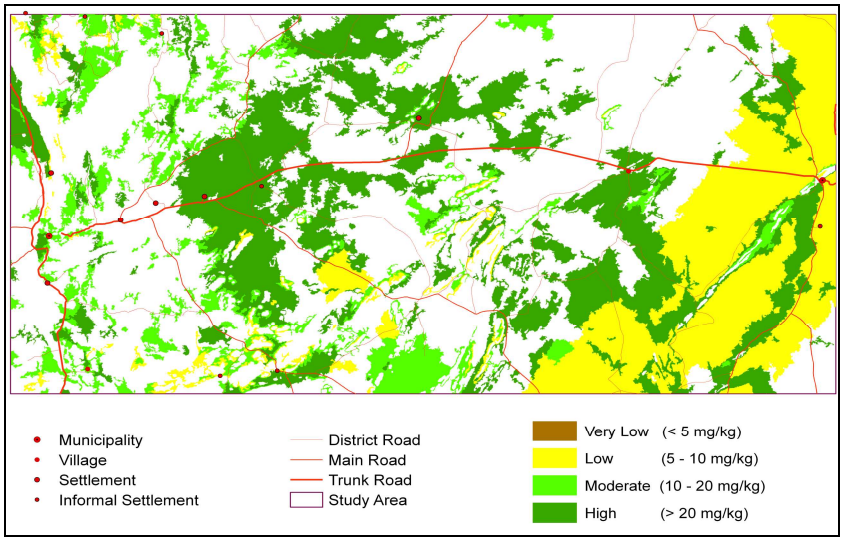

Figure 11.25. Spatial distribution of iron content (mg kg^{-1}) of topsoil

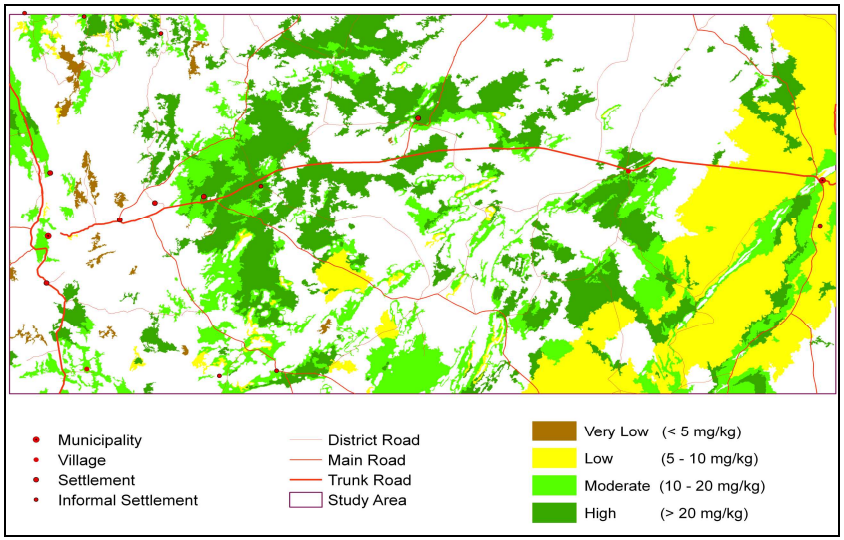

Figure 11.26. Spatial distribution of iron content (mg kg^{-1}) of subsoil

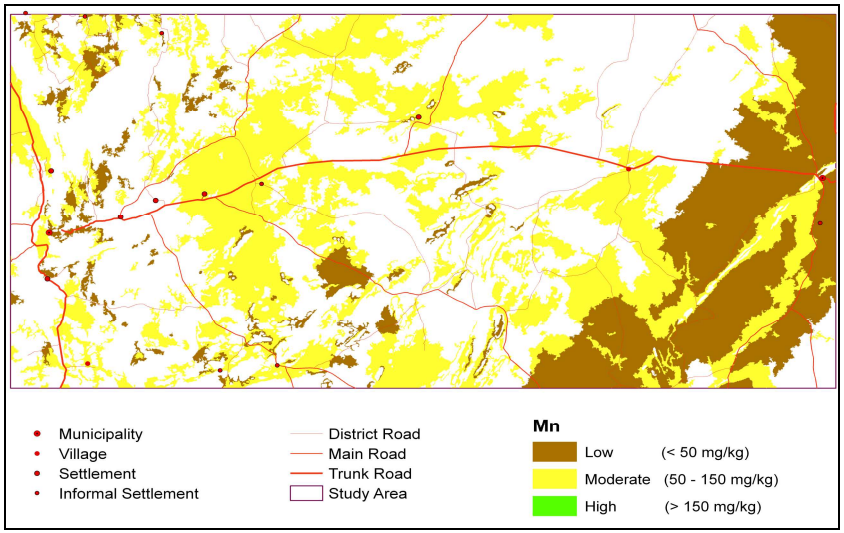

Figure 11.27. Spatial distribution of manganese content (mg kg^{-1}) of topsoil

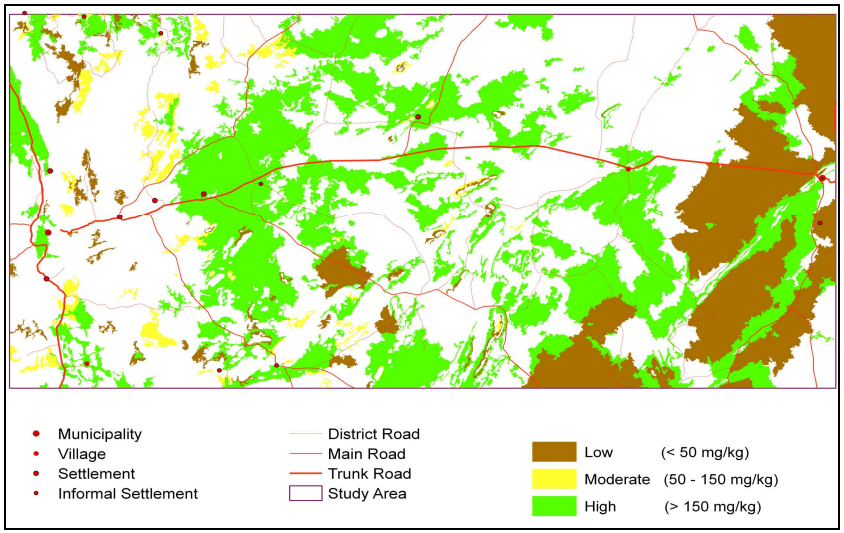

Figure 11.28. Spatial distribution of manganese content (mg kg^{-1}) of subsoil

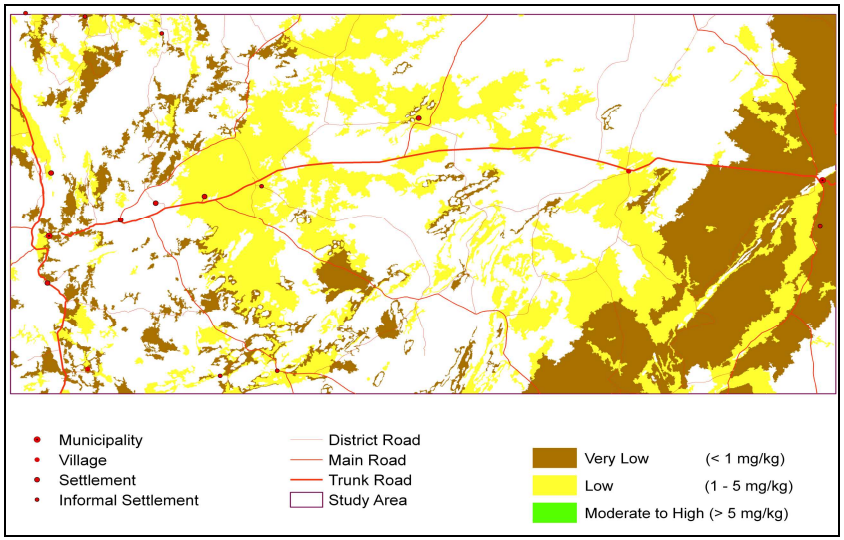

Figure 11.29. Spatial distribution of zinc content (mg kg^{-1}) of topsoil

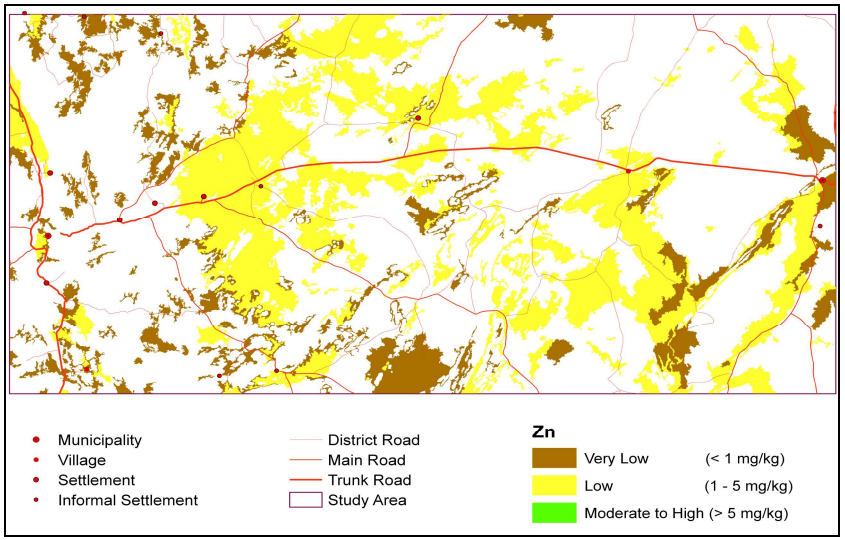

Figure 11.30. Spatial distribution of zinc content (mg kg^{-1}) of subsoil

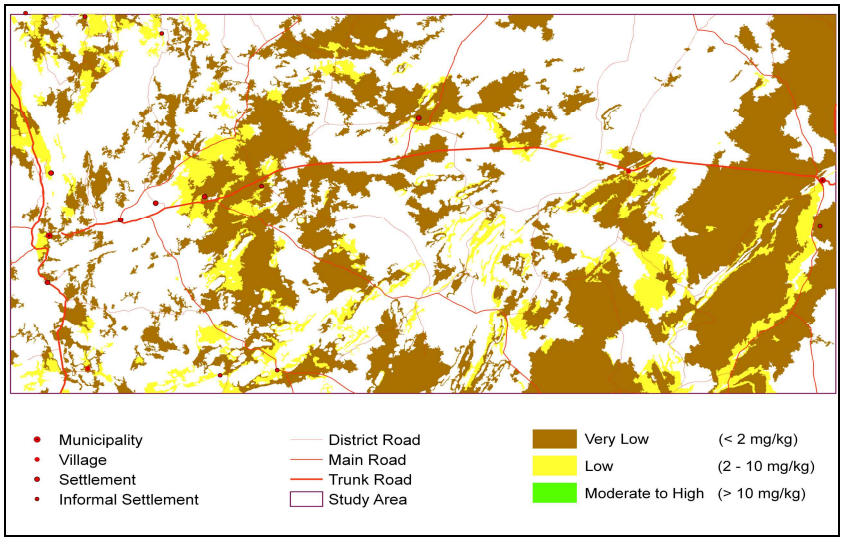

Figure 11.31. Spatial distribution of copper content (mg kg^{-1}) of topsoil

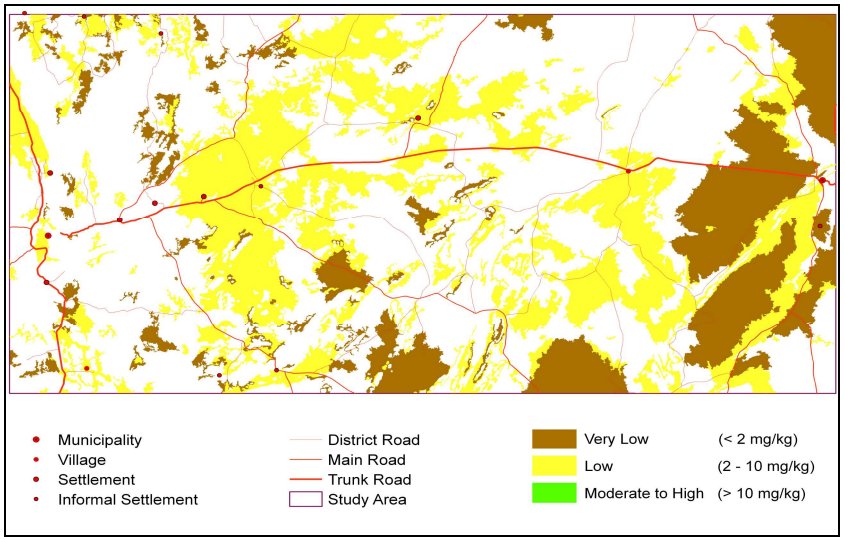

Figure 11.32. Spatial distribution of copper content (mg kg^{-1}) of subsoil

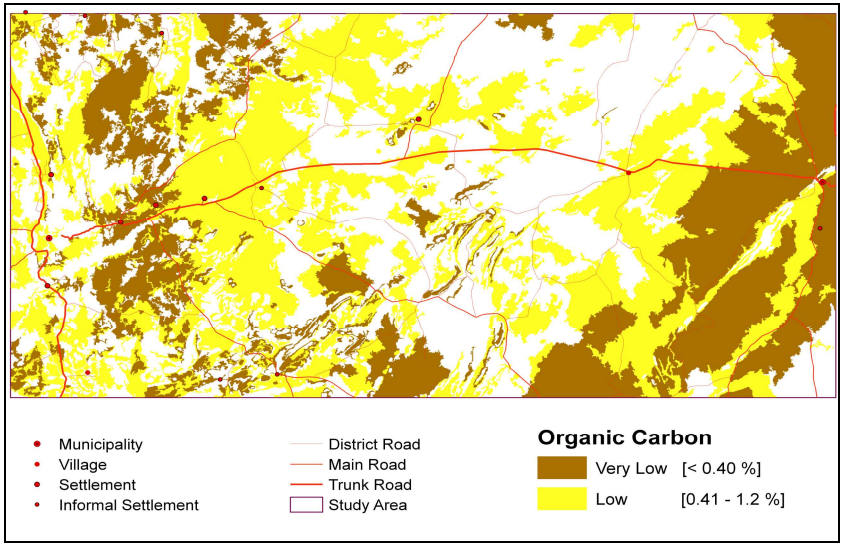

Figure 11.33. Spatial distribution of organic carbon content (%) of topsoil

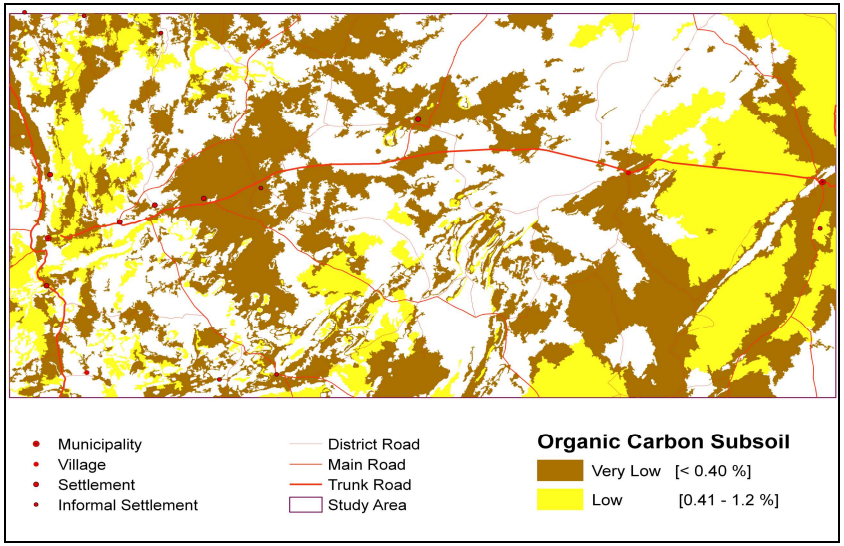

Figure 11.34. Spatial distribution of organic carbon content (%) of subsoil

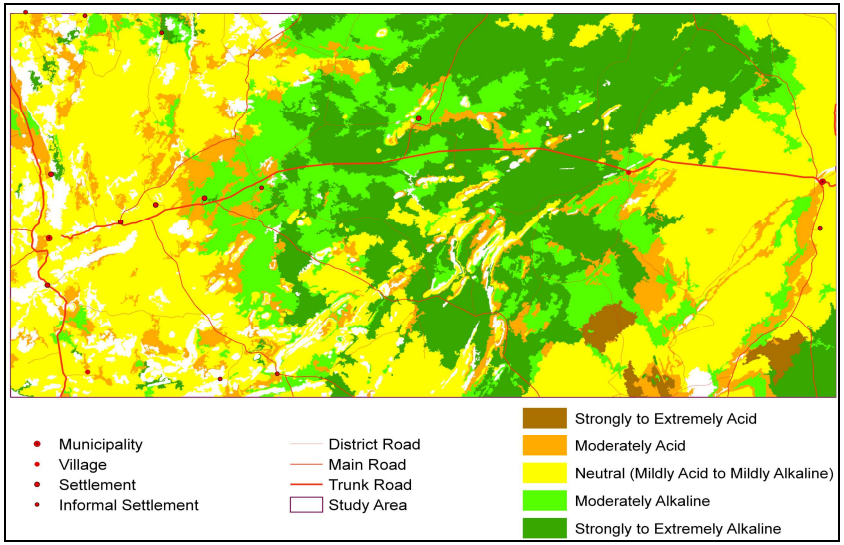

Figure 11.35. Spatial distribution of pH (H_2O) of topsoil

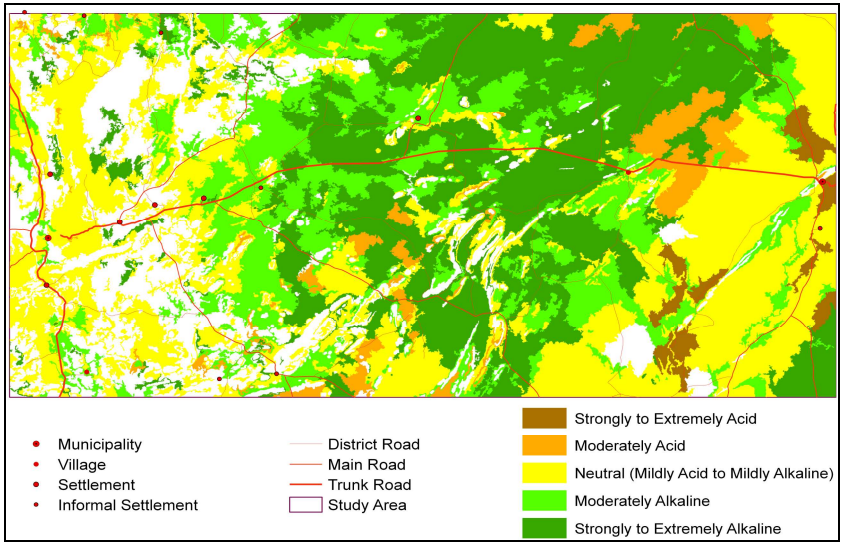

Figure 11.36. Spatial distribution of pH (H_2O) of subsoil

to clay plus silt, respectively. pH increases very slightly with depth, probably due to leaching of topsoil and accumulation of bases lower in the profile. The sandy Arenosols from the Kalahari are lowest in pH, as the result of leaching of bases from the topsoil, and the recorded values compare favourably with those from literature. Calcisols, by their very nature, are high in pH. Fluvisols also display high pH, most likely due to accumulation of bases along drainage channels as a result of both surface runoff and subsurface percolation of soil water. Soils formed on schist have relatively high pH as a result of the mineral composition of schist, while the quartz-rich Kalahari sands are slightly acidic. pH tends to increase with degree of dissection of the landscape. This could be ascribed to the fact that the highly dissected terrain of the study area occurs mainly on schist, quartzite and calcrete, whereas the less dissected areas, towards the east, are mainly covered with Kalahari sands.

11.2.17 PARTICLE SIZE

In 80 % of samples the sand content is between 60.3 and 89.7 %, silt content is between 4.6 and 25.2 %, and clay content is between 3.5 and 19.1 % (Figures 11.37 – 11.38). This agrees very well with values reported by other authors for locations close to the study area. The soils of the study area, thus, tend to be mainly sandy, sandy loam and loamy sand (Figures 11.39 – 11.40). This goes hand in hand with low water-holding capacity (Figure 11.46), low nutrient supply capacity, low organic matter levels, low susceptibility to water erosion, low levels of surface sealing, moderate susceptibility to wind erosion, good aeration and high rates of internal drainage. Primary minerals like quartz, feldspars and micas are highly prevalent in the study area. Sand content is strongly negatively correlated with silt, content clay content, exchangeable magnesium content, saturation, field capacity, available water and wilting point, while it is positively correlated with saturated hydraulic conductivity and bulk density. Silt content is strongly positively correlated with available water, less strongly with water saturation, field capacity and saturated hydraulic conductivity, and strongly negatively correlated with sand content and bulk density. Silt content is weakly positively correlated with coarse sand content, CEC, sum of exchangeable bases, exchangeable magnesium content and copper content, and weakly negatively correlated with very fine sand content. Clay is strongly negatively correlated with sand content, saturated hydraulic conductivity and bulk density. It is strongly positively correlated with exchangeable magnesium content, saturation, field capacity, wilting point, and weakly positively correlated with CEC, extractable magnesium, calcium and potassium content, exchangeable potassium content, sum of both extractable and exchangeable bases, manganese content, iron content, copper content and fluoride content. Topsoil contains more sand, less silt and less clay than subsoil, caused by eluviation of the finer material. Arenosols are, as per definition, poor in silt and clay, and high in sand content. Luvisols are relatively rich in silt and clay, but poor in sand, while Fluvisols are rich in silt, but poor in clay. The silt and clay content increases with an increase in the degree of dissection of the landscape, while the opposite is true for sand. Flat and almost flat areas have the highest sand content and lowest silt content of the different topographic classes, while the opposite is true for undulating, rolling, hilly and mountainous areas. Silt and clay content increases, and sand decreases, in the order aeolian, residual (weathered in situ), colluvial and alluvial material. Finer material is preferentially accumulated in colluvium and alluvium, and removed by wind erosion from aeolian material. Quartz-rich Kalahari sand have high percentages of sand-sized particles, while soils formed on schist are relatively rich in clay and silt sized particles.

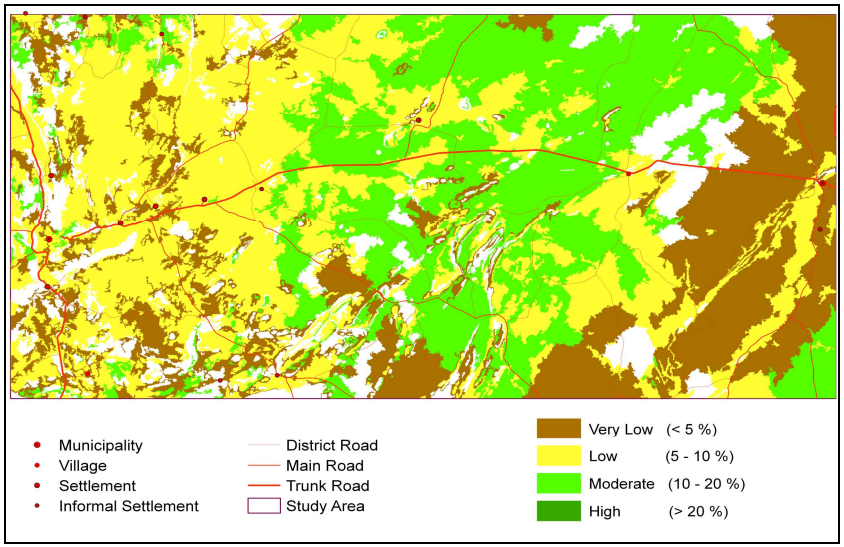

Figure 11.37. Spatial distribution of clay content (%) of topsoil

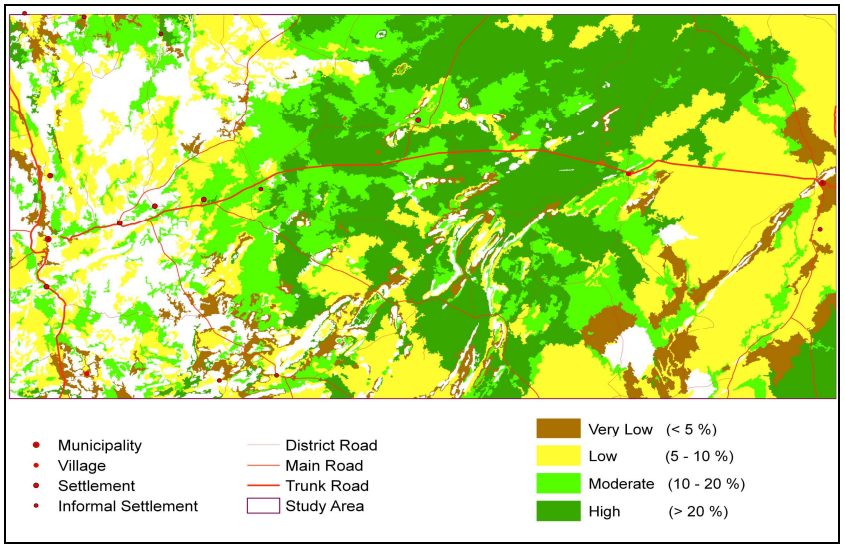

Figure 11.38. Spatial distribution of clay content (%) of subsoil

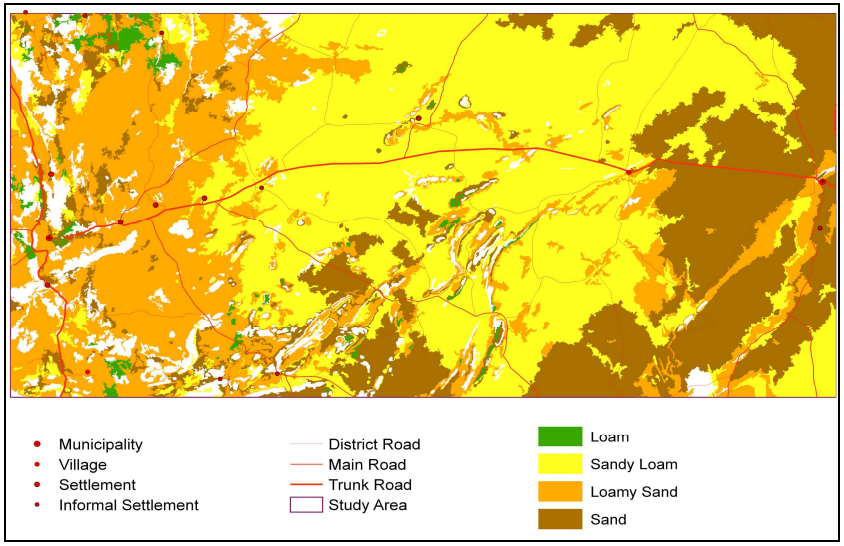

Figure 11.39. Spatial distribution of textural classes of topsoil

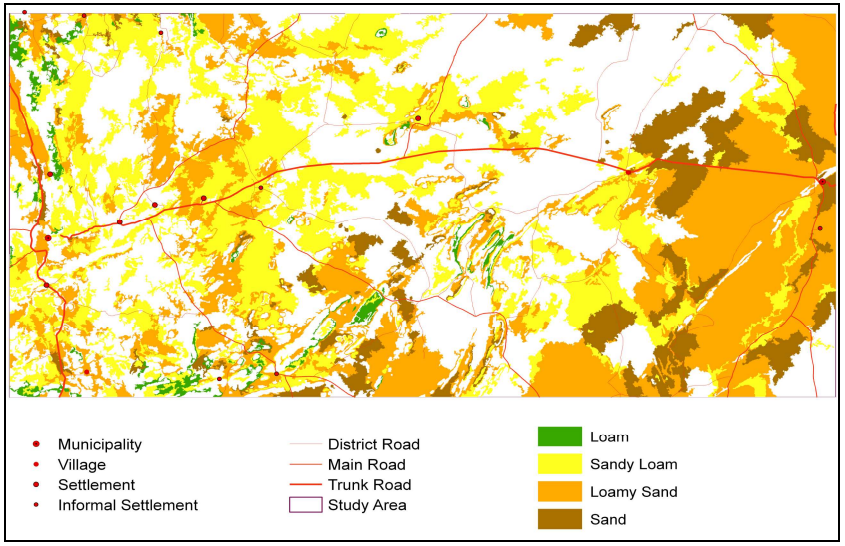

Figure 11.40. Spatial distribution of textural classes of subsoil

In 80 % of samples, the coarse sand content ranges from 3.5 to 34.5 %, the medium sand content from 20.5 to 37.3 %, the fine sand content from 38.7 to 54.5 % and the very fine sand content from 0 to 12.9 %. The fine sand fraction, thus, dominates, with very fine sand being least abundant. Topsoil contains relatively more coarse sand and less very fine sand than subsoil, most probably due to eluviation of the finer material. Fluvisols have a relatively high percentage of coarse and medium sand compared to the other soil groups, low fine sand percentage and no measurable very fine sand fraction. Arenosols are rich in medium, fine and very fine sand, but poor in coarse sand. Cambi-, Rego and Luvisols are also rich in fine and very fine sand fractions, and poor in coarse sand fractions. Calcisols have a relatively high percentage of very fine sand and low percentage of coarse sand, but a wide range of values for medium and fine sand. Soils formed from schist contain more coarse sand, fine sand and very fine sand, and less medium sand than those formed from Kalahari sand. The coarse sand content increases while fine and very fine sand content decreases with degree of dissection of the landscape. Coarse sand content is lowest when the landscape is flat or almost flat, while the opposite is true for fine and very fine sand content.

11.2.18 SEALING AND CRUSTING

Instances of sealing, crusting and hardening occur sporadically in the study area. Cracking is only found in pans, while self-mulching is not evident. No highly instable soils were encountered in the study area.

11.3 FERTILITY

The fertility status of a soil is to a large degree determined by the topsoil characteristics. While the more stable subsoil properties are emphasised in most soil taxonomic classification systems, the topsoil is usually more important in terms of ecology, food production, management practices and degradation control. Fertility is normally expressed as a function of soil organic matter, cation exchange capacity, base status and the amount of extractable phosphorus, potassium, calcium and magnesium (Bühmann, Beukes and Turner, 2006).

In general, the soils of the study area would be considered unsuitable to marginally suitable for rainfed crop production. However, the study area is climatologically unsuited for rainfed crop production, so the question of soil fertility for this landuse does not arise. The land flourishes under a system of extensive livestock production on large farms, where grazing is carefully managed. The natural vegetation has adapted throughout the aeons to the soils and climate. Species that are specifically adapted to low soil nutrient and soil water levels have established themselves, and are exploiting the niches provided by variations in the landscape, parent material and soils.

Figure 11.41 shows, in green, where topsoil pH is between 5.5 and 7.8, organic carbon content is above 0.5 % and plant-available phosphorus content is above 1 mg kg^{-1}. These would indicate the relatively more fertile soils. Areas where this combination of criteria is not met, where soils are relatively less fertile, are indicated in brown. Where insufficient analytical data were available, or inconsistency between data from different

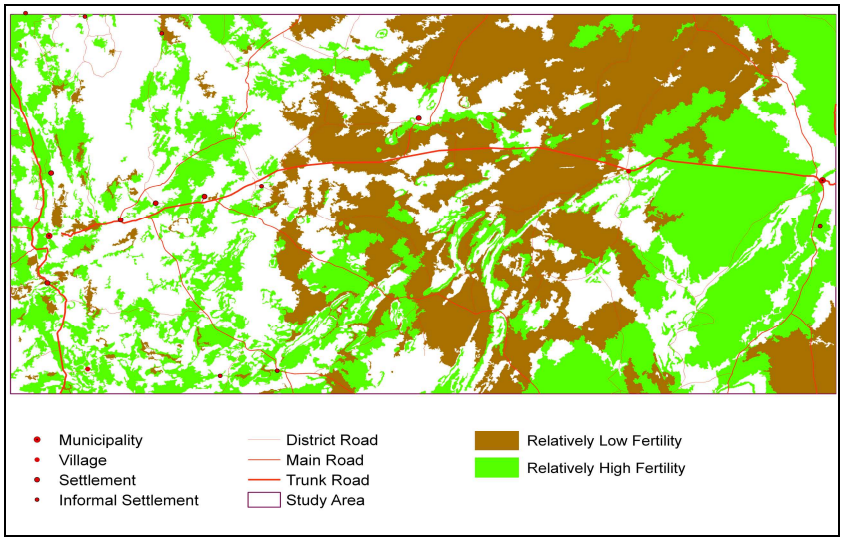

Figure 11.41. Spatial distribution of general fertility of topsoil

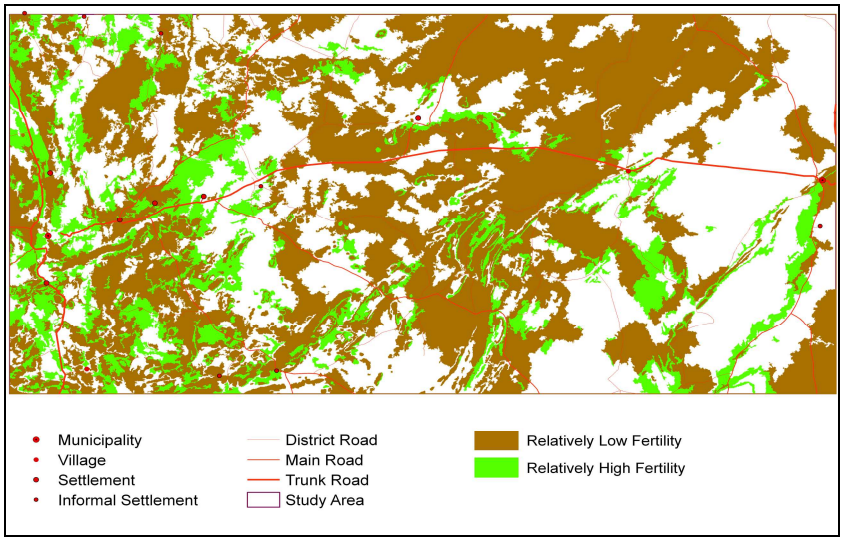

Figure 11.42. Spatial distribution of general fertility of subsoil

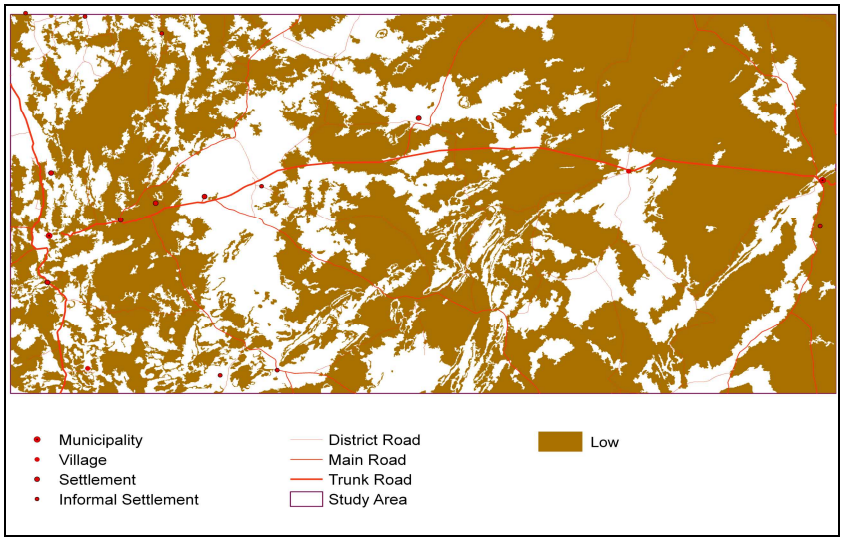

Figure 11.43. Spatial distribution of micronutrient fertility of topsoil

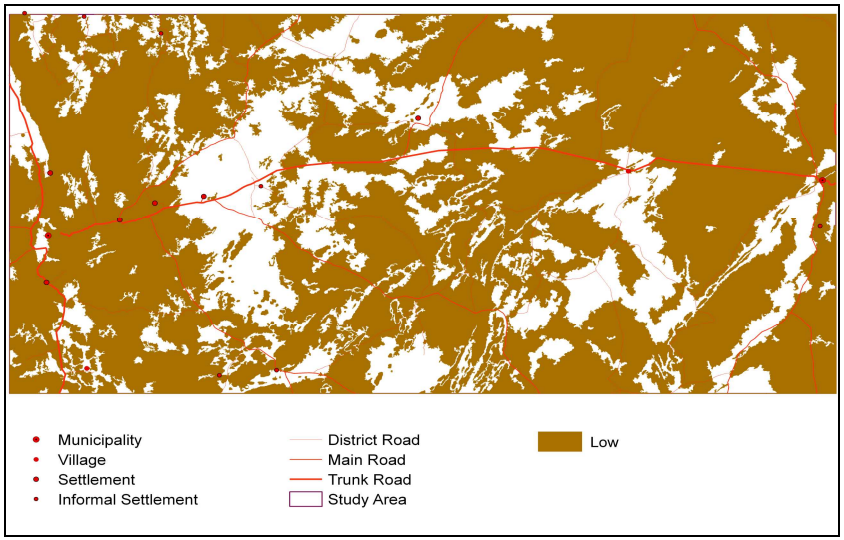

Figure 11.44. Spatial distribution of micronutrient fertility of subsoil

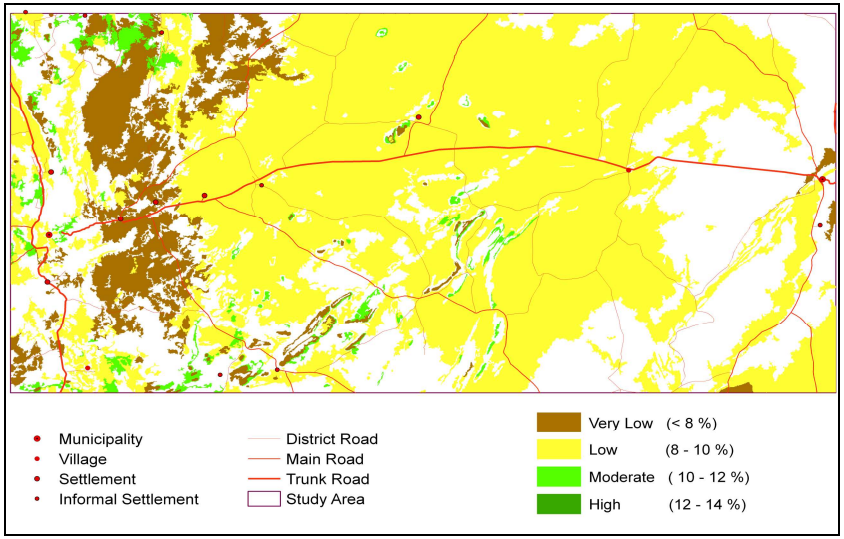

Figure 11.45. Spatial distribution of water-holding capacity (%) of topsoil

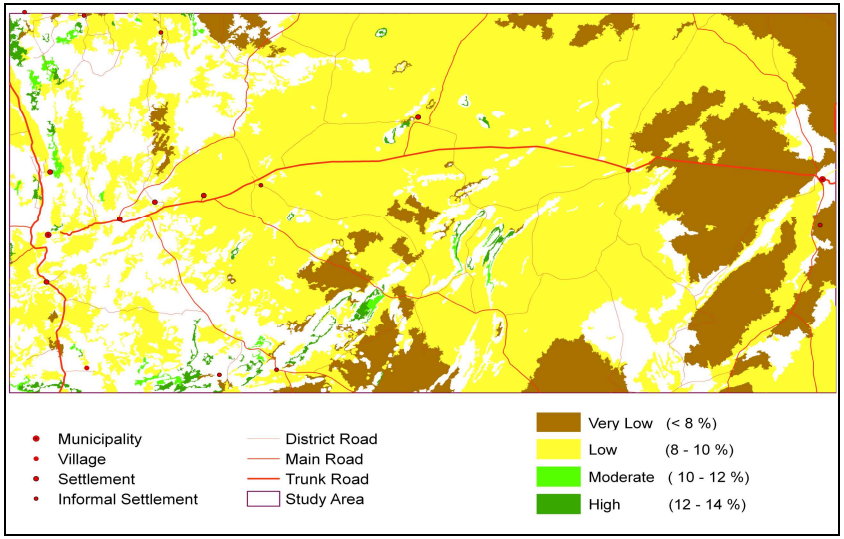

Figure 11.46. Spatial distribution of water-holding capacity (%) of subsoil

profiles within terrain units exists, extrapolation could not be done. These areas are indicated in white. Figure 11.42 is a similar combination of soil characteristics indicating relative fertility of subsoil, but the organic carbon requirement was replaced by cation exchange capacity of more than 1 $cmol_c\ kg^{-1}$.

Figures 11.43 – 11.44 were also constructed in a similar fashion. No areas met the criteria for moderate (Fe 10 – 20 mg kg^{-1}; Mn 50 – 150 mg kg^{-1}; Zn 1 – 5 mg kg^{-1}; Cu 2 – 10 mg kg^{-1}) and high (Fe > 20 mg kg^{-1}; Mn > 150 mg kg^{-1}; Zn > 5 mg kg^{-1}; Cu > 10 mg kg^{-1}) levels of micronutrients, so only areas with low (Fe ≤ 10 mg kg^{-1}; Mn ≤ 50 mg kg^{-1}; Zn ≤ 1 mg kg^{-1}; Cu ≤ 2 mg kg^{-1}) micronutrient levels are shown in brown.

Figures 11.45 – 11.46 show the water-holding capacity of the various terrain units, as calculated with pedotransfer functions (Hydraulic Properties Calculator website, based on the equations of Saxton *et al.*, 1986) using particle size distribution data. In the Khomas Hochland the plant-available water is limited by soil depth and in the Kalahari by soil texture. The transition zone has a somewhat better water-holding capacity, but it is still very low when compared to arable soils of temperate, sub-humid and humid zones elsewhere in southern Africa.

11.4 CONCLUSIONS

A number of chemical and physical characteristics of Namibian soils in a 22 790 km^2, two degree-square block between 17 – 19 ^oE and 22 – 23 ^oS in eastern central Namibia, had been investigated, and the fertility status established (Figures 11.41 – 11.44). The site and analytical information is available in digital format as spreadsheets and in a geographical information system, and in a variety of digital and printed maps.

The soils of the study area are very poor in organic matter, and thus in nitrogen, phosphorus and sulfur. Towards the west, where the high degree of dissection of the landscape allows fresh schistose parent material to be exposed to the elements, there is a source of nutrients, especially bases. The rate of weathering is, however, very slow as a result of low rainfall. Towards the east, where deep Kalahari sands with high quartz content dominate, deep-rooted plants are the main medium of bringing nutrients to the surface. Most soils are neither too alkaline nor too acid. Base status is high.

Although the fertility status is low, soil health is reasonably good and the natural vegetation has adapted to the soils and climate. At present, these remain in a healthy balance, with the exception of a few overgrazed and trampled farms and communal areas. The present climate does not permit rainfed agriculture, but if that should change or enough groundwater be available for irrigation, care will have to be taken when managing the soil. Conservation tillage methods, mulching, rotations with legume cover crops, incorporation of crop residues, application of efficient micro-organisms and drip irrigation would be advisable.

The methodology followed to delineate terrain units, with a combination of procedures involving digital elevation data and satellite imagery, seems to work well in the Namibian landscape. This study thus served as a successful proof-of-concept for the methodology, which can in future be rolled out for the remainder of the country.

TABLE OF AUTHORITIES

PRIMARY AUTHORITIES

AEZ Programme. (1999). PRELIMINARY AGRO-ECOLOGICAL ZONES. 69 pages. Addendum to *Agricola* 1998/1999. Agro-ecological Zoning Programme, Directorate of Agricultural Research and Training, Ministry of Agriculture, Water and Rural Development, Windhoek, Namibia.

Allison, L.E. and Moodie, C.D. (1965). CARBONATE. In: Black, C.A. (ed.), Methods of soil analysis, *Agronomy* 9: 1379–1396. American Society of Agronomy, Madison, USA.

Baker, D.E. (1972). SOIL CHEMISTRY OF MAGNESIUM. p. 1–39. In: Jones, J.B. (Jr.), Blount, M.C. and Wilkinson, S.R. (eds.), Magnesium in the environment: soils, crops, animals and man. Taylor County Publ. Co., Reynolds, USA.

Barber, S.A. (1994). SOIL NUTRIENT BIOAVAILABILITY – A MECHANISTIC APPROACH. 2nd edition. Wiley Interscience, John Wiley and Sons, Hoboken, New Jersey, USA.

Barnes, J.I. and De Jager, J.L.V. (1996). ECONOMIC AND FINANCIAL INCENTIVES FOR WILDLIFE USE ON PRIVATE LAND IN NAMIBIA AND IMPLICATIONS FOR POLICY. *South African Journal of Wildlife Research* 26(2): 37–46.

Bertram, S. and Broman, C.M. (1999). ASSESSMENT OF SOILS AND GEOMORPHOLOGY IN CENTRAL NAMIBIA. Minor Field Studies 71, 66 pages. Swedish University of Agricultural Sciences, Uppsala, Sweden.

Bertram, S. and Kempf, J. (2002). SOILS OF THE NEUDAMM HIGHLANDS, NAMIBIA – NEW APPROACHES TO SOIL CLASSIFICATION IN SEMI-ARID REGIONS. *Würzburger Geographische Arbeiten* 97: 59–84. Würzburg, Germany.

Bester, F.V. (1988). DIE BEPALING VAN DIE GRASPRODUKSIE VAN NATUURLIKE VELD. *Agricola* 6: 26-30.

Bester, F.V. (1996). BUSH ENCROACHMENT: A THORNY PROBLEM. *Namibia Environment* 1: 175–177.

Bester, F.V. (1997a). DEGREE OF NATURAL DIE-BACK OF BLACK THORN (*ACACIA MELLIFERA*) AND REGENERATION: SEEDLING ESTABLISHMENT. *Proceedings of the National Annual Agriculture Research Reporting Conference*, 19–21 August 1997, Windhoek, Namibia.

Bester, F.V. (1997b). REGENERATION OF BUSH ON BUSH-ERADICATED SITES IN THE THORN TREE SAVANNA. *Proceedings of the National Annual Agriculture Research Reporting Conference*, 19–21 August 1997, Windhoek, Namibia.

Bester, F.V. (1999a). MAJOR PROBLEM BUSH SPECIES AND BUSH DENSITIES IN NAMIBIA. *Agricola*, 10: 1–3.

Bester, F.V. (1999b). GRAZING REGISTER BASED ON THE BIOMASS CONCEPT. *Agri-Info* 1999: 10–12.

Bester, F.V. (2003). GRAZING REGISTER BASED ON THE BIOMASS CONCEPT. *Spotlight on Agriculture* 67, May 2003. Ministry of Agriculture, Water and Rural Development. Windhoek, Namibia.

Bethune. S., Griffin, M. and Joubert, D.F. (2004). NATIONAL REVIEW OF INVASIVE ALIEN SPECIES, NAMIBIA. Consultancy report for the Southern Africa Biodiversity Support Programme, Ministry of Environment and Tourism, Windhoek, Namibia.

Blackmer, A.M. (2000). BIOAVAILABILITY OF NITROGEN. p. D3–D18. In: Sumner, M.E. (ed.), Handbook of soil science. CRC Press, Taylor and Francis Group, Boca Raton, Florida, USA.

Blevins, D.G. (1994). UPTAKE, TRANSLOCATION AND FUNCTION OF ESSENTIAL MINERAL ELEMENTS IN CROP PLANTS. p. 259–275. In: Boote, K.J. *et al*. (eds.), Physiology and determination of crop yield. American Society of Agronomy, Madison, USA.

Bloom, P.R. (2000). SOIL pH AND pH BUFFERING. p. B333–B352. In: Sumner, M.E. (ed.), Handbook of soil science. CRC Press, Taylor and Francis Group, Boca Raton, Florida, USA.

Blümel, W.D. (1991). KALKKRUSTEN - IHRE GENETISCHE BEZIEHUNGEN ZU BODENBILDUNG UND ÄOLISCHER SEDIMENTATION. *Geomethodica* 16: 169–197. Basel, Switzerland.

Bower, C.A. and Wilcox, L.V. (1965). SOLUBLE SALTS. p. 933–951. In: Black, C.A. (ed.), Methods of soil analysis. *Agronomy* No. 9, American Society of Agronomy, Madison, USA.

Brady, N.C. and Weil, R.R. (2008). THE NATURE AND PROPERTIES OF SOILS. 14th edition. 992 pages. Prentice Hall, New Jersey, USA.

Bruce, R.C. (1999). CALCIUM. p. 247–254. In: Peverill, K.I., Sparrow, L.A. and Reuter, D.J. (eds.), Soil analysis: an interpretation manual. CSIRO Publishing, Collingwood, Australia.

Bühmann, C., Beukes, D.J. and Turner, D.P. (2006). PLANT NUTRIENT STATUS OF SOILS OF THE LUSIKISIKI AREA, EASTERN CAPE PROVINCE. *S. Afr. J. Plant Soil* 23(2), 93–98.

Buß, H.-J. (2006). LAND USE OPTIONS FOR NAMIBIAN FARMS – OPTIMAL MANAGEMENT STRATEGIES PROPOSED BY BIOECONOMIC MODELS. 201 pages. Wissenschaftsverlag Vauk Kiel KG. Kiel, Germany.

Camberato, J.J. and Pan, W.L. (2000). BIOAVAILABILITY OF CALCIUM, MAGNESIUM, AND SULPHUR. p. D53–D69. In: Sumner, M.E. (ed.), Handbook of soil science. CRC Press, Taylor and Francis Group, Boca Raton, Florida, USA.

Clarkson, D.T. and Hanson, J.B. (1980). FACTORS AFFECTING MINERAL ACQUISITION OF HIGHER PLANTS. *Annual Review of Plant Physiology* 21: 101–109.

Coetzee, M.E. (1998). GROWING PERIOD ZONES OF NAMIBIA. *Agri-Info.* Ministry of Agriculture, Water and Rural Development, Windhoek, Namibia.

Coetzee, M.E. (2001a). NAMSOTER – A SOTER DATABASE FOR NAMIBIA. Report. AEZ Programme, Ministry of Agriculture, Water and Rural Development, Windhoek, Namibia.

Coetzee, M.E., Beernaert, F. and Calitz, A.J. (1999). SOIL SURVEY OF UITKOMST RESEARCH STATION. *Agricola* 10: 17–25.

Costantini, E.A.C., Angelone, M. and Damiani, D. (2002). PHYSICAL, GEOCHEMICAL AND MINERALOGICAL INDICATORS OF AGING IN QUATERNARY SOILS OF CENTRAL ITALY. Abstracts of Symposium 49 "Paleosols as a memory for understanding landscape history and environmental problems" of the XVII World Congress of Soil Science, Bangkok, Thailand.

Curtis, B. and Mannheimer, C. (2005). TREE ATLAS OF NAMIBIA. 674 pages. National Botanical Research Institute, Ministry of Agriculture, Water and Forestry, Windhoek, Namibia

DeBolt, D.C. (1974). A HIGH SAMPLE VOLUME PROCEDURE FOR THE COLORIMETRIC DETERMINATION OF SOIL ORGANIC MATTER. *Commun. Soil Sci. Plant Anal*. 5: 131–137.

De Klerk, J.N. (2004). BUSH ENCROACHMENT IN NAMIBIA. Report on Phase 1 of the Bush Encroachment Research, Monitoring and Management Project. Ministry of Environment and Tourism, Windhoek, Namibia.

De Pauw, E. (1996). AGRO ECOLOGICAL ZONES OF NAMIBIA - FIRST APPROXIMATION. Technical Report 1. Project TCP/NAM/ 6611 (A). FAO, Rome, Italy.

De Pauw, E. and Coetzee, M.E. (1999). PRODUCTION OF AN AGRO-ECOLOGICAL ZONES MAP OF NAMIBIA (FIRST APPROXIMATION). PART I: CONDENSED METHODOLOGY. *Agricola* 10: 27–31.

De Pauw, E., Coetzee, M.E., Calitz, A.J., Beukes, H. and Vits, C. (1999). PRODUCTION OF AN AGRO-ECOLOGICAL ZONES MAP OF NAMIBIA (FIRST APPROXIMATION). PART II: RESULTS. *Agricola* 10: 33–43.

Di Gregorio, A. and Jansen, L.J.M. (1997). TECHNICAL DOCUMENT ON THE AFRICOVER LAND COVER CLASSIFICATION SCHEME. PART I. In: FAO AFRICOVER land cover classification. FAO, Rome, Italy.

Dobos, E., Daroussin J. and Montanarelle, L. (2005). AN SRTM-BASED PROCEDURE TO DELINEATE SOTER TERRAIN UNITS ON 1: 1 AND 1: 5 MILLION SCALES. 55 pages. EUR 21571 EN, Office for Official Publications of the European Communities, Luxembourg.

Dougill, A. and Cox, J. (1995). LAND DEGRADATION AND GRAZING IN THE KALAHARI - NEW ANALYSIS AND ALTERNATIVE PERSPECTIVES. Pastoral Development Network Series 38c, Rural Policy and Environment Group, Overseas Development Institute, UK.

Eijkelkamp. (1993). REVISED STANDARD SOIL COLOR CHARTS (commercial reproduction of the original Munsell soil color charts). Eijkelkamp Agrisearch Equipment, The Netherlands.

Ellis, F. (1988). DIE GRONDE VAN DIE KAROO. Unpublished PhD thesis. University of Stellenbosch, Stellenbosch, RSA.

Eriksen, J., Murphy, M.D. and Schnug, E. (1998). THE SOIL SULPHUR CYCLE. p. 39–74. In: Schnug, E. (ed.), Sulphur in agroecosystems. Springer.

Espach, C. (2006). RANGELAND PRODUCTIVITY MODELLING: DEVELOPING AND CUSTOMIZING METHODOLOGIES FOR LAND COVER MAPPING IN NAMIBIA. *Agricola* 16: 20–27.

Espach, C., Lubbe, L.G. and Ganzin, N. (2006). DETERMINING GRAZING CAPACITY IN NAMIBIA: APPROACHES AND METHODOLOGIES. *Agricola* 16: 28–39.

FAO. (1989). FAO-ISRIC SOIL DATABASE. World Soil Resources Report 64. FAO, Rome, Italy.

FAO. (1990). GUIDELINES FOR SOIL DESCRIPTION. 3rd edition (revised). 70 pages. FAO, Rome, Italy.

FAO. (1995). GLOBAL AND NATIONAL SOILS AND TERRAIN DIGITAL DATABASES – SOTER. PROCEDURES MANUAL. Van Engelen, V.W.P and Wen, T.T. (eds.), World Soil Resources Report 74 (Revision 1). UNEP, ISSS, ISRIC, FAO, Rome, Italy.

FAO. (1998a). WORLD REFERENCE BASE FOR SOIL RESOURCES. World Soil Resources Report 84. FAO, Rome, Italy.

FAO. (1998b). TOPSOIL CHARACTERIZATION FOR SUSTAINABLE LAND MANAGEMENT. 71 pages. Draft document. Land and Water Development Division, Soil Resources, Management and Conservation Service, FAO, Rome, Italy.

FAO. (2001). LECTURE NOTES ON THE MAJOR SOILS OF THE WORLD. World Soil Resources Report 94. FAO, Rome, Italy.

FAO-UNESCO. (1974). SOIL MAP OF THE WORLD 1 : 5 000 000. VOLUME I LEGEND. FAO, Rome, Italy.

FAO-UNESCO. (1977). SOIL MAP OF THE WORLD 1 : 5 000 000. VOLUME VI AFRICA. FAO, Rome, Italy.

FAO-UNESCO-ISRIC. (1988) (reprinted 1990). REVISED LEGEND OF THE FAO-UNESCO SOIL MAP OF THE WORLD. Food and Agriculture Organisation of the United Nations (FAO), United Nations Educational, Scientific and Cultural Organization (UNESCO), International Soil Reference and Information Centre (ISRIC). World Soil Resources Report 60. FAO, Rome, Italy.

Foth, H.D. (1990). FUNDAMENTALS OF SOIL SCIENCE. 8th edition. John Wiley and Sons, New York, USA.

Ganssen, R. (1960). DIE BÖDEN SÜDWESTAFRIKAS. *Die Erde* 91(2): 115–131.

Ganssen, R. (1963). SÜDWEST-AFRIKA. BÖDEN UND BODENKULTUR. VERSUCH EINER KLIMAPEDOLOGIE WARMER TROCKENGEBIETE. 160 pages. Dietrich Reimer, Berlin, Germany.

Ganssen, R. and Moll, W. (1961). BEITRÄGE ZUR KENNTNIS DER BÖDEN WARM-ARIDER GEBIETE, DARGESTELLT AM BEISPIEL SÜDWESTAFRIKA. *Z. Pflanzenern. Düngg. Bodenk* 94/139(1): 9–25.

Ganzin, N., Coetzee, M., Rothauge, A. and Fotsing, J.-M. (2005). RANGELAND RESOURCES ASSESSMENT WITH SATELLITE IMAGERY: AN OPERATIONAL TOOL FOR NATIONAL PLANNING IN NAMIBIA. *Geocarto International* 20(3): 33–42.

Gevers, T.W. (1932a). DIE GEOLOGISCHEN VERHÄLTNISSE DER UMGEBUNG WINDHUKS UNTER BESONDERER BERÜCKSICHTIGUNG DER HEISSEN QUELLEN. *J. S. W. A. Wiss. Ges*. 6: 75–80.

Gevers, T.W. (1932b). THE HOT SPRINGS OF WINDHOEK, SWA. *Transact. Geol. Soc. S. Afr.* 35: 1–28.

Gevers, T.W. (1934). THE GEOLOGY OF THE WINDHOEK DISTRICT IN SOUTH WEST AFRICA. *Transact. Geol. Soc. S. Afr.* 37: 221–251.

Gevers, T.W. (1942). THE MORPHOLOGY OF THE WINDHOEK DISTRICT, SOUTH WEST AFRICA. *S. Afr. Geogr. J.* 24: 45–64.

Giess, W. (1971). 'N VOORLOPIGE PLANTEGROEIKAART VAN SUIDWES-AFRIKA. *Dinteria* 4. Windhoek, Namibia.

Giess, W. (1998). A PRELIMINARY VEGETATION MAP OF NAMIBIA. 3rd revised edition. *Dinteria* 4. 112 pages. Windhoek, Namibia.

Goudie, A.S. (1973). DURICRUSTS IN TROPICAL AND SUBTROPICAL LANDSCAPES. Clarendon Press, Oxford, UK.

Goudie, A.S. (1983). CALCRETE. p. 93–132. In: Goudie, A.S. and Pye, K. (eds.), Chemical sediments and geomorphology. Academic Press, London, UK.

Goudie, A.S. and Thomas, D.S.G. (1985). PANS IN SOUTHERN AFRICA WITH PARTICULAR REFERENCE TO SOUTH AFRICA AND ZIMBABWE. *Zeitschrift für Geomorphologie* 29: 1–19.

Grünert, N. (2000). NAMIBIA – FASCINATION OF GEOLOGY. A TRAVEL HANDBOOK. 176 pages. Klaus Hess Publishers, Windhoek, Namibia and Göttingen, Germany.

Han, F.X. and Singer, A. (2007). BIOGEOCHEMISTRY OF TRACE ELEMENTS IN ARID ENVIRONMENTS. 366 pages. Springer.

Hartemink, A.E. and Hunting, J. (2008). LAND COVER, EXTENT, AND PROPERTIES OF ARENOSOLS IN SOUTHERN AFRICA. *Arid Land Research and Management* 22: 134–147.

Hegenberger, W. (1993). STRATIGRAPHY AND SEDIMENTOLOGY OF THE LATE PRECAMBRIAN WITVLEI AND NAMA GROUPS, EAST OF WINDHOEK. Memoir 17. Geological Survey of Namibia, Ministry of Mines and Energy, Windhoek, Namibia.

Heine, K. (1982). THE MAIN STAGES OF THE LATE QUATERNARY EVOLUTION OF THE KALAHARI DUNE SYSTEMS IN SOUTHERN AFRICA. *S. Afr. J. Sci*. 48: 374–375.

Helmke, P.A. (2000). THE CHEMICAL COMPOSITION OF SOILS. p. B3–B24. In: Sumner, M.E. (ed.), Handbook of soil science. CRC Press, Taylor and Francis Group, Boca Raton, Florida, USA.

Hendershot, W.H., Lalande, H. and Duquette, M. (1993). SOIL REACTION AND EXCHANGEABLE ACIDITY. p. 141–145. In: Carter, M.R. (ed.), Soil sampling and methods of analysis. Canadian Society of Soil Science and Lewis Publishers.

Hoffmann, K.H. (1983). LITHOSTRATIGRAPHY AND FACIES OF THE SWAKOP GROUP OF THE SOUTHERN DAMARA BELT, SWA/NAMIBIA. In: Miller, R. McG. (ed.), Evolution of the Damara Orogen of South West Africa/ Namibia.Geological Society of South Africa Special Publication 11: 43–63.

Hoffmann, K.H. (1989). NEW ASPECTS OF LITHOSTRATIGRAPHIC SUBDIVISION AND CORRELATION OF LATE PROTEROZOIC TO EARLY CAMBRIAN ROCKS OF THE SOUTHERN DAMARA BELT AND THEIR CORRELATION WITH THE CENTRAL AND NORTHERN DAMARA BELT AND THE GARIEP BELT. *Communs geol. Surv. Namibia* 5: 59–67.

Horsthemke, O. (2000). COMBATING INTRUDER BUSH – THE FINANCIAL DECISION. Doc 021/00. Namibia Agricultural Union, Windhoek, Namibia.

Howe, P., Heath, M. and Dobson, S. (2004). MANGANESE AND ITS COMPOUNDS: ENVIRONMENTAL ASPECTS. 63 pages. World Health Organization, United Nations Environmental Programme, International Labour Organisation, International Program on Chemical Safety, Inter-Organization Programme for the Sound Management of Chemicals.

ICC, MAWRD, AECI. (2000). PROJECT TO SUPPORT THE AGRO-ECOLOGICAL ZONING PROGRAMME (AEZ) IN NAMIBIA. Main Report 243 pages, Annexes 224 pages, 79 maps. Institut Cartogràfic de Catalunya (ICC), Namibian Ministry of Agriculture Water and Rural Development (MAWRD), Spanish Agency for International Cooperation (AECI). Windhoek, Namibia.

IDC. (2005). STUDY ON LAND PRODUCTIVITY AND ECONOMIC FARMING UNITS FOR THE MINISTRY OF AGRICULTURE, WATER AND FORESTRY. International Development Consultancy (IDC), in cooperation with Deutsche Gesellschaft für Technische Zusammenarbeit GmbH (GTZ). Windhoek, Namibia.

ISRIC. (1991). THE SOTER MANUAL. PROCEDURES FOR SMALL SCALE DIGITAL MAP AND DATABASE COMPILATION OF SOIL AND TERRAIN CONDITIONS. 92 pages. Van Engelen, V.W.P. and Pulles, J.H.M. (eds.). Working paper and preprint 91/3, International Soil Reference and Information Centre, Wageningen, The Netherlands.

ISRIC. (1993). GLOBAL AND NATIONAL SOILS AND TERRAIN DATABASES (SOTER): PROCEDURES MANUAL. UNEP-ISSS-ISRIC-FAO. International Soil Reference and Information Centre, Wageningen, The Netherlands.

ISSS Working Group RB. (1998). WORLD REFERENCE BASE FOR SOIL RESOURCES: INTRODUCTION. Deckers, J.A., Nachtergaele, F.O. and Spaargaren, O.C. (eds). 1st edition. ISSS-ISRIC-FAO. KULeuven Academic Press, Acco, Leuven, Belgium.

Jenness, J.S. (2004a). CALCULATING LANDSCAPE SURFACE AREA FROM DIGITAL ELEVATION MODELS. *Wildlife Society Bulletin* 32(3): 829–839.

Jenny, H. (1941). CALCIUM IN THE SOIL: III. PEDOLOGICAL RELATIONS. *Soil Sci. Soc. Am. Proc.* 6: 27–35.

Jenny, H. (1994). FACTORS OF SOIL FORMATION: A SYSTEM OF QUANTITATIVE PEDOLOGY. 281 pages. Courier Dover Publications.

Joubert, D.F., Rothauge, A. and Smit, G.N. (2008). A CONCEPTUAL MODEL OF VEGETATION DYNAMICS IN THE SEMIARID HIGHLAND SAVANNA OF NAMIBIA, WITH PARTICULAR REFERENCE TO BUSH THICKENING BY *ACACIA MELLIFERA*. *Journal of Arid Environments* 72(12): 2201–2210.

Kasch, K.W. (1983a). REGIONAL P-T VARIATIONS IN THE DAMARA OROGEN WITH PARTICULAR REFERENCE TO EARLY HIGH-PRESSURE METAMORPHISM ALONG THE SOUTHERN MARGIN. In: Miller, R. McG. (ed.), Evolution of the Damara Orogen of South West Africa / Namibia. *Geological Society of South Africa Special Publication* 11: 243–253.

Kasch, K.W. (1983b). CONTINENTAL COLLISION, SUTURE PROGRADATION AND THERMAL RELAXATION: A PLATE TECTONIC MODEL FOR THE DAMARA OROGEN IN CENTRAL NAMIBIA. In: Miller, R. McG. (ed.), Evolution of the Damara Orogen of South West Africa/ Namibia. *Geological Society of South Africa Special Publication* 11: 73–80.

Kasch, K.W. (1986). DELAMINATION AND SUTURE PROGRADATION IN THE SOUTHERN DAMARA OROGEN OF CENTRAL SOUTH WEST AFRICA/NAMIBIA. *South African Journal of Geology* 89: 215–222.

Kasch, K.W. (1988). LITHOSTRATIGRAPHY AND STRUCTURAL GEOLOGY OF THE UPPER SWAKOP RIVER AREA EAST OF OKAHANDJA, SWA / NAMIBIA. *Communications of the Geological Survey of South West Africa/Namibia* 4: 59–66.

Keller, G. and Warrack, B. (1997). STATISTICS FOR MANAGEMENT AND ECONOMICS. 4th edition. Duxbury Press, Pacific Grove, USA.

Kellner, K. (1986). 'N PLANTEKOLOGIESE STUDIE VAN DIE DAAN VILJOEN-WILDTUIN EN GEDEELTES VAN DIE PLASE CLARATAL EN NEUDAMM IN DIE HOOGLANDSAVANNA, SWA. 150 pages. MSc-thesis, Potchefstroom University for Christian Higher Education, South Africa.

Kempf, J. (1994). PROBLEME DER LAND-DEGRADATION IN NAMIBIA. AUSMASS, URSACHEN UND WIRKUNGSMUSTER. 270 pages. Würzburger Geographisch Manuskripte 31, Würzburg, Germany.

Kempf, J. (1999a). PEDO-GEOMORPHOLOGICAL STUDIES IN NAMIBIA. In: Focus Africa. Abstracts of the Third Biennial International Conference of the Society of South African Geographers, Windhoek, 5–9 July 1999: 39–40.

Kempf, J. (1999b). GEOMORPHOLOGICAL SIGNIFICANCE OF PEDOLOGICAL DEVELOPMENT IN CENTRAL NAMIBIA. [Poster] INQUA XV, Durban South Africa.

Kempf, J. (1999c). ZUR GEOMORPHOGENESE UND PEDOGENESE ZENTRAL-NAMIBIAS. PhD thesis. Würzburger Geographisch Manuskripte. Würzburg, Germany.

Kempf, J. 2008. PERS. COMM. University of Würzburg, Germany.

Killick, A.M. (2000). THE MATCHLESS BELT AND ASSOCIATED SULPHIDE MINERAL DEPOSITS, DAMARA OROGEN, NAMIBIA. *Communs geol. Surv. Namibia* 12: 73–80.

King, L.C. (1967). SOUTH AFRICAN SCENERY. A TEXTBOOK OF GEOMORPHOLOGY. 3rd edition – revised. 308 pages. Oliver and Boyd, Edinburgh, UK.

King, L.C. (1978). THE GEOMORPHOLOGY OF CENTRAL AND SOUTHERN AFRICA. p. 1–17. In: Werger, M. J. A. (ed.).

Klaassen, E.S. and Craven, P. (2003). CHECKLIST OF GRASSES IN NAMIBIA. 130 pages. Southern African Botanical Diversity Network Report No. 20. SABONET, Pretoria, RSA and Windhoek, Namibia.

Köppen, W. (1936). DAS GEOGRAPHISCHE SYSTEM DER KLIMATE. Handbuch der Klimatologie, Bd. 1, Teil C.

Kotze, E. and Du Preez, C.C. (2008). INFLUENCE OF LONG-TERM WHEAT RESIDUE MANAGEMENT ON ACIDITY AND SOME MACRONUTRIENTS IN AN AVALON SOIL. *S. Afr. J. Plant Soil* 25(1): 14–21.

Kukla, P.A. (1992). TECTONICS AND SEDIMENTATION OF A LATE PROTEROZOIC DAMARAN CONVERGENT CONTINENTAL MARGIN, KHOMAS HOCHLAND, CENTRAL NAMIBIA. 95 pages. *Memoirs of the Geological Survey of Namibia* No 12.

Kutuahupira J.T. and Mouton, H.D. (2006). SOIL SURVEY UNDER THE PILOT PROJECT 'QUANTIFICATION OF LAND PRODUCTION POTENTIAL'. Unpublished report of the AEZ Programme, Ministry of Agriculture, Water and Forestry, Windhoek, Namibia.

Kutuahupira, J.T., Mouton, H.D. and Beukes, H.A. (2003). SOIL SURVEY OF OTJINENE, EPUKIRO, GAM AND OKAKARARA. Report prepared for the Ministry of Agriculture, Water and Forestry and the Desert Research Foundation of Namibia, Windhoek, Namibia.

Kutuahupira, J,T., Mouton, H.G. and Coetzee, M.E. (2001a). SOIL SURVEY AT MAHENENE RESEARCH STATION. *Agricola* 12: 59–66.

Kutuahupira, J,T., Mouton, H.G. and Coetzee, M.E. (2001b). SOIL SURVEY OF SONOP RESEARCH STATION. *Agricola* 12: 67–72.

Lal, R. (2006). ENCYCLOPEDIA OF SOIL SCIENCE. 1600 pages. CRC Press.

Lancaster, I.N. (1978a). THE PANS OF SOUTHERN KALAHARI, BOTSWANA. *Geo. J.* 144: 81–98.

Lancaster, I.N. (1978b). COMPOSITION AND FORMATION OF SOUTHERN KALAHARI PAN MARGIN DUNES. *Zeitschrift für Gemorphologie, NF* 22: 148–169.

Lancaster, I.N. (1986). PANS IN THE SOUTHWESTERN KALAHARI: A PRELIMINARY REPORT. *Palaeocology of Africa* 17: 59–67.

Leigh, G. J. (ed.), Favre, H.A. and Metanomski, W.V. (1998). PRINCIPLES OF CHEMICAL NOMENCLATURE: A GUIDE TO IUPAC RECOMMENDATIONS. Blackwell Science Ltd., Oxford, UK.

Le Roux, P.A.L., Ellis, F., Merryweather, F.R., Schoeman, J.L., Snyman, K., Van Deventer, P.W. and Verster, E. (1999). RIGLYNE VIR KARTERING EN INTERPRETASIE VAN DIE GRONDE VAN SUID-AFRIKA.

Leser, H. (1971). LANDSCHAFTSÖKOLOGISCHE STUDIEN IM KALAHARISANDGEBIET UM AUOB UND NOSSOB (ÖSTLICHES SÜDWESTAFRIKA). 243 pp mit 96 Abbildungen. Franz Steiner Verlag, Wiesbaden, Germany.

Leser, H. (1982). NAMIBIA. LÄNDERPROFILE – GEOGRAPHISCHE STRUKTUREN, DATEN, ENTWICKLUNGEN. 259 pages. Ernst Klett, Stuttgart, Germany.

Loxton, Venn and Associates. (1971). CONSOLIDATED REPORT ON RECONNAISSANCE SURVEYS OF THE SOILS OF NORTHERN AND CENTRAL SOUTH WEST AFRICA IN TERMS OF THEIR POTENTIAL FOR IRRIGATION. Report for the Department of Water Affairs, Windhoek, Namibia.

Lubbe, L.G. (2005). TOWARDS AN UPDATED CARRYING CAPACITY MAP FOR NAMIBIA: A REVIEW OF THE METHODOLOGIES CURRENTLY USED TO DETERMINE CARRYING CAPACITY IN NAMIBIA. *Agricola* 15: 33–39.

Lubbe, L.G. (2006). PERS. COMM. Chief Agricultural Researcher: Subdivision Pasture Science, Ministry of Agriculture, Water and Forestry, Windhoek, Namibia.

Macvicar, C.N., De Villiers, J.M., Loxton, R.F., Verster, E., Lambrechts, J.J.N., Merryweather, F.R., Le Roux, J., Van Rooyen, T.H. and Harmse, J.H. von M. (1977). SOIL CLASSIFICATION. A BINOMIAL SYSTEM FOR SOUTH AFRICA. 150 pages. Department of Agricultural Development, Pretoria, RSA.

Malavolta, E. (1985). POTASSIUM STATUS OF TROPICAL AND SUBTROPICAL REGION SOILS. p. 163–200. In: Munson, R.E. (ed.), Potassium in agriculture. American Society of Agronomy, Madison, WI.

Mandelbrot, B.B. (1983). THE FRACTAL GEOMETRY OF NATURE. W. H. Freeman and Company, New York, USA.

Materechera, S.A., Mandiringana, O.T. and Mbokodi, P.M. (1998). ORGANIC MATTER, pH AND NUTRIENT DISTRIBUTION IN SOIL LAYERS OF A SAVANNA THORNVELD SUBJECTED TO DIFFERENT BURNING FREQUENCIES AT ALICE IN THE EASTERN CAPE. *S. Afr. J. Plant Soil* 15(3): 109–115.

MAWRD. (2000). QUALITY MANUAL. STANDARD OPERATING PROCEDURES OF THE AGRICULTURAL LABORATORY. Internal document, Ministry of Agriculture, Water and Rural Development, Windhoek, Namibia.

Mayland, H.F. and Wilkinson, S.R. (1989). SOIL FACTORS AFFECTING MAGNESIUM AVAILABILITY IN PLANT-ANIMAL SYSTEMS: A REVIEW. *J Anim Sci* 67: 3437–3444.

McCarthy, T. and Rubidge, B. (2005). THE STORY OF EARTH AND LIFE. A SOUTHERN AFRICAN, PERSPECTIVE ON A 4.6-BILLION-YEAR JOURNEY. 333 pages. Struik Publishers, Cape Town, RSA.

Medinski, T. (2007). SOIL CHEMICAL AND PHYSICAL PROPERTIES, INFILTRABILITY AND PLANT RICHNESS IN ARID SOUTH-WEST AFRICA. M.Sc. dissertation, University of Stellenbosch, Stellenbosch, RSA.

Mendelsohn, J., Jarvis, A. Roberts, C. and Robertson, T. (2002). ATLAS OF NAMIBIA. A PORTRAIT OF THE LAND AND ITS PEOPLE. 200 pages. Ministry of Environment and Tourism, Namibia and David Philip Publishers, Cape Town, RSA.

Mengel, K. and Kirby, E.A. (1987). PRINCIPLES OF PLANT NUTRITION. 306 pages. International Potash Institute. Worblaufen-Bern, Switzerland.

Mengel, K. and Kirkby, E.A. (eds.), Kosegarten, H. and Appel, T. (2001). PRINCIPLES OF PLANT NUTRITION. 849 pages. Springer.

Metson, A.J. (1974). MAGNESIUM IN NEW ZEALAND SOILS. I. SOME FACTORS GOVERNING THE AVAILABILITY OF SOIL MAGNESIUM: A REVIEW. *NZ J. Exp. Agric*. 2: 277–319.

Miller, R. McG. (1983). THE PAN-AFRICAN DAMARA OROGEN OF SOUTH WEST AFRICA/NAMIBIA. In: Miller, R. McG. (Ed.), Evolution of the Damara Orogen of South West Africa/Namibia. *Spec. Publ. Geol. Soc. S. Afr*. 11: 431–414.

Miller, W.P. and Miller, D.M. (1987). A MICRO-PIPETTE METHOD FOR SOIL MECHANICAL ANALYSIS. *Commun. Soil Sci. Plant Anal*. 18: 1–15.

Mokwunye, A.U. and Melsted, S.W. (1972). MAGNESIUM FORMS IN SELECTED TEMPERATE AND TROPICAL SOILS. *Soil Sci. Soc. Am. J*. 36: 762–764.

Monteith J.L. (1972). SOLAR RADIATION AND PRODUCTIVITY IN THE TROPICAL ECOSYSTEMS. *J. Appl. Ecol*. 9: 744–766.

Morris, C.D., Hardy, M.B. and Bartholomew, P.E. (1999). PRINCIPLES OF MANAGING VELD – STOCKING RATE. p186–193. In: Tainton, N.M. (ed.), Veld management in South Africa. University of Natal Press, Pietermaritzburg, RSA.

Mortvedt, J.J. (2000). BIOAVAILABILITY OF MICRONUTRIENTS. p. D71–D88. In: Sumner, M.E. (ed.), Handbook of soil science. CRC Press, Taylor and Francis Group, Boca Raton, Florida, USA.

Mosweu, S. (2008). SOIL RESOURCES DISTRIBUTION, WOODY PLANT PROPERTIES AND LAND USE IN A LUNETTE DUNE-PAN SYSTEM IN KALAHARI, BOTSWANA. *Scientific Research and Essay* 3(9): 242–256.

Müller, M.A.N. (1983). GRASSE VAN SUIDWES-AFRIKA/NAMIBIË. Direktoraat Landbou en Bosbou, Departement Landbou en Natuurbewaring. Windhoek, Namibia.

Mundy, G.N. (1984). EFFECTS OF POTASSIUM AND SODIUM APPLICATION TO SOIL ON GROWTH AND CATION ACCUMULATION OF HERBAGE. *Australian Journal of Agricultural Research* 35(1): 85–97.

Murphy, J. and Riley, J.P. (1962). A MODIFIED SINGLE SOLUTION METHOD FOR THE DETERMINATION OF PHOSPHATE IN NATURAL WATERS. *Anal. Chim. Acta* 27: 31–36.

Nash, D.J. (1995): STRUCTURAL CONTROL AND DEEP-WEATHERING IN THE EVOLUTION OF THE DRY VALLEY SYSTEMS OF THE KALAHARI, CENTRAL SOUTHERN AFRICA. *Africa Geoscience Review* 2: 9–23.

Nash, D.J. (1997). GROUNDWATER AS A GEOMORPHOLOGICAL AGENT IN DRYLANDS. p. 319–348. In: Thomas, D.S.G. (ed.), Arid zone geomorphology: process, form, and change in drylands. John Wiley and Sons, New York, USA.

Nash, D.J. and McLaren, S.J. (2003). KALAHARI VALLEY CALCRETES: THEIR NATURE, ORIGINS, AND ENVIRONMENTAL SIGNIFICANCE. Quaternary International 111: 3–22.

Nash, D.J., Shaw, P.A. and Thomas, D.S.G., (1994a). DURICRUSTS DEVELOPMENT AND VALLEY EVOLUTION: PROCESS-LANDFORM LINKS IN THE KALAHARI. *Earth Surface Processes and Landforms* 19: 299–317.

Nash, D.J., Shaw, P.A. and Thomas, D.S.G. (1994b). TIMESCALES, ENVIRONMENTAL CHANGE AND DRYLAND VALLEY DEVELOPMENT. p. 273–286. In: Millington, A.C., and Pye, K. (eds.), Environmental change in dryland: biogeographical and geographical, perspectives. John Wiley and Sons, New York, USA.

Nash, D.J., Shaw, P.A. and Thomas, D.S.G. (1994c). SILICEOUS DURICRUSTS AS PALAEOCLIMATIC INDICATORS: EVIDENCE FROM THE KALAHARI DESERT, BOTSWANA. *Palaeogeography, Palaeoclimatology, Palaeoecology* 112: 279–295.

Nelson, D.W. and Sommers, L.E. (1982). TOTAL CARBON, ORGANIC CARBON AND ORGANIC MATTER. p. 539–579. In: Page, A.L. *et. al.,* Methods of soil analysis Part 2. 2nd edition. *Agronomy* No. 9, American Society of Agronomy, Madison, WI, USA.

Netterberg, F. (1980). GEOLOGY OF SOUTHERN AFRICAN CALCRETES: TERMINOLOGY, DESCRIPTION, MACROFEATURES AND CLASSIFICATION. *Transactions, Geological Society of South Africa* 83: 255–283.

Non-Affiliated Soil Analysis Work Committee. (1990). HANDBOOK OF STANDARD SOIL TESTING METHODS FOR ADVISORY PURPOSES. Soil Science Society of South Africa, Sunnyside, Pretoria, RSA.

Olsen, S.R. and Dean, L.A. (1965). PHOSPHORUS. p. 1044–1046. In: Black, C. A. (ed.), Methods of soil analysis. *Agronomy* No. 9, American Society of Agronomy, Madison, WI, USA.

Papadakis, J. (1970a). CLIMATES OF THE WORLD. THEIR CLASSIFICATION, SIMILITUDES, DIFFERENCES AND GEOGRAPHIC DISTRIBUTION. Buenos Aires, Argentina.

Papadakis, J. (1970b). AGRICULTURAL POTENTIALITIES OF THE WORLD CLIMATES. Buenos Aires, Argentina.

Partridge, T.C. and Maud, R.R. (1987). GEOMORPHIC EVOLUTION OF SOUTHERN AFRICA SINCE THE MESOZOIC. *S. Afr. J. Geol.* 90: 179–208.

Partridge, T.C. and Maud, R.R. (1988). THE GEOMORPHIC EVOLUTION OF AFRICA: A COMPARATIVE REVIEW. In: Moon, B.P. and Dardis, G.F. (eds.), The geomorphology of southern Africa. Southern Book Publishers, Pretoria, RSA.

Petersen, A. (2008). PEDODIVERSITY OF SOUTHERN AFRICAN DRYLANDS. 388 pages. PhD dissertation. Hamburger Bodenkundliche Arbeiten. University of Hamburg, Germany.

Reuter, D.J. and Robinson, J.B. (eds.). (1997). PLANT ANALYSIS – AN INTERPRETATION MANUAL. CSIRO Publishing, Collingwood, Australia.

Rhoades, J.D. (1982). CATION EXCHANGE CAPACITY. p. 149–157. In: Page, A.L. *et al*. (eds.), Methods of soil analysis. *Agronomy* No. 9. 2nd ed. American Society of Agronomy, Madison, WI, USA.

Richards, L.A. (ed.). (1954). DIAGNOSIS AND IMPROVEMENT OF SALINE AND ALKALINE SOILS. U.S. Dep. Agric. Handbook No. 60.

Rowell, M.J. (2000a). CHANGING A LABORATORY METHOD: AN EXAMPLE CONCERNING PARTICLE SIZE ANALYSIS. *Agricola*, 11: 61–65.

Rowell, M.J. (2000b). MEASUREMENT OF SOIL ORGANIC MATTER: A COMPROMISE BETWEEN EFFICACY AND ENVIRONMENTAL FRIENDLINESS. *Agricola*, 11: 66–69.

Saggar, S. Hedley, M.J. and Phimsarn, S. (1998). DYNAMICS OF SULFUR TRANSFORMATIONS IN GRAZED PASTURES. In: Maynard, D.G. (ed.), Sulfur in the environment. 371 pages. CRC Press.

Saxton, K.E., Rawls, W.J., Romberger, J.S. and Papendick, R.I. (1986). ESTIMATING GENERALIZED SOIL-WATER CHARACTERISTICS FROM TEXTURE. *Soil Sci. Soc. Amer. J.* 50(4): 1031–1036.

Schaetzl, R.J. and Anderson, S. (2005). SOILS: GENESIS AND GEOMORPHOLOGY. 817 pages. Cambridge University Press, UK.

Schneider, G. (2004). THE ROADSIDE GEOLOGY OF NAMIBIA. 294 pages. Gebrüder Borntraeger. Berlin and Stuttgart, Germany.

Scholz, H. (1968a). DIE BÖDEN DER TROCHENEN SAVANNE SÜDWESTAFRIKAS. *Zeidschrift für Pflanzenernährung und Bodenkunde* 120(2): 118–130.

Scholz, H. (1968b). DIE BÖDEN DER FEUCHTEN SAVANNE SÜDWESTAFRIKAS. *Zeidschrift für Pflanzenernährung und Bodenkunde* 120(2): 209–221.

Scholz, H. (1973). SOME TYPICAL SOILS OF SOUTH WEST AFRICA. 6 pages. Lecture Manuscript. 5th International Congress of the South African Society for Soil Science in Salisbury/Rhodesia, February 1972. Windhoek, Namibia.

Sharpley, A. (2000). PHOSPHORUS AVAILABILITY. p. D18–D38. In: Sumner, M.E. (ed.), Handbook of soil science. CRC Press, Taylor and Francis Group, Boca Raton, Florida, USA.

Shaw, P.A. (1988). LAKES AND PANS. ARID LANDSCAPES. In: Moon, B.P. and Dardis, G.F. (eds.), The geomorphology of southern Africa. Southern Book Publishers, Johannesburg, RSA.

Shaw, P.A. (1997). GEOMORPHOLOGY OF THE WORLD'S ARID ZONES - AFRICA AND EUROPE. In: Thomas, D.S.G. (ed.), Arid zone geomorphology: process, form and change in drylands. 2nd edition. John Wiley and Sons,. New York, USA.

Shaw, P.A. and De Vries, J.J. (1988). DURICRUST, GROUNDWATER AND VALLEY DEVELOPMENT IN THE KALAHARI OF SOUTH-EAST BOTSWANA. *Journal of Arid Environments* 14: 245–254.

Shaw P.A. and Thomas S.G. (1997). PANS, PLAYAS AND SALT LAKES: In: Thomas, DSG (ed.), Arid zone geomorphology; process, form and change in drylands. John Wiley and Sons, New York, USA.

Shoenau, J.J. and Karamanos, R.E. (1993). SOIL SAMPLING AND METHODS OF ANALYSIS. In: Carter, M.E. (ed.). Canadian Society of Soil Science, Lewis Publishers.

Sims, T. (2000). SOIL FERTILITY EVALUATION. p. D113–D153. In: Sumner, M.E. (ed.), Handbook of soil science. CRC Press, Taylor and Francis Group, Boca Raton, Florida, USA.

Sims, J.R. and Haby, V.A. (1971. COLOURIMETRIC DETERMINATION OF SOIL ORGANIC MATTER. *Soil Science* 112: 137-141.

Skopp, J.M. (2000). PHYSICAL PROPERTIES OF PRIMARY PARTICLES. p. A3–A17. In: Sumner, M.E. (ed.), Handbook of soil science. CRC Press, Taylor and Francis Group, Boca Raton, Florida, USA.

Smit, P. (2002).GEO-ECOLOGICAL ANALYSIS OF NAMIBIAN LANDSCAPES INVADED BY *PROSOPIS*. Unpublished report. Windhoek, Namibia.

Smith, R.A., (1984). THE LITHOSTRATIGRAPHY OF THE KAROO SUPERGROUP IN BOTSWANA. *Bulletin of the Geological Survey Botswana*, vol. 26, 239 pages.

Soil Classification Working Group. (1991). SOIL CLASSIFICATION – A TAXONOMIC SYSTEM FOR SOUTH AFRICA. Memoirs on the Agricultural Natural Resources of South Africa No. 15. Department of Agricultural Development, Pretoria, RSA.

Soil Survey Staff. (1975). SOIL TAXONOMY: A BASIC SYSTEM OF SOIL CLASSIFICATION FOR MAKING AND INTERPRETING SOIL SURVEYS. USDA Handbook. 436. US Government Printing Office, Washinmgton, DC, USA.

Soil Survey Staff. (1998). KEYS TO SOIL TAXONOMY. 8th edition. US Government Printing Office, Washinmgton, DC, USA.

Sparks, D.L. (2000). BIOAVAILABILITY OF SOIL POTASSIUM. p. D38–D53. In: Sumner, M.E. (ed.), Handbook of soil science. CRC Press, Taylor and Francis Group, Boca Raton, Florida, USA.

Stevenson, F.J. (1991). ORGANIC MATTER – MICRONUTRIENT REACTIONS IN SOIL. p. 145–186. In: Mortvedt, J.J. (ed.), Micronutrients in agriculture. Soil Science Society of America, Madison, WI, USA.

Stevenson, F.J. (1994). HUMUS CHEMISTRY. 496 pages. 2nd edition. John Wiley and Sons, New York, USA.

Strohbach, B.J. (2001). VEGETATION SURVEY OF NAMIBIA. *Namibia Wissensschaftliche Gesellschaft / Namibia Scientific Society Journal* 49: 93–124. Windhoek, Namibia.

Summerfield, M.A. (1982). DISTRIBUTION, NATURE AND PROBABLE GENESIS OF SILCRETE IN ARID AND SEMI-ARID SOUTHERN AFRICA. In: Yaalon, D.H. (ed.), Aridic soils and geomorphic processes. *Catena*, supplement 1: 37–56.

Tate, R.L. (1987). SOIL ORGANIC MATER. 291 pages. John Wiley and Sons, New York, USA.

Thomas, G.W. (1982). EXCHANGEABLE CATIONS. p. 159–165. In: Page, A.L. *et al.* (eds.), Methods of soil analysis. *Agronomy* No. 9. 2nd ed. American Society of Agronomy, Madison, WI, USA.

Thomas, D.S.G. (1988). THE NATURE AND DEPOSITIONAL SETTING OF ARID AND SEMI-ARID KALAHARI SEDIMENTS. *Southern Afr. Journ. Arid Environ*. 14: 17–26.

Thomas, D.S.G. (ed.). (1997). ARID ZONE GEOMORPHOLOGY: PROCESS, FORM AND CHANGE IN DRYLANDS. 2nd edition. John Wiley and Sons, New York, USA.

Thomas, D.S.G. and Goudie, A. (eds.). (2000). THE DICTIONARY OF PHYSICAL GEOGRAPHY. 3rd edision. Blackwell Publishers, Malden, Massachusetts, USA.

Thomas, D.S.G., Nash, D.J., Shaw, P.A. and Van der Post, C. (1993). PRESENT DAY LUNETTE SEDIMENT CYCLING AT WITPAN IN THE ARID SOUTHWESTERN KALAHARI DESERT. *Catena*, 20: 515–527.

Thomas, D.S.G. and Shaw, P.A. (1991). THE KALAHARI ENVIRONMENT. Cambridge University Press, Cambridge, UK.

Troeh, F.R. and Thompson, L.M. (2005). SOILS AND SOIL FERTILITY. 489 pages. Blackwell Publishing.

Trollope, W.S.W., Trollope, L.A. and Bosch, O.J.H. (1990). VELD AND PASTURE MANAGEMENT TERMINOLOGY IN SOUTH AFRICA. *Die tydskrif van die Weidingsvereniging van Suid-Afrika* 7(1): 52–60.

Tucker, B.M. (1983). BASIC EXCHANGEABLE CATIONS. p. 401–416. In: Soils – An Australian viewpoint. CSIRO Division of Soils. CSIRO/Academic Press. Melbourne, Australia.

University of Stellenbosch (US). (2002). FERTILISERS AND PLANT NUTRITION. Class notes for Soil Science 244, B.Sc. Agric. Department of Soil Science, Faculty of Agricultural and Forestry Sciences, University of Stellenbosch, RSA.

USDA-SCS Staff. (1972). SOIL SURVEY LABORATORY METHODS AND PROCEDURES FOR COLLECTING SOIL SAMPLES. U.S. Gov. Print. Office, Washington, DC, USA.

Van der Watt, H.H. and Van Rooyen, T.H. (1995). A GLOSSARY OF SOIL SCIENCE. 2nd edition. Soil Science Society of South Africa, Pretoria, RSA.

Van Reeuwijk, L.P. (1992). PROCEDURES FOR SOIL ANALYSIS. 3rd edition. International Soil Reference and Information Centre, Wageningen, The Netherlands.

Van Reeuwijk, L.P. (2002) (ed.). PROCEDURES FOR SOIL ANALYSIS. 6th edition. Tech. Pap. 9, ISRIC, Wageningen, The Netherlands.

Vlek, P.L.G. and Harmsen, K. (1985). THE CHEMISTRY OF MICRONUTRIENTS IN SOIL. In: Vlek, P.L.G., Micronutrients in tropical food crop production. 260 pages. Springer.

Volk, O.H. and Leippert, H. (1971). VEGETATIONSVERHÄLTNISSE IM WINDHOEKER BERGLAND, SWA. *J. SWA Wiss. Ges*. 30: 5–44.

Walkley, A. and Black, I.A. (1934). AN EXAMINATION OF THE DEGTJAREFF METHOD FOR DETERMINING SOIL ORGANIC MATTER AND A PROPOSED MODIFICATION OF THE CHROMIC ACID TITRATION METHOD. *Soil Science* 37: 29–38.

Watts, N.L. (1980). QUATERNARY PEDOGENIC CALCRETES FROM THE KALAHARI (SOUTHERN AFRICA), MINERALOGY, GENESIS, AND DIAGENESIS. *Sedimentology* 27: 661–686.

Webb, J., Whinham, N. and Unwin, R.J. (1990). RESPONSE OF CUT GRASS TO POTASSIUM AND TO THE MINERAL SYLVINITE. *Journal of the Science of Food and Agriculture*, 53(3): 297–312.

Whitehead, D.C. (2000). NUTRIENT ELEMENTS IN GRASSLAND: SOIL-PLANT-ANIMAL RELATIONSHIPS. CABI Publishing, Wallingford, UK.

Wilkinson, M.J. (1988). ARID LANDSCAPES. In: Moon, B.P. and Dardis, G.F. The geomorphology of southern Africa. Southern Book Publishers, Johannesburg, RSA.

SECONDARY AUTHORITIES (QUOTED BY PRIMARY AUTHORITIES)

Beasom, S.L. (1983). A TECHNIQUE FOR ASSESSING LAND SURFACE RUGGEDNESS. *Journal of Wildlife Management* 47: 1163–1166. Quoted by Jenness (2004).

Berry, J.K. (2002). USE SURFACE AREA FOR REALISTIC CALCULATIONS. *Geoworld* 15(9): 20–1. Quoted by Jenness, 2004.

Bowen, H.J.M. (1966). TRACE ELEMENTS IN BIOCHEMISTRY. Academic Press, London, UK. Quoted by Helmke, In Sumner, 2000.

Bradford, G.R., Arkley, R.J., Pratt, P.F. and Blair, F.L. (1967). TOTAL CONTENT OF NINE MINERAL ELEMENTS IN FIFTY SELECTED BENCHMARK SOIL PROFILES OF CALIFORNIA. *Hilgardia* 38: 541–556. Quoted by Whitehead, 2000.

Casenave, A. and Valentin, C. (1989). LES ETATS DE SURFACE DE LA ZONE SAHÉLIENNE. INFLUENCE SUR L'INFILTRATION. Editions de l'ORSTOM. 229 pages. Paris. Quoted by FAO, 1989b.

Dampney, P.M.R. and Unwin, R.J. (1993). MORE EFFICIENT AND EFFECTIVE USE OF NPK IN TODAY'S CONDITIONS. In: Hopkins, A. and Younie, D. (eds.), Forward with grass into Europe. British Grassland Society Occasional Symposium 27: 62–72. British Grassland Society, Reading. Quoted by Whitehead, 2000.

Dickson, B. and Beier, P. (2006). QUANTIFYING THE INFLUENCE OF TOPOGRAPHIC POSITION ON COUGAR (*PUMA CONCOLOR*) MOVEMENT IN SOUTHERN CALIFORNIA, USA. *Journal of Zoology*, Zoological Society of London. Quoted by Jenness, 2006.

Guisan, A., Weiss, S.B. and Weiss, A.D. (1999). GLM VERSUS CCA SPATIAL MODELING OF PLANT SPECIES DISTRIBUTION. *Plant Ecology* 143: 107–122. Kluwer Academic Publishers. Quoted by Jenness, 2006.

Haynes, R.J. and Swift, R.S. (1984). AMOUNTS AND FORMS OF MICRONUTRIENT CATIONS IN A GROUP OF LOESSIAL GRASSLAND SOILS OF NEW ZEALAND. *Geoderma* 33: 53–62. Quoted by Whitehead, 2000.

Hobson, R.D. (1972). SURFACE ROUGHNESS IN TOPOGRAPHY: QUANTITATIVE APPROACH. p. 221–245. In: Chorley, R.J. (ed.), Spatial analysis in geomorphology. Harper and Row, New York, USA. Quoted by Jenness, 2004.

Hodgson, M.E. (1995). WHAT CELL SIZE DOES THE COMPUTED SLOPE / ASPECT ANGLE REPRESENT? *Photogrammetric Engineering and Remote Sensing* 61: 513–517. Quoted by Jenness, 2004.

Jenness, J.S. (2000). THE EFFECTS OF FIRE ON MEXICAN SPOTTED OWLS IN ARIZONA AND NEW MEXICO. Thesis, Northern Arizona University, Flagstaff, Arizona, USA. Quoted by Jenness, 2004.

Jones, K.B., Heggem, D.T., Wade, T.G., Neale, A.C., Ebert, D.W., Nash, M.S., Mehaffey, M.H., Hermann, K.A., Selle, A.R., Augustine, S., Goodman, I.A., Pedersen, J., Bolgrien, D., Viger, J.M., Chiang, D., Lin, C.J., Zhong, Y., Baker, J. and Van Remortel, R.D. (2000). ASSESSING LANDSCAPE CONDITIONS RELATIVE TO WATER RESOURCES IN THE WESTERN UNITED STATES: A STRATEGIC APPROACH. Environmental Monitoring and Assessment 64: 227–245. Quoted by Jenness, 2006

Lam, N.S.N. and De Cola, L. (1993). FRACTALS IN GEOGRAPHY. PTR Prentice-Hall, Englewood Cliffs, New Jersey, USA. Quoted by Jenness, 2004.

Laurie, S.H. and Manthey, J.A. (1994). THE CHEMISTRY AND ROLE OF METAL ION CHELATION IN PLANT UPTAKE PROCESSES. p.165–182. In: Manthey, J.A., Crowley, D.E., Luster, D.G. (eds.), Biochemistry of metal micronutrients in the rhizosphere. Lewis Publishers, Boca Raton, USA. Quoted by Whitehead, 2000.

Lindsey, W.L. (1979). CHEMICAL EQUILIBRIA IN SOILS. Wiley Interscience, New York, NY, USA. Quoted by Mortvedt, 2000.

Lorimer, N.D., Haight, R.G. and Leary, R.A. (1994). THE FRACTAL FOREST: FRACTAL GEOMETRY AND APPLICATIONS IN FOREST SCIENCE. United States Department of Agriculture Forest Service, North Central Forest Experiment Station, General Technical Report; NC-170. St. Paul, Minnesota, USA. Quoted by Jenness, 2004.

Parker, F.W. and Truog, E. (1920). THE RELATION BETWEEN THE CALCIUM AND THE NITROGEN CONTENT OF PLANTS AND THE FUNCTION OF CALCIUM. *Soil Sci*. 10: 49–56.

Paul, E.A. and Huang, P.M. (1980). CHEMICAL ASPECTS OF SOIL. p. 69-86. In: Hutzinger, O. (ed.), Handbook of environmental chemistry, Vol. 1 Part A. Springer Verlag, Berlin. Quoted by Whitehead, 2000.

Polidori, L., Chorowicz, J. and Guillande, R. (1991). DESCRIPTION OF TERRAIN AS A FRACTAL SURFACE, AND APPLICATION TO DIGITAL ELEVATION MODEL QUALITY ASSESSMENT. *Photogrammetric Engineering and Remote Sensing* 57: 1329–1332. Quoted by Jenness, 2004.

Scholz, H. (1968c). STUDIEN ÜBER DIE BODENBILDUNG ZWISCHEN REHOBOTH UND WALVIS Bay. Rheinischen Friedrich-Wilhelms-Universität, Bonn, Germany. Quoted by FAO-UNESCO, 1977.

Stevenson, F.J. (1986). CYCLES OF SOIL: CARBON, NITROGEN, PHOSPHORUS, SULFUR, MICRONUTRIENTS. 380 pages. John Wiley and Sons, New York, USA. Quoted by Whitehead, 2000.

Thomas, D.S.G. (1984). LATE QUATERNARY ENVIRONMENTAL CHANGE IN CENTRAL SOUTHERN AFRICA WITH PARTICULAR REFERENCE TO EXTENSIONS OF THE ARID ZONE. Unpublished DPhil thesis, University of Oxford, UK. Quoted by Thomas, 1997.

Weiss, A. (2001). TOPOGRAPHIC POSITION AND LANDFORMS ANALYSIS. Poster presentation, ESRI User Conference, San Diego, CA, USA. Quoted by Jenness, 2006

WEBSITES

IMA-Europe website: www.ima-eu.org

Mindat website: www.mindat.org

Webmineral website: www.webmineral.com

Hydraulic Properties Calculator website. http://staffweb.wilkes.edu/brian.oram/soil_watr.htm. Programming and web-realization by R Nelson, based on the work of K.E. Saxton *et al*, 1986.

SOFTWARE

AnalystSoft®. (2007). StatFi. Statistical analysis program. www.analystsoft. com

Behrens, T.M. (2005). Texture analysis and neighbourhood statistics for grids. Script for ArcView 3.2. University of Jena, Germany. http://arcscripts.esri.com

Behrens,T.M. (2005). DEMAT - DEM Analysis Tool. Script for ArcView 3.2. Institute for Soil Science and Soil Conservation, Justus-Liebig-University, Giessen, Germany. http://arcscripts.esri.com

Definiens Software®. (2006). Definiens Professional™ 5. Image analysis software. Definiens AG, Munich, Germany. www.definiens.com

DeLaune, M. (2003). Xtools. Script for ArcView 3.2. Oregon Department of Forestry. http://arcscripts.esri.com

ESRI®, Inc. (1999). ArcView™ 3.2. Including ArcView™ Image Analyst™, ArcView™ Spatial Analyst™, ArcView™ 3D Analyst™. Geographical information system software. Environmental Systems Research Institute, Inc. www.esri.com.

ESRI®, Inc. (2006). ArcGIS™ 9.2, including ArcMap™ 9.2, ArcCatalogue™ 9.2, Spatial Analyst™ 9.2, 3D Analyst™ 9.2, GeoStatistical Analyst™ 9.2. Geographical information system software. Environmental Systems Research Institute, Inc. www.esri.com.

Ganzin, N. (1999). Sustainable management of arid rangelands (SMAR) software.

Global Mapper Software, LLC. (2005). Global Mapper™ version 7.00. Elevation data processing software. www.globalmapper.com.

Hare, T. (2007). Grid Pig updated version 2.6. Script for ArcView 3.2. USGS - Flagstaff, Arizona. http://webgis.wr.usgs.gov/gridpig.htm, http://arcscripts.esri.com

Jenness, J. (2002). Surface Areas and Ratios from Elevation Grid (surfgrids.avx) version 1.2. Script for ArcView 3.2. Jenness Enterprises. www.jennessent. com/arcview/surface_areas.htm, http://arcscripts.esri.com

Jenness, J. (2004b). Surface Tools (surf_tools.avx). Script for ArcView 3.2. Jenness Enterprises. www.jennessent.com/arcview/surface_tools.htm, http://arcscripts. esri.com

Jenness, J. (2006a). Grid Tools (Jenness Enterprises), v. 1.7. Script for ArcView 3.2. Jenness Enterprises. www.jennessent.com, http://arcscripts.esri.com

Jenness, J. (2006b). Topographic Position Index (TPI) v. 1.3a. Script for ArcView 3.2. Jenness Enterprises. www.jennessent.com, http://arcscripts.esri.com

Leica®, LLC. (2006). ERDAS Imagine 9.1 Professional™. Image processing software. Leica Geosystems Geospatial Imaging, LLC. www.erdas.com, http://gi.leica-eosystems.com/documents/pdf/IMAGINEProfessionalDescription.pdf

Magadzire, T.T. (2006). Batch Grid Toolbox. Script for ArcView 3.2. USGS/ FEWSNET. http://arcscripts.esri.com

McVay, K.R. (1999). Grid Projector. Script for ArcView 3.2. http://arcscripts.esri.com

Microsoft® Corporation. (2003). Microsoft® Office Professional Edition 2003. www.microsoft.com

Patterson, W. (2004). Image-Tools version 2.6. Script for ArcView 3.2. Department of Fish and Game. http://arcscripts.esri.com

Petras, I. (2003). Basin1. Script for ArcView 3.2. Department of Water Affairs and Forestry, Pretoria, South Africa. http://arcscripts.esri.com

Raber, G. (1999). IMAGE GEOREFERENCING TOOLS. Script for ArcView 3.2. http: //arcscripts.esri.com

Saraf, A.K. (2002). GRID ANALYST EXTENSION version 1.1. Script for ArcView 3.2. Department of Earth Sciences, University of Roorkee, India. http://arcscripts. esri.com

Schaub, T. (2004). FEATUREDENSITY. Script for ArcView 3.2. CommEn Space. www.commenspace.org, http://arcscripts.esri.com

Schmidt, F. (2002). TOPOCROP. Script for ArcView 3.2. Precision Agriculture Project. www.preagro.de, http://arcscripts.esri.com

StatSoft®, Inc. (2004). STATISTICA™ data analysis software system version 7. www.statsoft.com.

Weigel, J. (2002). GRID CONVERTER 2.2. Script for ArcView 3.2. http://arc scripts.esri.com

Weigel, J. (2005). GRIDMACHINE 6.77. Script for ArcView 3.2. http://arcscripts.esri.com

MAPS AND DIGITAL DATA

Coetzee, M.E. (2001b). NAMSOTER – A SOTER DATABASE FOR NAMIBIA. Digital database. AEZ Programme, Ministry of Agriculture, Water and Rural Development. Windhoek, Namibia.

Du Pisani, A.L. (2005a). INTERPOLATION OF RAINFALL DATA FROM THE QLPP PILOT AREA. Unpublished data. AEZ Programme, Ministry of Agriculture, Water and Forestry. Windhoek, Namibia.

Du Pisani, A.L. (2005b). INTERPOLATION OF TEMPERATURE DATA FROM THE QLPP PILOT AREA. Unpublished data. AEZ Programme, Ministry of Agriculture, Water and Forestry. Windhoek, Namibia.

DWA. (1992). UPDATED ISOHYETAL RAINFALL MAP FOR NAMIBIA. Unpublished Report No. 11/1/8/H5, Hydrology Division, Department of Water Affairs. Windhoek, Namibia.

FAO. (1991). THE DIGITIZED SOIL MAP OF THE WORLD. World Soil Resources Report 67 (10 diskettes). FAO, Rome, Italy.

FAO. (1996). THE DIGITIZED SOIL MAP OF THE WORLD INCLUDING DERIVED SOIL PROPERTIES. CD-ROM. FAO, Rome, Italy.

FAO. (2003). SOIL AND TERRAIN DATABASE FOR SOUTHERN AFRICA (SOTERSAF). Land and Water Digital Media Series 25. ISRIC, FAO. Rome, Italy.

Geo Business Solutions. (2005). MTC CELLULAR PHONE COVERAGE MAP; NAMPOWER POWER NETWORK MAP. Windhoek, Namibia.

Geological Survey of Namibia. (2008). LITHOLOGY OF WINDHOEK (2216) AND GOBABIS (2218) MAP SHEETS - digital data. ArcView Shape format. Windhoek, Namibia.

MAWF. (2005). NAMIBIAN AGRICULTURAL RESOURCES INFORMATION SYSTEM (NARIS). Geographical information system. AEZ Programme, Ministry of Agriculture, Water and Forestry. Windhoek, Namibia.

Roads Authority. (2004). Roads of Namibia – digital data. ArcView Shape format. Windhoek, Namibia.

Strohbach, B.J. (2008). UNPUBLISHED VEGETATION DATA. National Botanical Research Institute, Ministry of Agriculture, Water and Forestry. Windhoek, Namibia

Surveyor General. (1972). 2217BA MECKLENBURG. 1: 50 000 scale topographical map. 2nd ed. Government Printer, Pretoria, RSA.

Surveyor General. (1972). 2217DD BERGZICHT. 1: 50 000 scale topographical map. 2nd ed. Government Printer, Pretoria, RSA.

Surveyor General. (1972). 2218AA OZOMBAHEBERG. 1: 50 000 scale topographical map. 2nd ed. Government Printer, Pretoria, RSA.

Surveyor General. (1972). 2218AB OMAKUARA. 1: 50 000 scale topographical map. 2nd ed. Government Printer, Pretoria, RSA.

Surveyor General. (1972). 2218AC OMITARA. 1: 50 000 scale topographical map. 2nd ed. Government Printer, Pretoria, RSA.

Surveyor General. (1972). 2218AD WITVLEI. 1: 50 000 scale topographical map. 2nd ed. Government Printer, Pretoria, RSA.

Surveyor General. (1972). 2218BA KEHORO. 1: 50 000 scale topographical map. 2nd ed. Government Printer, Pretoria, RSA.

Surveyor General. (1972). 2218BB HENNOPSRUST. 1: 50 000 scale topographical map. 2nd ed. Government Printer, Pretoria, RSA.

Surveyor General. (1972). 2218BC MARGARETENTAL. 1: 50 000 scale topographical map. 2nd ed. Government Printer, Pretoria, RSA.

Surveyor General. (1972). 2218BD GOBABIS. 1: 50 000 scale topographical map. 2nd ed. Government Printer, Pretoria, RSA.

Surveyor General. (1972). 2218DA HONITON. 1: 50 000 scale topographical map. 2nd ed. Government Printer, Pretoria, RSA.

Surveyor General. (1972). 2218DB DORINGVELD. 1: 50 000 scale topographical map. 2nd ed. Government Printer, Pretoria, RSA.

Surveyor General. (1972). 2218DC SCHÖNBORN. 1: 50 000 scale topographical map. 2nd ed. Government Printer, Pretoria, RSA.

Surveyor General. (1972). 2218DD SPATZENFELD. 1: 50 000 scale topographical map. 2nd ed. Government Printer, Pretoria, RSA.

Surveyor General. (1973). 2218CA OKOMBUKA. 1: 50 000 scale topographical map. 2nd ed. Government Printer, Pretoria, RSA.

Surveyor General. (1973). 2218CB AFGUNS. 1: 50 000 scale topographical map. 2nd ed. Government Printer, Pretoria, RSA.

Surveyor General. (1973). 2218CC OTJIMBONDONA. 1: 50 000 scale topographical map. 2nd ed. Government Printer, Pretoria, RSA.

Surveyor General. (1973). 2218CD NINA. 1: 50 000 scale topographical map. 2nd ed. Government Printer, Pretoria, RSA.

Surveyor General. (1976). 2217AA. 1: 50 000 scale topographical map. 2nd ed. Government Printer, Pretoria, RSA.

Surveyor General. (1976). 2217AB MIDGARD. 1: 50 000 scale topographical map. 2nd ed. Government Printer, Pretoria, RSA.

Surveyor General. (1976). 2217AC. 1: 50 000 scale topographical map. 2nd ed. Government Printer, Pretoria, RSA.

Surveyor General. (1976). 2217AD JG STRIJDOM. 1: 50 000 scale topographical map. 2nd ed. Government Printer, Pretoria, RSA.

Surveyor General. (1976). 2217BB OKAHUA. 1: 50 000 scale topographical map. 2nd ed. Government Printer, Pretoria, RSA.

Surveyor General. (1976). 2217BC SEEIS. 1: 50 000 scale topographical map. 2nd ed. Government Printer, Pretoria, RSA.

Surveyor General. (1976). 2217BD OTJIVERO. 1: 50 000 scale topographical map. 2nd ed. Government Printer, Pretoria, RSA.

Surveyor General. (1976). 2217CB BISMARCKBERGE. 1: 50 000 scale topographical map. 2nd ed. Government Printer, Pretoria, RSA.

Surveyor General. (1976). 2217CC ARIS. 1: 50 000 scale topographical map. 2nd Ed. Government Printer, Pretoria, RSA.

Surveyor General. (1976). 2217CD BRACK. 1: 50 000 scale topographical map. 2nd ed. Government Printer, Pretoria, RSA.

Surveyor General. (1976). 2217DA OTJIMUKONA. 1: 50 000 scale topographical map. 2nd ed. Government Printer, Pretoria, RSA.

Surveyor General. (1976). 2217DB OKAPANJE. 1: 50 000 scale topographical map. 2nd ed. Government Printer, Pretoria, RSA.

Surveyor General. (1976). 2217DC DORDABIS. 1: 50 000 scale topographical map. 2nd ed. Government Printer, Pretoria, RSA.

Surveyor General. (1981). 2218 GOBABIS. 1: 250 000 scale topographical map. 2nd ed. Government Printer, Pretoria, RSA.

Surveyor General. (1983). 2217CA WINDHOEK. 1: 50 000 scale topographical map. 2nd ed. Government Printer, Pretoria, RSA.

Surveyor General. (1984). 2216 WINDHOEK. 1: 250 000 scale topographical map. 2nd ed. Government Printer, Pretoria, RSA.